DOCUMENT RELEASE AND CHANGE FORM

Prepared For the U.S. Department of Energy, Assistant Secretary for Environmental Management
By Washington River Protection Solutions, LLC., PO Box 850, Richland, WA 99352
Contractor For U.S. Department of Energy, Office of River Protection, under Contract DE-AC27-08RV14800

TRADEMARK DISCLAIMER: Reference herein to any specific commercial product, process, or service by trade name, trademark, manufacturer, or otherwise, does not necessarily constitute or imply its endorsement, recommendation, or favoring by the United States government or any agency thereof or its contractors or subcontractors. Printed in the United States of America.

Release Stamp

DATE: Dec 01,2020

HANFORD RELEASE

1. **Doc No:** RPP-RPT-59197 **Rev.** 02

2. **Title:**
Analysis of Past Tank Waste Leaks and Losses in the Vicinity of Waste Management Area C at the Hanford Site, Southeast Washington

3. **Project Number:** T2R26 ☐N/A

4. **Design Verification Required:** ☐Yes ☒No

5. **USQ Number:** ☒ N/A RPP-27195

6. **PrHA Number** **Rev.** ☒ N/A

Clearance Review Restriction Type: public

7. **Approvals**

Title	Name	Signature	Date
Clearance Review	Aardal, Janis D	*Aardal, Janis D*	12/01/2020
Document Control Approval	Meinecke, Kathryn R	*Meinecke, Kathryn R*	12/01/2020
Originator	Bergeron, Marcel P	*Bergeron, Marcel P*	11/30/2020
Responsible Manager	Rutland, Paul L	*Rutland, Paul L*	11/30/2020

8. **Description of Change and Justification**

Updated version of RPP-RPT-59197. Rev. 1 that was originally cleared in October 2016.

9. **TBDs or Holds** ☒N/A

10. **Related Structures, Systems, and Components**

a. **Related Building/Facilities** ☒N/A	b. **Related Systems** ☒N/A	c. **Related Equipment ID Nos. (EIN)** ☒N/A

11. **Impacted Documents – Engineering** ☒N/A

Document Number	Rev.	Title

12. **Impacted Documents (Outside SPF):**

N/A

13. **Related Documents** ☒N/A

Document Number	Rev.	Title

14. **Distribution**

Name	Organization
Bergeron, Marcel P	CLOSURE & INTERIM MEASURES
Field, Jim G	PROCESS ENGINEERING
Lee, Kearn (Pat)	CLOSURE & INTERIM MEASURES
Parker, Dan	CLOSURE & INTERIM MEASURES
Rutland, Paul L	CLOSURE & INTERIM MEASURES
Singleton, Kristin M	CLOSURE & INTERIM MEASURES

INFORMATION CLEARANCE REVIEW AND RELEASE APPROVAL

Part I: Background Information

Title: Analysis of Impacts of Past Tank Waste Leaks and Losses in the Vicinity of Waste Management Area C at the Hanford Site, Southeast Washington

Publish to OSTI? ☐ Yes ☑ No

Information Category:
☐ Abstract ☐ Journal Article ☐ Summary
☐ Internet ☐ Visual Aid ☐ Software
☐ Full Paper ☑ Report ☐ Other

Trademark/Copyright "Right to Use" Information or Permission Documentation	Yes	NA
	☐	☑

Document Number: RPP-RPT-59197 Revision 2 Date: October 2020

Author: Bergeron, Marcel P

Part II: External/Public Presentation Information

Conference Name:

Sponsoring Organization(s): DOE

Date of Conference: Conference Location:

Will Material be Handed Out? ☐ Yes ☑ No Will Information be Published? ☐ Yes ☑ No *(If Yes, attach copy of Conference format instructions/guidance.)*

Part III: WRPS Document Originator Checklist

Description	*Yes*	*N/A*	*Print/Sign/Date*
Information Product meets requirements in TFC-BSM-AD-C-01?	☐	☑	
Document Release Criteria in TFC-ENG-DESIGN-C-25 completed? (Attach checklist)	☐	☑	
If product contains pictures, safety review completed?	☐	☑	

Part IV: WRPS Internal Review

Function	*Organization*	*Date*	*Print Name/Signature/Date*
Subject Matter Expert	WRPS	10/31/2020	Bergeron, Marcel P Workflow data attached
Responsible Manager	WRPS	09/21/2020	Rutland, Paul L Workflow data attached
Other:			

Part V: IRM Clearance Services Review

Description	*Yes*	*No*	*Print Name/Signature*
Document Contains Classified Information?	☐	☒	If Answer is "Yes," ADC Approval Required Print Name/Signature/Date
Document Contains Information Restricted by DOE Operational Security Guidelines?	☐	☒	Reviewer Signature: Print Name/Signature/Date
Document is Subject to Release Restrictions? *If the answer is "Yes," please mark category at right and describe limitation or responsible organization below:*	☐	☒	Document contains: ☐ Applied Technology ☐ Protected CRADA ☐ Personal/Private ☐ Export Controlled ☐ Proprietary ☐ Procurement – Sensitive ☐ Patentable Info. ☐ OUO ☐ Predecisional Info. ☐ UCNI ☐ Restricted by Operational Security Guidelines ☐ Other (Specify)
Additional Comments from Information Clearance Specialist Review? Replacement file addressed reviewer comments.	☐	☐	Information Clearance Specialist Approval APPROVED By Lynn M. Ayers at 8:56 am, Nov 12, 2020 Print Name/Signature/Date

When IRM Clearance Review is Complete – Return to WRPS Originator for Final Signature Routing (Part VI)

INFORMATION CLEARANCE REVIEW AND RELEASE APPROVAL

Part VI: Final Review and Approvals

Description	*Approved for Release*		*Print Name/Signature*
	Yes	*N/A*	
WRPS External Affairs	☒	☐	McCune, Hal C - IDMS workflow data attached
WRPS Office of Chief Counsel	☒	☐	Peters, Amber D - IDMS workflow data attached
DOE – ORP Public Affairs/Communications	☒	☐	Tyree, Geoff T - IDMS workflow data attached
Other: DOE OCC	☒	☐	King, Grace J - IDMS workflow data attached
Other: DOE ORP SME	☒	☐	Lobos, Rodrigo A - IDMS workflow data attached

Comments Required for WRPS-Indicate Purpose of Document:

Updated version of RPP-RPT-59197. Rev. 1 that was originally cleared in Oct of 2016.

APPROVED
By Lynn M. Ayers at 8:56 am, Nov 12, 2020

Approved for Public Release; Further Dissemination Unlimited

Information Release Station

Was/Is Information Product Approved for Release? ☒ Yes ☐ No

If Yes, what is the Level of Releaser? ☑ Public/Unrestricted ☐ Other (Specify) _____

Date Information Product Stamped/Marked for Release: 11/12/2020

Was/Is Information Product Transferred to OSTI? ☐ Yes ☒ No

Forward Copies of Completed Form to WRPS Originator

```
- <workflow name="(LMA) Normal - RPP-RPT-59197 Rev2" id="276501203">
  - <task name="Clearance Process" id="0" date-initiated="20200921T0704"
      performer="LYNN M AYERS" performer-id="212954838" username="h3998817">
      <comments>Please review for public release, the Rev 2 "Analysis of Impacts
        of Past Tank Waste Leaks and Losses in the Vicinity of Waste
        Management Area C at the Hanford Site, Southeast Washington,"
        submitted by Marcel Bergeron. Thank you, Lynn Ayers Information
        Clearance</comments>
    </task>
    <task name="Add XML" id="1" date-done="20200921T0704" />
    <task name="Manager Approval" id="41" date-due="20200924T0704" date-
      done="20200921T0751" performer="PAUL L RUTLAND" performer-
      id="140633218" username="h4494439" disposition="Approve"
      authentication="true" />
    <task name="Document Reviewer2" id="53" date-due="20200924T0750" date-
      done="20200921T0926" performer="AMBER D PETERS" performer-
      id="210402196" username="h3022486" disposition="Public Release"
      authentication="true" />
    <task name="Document Reviewer1" id="54" date-due="20200924T0750" date-
      done="20200923T1036" performer="HAL C MC CUNE" performer-
      id="226350486" username="h7687509" disposition="Public Release"
      authentication="true" />
  - <task name="Document Reviewer3" id="52" date-due="20200924T0750" date-
      done="20201005T1825" performer="RODRIGO A LOBOS" performer-
      id="232334741" username="h2488419" disposition="Public Release"
      authentication="true">
      <comments>Page 8/533 Scoping Case 1 (Case 1) evaluates the size of the
        tank C-105 leak. An upper bound and lower bound inventory were
        examined. The lower bound inventory analysis produced concentrations
        substantially below observed concentrations for 99Tc in observation
        wells. It was concluded based on the inventory analysis that the lower
        bound concentration estimate for 99Tc is inconsistent with observed
        concentration data, whereas the upper bound inventory estimate for 99Tc
        of 10 Ci in the tank C-105 leak waste was consistent with observed
        concentrations of 99Tc and thus the lower bound estimate is used for all
        other Scoping Cases. Should this be upper bound since the lower bound is
        inconsistent with observed concentration data?</comments>
    </task>
    <task name="Doc Owner Clearance Review" id="13" date-due="20201006T1826"
      date-done="20201020T1550" performer="MARCEL P BERGERON" performer-
      id="172635544" username="h0006384" disposition="Send On"
      authentication="true" />
    <task name="Milestone 1" id="24" date-done="20201020T1550" />
    <task name="ORP Document Reviewer2" id="58" date-due="20201022T1550"
      date-done="20201029T0856" performer="GRACE J KING" performer-
      id="211901436" username="h9807759" disposition="Public Release"
      authentication="true" />
    <task name="ORP Document Reviewer1" id="57" date-due="20201022T1550"
      date-done="20201030T1202" performer="GEOFFREY T TYREE" performer-
      id="6158846" username="h0068565" disposition="Public Release"
      authentication="true" />
    <task name="Doc Owner Reviews ORP Comments" id="61" date-
      due="20201102T1201" date-done="20201031T0653" performer="MARCEL P
      BERGERON" performer-id="172635544" username="h0006384"
      disposition="Send On" authentication="true" />
```

```
  <task name="Milestone 2" id="62" date-due="20201102T0653" date-
    done="20201031T0653" />
  <task name="Verify Doc Consistency" id="4" date-due="20201103T0653" date-
    done="20201106T0908" performer="LYNN M AYERS" performer-id="212954838"
    username="h3998817" disposition="Cleared" authentication="true" />
</workflow>
```

From: Bergeron, Marcel P
To: Ayers, Lynn M
Subject: Updates to RPP-RPT-59197, Rev. 2 for IDMS
Date: Tuesday, October 20, 2020 3:08:34 PM
Attachments: RPP-RPT-59197_Rev2_Clean_Final_10202020_compressed.pdf

---

Hi Lynn,

I have an update to the subject document for resubmission to RMAP which is attached. It has two updates:

- An update to page viii of the executive summary to address a comment from Rod Lobos
- An update to Figure 7-5 in Section 7

Hopefully the size of the file won't be a problem for you

Please give me a call if you have questions

Marcel

Marcel P. Bergeron
Principal Scientist, Closure and Interim Measures
marcel_p_bergeron@rl.gov
Office: (509) 376-4935
Cell: (509) 554-4924

washington river protection solutions
contractor to the United States Department of Energy

RPP-RPT-59197
Revision 2

Analysis of Impacts of Past Tank Waste Leaks and Losses in the Vicinity of Waste Management Area C at the Hanford Site, Southeast Washington

M. W. Kozak
S. Mehta
A. Ali
A. Mayenna
M. Weber
INTERA, Inc.

W. J. McMahon
CH2M HILL Plateau Remediation Company

M. P. Bergeron
J. G. Field
Washington River Protection Solutions, LLC

M. P. Connelly
TecGeo, Inc.

Date Published
October 2020

Prepared for the U.S. Department of Energy
Office of River Protection
Contract No. DE-AC27-08RV14800

Approved for public release; distribution unlimited

This page intentionally left blank.

VERSION HISTORY

Version	Date	Author	Change Description
Rev. 0	4-Oct-2016	M. Kozak et al.	Updates to initial draft in response to review comments provided by DOE-ORP and from WRPS.
Rev. 1	31-Oct-2016	M. Kozak et al.	Updates to Rev. 0 based internal review comments on past leaks analysis of tritium in Section 6.
Rev. 2	xx-Oct-2020	M. Kozak et al.	Updates to Rev. 1 in response to review comments provided by Washington State Department of Ecology and additional review comments from DOE-ORP

EXECUTIVE SUMMARY

The U.S. Department of Energy (DOE), Office of River Protection (ORP) is pursuing closure on the Single-Shell Tank (SST) Waste Management Area (WMA) C under Federal requirements and forthcoming State-approved closure plans and permits in accordance with the Hanford Federal Facility Agreement and Consent Order (HFFACO) (Ecology et al. 1989), Action Plan, Appendix I.

The Performance Assessment (PA) requirements for the closure process are outlined in Appendix I of the HFFACO. Appendix I of the HFFACO Action Plan contains language that broadens the scope of a "performance assessment" compared to its usual usage in the literature and in DOE Order 435.1, Radioactive Waste Management.

To distinguish between the two terms and avoid confusion, the term "performance assessment" is used in this document in the following manner:

- The broadened scope of the HFFACO Action Plan Appendix I analysis will be referred to as the "Appendix I Performance Assessment" (IPA)

- The simpler "performance assessment" (PA) will refer solely to the DOE O 435.1 definition of performance assessment.

Appendix I of the HFFACO Action Plan describes the waste retrieval and closure process that is to be implemented for the Hanford Site SST system. The four components of the IPA are illustrated in Figure ES-1. This document represents the right-most component in Figure ES-1 and is an analysis of past leaks that occurred at WMA C. Additionally, this document is used as an input to the Baseline Risk Assessment for WMA-C (RPP-RPT-58329, *Baseline Risk Assessment for Waste Management Area C*).

Figure ES-1. The Components of the Appendix I Performance Assessment.

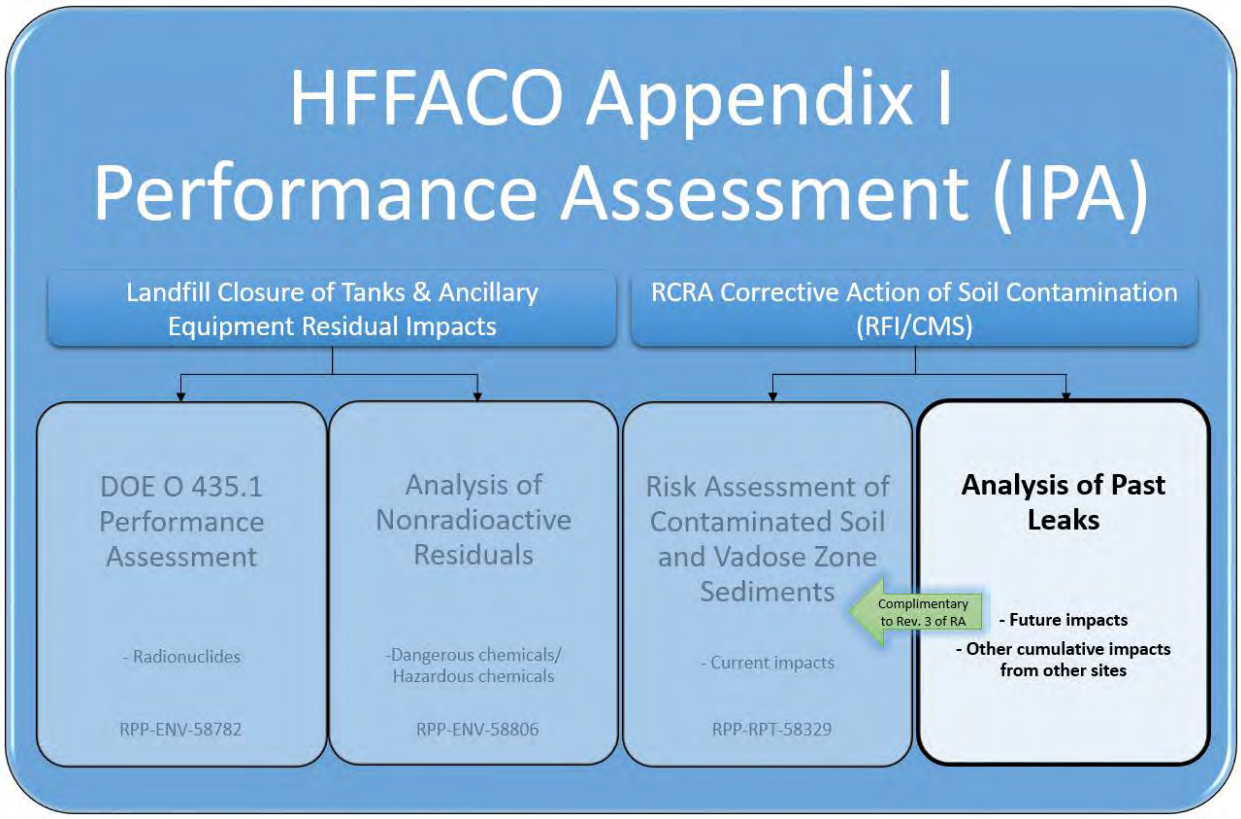

RA = Baseline Risk Assessment
HFFACO = Hanford Federal Facility Agreement and Consent Order
RCRA = Resource Conservation and Recovery Act of 1976
RFI/CMS = RCRA Facility Investigation/Corrective Measures Study

References:
DOE O 435.1, Radioactive Waste Management.
RPP-ENV-58782, *Performance Assessment of Waste Management Area C, Hanford Site, Washington*
RPP-ENV-58806, *Analysis of Post-Closure Groundwater Impacts of Hazardous Chemicals from Residual Wastes in Tanks and Ancillary Equipment at Waste Management Area C at the Hanford Site, Southeast Washington*..
RPP-RPT-58329, *Risk Assessment of Contaminated Soils and Vadose Zone Sediments Waste Management Area C at the Hanford Site, Southeast Washington*
.

The overall regulatory context of this document is provided in the Preface (p. 1-1). As indicated in the Preface, this document provides some supporting analyses for the risk assessment groundwater protection evaluation for soils contaminated by past leaks and releases from WMA C as documented in RPP-RPT-58329. Information presented in this document is expected to be used to support the evaluation of groundwater contamination under WMA C. This risk assessment evaluates overall impacts to human and ecological receptors from both non-radiological and radiological contaminants in contaminated soils at WMA C under current conditions, in the absence of actions to control or mitigate releases. Additionally, the risk

assessment is a support analysis to the *Resource Conservation and Recovery Act of 1976* (RCRA) Facility Investigation/Corrective Measures Study (FI/CMS) of WMA C. The analyses of past leaks included in this document are also intended to provide supporting information potentially relevant to the selection and specific implementation of groundwater mitigation measures being undertaken as a part of the *Comprehensive Environmental Response, Compensation, and Liability Act* (CERCLA) Remedial Investigation/Feasibility Study (RI/FS) effort in 200-BP-5-OU. As stated in Washington State Department of Ecology Letter 18-NWP-088, "Department of Ecology's (Ecology) Comments on the United States Department of Energy Submittal of the Phase 2 RCRA Facility Investigation Report (RFI), RPP-RPT-58339, Rev. 0 and Waste Management Area C Corrective Measures Study (CMS) Report, RPP-RPT-59379, Rev. 0," dated June 11, 2018:

- "Ecology approves the RFI and has determined there is a need to capture and remove contaminants of concern from the groundwater in WMA C. "

- "Ecology acknowledges that groundwater remediation will be managed through the 200-BP-5 and 200-PO-1 Comprehensive Environmental Response, Compensation, and Liability Act (CERCLA) Groundwater Operable Units. The proposed Feasibility Study for Interim Action will cite capture and removal of Tc-99 as the preferred alternative, with Tc-99 cited as a primary contaminant of concern for WMA C. A number of co-contaminants have also been identified for WMA C, including but not limited to cyanide, iodine-129, nitrate, and sulfate. Ecology expects that the co-contaminants identified in the Feasibility Study for Interim Action will be addressed incidentally with the CERCLA remediation."

The analysis of past leaks has been structured to meet several goals. First, the analysis is intended to be responsive to ideas and concerns expressed in the 2009 – 2011 PA scoping sessions (see Section 1.1.1), in which stakeholders identified specific features of WMA C that have the potential to influence the migration of contaminants. Second, the analysis is intended to be consistent, to the extent possible, with the PA (RPP-ENV-58782, *Performance Assessment of Waste Management Area C, Hanford Site, Washington*) and RCRA Closure Analysis (RCA) (RPP-ENV-58806, *RCRA Closure Analysis of Waste Management Area C, Hanford Site, Washington*) for disposal of residual wastes in WMA C. Data comparisons of this analysis and previous studies are intended to support confidence in the models used in those reports. A third goal is to provide an understanding of the key features and processes discussed in Sections 1.0 and 2.0 that influence the migration of contaminants, to aid in the design of the remedial strategy for groundwater at WMA C. Fourth, the goal is to use the understanding gained by modeling and analysis to provide a projection of the future evolution of the contamination beneath WMA C to be used as an input to the Baseline Risk Assessment (RPP-RPT-58329).

The strategy for this analysis of leaks at WMA C is to define and analyze a suite of scoping cases to evaluate the uncertainties associated with past leaks. These uncertainties can be broadly considered to originate from one of the following sources.

- Uncertainties exist in the timing, inventory, and volumes of leaks. These uncertainties have been discussed at length in Revision 4 of RPP-ENV-33418.

- Uncertainties exist in past actions taken to mitigate the surface manifestations of past leaks. In particular for several UPRs, water was added via firehose to surface contamination to wash it down into the soil column.

- Uncertainties exist in interpretations of the groundwater monitoring and vadose zone characterization data used to estimate current contamination levels resulting from the past leaks. The data represent specific locations and instances in time while the contamination continues to move.

- Uncertainties exist in the hydrogeological representation of the stratigraphy below WMA C. These uncertainties have been addressed in RPP-ENV-58782 and RPP-ENV-58806 by evaluating the consequences of alternative interpretations of the hydrogeology. This approach has continued to be used in the current document.

- Uncertainties exist in the effective values of parameters used in modeling groundwater flow and contaminant transport. These uncertainties are discussed in detail in RPP-ENV-58782 and RPP-ENV-58806.

- Uncertainties exist regarding the evolution of the groundwater system at WMA C over the past several decades, as discussed in Section 2.0. Anthropogenic water introduced south of WMA C created a gradient generally to the north, which has transitioned over recent decades to a gradient generally southward. The transition between these two states occurred approximately coincident with the arrival of the first contaminants at the water table. This feature of the groundwater system evolution complicates the interpretation of the observed contamination in groundwater wells at WMA C, as it is likely to have affected the trajectory of plumes moving in the aquifer.

The analyses of potential releases of contaminants in residual wastes presented in RPP-ENV-58782 and RPP-ENV-58806 were focused on future site conditions, and as a result did not directly address several of these sources of uncertainty; specifically, those associated with the leaks and that associated with the past evolution of the water table. However, in RPP-ENV-58782 and RPP-ENV-58806, a number of approaches to developing confidence in the data, assumptions, and methods were used, as follows:

- Many data were based on WMA C-specific site characterization, sampling, measurements and interpretations, including those for contaminant inventory, geology, hydrology and geochemistry. When data specific to WMA C were not available, data from nearby sites or comparable conditions, as well as data reported in the literature, were used.

- Data were upscaled to represent field-scale processes using scientifically accepted approaches that have been published in peer-reviewed journals. Upscaling techniques use information from small, core-scale measurements to develop parameters that are applicable to large, field-scale models.

- The process-based modeling software, Subsurface Transport Over Multiple Phases (STOMP)©[1] code (PNNL-12030, *STOMP Subsurface Transport Over Multiple Phases Version 2.0 Theory Guide*; Pacific Northwest National Laboratory, Queried 12/18/2015, [STOMP User Guide], http://stomp.pnnl.gov/user_guide/STOMP_guide.stm; PNNL-11216, *STOMP Subsurface Transport Over Multiple Phases Application Guide*), has been benchmarked and deemed suitable for use in this PA. The STOMP© code is the pre-authorized modeling software at the Hanford Site for vadose zone and near-field groundwater modeling (Internal memorandum 1301789, "Modeling to Support Regulatory Decision-making at Hanford"). The STOMP© code has previously been qualified for simulation use at Hanford by CH2M HILL Plateau Remediation Company (CHPRC) (CHPRC-00269, *STOMP Requirements Traceability Matrix CHPRC Build 4*).

- Sensitivity and uncertainty analyses were conducted to evaluate the effect of parameter uncertainties and alternative conceptual models on the overall performance of the system.

These approaches specifically address uncertainties in model conceptualizations and input parameters for groundwater flow and transport, but do not address uncertainties in past leaks and in past evolution of the groundwater table.

Consequently, the model used in RPP-ENV-58782 and RPP-ENV-58806 was adapted so that the water table was reflective of conditions at WMA C when first arrival of contaminants at the water table was observed. Model results have been compared to ^{99}Tc concentrations observed in groundwater monitoring wells around WMA C because ^{99}Tc is a key risk driver, and the contamination levels observed there are unambiguously the result of WMA C past leaks.[2] The concentration data for ^{99}Tc collected from groundwater monitoring wells have been used to evaluate and constrain the model inputs and assumptions that produce results that are consistent with the arrival times and concentration levels of ^{99}Tc observed historically in the vicinity of WMA C.

The results of the constrained model are then also compared with other contaminant concentration data as appropriate. The model is also used to project the consequences of past leaks to evaluate the future consequences of the past waste leaks and releases and to evaluate how the groundwater concentrations may change in the future.

Three approaches were used to evaluate and gain insight into the past leaks.

- The first approach was a set of scoping cases intended to examine uncertainties in the leaks themselves and in the vadose zone representation. In the scoping cases, the water table was assumed to be fixed, and directed in the same way as the prospective water table used for future analyses, but at a higher level, which allows the analysis to represent the shorter travel time in the vadose zone that would have existed when the plumes

[1] Subsurface Transport Over Multiple Phases (STOMP)© is copyrighted by Battelle Memorial Institute, 1996.
[2] Although it is possible that ^{99}Tc from the past leaks arrived in groundwater prior to the installation of well 299-E27-7 in 1982 and the RCRA groundwater monitoring well network in 1989, the concentration trends of ^{99}Tc currently observed in those monitoring wells appear to be consistent with the available information regarding the timing, size, and inventory of the leaks.

initially arrived. The Scoping Cases have been compared to the time of first arrival of the contamination at the water table. They have also been used for qualitative comparisons with the peak concentration of the groundwater plume. However, the Scoping Cases cannot represent the spatial distribution of contamination in the groundwater. The Scoping Cases are documented in Section 4.0.

- The second approach grew from stakeholder concerns about the potential effects of small-scale spatial heterogeneity on flow and transport in the vadose zone. A variety of modeling approaches and evaluations of data were used to assess the importance of heterogeneity at WMA C. The models used are related to the PA and RCA models, but use various approaches to represent spatial variability at WMA C. This approach is summarized in Section 5.0.

- The third approach was to introduce a time-varying water table to represent the likely evolution of the aquifer gradient over the simulation period. This model is used for direct comparisons with groundwater monitoring data and is documented in Section 6.0.

The first approach (Scoping Cases) is described in detail in Section 4.0. A summary of each of the scoping cases are as follows:

- Scoping Case 1 (Case 1) evaluates the size of the tank C-105 leak. An upper bound and lower bound inventory were examined. The lower bound inventory analysis produced concentrations substantially below observed concentrations for ^{99}Tc in observation wells. It was concluded based on the inventory analysis that the lower bound concentration estimate for ^{99}Tc is inconsistent with observed concentration data, whereas the upper bound inventory estimate for ^{99}Tc of 10 Ci in the tank C-105 leak waste was consistent with observed concentrations of ^{99}Tc and thus the upper bound estimate is used for all other Scoping Cases.

  Note: In this set of scoping cases (e.g., Case 1), an additional scoping case recommended by Ecology during their review of this document that doubled the tank C-105 leak volume and duration in a doubling of impacts predicted in at the fence line of WMA C.

- Scoping Case 2 (Case 2) investigated the effect of changing groundwater fluxes on the modeling results. It was found that the higher flux rates led to a greater dilution of plume concentrations at the water table, and it was concluded that the lower groundwater flux rate provides concentration levels of ^{99}Tc that are more consistent with monitoring data observed in key monitoring well locations.

- Scoping Case 3 (Case 3) investigated the effect of a higher recharge rate than used in the other scoping cases. It was found that the higher recharge rates led to early arrival of the plume at the water table compared to field observations. It was concluded that the higher recharge rate is not consistent with the arrival time observed in monitoring data. Case 3 also investigated the effect of a localized addition of water using a firehose to mitigate the operational hazard of leaks at UPRs -82 and -86, followed by the addition of gunite

caps on the UPRs. This analysis showed that this past practice has had little effect on the downward migration of waste releases from the three UPRs to groundwater at WMA C.

- Scoping Case 4 (Case 4) investigated a number of vadose zone parameters and conceptual models of potential interest, to evaluate the potential for heterogeneities in the vadose zone to affect the plume development migration. The variety of these cases led to several observations: (a) an alternative model with refined stratigraphy in the Hanford formation – sand sequence (H2 unit) did not significantly change results, (b) a highly heterogeneous model of the vadose zone showed early arrival times that appear to be inconsistent with observed arrival times in the field, (c) use of 95th percentile vadose zone hydraulic properties showed early arrival times that appear to be inconsistent with observed arrival times in the field, and (d) evaluations of both a hypothetical clastic dike and a poorly sealed borehole located near the tank C-105 leak had negligible effects on the results.

In summary, the three specific scoping cases (e.g., Cases 3a, 4b, and 4d produced results in which the arrival time of the calculated plume appears to be substantially earlier than the observations in the wells. The remaining Scoping Cases evaluated in Section 4.0 agreed well with observed arrival times, produced comparable results to each other, and none were obviously superior to others in terms of explaining the observation groundwater monitoring well data.

In Section 5.0, several bodies of work from multiple organizations are presented that explicitly evaluate vadose zone heterogeneities beneath WMA C . These conceptual models seek to understand the potential effects of heterogeneities on flow and contaminant transport. In Section 5.0, summaries are provided of the following bodies of work:

- Work by Pacific Northwest National Laboratory (PNNL) documented in PNNL-24740, *Alternative Conceptual Models of the Subsurface at WMA C;*

- Work by Washington River Protection Solutions, LLC (WRPS), PNNL, and INTERA Incorporated (INTERA) documented in RPP-RPT-61239, *Multiple Lines of Evidence and Modeling Results for Heterogeneous Alternative Conceptual Models of the Subsurface at Waste Management Area C*, in preparation; and

- Work by WRPS and INTERA completed at the request of Washington State Department of Ecology (Ecology) and documented in Appendix B of this document.

The transient water table analysis presented in Section 6.0 provides the best representation of the observation well data. However, it was necessary to make assumptions that approximate the magnitude and direction of groundwater flow in order to achieve the good agreement with data. These approximations are speculative but serve to provide insight into the evolution of the groundwater monitoring well data. Key factors that most strongly influenced the comparison with downgradient wells 299-E27-23 and 299-E27-21 were:

- The local direction of flow and hydraulic gradient at WMA C at the time the releases reach the water table.

- The northwesterly direction of flow inferred in other areas to the northwest of WMA C in the early year 2000 timeframe when releases from WMA C sources reached groundwater may not have been representative of local conditions at WMA C.

- Observations of ^{99}Tc concentrations seen historically in wells on the north, south, and southeast sides of the tank suggests that the primary directions of flow in the farm may have been variable ranging from southwest to southeast at the time when past releases started to impact groundwater.

- The time varying responses and concentration levels at individual monitoring wells is directly related to the timing of dynamic changes in the flow direction and hydraulic gradients as the water continues its return to more natural conditions.

The model analysis of transient flow conditions provided in Section 6.0 showed that the conceptual model involving the counterclockwise rotation of the hydraulic gradient from northwest to southeast provided the best representation of observed conditions in monitoring wells near WMA C. The associated numerical model results appear capable of approximating observed field data for the time of arrival of ^{99}Tc to groundwater and concentration levels of ^{99}Tc in groundwater. The model results also appear to explain qualitative features of the data, such as the sharp rise and fall of concentrations in individual wells. The model results include several assumptions regarding the timing and inventory of the past releases, and direction and magnitude of the hydraulic gradient during the time it could not be measured. The model results also appear to provide insight into the concentration levels and changes in concentration observed in monitoring wells since 2000. However, the model is not a unique representation of the data, and other models may also represent the data well. The model analysis was not intended to be predictive but rather used to gain some understanding the potential effects of transient water table changes on contaminant behavior.

The modeling is based on best estimates about the timing and magnitude of the leaks in WMA C (see Table 3-1). There is substantial uncertainty about these assumptions, and caution must be exercised in drawing too firm conclusions from modeling based on these assumptions. However, if the assumed leaks are indeed a reasonable representation of the actual leaks, the modeling allows some cautious insight into past monitoring observations and what may be expected in the future. These insights into past monitoring observations based on the modeling results are as follows:

- The tank C-105 leak appears to be the dominant source of ^{99}Tc observed in groundwater in the monitoring wells. According to the inventory estimates in RPP-RPT-42294, *Hanford Waste Management Area C Soil Contamination Inventory Estimates*, it is the only release large enough and early enough to bring about the concentration levels observed in the monitoring wells.

- Releases from UPR-81, UPR-82, and UPR-86, and the leak associated with tank C-110 are believed to have occurred later than the release from tank C-105, and the modeling results exhibit the implications of this. The concentration of ^{99}Tc in the wells located

nearest the UPRs is currently dominated by the tank C-105 leak. The results of modeling would suggest that ^{99}Tc attributed to the three UPRs peaks a few years after the concentration of ^{99}Tc peaks because of the tank C-105 leak. Therefore, the ^{99}Tc originating from the UPRs may be a secondary source that has not yet been observed because it has not yet reached the water table. There is a general lack of vadose characterization data and/or historical groundwater monitoring information in the general area of the UPRs that can be used to either support or refute the results realized in the modeling of UPR releases.

Given the uncertainties in the timing and ^{99}Tc inventory of the UPR releases, use of other modeling assumptions about the releases at the UPRs relative to the assumed releases at tank C-105 could lead to different modeling results and conclusions about their relative importance.

The modeling results indicate that as the water table returns to more natural conditions, the rotation of the gradient will continue to alter the primary movement of the plumes from primarily a southerly direction to a more southeasterly direction in the near future. The very high concentration levels of ^{99}Tc observed in wells 299-E27-23 and 299-E27-21, southwest and south of WMA C, respectively, may be observed in wells 299-E27-24 and 299-E27-14, which are located to the southeast of WMA C.

In the forward projection of the impacts of past waste releases into the future, sorbing and nonsorbing contaminants were treated differently. Nonsorbing contaminants (e.g., ^{99}Tc) have arrived or are arriving while the water table is in transition, at a higher level than will exist in the future. By contrast, sorbing contaminants are projected to arrive when the water table has returned to its projected long-term steady condition. As a result of this situation, the forward modeling of leaks has been undertaken using models with different water table heights for the sorbing and nonsorbing contaminants.

The forward projection results lead to several observations, as follow:

- Model results show that peak contaminant releases to the aquifer of mobile constituents like ^{99}Tc or nitrate originating from WMA C reach their peak values in the year 2020 to year 2030 timeframe. Peak contaminant releases to the aquifer of other mobile constituents like chromium modeled as hexavalent chromium originating from WMA C reach their peak values in about the same timeframe. Results also showed that fluxes of mobile contaminants from the vadose zone would continue to release to groundwater for decades (see Section 7.3.3).

- Consistent with the first observation, model results indicate that current high concentrations of ^{99}Tc below WMA C would decline but continue to be elevated over the next several decades as the contaminant source in the vadose zone becomes depleted.

- Contaminated groundwater, which is now impacted by releases from past waste leaks and losses at WMA C and in the future by upgradient sources in the B Complex area, will continue to migrate downgradient and will impact groundwater in local areas contained within the 200-PO-1 groundwater operable unit such as the A Complex area.

- There are not significant overlaps between releases from residual wastes in a closed WMA C and the releases from leaks.

Compared to the releases from WMA C past leaks or residual wastes, the releases from upgradient sources produce more significant concentrations of all contaminants other than ^{99}Tc than the release from WMA C past leaks or residual wastes. For ^{99}Tc, the groundwater concentrations associated with past leaks are the most significant.

TABLE OF CONTENTS

PREFACE 1-1

1.0 INTRODUCTION 1-1

1.1 BACKGROUND 1-1

1.1.1 Waste Management Area C Performance Assessment Scoping Process 1-6

1.1.2 Regulatory Context 1-8

1.2 PURPOSE AND SCOPE OF THE REPORT 1-10

1.2.1 Purpose 1-10

1.2.2 Scope 1-10

1.3 GENERAL FACILITY DESCRIPTION 1-12

1.4 PREVIOUS ASSESSMENTS 1-16

1.4.1 Single-Shell Tank Performance Assessment 1-17

1.4.2 Tank Closure and Waste Management Environmental Impact Statement Analysis of Waste Management Area C 1-17

2.0 BACKGROUND 2-1

2.1 INVENTORY ESTIMATES FOR PAST WASTE RELEASES TO THE VADOSE ZONE 2-1

2.1.1 Tank 241-C-101 2-3

2.1.2 Tank 241-C-104 2-7

2.1.3 Tank 241-C-105 2-9

2.1.4 Tank 241-C-108 2-9

2.1.5 Tank 241-C-110 2-10

2.1.6 Tank 241-C-111 2-10

2.1.7 Tank 241-C-112 2-11

2.1.8 UPR-200-E-81 2-11

2.1.9 UPR-200-E-82 2-11

2.1.10 UPR-200-E-86 2-12

2.1.11 216-C-8 French Drain 2-12

2.1.12 Surface Level Releases 2-13

2.1.13 Other Unplanned Releases 2-15

2.2 HYDROGEOLOGIC SETTING OF HANFORD'S CENTRAL PLATEAU ... 2-17

2.2.1 Geologic Setting and Stratigraphic Units 2-17

2.2.2 Unconfined Aquifer System 2-19

2.3 WASTE MANAGEMENT AREA C SITE CHARACTERIZATION 2-35

2.3.1 Geology of Waste Management Area C 2-36

2.3.2 Vadose Zone Characterization at Waste Management Area C 2-39

2.3.3 Unconfined Aquifer at Waste Management Area C 257

2.3.4 Recent Interpretations of Waste Management Area C Groundwater Chemistry 2-65

3.0 FEATURES FOR ANALYSIS 3-1

3.1 OVERVIEW OF ANALYSIS 3-1

3.2 ADAPTATION OF THE PERFORMANCE ASSESSMENT CONCEPTUAL AND NUMERICAL MODELS USED IN THE EVALUATION OF WASTE RESIDUAL IMPACTS 3-6

3.3 CONCEPTUAL MODEL OF SOURCE TERM RELEASES 3-12

3.4 VADOSE ZONE CONSIDERATIONS 3-12

3.5 AQUIFER CONSIDERATIONS 3-13

3.5.1 Flow Considerations 3-13

3.5.2 Transport Considerations 3-14

3.6 MATHEMATICAL MODELS 3-17

3.6.1 Source Term 3-17

3.6.2 Groundwater Flow and Contaminant Transport Equations 3-18

3.6.3 Implementation of the Groundwater Pathway in STOMP© 3-20

3.6.4 Key Assumptions in Past leaks Analysis 3-41

3.7 SUMMARY OF FEATURES AND DEFINITION OF SCOPING ANALYSIS CASES 3-42

4.0 SCOPING ANALYSES OF PAST WASTE RELEASES 4-1

4.1 CASE 1: EFFECT OF LEAK INVENTORIES AND VOLUMES 4-6

4.1.1 Case Description 4-7

4.1.2 Case Results 4-9

4.2 CASE 2: EFFECT OF CHANGES IN GROUNDWATER FLUX RATES 4-10

4.2.1 Case Descriptions 4-11

4.2.2 Case Results 4-13

4.3 CASE 3: EFFECT OF CHANGES IN RECHARGE CONDITIONS 4-16

4.3.1 Case Descriptions 4-17

4.3.2 Case Results 4-18

4.4 CASE 4: EFFECT OF CHANGING VADOZE ZONE PARAMETERS AND CONCEPTUALIZATION 4-22

4.4.1 Case Description and Model Implementation 4-23

4.4.2 Case Results 4-26

4.5 ADDITIONAL INVENTORY SCOPING CASE REQUESTED BY ECOLOGY 4-37

4.6 SUMMARY OF ANALYSIS CASES AND ASSOCIATED OBSERVATIONS 4-37

5.0 EVALUATIONS OF THE USE OF ALTERNATIVE CONCEPTUAL MODELS TO EVALUATE THE EFFECTS OF VADOSE HETEROGENEITY ON PLUME TRANSPORT 5-1

5.1 SUMMARY OF PREVIOUS WORK BY PACIFIC NORTHWEST NATIONAL LABORATORY AS DOCUMENTED IN PNNL-24740 5-1

5.2 SUMMARY OF PREVIOUS WORK ON ALTERNATIVE HETEROGENEOUS MODELS BEING DOCUMENTED IN RPP-RPT-61239 5-3

5.3 SUMMARY OF WORK ON WASHINGTON STATE DEPARTMENT OF ECOLOGY'S ADVOCACY MODELS DOCUMENTED IN APPENDIX B 5-16

6.0 EVALUATION OF THE EFFECTS OF TRANSIENT WATER TABLE 6-1

6.1 TRANSIENT MODEL DESCRIPTION AND IMPLMENTATION 6-1

6.1.1 Central Plateau Groundwater Model 6-2

6.1.2 Application of the Central Plateau Groundwater Model to Waste Management Area C 6-3

6.2 EVALUATION OF THE TRANSIENT WATER TABLE HYDRAULIC GRADIENT 6-6

6.3 RESULTS OF SELECTED TRANSIENT WATER TABLE MODELS 6-12

6.3.1 Results of the Assumed Clockwise Rotation of the Transient Hydraulic Gradient Model 6-12

6.3.2 Results of the Assumed Counter-Clockwise Rotation of the Transient Hydraulic Gradient Model 6-15

6.3.3 Summary 6-27

6.3.4 Conclusion 6-28

7.0 FUTURE IMPACTS OF PAST WASTE LEAKS AND RELEASES 7-1

7.1 APPROACH TO THE FORWARD PROJECTION 7-1

7.2 IDENTIFICATION OF CONTAMINANTS OF POTENTIAL CONCERN 7-2

7.3 FUTURE PROJECTIONS OF PAST WASTE LEAKS AND RELEASES 7-5

7.3.1 Results of Groundwater Pathway Evaluation: Time before Assumed Closure of Waste Management Area C in 2020 7-6

7.3.2 Results of Groundwater Pathway Evaluation: Time after Assumed Closure of Waste Management Area C in 2020 7-15

7.3.3 Results of Groundwater Pathway Evaluation: Contaminant Flux to Groundwater 7-32

7.4 DISCUSSION OF MONITORING RESULTS WITH PROJECT MODELING RESULTS FOR NITRATE, SULFATE, AND CHROMIUM 7-46

8.0 OTHER SOURCES OF CONTAMINATION AT WASTE MANAGEMENT AREA C 8-1

8.1 CONTRIBUTION OF CONTAMINATION ASSOCIATED WITH UPGRADIENT SOURCES 8-1

8.1.1 Technetium-99 8-3

8.1.2 Nitrate 8-3

8.1.3 Cyanide 8-16

8.1.4 Iodine-129 8-16

8.1.5 Uranium 8-16

8.2 CONTRIBUTION OF RESIDUAL WASTES 8-31

8.2.1 Technetium-99 8-31

8.2.2 Nitrate 8-31

8.2.3 Iodine-129 8-32

8.2.4 Uranium-238/Total Uranium 8-39

8.3 COMPARISON OF UPGRADIENT SOURCES, RESIDUAL WASTES, AND PAST LEAKS 8-39

8.3.1 Technetium-99 8-39

8.3.2 Nitrate 8-44

8.3.3 Cyanide 8-44

8.3.4 Iodine-129 8-44

8.3.5 Total Uranium 8-44

8.4 SUMMARY OF PEAK CONCENTRATIONS OF CONTAMINANTS OF POTENTIAL CONCERN 8-45

9.0 SUMMARY AND OBSERVATIONS 9-1

10.0 REFERENCES 10-1

APPENDICES

A Estimation of Potential Impacts From Past Releases of Cyanide at Waste Management Area C…… A-1
B Evaluation of Impacts of Vadose Zone Heterogeneities on Contaminant Transport at WMA C Using Washington State Department of Ecology's Advocacy Model……B-1
C Review Comment Record…… C-1
D Results of Additional Scoping Case Related to Past Leaks Analysis Proposed by Ecology …….D-1

LIST OF FIGURES

Figure 1-1. Hanford Site Tank Farms. 1-4

Figure 1-2. The Components of the Appendix I Performance Assessment. 1-5

Figure 1-3. Hanford Site and its Location in Washington State. 1-13

Figure 1-4. Location Map of Waste Management Area C and Surrounding Area. 1-15

Figure 1-5. Location Map of Unplanned Release Sites of Waste Management Area C. 1-16

Figure 2-1. Schematic of Process Used to Determine Vadose Zone Inventory. 2-2

Figure 2-2. Near Surface Spectral Gamma Activity in 241-C Tank Farm. 2-14

Figure 2-3. Surface Topography and Boundaries of the 200-BP-5 Groundwater Operable Unit. 2-19

Figure 2-4. Comparison of 200-BP-5 Operable Unit Hydrostratigraphy to Hanford Site Stratigraphy. 2-22

Figure 2-5. Representative Photos of the Hanford Formation, Cold Creek Unit, Ringold Unit E, Ringold Lower Mud Unit, and Basalt. 2-23

Figure 2-6. 200-BP-5 Operable Unit Near-Field Area Hydrogeology Depicting Truncation of Ringold Units on Uplifted Basalt. 2-24

Figure 2-7. Distribution of Hydrogeologic Units at the Water Table, 2009. 2-25

Figure 2-8. Discharge History for the 216-B Pond System and Gable Mountain Pond. 2-26

Figure 2-9. Discharge History for the 216-T Pond and 216-U Pond. 2-27

Figure 2-10a. Hind Cast Water Table Map of the Hanford Site, January 1944. 2-29

Figure 2-10b. Water Table Elevations for June 1987. 2-29

Figure 2-10c. Water Table Elevations for 2013. 2-29

Figure 2-11. Water Table Elevations at Groundwater Monitoring Wells Close to U-Pond (200 West Area) and B-Pond (200 East Area). 2-31

Figure 2-12. 200-BP-5 Operable Unit Pleistocene Paleo-Erosional Surface Topography. 2-33

Figure 2-13. Groundwater Contamination for 2013 which Originated within the Central Plateau along with Central Plateau Groundwater Interest Areas. 2-34

Figure 2-14. Waste Management Area C Tanks, Infrastructure, and Associated Unplanned Releases. 2-37

Figure 2-15. Fence Diagram Showing Cross-Sections through Waste Management Areas A-AX and C. 2-38

Figure 2-16. Fence Diagram of Alternative Geologic Models for Waste Management Area C. 2-41

Figure 2-17. Vadose Zone and Groundwater Monitoring Network for Waste Management Area C. 2-42

Figure 2-18. Three-Dimensional Perspective of Waste Management Area C Tanks and Drywells Showing Occurrence of Significant (>10 pCi/g) Cesium-137 Contamination in the Vadose Zone along with Technetium-99 at Borehole C4297. 2-45

Figure 2-19. Completed Phase 2 RCRA Facility Investigation Characterization Locations.... 2-46

Figure 2-20. Completed Transitional (Phase 1.5) Characterization Locations. 2-47

Figure 2-21. Moisture Content (% Vol) Measurements in Vadose Zone at Waste Management Area C. 2-60

Figure 2-22. Technetium-99 Concentrations above the Drinking Water Standard at Waste Management Area C Wells from January 2006 through December 2015. 2-72

Figure 2-23. Nitrate Concentrations above the Maximum Contaminant Level at Waste Management Area C Wells from January 2006 through December 2015. 2-73

Figure 2-24. Sulfate Concentrations above the Secondary Maximum Contaminant Level at Waste Management Area C Wells from January 2006 through December 2015. 2-74

Figure 2-25. Cyanide Concentrations in Waste Management Area C Wells from January 2006 through December 2015. 2-75

Figure 2-26. Technetium-99 Activity in Wells 299-E27-7, 299-E27-14, and 299-E27-24 on East and Southeast Side of Waste Management Area C. 2-76

Figure 2-27. Technetium-99 Activity in Wells 299-E27-4, 299-E24-13, and 299-E27-23 on West Side of Waste Management Area C. 2-77

Figure 2-28. Technetium-99-to-Nitrate Ratio Comparisons for Wells on West Side (299-E27-21 and 299-E27-23) and Southeast Side (299 E27-14 and 299-E27-23) of Waste Management Area C. 2-78

Figure 2-29. Cyanide-to-Nitrate Ratio Comparisons for Well 299-E27-14. 2-79

Figure 2-30. Bivariate Plots of Technetium-99/Nitrate Ratio Versus Nitrate by Year. 2-80

Figure 2-31. Bivariate Plots of Technetium-99/Sulfate Ratio Versus Sulfate by Year. 2-81

Figure 2-32. Bivariate Plots of Technetium-99/Chloride Ratio Versus Chloride by Year. 2-82

Figure 2-33. Conceptual Model for the Vadose Zone Flux Calculation. 2-84

Figure 2-34. Estimates of the Activity of Technetium-99 by Two Alternative Methods. 2-85

Figure 3-1. Schematic Conceptual Representation of Waste Management Area C and Contaminant Migration into the Environment along the Various Pathways Evaluated in the Performance Assessment. 3-8

Figure 3-2. Conceptual Model of the Waste Management Area C Site Showing Stratigraphy. 3-9

Figure 3-3. Evolution of the Groundwater Gradient In the Low-Level Waste Management Area-1 Monitoring Network. 3-10

Figure 3-4. Surface Conditions in and Around Waste Management Area C during the Construction and Operations Period. 3-11

Figure 3-5. Interpolated Numerical Three-Dimensional Post-Closure Alternative I Hydrogeologic Model. 3-23

Figure 3-6. Plan View of Waste Management Area C Performance Assessment Model Domain Showing the Horizontal Distribution and Surface Type of the Irregularly-Spaced Calculation Nodes. 3-26

Figure 3-7. Fence Diagram of Interpolated Numerical Three-Dimensional Post-Closure Alternative I Hydrogeologic Model. 3-27

Figure 3-8. Interpolated Numerical Three-Dimensional Post-Closure Alternative II Hydrogeologic Model. 3-28

Figure 3-9. Fence Diagram of Interpolated Numerical Three-Dimensional Post-Closure Alternative II Hydrogeologic Model. 3-29

Figure 3-10. Interpreted Extent of Paleo-channel Area Associated with the Ancestral Columbia River in 200 East Area in the Vicinity of Waste Management Area C. 3-36

Figure 3-11. Hindcast Water Table Map of the Hanford Site, January 1944. 3-36

Figure 3-12. Central Plateau Groundwater Model Calibration Results in the Vicinity of Waste Management Area C. 3-43

Figure 4-1. Decreases in Water Table Level with Time at Waste Management Area C, with a Projection to Future Conditions. 4-8

Figure 4-2. Points of Calculation for the Scoping Analyses. 4-9

Figure 4-3. Development of Technetium-99 Plumes over Selected Time Periods for Case 1a (Upper Bound Inventory for the Tank 241-C-105 Leak). 4-12

Figure 4-4. Concentrations at the Selected Points of Calculation for Case 1a (Upper Bound Inventory for the Tank 241-C-105 Leak). 4-13

Figure 4-5. Concentrations at the Selected Points of Calculation for Case 1b (Lower Bound Inventory for the Tank 241-C-105 Leak). 4-15

Figure 4-6. Concentrations at the Selected Points of Calculation for Case 2a (10th Percentile Groundwater Flux). 4-16

Figure 4-7. Concentrations at the Selected Points of Calculation for Case 2b (90th Percentile Groundwater Flux). 4-20

Figure 4-8. Surface Conditions in and Around Waste Management Area C during the Construction and Operations Period. 4-21

Figure 4-9. Concentrations at Selected Points of Calculation for Case 3a (150 mm/y Recharge). 4-24

Figure 4-10. Concentrations at Selected Points of Calculation for Case 3b (100 mm/y Recharge). 4-26

Figure 4-11. Concentrations at Selected Points of Calculation for Case 3c (Firehose Water Addition followed by Gunite Cover). 4-28

Figure 4-12. Depiction of Interpolated Numerical Three-Dimensional Model of Alternative Conceptual Model II for Scoping Case 4a. 4-29

Figure 4-13. Depiction of Interpolated Numerical Three-Dimensional Model of Heterogeneous Alternative Conceptual Model for Scoping Case 4b. 4-30

Figure 4-14. Depiction of Hypothetical Clastic Dike near Tank 241-C-105 Conceptualized for Scoping Case 4e. 4-32

Figure 4-15. Depiction of Hypothetical Unsealed Borehole Near Tank 241-C-105 Conceptualized for Scoping Case 4f. 4-33

Figure 4-16. Concentrations at Selected Points of Calculation for Case 4a (Alternative Geologic Model II). 4-34

Figure 4-17. Concentrations at Selected Points of Calculation for Case 4b (Alternative Heterogeneous Model). 4-36

Figure 4-18. Concentrations at Selected Points of Calculation for Case 4c (Median Hydraulic Properties). 4-38

Figure 4-19. Concentrations at Selected Points of Calculation for Case 4d (95th Percentile Hydraulic Properties). 4-39

Figure 4-20. Concentrations at Selected Points of Calculation for Case 4e (Clastic Dike)..... 4-41

Figure 4-21. Concentrations at Selected Points of Calculation for Case 4f (Borehole Preferential Pathway). 4-43

Figure 4-22. Technetium-99 Concentration Results A) at the WMA C Fence line and 100 m down gradient and B) at Fenceline Points of Calculation from Alternative Inventory Case Requested by Ecology. 4-44

Figure 4-23. Comparison of All Scoping Analysis Cases at 120 Meters Downgradient for the Tank 241-C-105 Past Release Location. 4-46

Figure 4-24. Comparison of Simulated Technetium-99 Concentrations from All Scoping Analysis Cases at 120 Meters Downgradient for the Tank 241-C-105 Past Release Location with Focus on First Arrival of Technetium-99 Concentrations Observed at Wells 299 E27-14 and 299-E27-23. 4-47

Figure 5-1. Analysis of the Geologic Logs for Sediment Texture within Each Hydrostratigraphic Unit..... 5-5

Figure 5-2. Histograms of Silt Particle Size for 31 Drywells at Waste Management Area C.... 5-6

Figure 5-3. Histograms of Moisture Content for the H2 Unit at Waste Management Area C. 5-7

Figure 5-4. Moisture Content Down Dip through Waste Management Area C from UPR-200-E-82. 5-8

Figure 5-5. Characterization Data from Borehole C4297 by Single Shell Tank 241-C-105.... 5-10

Figure 5-6. Comparison of Material Property Units for each of the Alternative Conceptual Models. 5-12

Figure 5-7. Comparison of Plume Spreading in 1995 for the Four Alternative Conceptual Site Models along a Southwest to Northeast Cross Section at the Location of the Single-Shell Tank 241-C-105 Unplanned Release. 5-13

Figure 5-8. Comparison of Plume Spreading in 1990 for the Four Alternative Conceptual Site Models along a Southwest to Northeast Cross Section at the Location of the UPR-200-E-82 Pipeline Leak Site. 5-13

Figure 5-9. Comparison of Instantaneous Technetium-99 Release at the Water Table for Single-Shell Tank 241-C-105 Unplanned Release for All Models. 5-15

Figure 5-10. Comparison of Instantaneous Technetium-99 Release at the Water Table for UPR-200-E-82 for All Models. 5-15

Figure 5-11. Depiction of Numerical Cross-Sectional Model of Fine-Grained Unit Alternative Conceptual Model. 5-17

Figure 5-12. Primary Case Results for EHM Cross-Sectional Model and FGU Cross-Sectional Model Comparing Mass Flux Arriving at the Water Table. 5-19

Figure 5-13. Comparison of Simulated (Primary Case) Technitium-99 Plume in the Vadose Zone in Year 1968 (First Row) and Year 1981 (Second Row) for EHM Cross-Sectional Model and FGU Cross-Sectional with Hss Hydraulic Properties for Fine-Grained Units. 5-20

Figure 5-14. Mass Flux Arriving at Water Table Showing the Effect of Hss and 31A Hydraulic Properties Used for the Fine-Grained Units. 5-21

Figure 5-15. Comparison of Simulated Technetium-99 Plume in the Vadose Zone in Year 1971 (First Row) to Year 2001 (Second Row) using FGU Cross-Sectional Model for the Primary Case (Hss Hydraulic Properties for Fine-Grained Units) and Sensitivity Case 1 (Sample 31A Hydraulic Properties for Fine-Grained Units). 5-22

Figure 6-1. Central Plateau Groundwater Model Calibration Results in the Vicinity of Waste Management Area C. 6-5

Figure 6-2. Alignment of the Central Plateau Groundwater Model and Waste Management Area C Unplanned Release Model Grids and Central Plateau Groundwater Model Hydraulic Head Interpolation Values Representing Calendar Year 2000 on a Triangular Mesh. 6-6

Figure 6-3. Waste Management Area C Unplanned Release Model Grid Hydraulic Head Boundary Averaging Values Representing Calendar Year 2000. 6-7

Figure 6-4. Inferred Direction of Flow During the Operations Period When the High Volume Discharge Facilities Operated. 6-11

Figure 6-5. Simulated Technetium-99 Plume in Groundwater Calendar Years 1998, 2000, 2002, 2005, 2010 and 2016 and Resulting from Waste Management Area C Unplanned Releases (Clockwise Rotation of the Hydraulic Gradient Based on Central Plateau Groundwater Model Boundary Conditions). 6-17

Figure 6-6. Comparison of Simulated Technetium-99 Concentrations in Groundwater to Measured Concentrations around the Northeast, Northwest, and Southwest of Waste Management Area C. Using Initial Conceptual Model with Clockwise Rotation of the Hydraulic Gradient. 6-20

Figure 6-7. Comparison of Simulated Technetium-99 Concentrations in Groundwater to Measured Concentrations around the Southwest and Southeast of Waste Management Area C. Using Initial Conceptual Model with Clockwise Rotation of the Hydraulic Gradient. 6-21

Figure 6-8. Simulated Technetium-99 Plume in Groundwater Calendar Years 1998, 2002, 2004, 2008, 2012 and 2016 and Resulting from Waste Management Area C Unplanned Releases (Counterclockwise Rotation of the Hydraulic Gradient). 6-23

Figure 6-9. Comparison of Simulated Technetium-99 Concentrations in Groundwater to Measured Concentrations around the Northeast, Northwest, and Southwest of Waste Management Area C. Conceptual Model with Counterclockwise Rotation of the Hydraulic Gradient. 6-25

Figure 6-10. Comparison of Simulated Technetium-99 Concentrations in Groundwater to Measured Concentrations around the Southwest and Southeast of Waste Management Area C. Conceptual Model with Counterclockwise Rotation of the Hydraulic Gradient. 6-26

Figure 7-1. Case 1a Past Leak Model Used for Nonsorbing Contaminants for the Forward Projection Compared to the Performance Assessment/RCRA Closure Analysis Model Used for the Sorbing Contaminants. 7-4

Figure 7-2. First-Arrival Time (in Calendar Year) of Radionuclides for Various K_d Values Based on Screening Analysis Using Subsurface Transport Over Multiple Phases. 7-13

Figure 7-3. Points of Calculation 100 Meters Downgradient of Waste Management Area C. 7-14

Figure 7-4. Concentration of Technetium-99 in Groundwater in the Points of Calculation at the Fenceline. 7-19

Figure 7-5. Concentration of Technetium-99 in Groundwater in the Points of Calculation 100 Meters Downgradient of the Fenceline. 7-20

Figure 7-6. Concentration of Tritium in Groundwater in the Points of Calculation at the Fenceline. 7-21

Figure 7-7. Concentration of Tritium in Groundwater in the Points of Calculation 100 Meters Downgradient of the Fenceline. 7-22

Figure 7-8. Concentration of Cobalt-60 in Groundwater in the Points of Calculation 100 Meters Downgradient of the Fenceline. 7-23

Figure 7-9. Concentration of Selenium-79 in Groundwater in the Points of Calculation 100 Meters Downgradient of the Fenceline. 7-24

Figure 7-10. Concentration of Nitrate in Groundwater in the Points of Calculation 100 Meters Downgradient of the Fenceline. 7-25

Figure 7-11. Concentration of Sulfate in Groundwater in the Points of Calculation 100 Meters Downgradient of the Fenceline. 7-26

Figure 7-12. Concentration of Chromium (as Cr^{+6}) in Groundwater in the Points of Calculation 100 Meters Downgradient of the Fenceline. 7-27

Figure 7-13. Concentration Contours of Technetium-99 along Cross-Section Planes through Unplanned Releases 200-E-81 and 200-E-82 and Tank Row 241-C-110, 241-C-107, 241-C-104 and 241-C-101 Corresponding to Year 2000. 7-28

Figure 7-14. Concentration Contours of Technetium-99 along Cross-Section Planes through Unplanned Releases 200-E-81 and 200-E-82 and Tank Row 241-C-110, 241-C-107, 241-C-104 and 241-C-101 Corresponding to Year 2016. 7-29

Figure 7-15. Concentration Contours of Nitrate along Cross-Section Planes through Unplanned Releases 200-E-81 and 200-E-82 and Tank Row 241-C-110, 241-C-107, 241-C-104 and 241-C-101 Corresponding to Year 2000. 7-30

Figure 7-16. Concentration Contours of Nitrate along Cross-Section Planes through Unplanned Releases 200-E-81 and 200-E-82 and Tank Row 241-C-110, 241-C-107, 241-C-104 and 241-C-101 Corresponding to Year 2016. 7-31

Figure 7-17. Concentration of Iodine-129 in Groundwater in the Points of Calculation at the Fenceline. 7-32

Figure 7-18. Concentration of Iodine-129 in Groundwater in the Points of Calculation 100 Meters Downgradient of the Fenceline. 7-33

Figure 7-19. Concentration of Tin-126 in Groundwater in the Points of Calculation 100 Meters Downgradient of the Fenceline. 7-36

Figure 7-20. Concentration of Uranium-238 in Groundwater in the Points of Calculation 100 Meters Downgradient of the Fenceline. 7-37

Figure 7-21. Concentration of Total Uranium in Groundwater in the Points of Calculation 100 Meters Downgradient of the Fenceline. 7-38

Figure 7-22. Concentration of Uranium-238 in Groundwater in the Points of Calculation at the Fenceline. 7-39

Figure 7-23. Concentration of Total Uranium in Groundwater in the Points of Calculation at the Fenceline. 7-40

Figure 7-24. Flux of Technetium-99 from the Vadose Zone that Enters Groundwater. 7-42

Figure 7-25. Flux of Nitrate from the Vadose Zone that Enters Groundwater. 7-43

Figure 7-26. Flux of Selenium-79 from the Vadose Zone that Enters Groundwater. 7-44

Figure 7-27. Flux of Uranium-238 from the Vadose Zone that Enters Groundwater. 7-45

Figure 8-1. 2013 200-BP-5 Operable Unit Consolidated Plume Map. 8-4

Figure 8-2. The Technetium-99 Plume at Year 2015 (Year 0 of the Simulation) for the Remedial Evaluation Case of 200-BP-5. 8-5

Figure 8-3. The Technetium-99 Plume at Year 2020 (Year 5 of the Simulation) for the Remedial Evaluation Case of 200-BP-5. 8-6

Figure 8-4. The Technetium-99 Plume at Year 2025 (Year 10 of the Simulation) for the Remedial Evaluation Case of 200-BP-5. 8-7

Figure 8-5. The Technetium-99 Plume at Year 2035 (Year 20 of the Simulation) for the Remedial Evaluation Case of 200-BP-5. 8-8

Figure 8-6. Remedial Evaluation Case Technetium-99 Concentrations at Waste Management Area C as a Function of Time. 8-9

Figure 8-7. The Nitrate Plume at Year 2015 (Year 0 of the Simulation) for the Remedial Evaluation Case of 200-BP-5. 8-10

Figure 8-8. The Nitrate Plume at Year 2025 (Year 10 of the Simulation) for the Remedial Evaluation Case of 200-BP-5. 8-11

Figure 8-9. The Nitrate Plume at Year 2030 (Year 15 of the Simulation) for the Remedial Evaluation Case of 200-BP-5. 8-12

Figure 8-10. The Nitrate Plume at Year 2035 (Year 20 of the Simulation) for the Remedial Evaluation Case of 200-BP-5. 8-13

Figure 8-11. Remedial Evaluation Case Nitrate Concentrations at Waste Management Area C as a Function of Time. 8-14

Figure 8-12. The Cyanide Plume at Year 2015 (Year 0 of the Simulation) for the Remedial Evaluation Case of 200-BP-5. 8-15

Figure 8-13. The Cyanide Plume at Year 2020 (Year 5 of the Simulation) for the Remedial Evaluation Case of 200-BP-5. 8-18

Figure 8-14. The Cyanide Plume at Year 2025 (Year 10 of the Simulation) for the Remedial Evaluation Case of 200-BP-5. 8-19

Figure 8-15. The Cyanide Plume at Year 2025 (Year 10 of the Simulation) for the Remedial Evaluation Case of 200-BP-5. 8-20

Figure 8-16. Remedial Evaluation Case Cyanide Concentrations at Waste Management Area C as a Function of Time. 8-21

Figure 8-17. The Iodine-129 Plume at Year 2015 (Year 0 of the Simulation) for the Remedial Evaluation Case of 200-BP-5. 8-22

Figure 8-18. The Iodine-129 Plume at Year 2025 (Year 10 of the Simulation) for the Remedial Evaluation Case of 200-BP-5. 8-23

Figure 8-19. The Iodine-129 Plume at Year 2035 (Year 20 of the Simulation) for the Remedial Evaluation Case of 200-BP-5. 8-24

Figure 8-20. The Iodine-129 Plume at Year 2045 (Year 30 of the Simulation) for the Remedial Evaluation Case of 200-BP-5. 8-25

Figure 8-21. Remedial Evaluation Case Iodine-129 Concentrations at Waste Management Area C as a Function of Time. 8-26

Figure 8-22. The Uranium Plume at Year 2015 (Year 0 of the Simulation) for the Remedial Evaluation Case of 200-BP-5. 8-27

Figure 8-23. The Uranium Plume at Year 2035 (Year 20 of the Simulation) for the Remedial Evaluation Case of 200-BP-5. 8-28

Figure 8-24. The Uranium Plume at Year 2045 (Year 30 of the Simulation) for the Remedial Evaluation Case of 200-BP-5. 8-29

Figure 8-25. The Uranium Plume at Year 2065 (Year 50 of the Simulation) for the Remedial Evaluation Case of 200-BP-5. 8-30

Figure 8-26. Remedial Evaluation Case Total Uranium Concentrations at Waste Management Area C as a Function of Time. 8-33

Figure 8-27. Groundwater Concentration of Technetium-99 at the Highest Point of Calculation 100 Meters Downgradient from Waste Management Area C. 8-34

Figure 8-28. Extent of Technetium-99 Plume in Groundwater 1,570 Years after Closure at the Time of the Maximum Concentration at the Point of Compliance. 8-35

Figure 8-29. Maximum Predicted Groundwater Concentration of Nitrate (K_d = 0 mL/g) at All Points of Calculation 100 Meters Downgradient from Waste Management Area C from Residual Wastes. 8-36

Figure 8-30. Extent of Nitrate Plume in Groundwater 1,375 Years after Closure at the Time of the Maximum Concentration at the 100-meter Point of Calculation. 8-37

Figure 8-31. Groundwater Concentration of Iodine-129 at All Points of Calculation 100 Meters Downgradient from Waste Management Area C from Residual Wastes. 8-38

Figure 8-32a. Predicted Groundwater Concentration of Uranium-238 at the Highest Point of Calculation 100 Meters Downgradient from Waste Management Area C. ... 8-41

Figure 8-32b. Predicted Groundwater Concentration of Total Uranium at the Highest Point of Calculation 100 Meters Downgradient from Waste Management Area C. ... 8-42

Figure 8-33. Results of the Past Leak Analysis for Technetium-99 at Points of Calculation 100 Meters Downgradient, Compared to Results from the Residual Waste Analysis and Upgradient Sources. 8-43

Figure 8-34. Results of the Past Leak Analysis for Nitrate at Points of Calculation 100 Meters Downgradient, Compared to Results from the Residual Waste Analysis and Upgradient Sources. 8-46

Figure 8-35. Results of the Past Leak Analysis for Iodine-129 at Points of Calculation 100 Meters Downgradient, Compared to Results from the Residual Waste Analysis and Upgradient Sources. 8-47

Figure 8-36. Results of the Past Leak Analysis for Total Uranium at Points of Calculation 100 Meters Downgradient, Compared to Results from the Residual Waste Analysis and Upgradient Sources. 8-48

LIST OF TABLES

Table 1-1. Data Packages Produced as a Part of the Waste Management Area C Performance Assessment Scoping Process. 1-7

Table 1-2. Reference Case Inventory of Past Leaks Assumed in the Single-Shell Tank Performance Assessment. 1-17

Table 1-3. Volumes of Past Leaks Assumed in the Single-Shell Tank Performance Assessment. 1-18

Table 1-4. Inventory of Past Tank Leaks and Unplanned Releases Assumed in the Tank Closure and Waste Management Environmental Impact Statement. 1-19

Table 1-5. Volumes of Past Leaks Assumed in the Tank Closure and Waste Management Environmental Impact Statement. 1-20

Table 2-1. Constituents Evaluated in the Hanford Defined Waste Model. 2-3

Table 2-2. Average Composition of Hanford Defined Model Chemical and Radiological Constituents for Selected Waste Types. 2-5

Table 2-3. Inventory Estimates for Releases at Waste Management Area C. 2-8

Table 2-4. Summary of Field Efforts Related to Areas Investigated in Waste Management Area C RCRA Facility Investigation. 2-48

Table 2-5. Hanford Environmental Information System Laboratory Qualifier Table. 2-51

Table 2-6. Summary Statistics for Volumetric Moisture Content in the Lithologic Units Underlying Waste Management Area C. 2-59

Table 2-7. Summary Statistics from January 1, 2006 to January 1, 2016 for Constituents Discussed in SGW-59669. 2-63

Table 3-1. Inventory of Technetium-99 Used for the Initial Analysis Cases. 3-13

Table 3-2. Distribution Coefficients (K_d) Values Used to Approximate the Transport of the Radionuclides in the Base Case. 3-15

Table 3-3. Base Case Recharge Rate (Net Infiltration) Estimates for Surface Conditions during the Pre-Construction, Operational, and Post-Closure Periods. 3-31

Table 3-4. Composite van Genuchten-Mualem Parameters for Various Strata at the Waste Management Area C Site Used in the Base Case Evaluations of Alternative Geologic Models I and II. 3-32

Table 3-5. Effective Bulk Density (E[ρb], g/cm^3) Estimates for Various Strata at Waste Management Area C Used in the Base Case Evaluations of Alternative Geologic Models I and II. 3-34

Table 3-6. Macrodispersity Estimates for Various Strata at Waste Management Area C Used in the Base Case Evaluations of Alternative Geologic Models I and II. 3-34

Table 3-7. Base Case Soil Hydraulic Properties for Aquifer Soil Type Used for Base Case at Waste Management Area C. 3-45

Table 4-1. Description of Past Tank Waste Release Scoping Cases. 4-3

Table 4-2. Comparison of the Technetium-99 Concentration Results at Selected Points of Calculation for Scoping Cases 1a and 1b. 4-14

Table 4-3. Comparison of the Technetium-99 Concentration Results at Selected Points of Calculation for Scoping Cases 2a and 2b. 4-19

Table 4-4. Assumed Recharge Rates (Net Infiltration) for Surface Conditions during the Pre-Construction, Operational Periods Used in Cases 1a, 1b, 3a, and 3b. 4-22

Table 4-5. Comparison of the Technetium-99 Concentration Results at Selected Points of Calculation for Scoping Cases 3a through 3d. 4-27

Table 4-6. van Genuchten-Mualem Parameters Corresponding to the Percentiles Selected for Cases 1a, 1b, 4c, and 4d from the Vertical Pore Water Velocity Cumulative Distribution Functions. 4-31

Table 4-7. Comparison of the Simulated Technetium-99 Concentration Results at Selected Points of Calculation for Scoping Cases 4a through 4f. 4-35

Table 4-8. Comparison of the Technetium-99 Concentration Results at Selected Points of Calculation for All Scoping Analysis Cases. 4-45

Table 5-1. Summary of Silt Particle Size Collected at Each Waste Management Area and the Vadose Zone Transport Field Study Site. 5-11

Table 6-1. Central Plateau Groundwater Model Hydraulic Head Interpolation Values and Waste Management Area C Unplanned Release Model Grid Boundary Rankings. 6-8

Table 6-2. Comparison of Central Plateau Groundwater Model Hydraulic Gradient Results (Magnitude and Direction) and Central Plateau Groundwater Model Results Modified to Rotate the Hydraulic Gradient Counterclockwise at Waste Management Area C. 6-14

Table 6-3. Central Plateau Groundwater Model Hydraulic Head Interpolation Values Modified to Rotate the Hydraulic Gradient Counterclockwise at Waste Management Area C, and Revised Model Grid Boundary Rankings. 6-15

Table 7-1. Leak Inventories of Contaminants of Concern Used in the Forward Projection Analyses. 7-11

Table 7-2. First-Arrival Time (in Calendar Year) of Radionuclides for Various K_d Values Based on Screening Analysis Using Subsurface Transport Over Multiple Phases. 7-13

Table 7-3. Width of the Nine Points of Calculation at the Waste Management Area C Fenceline. 7-15

Table 7-4. Summary Results of Radionuclides and Non-Radiological Contaminants that Arrive in Groundwater at the Waste Management Area C Fenceline before Closure..... 7-16

Table 7-5. Summary Results of Radionuclides and Non-Radiological Contaminants that Arrive in Groundwater at the Waste Management Area C Fenceline after Closure..... 7-41

Table 8-1. Peak Concentrations and Time of Peak of Arrival at Waste Management Area C from the Calculated Remedial Evaluation Case for Upgradient Sources. 8-16

Table 8-2. Comparison of Peak Concentrations and Approximate Calendar Year of the Occurrence of the Peak..... 8-49

LIST OF TERMS

Abbreviations and Acronyms

2-D	two-dimensional
3-D	three-dimensional
244-CR Vault	244-CR Process Tank Vault
ACM	alternative conceptual model
AEA	Atomic Energy Act
AMSL	above mean sea level
bgs	below ground surface
BRA	Baseline Risk Assessment
C Farm	WMA C Tank Farm
CCu	Cold Creek unit
CERCLA	Comprehensive Environmental Response, Compensation, and Liability Act of 1980
CFR	Code of Federal Regulations
CHPRC	CH2M HILL Plateau Remediation Company
CMS	Corrective Measures Study
COPC	constituent of potential concern
CPGWM	Central Plateau Groundwater Model
CRQL	contract required quantitation limit
CUL	cleanup level
CW	cladding waste
DOE	U.S. Department of Energy
DOE-ORP	U.S. Department of Energy, Office of River Protection
DQO	data quality objective

DWS	drinking water standard
DST	double-shell tank
Ecology	State of Washington Department of Ecology
EDTA	ethylenediaminetetraacetic acid
EHM	equivalent homogeneous medium
EIS	Environmental Impact Statement
ENM	Energy Northwest Columbia Generating Station
EPA	U.S. Environmental Protection Agency
ERDF	Environmental Restoration Disposal Facility
FS	Feasibility Study
GFAA	graphite furnace atomic absorption
H1 unit	Hanford formation – upper gravelly sequence
H2 unit	Hanford formation – sand sequence
H3 unit/CC_u/RF	undifferentiated Hanford formation (H3), Cold Creek unit and Ringold Formation
HDW	Hanford Defined Waste
HFFACO	Hanford Federal Facility Agreement and Consent Order
HRR	High Resolution Resistivity
HSU	hydrostratigraphic unit
HWMA	Hazardous Waste Management Act
IDF	Integrated Disposal Facility
IDL	instrument detection limit
INTERA	INTERA, Inc.
IPA	Appendix I Performance Assessment
K-U-T	potassium, uranium, thorium

LIGO	Laser Interferometer Gravitational Wave Observatory
LLWMA	Low-Level Waste Management Area
MCL	maximum contaminant level
MDA	minimum detectable activity
MDL	minimum detection limit
NAVD88	North American Vertical Datum of 1988
NRC	U.S. Nuclear Regulatory Commission
OU	operable unit
PA	performance assessment
PFP	Plutonium Finishing Plant
PoCal	point of calculation
PNNL	Pacific Northwest National Laboratory
PQL	practical quantitation limit
PUREX	Plutonium Uranium Extraction (facility)
RCA	RCRA Closure Analysis
RCRA	Resource Conservation and Recovery Act of 1976
REDOX	Reduction-Oxidation (facility)
RETC	RETention Curve (code)
RFI	RCRA facility investigation
RI	Remedial Investigation
RLM	Ringold Lower Mud Unit
Rtf	upper Ringold unit
Rwia	fluvial gravel unit A
Rwie	fluvial gravel unit E

SAP	Sampling Analysis Plan
SESP	Surface Environmental Surveillance Project
SGE	Surface Geophysical Exploration
SST	single-shell tank
SST PA	Single-Shell Tank Performance Assessment
STOMP	Subsurface Transport Over Multiple Phases (code)
TC&WM EIS	DOE/EIS-0391, “Final Tank Closure and Waste Management Environmental Impact Statement for the Hanford Site, Richland, Washington”
TEDF	Treated Effluent Disposal Facility
TIC	tentatively identified compound
TWINS	Tank Waste Information Network System
UPR	unplanned release
WIDS	Waste Information Data System
WMA	Waste Management Area
WRPS	Washington River Protection Solutions, LLC

LIST OF TERMS (cont.)

Waste Types

IX	ion exchange waste from the cesium recovery process at B Plant
P1	PUREX high-level waste (1956-1962)
P2	PUREX high-level waste (1963-1967)
CWP1	PUREX aluminum cladding waste (1956-1960)
CWP2	PUREX aluminum cladding waste (1961-1972)
CSR	waste from B Plant ion exchange cesium recovery
PSN	P2 supernate
PSS	PUREX sludge supernate derived from washing PUREX HLW sludges in 244-AR Vault or 241-A and 241-AX tanks

PREFACE

This document is the first of four volumes being written to support the performance assessment (PA) required under Section 2.5 of the Hanford Federal Facility Agreement and Consent Order (Ecology et al. 1989, hereinafter referred to as HFFACO) Appendix I for closure of the Hanford Site Tank Farms. The first single-shell tank (SST) farm being closed is Waste Management Area (WMA) C.

This particular volume contains an evaluation of the potential future impacts from selected radiological and hazardous chemicals and dangerous waste contaminants associated with past leaks and losses at WMA C. This evaluation includes specific analyses of past leaks that are intended to provide supporting information that could be relevant to the selection and specific implementation of groundwater mitigation measures being undertaken as a part of the Comprehensive Environmental Response, Compensation, and Liability Act (CERCLA) Remedial Investigation/Feasibility Study (RI/FS) effort in 200-BP-5-OU.

The other three volumes are as follows:

- A DOE O 435.1 Performance Assessment (RPP-ENV-58782, *Performance Assessment of Waste Management Area C, Hanford Site, Washington*) – An evaluation of the impacts from radioactive residual waste contaminants in tanks and ancillary equipment at a closed WMA C. The evaluation is needed by the U.S. Department of Energy (DOE) for closure of WMA C SSTs per DOE O 435.1, Radioactive Waste Management;

- A Hazardous Chemical Impact Analysis from Residual Wastes (RPP-ENV-58806, *Analysis of Post-Closure Groundwater Impacts from Hazardous Chemicals in Residual Wastes in Tanks and Ancillary Equipment at Waste Management Area C at the Hanford Site, Southeast Washington*); and

- A Risk Assessment of Contaminated Soils and Vadose Zone Sediments (RPP-RPT-58329, *Risk Assessment of Contaminated Soils and Vadose Zone Sediments at Waste Management Area C at the Hanford Site, Southeast Washington*, which is an evaluation of the impacts to human and ecological receptors from both non-radiological and radiological contaminants in soils at WMA C under current conditions, in the absence of actions to control or mitigate releases.

A more complete description of each of these documents is given in Section 1.1 of both RPP-ENV-58782 and RPP-ENV-58806.

1.0 INTRODUCTION

1.1 BACKGROUND

The U.S. Department of Energy, Office of River Protection (DOE-ORP) is pursuing closure on the SST WMA C under Federal requirements and forthcoming State-approved closure plans and permits in accordance with the HFFACO (Ecology et al. 1989), Action Plan, Appendix I. Waste Management Area C is located in the 200 East Area of the Central Plateau at Hanford and is one of 12 tank farms within 7 WMAs (A-AX, B-BX-BY, C, S-SX, T, TX-TY, and U) containing 149 SSTs and ancillary equipment built from 1943 to 1964 (see Figure 1-1).

The PA requirements for the closure process are outlined in Appendix I of the HFFACO. Appendix I of the HFFACO Action Plan contains language that broadened the scope of a "performance assessment." Section 2.5 of HFFACO Action Plan Appendix I states:

> "Ecology, as the lead agency for SST system closure, EPA, and DOE have elected to develop and maintain as part of the SST system closure plan <u>one performance assessment</u> for the purposes of evaluating whether SST system closure conditions are protective of human health and the environment for <u>all contaminants of concern</u>, both radiological and nonradiological. DOE intends that this performance assessment (PA) will document by reference relevant performance requirements defined by RCRA, HWMA, Clean Water Act, Safe Drinking Water Act, and the Atomic Energy Act of 1954 (AEA) and any other performance requirements that might be ARARs under CERCLA. <u>The PA is of larger scope than a risk assessment</u> required solely for nonradiological contaminants. The PA is expected to provide a single source of information that DOE can use to satisfy potentially duplicative functional and/or documentation requirements. <u>A PA will be developed for each WMA</u> and will incorporate the latest information available. These PAs will be approved by Ecology and DOE pursuant to their respective authorities. For Ecology approval means incorporation by reference, into the Site-Wide Permit through the closure plans.
>
> As <u>individual components are retrieved or characterized</u>, or other component closure activities are completed, <u>the resulting component characterization information will be incorporated into the WMA PA</u> to <u>determine its relative risk compared to the entire WMA performance.</u> In doing this, the Parties will be able to make interim closure decisions for individual components. Initially, the WMA PA will be based on assumptions and available data describing component characterization information. As each WMA proceeds toward closure, its respective PA will be updated to address all pertinent new results and findings – and will, as a minimum, incorporate the following results as they become available: actual volumes of tank waste residuals left after retrieval, results of

> leak investigations, new geologic and ancillary equipment waste characterization information, and the results of new barrier and tank residual stabilization and fill performance studies and tests. Final WMA closure decisions will be made after all components are retrieved and/or characterized, and all other component closure activities have been completed and a final WMA PA is completed."

Note: Underlining is added to emphasize key points in the scope of the HFFACO Action Plan Appendix I "performance assessment."

To distinguish between the two terms and avoid confusion, the term "performance assessment" will be used in this document in the following manner:

- The broadened scope of the HFFACO Action Plan Appendix I analysis will be referred to as the "Appendix I Performance Assessment" (IPA).

- The simpler "performance assessment" (PA) will refer solely to the DOE O 435.1 definition of performance assessment.

Appendix I of the HFFACO Action Plan describes the waste retrieval and closure process that is to be implemented for the Hanford Site SST system. The four components of the IPA are illustrated in Figure 1-2.

Figure 1-1. Hanford Site Tank Farms.

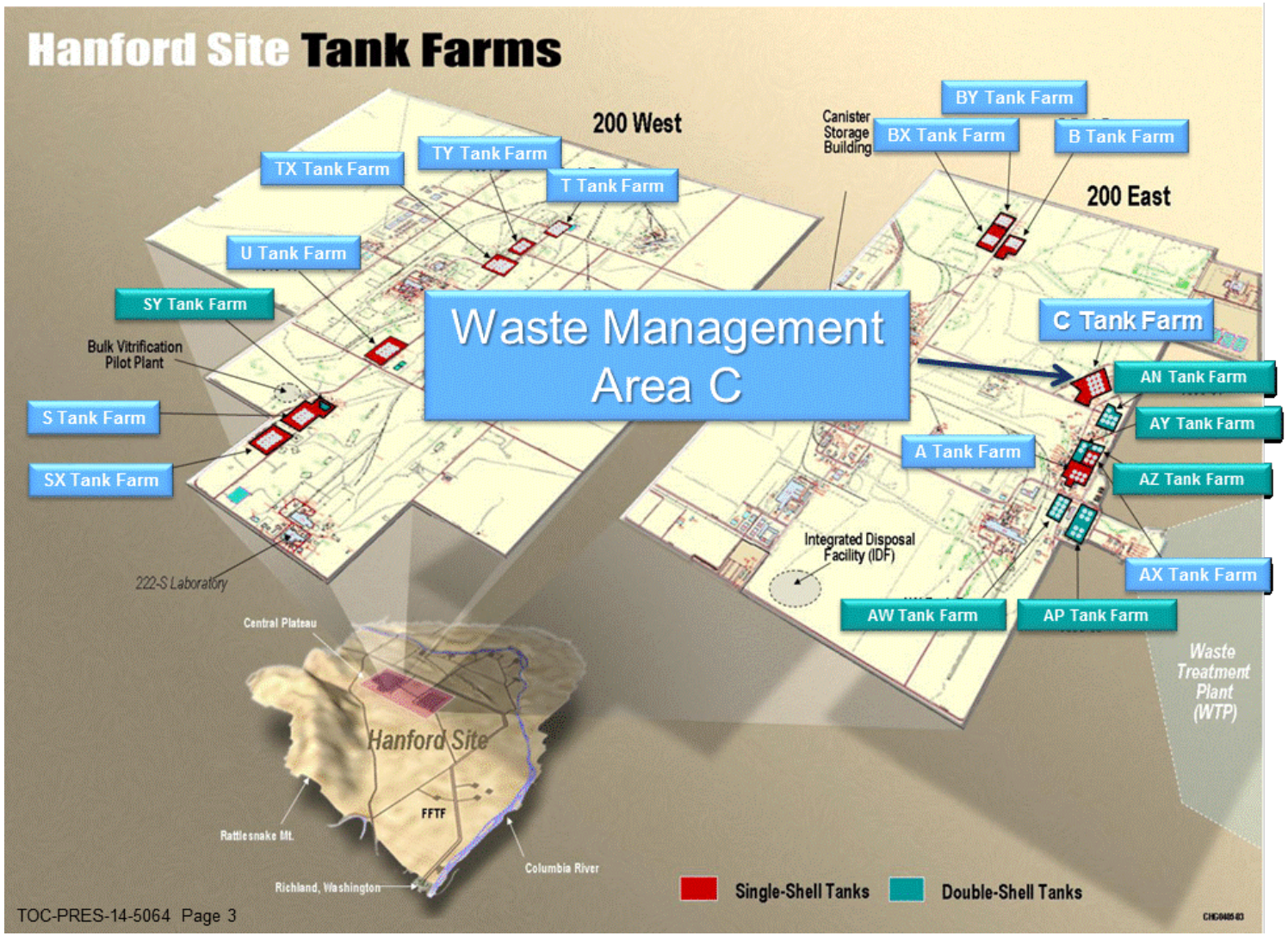

FFTF = Fast Flux Test Facility

Reference: TOC-PRES-14-5064-VA, "Waste Management Area C Performance Assessment (PA) Current Status."

Figure 1-2. The Components of the Appendix I Performance Assessment.

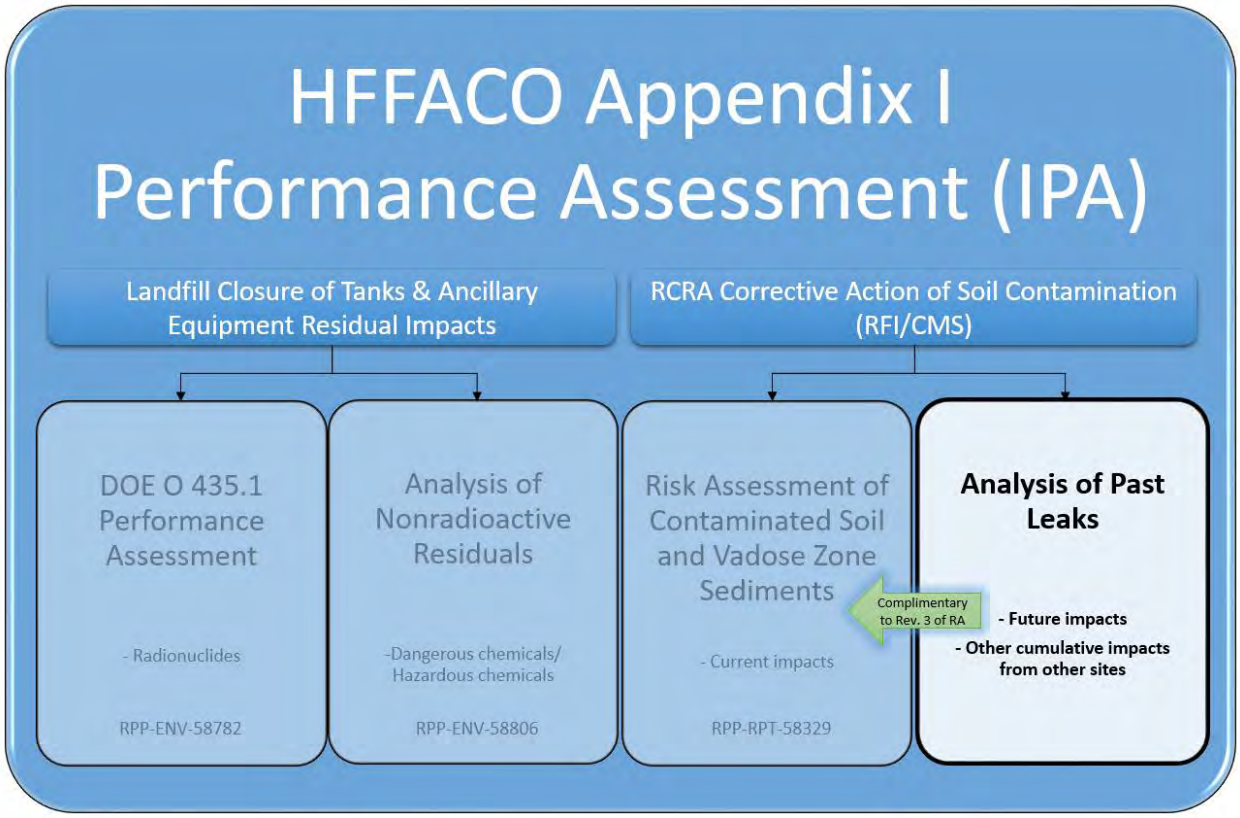

RA = Risk Assessment
HFFACO = Hanford Federal Facility Agreement and Consent Order
RCRA = Resource Conservation and Recovery Act of 1976
RFI/CMS = RCRA Facility Investigation/Corrective Measures Study

References:
DOE O 435.1, Radioactive Waste Management.
RPP-ENV-58782, *Performance Assessment of Waste Management Area C, Hanford Site, Washington*
RPP-ENV-58806, *Analysis of Post-Closure Groundwater Impacts from Hazardous Chemicals in Residual Wastes in Tanks and Ancillary Equipment at Waste Management Area C at the Hanford Site, Southeast Washington*.
RPP-RPT-58329, *Risk Assessment of Contaminated Soils and Vadose Zone Sediments Waste Management Area C at the Hanford Site, Southeast Washington.*

Closure decisions for the Hanford Site SST system soils will be made through the *Resource Conservation and Recovery Act of 1976* (RCRA) corrective action process. Corrective measures to address groundwater contamination are being undertaken by the CERCLA RI/FS effort in 200-BP-5-OU. The RCRA corrective action component of the IPA is documented in RPP-RPT-58339, *Phase 2 RCRA Facility Investigation Report for Waste Management Area C,* Rev. 0, and contain: 1) a baseline risk assessment; and 2) an analysis of past leaks.

- **Risk Assessment** – An evaluation of impacts to human and ecological receptors from both non-radiological and radiological contaminants in soils and vadose zone sediments at WMA C under current condition, in the absence of actions to control or mitigate releases. Under the U.S. Environmental Protection Agency (EPA), this is completed at contaminated waste sites prior to remediation activities to establish a need for action.

Initial versions of the risk assessment has been prepared (RPP-RPT-58329, Rev. 0 and Rev. 2). Revision 3 of this document will address both current and future impacts to human health and the environment.

- **Analysis of Past Leaks** – An evaluation of the future impacts from selected radiological and hazardous chemicals and dangerous waste contaminants associated with past leaks and losses at WMA C. This analysis of past leaks is intended to provide supporting information that could be relevant to the selection and specific implementation of groundwater mitigation measures being undertaken as a part of the CERCLA RI/FS effort in 200-BP-5-OU.

1.1.1 Waste Management Area C Performance Assessment Scoping Process

The foundation of the WMA C IPA was established in a scoping process that was conducted with regulatory agencies and stakeholders between 2009 and 2011. As a part of the scoping process, a series of working sessions were conducted that addressed the following technical topic areas:

- Residual Inventory (Detailed conceptual models and data related to residual waste inventories left in WMA C tanks and ancillary equipment at closure) (May 5-7, 2009)
- Assessment Context/General Conceptual Models (September 1-3, 2009)
- Soil Inventory (Detailed conceptual models and data on waste inventories released to the environment from historical releases during operations) (October 27-29, 2009)
- Engineered System #1 (Detailed conceptual models and data on natural recharge and waste release) (January 26-28, 2010)
- Natural System (Detailed conceptual models and data on vadose zone and groundwater flow and transport) (May 25-27, 2010)
- Engineered System #2 (Continuation discussion of detailed conceptual models, data, and characteristics of the engineered systems) (July 27-29, 2010)
- Exposure Scenarios (Detailed conceptual models and data on human health exposure scenarios) (September 28-30, 2010)
- Vadose Zone and Groundwater Flow and Transport Modeling (Use of numerical and system-level codes and models to support the PA) (January 25-27, 2011)
- Ecological Risk Assessment (Detailed conceptual models and data related to ecosystem risk assessments) (May 17-19, 2011).

Regulatory agency members who participated in the scoping process included representatives from DOE, EPA, the U.S. Nuclear Regulatory Commission (NRC), and Washington Department of Ecology (Ecology) as well as their contractors. Other participants in the working sessions included representatives of the tribal nations, other stakeholder groups, and members of the interested public.

The results of the WMA C IPA scoping process have been documented in a series of data package reports that were produced in the 2009 to 2011 scoping time frame. These data packages document the outcomes of working sessions held with relevant regulatory agencies and stakeholders. These working sessions were used to solicit input from the working session participants, and to obtain a common understanding concerning the scope, methods, and data to be used in the HFFACO Appendix I PA for WMA C. The listing of the current versions of each data package produced in each of the working sessions is summarized in Table 1-1.

Table 1-1. Data Packages Produced as a Part of the Waste Management Area C Performance Assessment Scoping Process.

Working Session Topical Area	Report Number (Year Published)	Current Revision No.	Title
Residual Inventory	RPP-RPT-42323 (2015)	3	Hanford C-Farm Tank and Ancillary Equipment Residual Waste Inventory Estimates
Assessment Context	RPP-RPT-41918 (2010)	0	Assessment Context for Performance Assessment for Waste in C Tank Farm Facilities after Closure
Soil Inventory	RPP-RPT-42294 (2016)	2	Hanford Waste Management Area C Soil Contamination Inventory Estimates
Engineered System #1	RPP-RPT-44042 (2010)	0	Recharge and Waste Release within Engineered System in Waste Management Area C
Engineered System #2	RPP-RPT-46879 (2011)	2	Corrosion and Structural Degradation within Engineered System in Waste Management Area C
Natural System	RPP-RPT-46088 (2010)	1	Flow and Transport in the Natural System at Waste Management Area C
Exposure Scenarios	RPP-RPT-47479 (2011)	1	Exposure Scenarios for the Waste Management Area C Performance Assessment
Numerical Codes	RPP-RPT-48490 (2011)	1	Technical Approach and Scope for Flow and Contaminant Transport Analysis in the Initial Performance Assessment of Waste Management Area C
Ecosystem Risk	RPP-RPT-49425 (2011)	1	Ecological Risk Assessment Approach for Hanford Waste Management Area C

Between the development of these data packages and today, updated information has become available for some of the inputs, and new conceptualizations and interpretations of data have been developed. In addition, stakeholders have expressed ideas and concerns to the project team that have led to the development of additional conceptual models and sensitivity analysis cases.

Specific areas associated with past leaks in which deviations or updates from the prior data packages occurred include the following:

- Estimates of leak inventories and volumes (RPP-ENV-33418, *Hanford C-Farm Leak Inventory Assessments Report*, Revision 4), soil inventories (RPP-RPT-42294, *Hanford Waste Management Area C Soil Contamination Inventory Estimates*, Revision 3), and groundwater plume extents and concentrations (DOE/RL-2015-07, *Hanford Site Groundwater Monitoring Report for 2014*; DOE/RL-2009-127, *Remedial Investigation Report for the 200-BP-5 Groundwater Operable Unit*; RPP-RPT-58297, *Screening-Level Evaluation of Groundwater Monitoring Data Collected in Vicinity of WMA C*) have been updated.

- Alternative models of the site stratigraphy and spatial variability have been implemented in collaboration with stakeholders.

- Vadose zone flow properties have been updated to better represent site-specific data.

- Aquifer flow properties have been updated to reflect new data and interpretations.

This updated information has been included in a performance assessment of tank residuals in RPP-ENV-58782.

1.1.2 Regulatory Context

The overall regulatory context of this document is provided in the Preface on p. 1-1. As indicated in the Preface, this document is a supporting analysis to the groundwater protection pathway part of the risk assessment of soils contaminated by past leaks and releases from WMA C documented in RPP-RPT-58329. This risk assessment evaluates impacts to human and ecological receptors from both non-radiological and radiological contaminants in soils at WMA C under current conditions, in the absence of actions to control or mitigate releases. Additionally, this document is a support analysis to the RCRA Facility Investigation/Corrective Measures Study (RFI/CMS) of WMA C.

An evaluation of groundwater protection from contaminated soil remaining within the vadose zone at WMA C is provided in RPP-RPT-58329.

Due to presence of soil contamination in the vadose zone at WMA C, the potential exists for future migration of these contaminants into the unconfined groundwater aquifer underneath WMA C. During Phase 2 characterization efforts conducted as a part of the RCRA Facility Investigation, the evaluation of soil and vadose zone characterization measurements were obtained for groundwater protection evaluation using exposure point concentrations (EPCs) developed from vadose site characterization data. Two combined steps were used to identify the specific hazardous chemical COPCs for groundwater protection considerations under the RCRA RFI/CMS of WMA C. They are summarized as follows:

- Step One (MTCA 3-Phase Partitioning Evaluation): Identification of hazard chemical contaminants of potential concern (COPCs) when their EPCs measured concentrations exceeded their corresponding cleanup levels (CULs) derived from the Fixed parameter three-phase partitioning model, also referred to as the MTCA three-phase partitioning model, as defined in *Washington Administrative Code* (WAC) 173-340-747, "Deriving Soil Concentrations for Ground Water Protection," subsection (3)(a) "Fixed parameter three-phase partitioning model". This evaluation compares soil concentrations protective of groundwater as calculated using the MTCA three-phase partitioning model with observed soil concentrations measured during the Phase 2 soil characterization efforts.

- Step Two (Background Evaluation): COPCs exceeding MTCA three-phase partitioning Model CULs that exceed background values are identified.

As a follow on to the groundwater protection evaluation, site-specific model analyses were performed to gain additional understanding and insight into the potential spatial and temporal impacts to groundwater that would be realized from selected non-radiological and radiological constituents associated with past waste leaks and losses from WMA C. These analyses are intended to provide information that could be relevant to the selection and specific implementation of potential groundwater mitigation measures as a part of the CERCLA RI/FS effort in 200-BP-5-OU. As stated in Ecology Letter 18-NWP-088, "Department of Ecology's (Ecology) Comments on the United States Department of Energy (USDOE) Submittal of the Phase 2 RCRA Facility Investigation Report for Waste Management Area C (RFI), RPP-RPT-58339, Revision 0, and Waste Management Area C Phase 2 Corrective Measures Study Report (CMS), RPP-RPT-59379, Revision 0" (18-NWP-088 – Letter), dated June 11, 2018:

- "Ecology approves the RFI and has determined there is a need to capture and remove contaminants of concern from the groundwater in WMA C."

- "Ecology acknowledges that groundwater remediation will be managed through the 200-BP-5 and 200-PO-1 Comprehensive Environmental Response, Compensation, and Liability Act (CERCLA) Groundwater Operable Units. The proposed Feasibility Study for Interim Action will cite capture and removal of Tc-99 as the preferred alternative, with Tc-99 cited as a primary contaminant of concern for WMA C. A number of co contaminants have also been identified for WMA C, including but not limited to cyanide, iodine-129, nitrate, and sulfate. Ecology expects that the co-contaminants identified in the Feasibility Study for Interim Action will be addressed incidentally with the CERCLA remediation."

As a part of these analyses, the groundwater concentrations estimated with site-specific modeling down gradient of WMA C described in this report were compared against Federal maximum contaminant levels (MCLs) or MTCA groundwater cleanup levels to identify constituents that have or could impact groundwater at WMA C in the future. The site-specific three-dimensional flow and transport model, developed to support the WMA IPA, was adapted to evaluate the potential impact of the groundwater for the following radiological and non-radiological contaminants – ^{99}Tc, ^{129}I, ^{60}Co, H_3, ^{238}U, ^{79}Se, ^{126}Sn, NO_3, SO_4, Cn, Cr, and total uranium. These

groundwater evaluations were performed to determine the arrival times and peak concentrations for those contaminants at nine (9) points of calculation down-gradient of the groundwater flow direction from WMA C fence line.

As a part of these analysis, the arrival times and overall magnitude of the contaminant concentrations impacts for selected non-radiological and radiological contaminants were evaluated to provide insight into when and how much they might impact the groundwater in the future. For contaminants that impacted the groundwater, the evaluation also identified the year of which the peak concentrations would potentially occur and would examine how long concentrations that exceed Federal MCLs or MTCA groundwater cleanup levels might persist.

These latter evaluations associated with past waste leaks and losses are presented in this document (RPP-RPT-59197). This information is needed to support the overall closure of WMA C SSTs per WAC 173-303-610, “Closure and Post-Closure.”

1.2 PURPOSE AND SCOPE OF THE REPORT

1.2.1 Purpose

This document provides an analysis of past leaks at WMA C using the model developed for the WMA C residual waste PA (RPP-ENV-58782) and RCA (RPP-ENV-58806). The report has several purposes.

First, the conceptual model developed for the performance assessment of residual contamination has been implemented to evaluate the ability of the model to represent observed field data for the time of arrival of contaminants to groundwater, concentrations of contaminants in groundwater, and the distribution of contaminants in the vadose zone. Although it is possible that contamination from the past leaks arrived in groundwater prior to the installation of well 299-E27-7 in 1982 and the RCRA groundwater monitoring well network in 1989, the concentration trends of ^{99}Tc currently observed in those monitoring wells appear to be consistent with available information regarding the timing, size, and inventory of the leaks. Second, the combination of field data and modeling were used to determine the bounds on input assumptions that are consistent with groundwater and soil monitoring data from past leaks. Third, the constrained model has been used to project future impacts from the past leaks. This part of the analysis will represent an input to additional analyses for the Appendix I PA.

1.2.2 Scope

The scope of this report is limited to an assessment of past leaks at WMA C, and is intended as a companion report to the radiological PA of residual contamination (RPP-ENV-58782) and the RCA for WMA C (RPP-ENV-58806).

In the remainder of Section 1, a general description is provided of WMA C, specifically focused on information germane to the past leaks. In addition, a description is provided of previous modeling efforts on past leaks.

In Section 2, a summary is provided of the general groundwater situation associated with the past leaks analysis, a summary of current estimates of the leaks themselves, and a summary of soil and groundwater data that are used for interpreting the groundwater model.

In Section 3, a description is provided of the model implemented for the past leaks analysis. The foundation of this model is the facility-specific groundwater model developed for the analysis of residual wastes at WMA C (RPP-ENV-58782 and RPP-ENV-58806). Section 3 therefore represents an interpretation of the site-specific data presented in Section 2, along with the general understanding of groundwater behavior presented in Section 2.

In Section 4, a series of scoping analysis cases are presented. These scoping analysis cases apply the site-specific WMA C groundwater model to the past leaks and compare calculations of arrival time of contamination and (to a lesser extent) groundwater concentrations to evaluate which model inputs are consistent with groundwater data. These comparisons are necessarily somewhat qualitative owing to the limitations of the data, but the comparisons are intended to be as quantitative as possible.

In Section 5, the results of several bodies of work from multiple organizations are presented that explicitly evaluate vadose zone heterogeneities beneath WMA C. These conceptual models seek to understand the potential effects of heterogeneities on flow and contaminant transport.

In Section 6, a set of transient model cases of past leak behavior are presented. The transient model analysis cases attempt to approximate the flow conditions that have existed at WMA C from its construction in 1944 to present day. During this time, referred to as the operations period, the hydraulic gradient, both in direction and magnitude, appears to have been highly variable, and flow appears to have occurred in several directions.

In Section 7, a set of forward calculations to evaluate the future consequences of the leaks are presented, to evaluate how the groundwater concentrations may change in the future based on the constraints on the scoping modeling analysis cases established in Section 4.

In Section 8, the results of the future impacts described in Section 6 are compared against future impacts from waste residuals anticipated to be left in tanks and ancillary equipment at closure and the potential impacts at WMA C from sources upgradient of WMA C.

A summary and conclusions from this analysis are presented in Section 9.

1.3 GENERAL FACILITY DESCRIPTION

The Hanford Site, a facility in the DOE nuclear waste complex, encompasses ~1,500 km^2 (~586 mi^2) northwest of the city of Richland along the Columbia River in southeastern Washington State, as shown in Figure 1-3. The Federal government acquired the Hanford Site in 1943 for the production of plutonium. Production of special nuclear materials continued until the 1980s. Since the 1990s, DOE has focused on environmental remediation of the Hanford Site.

Waste Management Area C (WMA C or the 241-C Tank Farm [C Farm]), part of the SST system, is located in the Central Plateau (see Figure 1-3), near the eastern edge of the 200 East Area. One of the first tank farms built, it was constructed in 1944 and 1945.

Figure 1-3. Hanford Site and its Location in Washington State.

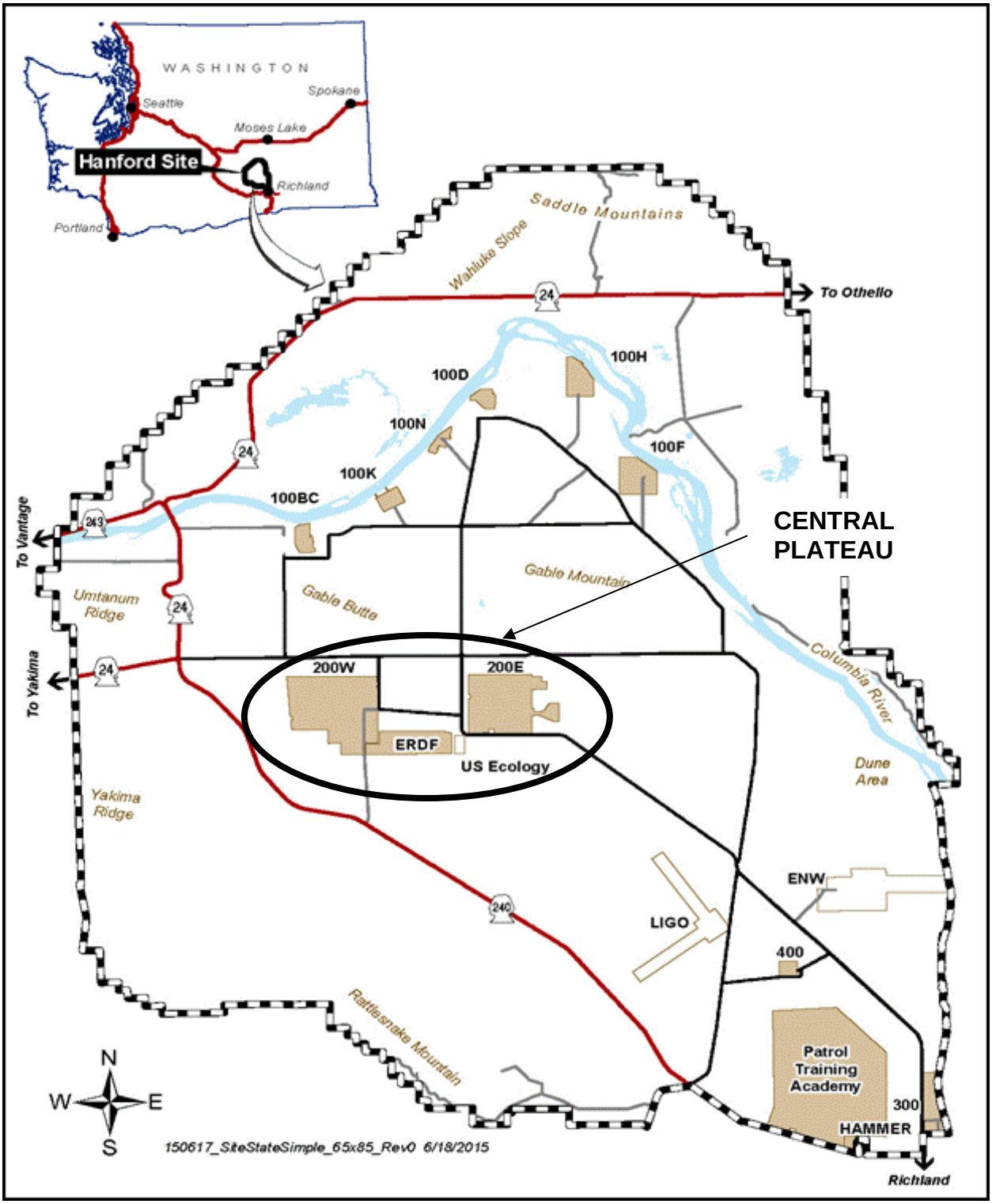

ENW = Energy Northwest Columbia Generating Station LIGO = Laser Interferometer Gravitational Wave Observatory
ERDF = Environmental Restoration Disposal Facility

The WMA C facility contains twelve 100-series tanks and four 200-series tanks (see Figure 1-4). The 100-series tanks are 23 m (75 ft) in diameter, with a maximum 5-m (16-ft) depth and 2,006,000-L (530,000-gal) design capacity. The 200-series tanks are 6 m (20 ft) in diameter with a maximum 7-m (24-ft) depth and 208,000-L (55,000-gal) design capacity. Only tanks 241-C-101 (C-101) through 241-C-106 (C-106) have concrete pits. The other 100-series tanks are equipped with centrally located salt well pump pits. The tanks sit below grade with at least 2 m (7 ft) of soil cover to provide shielding from radiation exposure to operating personnel. Tank pits are located on top of the tanks and provide access to the tanks, pumps, and associated monitoring equipment.

The SSTs were constructed in place with 0.95-cm (0.375-in.)-thick carbon steel (ASTM A283 Grade C) lining the bottom and 0.64-cm (0.25-in.)-thick carbon steel lining the sides of a reinforced-concrete shell. The tanks have concave bottoms (center of tanks lower than the perimeter) and a curving intersection of the sides and bottom, where the carbon steel plate is 0.8 cm (0.3125 in.) thick. The inlet and outlet lines are located near the top of the liners. There are four inlet lines on each tank, which are also known as nozzles. Pipelines from the diversion boxes to tanks C-101, 241-C-104 (C-104), 241-C-107 (C-107), 241-C-108 (C-108), 241-C-110 (C-110), and 241-C-111 (C-111) are supported by concrete viaducts. At ~3 m (~9 ft 10 in.) from the tank wall, the viaduct surface steps down and the void space between the pipes and the viaduct surface is grouted. At this point, the viaduct begins fanning out from 0.8 m (2 ft 8 in.) wide to 2.2 m (7 ft 4 in.) wide to support the spread placement of the fill lines through the tank wall. Tanks C-101, C-104, C-107, and C-110 each have one outlet line to the next tank in series. Tanks 241-C-102 (C-102), 241-C-105 (C-105), C-108, and C-111 each have one additional inlet line and one outlet line. Tanks 241-C-103 (C-103), C-106, 241-C-109 (C-109), and 241-C-112 (C-112) each have one additional inlet line from the previous tank in the series. The lines connecting each tank are also referred to as “cascade” lines since they allowed transfer of fluids between tanks using gravity flow.

To support the transfer and storage of waste within WMA C SSTs, there is a complex waste transfer system of pipelines (transfer lines), diversion boxes, vaults, valve pits, and other miscellaneous structures. These miscellaneous features of the tank farm are referred to in this document by the general term “ancillary equipment and components.”

The 244-CR Process Tank Vault (244-CR vault) is located south of the tanks. The vault is a two-level, multi-cell, reinforced-concrete structure constructed below grade, which contains four underground tanks along with overhead piping and equipment. Two tanks (TK-CR-001 and TK-CR-011) have a capacity of 170,343 L (45,000 gal) each. The other two tanks (TK-CR-002 and TK-CR-003) have capacities of 55,494 L (14,700 gal) each. This reference estimated a capacity of 170,343 L (45,000 gal) each for two tanks (TK-CR-001 and TK-CR-011) and a capacity of 55,494 L (14,700 gal) each for the other two tanks (TK-CR-002 and TK-CR-003). HNF-EP-0182, *Waste Tank Summary Report for Month Ending February 28, 2015*, currently lists the capacities of TK-CR-001 and TK-CR-011 as 151,400 L (40,000 gal) each and the capacities of TK-CR-002 and TK-CR-003 as 56,775 L (15,000 gal) each.

Figure 1-4. Location Map of Waste Management Area C and Surrounding Area.

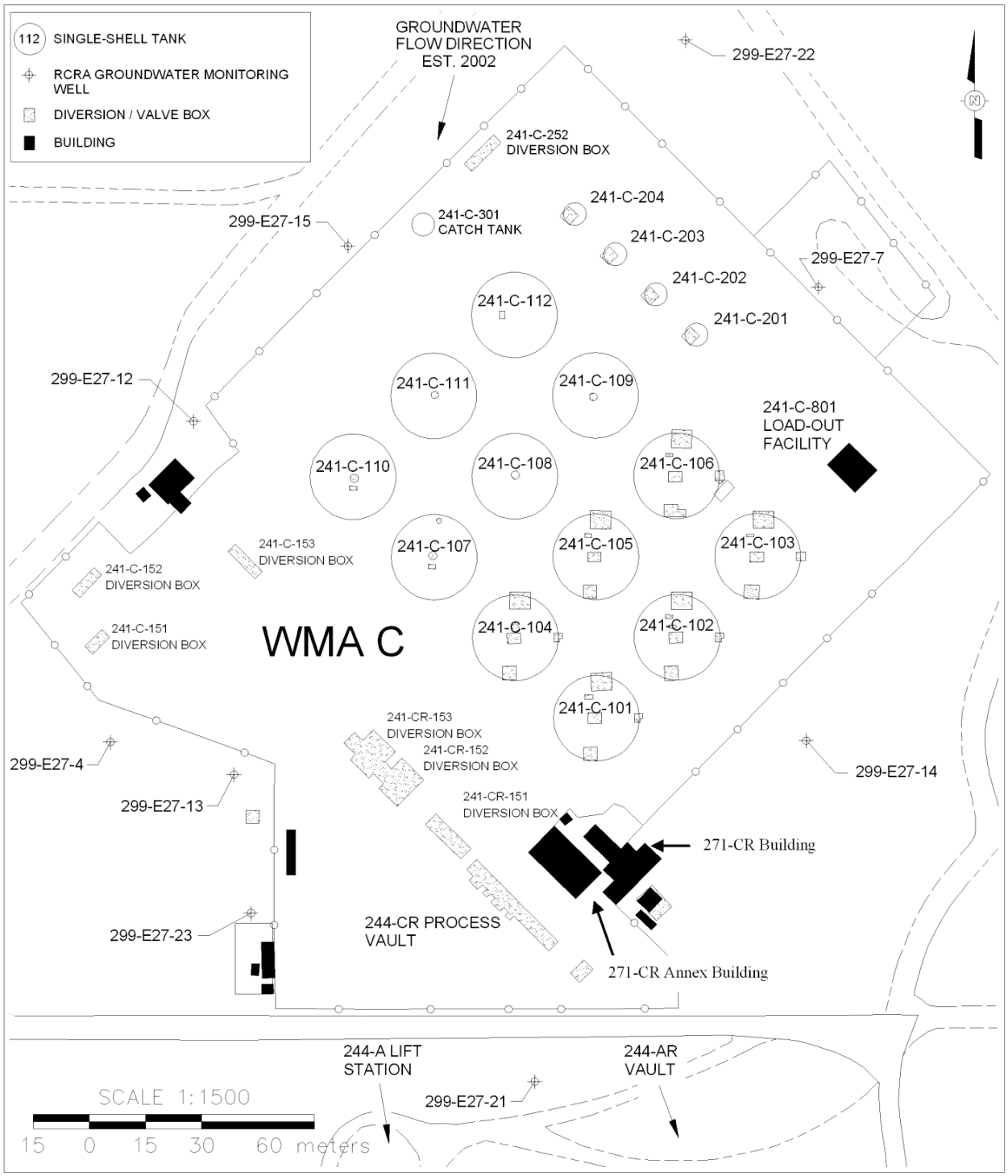

RCRA = Resource Conservation and Recovery Act of 1976 WMA = Waste Management Area

Figure 1-5. Location Map of Unplanned Release Sites of Waste Management Area C.

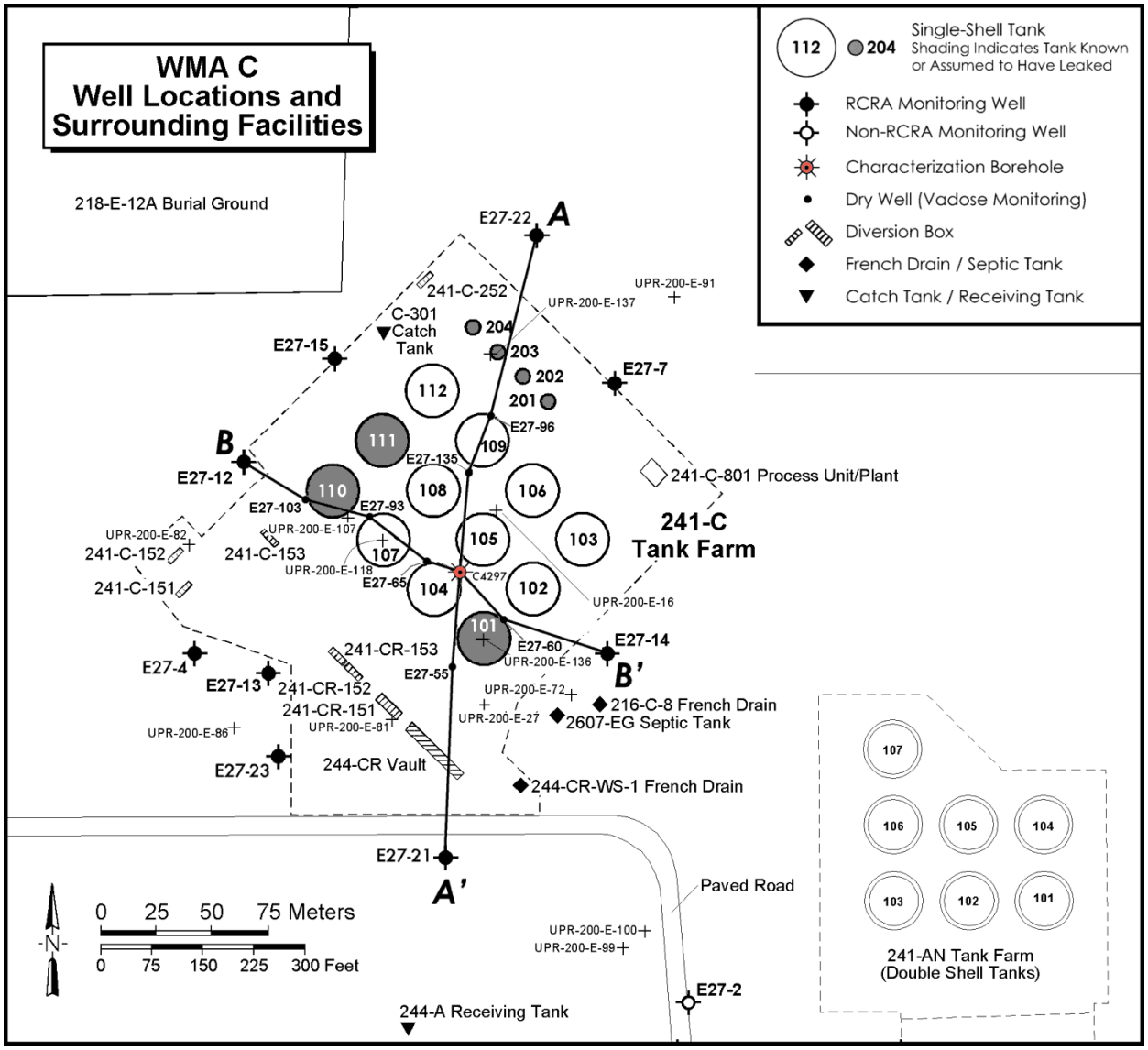

RCRA = Resource Conservation and Recovery Act of 1976 WMA = Waste Management Area

Fourteen unplanned releases (UPRs) have occurred within or near to WMA C (Figure 1-5). The largest ones are associated with leaks in pipelines or diversion boxes, with releases from inlet/outlet ports of the SSTs, or with leaks from the SSTs. Revision 4 of RPP-ENV-33418 provides the most recent estimates of the volumes and contaminant content of these releases. A summary of Revision 4 of RPP-ENV-33418 is provided in Section 2 of this document.

1.4 PREVIOUS ASSESSMENTS

Two principle assessments have been conducted that included consideration of past leaks at WMA C:

- DOE/ORP-2005-01, *Initial Single-Shell Tank System Performance Assessment for the Hanford Site*

- DOE/EIS-0391, *Final Tank Closure and Waste Management Environmental Impact Statement for the Hanford Site, Richland, Washington* (TC&WM EIS).

1.4.1 Single-Shell Tank Performance Assessment

The Single-Shell Tank Performance Assessment (SST PA) (DOE/ORP-2005-01) presented an analysis of the long-term impacts of residual wastes assumed to remain after retrieval of tank wastes and closure of the SST farms. The SST PA was intended to be a comprehensive evaluation of closure of all SST WMAs at Hanford, and included WMA C in its scope, but was not exclusively focused on it. The SST PA included four post-closure contamination sources consisting of tank residuals, ancillary equipment residuals, past UPRs, and hypothetical retrieval leaks. The SST PA assumed the presence of eight past tank leaks and four UPRs. The reference case inventories for past leaks assumed in the SST PA are presented in Table 1-2, and the assumed volumes are presented in Table 1-3. These values of the leak inventories were introduced as a source in the model at 40 m (130 ft) below surface at the start of the model (year 2000).

Table 1-2. Reference Case Inventory of Past Leaks Assumed in the Single-Shell Tank Performance Assessment.

Contaminant	Inventory	Contaminant	Inventory
Radionuclides (Ci)		Chemicals (kg)	
C-14	3.46E-1	Cr	1.11E2
Tc-99	6.93	NO_2	4.35E3
I-129	3.02E-2	NO_3	1.07E4
		U	7.88

Excerpted from DOE/ORP-2005-01, Initial Single-Shell Tank System Performance Assessment for the Hanford Site, Table 2-24.

This modeling approach was intended solely as a prospective, forward-looking analysis, and was not intended to mimic existing measured concentration data and arrival times of the plume at groundwater, and it did not match observed arrival times of ^{99}Tc at the water table.

1.4.2 Tank Closure and Waste Management Environmental Impact Statement Analysis of Waste Management Area C

The TC&WM EIS (DOE/EIS-0391) included in its scope an evaluation of all waste sources in the tank farm, including past tank leaks, retrieval leaks from the tanks, residual wastes, and UPRs associated with WMA. The inventory of the past tank leaks and UPRs used in the TC&WM EIS (see Section D.1.4 of Appendix D of DOE/EIS-0391) is presented in Table 1-4. It was assumed that all of the past leaks at WMA C occurred in 1946 and were associated with the volumes shown in Table 1-5.

Table 1-3. Volumes of Past Leaks Assumed in the Single-Shell Tank Performance Assessment.

Source	Volume (gal)*
241-C-101	1,000
241-C-105	1,000
241-C-110	2,000
241-C-111	5,500
241-C-201	550
241-C-202	450
241-C-203	400
241-C-204	350
UPR 200-E-81	36,000
UPR 200-E-82	2,600
UPR 200-E-86	18,500
UPR 200-E-107	5

Excerpted from DOE/ORP-2005-01, Initial Single-Shell Tank System Performance Assessment for the Hanford Site, Table 2-23.

* Conversion 1 gallon = 3.78541 liters

Table 1-4. Inventory of Past Tank Leaks and Unplanned Releases Assumed in the Tank Closure and Waste Management Environmental Impact Statement.

Contaminant	Inventory	Contaminant	Inventory
Past Tank Leaks			
Radionuclides (Ci)		Chemicals (kg)	
H_3	2.68E1	1-butanol	1.89E1
^{14}C	1.48E-1	Cr	4.15E1
^{99}Tc	6.61	Hg	2.12E-2
^{129}I	2.59E-3	NO_3	4.82E3
^{237}Np	2.30E-2	Pb	6.87
^{238}U	5.41E-3	U-total	2.88
Unplanned Releases			
Radionuclides (Ci)		Chemicals (kg)	
H_3	1.39E2	1-butanol	6.47E-1
^{14}C	1.90E-1	Cr	3.94E1
^{99}Tc	1.67	Hg	3.92E-3
^{129}I	2.48E-2	NO_3	9.68E3
^{237}Np	5.58E-3	Pb	2.16E1
^{238}U	1.49E-2	U-total	3.47E1

Excerpted from DOE/EIS-0391, *Final Tank Closure and Waste Management Environmental Impact Statement for the Hanford Site, Richland, Washington*, Tables M-18 and M-25.

Table 1-5. Volumes of Past Tank Leaks Assumed in the Tank Closure and Waste Management Environmental Impact Statement.

All tank leaks were assumed to occur in 1946.

Source	Volume (gal)*
241-C-101	20,000
241-C-110	2,000
241-C-111	5,500
241-C-201	550
241-C-202	450
241-C-203	400
241-C-204	350

Excerpted from DOE/EIS-0391, *Final Tank Closure and Waste Management Environmental Impact Statement for the Hanford Site, Richland, Washington,* Table M-4.

* Conversion 1 gallon = 3.78541 liters

2.0 BACKGROUND

This section of the report provides background information relevant to this past leak analysis including the following:

- Inventory estimates for past waste releases to the vadose zone;
- A summary of the hydrologic setting for the Central Plateau;
- A summary of vadose zone contamination;
- A summary of aquifer conditions and contamination; and
- A synopsis of recent interpretations of groundwater chemistry.

2.1 INVENTORY ESTIMATES FOR PAST WASTE RELEASES TO THE VADOSE ZONE

This section summarizes inventory estimates for past leaks and releases to the soil in WMA C. The technical basis for the inventory estimates is presented in RPP-ENV-33418 and inventories for the WMA C PA are presented in RPP-RPT-44294.

Inventory estimates from past releases were determined for those facilities or areas where there was an indication that a release occurred and for which a technical basis for a soil inventory estimate could be determined. The process to estimate tank leak inventories is shown in Figure 2-1 and is described in RPP-32681, *Process to Assess Tank Farm Leaks in Support of Retrieval and Closure Planning*. Information for WMA C SSTs, catch tanks, pits and diversion boxes and pipelines were reviewed to assess evidence of waste releases to the vadose zone.

The key parameters needed to estimate the inventory or mass of constituents released are: 1) the volume of a release; 2) the time a release occurred; and 3) the waste type and composition of waste released. For some tank leaks and unplanned releases (UPRs), historical records confirm the waste loss event and data provide a strong technical basis for time of leak event, leak volume, and composition of the waste estimates. However, for many tank leaks and UPRs few data are available, and existing data are often ambiguous and incomplete.

The inventory estimates in this report are based on information available as of September 1, 2014, and were calculated for chemical and radionuclide constituents included in RPP-19822, *Hanford Defined Waste Model – Revision 5.0* (HDW) model (Table 2-1). The HDW constituents account for over 99% of the chemical and radionuclide inventory (WHC-SD-WM-TI-731, *Predominant Radionuclides in Hanford Site Waste Tanks*).

The HDW Model is a spreadsheet-based engineering estimate of the chemical and radionuclide contents of the Hanford Site single-shell and double-shell tanks based on process reactor fuel irradiation records, separation plant dissolver charging records, separation plant and tank farm process flowsheets, and tank farm waste receipt and transfer records. The HDW includes waste

type composition estimates for solids and supernate for different process waste streams in the tank farms. The predominant supernatant waste types assumed to have been released from tanks and ancillary equipment in C Farm are from the Plutonium Uranium Extraction Plant (high-activity waste [P1 (1956-1962) and P2 (1963-1967)] and aluminum cladding waste [CWP1 (1956-1960) and CWP2 (1961-1972)]), B Plant (ion exchange cesium recovery waste [CSR]) and Stack condensate. The HDW estimates for these waste types, which are summarized in Table 2-2, provide the primary basis for the waste type composition estimates for waste released.

Figure 2-1. Schematic of Process Used to Determine Vadose Zone Inventory.

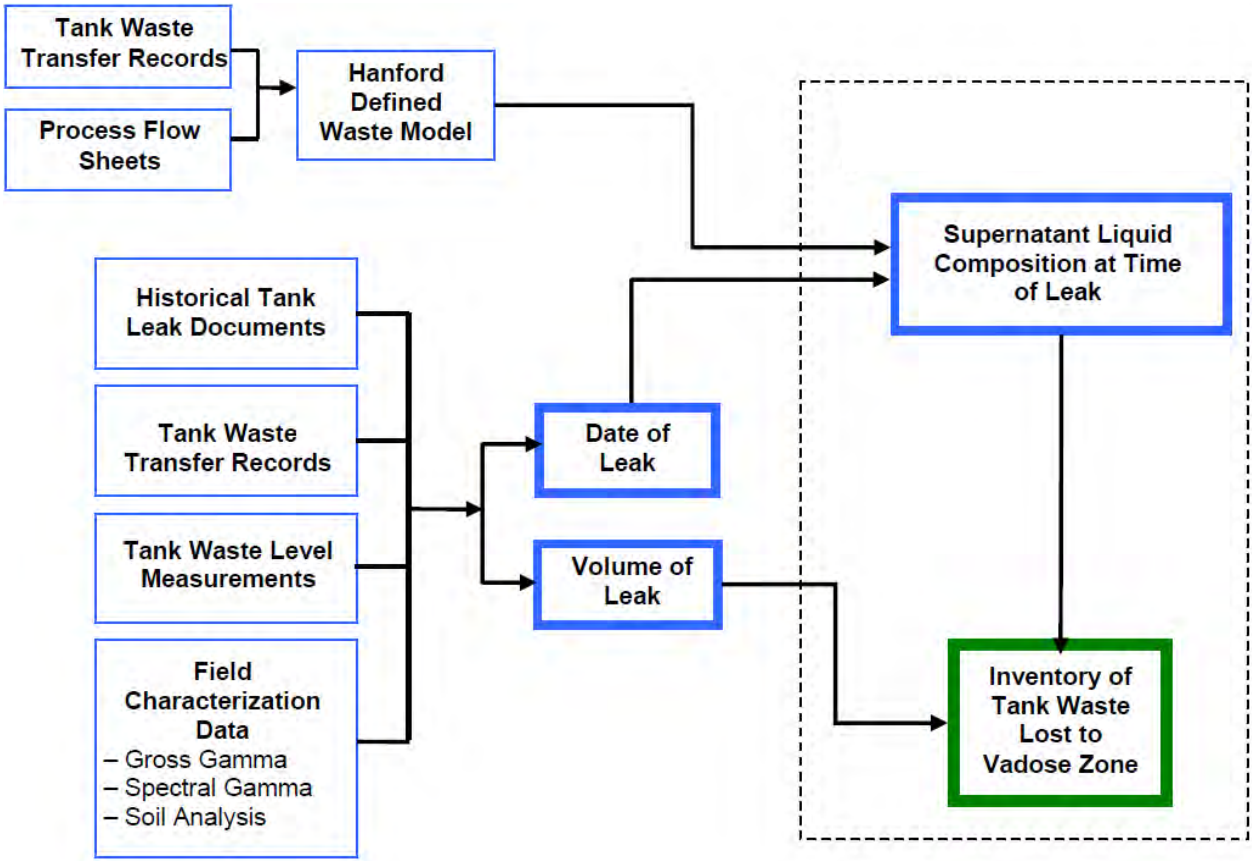

Note: Uncertainty exists in all these sources.

When sample data were identified that were considered representative of a waste release, the HDW values were adjusted based on the ratio of the analytical concentration and were only provided for a few constituents, but the values for all constituents were adjusted based on the ratio of ^{137}Cs concentrations or other selected analytes. This ratio is a multiplier or dilution factor comparing the HDW waste type to measured results. The ratio assumes that the differences between analytical values and HDW model values for ^{137}Cs are mostly due to water dilutions. The ^{137}Cs ratio is not constituent specific and may not apply equally to all constituents if the differences are due to other factors.

The following sections and Table 2-3 summarize the basis for inventory estimates for contaminant soil releases in WMA C. Additional information for each of the releases is provided in RPP-ENV-33418. These and other releases, not included in Table 2-3, were identified in

RPP-ENV-33418, Tables 6-2 and 6-3; however, volumes and inventories could only be estimated for releases shown in Table 2-3. Releases documented but not quantified include condensate discharges to the 244-CR-WS-1 drain, possible P1 and P2 waste discharges to the 241-C-801 drywell, and 11 additional UPRs from air emissions, pipelines, catch tanks and diversion boxes.

Table 2-1. Constituents Evaluated in the Hanford Defined Waste Model.

Chemicals			Radionuclides			
Na	Ag	Si	H_3	^{113m}Cd	^{228}Ra	^{237}Np
Al	Mn	F	^{14}C	^{125}Sb	^{227}Ac	^{238}Pu
Fe	Ca	Cl	^{59}Ni	^{126}Sn	^{231}Pa	^{239}Pu
Cr	K	CCl_4	^{63}Ni	^{129}I	^{229}Th	^{240}Pu
Bi	U-Total	Butanol	^{60}Co	^{134}Cs	^{232}Th	^{241}Pu
La	NO_3	Tributyl Phosphate	^{79}Se	^{137}Cs	^{232}U	^{242}Pu
Hg	NO_2	NPH	^{90}Sr	^{137m}Ba	^{233}U	^{241}Am
Zr	CO_3	NH_3	^{90}Y	^{151}Sm	^{234}U	^{243}Am
Pb	PO_4	$Fe(CN)_6$	^{93}Zr	^{152}Eu	^{235}U	^{242}Cm
Ni	SO_4		^{93m}Nb	^{154}Eu	^{236}U	^{243}Cm
			^{99}Tc	^{155}Eu	^{238}U	^{244}Cm
			^{106}Ru	^{226}Ra		

Reference: RPP-26744, *Hanford Soil Inventory Model*, Rev. 1.

A series of steady state flow and transport scoping cases evaluated as a part of the past leak analysis are summarized in Table 4-1 in Section 4. The effect of considering transient effects on flow and transport is fully described in Section 5. The focus in the scoping part of the analysis was on evaluating only ^{99}Tc. The rational for focusing on ^{99}Tc than other constituents is given at the end of Section 3.1.

A set of forward calculations to evaluate the future consequences of the past waste leaks and releases for selected constituents in the past leaks inventory are presented in Section 6 to evaluate how the groundwater concentrations may change in the future based on the constraints on the scoping modeling analysis cases established in Sections 4 and 5.

2.1.1 Tank 241-C-101

Tank C-101 was classified as a confirmed leaking tank in 1968 with a leak volume of ~75,600 L (~20,500 gal). The leak volume estimate appears to be based on a 34.3-cm (13.5-in.) liquid level decrease between January 1965 and September 1969 and a subsequent radioactivity increase in drywells (30-01-02, 30-01-06 and 30-01-09) around this tank. It appears that a portion of the

liquid level decrease was attributed to evaporation. Tank C-101 is fitted with a condensation unit to recycle condensate back into the tank. A 34.3-cm (13.5-in.) decrease in surface level corresponds to ~140,100 L (~37,000 gal). Further evaluations and field investigations indicate that some or all of the liquid level decrease may be attributed to a spare inlet release, cascade line release, or tank leak above 137.2 cm (54 in.) from the tank bottom.

The estimated waste release volume of ~140,100 L (~37,000 gal) is based on the liquid level decrease. Based on drywell readings and waste process history, the assumed waste types are 99% CWP1 and 1% P1 waste released from the spare inlet or near the inlet.

An informal integrity assessment for tank C-101 concluded, based on liquid level measurements, evaporation calculations, and low gamma activity in drywells, that the tank probably did not leak, and if it did leak the release point would have been high on the tank wall. Based on the integrity assessment, tank C-101 was retrieved using modified sluicing. Retrieval commenced on December 10, 2012 and ended on September 1, 2013. Although large volumes of water and supernate were added to the tank during sluicing operations, there was no indication of a leak during retrieval from the High Resolution Resistivity (HRR) leak detection monitoring system or other monitoring systems used.

1

Table 2-2. Average Composition of Hanford Defined Model Chemical and Radiological Constituents for Selected Waste Types. (3 sheets)

Constituent	Units	P1*	P2*	CWP1*	CWP2*	CSR*	Sr-Cs Rec (P2) Stack Drain**
$Al(OH)_4$ -	g/L	0.00E+00	0.00E+00	8.10E+01	5.97E+01	3.66E+01	0.00E+00
Bi	g/L	0.00E+00	0.00E+00	0.00E+00	0.00E+00	1.06E-03	0.00E+00
butanol	g/L	0.00E+00	0.00E+00	0.00E+00	0.00E+00	1.09E+00	0.00E+00
Ca	g/L	1.50E-01	1.50E-01	1.50E-01	1.50E-01	1.50E-01	6.32E-03
Cl-	g/L	5.15E-01	9.36E-01	2.47E-01	4.10E-01	2.49E+00	0.00E+00
CO_3--	g/L	2.25E-01	2.25E-01	2.25E-01	2.25E-01	1.11E+01	0.00E+00
Cr	g/L	4.18E-01	4.23E-01	1.60E-01	1.59E-01	1.65E+00	0.00E+00
DBP	g/L	0.00E+00	0.00E+00	0.00E+00	0.00E+00	3.10E+00	0.00E+00
F-	g/L	0.00E+00	0.00E+00	0.00E+00	0.00E+00	3.11E-02	0.00E+00
Fe	g/L	1.05E-01	1.05E-01	1.05E-01	1.05E-01	1.05E-01	4.80E-05
Hg	g/L	3.24E-04	3.24E-04	0.00E+00	0.00E+00	3.24E-04	8.48E-06
K	g/L	1.23E-01	2.24E-01	5.92E-02	9.82E-02	8.15E-01	9.65E-05
La	g/L	0.00E+00	0.00E+00	0.00E+00	0.00E+00	0.00E+00	0.00E+00
Mn	g/L	0.00E+00	0.00E+00	0.00E+00	0.00E+00	1.78E-02	7.07E-06
Na	g/L	1.66E+01	2.70E+01	5.47E+01	3.73E+01	9.55E+01	4.09E-04
NH_3	g/L	1.43E-01	5.23E-01	1.55E-03	3.15E-04	4.19E-01	0.00E+00
Ni	g/L	1.07E-01	1.07E-01	9.05E-02	8.99E-02	1.07E-01	0.00E+00
NO_2-	g/L	1.27E+01	2.83E+01	3.66E+01	1.31E+01	3.96E+01	0.00E+00
NO_3-	g/L	1.09E+01	7.44E+00	4.28E+01	4.26E+01	7.77E+01	9.08E-04
OH-	g/L	3.12E+00	3.14E+00	3.19E-01	3.19E-01	1.69E+01	
Pb	g/L	2.32E-02	1.49E-01	1.49E-01	1.49E-01	1.02E-01	1.46E-05
PO_4---	g/L	0.00E+00	0.00E+00	0.00E+00	0.00E+00	6.14E-01	0.00E+00
SiO_3--	g/L	8.02E-01	8.02E-01	8.02E-01	0.00E+00	8.02E-01	0.00E+00
SO_4--	g/L	4.22E+00	1.19E+01	8.52E-01	6.47E-01	9.04E+00	8.51E-04
Sr	g/L	4.55E-05	4.55E-05	1.17E-05	9.88E-06	4.62E-05	0.00E+00
TOC	wt%C	0.00E+00	0.00E+00	0.00E+00	0.00E+00	4.66E-01	
U total	g/L	3.10E-02	3.10E-02	3.10E-02	3.10E-02	3.10E-02	3.72E-07
Zr	g/L	0.00E+00	0.00E+00	0.00E+00	0.00E+00	1.46E-04	0.00E+00
density							

Table 2-2. Average Composition of Hanford Defined Model Chemical and Radiological Constituents for Selected Waste Types. (3 sheets)

Constituent	Units	P1*	P2*	CWP1*	CWP2*	CSR*	Sr-Cs Rec (P2) Stack Drain**
Constituent		Decayed to Year 2020					
H_3	Ci/L	1.33E-06	4.06E-06	5.73E-05	5.77E-05	6.76E-06	0.00E+00
^{14}C	Ci/L	2.44E-06	2.97E-06	1.57E-06	1.07E-06	3.77E-06	0.00E+00
^{59}Ni	Ci/L	6.12E-07	1.34E-06	6.19E-06	7.85E-06	7.02E-07	0.00E+00
^{60}Co	Ci/L	1.01E-06	1.97E-06	1.01E-06	1.70E-06	1.97E-06	0.00E+00
^{63}Ni	Ci/L	5.00E-05	1.13E-04	5.09E-04	6.64E-04	5.86E-05	0.00E+00
^{79}Se	Ci/L	2.39E-07	5.43E-07	6.52E-10	4.84E-10	4.50E-07	0.00E+00
^{90}Sr	Ci/L	1.57E-03	1.57E-03	4.03E-04	3.41E-04	1.57E-03	1.60E-05
^{90}Y	Ci/L	1.57E-03	1.57E-03	4.03E-04	3.41E-04	1.57E-03	1.60E-05
^{93}Zr	Ci/L	1.43E-05	3.23E-05	3.89E-08	2.79E-08	2.68E-05	0.00E+00
^{93m}Nb	Ci/L	5.23E-06	1.12E-05	1.44E-08	9.66E-09	9.56E-06	0.00E+00
^{99}Tc	Ci/L	7.50E-05	1.70E-04	2.84E-07	2.01E-07	1.44E-04	0.00E+00
^{106}Ru	Ci/L	9.29E-18	1.26E-16	9.55E-21	1.75E-18	1.00E-16	0.00E+00
^{103m}Cd	Ci/L	4.95E-06	1.47E-05	8.24E-07	7.94E-07	1.10E-05	0.00E+00
^{125}Sb	Ci/L	1.57E-08	7.38E-08	3.85E-11	1.78E-10	5.60E-08	0.00E+00
^{126}Sn	Ci/L	9.89E-07	2.26E-06	2.68E-09	2.00E-09	1.87E-06	0.00E+00
^{129}I	Ci/L	4.47E-09	1.02E-08	2.80E-07	1.75E-07	8.48E-08	0.00E+00
^{134}Cs	Ci/L	1.20E-10	1.71E-09	2.09E-13	2.31E-12	2.07E-11	0.00E+00
^{137}Cs	Ci/L	1.83E-01	4.69E-01	4.87E-04	4.08E-04	9.68E-03	1.93E-06
^{137m}Ba	Ci/L	1.63E-01	4.18E-01	4.35E-04	3.63E-04	8.63E-03	1.72E-06
^{151}Sm	Ci/L	6.35E-03	3.82E-03	2.38E-05	1.72E-05	5.10E-03	0.00E+00
^{152}Eu	Ci/L	4.15E-07	3.85E-07	1.42E-09	1.95E-09	4.15E-07	0.00E+00
^{154}Eu	Ci/L	1.76E-05	1.76E-05	5.90E-08	8.52E-08	1.76E-05	0.00E+00
^{155}Eu	Ci/L	2.33E-06	2.82E-06	7.44E-09	1.36E-08	2.36E-06	0.00E+00
^{226}Ra	Ci/L	9.35E-12	2.38E-11	8.51E-13	2.29E-12	2.08E-11	6.01E-15
^{227}Ac	Ci/L	2.29E-11	6.05E-11	2.28E-12	1.97E-10	6.79E-11	1.53E-14
^{227}Ra	Ci/L	5.90E-18	1.99E-17	9.33E-19	1.81E-09	9.93E-11	5.04E-21
^{229}Th	Ci/L	1.57E-13	1.45E-13	1.44E-15	4.88E-11	5.41E-12	3.66E-17
^{231}Pa	Ci/L	5.98E-11	1.69E-10	9.19E-12	1.81E-09	3.36E-10	4.28E-14
^{232}Th	Ci/L	5.98E-17	2.04E-16	1.14E-17	2.23E-10	1.51E-11	5.15E-20

Table 2-2. Average Composition of Hanford Defined Model Chemical and Radiological Constituents for Selected Waste Types. (3 sheets)

Constituent	Units	P1*	P2*	CWP1*	CWP2*	CSR*	Sr-Cs Rec (P2) Stack Drain**
^{232}U	Ci/L	5.72E-13	6.84E-13	3.92E-13	1.15E-09	2.16E-10	8.23E-15
^{233}U	Ci/L	4.86E-12	1.50E-12	2.24E-14	8.30E-08	1.61E-08	1.80E-14
^{234}U	Ci/L	1.01E-08	1.06E-08	1.01E-08	1.15E-08	1.10E-08	1.27E-10
^{235}U	Ci/L	4.32E-10	4.42E-10	4.30E-10	4.48E-10	4.61E-10	5.33E-12
^{236}U	Ci/L	2.23E-10	2.72E-10	2.30E-10	2.83E-10	2.99E-10	3.27E-12
^{237}Np	Ci/L	4.10E-07	4.57E-07	1.91E-09	1.34E-09	4.69E-07	2.38E-10
^{238}Pu	Ci/L	1.08E-07	2.08E-07	7.72E-08	1.05E-07	1.86E-07	1.92E-09
^{238}U	Ci/L	1.03E-08	1.03E-08	1.03E-08	1.03E-08	1.03E-08	1.24E-10
^{239}Pu	Ci/L	5.09E-06	5.03E-06	5.08E-06	5.05E-06	5.05E-06	4.63E-08
^{240}Pu	Ci/L	1.02E-06	1.23E-06	1.06E-06	1.19E-06	1.17E-06	1.13E-08
^{241}Am	Ci/L	6.53E-06	6.53E-06	6.38E-06	5.40E-06	6.53E-06	0.00E+00
^{241}Pu	Ci/L	1.80E-06	4.40E-06	1.84E-06	3.45E-06	3.91E-06	4.05E-08
^{242}Cm	Ci/L	3.37E-08	1.24E-08	1.13E-10	2.11E-10	2.30E-08	0.00E+00
^{242}Pu	Ci/L	3.20E-11	8.93E-11	3.30E-11	6.05E-11	8.02E-11	8.26E-13
^{243}Am	Ci/L	3.09E-09	3.58E-09	7.31E-11	1.48E-10	3.79E-09	0.00E+00
^{243}Cm	Ci/L	4.61E-10	5.21E-10	1.48E-12	7.70E-12	4.90E-10	0.00E+00
^{244}Cm	Ci/L	9.27E-09	9.28E-09	2.93E-11	1.81E-10	9.28E-09	0.00E+00

* Average estimates for these waste types from RPP-19822, *Hanford Defined Waste Model*, Rev. 5.
** Average estimate for this waste type taken from RPP-26744, *Hanford Soil Inventory Model*, Rev. 1.

P1 = Plutonium Uranium Extraction (PUREX) high-level waste (1956-1962)
P2 = PUREX high-level waste (1963-1967)
CWP1 = PUREX aluminum cladding waste (1956-1960)
CWP2 = PUREX aluminum cladding waste (1961-1972)
CSR =ion exchange cesium recovery waste

Reference: Appendix A of RPP-RPT-42294, *Hanford Waste Management Area C Soil Contamination Inventory Estimates*, Rev. 2.

2.1.2 Tank 241-C-104

Tank C-104 appears to be “sound” as previously classified. However, drywells show ^{137}Cs near the tank and ^{60}Co plumes that appear to extend from the tank cascade line and migrate outward and downward. The observed gamma activity in drywells is attributed primarily to cascade line releases from tank C-104 and may also be attributed to spare inlet overflows from tanks C-104 and tank C-105 and V103 pipeline leaks.

Table 2-3. Inventory Estimates for Releases at Waste Management Area C.

Waste Release	Waste Volume (gal)*	^{60}Co (Ci)	^{99}Tc (Ci)	^{129}I (Ci)	^{137}Cs (Ci)	$Fe(CN)_6$[1] (kg)	NO_3 (kg)	SO_4 (kg)	Total U[2] (kg)
241-C-101 (associated with UPR-200-E-136)	37,000	0.14	0.25	0.04	580	0	5,900	1.3	4.3
241-C-104	28,000	0.11	0.03	0.03	52	0	4,500	90	3.3
241-C-105	2,000 to 20,500	0.01 to 0.1	1 to 9.8	5.9E-4	2,700 to 27,000	0	3 to 430	690	0.18 to 1.8
241-C-108	18,000	0.07	0.02	0.02	33	0	2,900	58	2.1
241-C-110 (associated with UPR-2-00-E-107)	2,000	0.05	3.4	0.003	230	0	1,800	210	0.73
241-C-112	7,000	0.03	0.0075	0.007	13	0	1,100	23	0.82
UPR-200-E-81	36,000	0.9	0.11	0.1	220	0	23,000	350	17
UPR-200-E-82	2,600	0.01	1.3	7.5E-5	3,500	0	55	88	0.2
UPR-200-E-86	17,000	0.03	2.7	1.6E-4	7,400	0	120	190	0.5
216-C-8 French Drain	>32,000	0.0	0.0	0.0	0.3	0	0.15	0.14	6.0E-05
Surface Releases	1,000	0.004	0.001	0.001	1.9	0	160	3.2	0.12
Total	201,000	1.5	18	0.2	39,000	0	40,000	1,800	31

Note: Values are rounded to two significant digits.
Radionuclide values are decayed to January 1, 2020.
No $Fe(CN)_6$ was identified in the supernate for Hanford Defined Waste waste types.

1 The Fe(CN)6 was assumed to be insoluble and retained in the solids. However, as discussed in Section 2.3.3.3 of this report, low concentrations of cyanide from the tank farms have been observed in groundwater wells. Appendix A provides an estimate of the inventory of cyanide released at WMA C.

2 HDW model values for U-Total are the sum of U-isotope values. As shown in Table 2-2, U-235 is low enriched ~4% of U-238 Inventories of U isotopes are provided in Appendix C of RPP-RPT-42294.

References:
RPP-ENV-33418, *Hanford C-Farm Leak Inventory Assessments Report*.
RPP-19822, *Hanford Defined Waste Model*, Rev. 5.0.

* Conversion 1 gallon = 3.78541 liters

Tank C-104 was filled to ~2,120,000 L (~560,000 gal) of CWP1 waste in 1965. No transfer was identified; however, the surface level decreased to the spare inlet elevation of ~2,014,000 L (~532,000 gal) resulting in a possible ~106,000-L (~28,000-gal) release of CWP1 waste.

Waste retrieval operations for tank C-104 using a modified sluicing and chemical dissolution process began in January 2010 and were completed on August 17, 2012. Although large volumes of water and supernate were used for retrieval operations, there was no indication from any of the monitoring systems used of a tank leak during retrieval

2.1.3 Tank 241-C-105

Tank C-105 was classified as a "sound" tank for many years. However, a high-activity ^{137}Cs plume (greater than ~10^7 pCi/g) was observed in drywell 30-05-07 near the base of the tank when it was drilled in 1974. The drywell activity was previously attributed to a cascade line release. After further field investigations and review in 2010 it was concluded that the activity around tank C-105 is from several different sources. Probable sources of waste releases to the soil include: releases from the cascade line between tanks C-104 and C-105, a leak near the base of tank C-105, releases from spare inlet nozzles, condenser leaks and leaks from Pipeline V103 (RPP-ASMT-46452, *Tank 241-C-105 Leak Assessment Completion Report*). Based on direct push logging results obtained for the assessment, the integrity assessment panel concluded that the inlet cascade line to tank C-105 leaked and tank C-105 may have leaked, and the panel recommended that the tank classification be changed to "assumed leaker."

Waste retrieval operations using a mobile arm retrieval vacuum extraction system began in June 2014 and are ongoing. To date there has been no indication of a tank leak during retrieval.

The estimated tank leak/release volume ranged from ~7,570 to 77,600 L (~2,000 to 20,500 gal) of P2 supernate (PSN) based on the estimated size of the ^{137}Cs plume and a 1969 sample concentration of ^{137}Cs of 4.3 Ci/gal. The upper volume estimate, provided by the Nez Perce Tribe, assumes more extensive ^{137}Cs migration under the tank. The leak volumes would be proportionally lower if the waste concentration was higher, as measured in 1963 (RPP-ENV-33418, Appendix B2.0).

2.1.4 Tank 241-C-108

Tank C-108 has previously been designated as "sound." However, drywells show ^{137}Cs near the tank at 6.7 m (22 ft) below ground surface (bgs) and ^{60}Co plumes that appear to extend from the tank bottom and migrate out and downward. Because some cascade lines are known to have released waste during times when the tanks were overfilled, and because gamma activity was observed starting just at the depth of the cascade line and adjacent to it, it was assumed that the cascade line may be the source of the observed activity at ~6.7 m (~22 ft). However, drywell logging indicates continued migration of ^{60}Co in the soil over the past 40 years which appears to be from another source.

Based on geophysical logging measurements, an estimated ~68,140 L (~18,000 gal) of waste may have been released. Assuming the waste was Plutonium Uranium Extraction facility (PUREX) cladding, aluminum clad fuel (1956-1960) (CWP1) waste (the type of supernate in the tank in 1965), this equates to an estimated 50 Ci of ^{137}Cs and ~0.9 Ci of ^{60}Co that may have been released. Continued movement of the contaminant plume beneath the tank indicates that there may have been other waste releases and additional solutions (water) released.

In March 2012, tank C-108 waste retrieval was completed. During retrieval, drywell moisture monitoring and HRR monitoring are performed for leak detection. Although large volumes of supernate and other liquids were introduced to the tank during retrieval operations and liquid was recirculated in the tank to remove the remaining hard heel, no evidence of a leak during retrieval was detected by the drywell monitoring or the HRR leak detection systems; this supports the previous evaluations that the tank appears to be sound. This does not preclude the possibility of a small or slow tank leak or a release from another source that could not be detected by these methods.

2.1.5 Tank 241-C-110

Tank C-110 was declared as “questionable integrity” in 1977 following the discovery of unexplained gamma activity in drywell 30-10-09. In 1984, it was declared an “assumed leaker” with an estimated leak volume of ~7,570 L (~2,000 gal).

In 2008 an integrity assessment was conducted for tank C-110 (RPP-ASMT-38219, *Tank 241-C-110 Leak Assessment Report*). The assessment concluded that tank C-110 spare inlets were the apparent source for the waste release based on the tank’s stable liquid level surface bracketing the period when the drywell gross gamma peak was discovered, the natural decay of the drywell gross gamma peak following discovery, and an interior tank photo showing evidence of waste in and above the tank inlet line penetrations.

There was no liquid level decrease observed and less than 1,000 pCi/g ^{137}Cs activity in drywell 30-10-09 when it was first logged in 1975. The estimated ^{137}Cs inventory is based on 1975 sample results (0.32 Ci/gal). Because a liquid level decrease was not observed, a maximum spare spare inlet release of ~7,570 L (~2,000 gal) was assumed. The waste type released is assumed to be CSR supernate, the waste type in the tank in 1975.

Tank C-110 was retrieved using modified sluicing and an in-tank vehicle for mechanical and high-pressure water cleaning. Although large volumes of water and supernate were added to the tank during retrieval operations, there was no indication of a leak during retrieval from the HRR leak detection monitoring system or other monitoring systems used.

2.1.6 Tank 241-C-111

Tank 241-C-111 was designated as an “assumed leaker” in 1968, with a leak volume estimate of ~20,820 L (~5,500 gal) based on a liquid level decrease. A tank integrity assessment conducted

in 2008 concluded that tank C-111 likely did not leak and recommended that the tank C-111 leak integrity status be revised from "Assumed Leaker" to "Sound" (RPP-ASMT-39155, *Tank 241-C-111 Leak Assessment Report*). The report concluded that the most probable explanation for the 1965 to 1969 surface level decrease in tank C-111 was evaporation of the thermally hot waste.

Tank C-111 was sluiced in 2010 using modified sluicing. Although large volumes of water and supernate were added to the tank during sluicing operations, there was no indication of a leak during retrieval from the HRR leak detection monitoring system or other monitoring systems used. Consequently, no soil inventory was developed for tank C-111.

2.1.7 Tank 241-C-112

Tank C-112 started receiving waste in November 1946. Tank C-112 was suspected of leaking and liquid was pumped to tank C-103 in 1975 and 1976. Later surveillance could not confirm the suspected leak, and the tank is currently considered "sound." A ^{60}Co concentration peak was detected near tank C-112 in drywells 30-12-01 and 30-12-13. The drywells are near a known release from the tank C-112 saltwell pump pit and a transfer line leak from 252-C Diversion Box to tank C-112. Based on drywell data, an estimated ~26,500 L (~7,000 gal) of CWP1-B Plant ion exchange (IX) waste was released.

Waste retrieval operations for tank C-112 using modified sluicing began December 28, 2011 and were completed on January 31, 2014. Although large volumes of water and supernate were used for retrieval operations, there was no indication of a tank leak during retrieval from any of the monitoring systems used.

2.1.8 UPR-200-E-81

RHO-CD-673, *Handbook 200 Areas Waste Sites*, identifies UPR 200-E-81 (UN-216-E-9) as a ~136,275-L (~36,000-gal) line leak from the PUREX Plant to tank C-102 near the 241-CR-151 diversion box (see Figure 1-6). The source was determined to be a leak in an underground transfer line from the 202-A Building to tank C-102 via the 151-CR box. The PUREX Plant merged low-level waste flows into the remaining line available which carried organic wash and special run coating waste.

Based on RHO-CD-673, an estimated ~136,275 L (~36,000 gal) and 720 Ci of ^{137}Cs was released in 1969 (220 Ci decayed to 2020). Direct push holes were drilled, logged and sampled in the vicinity of the UPR in 2008 and 2009. The direct push results appear to be consistent with the estimated ~136,275-L (~36,000-gal) line leak and a CWP2 release.

2.1.9 UPR-200-E-82

UPR-200-E-82 is identified as a leak in cesium line V122 from tank C-105 to B Plant was discovered in December 1969, 10.7 m (35 ft) south of the 152-C diversion box (see Figure 1-6).

The pipeline leak was characterized shortly after the leak event in which waste from the pipe migrated to the surface and the site was covered with 0.6 m (2 ft) of back fill (ARH-1945, *B Plant Ion Exchange Feed Line Leak*). A gunite cap was installed over the release site, but not for 20 years after the leak.

Based on the ARH-1945 volume estimate of ~9,840 L (~2,600 gal) and a 1969 sample concentration of 4.3 Ci/gal of ^{137}Cs, an estimated 11,000 Ci of ^{137}Cs was released in 1969 (3,500 Ci decayed to 2020). Vertical direct push holes were drilled, logged and sampled in the vicinity of the UPR in 2008 and 2009. Three slant holes were also drilled under the site of the pipeline leak. The direct push results appear to be consistent with a~9,840-L (~2,600-gal) PSN line leak. Higher gamma activity was expected, but the high activity may be directly under the gunite cap and direct push holes may have been too deep to detect it.

2.1.10 UPR-200-E-86

UPR-200-E-86 (also UN-216-E-14) is identified as leakage from the 244-AR vault to the 151-C diversion box portion of the PUREX sludge supernate (PSS) line to tank C-106 (pipeline V108/812), discovered on February 25, 1971 (RHO-CD-673). The line is a 5.1-cm (2-in.) direct buried line, 2.4 m (8 ft) below grade. The leak appeared to have occurred at a carbon steel-stainless steel weld and was estimated to have a line loss of ~65,810 L (~17,385 gal) of PSS waste containing 1.35 Ci/gal of ^{137}Cs (decay date of February 1971) (RHO-CD-673).

Based on a volume estimate of 64,350 L (17,000 gal) of PSN and a 1971 sample concentration of 1.35 Ci/gal of ^{137}Cs, an estimated 23,000 Ci of ^{137}Cs may have been released (7,400 Ci decayed to 2020).

A number of vertical direct push holes were drilled, logged and sampled in the vicinity of the UPR in 2008 and 2009. Logging and sampling of the holes showed low levels of activity around the area of the suspected release, inconsistent with a release volume of ~64,350 L (~17,000 gal) of PSN waste. Although there was no evidence of a large PSN leak based on the direct push data, the volume and inventory of ~64,350 L (~17,000 gal) of PSN and 7,400 Ci of ^{137}Cs was determined to provide a bounding estimate for the line leak.

2.1.11 216-C-8 French Drain

The 216-C-8 French Drain is located ~22.9 m (~75 ft) southeast of the C Farm southeast perimeter fence and 250 ft east-northeast of the 244-CR vault (see Figure 1-6). The site is composed of a 1.8-m (6-ft)-diameter by 2.4-m (8-ft) -long concrete culvert, placed vertically 1.2 m (4 ft) below grade. The culvert is filled with gravel. It was placed into an 2.4-m (8-ft)-diameter by 4.8-m (16-ft) deep excavation. A 5.1-cm (2-in.)-diameter steel vent pipe was placed vertically through the center of the culvert and extended 0.9 m (3 ft) above the surface. The above-grade portion of the pipe has been removed.

Although process records are incomplete, a minimum of ~121,135 L (~32,000 gal) of treated 241-A Tank Farm Process Condensate ion exchange waste was discharged to the 216-C-8 French Drain from January 1960 through March 1965 (Interoffice memo 7G420-MEJ-06-007, "Waste Discharged to the 216-C-8 Crib" [Appendix C]). Waste sample analyses in 1961 showed a ^{137}Cs concentration of 2.57 µCi/L. The assumed waste type was Strontium - Cesium Recovery Stack drain waste from the B-Plant Process, designated in RPP-26744, *Hanford Soil Inventory Model*, Revision 1, as Sr-Cs Rec (P2) Stack Drain waste.

2.1.12 Surface Level Releases

Cross-section visualizations of near-surface gamma activity in C Farm from spectral gamma logging system drywell logging data show less than 10 pCi/g of ^{137}Cs activity at 0.6 m (2 ft) bgs across the farm (Figure 2-2). In general, the highest gamma activity levels were observed near tanks or where an inventory has been determined. This suggests that other, undocumented surface releases may have been smaller; contaminants have been flushed; or the waste lost contained lower levels of non-mobile gamma activity (i.e., ^{137}Cs).

Figure 2-2. Near Surface Spectral Gamma Activity in 241-C Tank Farm.

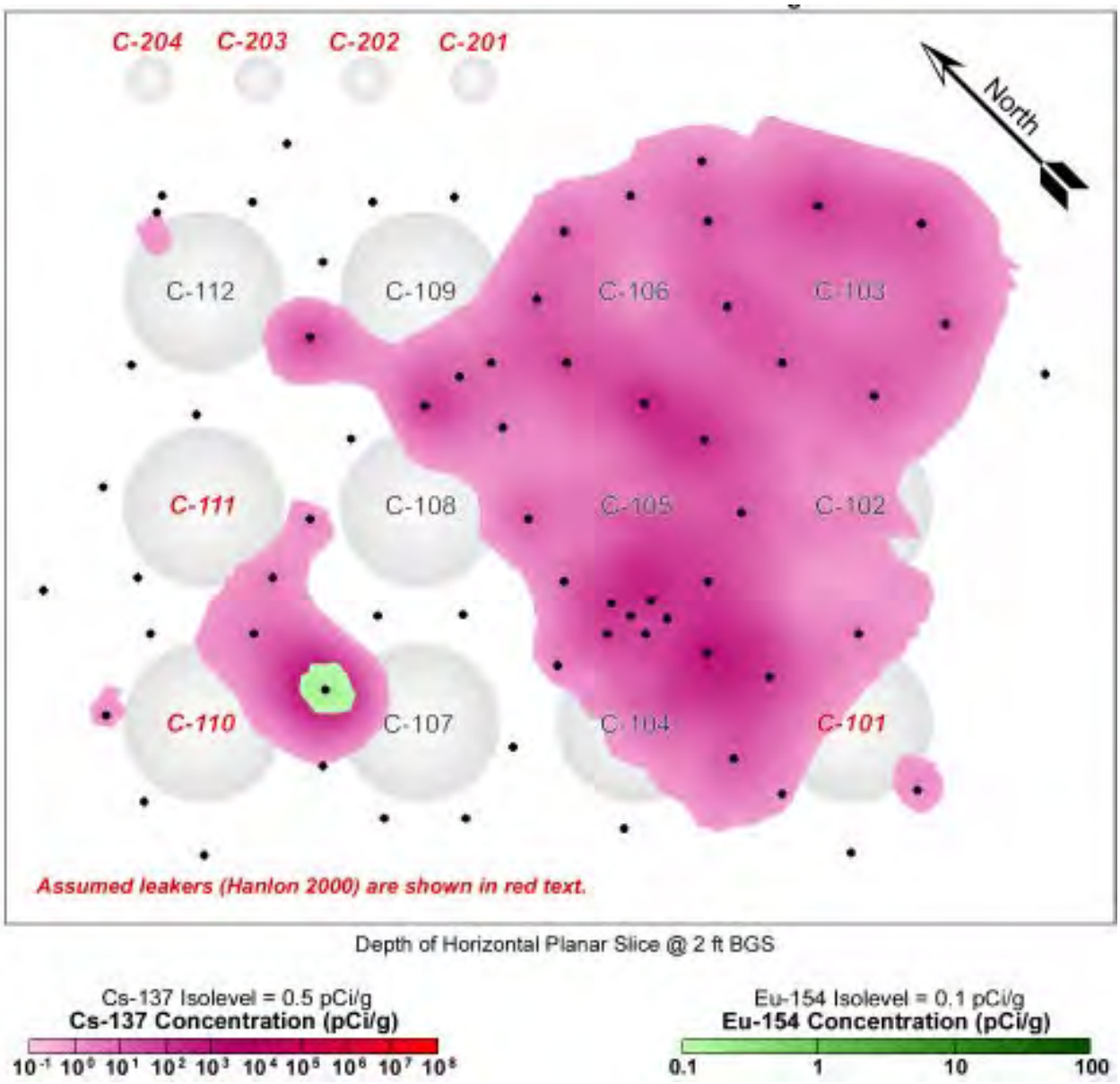

Reference: GJO-98-39-TARA/GJO-HAN-18, *Vadose Zone Characterization Project at the Hanford Tank Farms, Addendum to the C Tank Farm Report*.

A ^{137}Cs activity level of 10 pCi/g in the top 3.0 m (10 ft) of soil within the perimeter of the C Farm fence (an area of ~55,740 m^2 [~600,000 ft^2]) would result in a ^{137}Cs inventory of ~2 Ci (decayed to 2020). The associated volume of waste released based on this inventory and HDW, Rev. 5 waste type composition estimates ranges from ~38 L (~10 gal) for P1 waste to ~3,785 L (~1,000 gal) for CWP1 waste. For purposes of inventory estimates it is assumed that the waste released was predominantly CWP1. Table 2-1 shows the composition of CWP1 waste. Table 2-3 shows estimated WMA C surface inventories for selected constituents, inventories for other analytes are presented in Appendix A of RPP-RPT-42294.

2.1.13 Other Unplanned Releases

Sixteen UPRs have been documented within or adjacent to WMA C. Three of the UPRs (UPR-200-E-81, UPR-200E-82, and UPR-200-E-86) are discussed in Section 2.19, 2.1.10, and 2.11. Following are brief descriptions of the thirteen additional UPRs. All sixteen UPR's are summarized from the Waste Information Data System (WIDS) General Summary Reports (DOE/RL-88-30, *Hanford Site Waste Management Units Report*) and represent the best available information on the nature and extent of releases at the time of the data quality objective (DQO) (RPP-RPT-38152, *Data Quality Objectives Report Phase 2 Characterization for Waste Management Area C RCRA Field Investigation/Corrective Measures Study*). Locations of thirteen of the sixteen unplanned releases are provided in Figure 2-14. UPRs not posted on this figure include UPR-200-E-99, UPR-200-E-100, and UPR-200-E-135. A detailed description of all sixteen UPRs recorded in and near WMA C is provided in Appendix F of RPP-RPT-58339, *Phase 2 RCRA Facility Investigation Report for Waste Management Area C.*

- **UPR-200-E-16** is associated with waste site 200-E-133. UPR-200-E-16 is a surface spill associated with an over-ground transfer pipeline between tanks C-105 and C-108. The surface spill associated with this release is located 18 m (60 ft) northeast of tank C-105 and occurred in 1959. The spilled liquid was classified as cladding waste (CW) from the PUREX process and was an estimated 200 L (50 gal).

- **UPR-200-E-27** is associated with waste site 200-E-133. UPR-200-E-27 was a particulate release located east of the 244-CR Vault and extending east beyond the tank farm fenceline. DOE/RL-92-04 indicates the surface contamination was deposited in 1960 but does not identify the source(s) of the contamination. However, the November 1960 monthly report for the tank farm contractor reports the particulate contamination was due to work in C Farm diversion boxes and the 244-CR Vault (HW-67459, *Chemical Processing Department Monthly Report for November 1960*, pp. B-2 and B-3). Activity levels around the vault were on the order of 50 to 100 mrad/hr.

- **UPR-200-E-68** is associated with waste site 200-E-133. UPR-200-E-68 was a particulate release; wind-borne surface contamination spread from diversion box 241-C-151. Activity consisted of beta/gamma particulates, with readings ranging from 2,000 counts per minute to 5 rad per hour on the diversion box cover blocks and other surfaces in 200 East Area. The release occurred in 1985 and the waste site was subsequently decontaminated to background radiation levels or covered with clean soil for later decontamination (the source document is inconclusive). Sometime after the release, diversion box 241-C-151 was opened, flushed, and sprayed with Turco®[1] Fabrifilm to physically fix contamination to the structure surface.

- **UPR-200-E-72** occurred in 1985 and is located south of WMA C near the 216-C-8 French drain. The source of the contamination was attributed to buried contaminated waste. The waste posed little release potential because the contamination was fixed in

[1] TURCO is a trademark of Henkel Technologies, Corp., Rocky Hill, CT.

place with Turco® Fabrifilm. The source of the contamination was determined to be from the burial of previously undocumented contaminated material. The area was surrounded with a chain and posted as a "Surface Contamination Area"; however, the site is no longer marked or posted. The WIDS summary report (DOE/RL-88-30.) limits the description of the buried material to "Misc. Trash and Debris." Thus it is assumed that the contamination extends to the depth of the buried material, but the aerial extent and depth are not known. The volume of the contamination was not specified.

- **UPR-200-E-91** is located 30 m (100 ft) from the northeast side of the tank farm and resulted from surface contamination that migrated from WMA C. The date of the occurrence, its aerial extent, and the nature of the contamination are not specified. DOE/RL-92-04 states that the contaminated soil was removed, and the area was released from radiological controls.

- **UPR-200-E-99** is surface contamination that resulted from numerous piping changes associated with the 244-CR Vault. It is located south of 7th Street, directly south of the 244-CR Vault. This location was established as a release site in 1980, although the actual occurrence date is unknown. A radiological survey conducted in support of herbicide applications in 1981 found no detectable contamination in the release area. As a result of the radiological survey, surface contamination postings were removed on March 5, 1981, and the area was released from the radiation zone designation.

- **UPR-200-E-100** release area was determined due to windblown particulates and biological transport (rodent feces) from the tank farms and the 244-A Lift Station (DOE/RL-88-30) that occurred in the mid-1980s. It is located 60 m (197 ft) south and east of WMA C and surrounds the 244-A Lift Station.

- **UPR-200-E-107** resulted from a surface spill. The exact location of this release is unclear. The WIDS summary report (DOE/RL-88-30) states that the release was reported at the tank 241 CR-100. The original incident report states it occurred at the tank CR-110 in the 241 CR Farm. The report also states that the location should be tank C-110 in C Farm and states that a spill occurred on November 26, 1952, when a pump discharged an estimated 19 L (5 gal) of liquid to the ground surface during a pump installation. "Due to the magnitude of the ground contamination, it was decided to excavate a hole and blade the contamination earth into the hole" (RPP-RPT-29191, *Supplemental Information Hanford Tank Waste Leaks*, pp. 102).

- **UPR-200-E-115** is located east of C 1 Farm, south of 8th Street, across an unnamed gravel road. As a result of routine radiological surveys that confirmed radiological contamination in this area, the Dyncorp Integrated Soil, Vegetation and Animal Control group submitted a Waste Site Information Form to WIDS in 2000. The site was classified as "Discovery" until programmatic responsibility and ownership were determined in March 2001. No radiological surveys can be found to provide information about the radiological conditions inside the posted area. Very little is known about this posted area. During an interview with the Dyncorp Radiological Group in October 2000, an assumption was made that the release area was posted by the Tank Farm Contractor

East Tank Farm Radiological Control Group. A review of underground pipeline locations did not indicate a pipeline at this location. In 1980, a larger area of posted contamination (UPR-200- E-91) was located in the same vicinity. The contaminated soil from UPR-200-E-91 was removed in 1981. Because so much time has passed, it is difficult to determine if the two sites are related. In June 2004, UPR-200-E-115 was stabilized with gravel and posted as an "Underground Radioactive Material Area."

- **UPR-200-E-118** is associated with waste site 200-E-133. UPR-200-E-118 is located in the northeast portion of the tank farm and extends northward up to 305 m (1,000 ft) beyond the WMA C fence line. It was the result of an airborne release from tank C-107 that occurred in April 1957. The highest exposure rate was estimated at 50 mrem/hour at the ground surface (DOE/RL-92-04).

- **UPR-200-E-135** is located south and west of WMA C. This site was identified as contaminated vegetation which has subsequently been removed. The source of contamination is suspected to be an underground leaking pipeline in the area.

- **UPR-200-E-136** is associated with waste site 200-E-133. UPR-200-E-136 was a release in 1969 of 64,600 to 91,200 L (17,000 to 24,000 gal) of waste from tank C-101. The quantity and type of waste released from tank C-101 is uncertain (RPP-ENV-33418).

- **UPR-200-E-137** is associated with waste site 200-E-133. UPR-200-E-137 occurred when"water entered tank C-203, migrated through the saltcake, and either became entrained in the saltcake or leaked out of the tank." The leak was 1,520 L (400 gal) of PUREX HLW. The waste in tank C-203 was subsequently determined to be sludge and was retrieved to a double-shell tank (DST) in 2006. Subsequent review indicated that the water evaporated and was not released (RPP-ENV-33418).

2.2 HYDROLOGIC SETTING OF HANFORD'S CENTRAL PLATEAU

This section provides a brief description of the vadose zone and unconfined aquifer in the Hanford Site Central Plateau (refer to Figure 1-3). WMA C is located within the 200-BP-Groundwater Operable Unit (OU) inside the eastern boundary of the 200 East Area (Figure 2-3). For a more complete description of the site characteristics of the Central Plateau, see Section 3 of RPP-ENV-58782, or RPP-ENV-58806, or DOE/RL-2009-127, *Remedial Investigation Report for the 200-BP-5 Groundwater Operable Unit*, Draft A.

2.2.1 Geologic Setting and Stratigraphic Units

The vadose zone and unconfined aquifer in the vicinity of WMA C are contained within the suprabasalt sediments (Figure 2-4 and 2-5). The Ringold Formation comprises the oldest suprabasalt sediments, composed of fluvially-deposited, gravel-dominated sediments designated as units A, B/D, C, and E. These high-energy deposits may be intercalated with fine-grained lake-bed (lacustrine) or overbank deposits designated as the Ringold lower mud (RLM) unit and

the upper Ringold unit (Rtf). Within the WMA C near-field area, four sedimentary units are present (from oldest to youngest): fluvial gravel unit A (Rwia), RLM, fluvial gravel unit E (Rwie), and Rtf. These geologic units are designated as hydrostratigraphic units (HSUs) 9, 8, 5, and 4, respectively. Detailed lithologic descriptions of these units are provided in PNNL-12261, *Revised Hydrogeology for the Suprabasalt Aquifer System, 200-East Area and Vicinity, Hanford Site, Washington*, and PNNL-19702, *Hydrogeologic Model for the Gable Gap Area, Hanford Site*.

Rwia (HSU 9) is the oldest Ringold Formation unit and directly overlies the Elephant Mountain Basalt. The Rwia displays a relatively flat surface that dips toward the axis of the Cold Creek syncline (southerly). The Rwia is not present in the northern portion of the near-field area where the basalt surface has been structurally uplifted. This uplift created depositional thinning or exposed the older sediment to paleoflood removal (erosion) across this area (Figure 2-6). The Rwia ranges in thickness from over 30 m (100 ft) of the structure east and south of the 200 East Area to zero where it truncates within the near-field area. The position of the truncation boundary is approximate and is identified as the erosional limit of the post-Ringold fluvial incision from Pleistocene-age cataclysmic flooding that traversed the uplifted area. For the near-field area, Figure 2-6 depicts the stratigraphy and general structural and erosional relationships of the Ringold Formation and overlying Hanford formation sediment.

The Hanford formation (HSU 1) is the youngest geologic sequence within the 200-BP-5 OU. This unit consists of glaciofluvial sediment deposited during cataclysmic Ice Age flooding. HSU 1 is subdivided into three main facies (silt-, sand-, and gravel-dominated) that vary vertically and laterally across the region and are difficult to correlate from area to area. In the southern portion of the near-field area (southern 200 East Area), the Hanford formation sediments unconformably overly the older Ringold Formation units (Rwie, RLM, and Rwia) and may only comprise the very uppermost portion of the unconfined aquifer. In the other portions of the 200-BP-5 OU near-field area, the Hanford formation sediments were mainly deposited unconformably on top of basalt and form part or all of the sediment in the unconfined suprabasalt aquifer. The vadose zone in the 200-BP-5 OU near-field area is primarily composed of the Hanford formation. The thickness of the Hanford formation ranges from 0 m to more than 109 m (0 to more than 357 ft).

Clastic dikes are not known to exist in great numbers within the Hanford formation sediments of the 200-BP-5 OU but have been mapped extensively at the Hanford Site south of the 200-BP-5 OU (PNNL-14224, *Influence of Clastic Dikes on Vertical Migration of Contaminants in the Vadose Zone at Hanford*). Clastic dikes normally occur as cross-cutting, vertically oriented cracks or fissures in the formation that are typically filled with sand, silt, clay, and minor coarser debris. Their origin is not well understood but is likely associated with hydraulic ejection during or immediately following Pleistocene cataclysmic flooding, mass wasting, earthquakes, and other geologic processes. Clastic dikes occurring in vadose zone sediments have the potential to influence the movement of soil moisture and contaminants (BHI-01103, “Clastic Injection Dikes of the Pasco Basin and Vicinity – Geologic Atlas Series”), but no data exist about the potential influence of clastic dikes within the aquifer.

Figure 2-3. Surface Topography and Boundaries of the 200-BP-5 Groundwater Operable Unit.

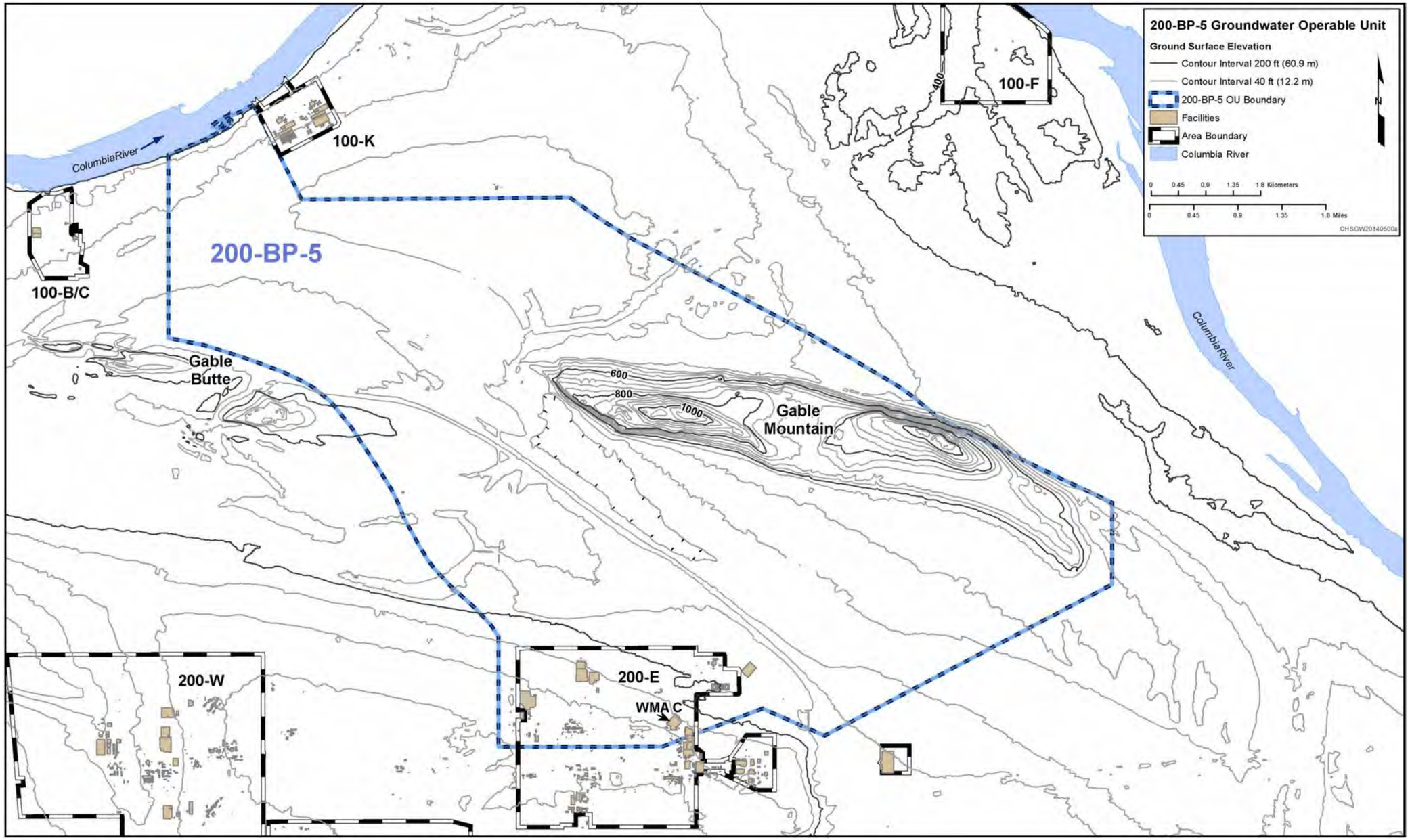

WMA = Waste Management Area

Holocene surficial deposits in the 200 East Area are dominated by very fine-grained to medium-grained, and occasionally silty, eolian sheet sands. These deposits have been removed or reworked over much of the area by past construction activities.

2.2.2 Unconfined Aquifer System

The base of the uppermost aquifer system is defined as the top of the uppermost basalt flow, with the top of the system being the water table. This aquifer system is bounded laterally by anticlinal basalt ridges and is ~152 m (~500 ft) thick near the center of the Pasco Basin. Within the Hanford Site, this uppermost aquifer system lies at depths ranging from less than 0.3 m (1 ft) below the ground surface near West Lake and the Columbia and Yakima Rivers (Figure 2-7), to more than 107 m (350 ft) in the central portion of the Cold Creek syncline. Groundwater in the unconfined aquifer at the Hanford Site generally flows from recharge areas in the elevated region near the western boundary of the Hanford Site toward the Columbia River on the eastern and northern boundaries. The Columbia River is the primary discharge area for the unconfined aquifer. The Yakima River borders the Hanford Site on the southwest and is generally regarded as a source of recharge.

The unconfined aquifer system underlying the Hanford Site exists within sediments deposited on top of the Columbia River Basalts. It is composed primarily of the Ringold Formation and overlying Hanford formation.

Figure 2-7 is a hydrogeologic map of the units present at the water table surface in 2009. In the 200 West Area, the water table occurs almost entirely in the Ringold Unit E gravels (Rwie, which corresponds to HSU 5), while in the 200 East Area, it occurs primarily in the Hanford formation and in the Ringold Unit A gravels (Rwia, which corresponds to HSU 9). Along the southern edge of the 200 East Area, the water table is in the Ringold Unit E gravels. The upper Ringold facies were eroded in most of the 200 East Area by the ancestral Columbia River and, in some places, by the Missoula floods that subsequently deposited Hanford gravels and sands on what was left of the Ringold Formation (DOE/RL-2002-39, Standardized Stratigraphic Nomenclature for Post-Ringold-Formation Sediments Within the Central Pasco Basin). Because the Hanford formation and possibly the Cold Creek unit (CCu) sand and gravel deposits are much more permeable than the Ringold gravels, the water table is relatively flat in the 200 East Area, but groundwater flow velocities are higher. Directly underneath WMA C, the unconfined aquifer occurs in the undifferentiated Hanford Gravels, CCu, and Ringold Formation (Figure 2-6).

Figure 2-4. Comparison of 200-BP-5 Operable Unit Hydrostratigraphy to Hanford Site Stratigraphy.

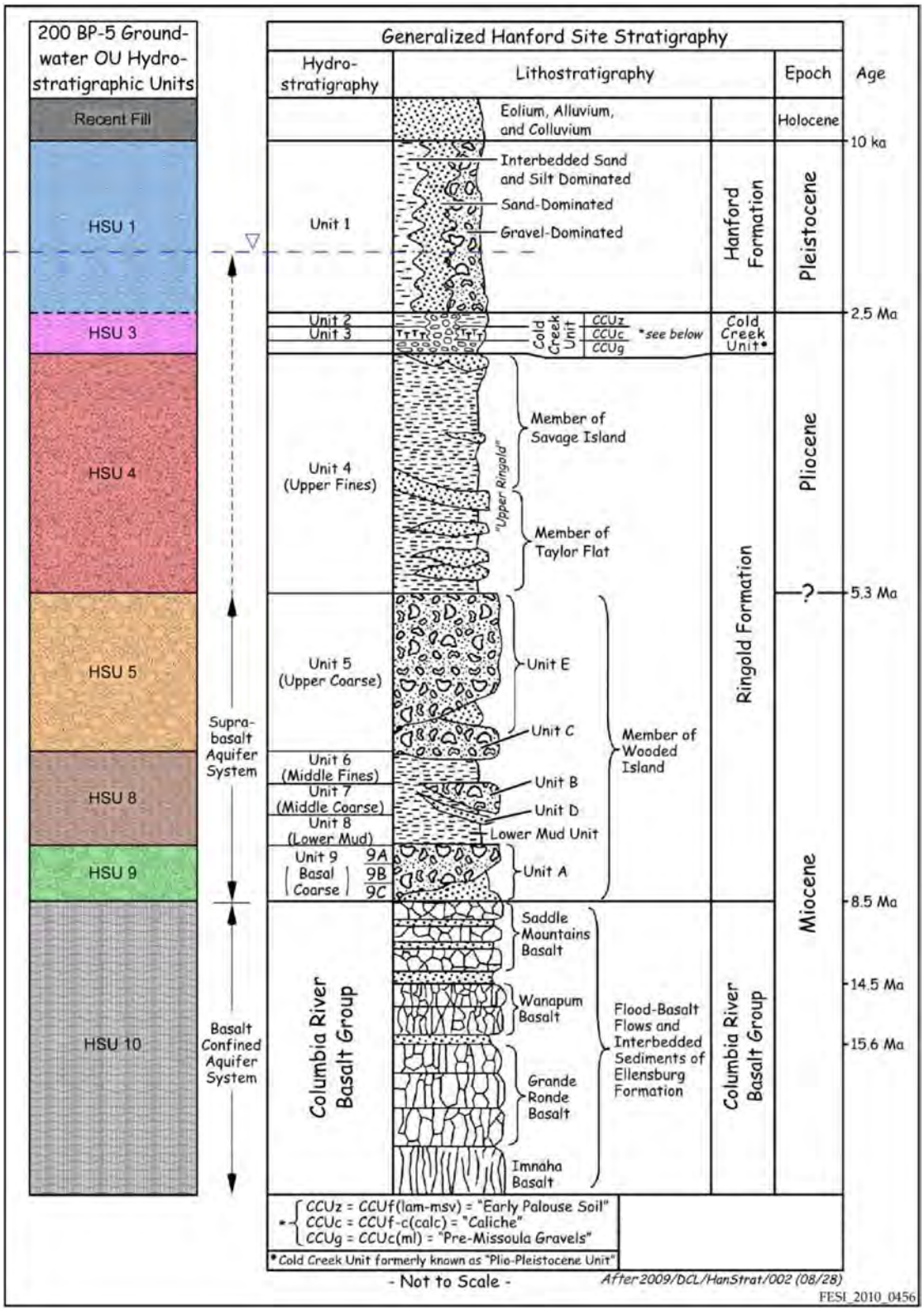

HSU = hydrostratigraphic unit OU = operable unit

Figure 2-5. Representative Photos of the Hanford Formation, Cold Creek Unit, Ringold Unit E, Ringold Lower Mud Unit, and Basalt.

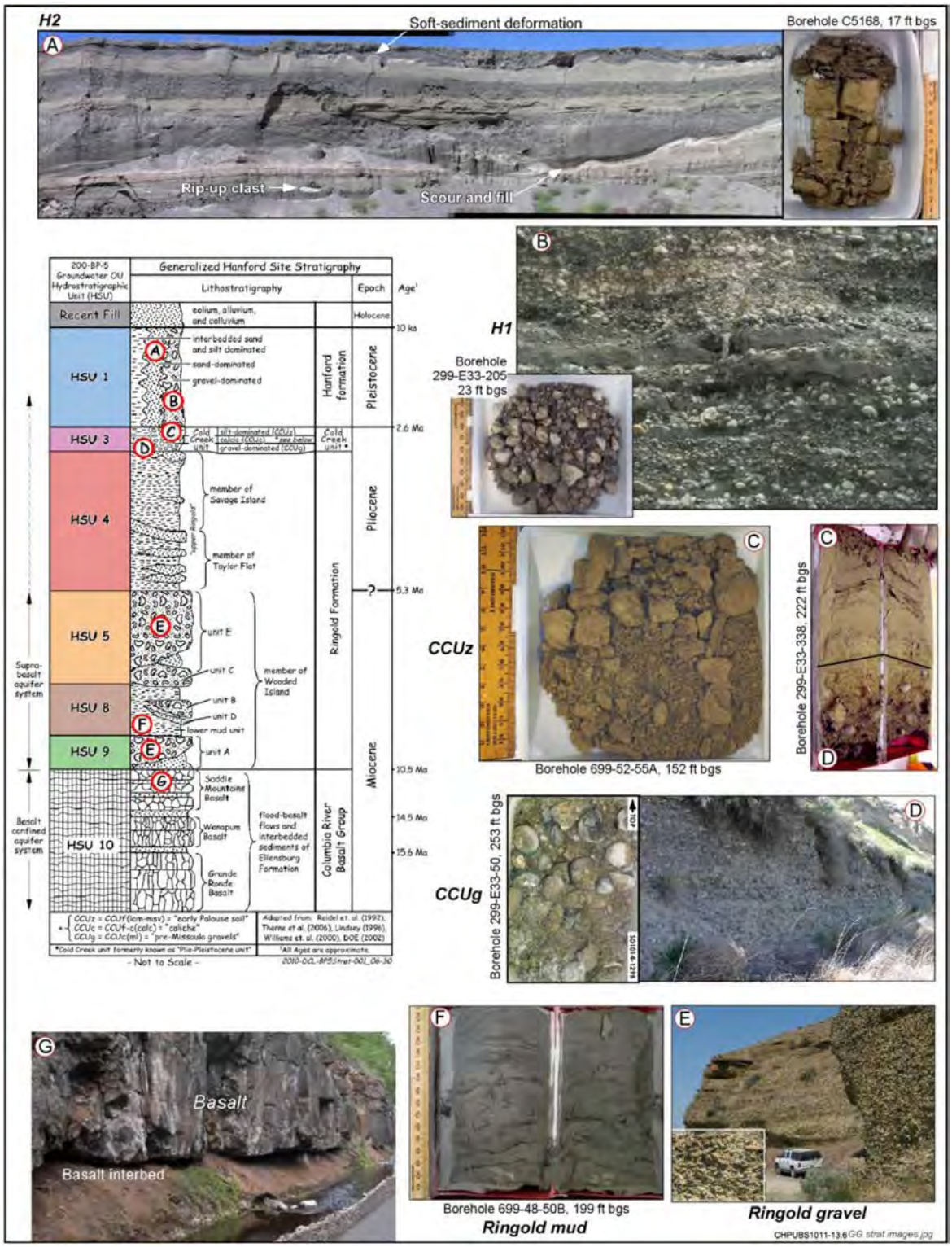

HSU = hydrostratigraphic unit OU = operable unit

Reference: PNNL-19702, "Hydrogeologic Model for the Gable Gap Area, Hanford Site."

Figure 2-6. 200-BP-5 Operable Unit Near-Field Area Hydrogeology Depicting Truncation of Ringold Units on Uplifted Basalt.

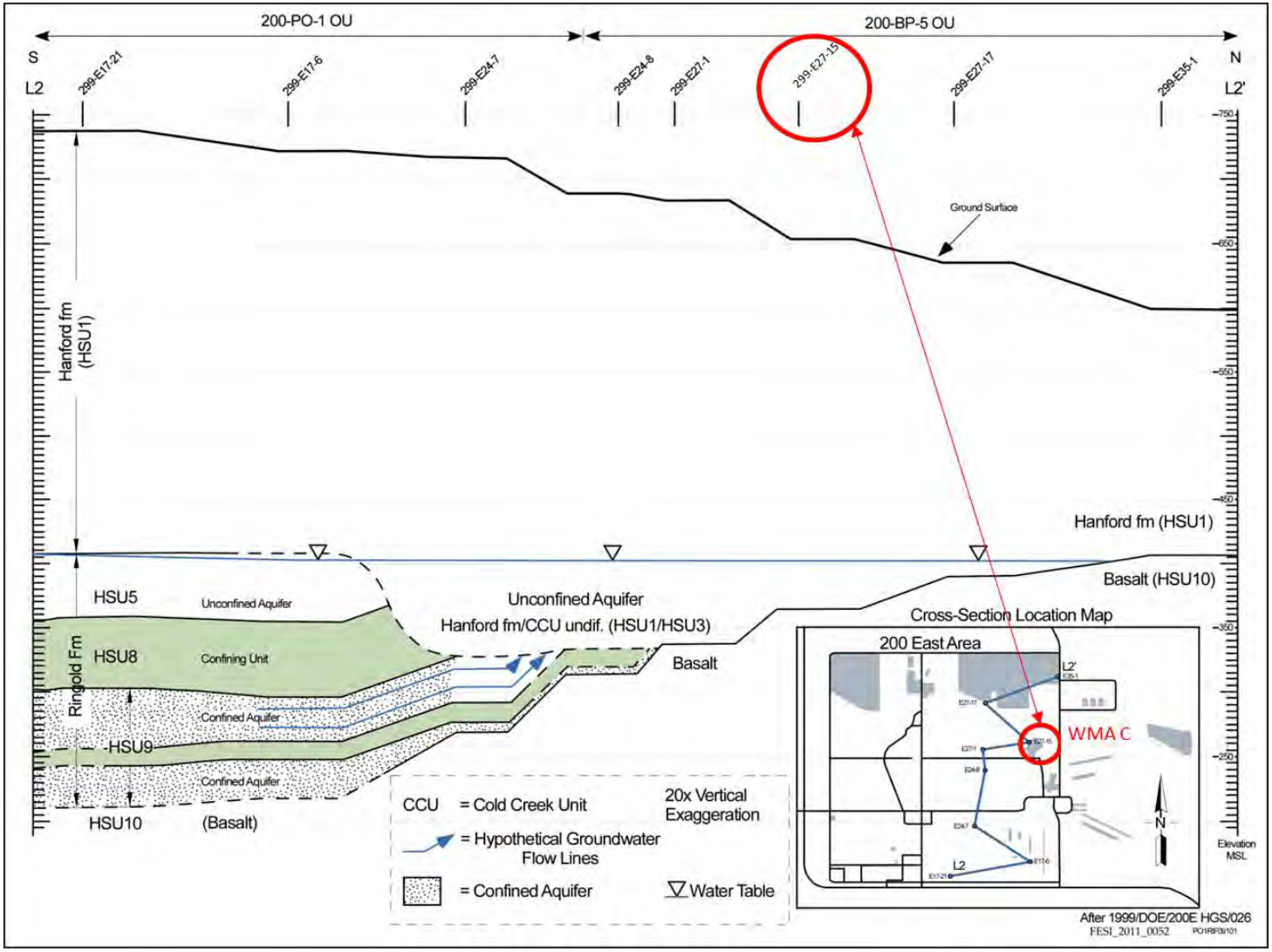

HSU = hydrostratigraphic unit OU = operable unit

Reference: PNNL-12261, "Revised Hydrogeology for the Suprabasalt Aquifer System, 200-East Area and Vicinity, Hanford Site, Washington."

Figure 2-7. Distribution of Hydrogeologic Units at the Water Table, 2009.

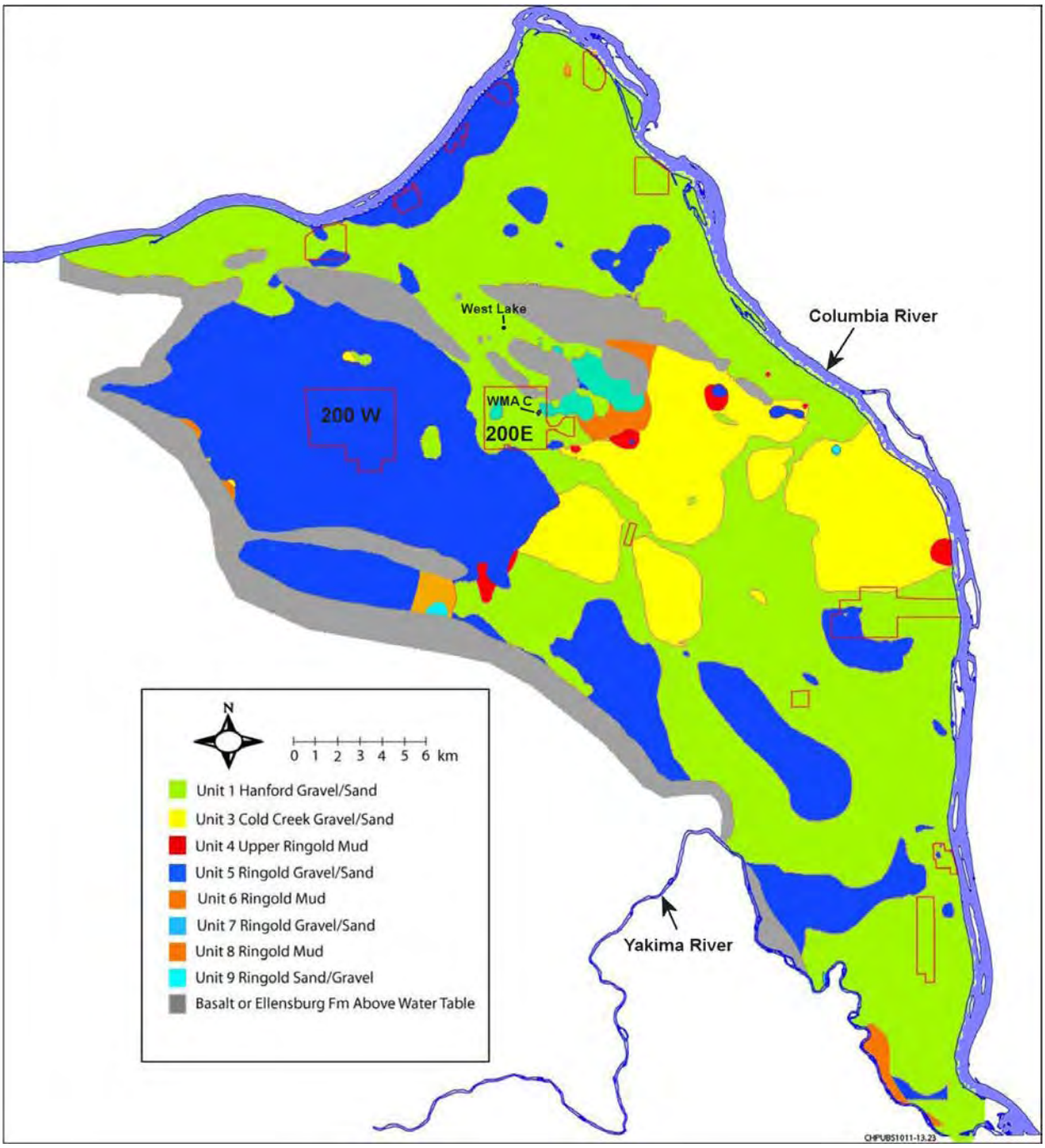

WMA = Waste Management Area

The hydrology of the 200 Areas has been strongly influenced by the discharge of large quantities of wastewater to the ground. Between 1944 and the mid-1990s, an estimated 1.68×10^{12} L (4.44×10^{11} gal) of liquid was discharged to disposal ponds, trenches, and cribs. Wastewater discharge has decreased since 1984 and currently only contributes a volume of recharge in the same range as the estimated natural recharge from precipitation. The largest volumes of discharge around the 200 East Area were to the 216-B Pond system, the 216-A-25 (Gable Mountain) pond system, and several of the PUREX cribs in the southeast corner of 200 East Area. Figure 2-8 shows the liquid discharge history for the two ponds. The Gable Mountain Pond is estimated to have received ~293 billion L (~77.4 billion gal) of effluent, while the 216-B Pond to have received ~256 billion L (~67.6 billion gal) of effluent. In the 200 West Area, the largest volumes of discharge were to the 216-T Pond system and the 216-U-10 Pond (Figure 2-9). The 216-T Pond system is estimated to have received ~424 billion L (~112 billion gal) of effluent (WHC-EP-0815, *Groundwater Impact Assessment Report for the 216-T-4-2 Ditch*), while the 216-U Pond to have received ~158 billion L (~41.5 billion gal) of effluent (WHC-EP-0707, *216-U-10 Pond and 216-Z-19 Ditch Characterization Studies*).

Figure 2-8. Discharge History for the 216-B Pond System and Gable Mountain Pond.

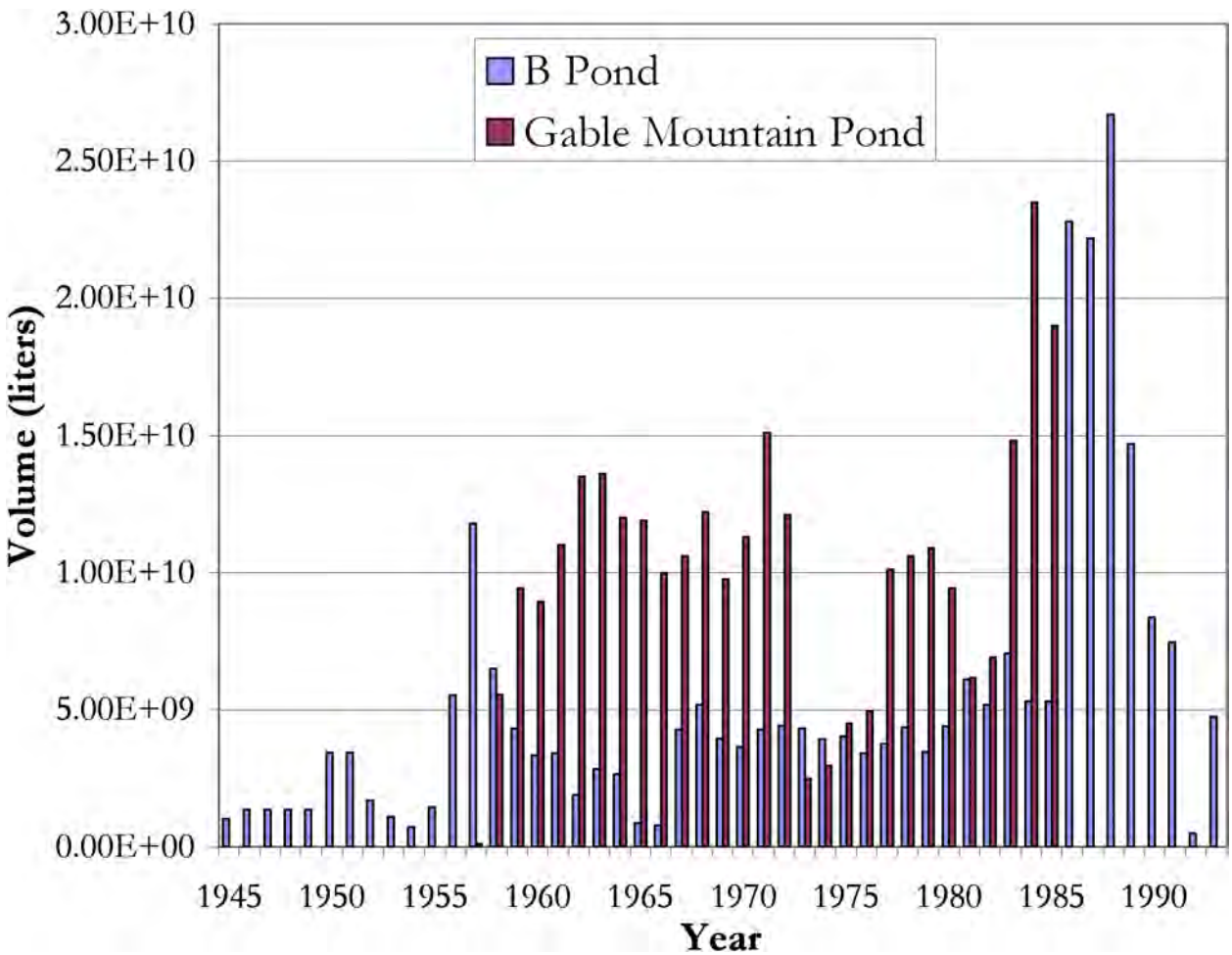

Figure 2-10 shows a series of water table elevation maps for the time periods representing pre-operational conditions, operational conditions, and present-day conditions for the Hanford Site. The first water table map (Figure 2-10a) is a hind cast map of water table elevations (ERDA-1538, *Final Environmental Impact Statement, Waste Management Operations, Hanford Reservation, Richland, Washington*) prior to the start of significant Hanford Site wastewater discharges. This water map includes the effects of limited irrigation near the former towns of White Bluff and Hanford, but not the effects of extensive irrigation now common in Cold and Dry Creeks. The 1944 water table contours indicate that groundwater flow is easterly toward the Columbia River with a relatively uniform hydraulic gradient (~1.5 m/km [~5 ft/mi]). Regional groundwater flow was generally toward the east-northeast, while flow north of Gable Mountain was more to the north.

Figure 2-9. Discharge History for the 216-T Pond and 216-U Pond.

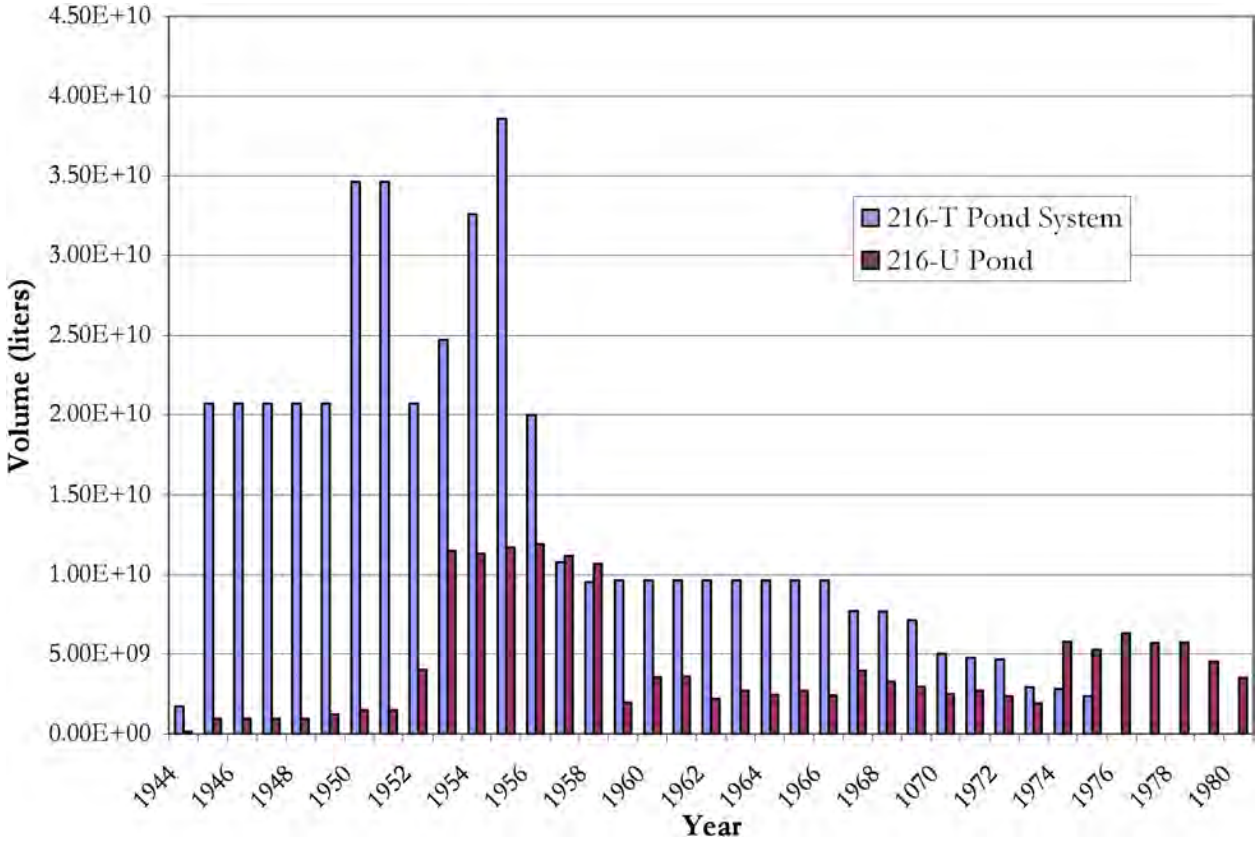

The pre-Manhattan Project water table in the 200 West Area and 200 East Area was ~123 m (~404 ft) and 120 m (394 ft) above sea level, respectively (BNWL-B-360, *Selected Water Table Contour Maps and Well Hydrographs for the Hanford Reservation, 1944-1973*). In the 200 West Area, the water-table elevation increased rapidly from 1949 to 1956, but appeared to stabilize between the late 1960s and the late 1980s. Water levels began to decline in the late 1980s when wastewater discharges in the 200 West Area were reduced. In the 200 East Area, the water table elevation increased rapidly from 1954 to 1963. The water table declined somewhat in the late 1960s and early 1970s, but then increased again in the early 1980s before

beginning a final decline throughout the 1990s when wastewater discharges in the 200 East Area were reduced.

During operations, water levels in the uppermost and unconfined aquifer rose as much as 26 m (85 ft) and 9 m (30 ft) beneath the 200 West Area and 200 East Area, respectively, because of artificial recharge caused by liquid waste disposed from the mid-1940s to 1995. Figure 2-10b shows water table mounding present in the 200 Areas for June 1987. The volume of water that was discharged to the ground at the 200 West Area was less than that discharged at the 200 East Area. However, the lower hydraulic conductivity of the aquifer near the 200 West Area inhibited groundwater movement in this area, resulting in a higher groundwater mound.

Figure 2-10a. Hind Cast Water Table Map of the Hanford Site, January 1944.

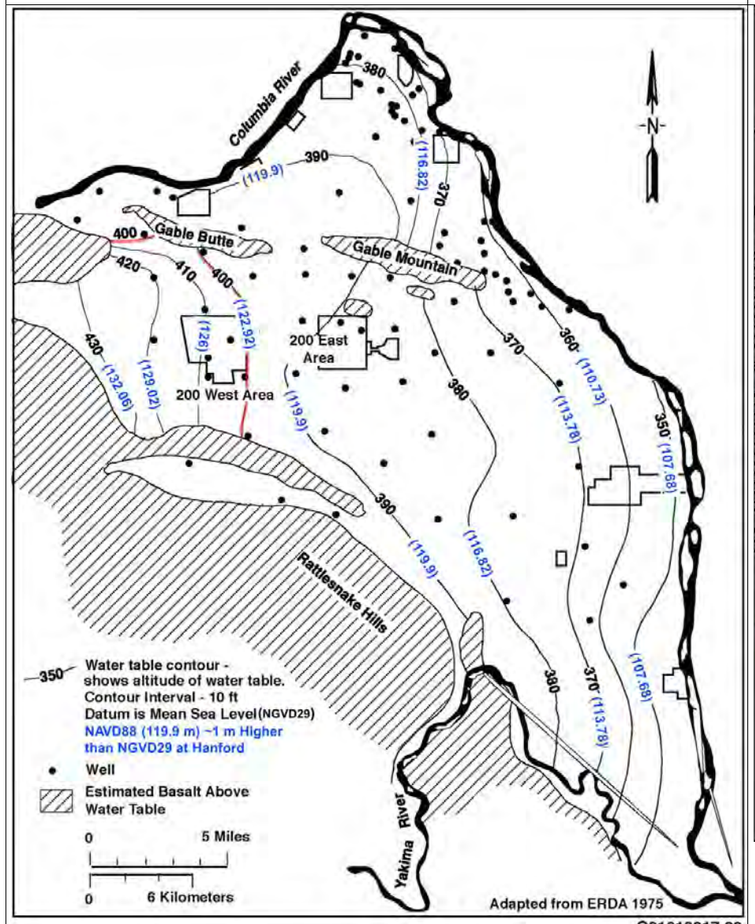

ERDA 1975 refers to ERDA-1538, "Final Environmental Impact Statement, Waste Management Operations, Hanford Reservation, Richland, Washington."

Note red contour line is to allow reader to follow changes for that contour interval through all three water table maps.

Figure 2-10b. Water Table Elevations for June 1987.

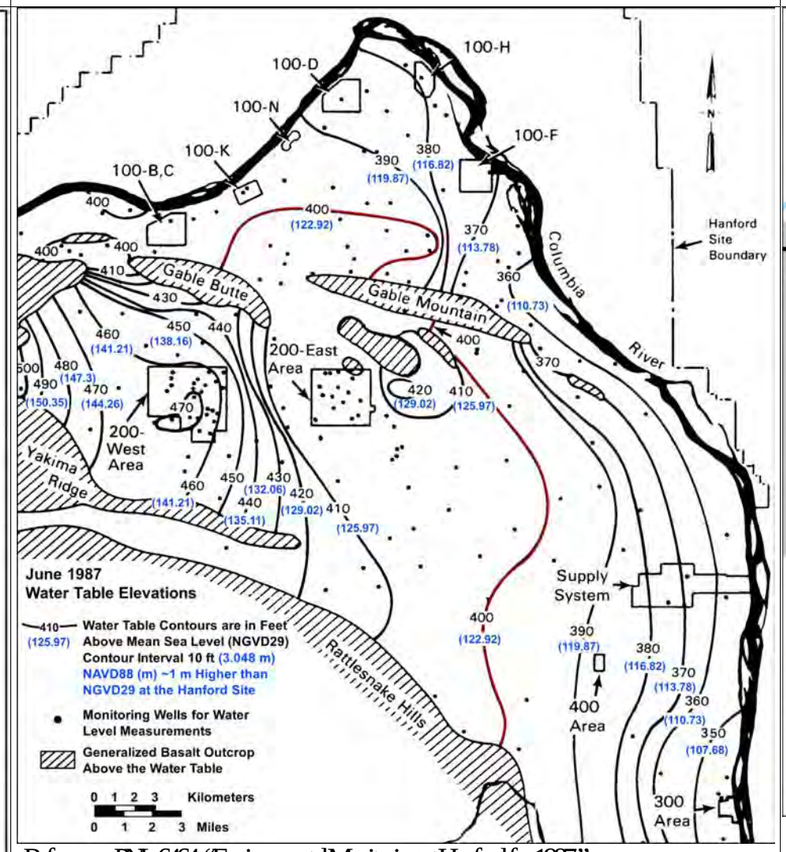

Reference: PNL-6464, "Environmental Monitoring at Hanford for 1987."

Figure 2-10c. Water Table Elevations for 2013.

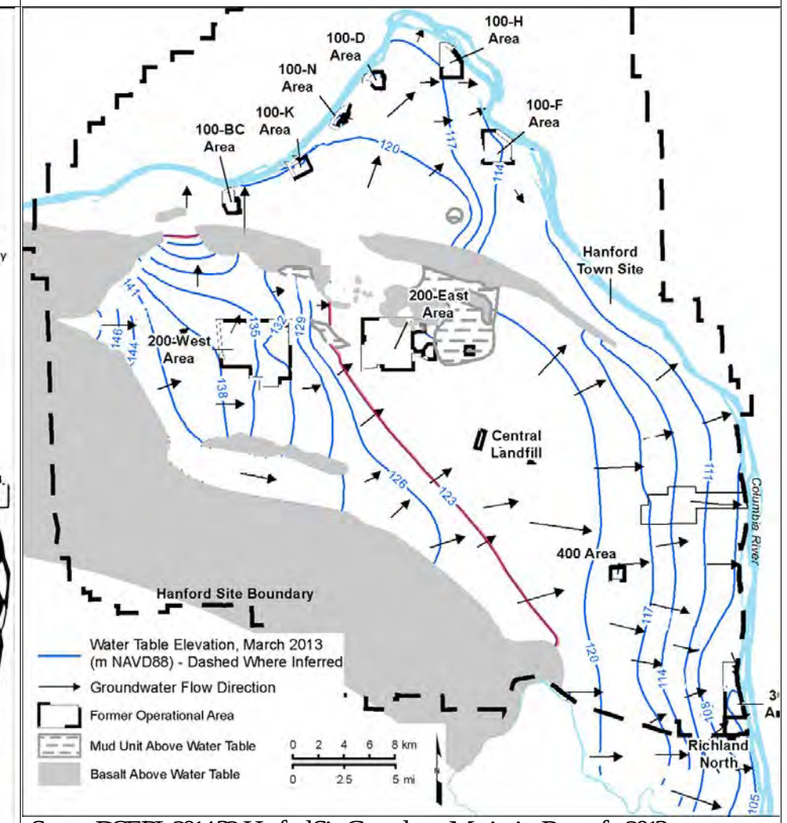

Source: DOE/RL-2014-32, Hanford Site Groundwater Monitoring Report for 2013.

1

Presently, groundwater in the unconfined aquifer generally flows from upland areas in the west toward the regional discharge area north and east along the Columbia River (Figure 2-10c). Steep hydraulic gradients occur in the western, eastern, and northern regions of the Site. Shallow gradients occur southeast of 100-FR and in a broad arc extending from west of 100-BC toward the southeast between Gable Butte and Gable Mountain (Gable Gap), through the 200 East Area and into the central portion of the Site. The reduction of wastewater discharges has caused water levels to drop significantly; however, a residual groundwater mound beneath the 200 West Area is still present today as shown by the curved water table contours near this area. Additionally, small groundwater mounds exist near the 200 Area Treated Effluent Disposal Facility (TEDF) and State-Approved Land Disposal Site wastewater disposal sites.

Comparing the approximate rate of water table decline in the 200 East Area with that in the 200 West Area shows that the rate of decline is three to four times faster in the 200 West Area. This is probably due, in part, to the greater increase in water level at U Pond than at B Pond. Also, the water table gradient is extremely flat in the 200 East Area, whereas the gradient is steeper beneath the 200 West Area. This indicates that a small increment of water table decline must be spread out over a much larger area in the 200 East Area than in the 200 West Area (Figure 2-11).

Figure 2-11. Water Table Elevations at Groundwater Monitoring Wells Close to U-Pond (200 West Area) and B-Pond (200 East Area).

With cessation of discharges to B Pond, the northward migration of contaminated groundwater from the 200 East Area slowed as the gradient decreased. By 2009, the unconfined aquifer presented a broad, relatively flat water table, with groundwater divide moving near the northern half of the 200 East Area around WMA C. At the flow divide, groundwater flow bifurcates to the northeast or southeast, essentially the travelling on either side of the remnants of the B Pond hydraulic mound. The exact location of this divide is variable and not easily identifiable. The water table in the 200 East Area is nearly flat and measurement uncertainties are greater than

actual water level differences between wells (DOE/RL-2010-11, *Hanford Site Groundwater Monitoring and Performance Report for 2009 Volumes 1 and 2*). By July 2011, groundwater flow within the unconfined aquifer in the southern portion of the 200-BP-5 OU (south of Gable Mountain) changed direction by 180 degrees compared to 2007. Since July 2011, the flow has maintained a south-southeast direction from the southern portion of Gable Gap into the northwest quarter of the 200 East Area (DOE/RL-2014-32, *Hanford Site Groundwater Monitoring Report for 2013*).

The dominant source of water in the unconfined aquifer beneath the 200 East Area and vicinity is inflow from the west. Formerly, the direction of groundwater flow diverged beneath the 200 East Area, with some water flowing toward the north through Gable Gap and some flowing southeast. The flow direction changed during 2011; since then flow has been toward the south and southeast across much of the 200 East Area. This change in flow directions is important because contaminant plumes located in the northwest corner of the 200 East Area located near and under the B Complex (WMA B-BX-BY and nearby Cribs) could flow under WMA C.

The distribution of hydrogeologic units within the unconfined aquifer is a result of Miocene-Pliocene Age geologic uplift and subsequent ancestral Columbia River and Pleistocene cataclysmic flooding and erosion. Highly turbulent floodwaters eroded channels into the basalt flow tops that typically filled with coarse-grained highly permeable channel fill. One such high-permeability channel exists below the water table at WMA C (Figure 2-12). These channel fill structures are often the location of preferential groundwater flow and contaminant migration when the orientation of the channel feature and the direction of groundwater flow align. This allows significant groundwater movement through the unconfined aquifer.

Groundwater velocity in the unconfined aquifer is dependent upon the hydraulic conductivity and effective porosity of the aquifer sediments and the gradient of the water table. In those areas where both Hanford formation and Ringold Formation occur in the unconfined aquifer, the hydraulic conductivity of the Hanford formation gravel-dominated facies (HSU 1) is generally a couple of orders of magnitude higher than the Ringold Formation unit E gravel-dominated facies (HSU 5) (
Figure 2-7), and several orders of magnitude higher than that of the RLM (HSU 8). Groundwater in the southern part of 200-BP-5 Groundwater OU flows south and then east around the HSU 8 low-permeability barrier as it moves toward the Columbia River.

The 200-BP-5 groundwater and concurrent contaminant plumes (Figure 2-13) have migrated toward the Columbia River in two general directions. The groundwater divide beneath the 200 East Area bifurcated contaminant plume movement either northwest through Gable Gap or southeast toward the Columbia River:

- Plumes in the northwestern portion of the 200 East Area generally moved northwest toward Gable Gap in the past, but now may be moving to the southeast

- Plumes further south in the 200 East Area moved southeast toward the Columbia River.

Figure 2-12. 200-BP-5 Operable Unit Pleistocene Paleo-Erosional Surface Topography.

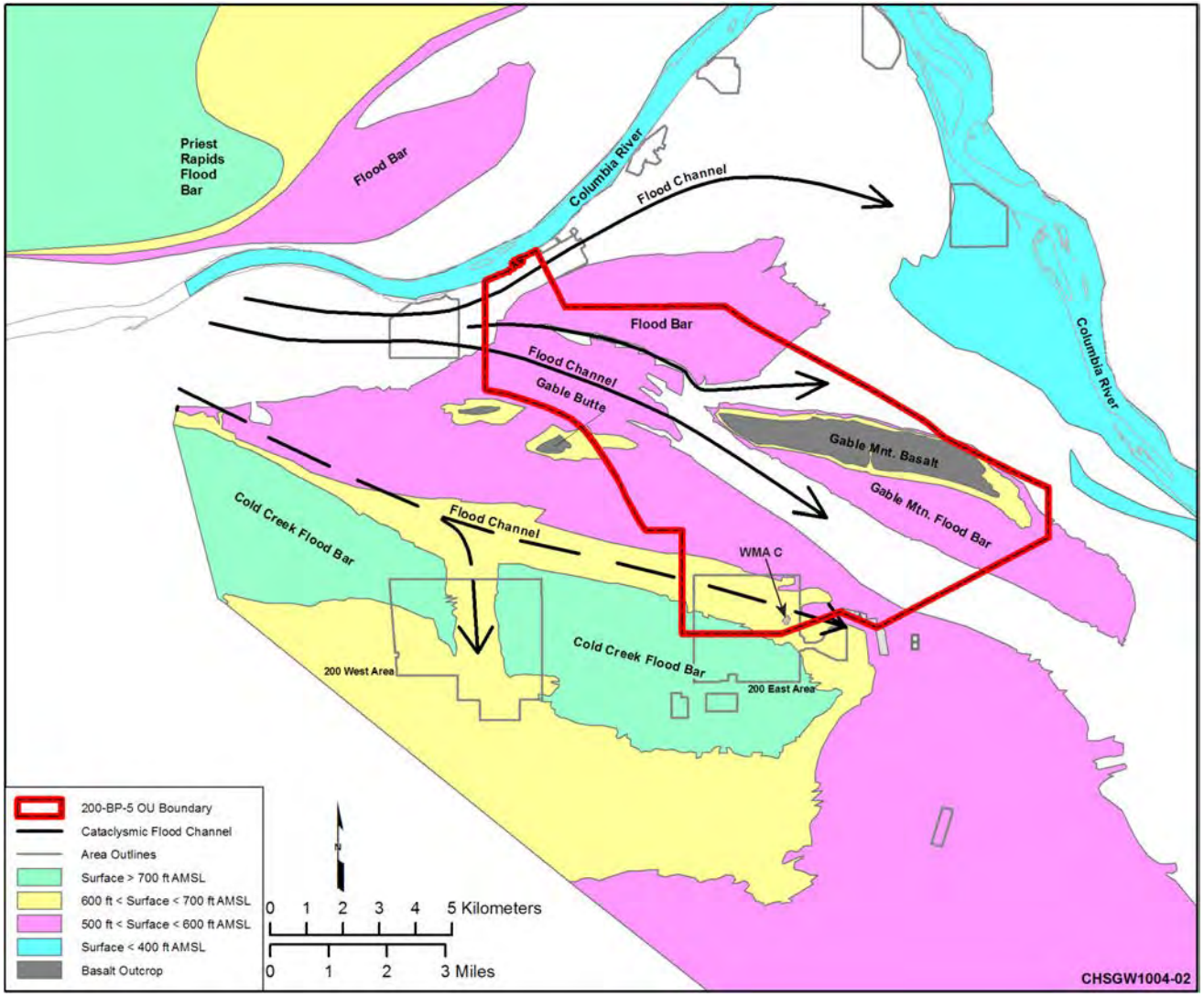

AMSL = above mean sea level OU = operable unit WMA = Waste Management Area

Reference: PNNL-12261, *Revised Hydrogeology for the Suprabasalt Aquifer System, 200-East Area and Vicinity, Hanford Site, Washington.*

Figure 2-13. Groundwater Contamination for 2013 which Originated within the Central Plateau along with Central Plateau Groundwater Interest Areas.

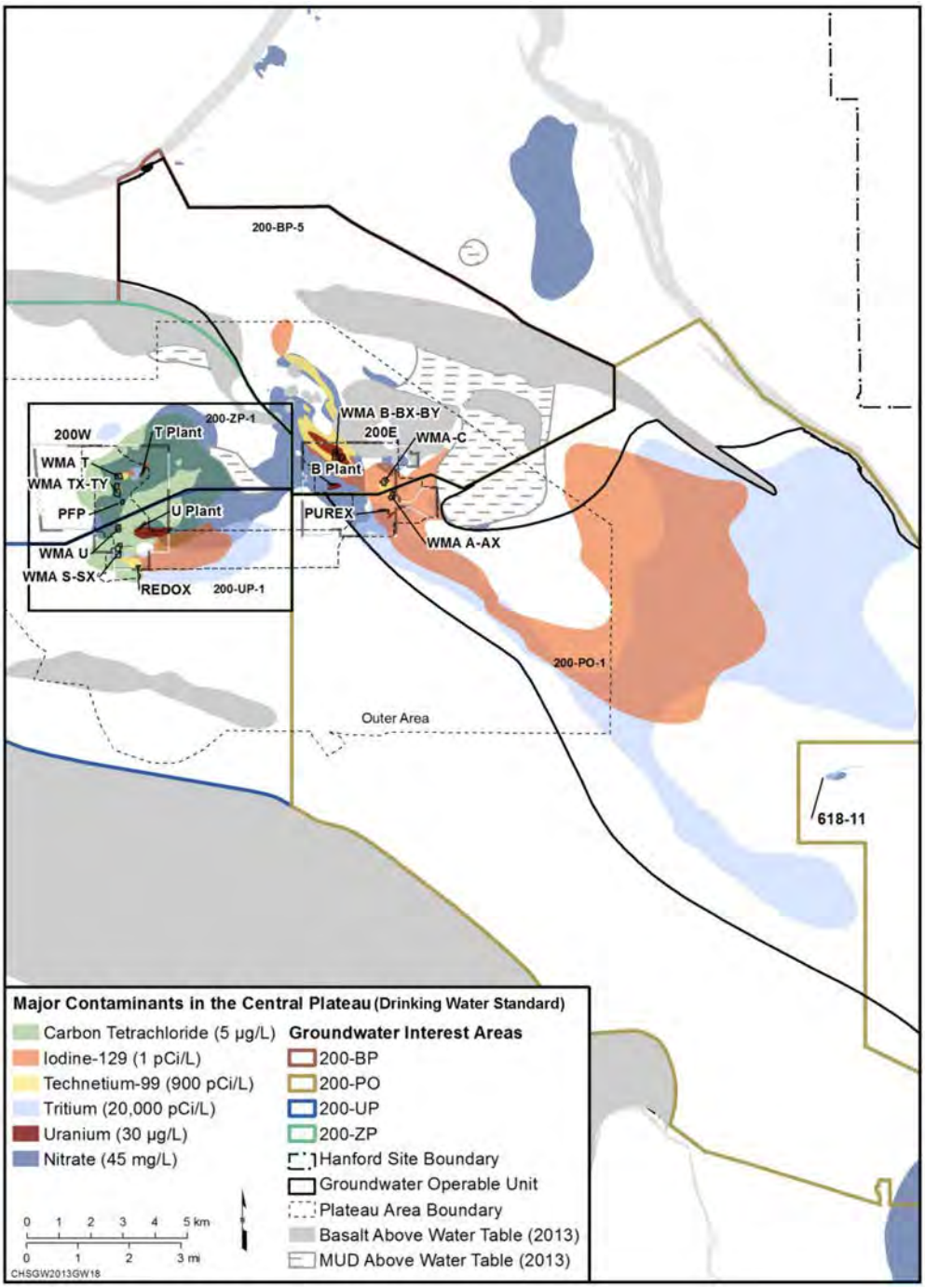

Reference: DOE/RL-2014-32, *Hanford Site Groundwater Monitoring Report for 2013*.
Additional Reference: See Figure 2.1-1 of the Hanford Site Groundwater Monitoring for FY 2005. https://www.pnnl.gov/main/publications/external/technical_reports/PNNL-15670.pdf

PFP = Plutonium Finishing Plant
PUREX = Plutonium Uranium Extraction (facility)
REDOX = Reduction-Oxidation (facility)
WMA = Waste Management Area

The geometries of most of the contaminant plumes were first established when gradients were steeper and more groundwater flow occurred to the northwest toward the Gable Gap. In 2007 and 2008, stage fluctuations on the Columbia River appeared to cause flow reversals within the unconfined aquifer beyond the Gable Gap. These temporary groundwater flow reversals, and the current nearly flat water table beneath the 200 East Area, strongly suggest that 200 East Area groundwater and contaminant plumes may move very slowly, stagnate or even reverse seasonally. The flat horizontal gradient measured in 2009 indicates a significant slowing or stalling of the movement of 200-BP-5 contaminant plumes compared to movement in the mid-1990s.

The velocity of groundwater is proportional to the horizontal gradient, and the decline in the horizontal gradients to nearly zero in the aquifer around WMA C indicates significantly lower groundwater velocities during recent years. After cessation of non-permitted liquid disposal to cribs, ponds, and ditches in the mid-1990s, the artificially elevated water table rapidly declined. The water table throughout most of the 200-BP-5 Groundwater OU continues to decline at present but shows indications of stabilization in recent years. The current horizontal gradient is so small that scientists can barely detect differences in groundwater elevation in the unconfined aquifer around WMA C. For example, the regional gradient to the southeast from the 200 East Area (across the 200-BP-5 and 200-PO-1 Groundwater OUs) has been estimated to be 1.8×10^{-5} m/m, which translates to a difference of less than 2 cm across a kilometer (DOE/RL-2008-66, *Hanford Site Groundwater Monitoring for Fiscal Year 2008*).

2.3 WASTE MANAGEMENT AREA C SITE CHARACTERIZATION

This section provides a brief summary of the characterization of the vadose zone and unconfined aquifer in and around WMA C, including contamination in both the vadose zone and unconfined aquifer. Since the late 1990s there has been an extensive effort to characterize the vadose zone and unconfined aquifer around WMA C. These efforts are described in numerous documents including, but not limited to, DOE/ORP-2008-01, *RCRA Facility Investigation Report for Hanford Single-Shell Tank Waste Management Areas*, Appendix L; DOE/RL-2014-32; GJO-98-39-TAR/GJO-HAN-18, *Hanford Tank Farms Vadose Zone: C Tank Farm Report*; GJO-98-39-TARA/GJO-HAN-18, *Hanford Tank Farms Vadose Zone: Addendum to the C Tank Farm Report*; RPP-PLAN-39114, *Phase 2 RCRA Facility Investigation/Corrective Measures Study Work Plan for Waste Management Area C*; RPP-RPT-56356, *Development of Alternative Digital Geologic Models of Waste Management Area C*; and RPP-RPT-58339. For more detailed information, please refer to the characterization documents.

The principal driver for site characterization at WMA C is a number of confirmed or suspected waste loss events which occurred in WMA C (labeled as UPRs in Figure 2-14) during its operational history. These included suspected tank leaks and known waste losses from waste transfer piping systems. The current understanding of contaminant occurrences and environmental conditions at WMA C is described in RPP-ENV-33418 and DOE/ORP-2008-01 and summarized in Section 2.1 of this document. The primary contamination zones currently identified in WMA C include a localized high ^{137}Cs activity zone near the bottom of the

southwest part of tank C-105 and three UPRs near waste transfer pipelines and diversion boxes in the southwest part of WMA C. Sampling at groundwater wells 299-E27-21 and 299-E27-23 along the southern boundary of WMA C (Figure 2-14) had results for ^{99}Tc at concentrations greater than 25 times the drinking water standard (DWS) of 900 pCi/L.

2.3.1 Geology of Waste Management Area C

The geology of WMA C is summarized from the information provided in DOE/ORP-2008-01; DOE/RL-2009-127 Draft A; RPP-RPT-46088, *Flow and Transport in the Natural System at Waste Management Area C*; and RPP-RPT-56356. A generalized fence diagram through WMAs A-AX and C is shown in Figure 2-15.

Six stratigraphic units lie within WMAs A-AX and C. From oldest to youngest, the primary geologic units are:

- Columbia River Basalt Group
- Undifferentiated Hanford lower gravelly sequence (H3 unit)/Cold Creek/Ringold formations
- Hanford formation – sand sequence (H2 unit)
- Hanford formation – upper gravelly sequence (H1 unit)
- Backfill
- Recent deposits.

The general characteristics of these units are described in more detail in RPP-RPT-46088 and RPP-RPT-56356. At WMA C, it is not possible to separate out the Ringold Formation, CCu and the lower gravely sequence of the Hanford formation (H3). In the vicinity of WMA C, this unit is referred to as undifferentiated H3, CCu and Ringold Formation ($H_3/CC_u/RF$) because of the scouring within the paleochannel underlying WMA C (Figure 2-12). The SSTs at WMA C were emplaced in an excavation of the Hanford formation sediments of the upper, gravel-dominated (H1) unit. This excavation may also locally intercept the upper portions of the sand-dominated Hanford (H2) unit. Once the tanks were built, the excavation was backfilled with reworked sediments of the upper, gravel-dominated (H1) unit. The water table or the unconfined aquifer's surface lies ~60 m (~200 ft) below the bottom of the tank farms excavations within the undifferentiated $H_3/CC_u/RF$.

The geologic strata underlying WMA C was characterized in conjunction with soil sampling and borehole logging for radionuclides and hazardous waste constituents as part of the Phase 1 and 2 RCRA Facility Investigations at WMA C. The borehole and geologic logging were used to identify the elevations of tops of the geologic units in the vicinity of WMA C. Specifically, potassium, uranium, thorium (K-U-T) data from geophysical logs were used to map the tops of

the different geologic units at WMA C (RPP-RPT-56356). Two alternative geologic models were developed based on these data.

Figure 2-14. Waste Management Area C Tanks, Infrastructure, and Associated Unplanned Releases[1].

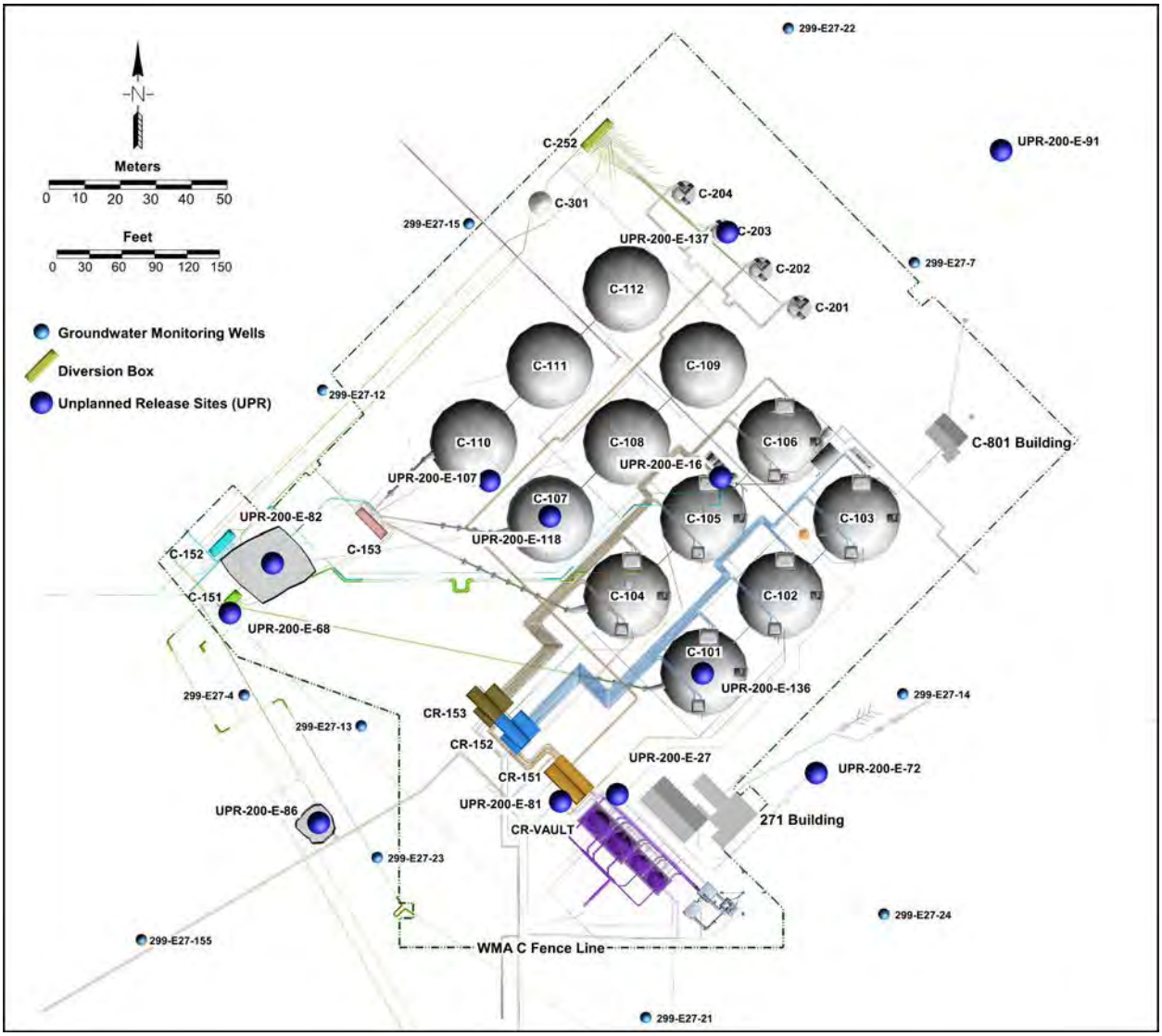

WMA = Waste Management Area

[1] Only thirteen of the sixteen unplanned releases are provided in this figure. UPRs not posted include UPR-200-E-99, UPR-200-E-100, and UPR-200-E-135. Brief descriptions of all sixteen unplanned releases are provided in Sections 2.1.8, 2.1.9, 2.110, and 2,1,13.

Figure 2-15. Fence Diagram Showing Cross-Sections through Waste Management Areas A-AX and C.

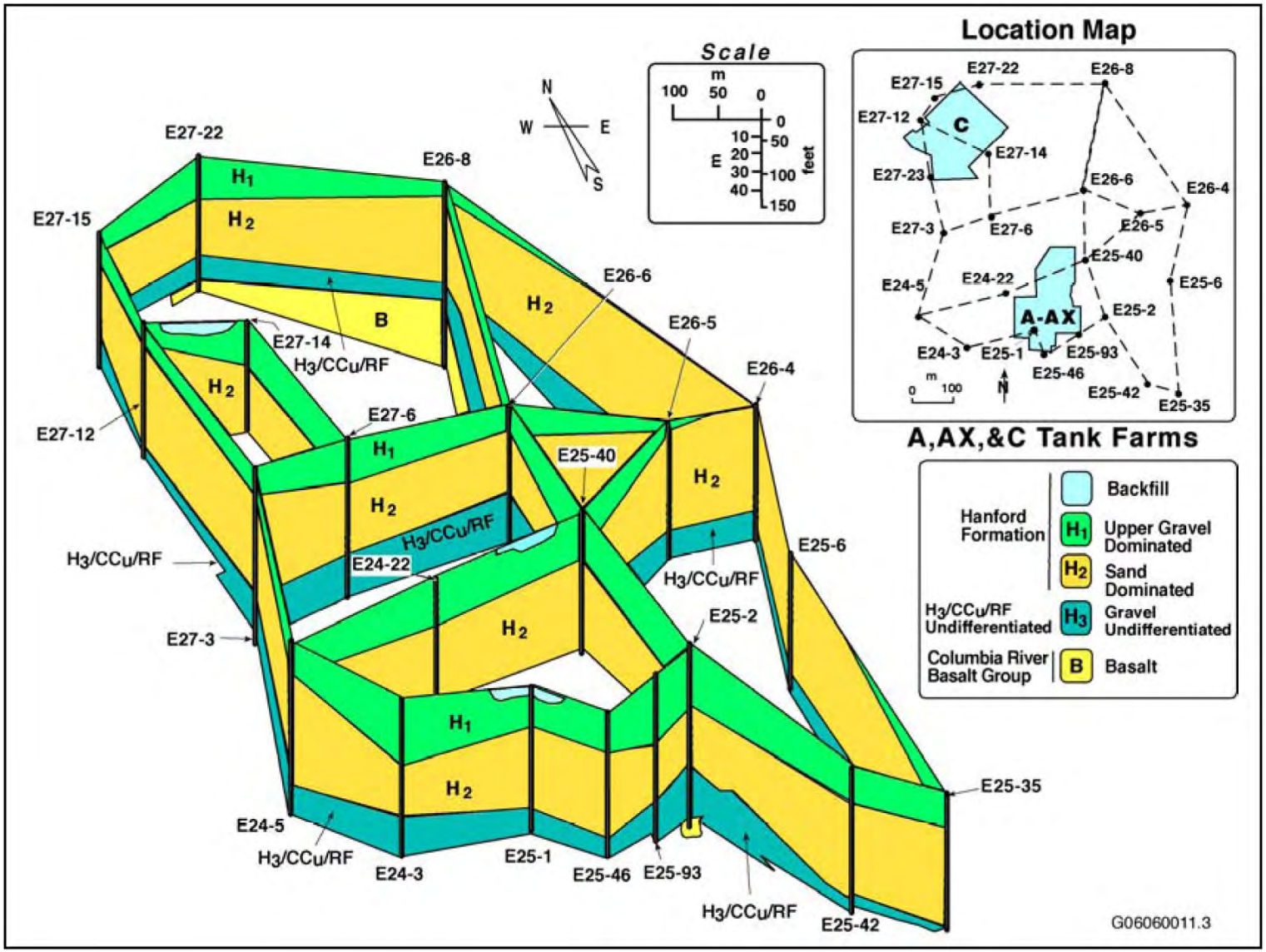

$H_3/CC_u/RF$ = undifferentiated Hanford Formation, Cold Creek unit and Ringold Formation

The major difference between these two alternative geologic models is whether or not a sandy gravel facies is to include a silt layer identified at the bottom of the H2 subunit in the vicinity of WMA C. The K-U-T data (i.e., a lower gross gamma and potassium count) indicates that there is a coarsening of the sand at the bottom of the H2 unit turning more into a sandy gravel. Underlying this sandy gravel facies is a silt unit with a strong potassium peak and occasional strong natural uranium peak. The difficulty in making this determination is that there are few direct pushes or drywells that are at a sufficient depth to obtain both good geophysical logs and geologic logs (with drill cuttings). The drill cuttings from some of the nearby groundwater wells indicated that there was definite fining of the sands along with some silt found at the vertical location as indicated by the K-U-T data in the geophysical logs, but a competent silt layer was not observed. Alternative Geologic Model I does not include the sandy gravel and underlying silt unit with the H2 unit, while Alternative Geologic Model II does include them. The existence of these layers could cause increased lateral movement in the vadose zone. A series of fence diagrams showing the differences between the two models within WMA C is given in RPP-RPT-56356. The fence diagram for both these models running southwest to northeast through the center of WMA C is given in Figure 2-16.

Additional conceptual models are being developed with detailed heterogeneous representations of the geologic framework at WMA C. One is a facies-based model based primarily on a geostatistical analysis of the K-U-T data collected in selected direct push boreholes within WMA C; the other is based on geostatistical evaluations of volumetric moisture content measured in multiple direct push boreholes and drywells within WMA C. The work that was done by PNNL on alternative conceptual models of heterogeneity with some intercomparison of selected modeling simulation results taken from the PA effort has been documented in PNNL-24740.

2.3.2 Vadose Zone Characterization at Waste Management Area C

Since the late 1990s, there have been the following three major campaigns to characterize the vadose zone at WMA C:

1) Log the existing drywells around each of the 100-series SSTs to provide baseline characterization, which took place in the late 1990s

2) Phase 1 RCRA Facility Investigation, which took soil samples close to the high ^{137}Cs activity found near SST 241-C-105 and to probe underneath the gunite cap at UPR-200-E-82 where a pipeline failure lead to the loss of PSN waste (4.3 Ci/gal of ^{137}Cs)

3) Phase 2 RCRA Facility Investigation, in which site characterization data was collected at the 23 sites across the farm.

The results of these characterization efforts are summarized in the following sections.

2.3.2.1 Drywell Monitoring at Waste Management Area C. Waste Management Area C has 70 drywell monitoring boreholes (see Figure 2-17) available for leak detection monitoring and to provide access for limited vadose zone characterization (e.g., geophysical logging). These drywells were drilled from 1944 to 1982. In 1997, C Farm drywells were logged using a high-resolution spectral gamma logging system. This effort was part of the baseline characterization for WMA C. Results are documented in GJO-98-39-TAR/GJO-HAN-18 and its associated addendum GJO-98-39-TARA/GJO-HAN-18. The depth ranges for most of these drywells is between 30.5 and 45.7 m bgs (100 and 150 ft bgs). The deepest drywell in WMA C is 47.2 m bgs (155 ft bgs) (30-00-03), and the maximum logged depth is 43.6 m bgs (143 ft bgs) (30-04-08).

The major gamma-emitting contaminants associated with WMA C are ^{137}Cs and ^{60}Co with lesser amounts of ^{154}Eu. These contaminants are located mostly in and around areas of confirmed or suspected tank and pipeline leaks. Although most of the drywells are deeper than the surrounding contamination, some zones of contamination extend deeper than nearby drywells. Consequently, the depth of vadose zone contamination is not known in some areas of WMA C.

Figure 2-18 provides a visualization of the vadose zone contamination beneath WMA C as represented by Cs-137 data and the ^{99}Tc at borehole C4297. This figure is a three-dimensional (3-D) perspective of WMA C providing locations of tanks and associated drywells. Tanks are considered to be leakers based on information in HNF-EP-0182, *Waste Tank Summary Report for Month Ending February 28, 2015*, Rev. 326. For ^{137}Cs, each drywell is represented with a single vertical line. Shaded rings around the drywells indicate the level of vadose zone contamination based on spectral gamma logging results. Only the more significant soil contamination zones (i.e., ^{137}Cs contamination levels greater than 10 pCi/g) are shown.

Spectral gamma logging data provided in Figure 2-18 indicate the presence of contamination in the region between tanks C-104 and C-105. The most concentrated contamination occurs at drywell 30-05-07 on the southwest side of tank C-105 (Figure 2-18), where two high ^{137}Cs concentration zones occur at and below the tank bottom (DOE/ORP-2008-01).

Figure 2-16. Fence Diagram of Alternative Geologic Models for Waste Management Area C.

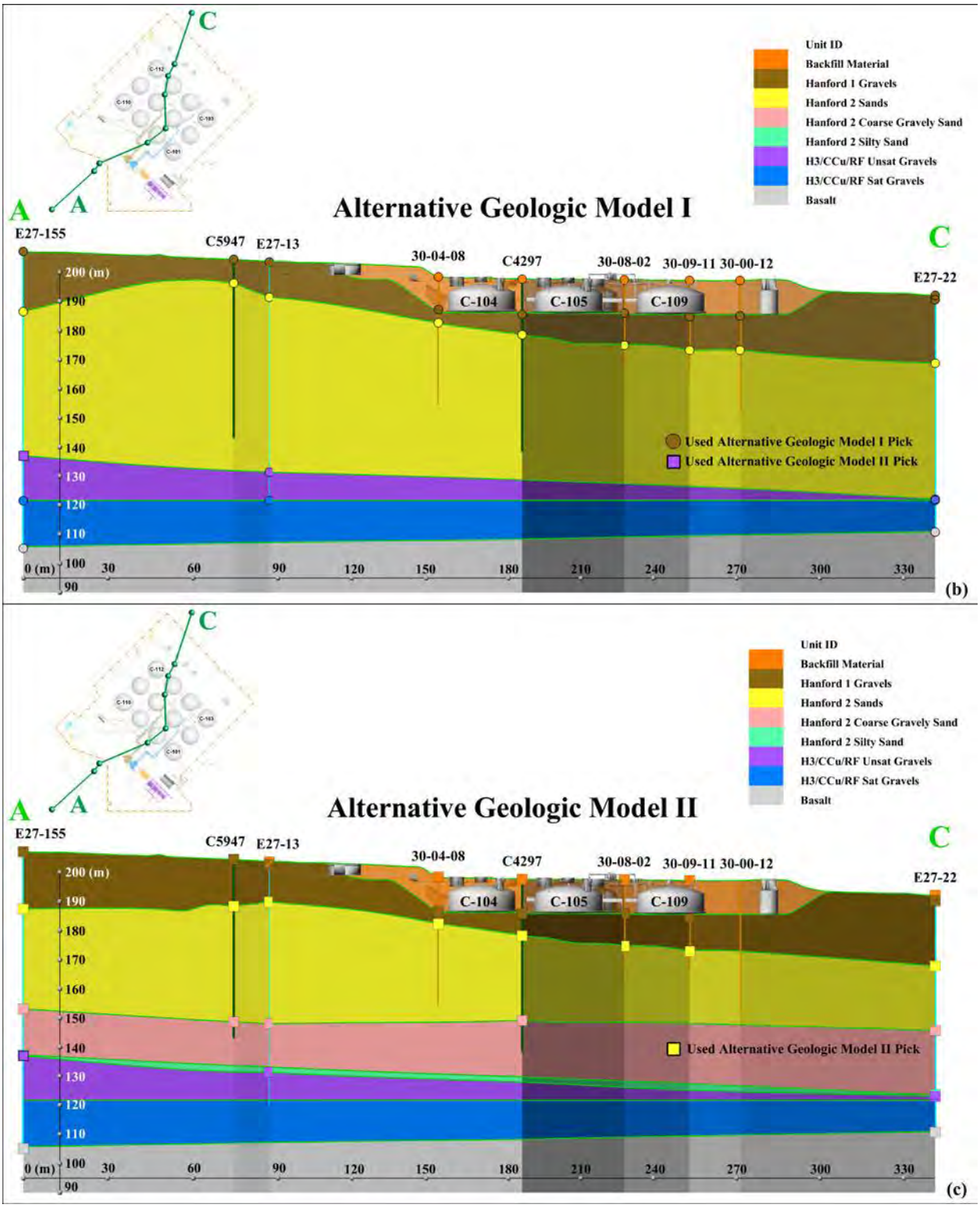

H3/CCu/RF = undifferentiated Hanford Formation, Cold Creek unit and Ringold Formation

Figure 2-17. Vadose Zone and Groundwater Monitoring Network for Waste Management Area C.

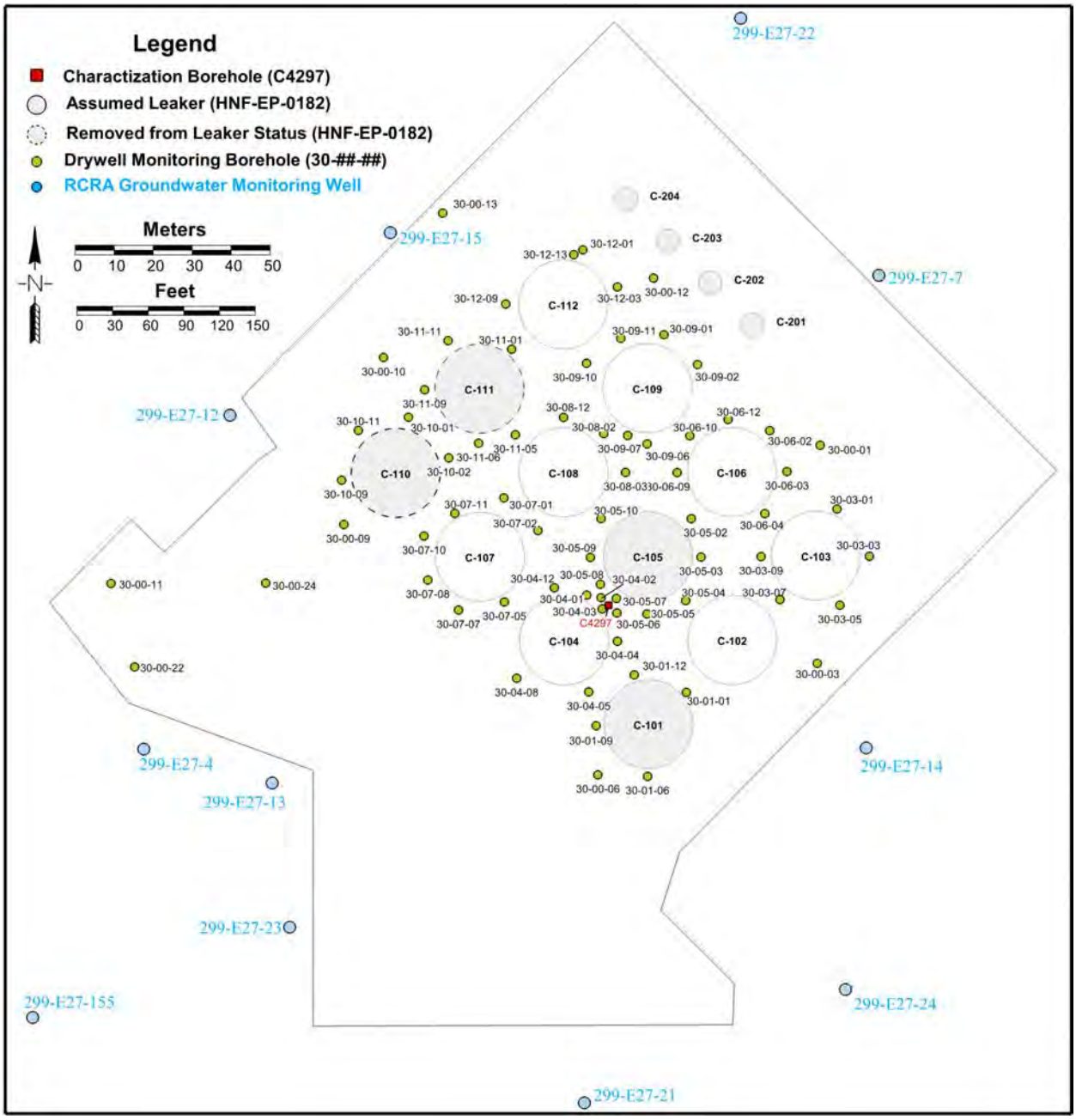

Reference: HNF-EP-0182, "Waste Tank Summary Report for Month Ending September 30, 2013," Rev. 306.

RCRA = Resource Conservation and Recovery Act of 1976

2.3.2.2 Phase 1 RCRA Facility Investigation Characterization Activities and Results. In 2004, vadose characterization activities were conducted at WMA C in support of the RCRA corrective action. The first phase concentrated on characterizing an area of high Cs-137 concentrations observed in drywells at the depth of the base of tank C-105 below the cascade line

running between tanks C-104 and C-105 and the pipeline leak known as UPR-200-E-82 close to the 241-C-152 diversion box. The characterization borehole drilled next to tank C-105 was the deepest characterization within WMA C at 59.9 m (196.5 ft) bgs at the time. Results from soil sampling show the greatest concentration of ^{99}Tc (8.4 pCi/g) and nitrate (20 µg/g) at 41.1 to 47.2 m bgs (135 to 155 ft bgs). Also shown on Figure 2-18 are sample locations showing where the more mobile ^{99}Tc was found in characterization borehole C4297.

Slant direct pushes underneath the gunite cap at UPR-200-E-82 found ^{99}Tc (28.6 pCi/g) and nitrate (19.7 µg/g) centered below the pipeline leak at 23.5 m bgs (77 ft bgs). Complete results of the first phase of characterization are documented in DOE/ORP-2008-01 Appendix L and in RPP-35484, *Field Investigation Report for Waste Management Areas C and A-AX*.

2.3.2.3 Phase 2 RCRA Facility Investigation Characterization Activities. The second phase started in 2008 and characterization data was collected per the work plan (RPP-PLAN-39114). For Phase 2, site characterization data was collected at the 23 sites identified in Figure 2-19. Each characterization site was given a letter map designation. The site characterization activities for Phase 2 included the following:

- Soil collection and analysis through direct push boreholes technology
- Geophysical logging at drywell boreholes and groundwater monitoring wells
- Surface Geophysical Exploration
- Tissue sampling for ecological risk assessment
- Possible sampling of vadose zone during the installation of any new groundwater wells within ~30 m (~100 ft) of WMA C.

RPP-PLAN-39114 provides a complete description of what was to be collected at each of these sites. During the preparation of the work plan for the Phase 2 characterization, a transitional characterization (Phase 1.5) effort was undertaken and vadose zone characterization took place at two past UPR sites (UPR-200-E-81 and UPR-200-E-86) (Figure 2-20). This transitional characterization effort was called “near-term characterization” and focused on the deployment of hydraulically-driven direct push technology to push boreholes (i.e., Phase 1.5) for geophysical logging, placement of deep electrodes, and to collect soil samples. The results of both the transitional characterization and the Phase 2 vadose zone characterization efforts are given in RPP-RPT-58339 and are summarized in the following section.

2.3.2.4 Overview of Characterization Results from RCRA Facility Investigations. As a part of the Phase 2 RCRA Facility Investigation (RFI)/Corrective Measures Study (CMS), a significant amount of work has been performed to characterize contamination in the vadose zone within and around WMA C. The area shows evidence of widespread shallow and deep contamination and a discontinuity between soil constituents and groundwater contamination, and

there continues to be a limited understanding of the linkage between sources and contaminants at WMA C. In general, contamination has been found from the surface to depths of ~73 m (~240 ft) bgs. It is difficult to make specific correlations because the various waste releases have occurred in near proximity and in an area of up to 7 hectares (16 acres).

Several observations could be made from the Phase 2 RFI characterization efforts. For instance, gamma logging showed higher gamma spectra near the soil surface and near locations of suspected waste losses, confirming that waste had entered the soil and that many gamma-emitting radionuclides did not show significant mobility. Moisture logging showed layers of higher moisture interspersed with lower moisture. These observations were consistent with expectation of high moisture content with finer grain size. Although the Surface Geophysical Exploration (SGE) campaign did not determine conclusively whether individual 200-series tanks leaked, it did identify that soil anomalies in the area suggested the possible presence of elevated moisture and/or possible contamination (e.g., UPR-200-E-81).

It should be noted that the placement of all the characterization boreholes was limited because of the tanks, ancillary equipment, and complex infrastructure located at the tank farm. Most direct push boreholes are vertical however, a number of angled direct push boreholes were placed in the vicinity of UPR-82 and Sites A, B, and J. Very few data have been collected directly below the tanks.

As identified, Phase 2 sampling efforts did not represent a random statistical sampling scheme at WMA C. The Phase 2 investigation targeted locations where contamination was expected to be found based on historic records of waste losses. Table 2-4 provides an overview of the areas investigated at WMA C.

For the most part, sampling did not show high concentrations of mobile constituents in any specific depth range. The following observations should be noted.

- Many sampling locations showed concentrations of mobile constituents somewhat above background (37 out of 45 constituents), suggesting for the most part that mobile constituents had migrated through the region, to greater depths.

- Increased concentrations of some mobile contaminants above background were found in samples from all depths.

- As the Phase 2 RFI characterization was proceeding, the groundwater monitoring program was finding additional evidence that waste from the WMA C facilities had reached groundwater (see Section 2 of RPP-RPT-58339).

- Information collected in and near other tank farms suggested that geologic layers in the soil have the potential to provide lateral movement of water and mobile contaminants.

Figure 2-18. Three-Dimensional Perspective of Waste Management Area C Tanks and Drywells Showing Occurrence of Significant (>10 pCi/g) Cesium-137 Contamination in the Vadose Zone along with Technetium-99 at Borehole C4297.

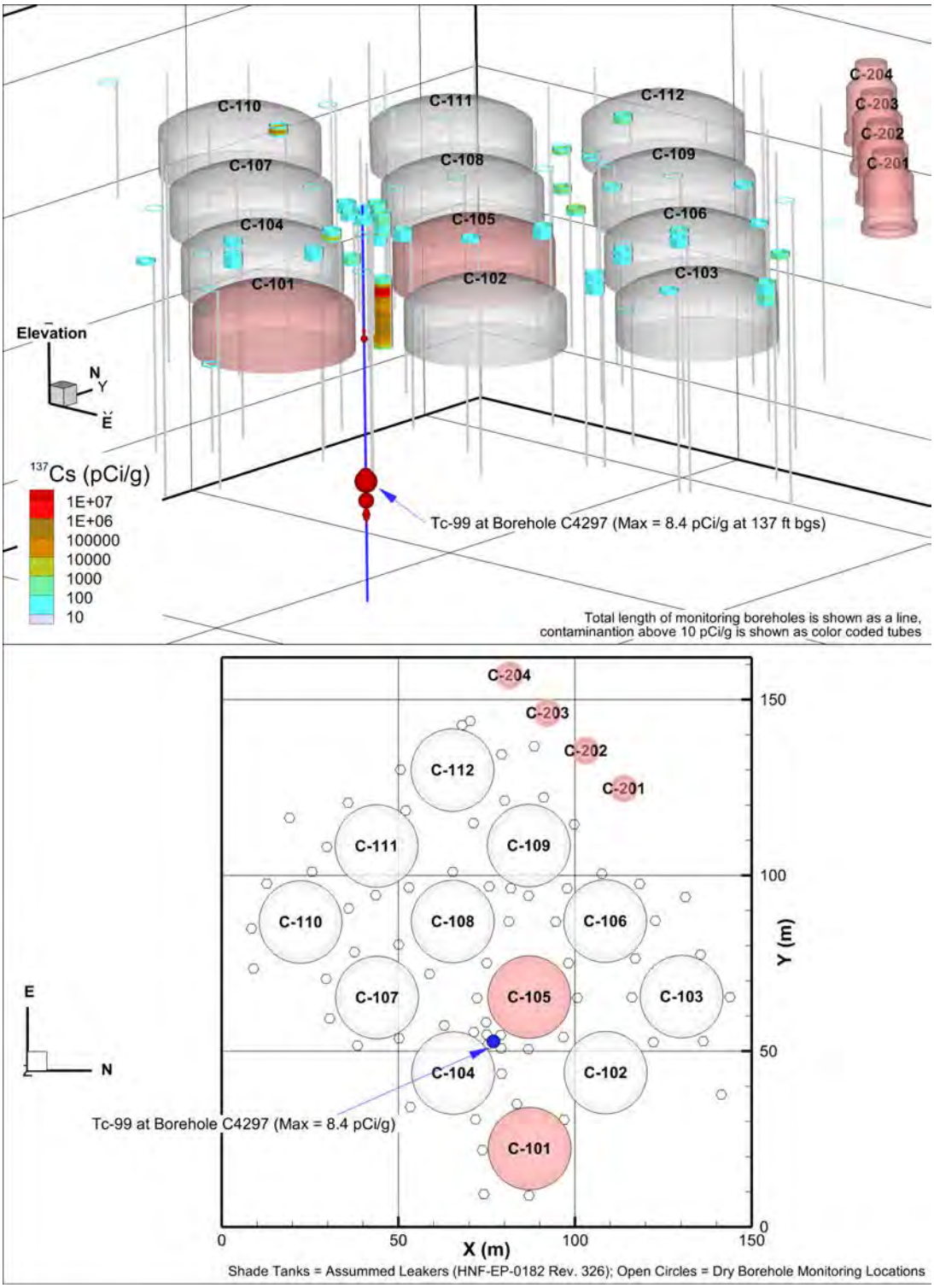

Reference: HNF-EP-0182, "Waste Tank Summary Report for Month Ending February 28, 2015," Rev. 326.

Figure 2-19. Completed Phase 2 RCRA Facility Investigation Characterization Locations.

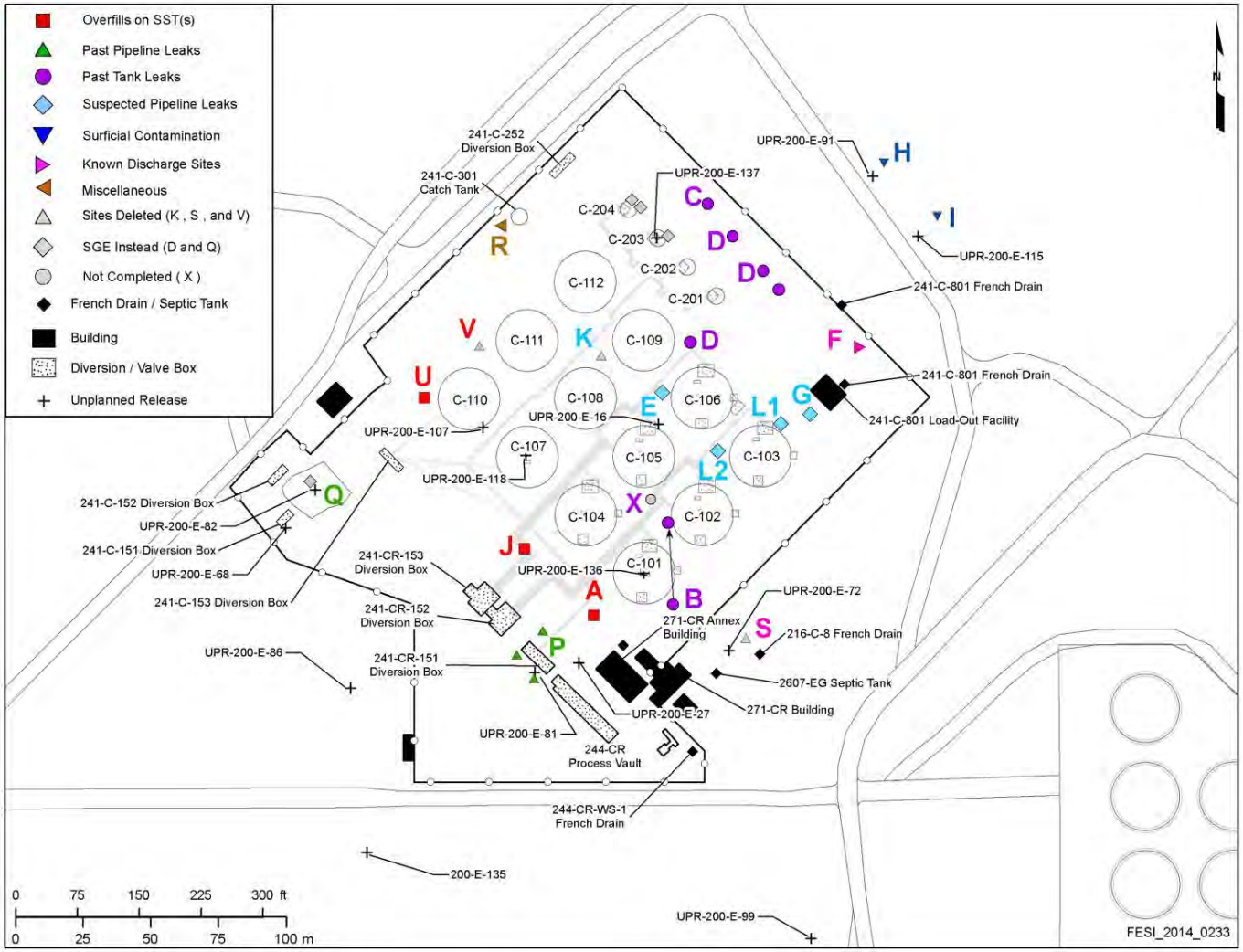

RCRA = Resource Conservation and Recovery Act of 1976 SGE = Surface Geophysical Exploration WMA = Waste Management Area

Reference: HNF-EP-0182, "Waste Tank Summary Report for Month Ending July 31, 2014," Rev. 319

Figure 2-20. Completed Transitional (Phase 1.5) Characterization Locations.

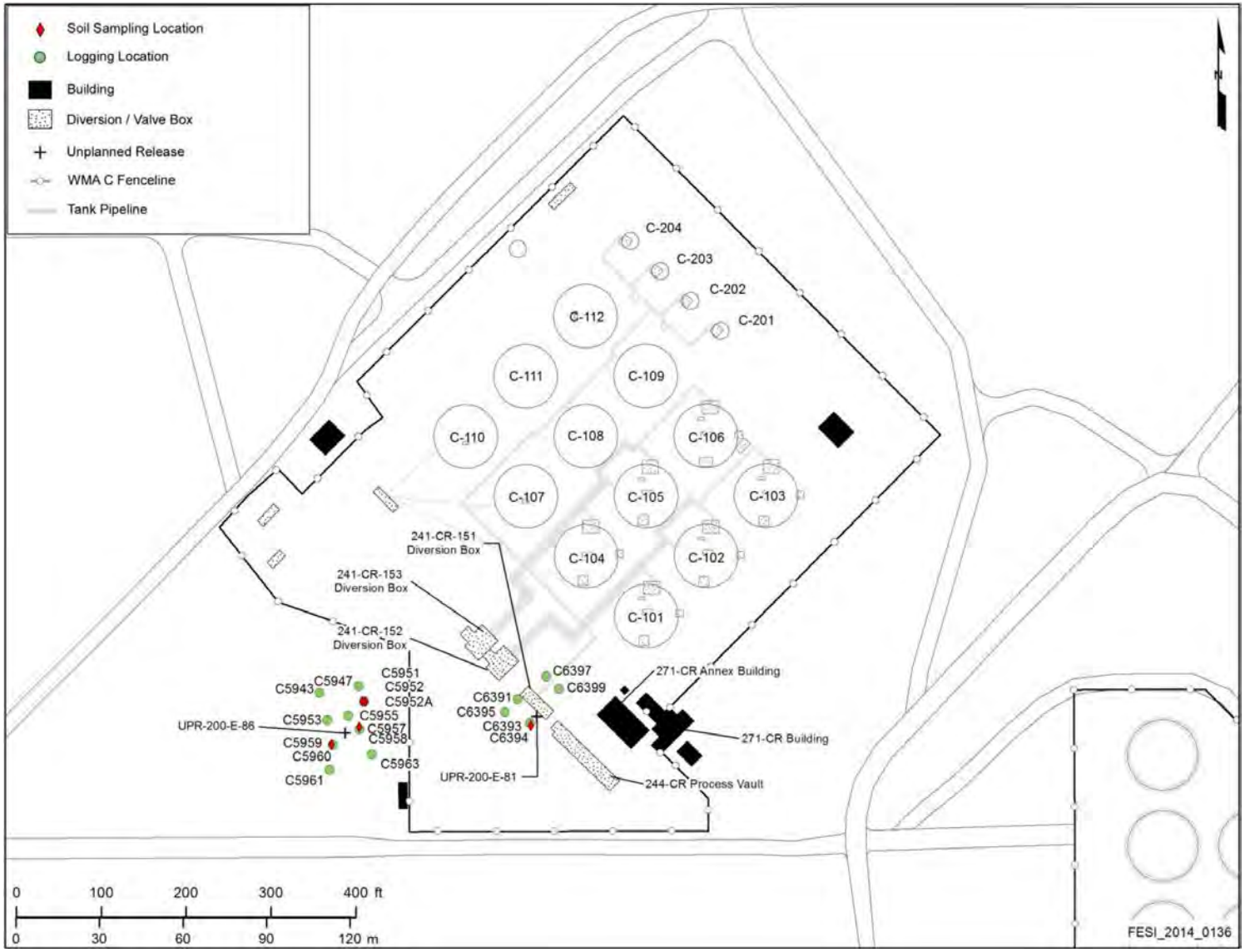

WMA = Waste Management Area

Table 2-4. Summary of Field Efforts Related to Areas Investigated in Waste Management Area C RCRA Facility Investigation. (2 sheets)

Area Investigated	Field Efforts[1]
Tank 241-C-101	• Group A + B Direct Push Logging • Group A + B Analytical • Drywell Logging (30-01-01, 30-01-01, 30-01-06, and 30-01-09) • Site O Surface Geophysical Exploration
Area between Tanks 241-C-103 (C-103) and 241-C-106 (C-106)	• Group L1 + L2 Direct Push Logging • Group L1 + L2 Analytical • Drywell Logging (30-00-01, 30-03-01, 30-03-03, 30-03-05, 30-03-07, 30-03-09, 30-06-02, 30-06-03, 30-06-04, 30-06-09, 30-06-10, and 30-06-12) • Site O Surface Geophysical Exploration
Tank C-103 and Building C-801 and the building's chemical drain	• Group F + G Direct Push Logging • Group F + G Analytical • Drywells Logging (30-03-01, 30-03-03, 30-03-05, 30-03-07, and 30-03-09) • Site O Surface Geophysical Exploration
Tank 241-C-104	• Site J Direct Push Logging • Site J Analytical • Site M Drywell Logging (30-04-01, 30-04-02, 30-04-03, 30-04-04, 30-04-05, 30-04-08, 30-04-12, and 30-05-06) • Site O Surface Geophysical Exploration
Tank 241-C-105	• C4297 Analytical and Logging • C7469 Direct Push Logging • Drywell Logging (30-05-02, 30-05-07, and 30-05-08)
Area between Tanks C-106 and 241-C-109	• Site E Direct Push Logging • Site E Analytical • Site M Drywell Logging (30-00-01, 30-06-02, 30-06-03, 30-06-04, 30-06-09, 30-06-10, 30-06-12, 30-09-01 ,30-09-02, 30-09-06, 30-09-10, and 30-09-11) • Site O Surface Geophysical Exploration
Tank 241-C-108	• Drywell Logging (30-05-10, 30-07-01, 30-07-02, 30-08-02, 30-08-03, 30-08-12, and 30-09-07)
Tank 241-C-110	• Site U Direct Push Logging • Site U Analytical • Site M Drywell Logging (30-00-09, 30-10-01, 30-10-02, 30-10-09, and 30-10-11) • Site O Surface Geophysical Exploration
Tank 241-C-111	• Drywell Logging (30-11-01, 30-11-05, 30-11-06, 30-11-09, and 30-11-11)
Tank 241-C-112	• Drywell Logging (30-00-12, 30-12-01, 30-12-03, 30-12-09, and 30-12-13)
C-200s tanks	• Group C + D Direct Push Logging • Site C Analytical • Group C + D Surface Geophysical Exploration
UPR-81	• Phase 1.5 and Phase 2 Site P Direct Push Logging • Phase 1.5 and Phase 2 Site P Analytical • Site N Surface Geophysical Exploration

Table 2-4. Summary of Field Efforts Related to Areas Investigated in Waste Management Area C RCRA Facility Investigation. (2 sheets)

Area Investigated	Field Efforts[1]
UPR-82	• Pre-RFI Analytical Locations 5 and 10 identified in ARH-1945[2] • Phase 1 Direct Push Logging • Phase 1 Analytical • Site Q Direct Push Logging • Site N Surface Geophysical Exploration
UPR-86	• Phase 1.5 Direct Push Logging • Phase 1.5 Analytical • 299-E27-20 (Site Z) Analytical • Site N Surface Geophysical Exploration
URP-91 and URP-115	• Group H + I Direct Push Logging • Group H + I Analytical • Site O Surface Geophysical Exploration
Area near C-301 catch tank	• Site R Direct Push Logging • Site R Analytical • Site O Surface Geophysical Exploration

[1] Investigation groups and sites and associated direct push borehole locations are provided in Figure 2-19. Approximately 70 drywells were logged in Waste Management Area C, not all are listed in this table. Location of these drywells are provided in Figure 2-17.

[2] ARH-1945, *B Plant Ion Exchange Feed Leak*, summarizes the results of a historical investigation performed at UPR-200-E-82-27 in the early1970s to evaluate an unplanned release of liquid waste containing ^{137}Cs.

RCRA = Resource Conservation and Recovery Act of 1976

While push hole logging was conducted at several UPR sites, it is worthy to note that the equipment is limited to radioactive levels below a certain activity for safety precautions. Thus, the “hottest” zones may not have been sampled at a few locations. However, decisions on sampling due to high levels of radiation was not a pervasive problem in the Phase 2 characterization efforts. Changes to original planned borehole locations due to high radiation levels occurred in only two instances. Decisions to not pursue the planned direct push borehole Q through the gunite cap at UPR-82 during the Phase 2 characteristic work plan was directly influenced by the knowledge of likely occurrence of high radiation under the gunite at this past release site. Although a vertical push through the gunite cap had been proposed, it was not implemented due the need to implement radiological control requirements to facilitate the sampling. Instead, four direct push holes were placed to a depth of 61 m (200 ft), one on each side of the unplanned release, and multi-depth electrodes were placed. The basis for this decision is provided in RPP PLAN 39114.

Results of the Phase 2 investigation confirm the expectation that a number of immobile waste constituents remain near sources of waste releases. Mobile constituents have moved into the vadose zone to varying depths as a result of the waste release and geochemical processes. In addition to vertical movement of the contamination, lateral migration is also suspected.

Although there may be a preferential direction in some parts of the tank farm, spreading in other directions due to smaller lenses of less permeable soil cannot be ruled out.

With respect to data gaps, only Site X could not be accessed during the field investigation. Specifically, Site X, which was to be located near tank C-105, was added to Revision 2 of the work plan to better define the area of contamination associated with a historic waste loss from tank C-105. The goal of the investigation was to gain information about a contamination under the tank, which was thought to be accomplished with an angled direct push under the tank. However, based on the available information already collected from WMA C, it is not certain if this additional field information is needed, or if it will be of value. The area continues to be difficult to access and it is thought that model analysis of past leaks may provide any additional information, if needed. Therefore, no further field characterization is recommended at this site.

Additionally, as identified, direct pushes at Site R were completed to assess a potential waste release from the catch tank. Characterization data obtained through the field effort yielded less than expected contamination levels (i.e., minimal soil background exceedances). It is understood that additional information may be required to make retrieval and closure decisions for C-301 catch tank, beyond the scope of the characterization covered in the Phase 2 RFI; however, it is believed that no further soil characterization around the C-301 catch tank is needed.

2.3.2.5 General Observations of Phase 1 and 2 Vadose Zone Characterization Results for Selected Contaminants of Potential Concern. Following is a summary of general observations of selected constituents of potential concern (COPCs) in different investigation areas at WMA C. The selected COPCs represent three classes of constituent mobility:

- Mobile constituents (K_d = 0 mL/g which include ^{99}Tc, nitrate, sulfate, and chromium)
- Slightly sorbed constituents (K_ds between 0.2 to 0.6 mL/g including ^{129}I, ^{60}Co, and uranium)
- Sorbed constituents (K_ds > 0.6 mL/g including ^{137}Cs, ^{90}Sr, and tributyl phosphate).

2.3.2.5.1 Mobile Constituents (K_d = 0 mL/g).

Technetium-99: In the Phase 2 RFI/CMS investigation, ^{99}Tc was detected in 16 samples from six Investigation Sites/Groups. The maximum reported value was a non-detect result of 76 [BYUJ][2] pCi/g from Investigation Group L1+L2 at a depth of 35 m (115 ft) bgs (deep); however, the highest detected value was 53.5 [Y] pCi/g from Site U at a depth of 39 m (129 ft) bgs (deep).

Technetium-99 was detected in Phase 2 WMA C shallow and deep soil samples as follows.

[2] Flag(s) for laboratory qualifier on the results will be enclosed in []; please see Table 2-5 and HNF-38155, "HEIS Sample, Result, and Sampling Site Data Dictionary" for meaning on the laboratory qualifiers.

- Shallow (≤ 5 m [15 ft] bgs) depths only: none.

- Deep (>5 m [15 ft] bgs) depths only: Investigation Groups A+B, F+G, L1+L2 and Sites R and U.

- Both shallow (≤ 5 m [15 ft] bgs) and deep (> 5 m [15 ft] bgs) depths: Investigation Group P.

Technetium-99 was below detection at all other Investigation Sites/Groups and depths. At borehole C4297 (Phase 1 Characterization), ^{99}Tc was reported for 98 of 110 soil samples analyzed for radionuclides. All detectable results for ^{99}Tc were found at depths below 5 m (17 ft) bgs. Concentrations ranged from -8.48 pCi/g to 8.42 pCi/g, with the maximum concentration occurring at depth of 41.68 m (136.75 ft) bgs. Enriched or elevated concentrations of ^{99}Tc were found at depths between 12.4 and 20.9 m (40.8 and 66.2 ft) bgs and between 40.77 and 49 m (133.75 and 159 ft) bgs. At depths between 12.4 and 20.2 m (40.8 and 66.2 ft) bgs, ^{99}Tc was coincident with elevated concentrations of ^{238}U and ^{60}Co. Co-occurrence of maximum concentrations of ^{99}Tc and nitrate were observed between 41 and 46 m (135 and 150 ft) bgs.

Table 2-5. Hanford Environmental Information System Laboratory Qualifier Table. (2 sheets)

A laboratory-generated character string containing codes in combinations that qualify the associated result. Different forms have different permitted combinations of valid qualifiers; however, B and U are mutually exclusive qualifiers on all forms. The valid qualifier codes and their translations are as follows.	
CODE	TRANSLATION
*	INORGANICS – Duplicate analysis not within control limits.
+	INORGANICS – Correlation coefficient for Method of Standard Additions is < 0.995.
>	WETCHEM – Result greater than quantifiable range or greater than upper limit of the analysis range.
A	ORGANICS – Valid for tentatively identified compounds (TICs) only: The TIC is a suspected aldol-condensation product.
B	INORGANICS and WETCHEM – The analyte was detected at a value less than the contract required detection limit, but greater than or equal to the instrument detection limit (IDL)/minimum detection limit (MDL) (as appropriate). ORGANICS – The analyte was detected in both the associated quality control (QC) blank and in the sample. RATIONUCLIDES (HEISPROD/PNLGW) – The associated QC sample blank has a result >= 2X the minimum detectable activity (MDA) and, after corrections, result is >= MDA for this sample. Surface Environmental Surveillance Project (SESP) – The associated QC sample blank has a result >= MDA and, after corrections, result is >= MDA for this sample.
C	INORGANICS/WETCHEM: The analyte was detected in both the sample and the associated QC blank, and the sample concentration was <= 5X the blank concentration. ORGANICS (PESTICIDE only) – The identification of a pesticide confirmed by gas chromatograph/mass spectrometer (GC/MS).
D	ORGANICS/WETCHEM – Analyte was identified in an analysis at a secondary dilution factor (i.e., dilution factor different than 1.0).
E	INORGANICS – Reported value is estimated because of interference. See comment on cover page,

Table 2-5. Hanford Environmental Information System Laboratory Qualifier Table. (2 sheets)

	hardcopy case narrative, or specific FORM I. ORGANICS – Concentration exceeds the calibration range of the GC/MS. Not applicable for PESTICIDES/PCBs.
J	ALL – The reported value is an estimate. Analyte was analyzed for and detected, but has potentially larger associated error factors in the result. If this qualifier is applied for any reason other than results reported close to the analytical detection limit, an explanation must be provided in the associated hardcopy Sample Data Summary Package and/or case narrative.
L	MDL <= value < contract required quantitation limit (CRQL) [RETIRED]
M	INORGANICS – Duplicate precision criteria not met.
N	ALL (except GC/MS based analysis) – Spike sample recovery is outside control limits. ORGANICS (GC/MS only) – Presumptive evidence of compound based on mass spectral library search.
P	ORGANICS (PCB only) – Aroclor target analyte with greater than 25% difference between column analyses.
Q	ORGANICS (Dioxins only) – Estimated maximum concentration. Used if one of the qualitative identification criteria is not met (e.g., Cl isotopic rations outside theoretical range.)
S	INORGANICS – Reported value determined by the Method of Standard Additions.
CODE	TRANSLATION
U	ALL – Analyzed for but not detected above limiting criteria. NOTE: Limiting criteria may be any of the following: value reported < 0; value reported < counting error; value reported < total analytical error; value_rptd <=contract MDL/IDL/MDA/practical quantitation limit (PQL).
W	INORGANICS – Post-digestion spike recovery for graphite furnace atomic absorption (GFAA) out of control limit. Sample absorbency < 50% of spike absorbency.
X	ALL – Other specific flags and notes required to properly qualify the result are described in the hardcopy Sample Data Summary Package and/or Case narrative. Additional information may be found in the RESULT_COMMENT field for this record.
Y	Same as X if more than one flag is required.
Z	Same as X and Y if more than two flags are required.
NOTE: If no qualifier code is reported with the analytical result, then the value reported is believed to be reliable without qualification.	
This Field is in the RESULT Table	

Nitrate: In the Phase 2 RFI/CMS investigation, nitrate was reported above background in eight samples at WMA C. The maximum concentration (198,000 µg/kg) was reported at Investigation Area Group F+G at a depth of 38 m (126 ft) bgs.

The distribution of concentrations above background for shallow and deep soils is as follows.

- Shallow (≤ 5 m [15 ft] bgs) depths only: Investigation Group H+I.

- Deep (>5 m [15 ft] bgs) depths only: Investigation Groups A+B, F+G, L1+L2, P, and Site U.

- Both shallow (≤ 5 m [15 ft] bgs) and deep (> 5 m [15 ft] bgs) depths: none.

Nitrate results for all other locations were less than background or were below detection. At borehole C-4297 (Phase 1 Characterization), nitrate was detected in 51 of 72 soil samples with concentrations ranging from below detection to 19.5 µg/g (RPP-35484). The greatest number of nitrate detections were reported at depths below 18 m (60 ft) bgs. Only one of the 51 detected concentrations of nitrate (0.52 µg/g) was reported in shallow (≤5 m [15 ft] bgs) soil samples. The maximum nitrate concentration of 19.5 µg/g was reported at a depth of 41.68 m (136.75 ft) bgs. The highest concentrations of nitrate were reported between two depth intervals; between 40.77 and 41.68 m (133.75 and 136.75 ft) bgs, and between 46.2 and 49.15 m (151.6 and 161.25 ft) bgs. Elevated nitrate concentrations in the 40.77 and 41.68 m (133.75 and 136.75 ft) bgs interval were co-located with maximum concentrations of sulfate and calcium.

Sulfate: In the Phase 2 RFI/CMS investigation, sulfate was reported above background in three samples collected during Phase 2. The maximum concentration was 592,000 µg/kg from Investigation Group A+B at a depth of 4.3 m (14.2 ft) bgs (shallow).

Sulfate exceeded background in Phase 2 WMA C soils as follows.

- Shallow (≤ 5 m [15 ft] bgs) depths only: Investigation Group H+I.

- Deep (>5 m [15 ft] bgs) depths only: none.

- Both shallow (≤ 5 m [15 ft] bgs) and deep (> 5 m [15 ft] bgs) depths: Investigation Groups A+B.

Results for all other locations were less than background or were below detection. At borehole C-4297 (Phase 1 Characterization), sulfate concentrations were reported for 72 soil samples. The highest concentrations of sulfate (80.9 µg/g to 104 µg/g) were reported at depths ranging from 40.77 to 41.68 m (133.75 and 136.75 ft) bgs, coincident with elevated concentrations of nitrate and calcium.

Chromium: Chromium, a dangerous waste constituent, was reported above background in 29 samples from nine Investigation Sites/Groups. The maximum concentration of chromium was 44,500 µg/kg from Site U at a depth of 48 m (158 ft) bgs (deep).

Chromium exceeded background in Phase 2 WMA C soils as follows.

- Shallow (≤ 5 m [15 ft] bgs) depths only: none.

- Deep (>5 m [15 ft] bgs) depths only: Investigation Groups A+B, F+G, H+I, L1+L2, and Sites C, E, and J.

- Both shallow (≤ 5 m [15 ft] bgs) and deep (> 5 m [15 ft] bgs) depths: Investigation Groups H+I, P, and Site U.

Chromium was not reported above background at Site R.

Cyanide: Cyanide was not detected in any soil samples collected during the Phase 2 soil investigation. The detection limit for cyanide was 0.5 mg/kg. Further discussion of cyanide can be found in Section 2.3.3.3, Groundwater Contamination.

2.3.2.5.2 Slightly Sorbed Constituents (K_ds between 0.2 to 0.6 mL/g).

Iodine-129: In the Phase 2 RFI/CMS investigation, ^{129}I was detected in one sample at a concentration of 0.808 [B] pCi/g from Investigation Group P at a depth of 2 m (6 ft) bgs (shallow). Iodine-129 results for all other locations and depths were below detection. Note that ^{129}I contamination in groundwater is present throughout the east half of the 200 East Area and are believed to be from liquid waste facilities in the northern portion of the 200-PO-1 OU (DOE/RL-2011-01, *Hanford Site Groundwater Monitoring Report for 2010*).

Cobalt-60: Cobalt-60 was reported above background in 138 samples across all locations and depths. However, all results were reported as non-detects. The maximum reported concentration was 3.13 [U] pCi/g from Investigation Group P at a depth of 2 m (7 ft) bgs (shallow).

A summary of results for gross gamma and spectral gamma logging results relevant to Co-60 in drywells and direct push boreholes in each of the investigation areas of the RFI are discussed in Section 5.2 of the RFI (RPP-RPT-58339, Rev. A). All logs used in the RFI are provided in Appendix T of the RFI (RPP-RPT-58339, Rev. A).

Cobalt-60 was reported above background in 138 samples across all locations and depths. However, all results were reported as non-detects. The maximum reported concentration was 3.13 [U] pCi/g from Investigation Group P at a depth of 2 m (7 ft) bgs (shallow).
In borehole C-4297 (Phase 1 Characterization), low levels of ^{60}Co (<1 pCi/g) were found at depths from 12 to 20 m (40 to 65 ft) bgs.

Note that detection limits were established during the DQO process and it was understood that based on the limited soil collected through the direct push process that some detection limits would be above site soil background levels. Table 5-4 (Page 5-21) of the RFI identifies the constituents with detection limits established above site soil background levels. Cobalt-60 was one of the constituents having detection limit issues (background level 0.0084 [0.01] pCi/g with a detection limit of 0.05 pCi/g).

In borehole C-4297 (Phase 1 Characterization), low levels of ^{60}Co (<1 pCi/g) were found at depths from 12 to 20 m (40 to 65 ft) bgs.

Uranium: Uranium was reported above background in 44 samples from three Investigation Sites/Groups. All results were reported as non-detects. The maximum concentration was 101,000 ug/kg U at Investigation Group P from a depth of 5 m (15 ft) bgs (shallow).

Uranium exceeded background in Phase 2 WMA C soil samples as follows.

- Shallow (≤ 5 m [15 ft] bgs) depths only: none.
- Deep (> 5 m [15 ft] bgs) depths only: none.
- Both shallow (≤ 5 m [15 ft] bgs) and deep (> 5 m [15 ft] bgs) depths: Investigation Groups F+G, L1+L2, P.

Uranium results for all other locations were less than background or were below detection.

For uranium, the DQO identified the target detection limit of 1,000 µg/kg (1 mg/kg) and the Sampling Analysis Plan (SAP) identified a required detection limit of 500 µg/kg (0.5 mg/kg). Background for uranium is 3,210 µg/kg (3.21 mg/kg). It should also be noted that the SAP also identified that isotopic uranium analysis may be substituted for total uranium as long as the required detection limit is met. Appendix M of the RFI (Data Quality Assessment) identified the detection limit issues with uranium analysis. Table M-25 provides uranium results estimated from isotopic ratios of uranium radioisotopes. All of the total uranium results (determined from isotopic uranium) were below background with the exception of one sample at Site P (C6404) at a depth of 13 m (43 ft) bgs and a concentration of 6440 µg/kg.

Uranium and ^{60}Co is not observed in groundwater in concentrations to contribute significantly to current risk. The overall risk contribution from uranium is expected to low in the future due to the combination of its affinity to be sorbed on Hanford Site sediments and their inventories. In the case of ^{60}Co, its overall risk contribution is expected to low in the future due to its short half-life, low inventory, and its apparent affinity for small amounts of sorption onto Hanford Site sediments

2.3.2.5.3 Sorbed Constituents (K_d > 0.6 mL/g).

Cesium-137: Cesium-137 was reported above background in 34 samples from eight Investigation Sites/Groups. The maximum concentration was 73.1 pCi/g from Investigation Group P at a depth of 5 m (15 ft) bgs (shallow).

Cesium-137 exceeded background in Phase 2 WMA C soil samples as follows.

- Shallow (≤ 5 m [15 ft] bgs) depths only: Investigation Groups A+B, L1+L2, and Sites C, E, J, and U.
- Deep (> 5 m [15 ft] bgs) depths only: none.

- Both shallow (≤ 5 m [15 ft] bgs) and deep (> 5 m [15 ft] bgs) depths: Investigation Groups F+G and P.

Cesium-137 results for Investigation Group H+I and Site R were less than background or below detection.

In borehole C-4297 (Phase 1 Characterization), detailed characterization showed that ^{137}Cs was detected between the ground surface and 6 m (19 ft) in depth at concentrations up to 1,700 pCi/g. The log report states that the profile of the gamma log between 3 and 5 m (11 and 16 ft) bgs is suggestive of a point source of contamination such as a pipeline and may be waste inside a nearby pipeline. No significant ^{137}Cs activity was observed below the base of the tank.

Cesium-137 is one of the key constituents identified in spectral gamma logging in drywells and direct push boreholes. A summary of results for these logging results relevant to ^{137}Cs in drywells and direct push boreholes in each of the investigation areas of the RFI are discussed in Section 5.2 of the RFI (RPP-RPT-58339, Rev. A). All logs used in the RFI are provided in Appendix T of the RFI (RPP-RPT-58339, Rev. A).

Nickel: In the Phase 2 RFI/CMS investigation, nickel was reported above background in nine samples from Investigation Groups E, L1 + L2, P and U at WMA C. The maximum concentration (30,600 µg/kg) was reported at Investigation Area Group P at a depth of 8 m (126 ft) bgs.

Nickel was reported above background as follows:

- Two samples from Investigation Group E from borehole C7672. The maximum concentration was 25,300 µg/kg at a depth of 23 m (74 ft) bgs (H2). The maximum depth of detection was 23 m (74 ft) bgs (H2).

- One sample from Investigation Group L1 + L2 from borehole C7670 at a concentration of 20,200 µg/kg and a depth of 12 m (40 ft) bgs (backfill).

- Five samples from Investigation Group P. The maximum reported concentration was 30,600 µg/kg at a depth of 8 m (26 ft) bgs (H1) from borehole C6392. The maximum depth of detection above background was 52 m (170 ft) bgs (H2) at borehole C6394.

- One sample from Investigation Group U from borehole C7676 with a concentration of 29,400 µg/kg at a depth of 48 m (158 ft) bgs (H2).

Further discussion of nickel can be found in Section 2.3.3.3, Groundwater Contamination.

Strontium-90: Strontium-90 was reported above background in 141 samples from all Investigation Sites/Groups. The maximum concentration was 141 pCi/g from Investigation Group P at a depth of 3 m (11 ft) bgs (shallow). Some results exceeding background were reported as non-detects.

Strontium-90 exceeded background in Phase 2 WMA C soil samples as follows.

- Shallow (≤ 5 m [15 ft] bgs) depths only: none.
- Deep (> 5 m [15 ft] bgs) depths only: Investigation Sites R, and U.
- Both shallow (≤ 5 m [15 ft] bgs) and deep (>5 m [15 ft] bgs) depths: Investigation Groups A+B, E, F+G, H+I, P, and Site J.

Tributyl Phosphate: Tributyl phosphate was not detected or was detected below background at all locations during the Phase 2 RFI/CMS investigation.

2.3.2.6 Moisture Content Results. Moisture content data from both neutron logging and laboratory analyses were collected during both Phase 1 and 2 characterization efforts of the RCRA facility investigation. A statistical summary of this moisture content data is provided here. The reader is referred to Appendix B for additional detailed information about this moisture content data and its use in the PA model development process.

The neutron logging data came from two drywells and 63 direct push boreholes. Laboratory measured moisture content (weight % converted to volumetric moisture content) came from one groundwater well (299-E27-22) and one characterization borehole (C4297).

The spacing for the neutron logging of moisture content varied from 0.05 m to 0.15 m (~0.15 ft to 0.5 ft). The spacing on the laboratory samples was greater. A total of 32,912 measurements were made and moisture content ranged from 0.11 to 30.64 volumetric percent, with a mean of 5.69 and a median of 5.09. Furthermore, the formations were identified in each well/borehole/direct push and a statistical analysis of volumetric moisture content data was run for each formation (Table 2-6). The locations for the moisture content measurements are shown in Figure 2-21.

An alternative conceptual model was developed looking at this type of moisture content information. The development of this specific model is provided in Appendix F of RPP-ENV-58806, and RPP-ENV-58782. This model is one of the many alternative conceptual models (ACMs) considered in the scoping analysis of leaks described in Section 4 of this document. An alternative conceptual was also developed by Pacific Northwest National Laboratory (PNNL) based on the same moisture content information. The development of that model is summarized in PNNL-24740.

2.3.3 Unconfined Aquifer at Waste Management Area C

The unconfined aquifer underlying WMA C has been monitored on a quarterly basis since 1992. This section provides a summary of the flow conditions underlying WMA C, a brief description of the monitoring network, a summary of the contamination observed in the unconfined aquifer, and a brief interpretation of the results.

2.3.3.1 Groundwater Flow Conditions. The water table or potentiometric surface lies ~60 m (~200 ft) below the bottom of the tank farm excavations within the undifferentiated $H_3/CC_u/RF$ located in the paleochannel (Figure 2-6 and Figure 2-12). The aquifer materials consist dominantly of sandy gravel or silty sandy gravel. The water table elevation beneath WMA C is ~122 m (!400 ft) North American Vertical Datum of 1988 (NAVD88) with ~77 m (~255 ft) of vadose zone. The aquifer thickness, based on the top of basalt at 108 m (355 ft), is ~13.4 m (~44 ft).

Scouring of suprabasalt sediments in the paleochannels is evident in that, along much of its path, only the Hanford formation overlies the top of the basalt (Figure 2-6). Hanford formation material makes up almost entirely the material within the paleochannels in general, as well as all of the material within the paleochannel at the WMA C water table. Removal of pre-Hanford formation suprabasalt sediments, with the possible exception of a thin layer of CCu beneath the eastern half of WMA C, is apparent. This suggests that the width of the paleochannel beneath WMA C is over 500 m (1640 ft). Wells 299-E27-14 and 299-E27-15 penetrate the Hanford formation within the paleochannel beneath WMA C.

Hydraulic conductivity values reported for the aquifer in this area vary considerably, ranging from 0.04 (silt lenses within the sandy gravel) to 6,900 m/day (0.13 to 22,640 ft/day). Additional hydraulic property data from aquifer testing at wells near WMA C is provided in RPP-RPT-46088. More recently, additional large-scale hydraulic property data are derived from The Central Plateau Groundwater Model (CPGWM) (CP-47631, *Model Package Report: Central Plateau Groundwater Model Version 3.3*, Rev. 0) incorporates the large-scale geologic and hydrogeologic features, and provides estimates of water levels, hydraulic gradients, and groundwater flows throughout the 200 West and 200 East Areas for current and expected future groundwater conditions. The CPGWM provides calibrated hydraulic conductivity estimates for the model layers and HSUs present within the aquifer in the vicinity of WMA C. The thicknesses of the different aquifer HSUs are mapped from the CPGWM onto the WMA C RCRA closure analysis model flow domain. An averaging scheme weighted according to HSU thickness provides estimates of the equivalent homogeneous medium (EHM) effective saturated hydraulic conductivity and the hydraulic gradient. The weighted average of hydraulic conductivity of the CPGWM HSUs mapped onto the WMA C flow domain indicates that the effective saturated hydraulic conductivity is ~11,000 m/day (~32,808 ft/day). The basis for the development pf this estimated effective saturated hydraulic conductivity is found in Section C3.2 of Appendix C of RPP-ENV-58806, *RCRA Closure Analysis of Tank Waste Residuals Impacts at Waste Management Area C*.

Table 2-6. Summary Statistics for Volumetric Moisture Content in the Lithologic Units Underlying Waste Management Area C.

Unit	Count of Wells	Count of Measurements	Minimum (Vol %)	Maximum (Vol %)	Average (Vol %)	Median (Vol %)	Mode (Vol %)	Standard Deviation	Variance
Backfill	52	4,052	0.11	30.61	8.09	7.48	6.20	3.71	13.75
H1	66	7,977	0.13	30.64	5.88	4.72	3.26	3.67	13.47
H2	64	20,876	1.06	26.32	5.15	4.96	4.89	1.82	3.30
H3	1	7	5.54	7.09	6.18	6.01	Too Few	0.65	0.43
Waste Management Area C	67	32,912	0.11	30.64	5.69	5.09	4.89	2.82	7.95

Figure 2-21. Moisture Content (% Vol) Measurements in Vadose Zone at Waste Management Area C.

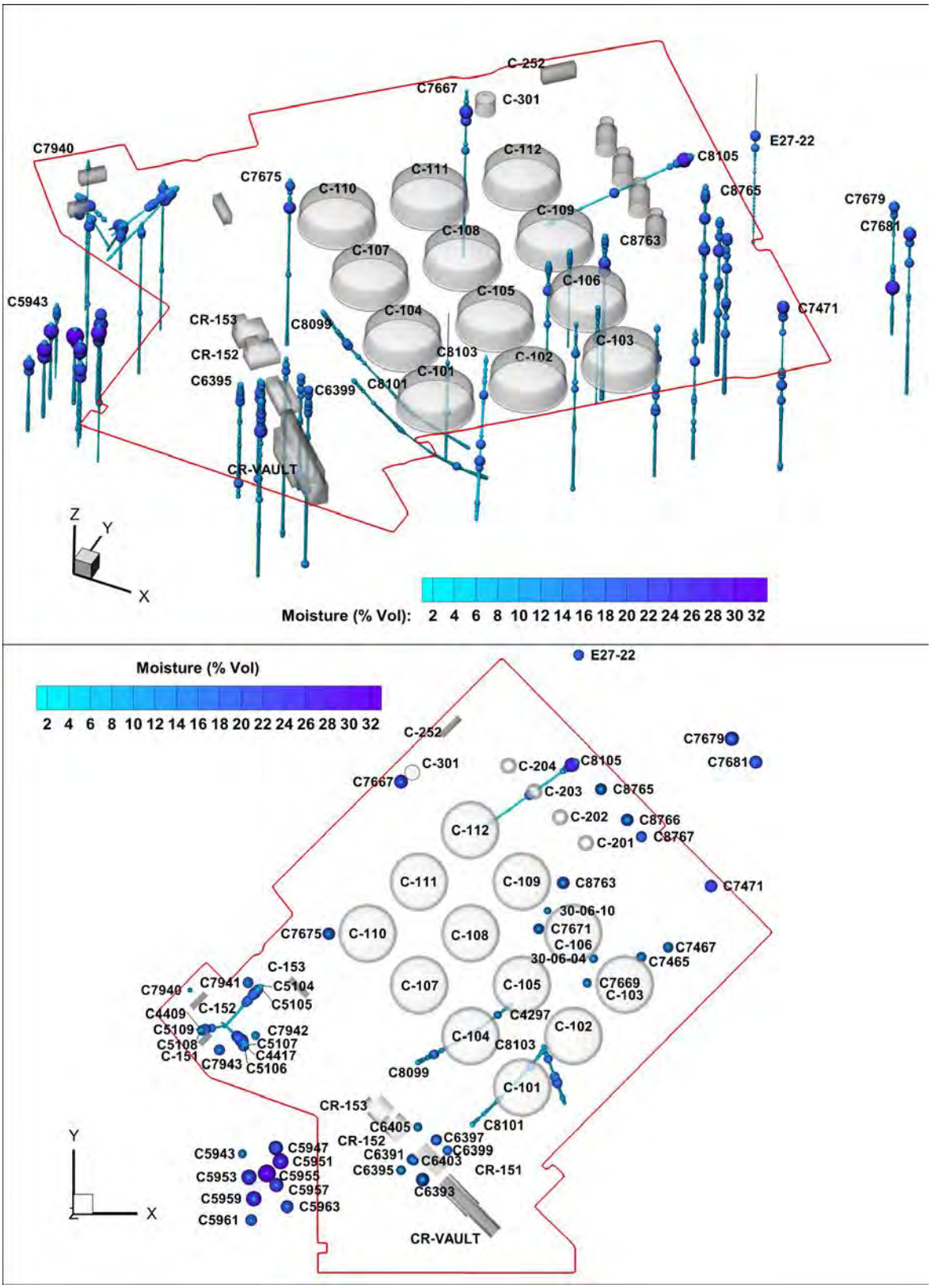

Currently, the general groundwater flow direction in the unconfined aquifer beneath WMA C is to the south/southeast. The water table is very flat overall, with an estimated hydraulic gradient between 1×10^{-5} to 2×10^{-5} m/m; the estimated groundwater flow velocity ranges from 0.2 to 0.4 m/day (0.7 to 1.3 ft/day) (RPP-RPT-46088). Those hydraulic gradient estimates are also consistent with those recently reported in SGW-54165, *Evaluation of the Unconfined Aquifer Hydraulic Gradient Beneath the 200 East Area, Hanford Site*, for the unconfined aquifer near the Integrated Disposal Facility (IDF) and PUREX cribs. Also coincident with the flow change are decreasing concentrations of other contaminants in monitoring wells west of C Farm, indicating a change in flow direction. These observations and other interpretations discussed in SGW-58561, *WMA C Quarterly October through December 2014 Quarterly Groundwater Monitoring Report*, provide sufficient evidence for the determination of a south to southeast flow direction at WMA C. These estimates are also consistent with the CPGWM.

The discharge of large volumes of wastewater in the early 1950s to B Pond (Figure 2-8) raised the water table in the vicinity of WMAs C and A-AX as much as 4.9 m (16 ft) above the pre-Hanford Site operations level (*PNNL-14548, Hanford Site Groundwater Monitoring for Fiscal Year 2003*). The corresponding flow direction underneath WMA C at this time was toward the southwest (DOE/ORP-2008-01, Appendix H). Water levels began to decline in the late 1980s when wastewater discharges were reduced. The decline has become even more pronounced since other effluent discharges throughout the 200 Areas ceased in 1995 (Figure 2-11). Water levels are expected to continue declining within the region surrounding WMAs A-AX and C, with the flow direction changing to the southeast. With the change in flow direction, contamination originating in the B Complex in the northwest corner of 200 East may flow underneath WMA C in the not too distant future.

2.3.3.2 Groundwater Monitoring. Quarterly groundwater monitoring was initiated at WMA C in 1992 in accordance with WHC-SD-EN-AP-012, *Interim-Status Groundwater Monitoring Plan for the Single-Shell Tanks*. The initial well network consisted of five wells: 299-E27-7, 299-E27-12, 299-E27-13, 299-E27-14, and 299-E27-15 (see Figure 2-17). These wells were used for quarterly groundwater monitoring beginning in March 1992 and continued until the Fall of 1993. In the Spring of 1994, semi-annual sampling began for indicator parameter evaluation. Monthly sampling began in June 1998 to prepare for sluicing at tank C-106. The monthly sampling was scaled back to bi-monthly in 2000 and then returned to quarterly sampling in 2001. In 2001, a new monitoring plan, PNNL-13024, *RCRA Groundwater Monitoring Plan for Single-Shell Tank Waste Management Area C at the Hanford Site*, was initiated and required additional wells to ensure adequate monitoring network coverage for WMA C. Wells 299-E27-4, 299-E27-21, 299-E27-22, and 299-E27-23 (Figure 2-17) were subsequently added to the network.

In 2009, WMA C was placed in assessment monitoring because of the exceedance of the critical mean for the indicator parameter specific conductance. In addition, the dangerous constituent cyanide has been found in groundwater beneath WMA C, albeit at levels much lower than the DWS. To meet quarterly RCRA assessment requirements, a new monitoring plan (DOE/RL-2009-77, *Groundwater Quality Assessment Plan for the Single-Shell Tank Waste Management Area C*) was developed which superseded PNNL-13024. Currently, assessment

monitoring is being completed in accordance with DOE/RL-2009-77. Three wells (299-E27-24, 299-E27-25, and 299-E27-155; see Figure 2-17) were added to the network per DOE/RL-2009-77. Well 299-E27-25 is not shown on Figure 2-17; it is located ~170 m (~550 ft) northeast of the northeast fenceline of WMA C. The WMA C groundwater monitoring network now is composed of the following 12 wells:

299-E27-4	299-E27-7	299-E27-12	299-E27-13	299-E27-14	299-E27-15
299-E27-21	299-E27-22	299-E27-23	299-E27-24	299-E27-25	299-E27-155

In addition to meeting the quarterly assessment requirements, quarterly monitoring is also done to meet the requirements of External letter 04-TPD-083, "Agreement on Content of Tank Waste Retrieval Work Plans," in which quarterly groundwater monitoring sample results are to be provided to Ecology during tank retrievals. To meet the sampling requirements, the groundwater monitoring analyses include RCRA and AEA constituents from the following: anions, cyanide, metals ^{99}Tc, gross beta, total uranium, and low-level gamma scan. The most recent quarterly monitoring report is SGW-59669, *WMA C Quarterly October Through December 2015 Quarterly Groundwater Monitoring Report*.

2.3.3.3 Groundwater Contamination. In SGW-59669, the results of sampling for 129 constituents across the WMA C monitoring network are provided. In that report, six analytes (i.e., cyanide, nickel, nitrate, sulfate, ^{99}Tc, and uranium) are discussed in detail.

Table 2-7 provides summary statistics for these analytes for the past ten years. It also identifies the date at which the maximum for a particular analyte was collected and in which monitoring well the maximum was collected.

Observations of elevated concentrations of nitrate, sulfate, and ^{99}Tc appear to be associated with past releases from WMA C because these constituents are much higher in the downgradient wells compared to upgradient wells, and they exceed their respective groundwater DWSs/maximum contaminant levels (MCLs). Additionally, cyanide, which is a dangerous waste constituent, is also found in the aquifer at levels above detection limit, which well below the DWS of 200 µg/L. but above the WAC 173-340-720 Method B groundwater cleanup level for cyanide (hazard quotient = 1) is 9.6 µg/L for CN- and 4.8 µg/L for hydrogen cyanide (HCN) in some wells. The measured cyanide concentration was 14.9 µg/L in December 2015 at well 299-E27-14. Only ^{99}Tc, nitrate, sulfate, and cyanide are discussed further in this section. Technetium-99 exceeded the DWS by a factor of almost 30. For discussions and interpretations of the overall trends of other constituents in monitoring wells in the vicinity of WMA C, the reader is referred to SGW-59669.

1

Table 2-7. Summary Statistics from January 1, 2006 to January 1, 2016 for Constituents Discussed in SGW-59669*.

Constituent	Maximum	Minimum	Average	Standard Deviation	Unit	Maximum Collected on	Maximum Found at Well	Filtered	Location Count	Location Count Detect	Count	Rejects	Detects
Cyanide	41	1.8	9.5	7.2	µg/L	6/11/2009	299-E27-7	N	12	12	488	7	185
Nickel	191	0.47	12	16	µg/L	9/4/2015	299-E27-4	Y	12	12	476	5	191
Nickel	293	0.23	16	24	µg/L	9/4/2015	299-E27-4	N	12	12	426	6	212
Nitrate	118,000	8,280	37,771	21,262	µg/L	9/7/2012	299-E27-14	N	12	12	509	4	505
Sulfate	345,000	45,600	162,980	75,535	µg/L	5/14/2010	299-E27-24	N	12	12	509	5	504
^{99}Tc	26,700	7.0	3,854	5,496	pCi/L	12/8/2015	299-E27-21	N	12	11	498	3	460
Uranium	9.9	3.4	5.5	2.3	µg/L	12/10/2013	299-E27-155	Y	12	12	18	1	17
Uranium	10.8	1.8	3.8	1.6	µg/L	9/7/2012 & 3/6/2013	299-E27-14	N	12	12	445	11	434

*Values reported do include those that are suspect or have been rejected by user.

Reference: SGW-59669, *WMA C Quarterly October Through December 2015 Quarterly Groundwater Monitoring Report*.

A number of other constituents have been detected at concentration levels near or just above background in groundwater wells near C-Farm. Some examples of these types of constituents include arsenic, chromium, nickel, uranium, and tritium. Concentration levels of these constituents may be reflective of background levels but could also reflect the potential local influences in groundwater from past releases or losses from WMA C tanks and/or ancillary facilities. In addition, past interpretations of well monitoring results in the general area of WMA C do show that groundwater in the vicinity of WMA C has been impacted by both local and up gradient plumes that could also have some potential influence on observed concentration levels for some of these constituents. Current groundwater contamination in vicinity of WMA C has been evaluated as a part of a broader remedial investigation/feasibility study for the 200-BP-5 OU (Site 200-BP-5 OU RI) (DOE/RL-2009-127, *Remedial Investigation Report for the 200-BP-5 Groundwater Operable Unit, Draft A*). The feasibility study part of this evaluation is leading to the development of interim measures designed to mitigate current contamination in groundwater at WMA C as well as other areas of contaminated groundwater within the 200-BP-5 OU.

It should be noted that interpretations of some aspects of groundwater concentration monitoring results, described in the following sections, have been or are generally used to infer that sources for the monitoring well impacts have originated from past source releases from WMA C. However, because the lack of groundwater monitoring wells within the tank farm area and the uncertainties associated with historical knowledge of both natural and anthropogenic sources of recharge, and the past directions and rates of groundwater flow in the unconfined at WMA C, attempts to attribute the impacts observed in groundwater wells to specific source leaks or releases that have occurred in or in the general vicinity of WMA C is not considered to be feasible with current state of data and information

Technetium-99: In December 2015, ^{99}Tc had concentrations exceeding the 900 pCi/L DWS in 7 of the 11 monitoring wells surrounding WMA C (Figure 2-22). However, in 2006 only 4 of the 11 wells exceeded the DWS. Three of these wells (299-E27-4, 299-E27-13, and 299-E27-23) are located just outside the south central region of WMA C (Figure 2-17). The other well that exceeded the DWS is well 299-E27-14, located east of WMA C. Two new wells (299-E27-155 and 299-E27-4) placed to the south and east of WMA C after 2006 also showed ^{99}Tc concentrations above the DWS when they were installed. The ^{99}Tc in the groundwater in that region appears to be centered on well 299-E27-23 with the trend in that well increasing from ~5,000 pCi/L in late 2006 to ~26,000 pCi/L by April 2012. Since then, the trend at the well has been decreasing, falling to ~3,400 pCi/L by December 2014. This decline is associated with changes in the flow direction to the east and southeast. The resulting change in flow direction and sampling in downgradient wells (299-E27-21) from well 299-E27-23 show the concentration of ^{99}Tc increasing in this well, indicating plume movement to the east-southeast. The highest ^{99}Tc concentration found in WMA C was in December of 2015 with a value of 26,700 pCi/L at well 299-E27-21. At well 299-E27-14, ^{99}Tc concentrations ranged between 1,500 and 2,600 pCi/L from 2006 to late 2012. However, in early 2013 they started increasing, peaking in June of 2013 at 10,700 pCi/L and decreasing since then; the ^{99}Tc concentration had decreased to 2,620 pCi/L by December 2015. Finally, well 299-E27-24 (installed in 2010) shows an initial ^{99}Tc concentration of 2,100 pCi/L that raises to a peak of 5,100 pCi/L in September of 2013,

with it slowly dropping to 3,800 pCi/L in December 2015. Based on evaluation of ^{99}Tc to nitrate ratios, it is believed the ^{99s}Tc found at wells 299-E27-14 and 299-E27-24 is from a different source than ^{99}Tc found in the south central region of WMA C (299-E27-4, 299-E27-21, and 299-E27-23). A full discussion of this topic is provided in Section 2.3.4. The specific sources (i.e., tank and/or pipeline) of ^{99}Tc in the groundwater at WMA C has not been identified.

Wells 299-E27-24 and 299-E27-155, which are screened along the bottom of the unconfined aquifer, indicate that ^{99}Tc has migrated throughout the unconfined aquifer. Contamination has also reached the bottom of the aquifer. Depth-discrete samples were taken from wells 299-E27-4, 299-E27-21, and 299-E27-23 in 2010. Like well 299-E27-155, which had depth-discrete samples taken during drilling, the samples taken at wells 299-E27-4 and 299-E27-21 showed increasing contamination with depth. Well 299-E27-23 generally had steady concentrations of around 20,000 pCi/L throughout its depth profile.

The vertical distribution of a plume is affected or influenced by hydrophysical, hydrologic, and geochemical processes. Hydrophysical processes include the rate at which the contaminant enters the aquifer and the volume of water transporting the contaminant. Higher rates and larger volumes provide more of a vertical gradient to the contaminant movement than lower rates and smaller volumes. Hydrologic processes include the irregularly shaped aquifer geometry that may physically control flow paths, and spatially heterogeneous hydrogeologic units that influence transport. Either of these processes may facilitate or impede flow to create vertical gradients and other multidimensional contaminant transport and spreading within the aquifer. Geochemical processes include contaminant solution density, and state (e.g., non-aqueous liquid that may sink or float in water) occurring in the groundwater. The specific factors affecting the increasing contamination with depth observed at wells 299-E27-23 and 299-E27-21 while these wells were being drilled is unknown.

Gross beta measurements were not considered in our analyses. Gross beta has been detected in well 299-E27-7 since 1984. Gross beta was first detected in this well about 24 pCi/l in March 1984 and observed at levels ranging between 3 and 7 pCi/l. ^{99}Tc was first detected in this well in July 1991 and relatively low levels until it began to rise in 1998, reaching its' peak of 2760 pCi/l in January 2002. After this peak time, ^{99}Tc concentration decreased back down to low levels although they were found at slightly higher levels than observed prior to the rise in concentrations in 1998. While there appears to general correlation between ^{99}Tc and gross beta results during the overall time frame, this specific analysis focused on observations for ^{99}Tc and does not consider the early low trends on gross beta observations.

Nitrate: General trends for nitrate in wells in the vicinity of WMA C are provided in Figure 2-23. Nitrate concentrations at eight WMA C wells have exceeded 45 mg/L MCL over the past 10 years. Two of the three wells, 299-E27-14 and 299-E27-24, are downgradient of WMA C. The greatest nitrate concentration (118 mg/L) was at well 299-E27-14 in 2012, located on the southeast side of WMA C. Based on concentrations at well 299-E27-24, which was installed in the lower portion of the unconfined aquifer ~66 m (~216.5 ft) south of well 299-E27-14 in 2010, the plume extends throughout the 15.5-m (50.9-ft)-thick aquifer. The nitrate concentrations in well 299-E27-24 have been stable, ranging between 65.5 and 73.5 mg/L since sample collection began in 2010. Wells slightly in the southern part of the WMA C farm,

(299-E27-4, 299-E27-21, and 299-E27-21) only slightly exceed the MCL ranging between ~35 to 50 mg/L. Well 299-E27-155 was installed in the last quarter of 2007. Nitrate values from this well stayed at ~50 mg/L from 2008 to the beginning of 2014 before dipping 24 mg/L in late 2013, then raising to 66 mg/L at the end of 2015. In addition to these wells, an upgradient monitoring well (off the map to the north of WMA C) was installed in 2010. The nitrate trend in this well has shown a steady increase from 36 mg/L (April 6, 2010) to over 57 mg/L (December 10, 2015). This well is cross gradient of WMA C and is affected by migrating contaminant plumes to the north.

Currently, nitrate concentrations do not exceed the DWSs in upgradient wells (299-E27-7, 299-E27-22, and 299-E27-25), suggesting a source within C Farm. Furthermore, nitrate concentrations at well 299-E27-14 are more than double past and present upgradient well concentrations.

Sulfate: General trends for sulfate in wells in the vicinity of WMA C are provided in Figure 2-24. Over the past 10 years, sulfate concentration exceeded the secondary MCL for sulfate of 250 mg/L in only three wells (299-E27-7, 299-E27-14, and 299-E27-24). For well 299-E27-7, it was a one-time occurrence in February 2016. From June 2010 to December 2015, sulfate concentrations do not exceed the DWSs in upgradient wells 299-E27-7 and 299-E27-14 which suggests a source of sulfate within C Farm. However, in upgradient well 299-E27-25, sulfate concentration exceeded the secondary MCL for sulfate of 250 mg/L in December 2010 with a value of 259 mg/L, and by December 2015 has gradually increased 320 mg/L. This upstream sulfate plume may impact WMA C sometime in the future.

Cyanide: The dangerous waste constituent cyanide was detected at four WMA C wells in December 2014 at concentrations far below the 200 µg/L DWS. A possible reason for the increased number of wells with detectable cyanide between June and December 2014 is that the detection limit for cyanide decreased from 4 to 1.67 µg/L. In December of 2015, two wells (299-E27-14 and 299-E27-24) had concentrations approaching 15 µg/L, while two wells (299-E27-4 and 299-E27-23) had concentrations at or below 5 µg/L (Figure 2-25). The other well (299-E27-7) had historically the highest value (40.7 µg/L) in 2009, but levels had fallen in that well to less than 5 µg/L by 2012. Concentrations at well 299-E27-4 are generally near the detection level but were higher in December of 2009, 2011, and 2014 (10.4, 7.98, and 7.9 µg/L, respectively). Remnant levels of low cyanide concentrations appear to be present sporadically beneath the eastern and western portions of the C Farm facility, while more persistent concentrations exist to the southeast (wells 299-E27-14 and 299-E27-24) as can be seen in Figure 2-25. As discussed in DOE/RL-2009-77, the source of cyanide in groundwater is likely be related to past releases from WMA C, but a specific tank/leak source within WMA C has not been identified.

More discussion that estimates of inventories and potential impacts from past releases of cyanide at WMA C are provided in Appendix A.

2.3.4 Recent Interpretations of Waste Management Area C Groundwater Chemistry

This section summarizes results of evaluation of ~10 years of analytical groundwater data as part of an effort by the BP-5 Remedial Investigation (RI) that examined recent impacts to groundwater at WMA C. This specific evaluation was used to support one of two approaches in the BP-5 RI to estimate the magnitude of potential fluxes from the vadose zone at WMA C to groundwater based on the evaluation of recent data and information collected at wells located in the vicinity of WMA C. The estimates of contaminant fluxes developed as a part of these efforts were used in the BP-5 RI as a basis for source term estimated used in contaminant fate and transport model simulations that examine the potential for future impacts to groundwater from continuing sources within the vadose zone resulting from past tank waste releases at WMA C. The specific evaluation of groundwater data and information provided in this subsection is described in ECF-Hanford-13-0037, *Development of Source Terms for Inclusion in Fate and Transport Modeling for Remedial Investigation/Feasibility Studies of the 200-BP-5 and 200-PO-1 Groundwater Operable Units.* This evaluation provide published information about the recent estimate of mass flux of ^{99}Tc and other constituents from the vadose zone to the saturated zone at WMA C, The results of the contaminant fate and transport modeling are described in detail in ECF-Hanford-13-0031, *Fate and Transport Modeling for Baseline Conditions for Remedial Investigation/Feasibility Studies of the 200-BP-5 and 200-PO-1 Groundwater Operable Units*.

2.3.4.1 Technical Approach. The concentration trends used in this evaluation were based on the last 10 years of concentrations in groundwater monitoring wells in the vicinity of WMA C. The focus of this approach was on large changes in concentrations for selected analytes—^{99}Tc, nitrate, sulfate, and chloride—that provide insight into relative contribution from past releases from WMA C. The following steps were undertaken in this calculation approach.

- Year 2008, 2010, and 2012 datasets were selected for this calculation. The groundwater concentrations of ^{99}Tc, nitrate, sulfate, and chloride were analyzed for these years. Time histories for the first three analytes are presented in Figure 2-22. Trends for chloride are not provided here but can be found in ECF-Hanford-13-0037. These trends are described as part of the groundwater contamination section.

- Identified possible plume source areas for ^{99}Tc within the WMA C aquifer.

- The median concentration values were calculated for each analyte for each year and bivariate plots were drawn for the analytes. The bivariate plots with median concentrations were developed and evaluated to identify overall trends in chemistry and calculate mixing lines between the end-member waters and upgradient water types.

- Used information based on bivariate plots and dilution lines along with the long-term observed concentration trends to identify different plume source zones that could be influencing concentration trends seen in monitoring wells in the vicinity of WMA C.

- Provided estimates of ^{99}Tc fluxes to the unconfined aquifer.

2.3.4.2 Technetium-99 Source Areas within the Groundwater at Waste Management Area C. Well data suggest two sources for the contamination: 1) on the western side of WMA C, which appears to be migrating to the southeast as of 2012; and 2) in the southeast of WMA C. The wells which can be associated with the southeastern plume are wells 299-E27-14, 299-E27-24, and 299-E27-7. The wells associated with the western plume are wells 299-E27-13, 299-E27-23, and 299-E27-4. The data suggest that the contamination in the southeast comes from a different source than the contamination in the west. The three major lines of evidence for this are as follows.

- The concentration trends are different: the southeastern wells 299-E27-14 and 299-E27-24 display a nearly stable ^{99}Tc trend (Figure 2-26), while the western wells 299-E27-13 and 299-E27-23 show increasing values from approximately 2000 to 2010, then decreasing from approximately 2010 to 2015 (Figure 2-27).

- The ^{99}Tc-to-nitrate ratios are different: the southeastern wells, 299-E27-14 and 299-E27-24, display a nearly stable ^{99}Tc-to-nitrate ratio of ~50 through 2012. Wells beneath the BY crib display a similar ratio, suggesting a similar source material. The western wells 299-E27-13 and 299-E27-23 show a five-fold increase in the ^{99}Tc-to-nitrate ratio after 2008 (Figure 2-28).

- There is more cyanide present in the southeast than the west: wells 299-E27-14 and 299-E27-24 are impacted by a ferrocyanide-derived waste, while analysis of the contamination in the western wells is more representative of a PUREX-derived liquid waste (Figure 2-25).

A change in groundwater flow appears to have shifted the center of the western plume. From 2012 to 2013, the center of the western plume seems to have shifted from well 299-E27-23 to well 299-E27-21 (Figure 2-13). The ^{99}Tc concentration increases at well 299-E27-21 as it decreases in well 299-E27-23. Furthermore, the technetium-to-nitrate ratio at the presumed new center of the plume in well 299-E27-21 was, in December 2013, nearly identical to the technetium-to-nitrate ratio at well 299-E27-23 near its peak in 2010, indicating a change in groundwater flow direction sometime in mid-2011.

Technetium-99, the contamination to the southeast of WMA C appears to be sourced from ferrocyanide-derived waste. The highest concentrations of nitrate occur in the southeast as well, near well 299-E27-14. From a measurement of 12.4 mg/L in Fall 1998, the concentrations at well 299-E27-14 increased until finally reaching the DWS in 2003, with peaks occurring in the Fall after 2006 (Figure 2-23). Nitrate concentrations at well 299-E27-24, which is ~60 m (~197 ft) south of well 299-E27-14, average ~70 mg/L, ~20 to 30 mg/L less than those at well 299-E27-14. The cyanide-to-nitrate ratio indicates these wells are contaminated from a local, similar source (Figure 2-29).

2.3.4.3 Evaluation of Bivariate Plots and Mixing Lines Using Selected Chemical Concentration Ratios. Following is a brief discussion of results of the bivariate plot and mixing line evaluation for ^{99}Tc/nitrate versus nitrate and ^{99}Tc/sulfate versus sulfate summarized in ECF-Hanford-13-0037. An evaluation of bivariate and mixing lines for nitrate/chloride versus chloride was also done as a part of the ECF-Hanford-13-0037 analysis but is not provided in the section. The reader is referred to ECF-Hanford-13-0037 for more information on the latter analysis.

2.3.4.3.1 Evaluation of Technetium-99/Nitrate Ratio Versus Nitrate. Bivariate plots of ^{99}Tc/nitrate ratio versus nitrate by year, provided in Figure 2-30, were used to examine overall trends in these specific constituents and evaluate mixing lines between the end-member waters and upgradient water types.

From the bivariate plots of ^{99}Tc/nitrate versus nitrate, three different end-member waters (reflecting varying sources) were identified and mixing lines were calculated between the end-member waters and the upgradient water type characterized in this case by chemical concentrations found in well 299-E27-12.

In 2008, the characteristics of the end-member waters were associated with wells 299-E27-23, 299-E27-155, and 299-E27-14. The concentrations from wells that fall along the mixing lines can be explained by dilution of the end-member water with the uncontaminated upgradient water.

By 2010, bivariate plots show end-member waters were still associated with wells 299-E27-23, 299-E27-155, and 299-E27-14. However, because of large increases in ^{99}Tc observed in well 299-E27-23 and associated with well 299-E27-13, the magnitude of the ratios for these two wells are much larger than seen in 2008.

By 2012, bivariate plots show end-member waters were still associated with wells 299-E27-23, 299-E27-155, and 299-E27-14. However, some shifting of the position of two wells, 299-E27-13 and 299-E27-21, is observed. With the decline in ^{99}Tc concentrations in well 299-E27-13, the position of this well shifts to come closer to the mixing line between wells 200-E27-12 and 299-E27-155. As ^{99}Tc concentrations begin to increase in well 299-E27-21, its position on the plot shifts from the mixing line between well 299-E27-12 to well 299-E27-14 to a location just above the mixing line between wells 200-E27-12 and 299-E27-155.

By 2013, bivariate plots show some shifts in some of the wells in response to changing ^{99}Tc concentration levels in wells 299-E27-23 and 299-E27-21 that result from changing groundwater conditions from a southwesterly flow to a more south-southeast direction. By 2013, end-member waters are associated with wells 299-E27-21, 299-E27-155, 299-E27-4, and 299-E27-14. At this time, well 299-E27-23 fell on the mixing line between wells 299-E27-12 and 299-E27-21. The increase in ^{99}Tc/nitrate ratios in wells 299-E27-14 and 299-E27-24 seems to correlate with corresponding increasing ^{99}Tc concentrations in these wells in 2013.

2.3.4.3.2 Evaluation of Technetium-99/Sulfate Ratio Versus Sulfate. To complement the bivariate plots of ^{99}Tc/nitrate versus nitrate presented in the previous section, the BP-5 RI evaluation also examined bivariate plots of ^{99}Tc/sulfate versus sulfate. The resulting bivariate plots of these constituents are provided in Figure 2-31.

From the bivariate plots of ^{99}Tc/sulfate versus sulfate, three different end-member waters (reflecting varying sources) were also identified and mixing lines were calculated between the end-member waters and the upgradient water type characterized by chemical concentrations found in well 299-E27-12. The identification of three different end members and the shifting of the relative positions of wells among the mixing lines were nearly identical to those found using the ^{99}Tc/nitrate versus nitrate plots. This is supporting evidence in the strong correlation of nitrate and sulfate in this evaluation.

2.3.4.3.3 Nitrate/Chloride Ratio Versus Chloride. The BP-5 RI also examined bivariate plots of nitrate/chloride versus chloride to evaluate overall trends in these specific constituents. Results of these bivariate plots by year are provided in Figure 2-32.

Figure 2-22. Technetium-99 Concentrations above the Drinking Water Standard at Waste Management Area C Wells from January 2006 through December 2015.

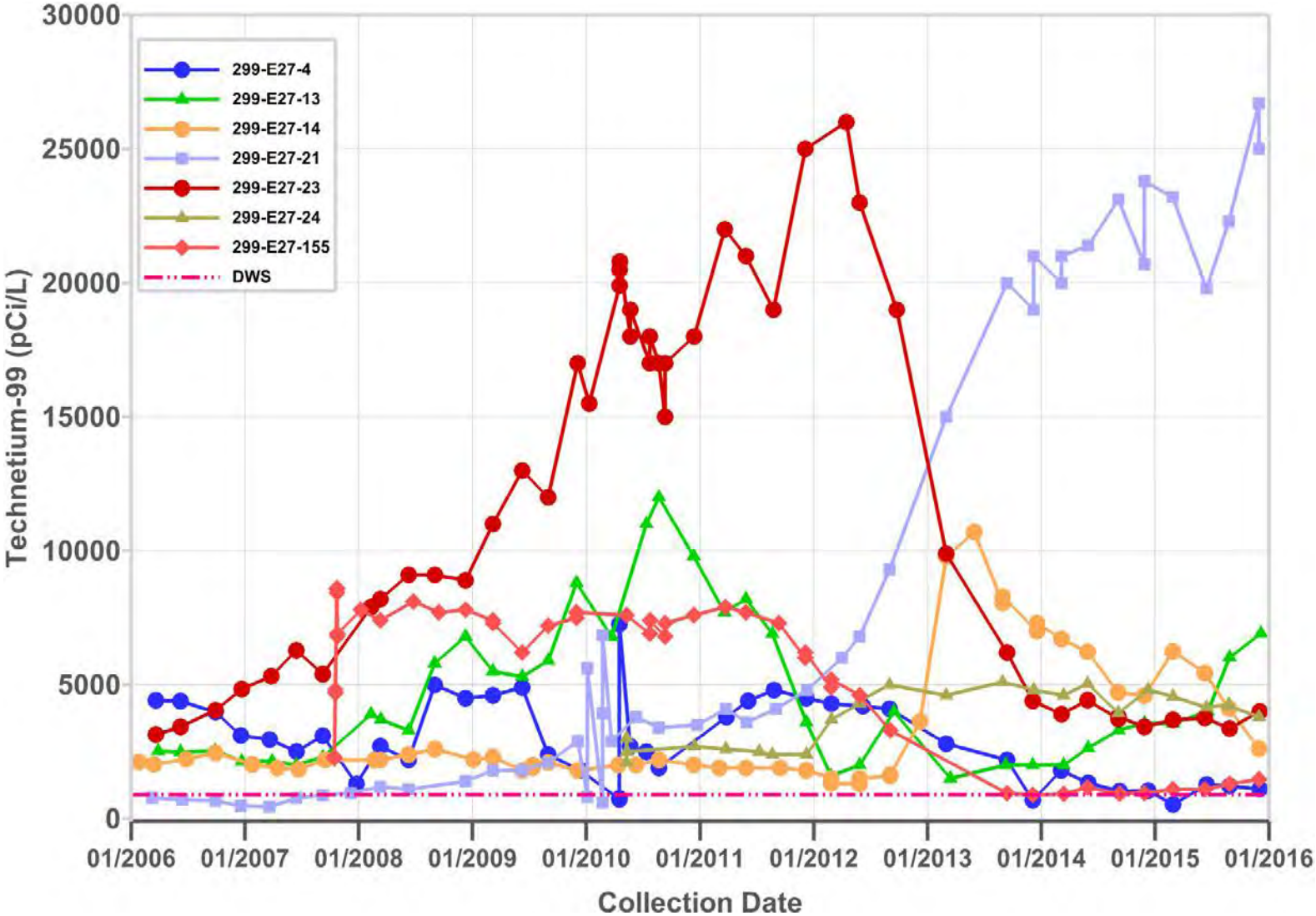

DWS = drinking water standard

Figure 2-23. Nitrate Concentrations above the Maximum Contaminant Level at Waste Management Area C Wells from January 2006 through December 2015.

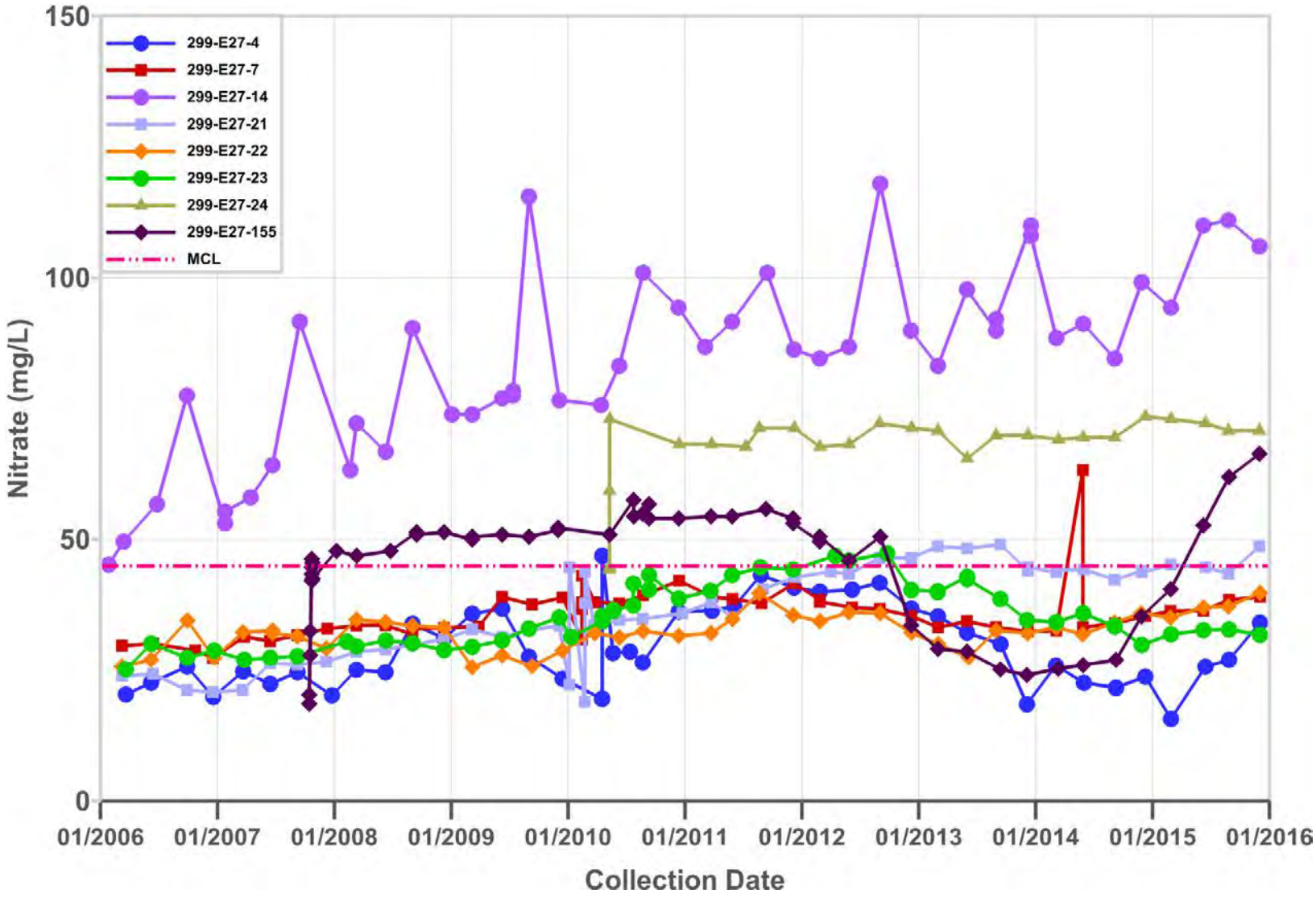

MCL = maximum contaminant level

Figure 2-24. Sulfate Concentrations above the Secondary Maximum Contaminant Level at Waste Management Area C Wells from January 2006 through December 2015.

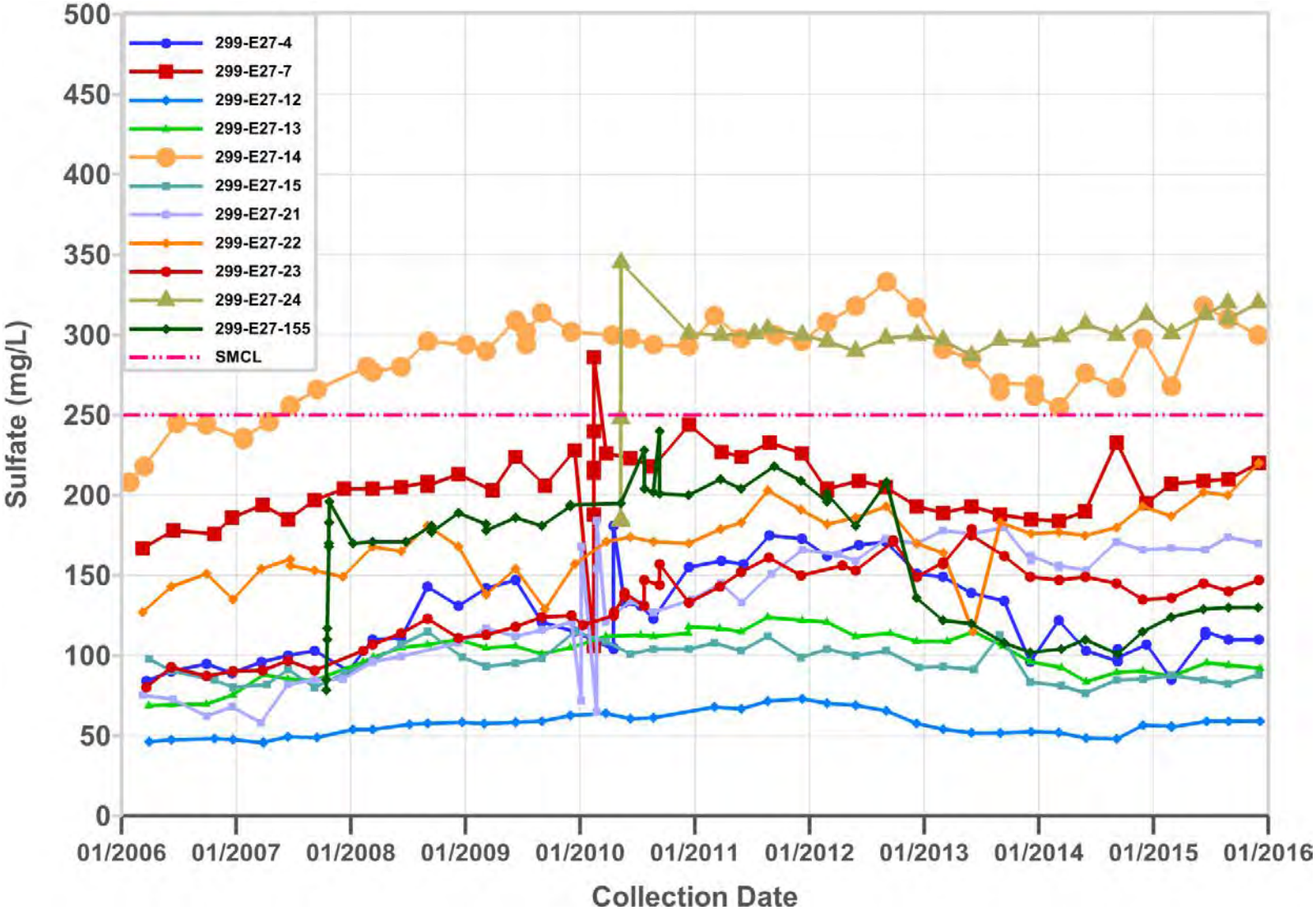

SMCL = Secondary maximum containment level

Figure 2-25. Cyanide Concentrations in Waste Management Area C Wells from January 2006 through December 2015.

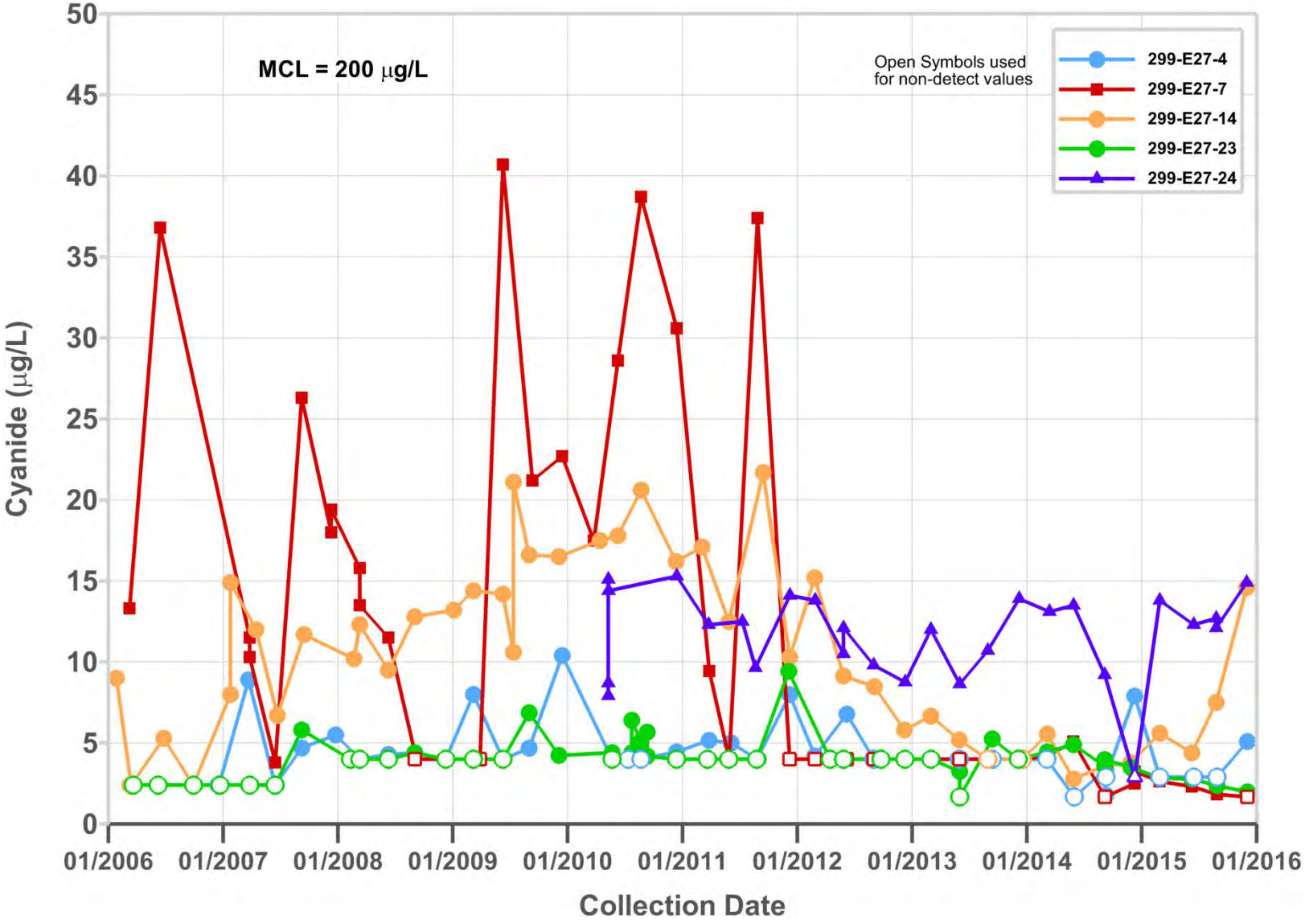

MCL = maximum contaminant level

Figure 2-26. Technetium-99 Activity in Wells 299-E27-7, 299-E27-14, and 299-E27-24 on East and Southeast Side of Waste Management Area C.

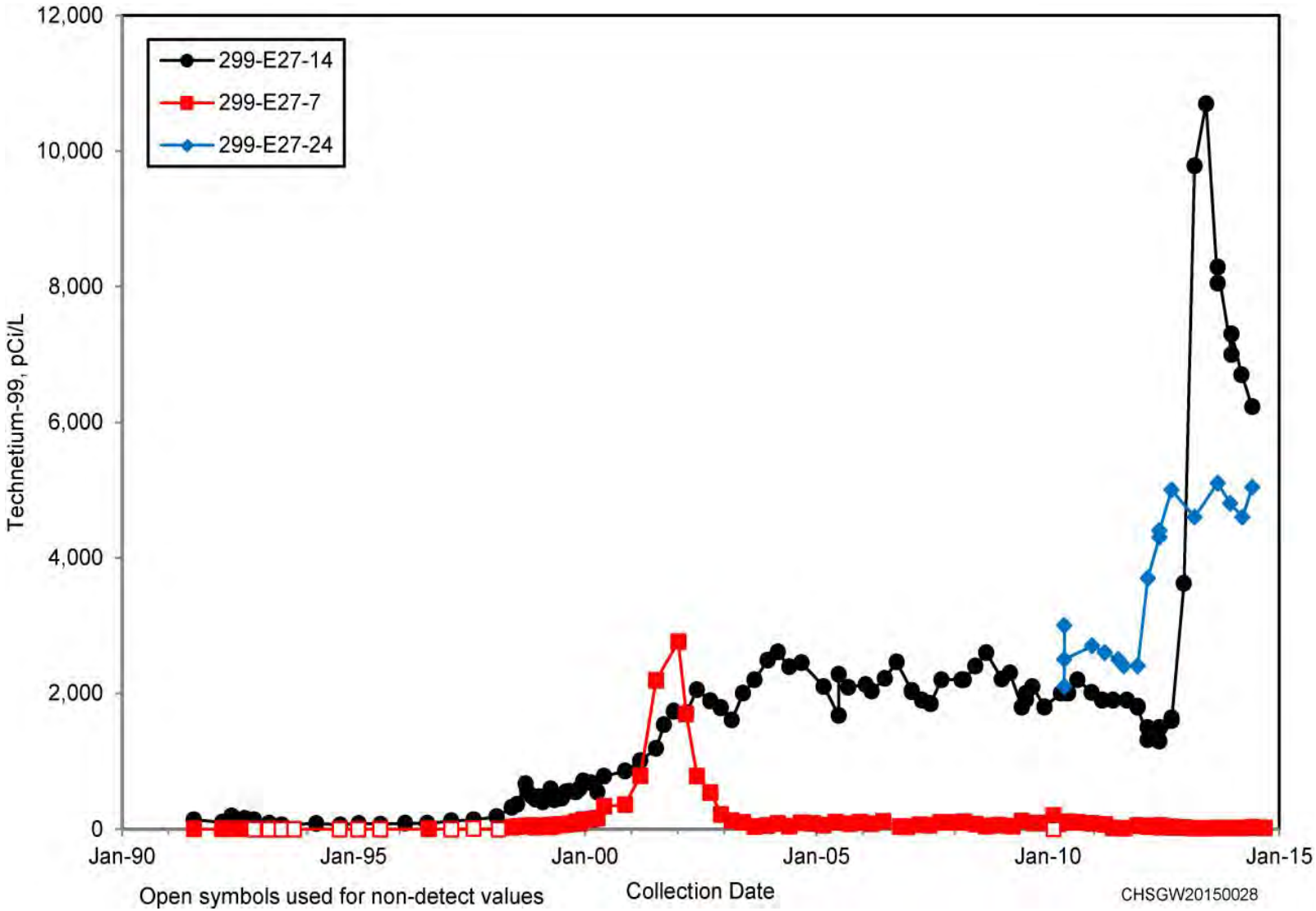

Reference: DOE/RL-2009-127, *Remedial Investigation Report for the 200-BP-5 Groundwater Operable Unit*, Draft A.

Figure 2-27. Technetium-99 Activity in Wells 299-E27-4, 299-E24-13, and 299-E27-23 on West Side of Waste Management Area C.

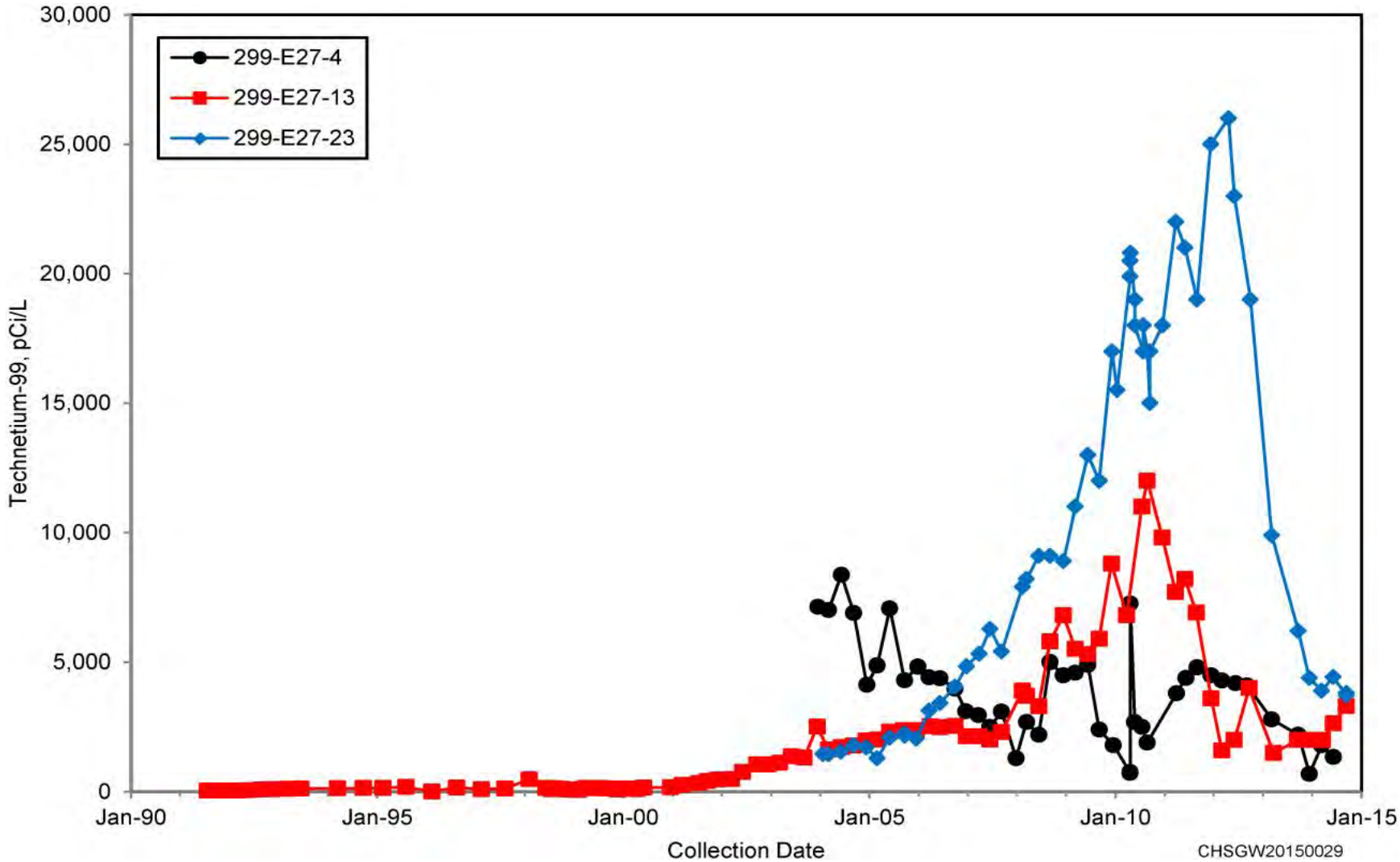

Reference: DOE/RL-2009-127, *Remedial Investigation Report for the 200-BP-5 Groundwater Operable Unit*, Draft A.

Figure 2-28. Technetium-99-to-Nitrate Ratio Comparisons for Wells on West Side (299-E27-21 and 299-E27-23) and Southeast Side (299-E27-14 and 299-E27-23) of Waste Management Area C.

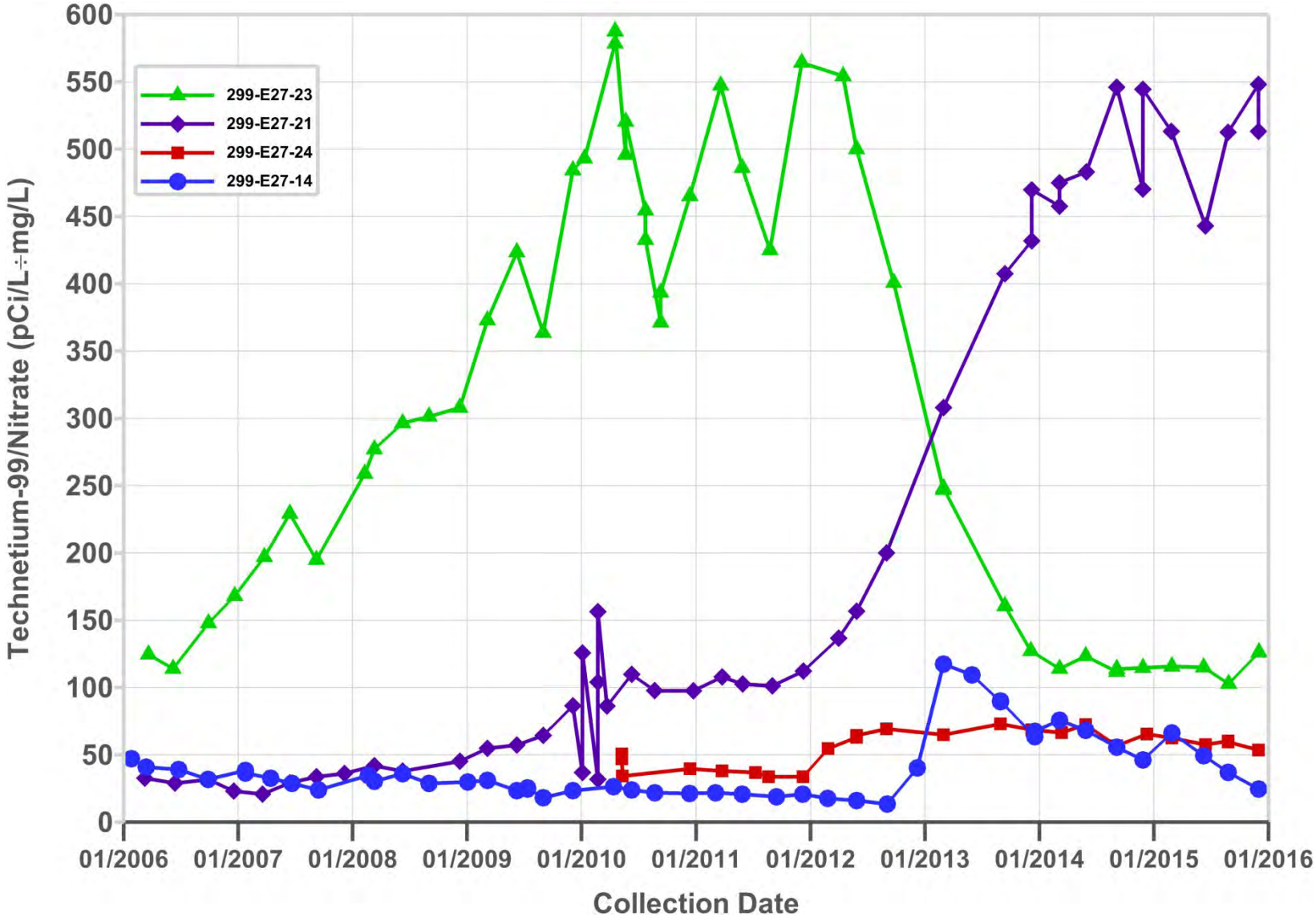

Figure 2-29. Cyanide-to-Nitrate Ratio Comparisons for Well 299-E27-14.

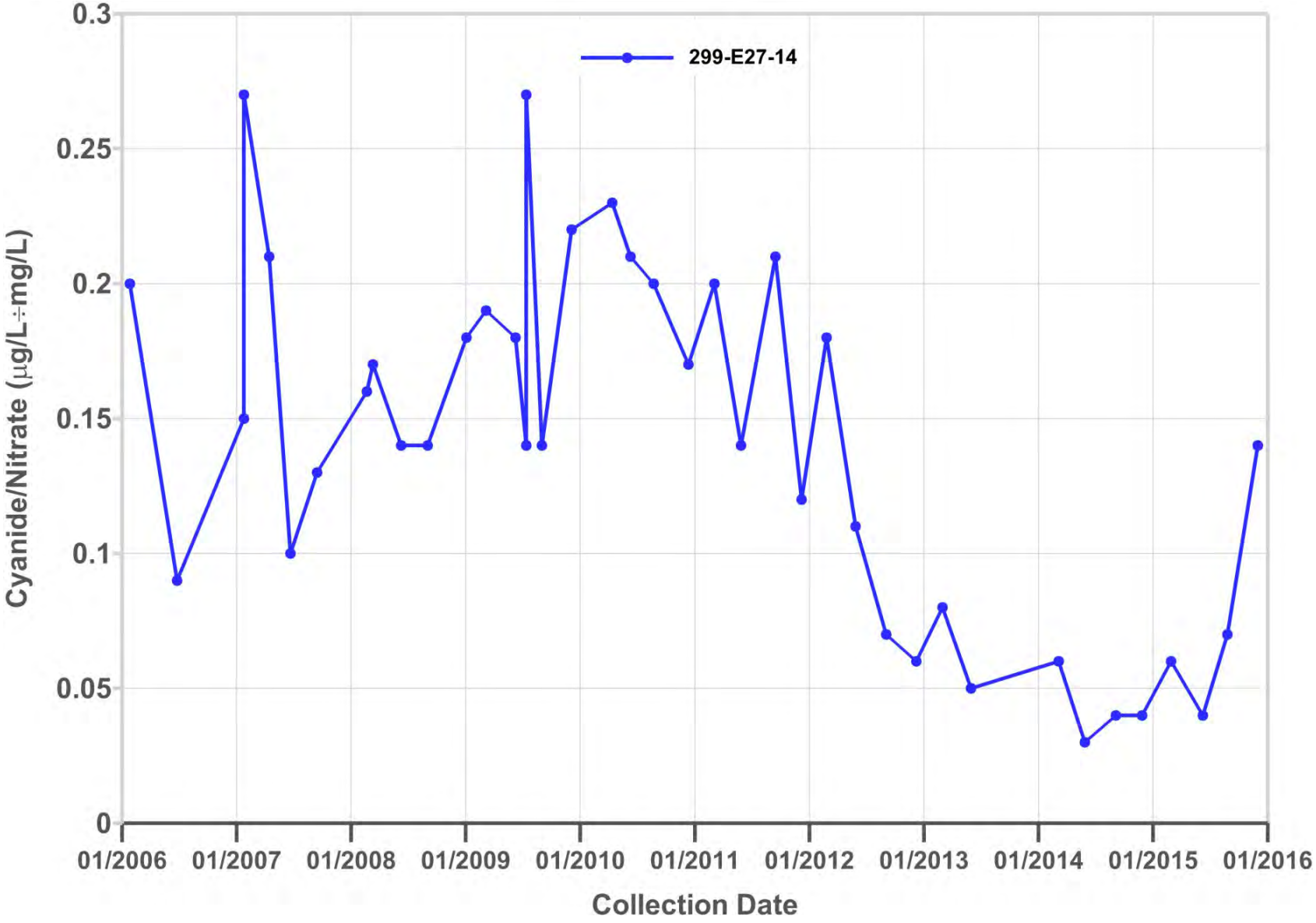

Figure 2-30. Bivariate Plots of Technetium-99/Nitrate Ratio Versus Nitrate by Year.

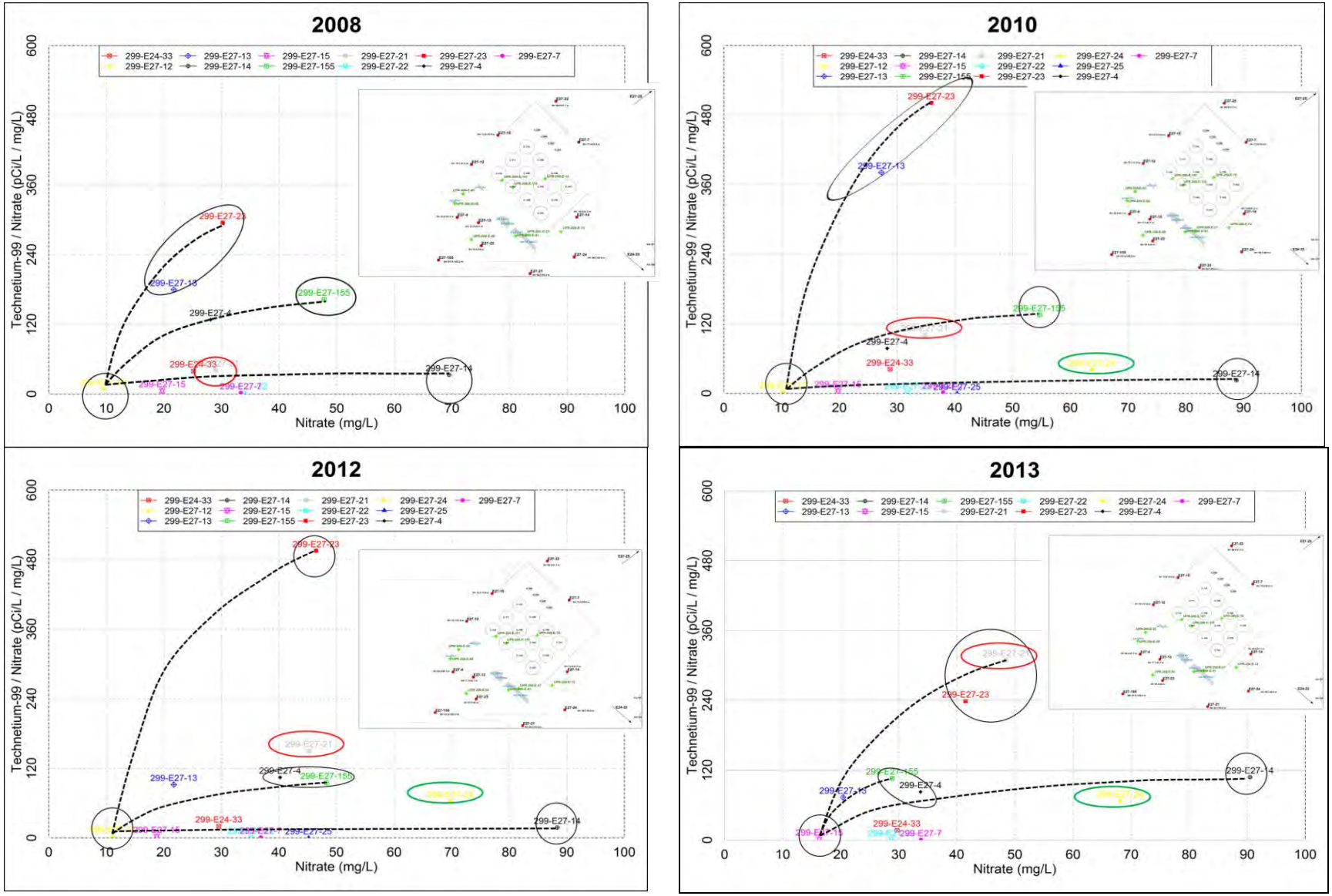

Figure 2-31. Bivariate Plots of Technetium-99/Sulfate Ratio Versus Sulfate by Year.

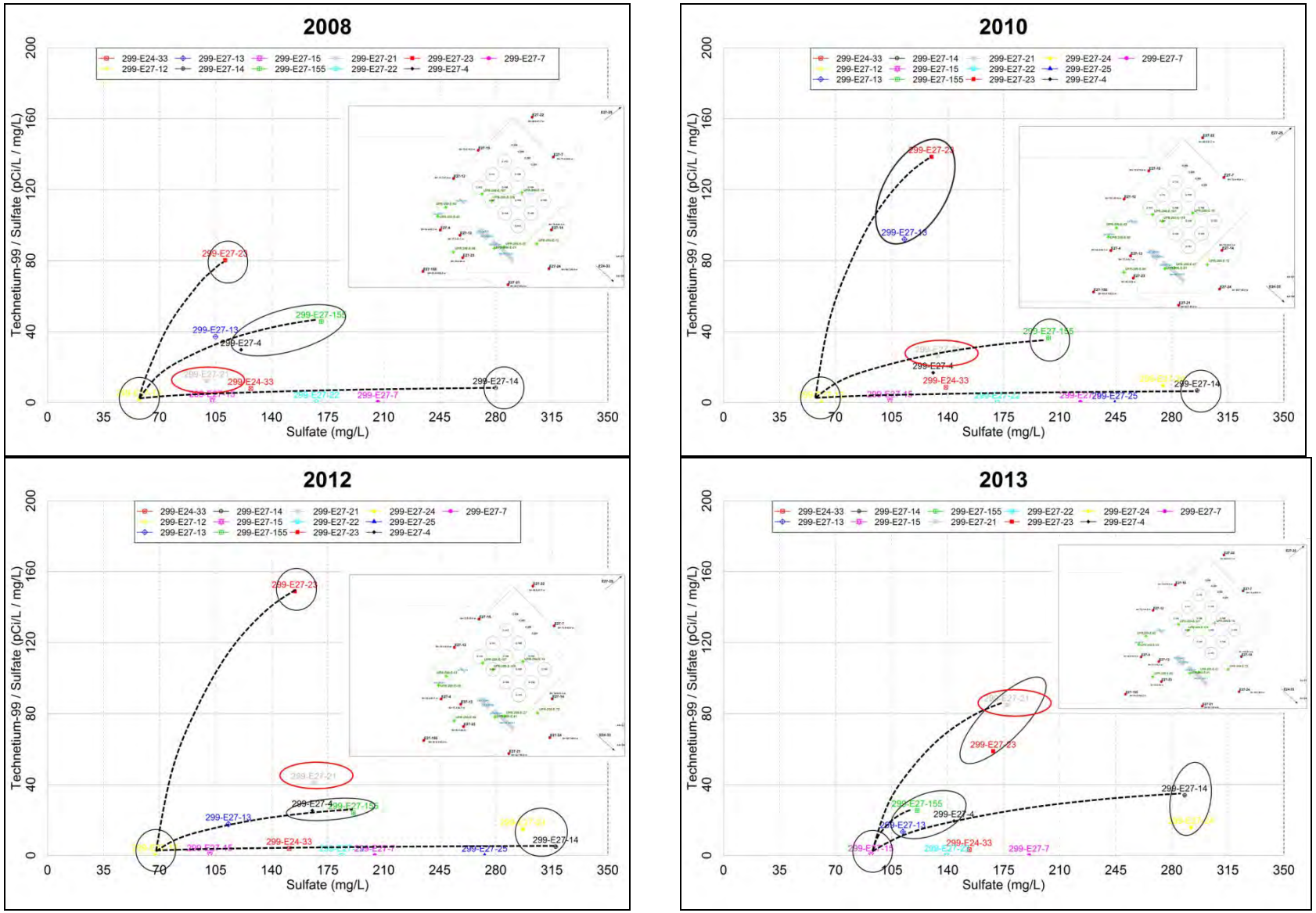

Figure 2-32. Bivariate Plots of Technetium-99/Chloride Ratio Versus Chloride by Year.

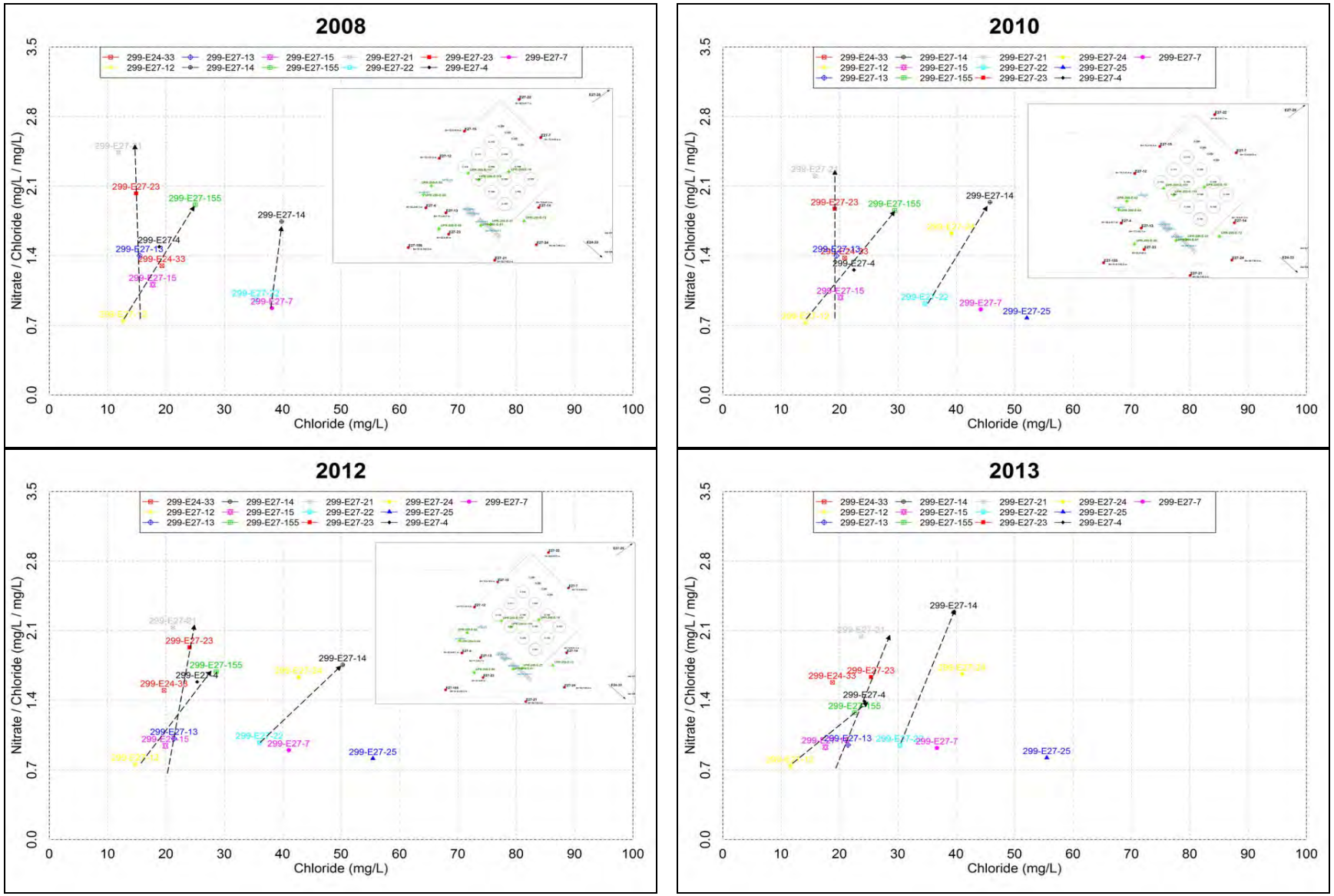

From the bivariate plots of nitrate/chloride versus chloride, three different end-member waters (reflecting varying sources) were identified and mixing lines were calculated between the end-member waters and the upgradient water type. The identification of three different end members and the shifting of the relative positions of wells among the mixing lines were different to those found using the other bivariate plots of ^{99}Tc/nitrate versus nitrate and ^{99}Tc/sulfate versus sulfate.

2.3.4.4 Estimates of Technetium-99 Flux from the Vadose Zone. Two independent methods have been used for estimating ^{99}Tc flux from the vadose zone to the saturated zone in the WMA C vicinity (ECF-Hanford-13-0037; DOE/RL-2009-127, Draft A).

2.3.4.4.1 Method 1: Plume Volume from Annual Groundwater Monitoring Reports. This approach takes the plume shapes defined by the Annual Groundwater Monitoring Reports of the past five years and assumes they are correct and uniform through the saturated thickness. The activity and mass are calculated for each year, and then the difference in activity and mass between each year is the amount added or reduced each year.

This approach is relatively simple and quick. It uses data and interpretations that have been published. The possibility of combining sub-plumes into one large plume, as well as the bias towards increased plume areas where data are scarce, mean this approach is more likely to over-estimate plume volume (ECF-Hanford-13-0037).

2.3.4.4.2 Method 2: Interpreted Plume Approach. The interpreted plume method uses data from at least the past ten years to create site conceptual models that take account of flow paths and major ion chemistry in order to determine the plume extent. This approach acknowledges that the lower-concentration parts of the plume are not as easily constrained or understood as the zone of high concentration. The more easily understood zone of high concentration is then used as the control volume, and the mass flux is derived based on the flow rate through the control volume, which causes changes in the dissolved concentration. The observed changes in the dissolved concentration define the mass flux.

This approach is more complex than the first estimation method, but can be distilled to a simple conceptual model as seen in Figure 2-33. Mass flux in the saturated zone is controlled by the inflow of water as well as the mass coming in from the vadose zone. The basis of this conceptual model is that the persistence of some plumes is due to continued mass coming in from the vadose zone, as the water flowing through the system would tend to move the contamination out of the control volume, so any mass output would have to be replaced by mass input from the vadose zone to maintain concentrations in the control volume.

This approach assumes Dupuit conditions in an unconfined aquifer, which assumes (ECF-Hanford-13-0037):

- The water table or free surface is only slightly inclined

- Streamlines may be considered horizontal and equipotential lines are vertical
- Slopes of the free surface and hydraulic gradient are equal.

Figure 2-33. Conceptual Model for the Vadose Zone Flux Calculation.

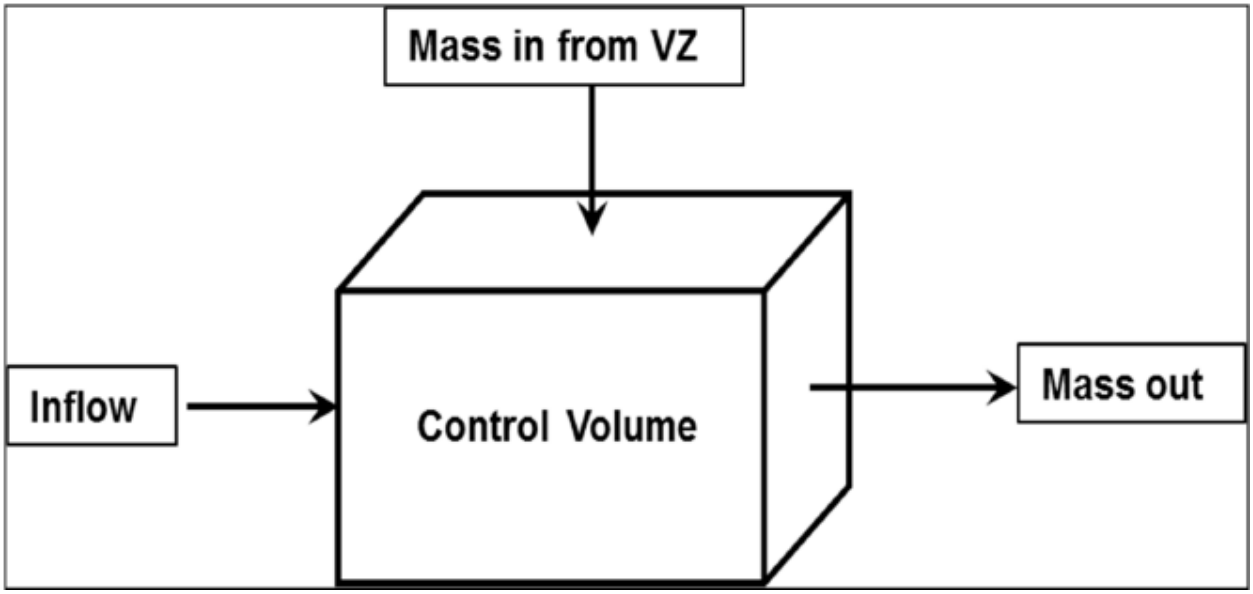

VZ = vadose zone

The groundwater flow equation of continuity is used:

$$\frac{\partial^2 h_x}{\partial x^2} + \frac{\partial^2 h_y}{\partial y^2} + \frac{\partial^2 h_z}{\partial z^2} = 0$$

where h_x, h_y, and h_z are the hydraulic head in the x, y, and z directions. The mass balance equation is also used:

$$\left(\frac{M}{\Delta t}\right)_{UZ} = (Q_s \Delta C)_{SZ}$$

where the left side is the mass flux from the vadose zone (g/yr or Ci/yr) and the right side is the saturated zone mass flux defined by flow rate (Q_x) times the change in concentration (ΔC). Further discussion of the appropriate application of the above equations can be found in ECF-Hanford-13-0037, Section 2.

2.3.4.4.3 Flux Estimation. In the first method, using information from the Groundwater Annual Reports, the calculated total activity residing in the saturated zone is estimated to be ~1 Ci, and it shows an increasing trend (see Figure 2-34). It has been concluded that this value is an overestimate, owing to the extrapolation of the plume area to regions where information is not available (ECF-Hanford-13-0037). Using this method, the average increase in ^{99}Tc activity from year 2008 to year 2012 is calculated to be ~0.17 Ci per year. It was assumed that 6 Ci of ^{99}Tc remains in the vadose zone (ECF-Hanford-13-0037 based this estimate on the data provided in

RPP-ENV-33418). It was concluded from these values that it will take about 35 years for the ^{99}Tc in the vadose zone to be released into the saturated zone, assuming uniform flux (ECF-Hanford-13-0037).

Figure 2-34. Estimates of the Activity of Technetium-99 by Two Alternative Methods.

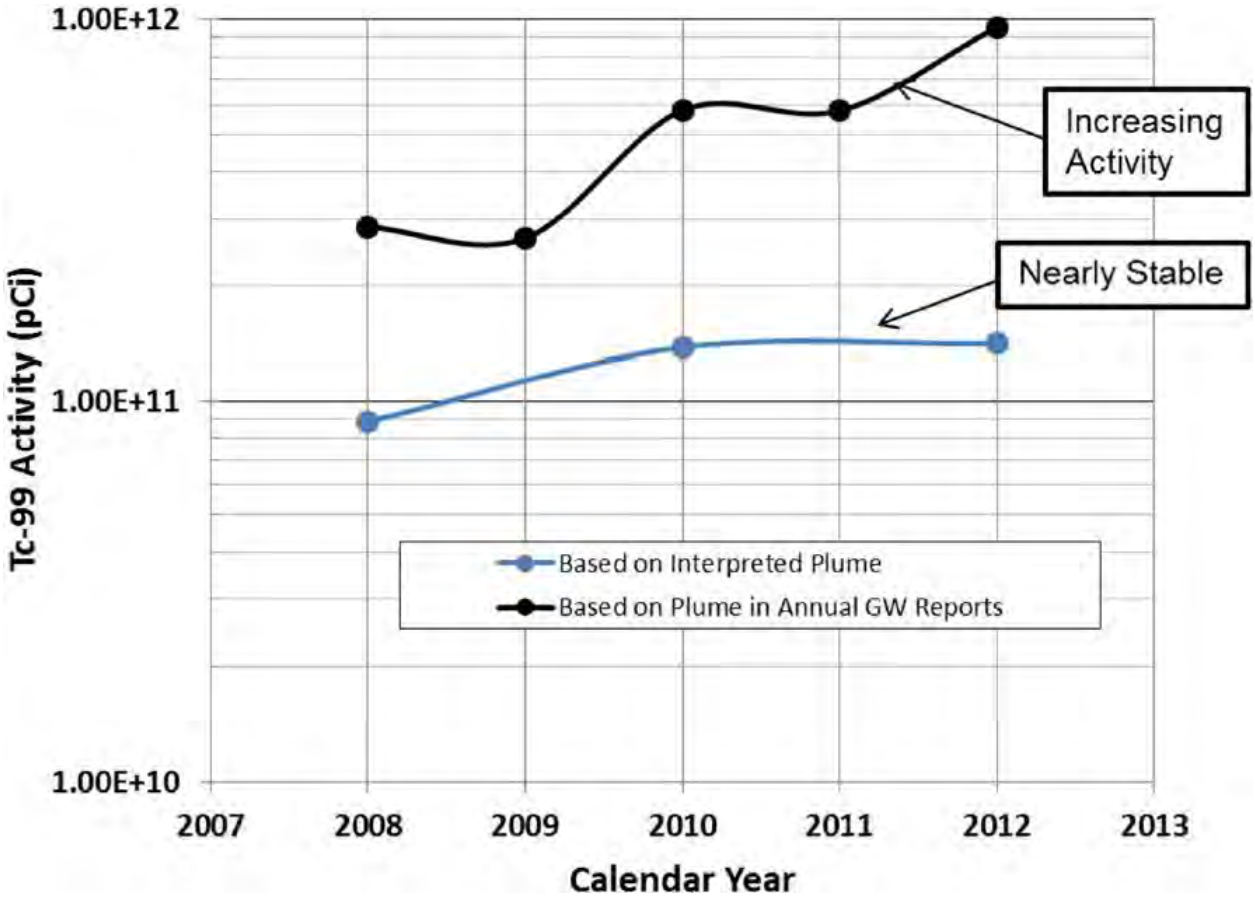

Reference: ECF-Hanford-13-0037, *Development of Source Terms for Inclusion in Fate and Transport Modeling for Remedial Investigation/Feasibility Studies of the 200-BP-5 and 200-PO-1 Groundwater Operable Units.*

In the second method, which combined site-specific conceptual models to evaluate a mass balance for ^{99}Tc, the current total activity residing in the saturated zone was estimated to be ~0.14 Ci. Using this method, the activity in the control volume is calculated to have reached a steady state, meaning that the rate at which ^{99}Tc is being transported downgradient is approximately equal to the rate at which it is being transported from the vadose zone to the saturated zone (see Figure 2-34). This rate was estimated to be 0.1 Ci per year (ECF-Hanford-13-0037). Using the estimate of 6 Ci of ^{99}Tc remaining in the vadose zone (see above), it will take approximately 60 years to be released to the saturated zone.

The results of this analysis provide a summary of recent interpretations based on WMA C groundwater chemistry undertaken by the 200-BP-5 Remedial Investigation.

This page intentionally left blank.

3.0 FEATURES FOR ANALYSIS

The analysis of past leaks has been structured to meet several goals. First, the analysis is intended to be responsive to ideas and concerns expressed in the 2009 – 2011 PA scoping sessions (see Section 1.1.1), in which specific features of WMA C were identified as requiring particular attention because of their potential to influence the migration of contaminants from WMA C. Second, the analysis is intended to be consistent, to the extent possible, with the PA (RPP-ENV-58782) and RCA (RPP-ENV-58806) for disposal of residual wastes in WMA C. Third, the goal is to provide an understanding of the key features and processes discussed in in the data packages produced for the scoping sessions (see Section 1.1.1) that influence the migration of contaminants. Fourth, the goal is to use the understanding gained by the analysis to provide a projection of the future evolution of the contamination beneath WMA C.

This section provides an overview of the model interpretation of the site description and data +presented in Sections 1 and 2. This section describes the conceptual models of WMA C relevant to the assessment of past leaks, and the implementation of associated mathematical models. The information related to the analysis and modeling approach is presented in the following subsections:

- Overview of analysis;
- Adaptation of the PA conceptual and numerical models used in the evaluation of waste residual impacts;
- Conceptual model of source term releases;
- Aquifer considerations; and
- Mathematical models.

3.1 OVERVIEW OF ANALYSIS

The strategy for this analysis of leaks at WMA C has been to define and analyze a suite of scoping cases to evaluate the uncertainties associated with past leaks. The approach has been to compare model results to key data in the groundwater monitoring. No specific adjustments or calibrations to the model to match historical observations were performed; the model was run for a variety of alternative assumptions and input parameters, to evaluate which inputs provided results that were consistent with data, and which inputs provided results that were inconsistent with data. These key uncertainties in the analysis of past leaks can be broadly considered to originate from one of the following sources:

- Uncertainties exist in the timing, inventory, and volumes of leaks. These uncertainties have been discussed at length in Revision 4 of RPP-ENV-33418 during operational waste transfers. These uncertainties include:
    - Limitations found in tank process reports and assessments;
    - Difficulties in interpreting in-tank liquid level measurements using different types of measurement devices;
    - Gaps in waste transfer records;
    - Moisture monitoring data;
    - Logging data;
    - Limited well spacing and frequency of logging;
    - Multiple probe types provide different results;
    - Limited vadose zone sampling and analysis; and
    - Multiple potential sources for some leaks.
- Uncertainties exist in past actions taken to mitigate the surface manifestations of past leaks. For several UPRs, water was added via firehose to surface contamination to wash it down into the soil column. Alternative scoping cases that examine to the potential effects of increases in recharge include Cases 3a, 3b, and 3c (See Table 4-1 for descriptions of these cases). Results from these alternative scoping cases are discussed in Section 4.3.
- Uncertainties exist in interpreting the groundwater monitoring and vadose zone characterization data based on the interpretation of contamination levels observed in groundwater and the vadose zone resulting from past leaks. This uncertainty exists because data represents specific point locations in the subsurface and needs to be interpolated in space and time for development of the interpretations.
- Uncertainties exist in the hydrogeological representation of the stratigraphy below WMA C (RPP-RPT-56356). These uncertainties have been addressed in RPP-ENV-58782 and RPP-ENV-58806 by evaluating the consequences of alternative interpretations of the hydrogeology. This approach has continued to be used in this document. Alternative scoping cases that examine to the potential effects of alternative conceptual models of the hydrogeologic framework include Cases 4a through 4f (See Table 4-1 for descriptions of these cases). Results from these alternative scoping cases are discussed in Section 4.4.

- Uncertainties exist in the effective values of parameters used in modeling groundwater flow and contaminant transport. These uncertainties are discussed in detail in RPP-ENV-58782 and RPP-ENV-58806.

- Uncertainties exist regarding the evolution of the groundwater system at WMA C over the past several decades, as discussed in Section 2. Anthropogenic water introduced south of WMA C created a gradient generally to the north, which has transitions over recent decades to a gradient generally southward. The transition between these two states occurred approximately coincident with the arrival of the first contaminants at the water table. The feature of the groundwater system evolution introduces additional uncertainties about the trajectory of plumes moving in the aquifer. In addition, it is acknowledged that a compliant groundwater monitoring network was not present at WMA C until 1989, almost a decade after most tanks stopped operating. This lack of monitoring information before 1989 introduces another element of uncertainty when evaluating model results against monitoring observations.

The analyses of potential releases of contaminants in residual wastes presented in RPP-ENV-58782 and RPP-ENV-58806 were focused on future site conditions. Peak impacts from the residual wastes were shown to occur thousands to tens of thousands of years in the future, and this conclusion was very robust to alternative assumptions and input parameters. However, since the impacts from residual wastes will occur so far in the future, it is not possible to directly compare model outputs with field data for groundwater concentrations. Therefore, by using the same model developed for residual waste analyses to evaluate past leaks, there is the potential to develop confidence in the model by comparing the results to current groundwater contamination data.

A complication arises because the two analyses are focused on different time periods; the prospective residual waste analyses look forward in time over thousands of years, whereas the past leaks analyses look to the past to model the time between the leak occurred and today. The complication is that conditions in these two time periods are somewhat different. In particular, the residual waste analyses did not directly address several sources of uncertainty that affect the past leaks analyses. Additionally, uncertainties associated with the past evolution of the water table from water discharges in both the 200 East and 200 West areas was not addressed. These effects are projected to be inconsequential for analyses of future conditions.

Therefore, in viewing the analyses in RPP-ENV-58782 and RPP-ENV-58806, there are some parts of the analysis that can be tested using comparisons with leak data, and there are some parts of the model that cannot be tested. A number of approaches to developing confidence in the data, assumptions, and methods were used in the residual waste analyses that also have direct applicability to the past leaks analyses and as a result did not directly address several of these sources of uncertainty. Specifically, the future analysis does not address those associated with the UPRs at WMA C and those associated with the past evolution of the water table, as water was discharged in both the 200 East and 200 West areas. However, in RPP-ENV-58782 and RPP-ENV-58806, a number of approaches were used to develop confidence in the data, assumptions, and methods, they are as follows.

- To the extent possible, data were based on WMA C-specific site characterization, sampling, measurements, and interpretations, including those for contaminant inventory, geology, hydrology and geochemistry. For estimates of contaminants inventories, due to the lack of specific data on specific waste compositions in a tank or in ancillary equipment at the suspected time of the leak, this analysis needed to rely on approaches used in the leak assessment process which involved the use of best basis inventory template compositions developed for waste types suspected to have been in the tank at the time of the suspected leak(s). When characterization data specific to WMA C were not available, data from nearby sites or comparable conditions, as well as data reported in the literature, were used. In all cases, when data are used that are not WMA C-specific, the basis for the use of these alternative sources of information is explained, providing the logical link for their use at WMA C

  Data were upscaled to represent field-scale processes using scientifically accepted approaches that have been published in peer-reviewed journals. Upscaling techniques use information from small, core-scale measurements to develop parameters that are applicable to large, field-scale models. Details of approaches to upscaling vadose-zone parameters are presented in Appendix B of RPP-ENV-58782 and RPP-ENV-58806. Details of the relationship between local-scale measurements of aquifer properties and the upscaled model representation are presented in Appendix C of RPP-ENV-58782 and RPP-ENV-58806.

- The process-based modeling software, Subsurface Transport Over Multiple Phases (STOMP)©[1] code (PNNL-12030, *STOMP Subsurface Transport Over Multiple Phases Version 2.0 Theory Guide*; Pacific Northwest National Laboratory, Queried 12/18/2015, *[STOMP User Guide]*, http://stomp.pnnl.gov/user_guide/STOMP_guide.stm; PNNL-11216, *STOMP Subsurface Transport Over Multiple Phases Application Guide*), has been benchmarked and deemed suitable for use in this PA. The STOMP© code has previously been qualified for simulation use at Hanford by CHPRC (CHPRC-00269, *STOMP Requirements Traceability Matrix CHPRC Build 4*). Sensitivity and uncertainty analyses were conducted to evaluate the effect of parameter uncertainties and alternative conceptual models on the overall performance of the system.

- One of the most important aspects of the tank waste residual analysis that is relevant is the good general agreement between modeled volumetric moisture results with average field measured volumetric moisture contents for the various hydrogeologic units in the vadose zone at WMA C. The agreement of modeled moisture contents with field measured values provides some confidence that the developed flow and transport process models being used here will produce reasonable flow and transport results in the vadose zone.

- Another aspect that is relevant in the tank waste residual analysis is the demonstration of very good agreement of simulated contaminant fluxes at the water table between the

[1] Subsurface Transport Over Multiple Phases (STOMP)© is copyrighted by Battelle Memorial Institute, 1996.

WMA C PA model and the Tank Closure and Waste Management EIS model (See Appendix G of RPP-ENV-58782 and RPP-ENV-58805) when the same inventories and release models used for Alternative 2b are evaluated in both models.

These approaches specifically address uncertainties in model conceptualizations and input parameters for groundwater flow and transport, but do not address uncertainties in past leaks and in past evolution of the groundwater table.

Consequently, the model used in RPP-ENV-58782 and RPP-ENV-58806 was adapted for the past leaks scoping analyses such that the water table was reflective of conditions at WMA C when first arrival of contaminants at the water table was observed. During the time between when the leaks occurred and when they arrived at the water table, the aquifer was elevated from the addition of water in both 200 East and 200 West Areas. In addition to the water table elevation, it is believed that the flow direction was variable during this time, generally changing from flow to the northwest, shifting to the southeast, with the timing of the shift coinciding with the arrival of contaminants at the water table.

Two approaches were used to address the complications the shifting water table causes for the modeling. In the first approach, the water table was assumed to be fixed or at steady state, and directed in the same way as the prospective water table used for future analyses, but at a higher level, which allows the analysis to represent the shorter travel time in the vadose zone that would have existed when the plumes initially arrived. This approach is intended to represent the time of first arrival and the peak of the groundwater plume but is not necessarily to represent the spatial distribution of contamination in the groundwater. Therefore, this first approach can be used to test the model representation of the leaks and vadose-zone behavior, separate from the complications the shifting aquifer causes. The second approach was to introduce a time-varying or transient water table to represent the likely evolution of the aquifer gradient over the simulation period. This second approach requires the introduction of speculation regarding the timing, orientation, and magnitude of the aquifer gradient since these are all unknown. However, it has the benefit that the resulting model can be directly compared to all aspects of the groundwater concentration data. Both approaches are described in more detail in Section 4.

The model was initially compared to ^{99}Tc concentrations in groundwater, since ^{99}Tc is a key risk driver and the contamination levels observed in groundwater monitoring wells are considered to be the result of WMA C past leaks. The ^{99}Tc concentration data observed in groundwater monitoring wells have been used to evaluate the input conditions that are consistent with the arrival times and concentration levels of ^{99}Tc observed historically in the vicinity of WMA C. As discussed in the preceding paragraph, the static water table analyses were compared to the first arrival time and are intended to evaluate how well the model performed in representing the leaks and the vadose zone. Whereas the dynamic water table analyses are intended to test the overall model behavior. The resulting constrained model was then also compared with other contaminant data as appropriate.

3.2 ADAPTATION OF THE PERFORMANCE ASSESSMENT CONCEPTUAL AND NUMERICAL MODELS USED IN THE EVALUATION OF WASTE RESIDUAL IMPACTS

The foundation of the conceptual models used in this document is the model(s) developed for the analysis of releases associated with residual wastes as described in RPP-ENV-58782 and RPP-ENV-58806. The basis for that model is reviewed in this section as it is applied to the past leaks analysis. The initial basis for the model has been the Base Case model in RPP-ENV-58782 and RPP-ENV-58806, with appropriate changes to the depth to the water table to reflect the conditions that existed when data showed the leaks arriving at the water table. This change was made to improve the correlation of the calculated and observed first arrival of contaminants at the water table. This initial basis forms the first analysis case to be evaluated (see Section 4); additional scoping analysis cases have been carried out to explore the effects of alternative conceptual models and input assumptions. These alternative analysis cases have also been described in Section 4.

The WMA C PA methodology (RPP-ENV-58782 and RPP-ENV-58806) uses conceptual models that are based on the physical system and expected contaminant migration pathways. Figure 3-1 provides a schematic representation of both WMA C at closure and the contaminant migration into the environment along the various pathways evaluated in the PA. The WMA C site is composed of both man-made and natural components that are represented in the model. The man-made components of the system that influence contaminant migration include a closure surface barrier, the WMA C tanks, pipelines, and infrastructure, and the distribution of waste in those components. The natural components of the system that influence contaminant migration are a number of mostly horizontal to slightly dipping (to the northeast) stratigraphic layers within the saturated and unsaturated zones, net infiltration resulting from rainfall, and any antecedent moisture conditions (and contaminants) within WMA C or from adjacent sites. Figure 3-2 illustrates the major stratigraphic units for the thick vadose zone at WMA C.

The water table at WMA C is located within the undifferentiated Hanford formation and Cold Creek gravels, and, during Hanford operations, was strongly influenced by large volumes of liquids that were discharged to the subsurface at major waste water discharge facilities located in and around 200 East Area, raising the groundwater elevation in the 200 East Area and vicinity (Figures 2-10 and 2-11). Since the termination of processing operations, the groundwater mounds in the 200 East Area have been dissipating and groundwater flow velocities have slowed. Since the groundwater gradient in the area is so flat, the groundwater monitoring network at WMA C does not have sufficient resolution to use data to directly show the timing and magnitude of the groundwater gradient at WMA C. However, the effect can be illustrated using the nearby low-gradient Low-Level Waste Management Area (LLWMA)-1 monitoring network shown in Figure 3-3. In the period prior to about 2007 to 2008, the gradient orientation at LLWMA is approximately north. Then comes a period between 2008 and mid-2011 when the gradient is ambiguous, variable, and for the most part statistically indeterminate. Since that time, the gradient has been approximately south as it returns to its natural gradient as the water mounds dissipate.

A similar pattern of behavior is believed to have occurred at WMA C, with minor differences in the timing of changes, and in the magnitude and orientation of the gradient. As noted above, reliable determination of the gradients at WMA C is not possible because they are so flat that gradient determination requires special methods. The existing estimates of the hydraulic gradient appear to be sufficient for the purpose of the IPA. Adding transducers would not provide particularly useful information applicable to the past leak breakthrough time frame, and the impacts from the tank residuals are not projected to occur for thousands of years. Consequently, analysis of the behavior of the aquifer during this time period is best undertaken using modeling.

Figure 3-4 shows an aerial view of WMA C, and surrounding disturbed, undisturbed, and resurfaced areas.

Figure 3-1. Schematic Conceptual Representation of Waste Management Area C and Contaminant Migration into the Environment along the Various Pathways Evaluated in the Performance Assessment.

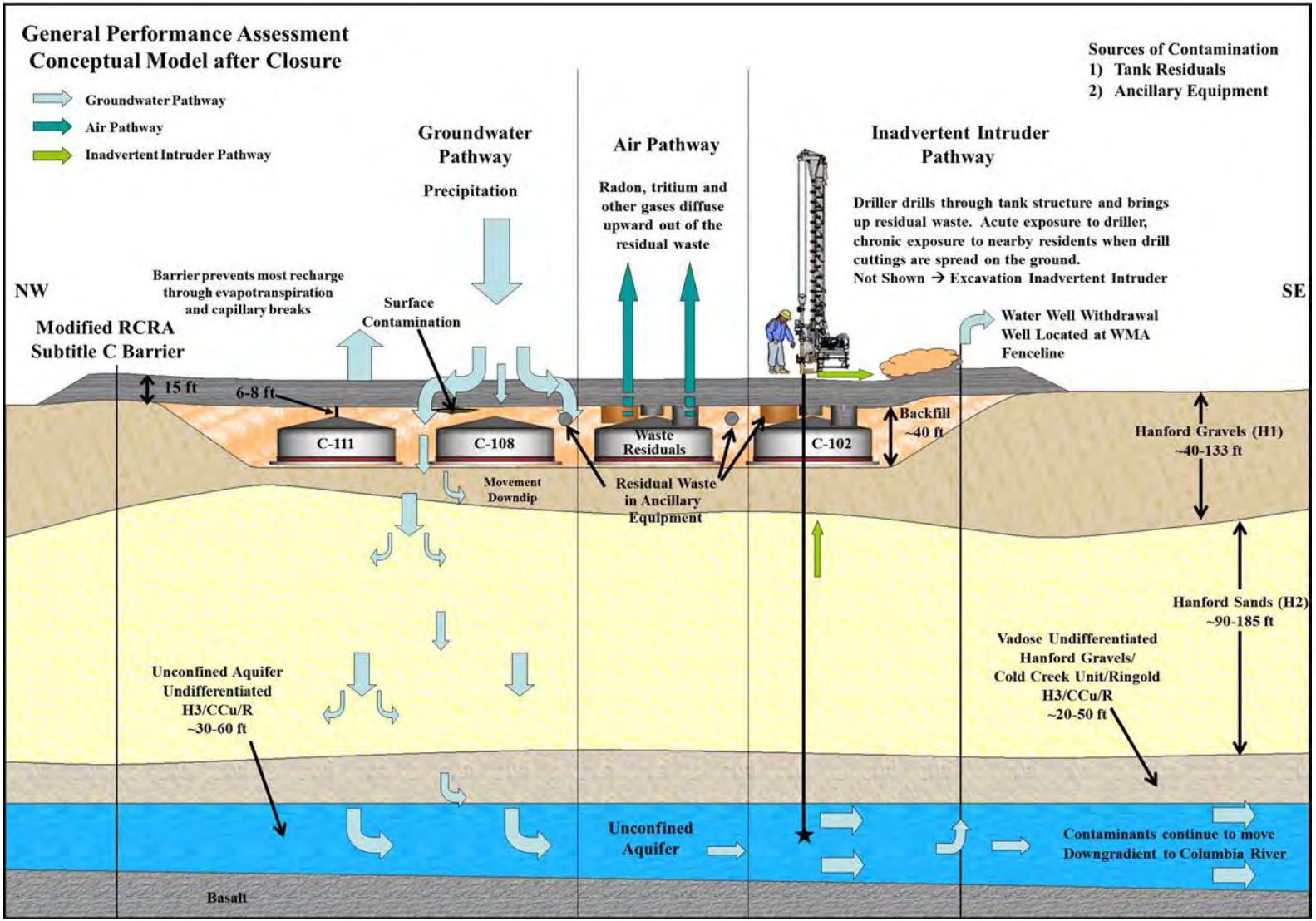

RCRA = Resource Conservation and Recovery Act of 1976 WMA = Waste Management Area

Figure 3-2. Conceptual Model of the Waste Management Area C Site Showing Stratigraphy.

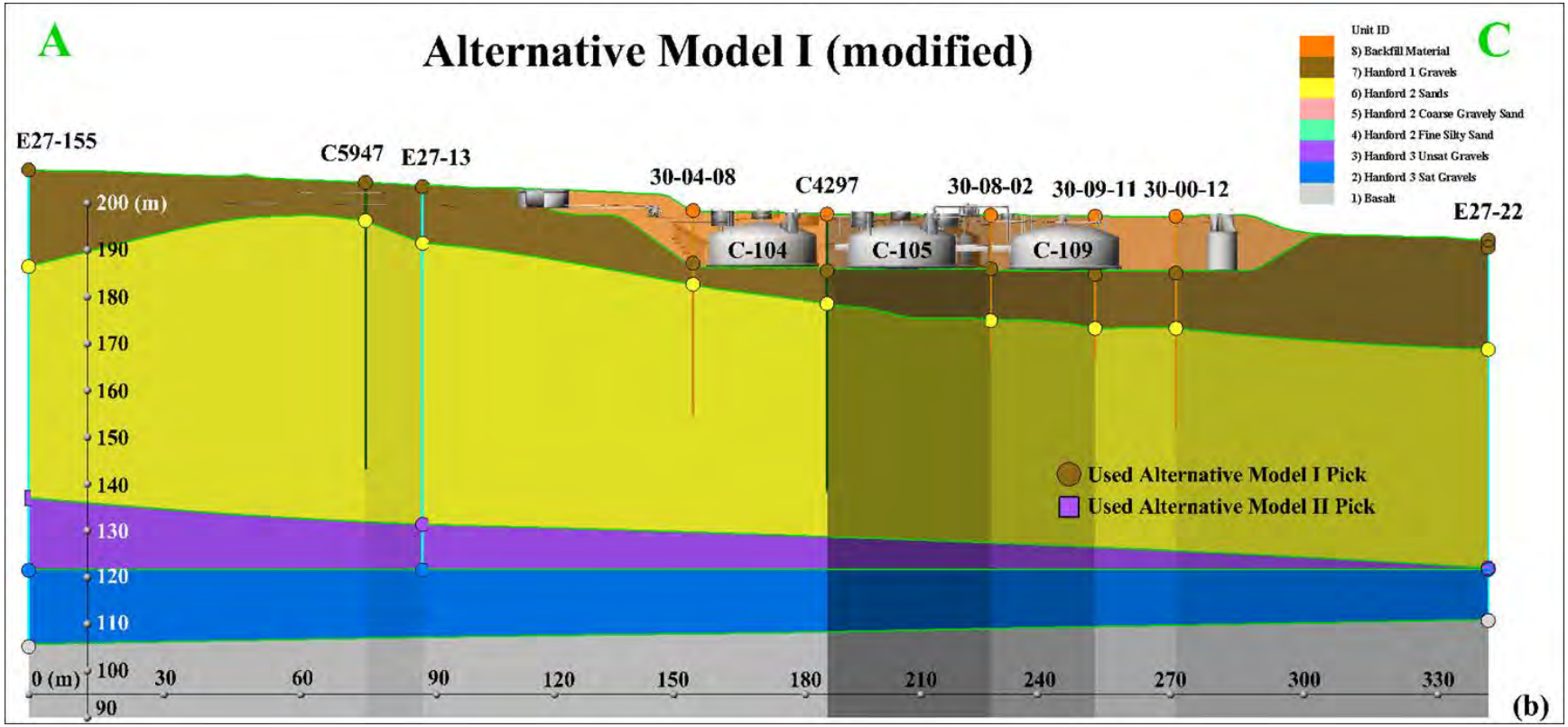

Figure 3-3. Evolution of the Groundwater Gradient in the Low-Level Waste Management Area-1 Monitoring Network. The gradient at the nearby Waste Management Area C evolved in a similar manner and timescale.

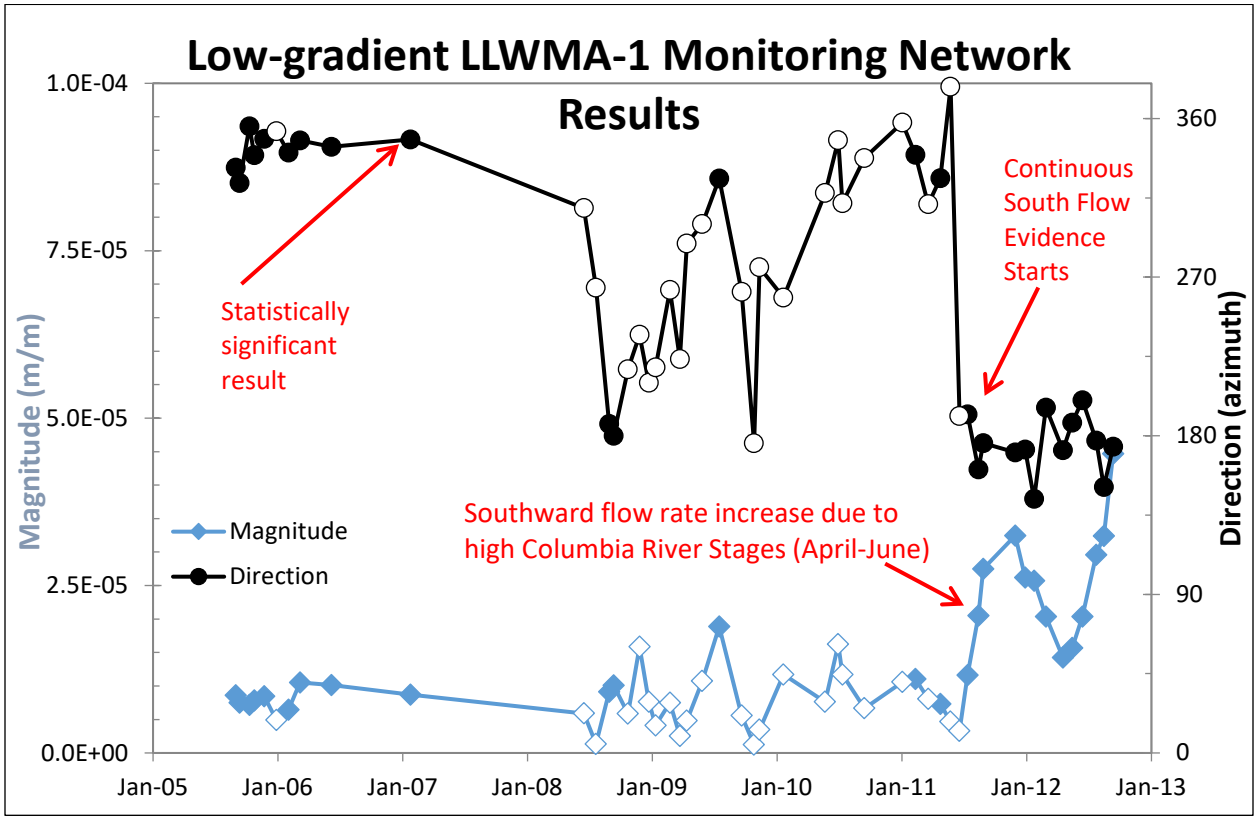

Excerpted from SGW-54165, *Evaluation of the Unconfined Aquifer Hydraulic Gradient Beneath the 200 East Area, Hanford Site*.

LLWMA-1 = Low-Level Waste Management Area 1

As discussed in RPP-ENV-58782 and RPP-ENV-58806, the conceptual models and relevant parameters for fate and transport modeling have been developed for the following four time periods:

- Pre-operations and initial construction period (before 1945) representing the time when the tank farm ground remained undisturbed from the Hanford Manhattan Project mission;
- Operations period representing tank farm construction, current, and immediate future conditions of the tank farm (1945 to 2020);
- Closure and post-closure period during the assumed design life of the intact surface barrier (2020 to 2520) when the tanks become grouted and radionuclides begin to diffuse out of the grout; and
- Post-closure period beyond assumed design life of the surface barrier (2520 to 12120) when the performance of the surface barrier is assumed to degrade.

Figure 3-4. Surface Conditions in and Around Waste Management Area C during the Construction and Operations Period.

WMA = Waste Management Area

The second of these time periods is most relevant for the analysis of past leaks. The third and fourth time periods are relevant to the future projection of leak contamination into the future.

For WMA C vadose zone modeling, small-scale laboratory measurements provide the basis for hydraulic properties used to predict the large, field-scale flow behavior (Appendix B of RPP-ENV-58782 and RPP-ENV-58806). Each heterogeneous geologic unit is replaced by an EHM with macroscopic flow properties. With each heterogeneous unit assigned its upscaled or effective hydraulic properties, the simulated flow fields predict the bulk or mean flow behavior at the field scale. Upscaling, in effect, accounts for the differences in scale between small, core-scale measurements and large, field-scale modeling. The radionuclides travel through the vadose zone until they reach the water table and the unconfined aquifer. The unconfined aquifer is also treated as an EHM, and an equivalent saturated hydraulic conductivity is estimated for the undifferentiated Hanford gravels and CCu sediments (Appendix C of RPP-ENV-58782 and RPP-ENV-58806) through the use of a calibrated large-scale model.

3.3 CONCEPTUAL MODEL OF SOURCE TERM RELEASES

The source term for the leaks analysis is derived from current estimates of past leaks in Revision 4 of RPP-ENV-33418. A summary of these current estimates is provided in Section 2.1. For the purpose of carrying out calculations, it is necessary to make specific assumptions on inventory, volume, and timing that can be input into STOMP© as the source term for the analysis. As discussed in Section 2.1, there is substantial uncertainty in leak estimates, but the current estimates of ^{99}Tc contained in Revision 4 of RPP ENV-33418 (mentioned in the first sentence of the section) provide the basis for the inventory of ^{99}Tc used in the past leak analysis. This inventory is summarized in Table 3-1. Scoping analyses presented in Section 4 have been used to evaluate alternative assumptions about, specifically, the tank C-105 leak.

3.4 VADOSE ZONE CONSIDERATIONS

The vadose zone underlying WMA C consists of heterogeneous layers of sediments that vary in thickness at different locations. Alternative conceptual models described in RPP-ENV-58782 and RPP-ENV-58806 present results from several alternative representations of the spatial variability of these sedimentary units to evaluate the consequences of these alternative representations. These alternative representations have been carried forward into this document.

Features such as clastic dikes and man-made structures (i.e., monitoring wells) can allow water and contaminants to bypass vadose zone continuum fate and transport processes. Clastic dikes (anomalous, subvertical linear features composed of layers of differing particle size distributions) occur in the vadose zone, extend up to tens of meters in length, and crosscut the major layers. At the Hanford Site, there is little evidence of enhanced transport in these preferential pathways in arid and semiarid climates with low-water flux in the vadose zone, particularly where soils are coarse-grained such as in Hanford formation sediments (“Influence of Clastic Dikes on Vertical Migration of Contaminants at the Hanford Site” [Murray et al. 2007]).

Table 3-1. Inventory of Technetium-99 Used for the Initial Analysis Cases.

Tank/Unplanned Release	Waste Release Volume, gal*	^{99}Tc, Ci	Time of release
Tank 241-C-101 (associated with UPR-200-E-136)	37,000	0.25	Continuous release 1965 – 1969
Tank 241-C-104	28,000	0.03	Acute release 1965
Tank 241-C-105	2,000 to 20,500	10	Continuous release 1963 – 1967
Tank 241-C-108	18,000	0.02	Acute release 1965
Tank 241-C-110 (Associated with UPR-2-00-E-107)	2,000	3.4	Continuous release 1971 – 1972
Tank 241-C-112	7,000	0.0075	"prior to 1972" taken as acute release 1965
UPR-200-E-81	36,000	0.1	Acute release 1969
UPR-200-E-82	2,600	1.3	Acute release 1969
UPR-200-E-86	17,000	2.7	Acute release 1971
Surface Releases	1,000	0.001	"Unknown" taken as acute release 1965
Tank 216-C-8	32,000	0.0	Continuous release 1960 – 1965
Total	169,100	17.5	

* Conversion 1 gallon = 3.78541 liters

However, these features may form preferentially faster flow pathways under conditions closer to saturation, such as may have potentially occurred following leak releases. As a result, a specific analysis case has been set up to evaluate the potential effect of a clastic dike on transport of contaminants from past leaks through the vadose zone (see Section 4.4).

Similarly, the presence of man-made features such as exploratory boreholes and drywells has been speculated to provide a potential fast path for contamination from past leaks. Consequently, an alternative modeling case has been established to evaluate these effects (see Section 4.4).

3.5 AQUIFER CONSIDERATIONS

3.5.1 Flow Considerations

As discussed in RPP-ENV-58782 and RPP-ENV-58806, estimates of hydraulic properties are based on the groundwater flux in the aquifer around WMA C according to the CPGWM calibration reported in CP-47631, *Model Package Report: Central Plateau Groundwater Model Version 6.3.3*.

3.5.2 Transport Considerations

The effective transport parameter (i.e., macrodispersivity, bulk density, and diffusivity) estimates used in the base case associated with the WMA C PA (RPP-ENV-58782) and the RCA (RPP-ENV-58806) provide the basis for transport parameters used in this analysis. The basis for the distribution coefficients (K_d) values used to approximate the transport of the radionuclides and chemical contaminants in this analysis (see Table 3-2) also rely on the same estimates for these parameters used in the base case from the PA and RCA.

PNNL-17154, *Geochemical Characterization Data Package for the Vadose Zone in the Single-Shell Tank Waste Management Areas at the Hanford Site*, indicates that K_d values are typically lower for materials that contain significant amounts of gravel and should be corrected according to the following equation:

$$\mathrm{K}_d(\text{gravel corrected}) = (1.0 - \text{weight fraction gravel}) \times \mathrm{K}_d(\text{value determined using} < 2\text{mm material} \quad (3\text{-}1)$$

The gravel weight fractions for the Backfill, Hanford H1/H3, and Hanford H2 HSUs are 0.54, 0.42, and 0.20, respectively (see Appendix B of RPP-ENV-58782).

The K_d-based (linear isotherm) sorption model is best used to represent adsorption processes when contaminant concentrations are low relative to the adsorption capacity, and the variability in mineralogy and geochemical conditions are minimal along the flow path. Since the K_d value is a lumped parameter, it neglects any time varying and spatially varying chemical conditions that would likely happen near the origin of the tank leak.

Some examples of geochemical factors that could influence the mobility of selected constituents in the near field environment impacted by tank wastes could include:

- The presence of synthetic chelating agents such as EDTA in some tank wastes that could affect the overall mobility of certain constituents like ^{60}Co and cyanide or other metals like Plutonium and Americium.

- The presence of high sodium concentrations and other constituents found in some tank wastes could affect the overall ion exchange and adsorption process. This could lead to the enhanced mobility of typically immobile constituents like ^{137}Cs and other metals.

- The direct dissolution of soil components by high pH tank wastes that could impact the potential overall porosity and hydraulic properties of vadose zone sediments.

A detailed discussion of important geochemical processes that could affect the overall mobility and transport of key constituents of concern found in tank wastes is provided in Section 6 of PNNL-16663, *Geochemical Processes Data Package for the Vadose Zone in the Single-Shell Tank Waste Management Areas at the Hanford Site*.

However, it is also recognized from various soil characterization studies that the waste stream-sediment interactions that occur within a short distance of the leak lead to complex mineral dissolution and precipitation reactions that buffer the pH and thereby reduce the variability in local geochemical conditions (from ambient conditions) within a short distance.

A discussion of geochemical studies of vadose zone sediments in the vicinity of a postulated leak at tank C-105 and tank waste losses in the vicinity of the 200-UPR-82, are provided in Sections 3.3.1 and 3.3.2 of PNNL-17154. This discussion has provided considerable evidence that these geochemical effects that could have potentially affected the mobility of constituents of normally immobile metal constituents would have been limited to shallow depths that directly came into contact with tank wastes in these locations.

Given that the vadose zone is much thicker than the extent of the reaction front over which buffering occurs for the majority of the transport distance in the vadose zone, a K_d-based sorption model is deemed adequate due to large sorption capacity compared to the contaminant concentrations. For more details of this approach and applicability of empirical K_d model, see the discussion in PNNL-17154.

For WMA C, the K_d values that were chosen are representative of low-salt, near-neutral waste chemistry assuming "intermediate" impact zones. “Intermediate” impact zones are defined as zones (or areas) in which the acidic or basic nature of the released waste was expected to have been largely neutralized by reaction with the natural sediment. However, if the focus of evaluation were on contaminant transport near the leak location at the time of leak, use a more sophisticated sorption model would be warranted. Given that this was not the objective of the study for the time scales and length scales of evaluation undertaken, a K_d-based model is deemed appropriate.

As with any other parameter, the K_d value is uncertain and can vary. The values chosen here (shown in Table 3-2) are the best estimate values. To eliminate confusion, it is clarified and acknowledged that there is uncertainty in these estimates (i.e., PNNL-17154 [Table 3-9], provides a minimum and maximum estimates of K_d values in addition to the best estimate).

Table 3-2. Distribution Coefficients (K_d) Values Used to Approximate the Transport of the Radionuclides in the Base Case. (2 sheets)

Element or Contaminant	Base Case K_d (mL/g)				
	< 2mm Material	Backfill	Hanford H1/H3	Hanford H2	Reference
Ac	350	NM	NM	NM	PNNL-16663
Al	1,500	NM	NM	NM	RPP-RPT-46088
Am	600	NM	NM	NM	PNNL-17154
B	3	NM	NM	NM	RPP-RPT-46088
C	1	0.46	0.58	0.8	PNNL-17154
Cm	350	NM	NM	NM	PNNL-16663

Table 3-2. Distribution Coefficients (K_d) Values Used to Approximate the Transport of the Radionuclides in the Base Case. (2 sheets)

Element or Contaminant	Base Case K_d (mL/g)				
	< 2mm Material	Backfill	Hanford H1/H3	Hanford H2	Reference
CN	0	NM	NM	NM	RPP-RPT-46088
Co	0	0	0	0	PNNL-17154
Cr	0	0	0	0	PNNL-17154
Cs	100	NM	NM	NM	PNNL-17154
Eu	10	NM	NM	NM	PNNL-17154
F	0	0	0	0	PNNL-17154
Fe	25	NM	NM	NM	RPP-RPT-46088
H	0	0	0	0	PNNL-17154
Hg	52	NM	NM	NM	RPP-RPT-46088
I	0.2	0.09	0.12	0.16	PNNL-17154
Mn	65	NM	NM	NM	RPP-RPT-46088
Nb	0	0	0	0	PNNL-16663
Ni	3	1.4	1.7	2.4	PNNL-17154
NO_2	0	0	0	0	PNNL-17154
NO_3	0	0	0	0	PNNL-17154
Np	10	NM	NM	NM	PNNL-17154
Pa	300	NM	NM	NM	PNNL-17154
Pb	10	NM	NM	NM	PNNL-17154
Pu	600	NM	NM	NM	PNNL-17154
Ra	10	NM	NM	NM	PNNL-17154
Rn	0	0	0	0	No relevant information available
Se	0.1	0.05	0.06	0.08	PNNL-17154
Sm	10	NM	NM	NM	PNNL-17154
Sn	0.5	0.23	0.29	0.4	PNNL-17154
Sr	10	NM	NM	NM	PNNL-17154
Tributyl Phosphate	1.89	NM	NM	NM	RPP-RPT-46088
Tc	0	0	0	0	PNNL-16663
Th	300	NM	NM	NM	PNNL-16663
U	0.6	0.28	0.35	0.48	RPP-RPT-46088

Table 3-2. Distribution Coefficients (K_d) Values Used to Approximate the Transport of the Radionuclides in the Base Case. (2 sheets)

Element or Contaminant	Base Case K_d (mL/g)				
	< 2mm Material	Backfill	Hanford H1/H3	Hanford H2	Reference
Zr	300	NM	NM	NM	PNNL-16663

NM = not included in the 3-D modeling because the results of screening indicated the element or contaminant does not arrive at the water table within 10,000 years.

References:
PNNL-16663, *Geochemical Processes Data Package for the Vadose Zone in the Single-Shell Tank Waste Management Areas at the Hanford Site*.
PNNL-17154, *Geochemical Characterization Data Package for the Vadose Zone in the Single-Shell Tank Waste Management Areas at the Hanford Site*.
RPP-RPT-46088, *Flow and Transport in the Natural System at Waste Management Area C*.

3.6 MATHEMATICAL MODELS

This section presents development and implementation of mathematical models that are used to evaluate flow and radionuclide transport. The mathematical models and their implementation are described in RPP-ENV-58782 and RPP-ENV-58806. There is no difference between the STOMP© mathematical models implemented in those reports and the one used here. However, given the additional complexity (i.e., release from the tank structure) of the residual waste PA, in which additional models and features in STOMP© were described, the additional mathematical models specific to the leaks analysis have been added to this section, along with a description of the mathematical implementation of the leak source term.

3.6.1 Source Term

The source term is input directly as a mass of contamination and associated water volume into the STOMP© model at nodes representing the estimated location of the leak. As indicated in Section 2, the tank leaks appear to be associated with cascade lines or spare inlets that occur at or above the shoulders of the tanks. Therefore, source term is applied to the nodes representing the elevation of the tanks approximately halfway between their base and top for the estimated duration of the occurrence. The masses and volumes of the leaks are discussed in Section 2.1.

3.6.2 Groundwater Flow and Contaminant Transport Equations

Analyses were conducted using the STOMP© code, which was used to simulate 3-D flow and contaminant transport through the vadose zone and unconfined aquifer system. To calculate water flow, STOMP© includes the assumption that the vadose zone and unconfined aquifer system can be represented and approximated by an equivalent porous continuum. STOMP© solves the conservation of mass equation using a finite difference approximation to Richards' equation (Soil Physics, 6th edition [Jury and Horton 2004]) that calculates fluid flow entering, exiting, and accumulating within the finite numerical volumes as follows:

$$\frac{\partial\theta}{\partial t} = \sum \frac{\partial}{\partial x}\left[K(\theta)\frac{dh}{d\theta}\frac{\partial\theta}{\partial \mathrm{x}}\right] + \frac{\partial}{\partial y}\left[K(\theta)\frac{dh}{d\theta}\frac{\partial\theta}{\partial y}\right] + \frac{\partial}{\partial z}\left[K(\theta)(\frac{dh}{d\theta}\frac{\partial\theta}{\partial z} + 1)\right] \pm S \qquad (3\text{-}2)$$

Where:

$\partial\theta/\partial t$	=	the change in soil moisture content through time
$dh/d\theta$	=	the slope of the soil matric potential-moisture retention relationship curve (cm)
$\partial\theta/\partial\{x, y, z\}$	=	the changes in soil moisture content through space in each direction (1/cm)
$K(\theta)$	=	the hydraulic conductivity (cm/s), which may be anisotropic and is, as expressed, dependent on moisture content
S	=	the amount of water added (source) or subtracted (sink) per unit volume through time (1/s).

Moisture content is a function of soil matric potential, and the soil matric potential-moisture retention relationship is described for each HSU using the following empirical relationship ("A Closed-form Equation for Predicting the Hydraulic Conductivity of Unsaturated Soils" [van Genuchten 1980]; EPA/600/2-91/065, *The RETC Code for Quantifying the Hydraulic Functions of Unsaturated Soils*):

$$\theta(h) = \theta_r + (\theta_s - \theta_r)\{1 + [\alpha h]^n\}^{-m} \qquad (3\text{-}3)$$

Where $\theta(h)$ is the moisture content, here expressed explicitly as a function of the soil matric potential, and the other terms are defined as follows:

θ_r = residual moisture content (dimensionless)
θ_s = saturated moisture content (dimensionless)
α = a fitting parameter related to the air entry or bubbling pressure of the soil (cm-1)
n = a fitting parameter related to the shape of the retention curve (dimensionless). This parameter is fixed for each HSU.
m = a fitting parameter related to the shape of the retention curve assumed equal to 1 - 1/n, per the recommendation in van Genuchten, 1980.

Combining the van Genuchten model with Mualem's (1976) model ("A New Model for Predicting the Hydraulic Conductivity of Unsaturated Porous Media") for unsaturated conductivity produces the following relationship for hydraulic conductivity and soil matric potential:

$$K(h) = \frac{K_s\{1-(\alpha h)^{mn}[1+(\alpha h)^n]^{-m}\}^2}{[1+(\alpha h)^n]^{ml}} \qquad (3\text{-}4)$$

Where *K(h)* is the hydraulic conductivity (cm/s), which is, as expressed, dependent on the soil matric potential; K_s is the saturated hydraulic conductivity (cm/s); and *l* is a pore-connectivity parameter (dimensionless) that accounts for the alignment of pores in the direction of flow, and for the flow path tortuosity. Mualem (1976) estimates the pore-connectivity to be ~0.5 for many soils, and it is assumed to equal 0.5 in this analysis.

Within STOMP©, tension-dependent anisotropy provides a framework for upscaling small-scale measurements to the effective (upscaled) properties for the large-scale vadose zone (Section 6.4 and Appendix B of RPP-ENV-58782 and RPP-ENV-58806). Each heterogeneous geologic unit is represented in the model by an EHM with macroscopic flow and transport properties. With each heterogeneous unit assigned its upscaled or effective hydraulic properties, the simulated flow fields predict the bulk or mean flow behavior at the field scale. Upscaling, in effect, accounts for the differences in scale between small, core-scale measurements and large, field-scale modeling. Tension-dependent anisotropy provides a framework for upscaling small-scale measurements to the effective (upscaled) properties for the large-scale, macroscopic vadose zone. The stochastic model developed in "Application of Stochastic Methods to Transient Flow and Transport in Heterogeneous Unsaturated Soils" (Polmann 1990) is used to evaluate and apply tension-dependent anisotropy for the HSUs at WMA C. Details about the development of the Polmann stochastic tension-dependent anisotropy model and its application to the HSUs at WMA C are presented in Appendix B, Section B.3.2 of RPP-ENV-58782 and RPP-ENV-58806.

Contaminant transport in STOMP© is described by the conventional advective-dispersive transport solution to the conservation of mass equation described in Soil Physics,5th edition [Jury et al. 1991] and applied to finite difference volumes:

$$\frac{\partial}{\partial t} M_c = \frac{\partial}{\partial x}(J_x\, C_l) + \frac{\partial}{\partial y}(J_y\, C_l) + \frac{\partial}{\partial z}(J_z\, C_l) + \frac{\partial}{\partial x}\left(D_e \frac{\partial C_l}{\partial x}\right) + \frac{\partial}{\partial y}\left(D_e \frac{\partial C_l}{\partial y}\right) + \frac{\partial}{\partial z}\left(D_e \frac{\partial C_l}{\partial z}\right) - M_c \frac{ln(2)}{t^{1/2}} \qquad (3\text{-}4)$$

Where:

$\frac{\partial}{\partial t} M_c$ = the change in contaminant mass or activity present in the finite volume (g or Ci) through time and the mass or activity is calculated according to the equation ($\rho_b\, C_a + \theta\, C_l$)

ρ_b = soil bulk density (g/cm^3)

C_a = adsorbed solute concentration (g or Ci per g soil)

θ = moisture content (dimensionless), and as discussed previously, dependent on the soil matric potential

C_l = dissolved solute concentration (g or Ci per mL water)

$J_{x,y,z}$ = fluxes of water carrying contaminants into or out of the finite volume (cm/s) that cross the planes normal to the x, y, and z directions, respectively

D_e = effective dispersion/diffusion coefficient (cm^2/s); note that the entire terms represent the flux of solutes that crosses the planes normal to the x, y, and z directions, respectively, because of diffusion and dispersion

$\frac{\partial c_l}{\partial\{x,y,z\}}$ = the change in dissolved solute concentration through space in the x, y, and z directions, respectively; note that the entire terms represent the flux of solutes that crosses the planes normal to the x, y, and z directions, respectively, because of diffusion and dispersion

$t^{1/2}$ = radioactive half-life(s), the entire term represents the mass of solute lost to radioactive decay.

In Equation 3-4, positive is used to indicate solute entering the finite volume, and negative is used to indicate what is exiting or lost to decay. The adsorbed and dissolved solute concentrations are related through an equilibrium linear sorption coefficient (K_d [mL water per g soil]) formulation: $C_a = K_d C_l$. No temperature effects are considered for the vadose zone model (i.e., the model used is isothermal).

3.6.3 Implementation of the Groundwater Pathway in STOMP©

This section describes the implementation of STOMP© in the WMA C PA for evaluation of the groundwater pathway. This model is the starting point for the scoping analyses presented in Sections 4 and 5. The scoping analyses have the same general structure but have been modified from the model described here to address alternative assumptions in the representation of the transport of contaminants from the leaks. These alternative assumptions include differing hypotheses about the leaks themselves, the geological setting (including consideration of highly heterogeneous representations of the subsurface), and a number of hydrological parameters. In addition, the aquifer gradient changed in magnitude and direction when the leaks were arriving at the water table; consequently, separate scoping analyses have been developed to represent that effect. The model described in this section forms the basis for all these subsequent alternative models.

In the current analysis, it has not been possible to run fully probabilistic analyses of parameter uncertainty because of the large simulation times associated with running the numerical representation of the vadose zone and aquifer systems. Instead, parameter uncertainties have been addressed by performing a range of deterministic calculations that span the range of the parameter uncertainties. The parameters selected in a few of the scoping cases were based on evaluation of uncertainty distributions developed for conducting the uncertainty analysis performed in the RPP-ENV-58782. While this approach is limited in its ability to represent the full parameter space, it illustrates the effects of uncertainties associated with each input parameter..

DOE/RL-2011-50, *Regulatory Basis and Implementation of a Graded Approach to Evaluation of Groundwater Protection*, contains the description of the generalized models, conditions, and

parameters applicable to the Hanford Site vadose zone, which were refined and augmented for the WMA C PA evaluation, and used here.

The site-specific STOMP© model components for the WMA C PA evaluation are:

- Model domain and boundary conditions,
- Hydrogeologic model,
- Source term,
- Recharge,
- Vadose zone hydrogeology and fluid transport,
- Groundwater domain and characteristics, and
- Geochemistry.

The model domain and boundary conditions are included in the list above to emphasize the fundamental nature of boundary conditions used in the modeling.

The following subsections for the individual conceptual model components provide the basis, rationale, and references for the base case values. These base case values have been used as the initial input parameters for this document, with alternative assumptions and input parameters used as appropriate to show the range of possible outcomes for the range of input uncertainties identified in RPP-ENV-58782 and RPP-ENV-58806. The base case parameters represent single representative values selected for use in deterministic runs of the model, selected from the ranges of plausible parameter values identified in RPP-ENV-58782 and RPP-ENV-58806. These values may differ from parameter estimates for other Hanford Site modeling performed for different purposes or areas of the Hanford Site, or at different scales.

3.6.3.1 Model Domain and Boundary Conditions. The model domain and boundary conditions establish both a framework and limiting conditions for the numerical model. The model domain for flow and transport in the vadose zone is represented numerically in 3-D space, with one of the horizontal axes aligned in the general direction of groundwater flow. Aligning an axis with the general direction of groundwater flow allows concentrations to be calculated more easily downgradient of the waste sites. The numerical model adapts the physical elements of the conceptual model to a Cartesian grid, and also assigns numerical values to the parameters used in algorithms to represent the physical and geochemical systems and processes.

The WMA C model domain is 737.9 m (2,421 ft) northwest to southeast by 795.3 m (2,609 ft) southwest to northeast by 116 m (381 ft), vertically, extending ~12 m (~39 ft) below the water table (Figure 3-5 shows the extent of the model domain). The southwestern and northwestern boundaries of the model are 574656.09 m, 136454.41 m, and 575218.45 m, 137016.78 m, respectively (Lambert Coordinate system easting, NOAA Manual NOS NGS 5, “State Plane Coordinate System of 1983”). The southeastern and northeastern boundaries are 575177.86 m, 135932.64 m, and 575740.22 m, 136495.00 m, respectively. The vertical base elevation of the model is nominally 95 m (312 ft) (NAVD88), although the bottom and top of the model domain vary spatially according to the top of basalt elevation and surface relief, respectively (RPP-RPT-56356).

The horizontal node spacing varies between 3.0 m and 20 m (9.8 ft and 65.6 ft) to optimize the discretization in the areas attempting to approximate the slopes associated with construction of WMA C and the 100-series tanks without overwhelming the available computational resources. Figure 3-6 shows the plan view distribution of the calculation nodes. The vertical spacing in the vadose zone ranged between 1 m and 1.25 m (3.28 ft and 4.10 ft) except around the water table, where the spacing decreased to 0.5 m (1.6 ft) to capture the impact of the capillary fringe above the water table. The total number of nodes in the modeled rectangular prism equals 736,653. During the pre-operational phase, the number of active nodes equals 640,565 with 96,088 inactive. Inactive nodes represent space where no flow occurs (e.g., above ground surface, within basalt, or within intact tanks). During the operational and post-closure phases, the number of active nodes equals 637,543 with 99,110 inactive, the increase in inactive nodes attributed to the inactivation of the tank and ancillary equipment nodes within the WMA C excavation.

Figure 3-5. Interpolated Numerical Three-Dimensional Post-Closure Alternative I Hydrogeologic Model.

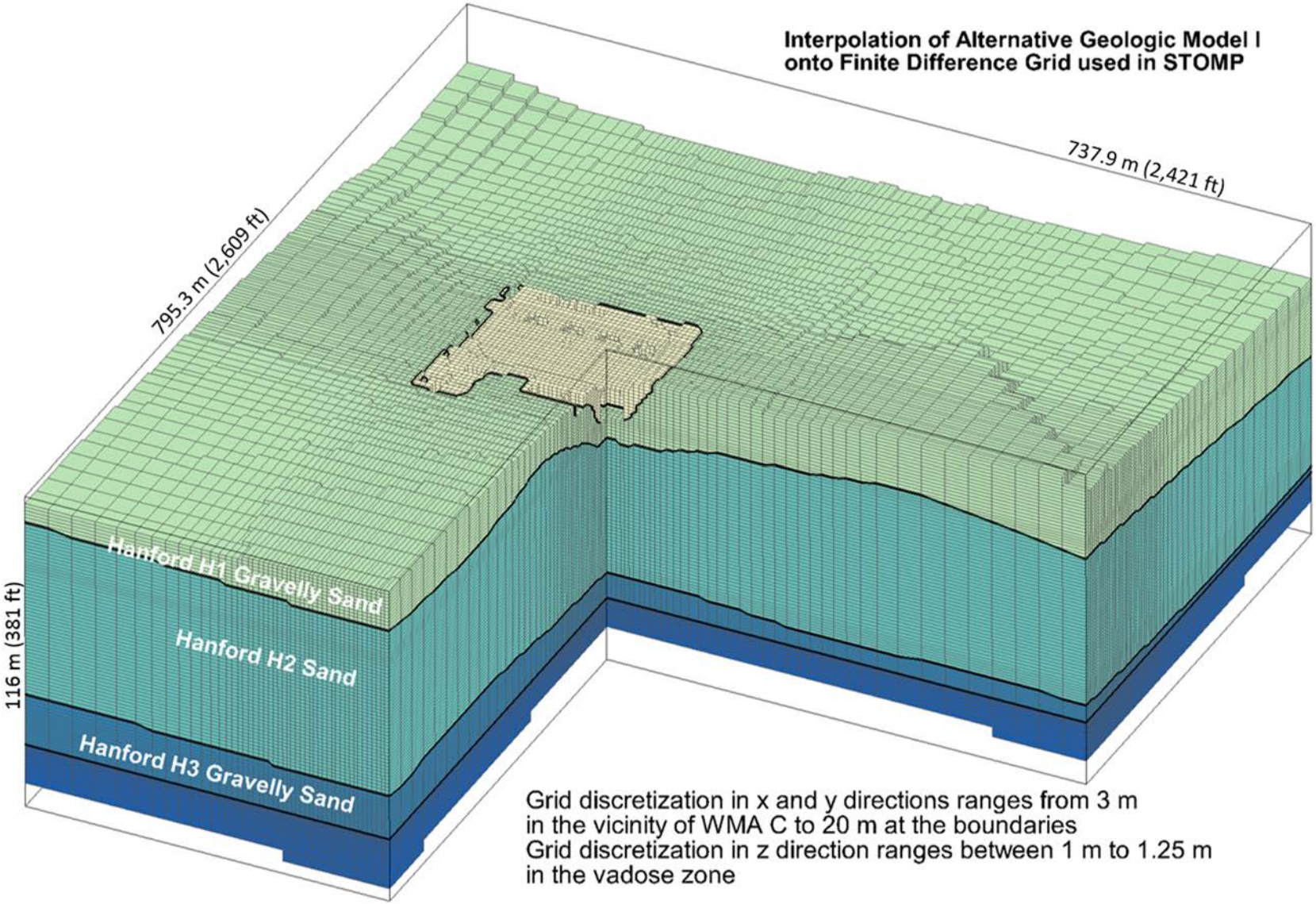

STOMP = Subsurface Transport Over Multiple Phases (computer code) WMA = Waste Management Area

A specified-flux boundary condition was applied at the surface to simulate recharge. Recharge rates varied spatially and temporally along the upper boundary, depending on surface conditions, the presence of WMA C and other facilities, and the time of WMA C operations and surface conditions simulated (RPP-RPT-44042, *Recharge and Waste Release within Engineered System in Waste Management Area C*). The bottom boundary of the unsaturated (vadose) zone is the water table, and the bottom of the model (aquifer) was defined as a no-low boundary condition. Boundary conditions at the sides of the model domain were assumed to be no flow in the vadose zone and prescribed flux and prescribed head in the aquifer on the upgradient and downgradient boundaries, respectively. The boundary condition in the aquifer on the upgradient boundary was assumed to be prescribed flux, calculated on the basis of the hydraulic conductivity and gradient, and independent of recharge. The prescribed flux boundary condition value includes a factor to account for the varying thickness of the unconfined aquifer and uneven surface of the underlying basalt. To account for the non-uniform aquifer thickness from the underlying basalt boundary, the nominal flux rate was calculated as the product of the hydraulic conductivity and gradient (base case values of 11,000 m/day [6.8 mi/day] and 2×10^{-5} m/m [6.6×10^{-5} ft/m], respectively), and was proportioned according to the ratio of the average aquifer cross-sectional area throughout the model domain (9,440 m^2 [2.3 acres]) and the aquifer area along the upgradient boundary (6,151 m^2 [1.5 acres]) where the prescribed flux is applied. The hydraulic conductivity value for the WMA C analysis is derived from estimates developed within the CPGWM (CP-47631, 2015, *Model Package Report: Central Plateau Groundwater Model Version 6.3.3*) that range between 5,802 m/day (3.6 mi/day) and 17,000 m/day (10.6 mi/day). Using those hydraulic conductivity estimates and a layer thickness weighted averaging scheme, the effective hydraulic conductivity is estimated to be 11,000 m/day (6.8 mi/day) for the entire aquifer around WMA C. Incidentally, CP-47631 (2015) predates DOE/RL-2015-75 (2016) and therefore does not include those results as part of the CPGWM Version 6.3.3 calibration. The aquifer cross-sectional area refers to the area perpendicular to the direction of groundwater flow. The aquifer cross-sectional area varies from the northwest to southeast boundaries because of the uneven top of the basalt.

3.6.3.2 Hydrogeologic Model. The hydrogeologic conceptual model developed for the WMA C PA (RPP-RPT-46088 and RPP-RPT-56356) provides the information basis and data necessary to prepare the 3-D geologic inputs used in the 3-D numerical model. Each node in the numerical model represents a unique set of horizontal (x and y) coordinates and vertical (z) elevation. A node is assigned the hydrogeologic properties associated with the HSU identified in the RPP-RPT-56356 geologic models as existing in the space represented by the node coordinates and elevation.

Figure 3-5 shows the geologic interpretation prepared by Washington River Protection Solutions, LLC (WRPS) staff and identified as Alternative Model I as interpolated onto the numerical grid used in the fate and transport model. The fence diagram, given in Figure 3-7, shows some internal cross-sections of the geology to illustrate the shape and layering of the hydrogeologic units. Figures 3-8 and 3-9 show the geologic interpretation prepared with input from technical staff of the Nez Perce and identified as Alternative Model II. Alternative Model II includes the separation of the Hanford H2 sand unit into three distinct subunits: the Hanford H2 sand, the Hanford H2 gravelly sand, and the Hanford H2 fine or silty sand. Explanation of the basis and the development of the two geologic interpretations is presented in RPP-RPT-56356. The

scoping analysis includes evaluation of an additional alternative geologic model that is identical to Alternative Model I, except that a clastic dike is assumed to exist under tanks C-102, C-105, C-108, and C-111, and another is assumed to exist under tanks C-110, C-111, and C-112. These clastic dikes extend the length and width, respectively, of WMA C, and extend from the bottom of the WMA C excavation to the capillary fringe of the aquifer.

For one of the cases used the scoping analysis (i.e., heterogeneous model; see Case 4b in Table 4-1 in Section 4), the assignment of vadose zone hydraulic properties based on moisture contents represented an alternative conceptual model to the base case. Details of the development of this model and how vadose zone properties were assigned to various hydrologic units in this specific model is described in Appendix F of RPP-ENV-58782 and RPP-ENV-58806). This case is meant to examine the effect of heterogeneous treatment of hydraulic properties of sediments in the vadose zone on impacts of past releases.

The bulk or mean water flow and contaminant transport in the vadose zone, according to the model results, do appear to remain within the WMA C perimeter fence. However, the models' construct in and of itself does not contain contamination within the perimeter fence. The model simulates contaminants associated with the sources moving through the vadose zone in accordance with the hydraulic and transport parameters used in the mathematics of the flow and transport equations. The EHM approach addresses bulk or mean water flow and contaminant transport, in accordance with the intent of the analysis.

Figure 3-6. Plan View of Waste Management Area C Performance Assessment Model Domain Showing the Horizontal Distribution and Surface Type of the Irregularly-Spaced Calculation Nodes.

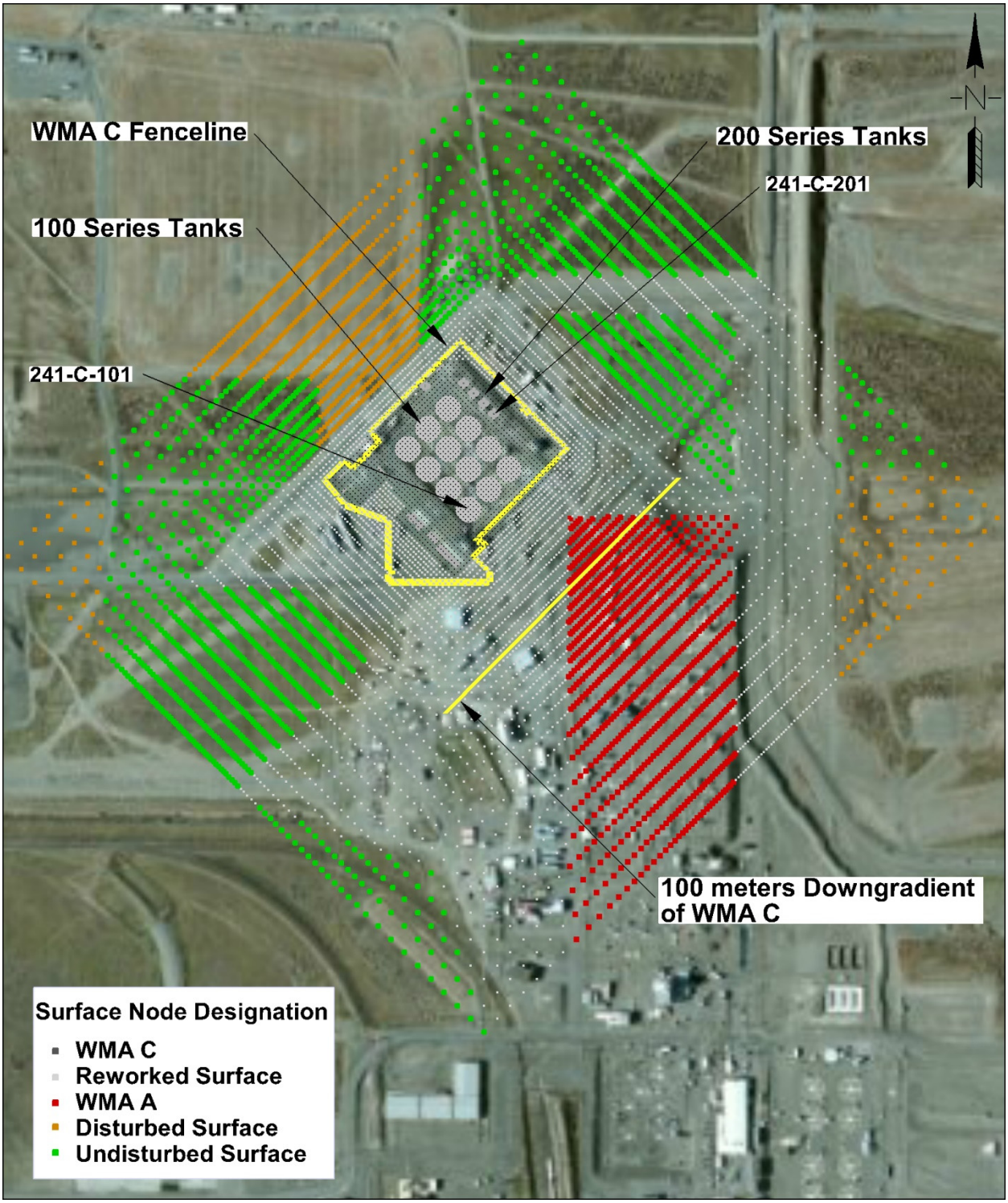

The resolution increases in the area of Waste Management Area C.

WMA = Waste Management Area

Figure 3-7. Fence Diagram of Interpolated Numerical Three-Dimensional Post-Closure Alternative I Hydrogeologic Model.

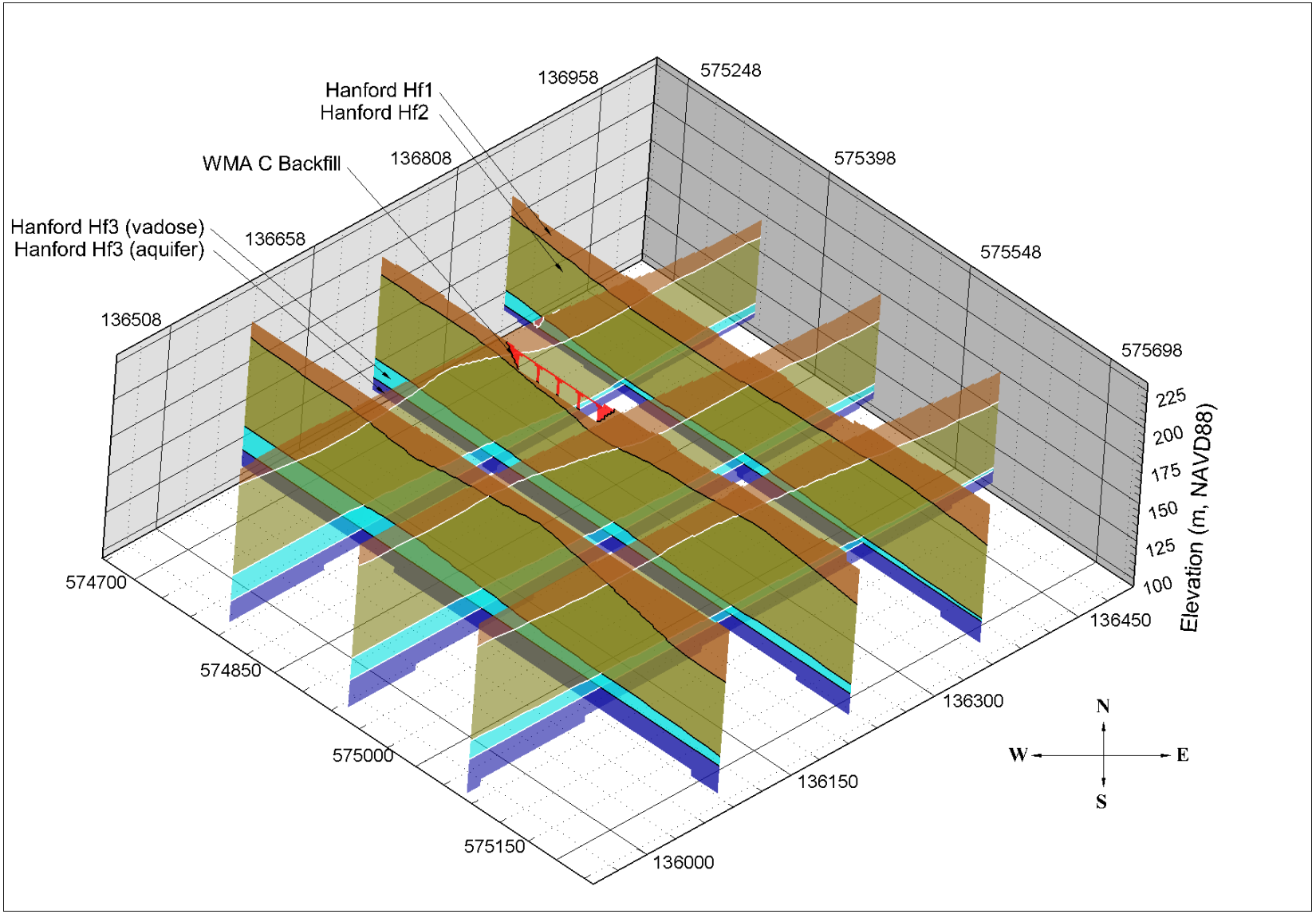

NAVD88 = North American Vertical Datum of 1988, WMA = Waste Management Area, Hf = Hanford formation

Figure 3-8. Interpolated Numerical Three-Dimensional Post-Closure Alternative II Hydrogeologic Model.

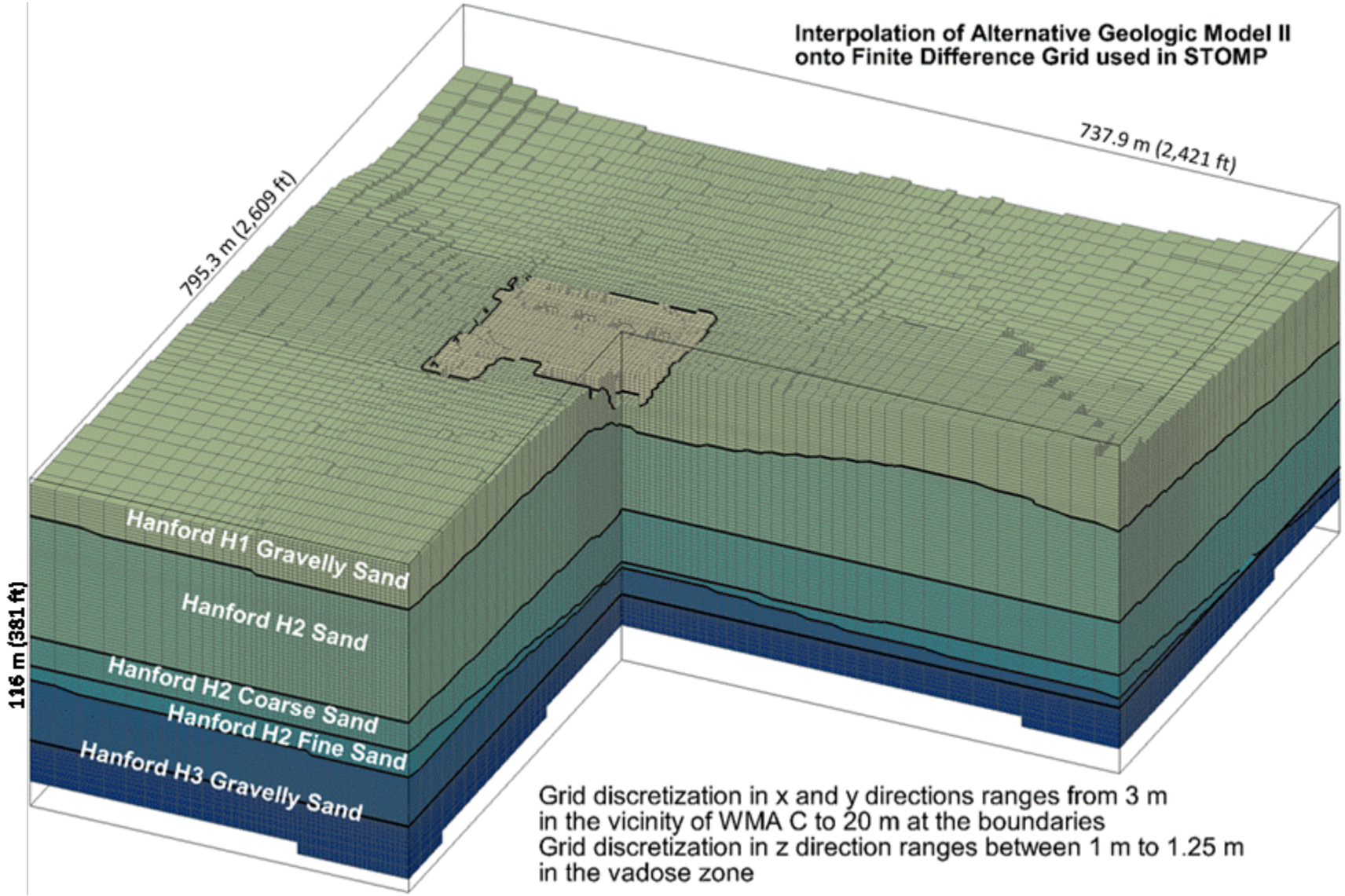

STOMP = Subsurface Transport Over Multiple Phases (computer code) WMA = Waste Management Area

Figure 3-9. Fence Diagram of Interpolated Numerical Three-Dimensional Post-Closure Alternative II Hydrogeologic Model.

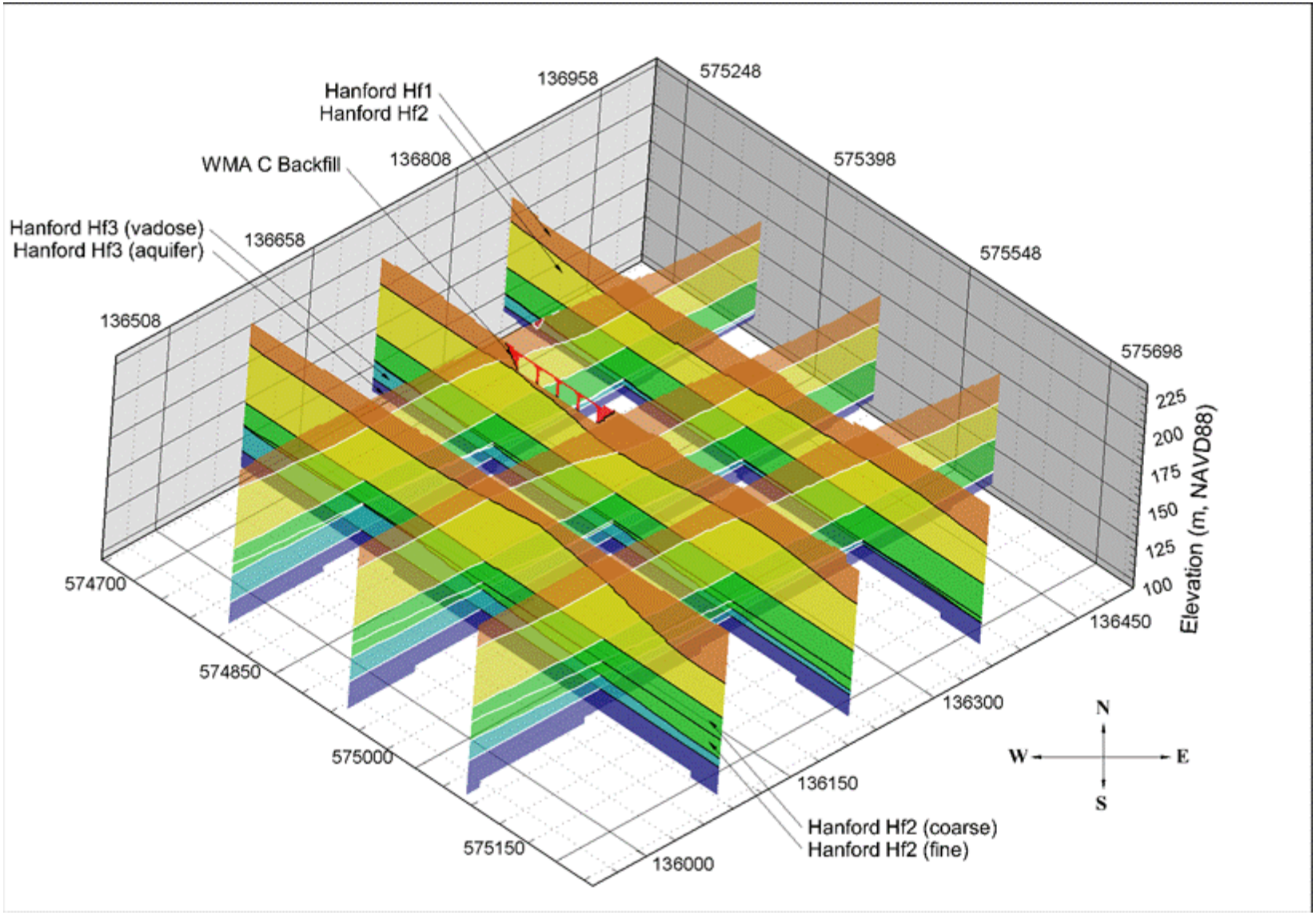

Hf = Hanford formation VD88 = North American Vertical Datum of 1988 WMA = Waste Management Area

3.6.3.3 Recharge. The magnitude of recharge for soils at the Hanford Site varies as a function of the soil type, condition of the vegetation cover, and soil integrity (e.g., disturbed versus undisturbed). The range of recharge values reported in RPP-RPT-44042 represents distinct populations of data based on lysimetry and isotopic measurements, and interpretation—and, in some instances, extrapolation—by Hanford Site subject matter experts. The natural background recharge rates represent a population for natural vegetated conditions. The range of values for operational conditions represents a population of recharge rates for vegetation-free disturbed soil.

The final design for the surface barrier for WMA C at closure has not been developed. The surface barrier is expected to function comparably to a modified RCRA Subtitle C barrier (Section 3.2.1.2.2), which PNNL-16688, *Recharge Data Package for Hanford Single-Shell Tank Waste Management Areas*, indicates should function similarly to the Prototype Hanford Barrier. Summary of data collected over 13 years at the Prototype Hanford Barrier (PNNL-17176, *200-BP-1 Prototype Hanford Barrier Annual Monitoring Report for Fiscal Years 2005 Through 2007*; DOE/RL-93-33, *Focused Feasibility Study of Engineered Barriers for Waste Management Units in the 200 Areas*) indicates that infiltration through the prototype is much less than 0.1 mm/yr (0.004 in./yr), and evaluations of the design using lysimeter data indicate that the barrier is capable of limiting recharge to this amount even with a complete lack of vegetation ("Multiple-Year Water Balance of Soil Covers in a Semiarid Setting" [Fayer and Gee 2006]). However, for base case simulations involving WMA C PA with a functioning surface barrier, a base case recharge rate of 0.5 mm/yr (0.02 in./yr) is assumed, which is consistent with the drainage design specification in DOE/RL-93-33.

At the end of 500 years, the surface barrier performance is assumed to degrade to permit an infiltration rate of 3.5 mm/yr (0.14 in./yr) and maintain that infiltration rate for the remainder of the simulation for the base case. No quantifying data are available for specifying the performance of the barrier top after its design life, but the performance of the surface barrier in limiting recharge is not expected to diminish appreciably (PNNL-16688). According to PNNL-13033, *Recharge Data Package for the Immobilized Low-Activity Waste 2001 Performance Assessment*, not even the erosion of the silt loam layer and deposition of dune sand on the barrier is likely to alter the barrier performance significantly. The value of 3.5 mm/yr (0.14 in./yr) corresponds to the recharge in an undisturbed area, which indicates that native vegetation is assumed to reclaim the land.

Although the side slopes and berm are likely to function and perform differently than the surface of the barrier, they are included as part of the barrier surface. The impact of the side slopes on the overall recharge rate is expected to be relatively negligible. The sandy gravel/gravelly sand barrier side slope and berm are assumed eventually to resemble a Burbank loamy sand, and if that assumption is valid, then PNNL-16688 indicates that the long-term recharge rate for that soil type is 1.9 mm/yr (0.07 in./yr), which is less than the 3.5 mm/yr (0.14 in./yr) used in the analysis for the degraded barrier surface. Table 3-3 presents a summary of the base case recharge rates applied to the different surface types present within the WMA C model domain.

3.6.3.4 Vadose Zone Hydrogeology and Transport. The vadose zone hydrogeology and transport information presented here is a brief summary of the information presented in RPP-ENV-58782 and RPP-ENV-58806. Those reports include detailed discussion and description of the data available and the methods used to develop the base case parameters, and sensitivity and uncertainty distributions and percentile values.

Table 3-3. Base Case Recharge Rate (Net Infiltration) Estimates for Surface Conditions during the Pre-Construction, Operational, and Post-Closure Periods.

Period	Waste Management Area (WMA) C Region and Surface Condition	Base Case Value of Recharge Rate (mm/yr)
Pre-construction (before 1944)	Undisturbed region (Rupert sand with vegetation)	3.5
Operational period (1945 to 2020)	Undisturbed region (Rupert sand with vegetation)	3.5
	WMA C Surface region (Gravel without vegetation)	100
	WMA A Surface region (Gravel without vegetation)	100
	Disturbed revegetated region (Rupert sand with vegetation)	22
	Disturbed un-revegetated region (Rupert sand with no vegetation)	63
Early post-closure (2020 to 2520)	Undisturbed region (Rupert sand with vegetation)	3.5
	WMA C Surface region (Surface barrier with vegetation)	0.5
	WMA A Surface region (Surface barrier with vegetation beginning in 2050)	0.5
	Disturbed revegetated region (Rupert sand with vegetation beginning in 2050 with vegetation recovery completed in 2080)	3.5
	Disturbed un-revegetated region (Rupert sand with no vegetation until vegetation recovery begins in 2050 and completes in 2080)	3.5
Late post-closure (2520 to 3020 and beyond)	Undisturbed region (Rupert sand with vegetation)	3.5
	WMA C Surface region (Surface barrier with vegetation)	3.5
	WMA A Surface region (Degraded surface barrier with vegetation begins in 2550)	3.5
	Disturbed revegetated region (Rupert sand with vegetation recovery completed in 2080)	3.5
	Disturbed un-revegetated region (Rupert sand with vegetation recovery completed in 2080)	3.5

The flow and transport pathway process used for the WMA C vadose zone modeling is porous media continuum flow. The porous media continuum assumption and the soil relative permeability/saturation/capillary pressure relations provide the basis for vadose zone flow and

transport modeling (PNNL-11216, PNNL-12030). The vadose zone at the Hanford Site is composed of sediments ranging in particle size associated with gravels to silts or clays. In the model domain, the hydraulic properties describing fluid transport characteristics associated with each geologic layer (also referred to as HSUs) are approximated by average upscaled values, with each unit having different flow and transport parameter values (hydraulic conductivity, bulk density, and dispersivity). The EHM parameters associated with the different HSUs are assigned to each node where the interpolation of the geologic models in RPP-RPT-56356 onto the model grid indicates where each HSU exists. The model describes bulk (or mean) flow and radionuclide transport behavior in the vadose zone, limiting the evaluation to estimating overall and eventual radionuclide impacts to groundwater. Porous media continuum transport in unsaturated media of this type is regarded as the fundamental process and feature for modeling contaminant fate and transport behavior in the vadose zone at the Hanford Site (DOE/RL-2011-50).

Table 3-4 lists the upscaled composite-fitted van Genuchten-Mualem (van Genuchten 1980; Mualem 1976; EPA/600/2-91/065) base case parameters for the various strata at the WMA C site. A stochastic model of variable moisture or tension-dependent anisotropy provides the framework for upscaling small-scale measurements to the effective (upscaled) properties for the large-scale vadose zone (Polmann 1990). The upscaling processes factor the inherent spatial variability that occurs on different scales in heterogeneous media into the field scale parameter estimates ("Stochastic analysis of moisture plume dynamics of a field injection experiment" [Ye et al. 2005], "Estimation of effective unsaturated hydraulic conductivity tensor using spatial moments of observed moisture plume" [Yeh et al. 2005]). Specific upscaled flow parameters include moisture retention, and saturated and unsaturated hydraulic conductivity. Upscaled transport parameters include bulk density, diffusivity, sorption coefficients, and macrodispersivity.

Table 3-4. Composite van Genuchten-Mualem Parameters for Various Strata at the Waste Management Area C Site Used in the Base Case Evaluations of Alternative Geologic Models I and II.

Strata	Number of Samples	θ_s	θ_r	α (1/cm)	n	ℓ^c	Fitted K_s (cm/s)
Backfill (Gravelly)	10	0.138	0.010	0.021	1.374	0.5	5.60E-04
Hanford H1/H3 (Gravel-dominated)	15	0.171	0.011	0.036	1.491	0.5	7.70E-04
Hanford H2 (Sand-dominated)	44	0.315	0.039	0.063	2.047	0.5	4.15E-03
Hanford H2 –Gravel/coarse sand subunit*	not applicable	0.265	0.002	0.108	1.724	0.5	1.68E-02
Hanford H2 – Silty-sand subunit*	not applicable	0.354	0.029	0.040	1.633	0.5	1.79E-03

*Hydraulic properties of these units are only used in numerical model simulation of Alternative Geologic Model II. As an initial estimate of these properties, the hydraulic properties associated with the 5th and 95th percentile realizations of unsaturated hydraulic conductivity curves developed in the Uncertainty and Sensitivity Analysis for the Hanford H2 sand unit were considered to be representative of the Hanford H2 silty sand and the Hanford H2 gravel/coarse sand subunits, respectively.

Estimated unsaturated conductivities, based on saturated conductivity and the van Genuchten retention model, can differ by up to several orders of magnitude with measured conductivities at the dry end (e.g., "Evaluation of van Genuchten-Mualem Relationships to Estimate Unsaturated Hydraulic Conductivity at Low Water Contents" [Khaleel et al. 1995]). Therefore, unlike the conventional approach, the unsaturated conductivities are not based on predictions using the measured retention curve and the measured saturated conductivity. Rather, the soil hydraulic properties are based on a simultaneous fit of moisture retention and unsaturated conductivity data, and all five unknown parameters θ_r, θ_s, α, n, and K_s, with m=1-1/n (van Genuchten 1980) were fitted to the data via a code named RETention Curve (RETC) (EPA/600/2-91/065). Thus, in order to obtain a better agreement with experimental data for the region of interest (i.e., relatively dry moisture regime), K_s is treated as a fitted parameter during the curve fitting process. This is considered appropriate because the WMA C PA predictions are needed for the relatively dry moisture regime observed in the field, rather than for the saturated or near-saturated regime. The pore size distribution factor, ℓ, was kept fixed at 0.5 during the simultaneous fitting.

For the Alternative Geologic Model II evaluation, the Hanford H2 gravel/coarse sand subunit was assumed to be more transmissive, and the Hanford H2 silty sand less transmissive, than the Hanford H2 sand. Therefore, as an initial estimate of these properties, the hydraulic properties associated with the 5th and 95th percentile realizations of unsaturated hydraulic conductivity curves developed for the Hanford H2 sand unit were considered representative of the Hanford H2 gravel/coarse sand and the Hanford H2 silty sand subunits, respectively.

The effective transport parameter (i.e., macrodispersivity, bulk density, and diffusivity) estimates used in the base case and sensitivity cases are presented. Because of natural variability, the transport parameters are all spatially variable. The purpose is similar to the upscaled flow parameters, to evaluate the effect of such variability on the large-scale transport process. Effective bulk density (ρ_b) estimates are needed to calculate retardation factors for different species. The average ρ_b, E[ρ_b] estimates for various strata at WMA C are presented in Table 3-5. These estimates are derived from bulk density sample values listed in RPP-ENV-58782 and RPP-ENV-58806, Appendix B. The values of macrodispersivity applicable to the scale of the WMA C PA model for the base case evaluation are shown in Table 3-6.

It is assumed that the effective, large-scale diffusion coefficients for all strata in the vadose zone at the WMA C site are a function of volumetric moisture content, θ, and can be expressed using the Millington-Quirk ("Permeability of Porous Solids" [Millington and Quirk 1961]) empirical relation:

$$D_e(\theta) = D_0 \frac{\theta^{10/3}}{\theta_s^2} \tag{6-15}$$

Where:

$D_e(\theta)$ = the effective diffusion coefficient of an ionic species
D_0 = the effective diffusion coefficient for the same species in free water

θ = the localized volumetric moisture content
θ_s = the localized volumetric moisture content at saturation.

The tortuosity formulation in the Millington-Quirk model is based on theoretical considerations absent from other empirical models, and accounts for the ranges of moisture contents present in the vadose zone around WMA C. The molecular diffusion coefficient for all species in pore water is assumed to be 2.5×10^{-5} cm^2/sec (6.98×10^{-4} in.^{2}/sec) (WHC-SD-WM-EE-004, *Performance Assessment of Grouted Double-Shell Tank Waste Disposal at Hanford*), which is consistent with, and representative of, values used in other Hanford PAs (WHC-EP-0645, *Performance Assessment for the Disposal of Low-Level Waste in the 200 West Area Burial Grounds*; BHI-00169, *Environmental Restoration Disposal Facility Performance Assessment*; WHC-SD-WM-TI-730, *Performance Assessment for the Disposal of Low-Level Waste in the 200 East Area Burial Grounds*; WHC-SD-WM-EE-004, and DOE/ORP-2000-24, *Hanford Immobilized Low-Activity Waste Performance Assessment: 2001 Version*).

Table 3-5. Effective Bulk Density (E[ρ_b], g/cm^3) Estimates for Various Strata at Waste Management Area C Used in the Base Case Evaluations of Alternative Geologic Models I and II.

Strata	E[ρ_b]
Backfill (Gravelly)	2.13
Hanford H1/H3 (Gravel-dominated)	2.05
Hanford H2 (Sand-dominated)	1.71
Hanford H2 – Gravel/coarse sand subunit*	1.88
Hanford H2 – Silty-sand subunit*	1.94

*Effective bulk densities of these units are only used in numerical model simulation of Alternative Geologic Model II.

Table 3-6. Macrodispersity Estimates for Various Strata at Waste Management Area C Used in the Base Case Evaluations of Alternative Geologic Models I and II.

Strata	A_L (cm)	A_T (cm)
Backfill (Gravelly)	~20	2.0
Hanford H1/H3 (Gravel-dominated)	~20	2.0
Hanford H2 (Sand-dominated)	~25	2.5
Hanford H2 –Gravel/coarse sand subunit*	~25	2.5
Hanford H2 – Silty-sand subunit*	~25	2.5

*Macrodisperisivities of these units are only used in numerical model simulation of Alternative Geologic Model II.

3.6.3.5 Groundwater Domain and Characteristics. The groundwater in the aquifer system in the vicinity of WMA C has been studied extensively as part of the site characterization that is discussed in RPP-RPT-46088 and Section 2 of this document. The groundwater conceptual model for WMA C includes the uppermost unconfined aquifer system that exists within a paleo-channel area eroded by the cataclysmic floods of the Pleistocene age (see Figure 3.10). The base of the aquifer is the underlying basalt surface. The undifferentiated lower sands and gravels associated with the Hanford formation, CCu, and the Ringold Formation (Unit A) that comprise the aquifer sediments are simply categorized as saturated Hanford H3 sediments in the model. The thickness of the uppermost aquifer beneath WMA C is ~12 m (~39 ft).

Figure 3-10. Interpreted Extent of Paleo-channel Area Associated with the Ancestral Columbia River in 200 East Area in the Vicinity of Waste Management Area C

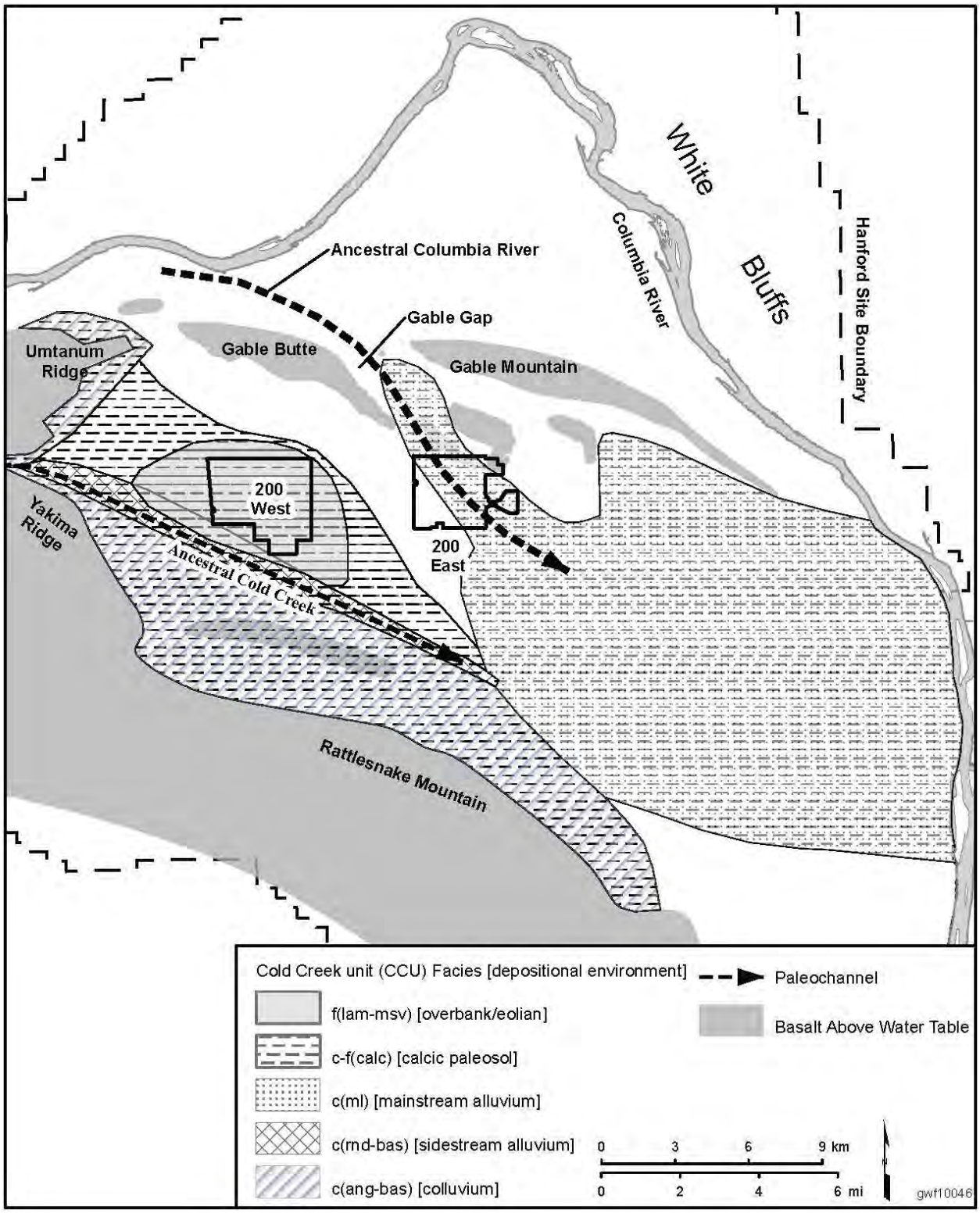

Reference: DOE/RL-2011-118, *Hanford Site Groundwater Monitoring for 2011*, Appendix E.

Historically, groundwater flow beneath WMA C was difficult to measure because of the scarcity of monitoring wells, the presence of the hydraulic divide, the hydraulic gradient is very small, and the hydraulic conductivity is very high in this region of the Hanford Site. For example, well 299-E27-7 had been considered an upgradient well, but groundwater contamination detected at this well in the late 1990's raised concern of the representativeness as an upgradient well for WMA C (DOE/RL-2016-67). In addition, the variable operational liquid discharges at 216-B-3 Pond system and other large discharge sites in 200 East Area impacted the water table. The direction of flow appeared to be primarily to the southwest during operations, although the water table maps were essentially indeterminate with respect to magnitude of the gradient (BNWL-B-360, *Selected Water Table Contour Maps and Well Hydrographs for the Hanford Reservation, 1944-1973*). During the 2000's, groundwater flow direction appears to have been predominantly to the southwest, with a shift to the south-southwest based on observed contaminant migration (DOE/RL-2009-77). The uneven surface of the basalt bottom of the aquifer also contributes to the difficulty of estimating quantity of flow. The aquifer thickness appears to vary by about ~5.5 m (~18 ft) in the vicinity of WMA C based on the top of basalt contacts in wells 299-E27-7, 299-E27-22, and 299-E27-155 (DOE/RL-2009-77).

The current WMA C monitoring well network consists of three upgradient wells, seven downgradient wells, and two cross-gradient wells (DOE/RL-2016-67). The water table continues to recover from the operational liquid discharges, and the projected equilibrium state is expected to be similar to its pre-Hanford behavior described in Section 3.1.9.2 and Appendix C of RPP-ENV-58782 and RPP-ENV-58806. As a result of these forecasted changes, the post-closure position of the water table and associated hydraulic gradient can only be evaluated through modeling. Consequently, the groundwater flux in the aquifer beneath WMA C is calculated on the basis of the aquifer hydraulic properties, and the hydraulic gradient projected to exist in the future.

The hydraulic heads around WMA C are expected to continue declining slowly (Figure 2-11) until they stabilize around 119.5 m (392 ft) (CP-47631). This stabilization is estimated to occur approximately 100 years into the future (CP-47631). The gradient is generally expected to slope from northwest to southeast with a value of approximately 0.00002 m/m, which is close to the one estimated to have existed prior to start of Hanford operations (Figure 3-11). Appreciable changes in hydraulic gradient are not expected in the future while land use remains as forecast and once the hydraulic heads stabilize.

Appendix A of CP-47613, Rev. 2 (CPGWM version 6.3.3), provides hydrograph comparisons of measured data and the calibrated modeled results for several wells, including the following wells located near WMA C: 299-E27-12, 299-E27-13, 299-E27-14, 299-E27-15, and 299-E27-21. Figures 4-43 through 4-45 of CP-47813 provide information regarding the overall performance of the model calibration in matching the measured data. Figure 4-43 presents the calibration misfit probability density for the two temporal data sets used in the calibration (1948 to 1953 and 2000 to 2009). Figure 4-44 presents the calibration misfit cumulative probability curve. Figure 4-45 provides a comparative view of the model results and measured data. Additionally, Table 4-10 in CP-47613, Rev. 2, includes the calibration statistics, indicating that the average error and root mean square error were 0.03 m (1.2 in.) and 0.86 m (33.9 in.), respectively. Figure 3-12 provides examples of the calibrated fit at wells 299-E27-14 and 299-E27-15 around WMA C.

Groundwater flow beneath WMA C has been historically difficult to measure because the hydraulic gradient is very small, and the hydraulic conductivity is very high in this region of the Hanford Site. In addition, the water table continues to recover from the operational liquid discharges at 216-B-3 Pond system and other large discharge sites in 200 East Area. This has led to changes in the direction of and magnitude of the groundwater flow beneath WMA C that occurred concurrent with the transport of leak contaminants in vadose zone and their arrival at the water table. Specific details of the changing aquifer gradient are difficult to establish and has been inferred from three lines of evidence. 1) As discussed in Section 2.3.3, a variety of contaminants have been detected below WMA C, so there is the potential that the locations and timing of arrival of groundwater plumes could be used to infer information about the groundwater flow system. However, it has not been possible to unambiguously identify contaminant concentrations in groundwater wells with specific leaks (see Section 2.3.4). The strongest association in the groundwater monitoring data is that ^{99}Tc in groundwater is unambiguously derived from WMA C, and furthermore, because of the high concentrations in groundwater, the majority of the ^{99}Tc in groundwater is probably derived from the largest WMA C leak, the tank C-105 leak. As a result of these observations, scoping calculations used to test the model (see Sections 4 and 5) are focused on ^{99}Tc groundwater data. 2) As discussed in Section 3.2, measured hydraulic head data at WMA C does not have sufficient resolution to show the timing and magnitude of the changes in groundwater gradient at WMA C. However, the general behavior of the water table is believed to be reasonably represented using the nearby low-gradient LLWMA-1 monitoring network, as shown in Figure 3-3. This line of evidence suggests that the aquifer was directed in a generally northerly direction until approximately 2008, after which it underwent a transition for several years that may have included several reversals of direction, ending with the gradient directed in a generally southerly direction following about 2011 (Figure 3-3). This interpretation is broadly consistent with interpretations of the groundwater system in the 200 East Area in successive Hanford Site annual groundwater monitoring reports during this period.

For instance, the 2006 annual report, PNNL-16346, *Hanford Site Groundwater Monitoring for Fiscal Year 2006*, Figure 2.1-2, shows an interpreted gradient that is somewhat ambiguous under 200 East Area, but generally directed northerly or northeasterly. By contrast, the 2016 Annual report, DOE/RL-2016-66, *Hanford Site RCRA Groundwater Monitoring Report for 2016*, Figure 10-4 shows an interpreted gradient unambiguously directed from the northwest to the southeast. Between these two reports, the interpreted groundwater system shows generally ambiguous flow directions to the northeast or east under 200 East Area. However, the 2012 annual report, DOE/RL-2013-22, *Hanford Site Groundwater Monitoring Report For 2012*, identifies that the change in flow direction was identified unambiguously. DOE/RL-2013-22 states “A recent flow direction change in the northwest corner of the 200 East Area appears to be the driver for the changing flow direction at WMA C. Groundwater flow in the northwest corner of 200 East Area has changed from predominantly northwest to southeast. This flow direction change coincides with ^{99}Tc increases in wells 299-E27-21 and 299-E27-24 at WMA C. These wells are located southeast of well 299-E27-23, where ^{99}Tc activity has exceeded 10 times the drinking water standard since 2008. Also coincident with the flow change are decreasing concentrations of other contaminants west of the 241-C tank farm, indicating a change in flow direction.” 3) The third line of evidence for the transient behavior of the groundwater system beneath WMA C

comes from the Central Plateau Groundwater Model (CPGWM). The development of CPGWM incorporates over 30 years of experience on development and application of groundwater models for the Central Plateau [PNL-10886, *Development of a Three-Dimensional Ground-Water Model of the Hanford Site Unconfined Aquifer System: FY 1995 Status Report*; PNNL-13641, *Uncertainty Analysis Framework – Hanford Site-Wide Groundwater Flow and Transport Model*; PNNL-14398, *Transient Inverse Calibration of the Site-Wide Groundwater Flow Model (ACM-2): FY 2003 Progress Report*; PNNL-14753, *Groundwater Data Package for Hanford Assessments*; and PNNL-12261, *Revised Hydrogeology for the Suprabasalt Aquifer System, 200-East Area and Vicinity, Hanford Site, Washington*]. The CPGWM incorporates the large-scale geologic and hydrogeologic features and provides estimates of water levels, hydraulic gradients, and groundwater flows throughout the 200 West and 200 East Areas, for past, current, and expected future groundwater conditions. Simulated water levels have been compared to observed values for wells located upgradient (well 299-E27-15) and downgradient (well 299-E27-14) of WMA C (Figure 3-12). The observed heads and CPGWM simulated heads, representing a time span of over 20 years, compare well providing confidence in the predictive capabilities of the CPGWM. The results of the CPGWM broadly support the conceptual framework of a shift in gradient from generally northerly or northwesterly, to a gradient directed southeasterly. Since the CPGWM represents a larger scale than the local area near WMA C, additional effort was needed to evaluate the local implications of the CPGWM on groundwater at WMA C; these additional evaluations are described in Section 5.

While these lines of evidence provide a general basis for the aquifer behavior at WMA C at times relevant to the assessment of past leaks, considerable challenges remain. The hydraulic heads, head gradients, and gradient orientations are significantly uncertain and change on the same time scales as the arrival of the plumes from the vadose zone. In the face of these uncertainties, the system representation has been undertaken in the following two ways:

1) A scoping case has been implemented that approximates the understanding of the changes in the water table as a function of time based on the above lines of evidence. This scoping case includes an initial time period with groundwater flow directed to the northwest, followed by a period in which groundwater flow transitions to the southeast, and a final period in which groundwater flow remains directed to the southeast. Two variants have been analyzed, one in which the transition occurs by a clockwise rotation of the aquifer gradient, and one in which the transition occurs by a counterclockwise rotation. This scoping case and the assumptions regarding the flow transition are documented in Section 5. It is emphasized that this scoping case is the only one developed for this report that is intended to represent the groundwater data in timing, concentration, shape of the breakthrough curves, and location of the wells.

2) All other scoping analyses have assumed a constant steady-state aquifer gradient magnitude and orientation. These scoping analyses are documented in Section 4. The conditions of these scoping cases have been chosen to be consistent with the long-term gradient assumed in RPP-ENV-58782 and RPP-ENV-58806 with hydraulic heads representative of past conditions to take account of the shorter travel distance in the vadose zone compared to the post-closure period. These scoping cases are intended primarily to assess the ability of the model to represent the time of first arrival of

contaminants at the water table. Evaluating the time of first arrival allows an examination of the ability of the model to represent the leaks themselves, and contaminant transport through the vadose zone, without the complications introduced by the transient aquifer conditions. Therefore, it is emphasized that the primary metric of interest in the scoping analyses in Section 4 is the time of first arrival. The breakthrough curves at specific well locations (including peak concentration and shape of the breakthrough curve), are primarily influenced by the transient aquifer conditions, which are evaluated in Section 5.

Within the WMA C flow domain, the weighted average of hydraulic conductivity derived from the CPGWM is ~11,000 m/day (~33,000 ft/day). Thus, the base case horizontal saturated hydraulic conductivity for the aquifer is estimated to be 11,000 m/day (33,000 ft/day). The CPGWM estimate of vertical anisotropy ratio of 0.1 is also incorporated in the WMA C base case. The estimates of hydraulic properties from calibration of the CPGWM were derived by matching water levels in the unconfined aquifer as the regional water table rose and fell in response to major increases and declines in discharges at waste water facilities in the central plateau between 1944 and 2008. Because the calibration is performed to long-term, larger scale transient changes to the water table in response to major changes in waste water discharges to the unconfined aquifer in the central plateau, hydraulic properties derived from this calibrated model effort is regarded as more reliable than hydraulic properties derived from smaller scale direct measurements by permeameter, slug, or pump tests. Additional discussion on this specific topic is provided in Appendix C of RPP-ENV-58806.

Table 3-7 presents a summary of the aquifer base case hydraulic parameters for the Hanford H3 – aquifer. The aquifer, identified as Hanford H3 – aquifer, is separated from that portion of the Hanford H3 above the water table, reflecting the distinctly different saturation conditions. The basis for the development of this estimated effective saturated hydraulic conductivity is found in Section C3.2 of Appendix C of RPP-ENV-58806.

Hydraulic conductivity estimates from various investigations on the aquifer within the 200 East Area are presented in Figure C-6 of RPP-58782. While groundwater flow can vary spatially due to local changes in hydraulic properties, the peak concentration at a particular location appears to correlate strongly to the mean groundwater flux (i.e., the rate of flow that occurs in a single direction), even in a heterogeneous aquifer (ITRC 2010, "Use and Measurement of Mass Flux and Mass Discharge," Interstate Technology & Regulatory Council; NUREG/CR-6767, *Evaluation of Hydrologic Uncertainty Assessments for Decommissioning Sites Using Complex and Simplified Models*). Permeameter, slug, and even aquifer pumping tests are limited in their ability to quantify spatial averages or trends, and are less likely to produce central measures of flow magnitudes than a regional model, but are important data included during model calibration (ITRC 2010). Measurements of hydraulic conductivity appear to be dependent on the test scale, and increase as the scale increases, particularly in heterogeneous media ("Scale Dependency of Hydraulic Conductivity Measurements" [Rovey and Cherkauer 1995]; "Scale Dependency of Hydraulic Conductivity in Heterogeneous Media" [Schulze-Makuch et al. 1999]). In-situ measures of aquifer flow and hydraulic properties inferred from hydraulic testing represent relatively small areas compared to the overall scale and dimensions of the model domain, and therefore do not provide representative results appropriate for the field scale (ITRC 2010).

3.6.3.7 Sorption Characteristics. The scoping analysis cases presented in Section 4 focus on ^{99}Tc, for which an assumption of zero sorption is appropriate. For forward calculations, base-case K_d values for other contaminants described in RPP-ENV-58782 and RPP-ENV-58806 are used.

3.6.4 Key Assumptions in Past leaks Analyses

In this section, a set of key assumptions used in the base case analysis of the past leaks analysis is listed. They are as follows:

- In the base case, the land use and land cover, including the barrier, remain shrub steppe indefinitely after closure.
- Alternative infiltration rates are included in alternative analysis cases, which are intended to address a variety of potential past recharge conditions.
- The design life of the cover is assumed to be 500 years in the base case, following which the infiltration through the cover is assumed to return to the site-wide average infiltration rate for undisturbed soil.
- These scoping analyses summarized in Section 4 evaluate the release of past leaks and waste losses summarized in Table 2.3. This future prediction analyses, summarized in Section 7 evaluate the inventories and timing of releases of past leaks and waste losses as summarized in Table 7.1.
- Radionuclide and chemical release mechanisms from the sources are assumed to occur at the approximate location of the past leaks and losses.
- Release from one WMA C solute source and migration are independent of other solute transport and source terms in the model.
- The vadose zone is modeled as an aqueous-gas porous media system where flow and transport through the gas phase are assumed to be negligible.
- Details of the development of this model and how vadose zone properties were assigned to various hydrologic units in this specific model is described in Appendix F of RPP-ENV-58782 and RPP-ENV-58806). A range of vadose zone hydraulic properties evaluated in the some of the scoping cases, including an alternative heterogeneous model representation of the vadose zone, are also discussed in this appendix.
- The basis for the development of this estimated effective saturated hydraulic conductivity is found in Section C3.2 of Appendix C of RPP-ENV-58806. A range of groundwater hydraulic properties evaluated in the some of the scoping cases are also discussed in Appendix C of RPP-ENV-58806.

- Groundwater flow beneath WMA C in the steady state scoping and future projection analyses is assumed to be northwest to southeast and parallel to the four tank arrays of 100-series tanks and the four 200-series tanks in WMA C.

- Transport of contamination from the past leaks is assumed to be controlled by sorption and they migrate through the underlying vadose zone and the unconfined aquifer.

- Distribution coefficients (K_d) are used to represent sediment-contaminant chemical interaction that best represent plausible levels of reactivity. The K_d values are chosen assuming low-salt, near-neutral waste chemistry in the vadose and saturated zone. Justification for the selected parameter values is found in RPP-RPT-46088 and PNNL-16663.

3.7 SUMMARY OF FEATURES AND DEFINITION OF SCOPING ANALYSIS CASES

As discussed in Section 3.1, uncertainties exist in a number of the features associated with modeling past leaks at WMA C. As part of the scoping sessions held in 2009 through 2011, a set of topics were identified that need to be explored through scoping analysis cases. These issues can be broadly thought of belonging to one of the following three categories.

- Topics associated with past leaks: inventory, volume, timing, and location.

- Topics associated with the vadose zone: the effects of soil heterogeneity, the effects of alternative conceptualizations of the geological media, the effects of man-made features such as dry wells, and the potential effects of unknown features such as a clastic dike under WMA C.

- Topics associated with the saturated zone evolution in time during the operational period and its effect on the observed changes in patterns of contamination at the monitoring wells.

Figure 3-11. Hindcast Water Table Map of the Hanford Site, January 1944.

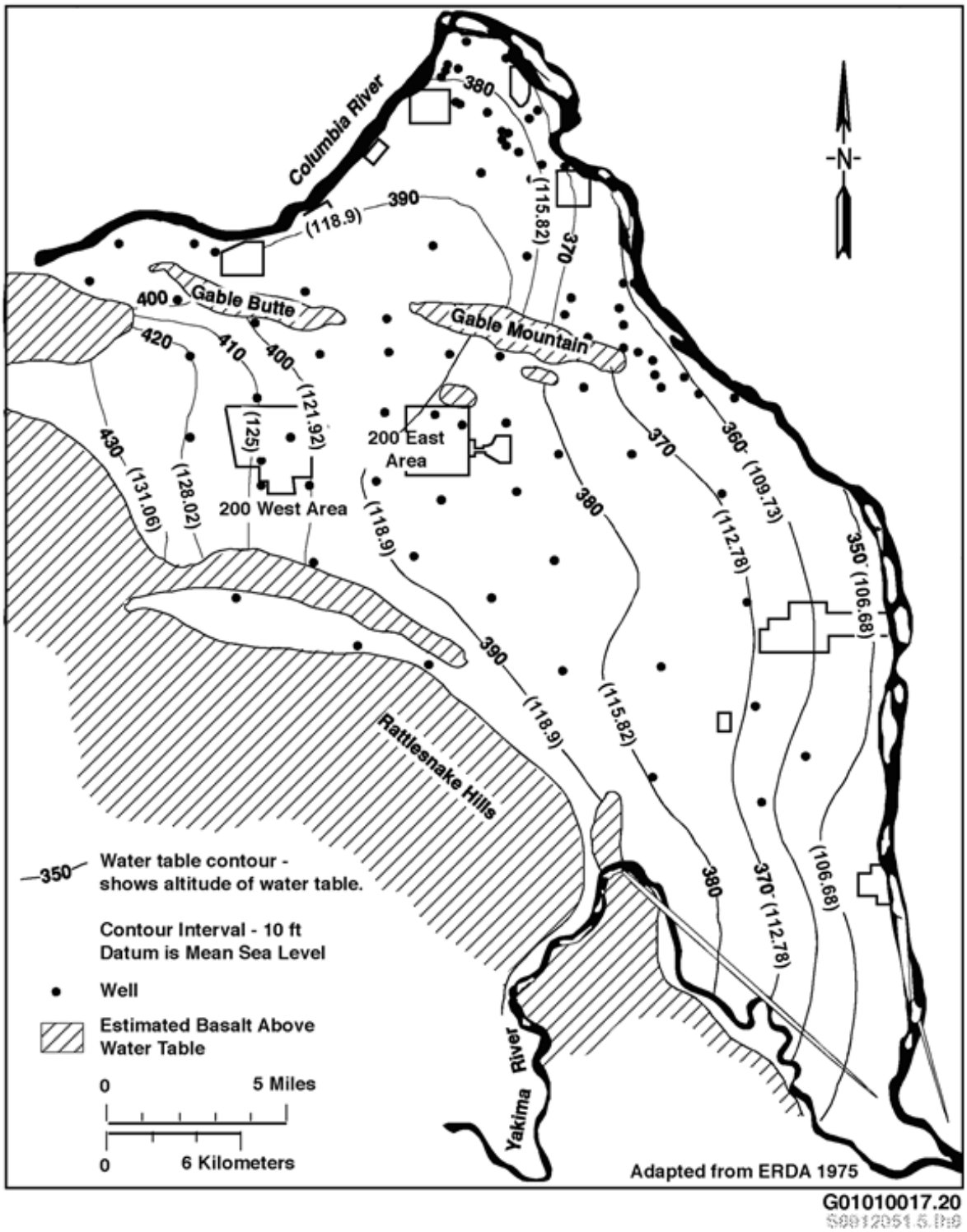

ERDA 1975 = ERDA-1538, *Final Environmental Statement, Waste Management Operations, Hanford Reservation, Richland, Washington*.

Reference: WHC-SD-ER-TI-003, *Geology and Hydrology of the Hanford Site: A Standardized Text for Use in Westinghouse Hanford Company Documents and Reports*.

Figure 3-12. Central Plateau Groundwater Model Calibration Results in the Vicinity of Waste Management Area C.

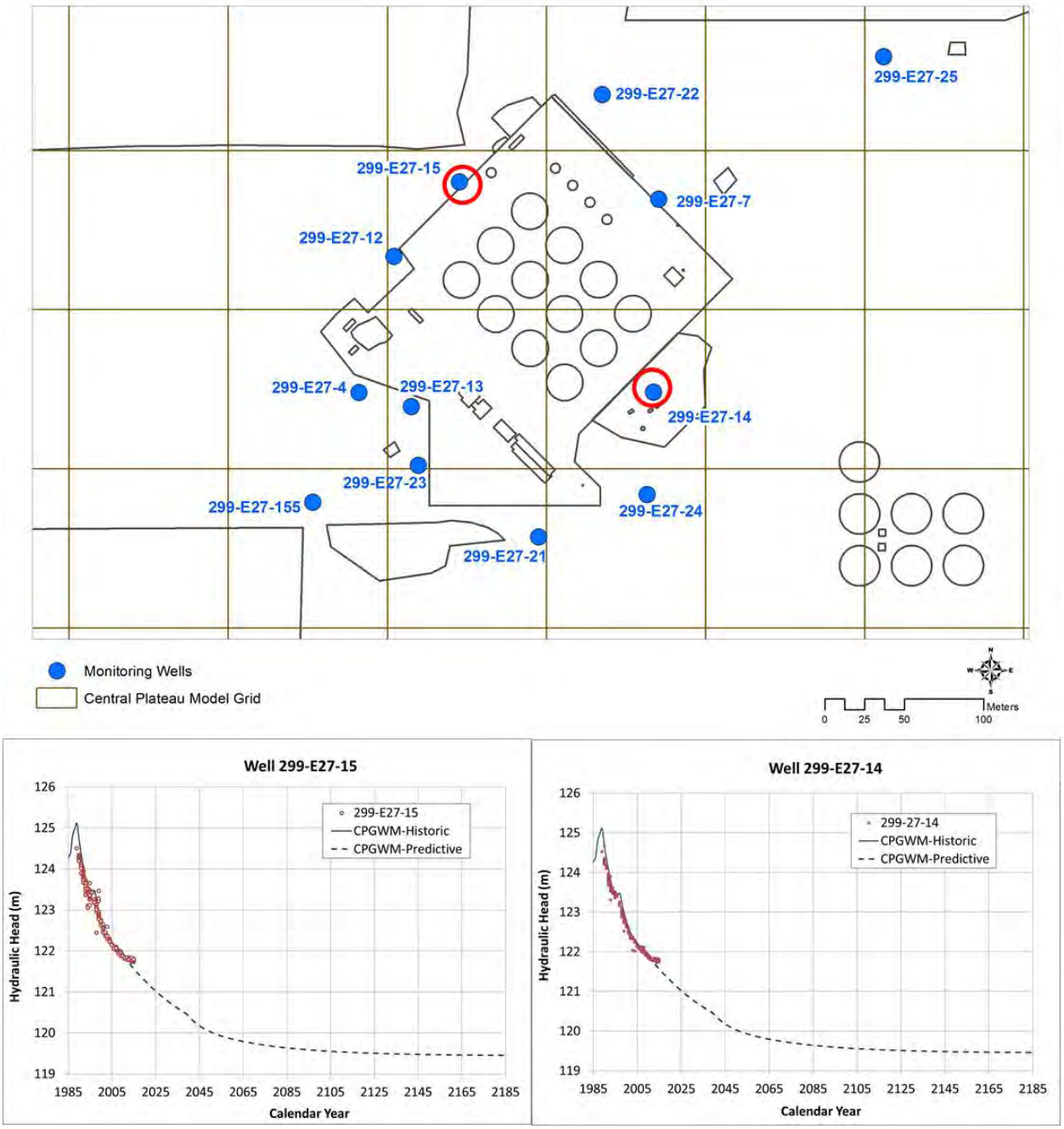

CPGWM = Central Plateau Groundwater Model

Reference: CP-47631, *Model Package Report: Central Plateau Groundwater Model Version 6.3.3*.

To address these topics, a suite of scoping analysis cases has been identified and are described in Section 4.

Table 3-7. Base Case Soil Hydraulic Properties for Aquifer Soil Type Used for Base Case at Waste Management Area C.

Aquifer Soil Type	Total Porosity	Saturated Moisture Content	Horizontal Saturated Hydraulic Conductivity[a] (m/day)	Longitudinal Dispersivity[b] (m)	Aquifer Hydraulic Gradient (m/m)	Average Aquifer Water Flux ($m^3/day/m^2$)
Hanford H3 (aquifer)	0.20	0.20	11,000	10.5	0.00002	0.22

[a] Vertical Saturated Hydraulic Conductivity assumed equal to 1/10 of the Horizontal Saturated Hydraulic Conductivity.
[b] Transverse dispersivity assumed to be equal to 1/10 of the longitudinal dispersivity.

Reference: RPP-RPT-46088, *Flow and Transport in the Natural System at Waste Management Area C.*

This page intentionally left blank.

4.0 SCOPING ANALYSES OF PAST WASTE RELEASES

In this section, a series of scoping analysis cases are described that use the PA model developed for the assessment of potential future releases from residual wastes, documented in RPP-ENV-58782 and RPP-ENV-58806, with appropriate adaptations to represent past conditions at WMA C. Sources of contamination have been introduced into the model to represent the occurrence of the past leaks at the times at which they are believed to have occurred. The model was then run forward to the present to evaluate how well the models represent field data for ^{99}Tc in groundwater wells.

As discussed in Section 3, the groundwater concentration data are significantly affected by the way the water table changed during this time period, and the specific way the water table changed is not well known. Instead, it has been inferred from several lines of evidence. This feature of the modeled system introduces substantial complexities to the modeling and interpretation of the data. Consequently, a set of scoping analyses were developed to evaluate the system behavior without this complexity. This was accomplished by developing scoping cases with a static water table, which are intended only to evaluate processes in the vadose zone. These scoping cases are presented in this section. Scoping cases that evaluate the entire system behavior, including the changing water table, are presented in Section 6.

The focus of the analysis cases presented in this section is to provide improved understanding of the phenomena and parameters in the vadose zone that have led to the current state of contamination below and near WMA C. The focus of the analysis cases reported in this section is on ^{99}Tc contamination, which is unambiguously the result of past UPRs from WMA C. Groundwater in the vicinity of WMA C has also seen impacts by other COPCs (e.g., nitrate, sulfate, for example), but ^{99}Tc is the contaminant that accounts for the majority of the past and current dose and risk impacts to groundwater at WMA C. The focus of the analysis cases presented in this section is to provide improved understanding of the phenomena and parameters in the vadose zone that have led to the current state of contamination below and near WMA C. The focus of the analysis cases reported in this section is on ^{99}Tc contamination, which is unambiguously the result of past UPRs from WMA C.

The goal of the scoping analyses is to match, to the extent possible, the first arrival times of contamination at the water table and general concentration levels as observed in monitoring wells[1]. The first arrival is primarily influenced by the behavior of the leaks themselves, and by flow and transport behavior in the vadose zone. Changes in the saturated zone affect time to the first arrival only in that the changing height of the water table (hence thickness of the vadose zone) needs to be considered. Since changes in the water table are not included in the scoping analyses presented in this section, they should not be expected to (and indeed do not) provide good comparisons with either the peak concentrations in well data or the general shapes of the

[1] The monitoring network was started in 1989, with subsequent additions. There are, therefore, no observations prior to that time with which to compare. Any contamination that may have reached groundwater during that time is not included in the current assessment. There is no evidence suggesting that any such contamination occurred.

breakthrough curves (sharp rises and falls in concentration). These features of the data are believed to be associated with shifts in the direction of the groundwater flow. This aspect of the breakthrough curves is not well represented by the scoping cases presented in this section, since they all assume a constant groundwater flow rate and direction. Analyses that take account of the changing water table are presented in Section 6, and those analyses are intended to provide insight into the rapid rise and fall of observed data, and how the plume has moved between wells.

The scoping analyses presented in this section evaluate changes in calculated groundwater impacts that result from changes in input parameter estimates or changes to a conceptual model, such as the interpretation of the hydrogeologic units. The range of analysis cases are generally intended to evaluate changes in parameters and modeling assumptions, which demonstrate the effect that alternative assumptions and estimates have on the groundwater arrival times and concentrations in and around the tank farm. To emphasize, the scoping cases in this section are focused solely on alternative assumptions about conditions in the vadose zone. Refer to Section 6 for the complete model that accounts for all the relevant phenomena.

The set of scoping analyses is presented in Table 4-1. The table includes a brief explanation of each scoping analysis to provide insight into the alternative assumptions it is intended to evaluate. Because these scoping cases involve changes to the underlying flow field, the analysis was best done using a process model and STOMP© was used to perform the calculations.

In Table 4-1, the scoping analyses represent categories of uncertainty. The scoping cases can be grouped in four categories: 1) changes to estimates of UPR volume and inventory; 2) changes in groundwater flow rate (hence dilution) in the saturated zone; 3) changes in recharge; and 4) changes in vadose zone geology and hydrologic parameters. The first set of scoping simulations (Cases 1a and 1b) addresses the range of estimated ^{99}Tc inventory and the leak volume. The set of groundwater flux cases (Case 2a and 2b) correspond to altered aquifer flow rates that produce lower and upper confidence limits of aquifer dilution. The set of recharge-related scoping analyses (Cases 3a –3c) address elements associated with the magnitude of the net infiltration through the tank farm surface and surrounding disturbed ground. The set of vadose zone cases (Cases 4a-4f) examine the impacts of changes in the hydrologic parameters and spatial heterogeneity in the vadose zone. This fourth set of scoping cases considers the evaluation of a range of cases:

- Case 4a – a case to represent Alternative Geologic Model II;
- Case 4b – a case to represent a heterogeneous representation of the vadose zone;
- Cases 4c and 4d – cases to represent upper and lower confidence limits for vadose zone hydraulic properties;
- Case 4e – a case to represent a hypothesized presence of a clastic dike within the WMA C fenceline, and

- Case 4f – a case to represent a hypothesized existence of an unsealed or poorly sealed borehole in the tank farm.

Table 4-1. Description of Past Tank Waste Release Scoping Cases. (2 sheets)

Scoping Case (Abbreviation)	Scoping Case Description and Purpose
Case 1a[1] (Hi_inv)	Assumes prescribed invariant aquifer boundary conditions, similar to the base case of the DOE 435.1 PA and RCRA Closure Analysis, with a modification to account for the increased water table elevation in the WMA C area under current conditions. The water table has been set to approximate current conditions of ~122.25 m (~401 ft) above Mean Sea Level. The hydrogeologic framework, vadose zone, and groundwater flow and transport parameters remain unchanged from the base case of the DOE 435.1 PA and RCRA Closure Analysis. This case also assumes current estimates of leak inventories and volumes that includes the upper bound inventory (9.8 Ci) and volume 77,600 L (20,500 gals) developed for tank 241-C-105 (tank C-105).
Case 1b (Lo_inv)	This case is similar to Case 1a but assumes current estimates of leak inventories and volumes that includes the lower bound inventory (1 Ci) and volume 7,570 L (2,000 gals) developed for tank C-105.
Cases Related to Changes in Groundwater Flux Rates	
Case 2a (GWflux_10%)	Assumes same parameterization and past leak volumes and inventories as Case 1a but with the aquifer flux set at 10th percentile values used in the uncertainty analysis developed for the DOE 435.1 PA. This case corresponds to altered aquifer flow producing minimal aquifer dilution compared to Hi_inv.
Case 2b (GWflux_90%)	Assumes same parameterization and past leak volumes and inventories as Case 1a but with the aquifer flux set at 90th percentile values used in the uncertainty analysis developed the DOE O 435.1 PA. This case corresponds to altered aquifer flow producing a higher level of aquifer dilution compared to Hi_inv.
Cases Related to Changes in Recharge Rates	
Case 3a (EnhanceRech_150)	Assumes same parameterization and past leak volumes and inventories as Case 1a but with a recharge rate of 150 mm/yr (5.9 in./yr) applied for the tank farm area within the WMA C model domain to evaluate effect of increased recharge inside of the tank farm area on past releases.
Case 3b (EnhanceRech_100)	Assumes same parameterization and past leak volumes and inventories as Case 1a but with a recharge rate of 100 mm/yr (3.9 in./yr) for all areas within the WMA C model domain to evaluate effect of increased anthropogenic recharge outside of the tank farm area on past releases.
Case 3c (Gunite_Cap)	Assumes same parameterization and past leak volumes and inventories as Case 1a but some local changes at UPRs-E-81, -82, and -86. These changes include an additional 1,135 Lpm (300 gpm) of wash water for 4 hours at the time of release (a one-time addition of 272,550 L [72,000 gal]). Twenty years after UPRs-E-82, and -86, a gunite cap was applied to those two surfaces which is assumed to change the infiltration at those UPRs to 1 mm/yr (0.04 in./yr) (UPR-E-81 includes does not have a gunite cap). The case investigates the effects of potential localized water use and caps at selected UPRs on those past releases.

Table 4-1. Description of Past Tank Waste Release Scoping Cases. (2 sheets)

Scoping Case (Abbreviation)	Scoping Case Description and Purpose
Cases Related to Changes in Vadose Zone Parameters/Conceptualizations	
Case 4a[1] (ACM_II)	Assumes the same parameterization and past leak volumes and inventories as Case 1a but with the geologic interpretation using the picks for the top of the units supplied by Nez Perce staff for Alternative Geologic Model II. This case examines the effect of a finer alternative treatment of major hydrogeologic units in the vadose zone on past releases.
Case 4b (ACM_hetero)	Assumes vadose zone parameterization in the heterogeneous (i.e., based on moisture contents in the vadose zone underlying WMA C) hydrogeologic model interpretation developed for use in DOE O 435.1 PA and RCRA Closure Analysis with Case 1a leak volumes and inventories. This case examines the effect of heterogeneous treatment of sediments in the vadose zone on past releases. Since this scoping analysis was completed, the results for other alternative representations of subsurface heterogeneity at WMA C have been developed. A summary of these additional developmental efforts and associated modeling results are presented and discussed in Section 5 of this document.
Case 4c (vzprop_50%)	Assumes same parameterization and past leak volumes and inventories as Case 1a but with vadose zone hydraulic properties at the 50th percentile values as set in the uncertainty analysis developed for the DOE Order 435.1 PA. This case evaluates the effect on past releases of higher vadose zone hydraulic properties than used in Case 1a.
Case 4d (vzprop_95%)	Assumes same parameterization and past leak volumes and inventories as Case 1a but with vadose zone hydraulic properties at the 95th percentile values as set in the uncertainty analysis developed for the DOE Order 435.1 PA. This case evaluates the effect on past releases of lower vadose zone hydraulic properties than used in Case 1a.
Case 4e (ACM_dike)	Assumes same parameterization and past leak volumes and inventories as Case 1a but with a hypothetical clastic dike placed below tank C-105. This case evaluates the effect on past releases of a possible preferential pathway for contaminants in the vicinity of tank C-105. The key assumptions and model implementation of the hypothetical clastic dike simulated in this case is described in Section 4.4 below.
Case 4f (ACM_borehole)	Assumes same parameterization and past leak volumes and inventories as Case 1a but with the additional assumption of an inadequately sealed borehole at well 299-E27-70 (drywell 30-05-02), located near the past tank leak near tank C-105. This case evaluates the effect on past releases for another possible type of preferential pathway for contaminants in the vicinity of tank C-105. The key assumptions and model implementation of the hypothetical unsealed borehole simulated in this case is described in Section 4.4 below.

PA = performance assessment
RCRA = Resource Conservation and Recovery Act of 1976
UPR = unplanned release
WMA = Waste Management Area

Reference: DOE 435.1, Radioactive Waste Management.

1 As a part of the comment resolution process with Ecology, a request was made by Ecology staff to evaluate an alternative inventory case that examined the groundwater impacts of doubling the release duration, the ^{99}Tc inventory, and the waste volume associated with the tank C-105 leak that were assumed in Case 1a. A complete description of Ecology's requested alternative to Case 1a is provided in Appendix D.

For all these analysis cases, the STOMP©-based model developed for the PA and RCA of residual wastes has been modified to match the approximate water table elevation that currently exists. This modification was made to approximate the depth to the water table that existed when the plumes arrived at the water table, so that this model will represent the time of first arrival at the water table of past leaks better than the base-case PA and RCA model. The decline in the water table and its effect on the gradient and orientation of the flow have been discussed in Section 2.5. In the scoping analyses these changes are not evaluated; instead, the water table is assumed to be static, at its current level, for the duration of the analysis.

It is worth noting that Case 1 represents a minimal change from the PA and RCA model, in which the height of the water table is changed to current conditions, and the leaks have been introduced, but the structure of the model and all other parameters remain the same. The other cases represent additional changes to the model structure or parameter values.

The hydraulic heads around WMA C are expected to continue declining slowly, as shown in Figure 4-1, until they stabilize around year 2130 at 119.5 m (392 ft) Above Mean Sea Level (AMSL). The stable projected long-term aquifer conditions were evaluated in the radiological PA of residual contamination (RPP-ENV-58782) and the RCA for WMA C (RPP-ENV-58806).

For the scoping analyses, the water table elevation in the WMA C area has been set to approximate current conditions, around 122 m (404 ft) (Figure 4-1); the boundary condition of the 3-D STOMP© model developed for the PA/RCA has been changed to 122.50 m (401.9 ft) AMSL. This change in the model was implemented by updating the model boundary conditions. The updated water table location resulted an average 14-m (46-ft)-thick saturated zone in these analysis cases. Everything else in the model has been kept the same as the PA/RCA model (RPP-ENV-58782, RPP-ENV-58806).

The scoping analyses discussed in this section do not attempt to include the effects that the changes in hydraulic gradient magnitude and direction have introduced to the groundwater flow field since Hanford Site began discharging large quantities of liquid. The direction has rotated 180 degrees since the startup of operations, and the gradient has been highly variable and very difficult to measure. Instead, the scoping analyses are based on a static gradient magnitude and direction. Therefore, the analyses in this section are primarily intended to evaluate parameters associated with the leaks themselves, and with the vadose zone. The primary metric of interest for these scoping analyses is the time of arrival of the plume at the water table; the time of arrival is not affected by the orientation of the aquifer gradient. Aquifer concentrations are only a secondary metric of interest in these scoping analyses, allowing a qualitative comparison of the magnitude of the concentration, without an expectation that the model will produce a good match to concentration results. To match concentration results, the effect of the changing aquifer must be built into the model; such an analysis is presented in Section 6.

As a result of the complicating effect of the variable water table on monitoring data, it is not appropriate to compare the model results at the location of the monitoring wells. The static gradient applied in the model is not necessarily oriented in the same direction as the real water table at any given time in the analysis. Instead, the model is used to calculate concentrations as fixed distances from the releases, and this is used as an indicator of the effect of distance from

the leak on groundwater concentrations. Since the tank C-105 leak is the predominant source in the tank farm, a distance of 60 m (197 ft) was selected as one distance used in the scoping analyses. This represents both the approximate distance from the tank C-105 leak to the WMA C fenceline in a southeasterly direction, and also the approximate distance to monitoring well 299-E27-14 (see Figure 4-2). Concentrations were also calculated at 60 m (197 ft) downgradient from the WMA C fenceline, representing the approximate distance to monitoring well 299-E27-24 (see Figure 4-2), and at 20 m (66 ft), which provides an upper bound concentration for the calculation taking account of the dilution that occurs as the plume moves downgradient in the aquifer. The 60-m (197-ft) distance from tank C-105 to the fenceline and the additional 60 m (197 ft) downgradient from the WMA C fenceline, represent the approximate distance to monitoring wells 299-E27-23 and 299-E27-21, two other locations where significant concentrations of ^{99}Tc have been observed.

These points of calculation (PoCals) primarily focus on the tank C-105 leak, and the calculated concentrations largely represent the contribution of the tank C-105 leak. However, in all scoping analysis cases the entire inventory of all leaks is implemented.

4.1 CASE 1: EFFECT OF LEAK INVENTORIES AND VOLUMES

The scoping cases presented in this subsection represent an attempt to compare alternative modeling assumptions about leak inventories and volumes to field data, with a view to identifying modeling assumptions that are either consistent or inconsistent with monitoring data. Monitoring data do not exist prior to 1989, and comparisons of the model with data are only made subsequent to that time. The cases have been run as blind trials; that is, the inputs are best estimates derived as discussed in Sections 2 and 3, and the models run in a forward manner from the time of the leaks to today. There are no fitting parameters in the model, and no adjustments to model inputs have been made to improve the comparisons. The intent is to identify which sets of inputs are contradicted by data, and hence develop improved understanding of the implications of various alternative assumptions on the comparison between the model and data.

As discussed in the introduction of Section 4, because of the complicating effect of the time-varying water table on monitoring data, it is not appropriate to compare the model results in this section at the location of the monitoring wells. The static gradient applied in the models discussed in this section is not necessarily oriented in the same direction as the real water table at any given time in the analysis. Instead, the model is used primarily for comparison with time of arrival of the plume, and secondarily to calculate concentrations as fixed distances from the releases, and this is used as an indicator of the effect of distance from the leak on groundwater concentrations. Model comparisons with the changing water table are presented in Section 6, along with comparisons with field data.

4.1.1 Case Descriptions

The purpose of Case 1 is to evaluate the effect of leak inventory and volume on peak concentrations and arrival time at the aquifer. Given the dominance of the tank C-105 leak in terms of total ^{99}Tc released, the focus of this case is on the inventory and volume of the tank C-105 leak. Case 1a uses upper bound leak inventories and volumes based on an assumed upper bound inventory for the tank C-105 waste loss of 9.8 Ci and an upper bound leak volume of 77,600 L (20,500 gal). Case 1b uses the lower bound leak inventories and volumes based on an assumed lower bound inventory for the tank C-105 waste loss of 1.0 Ci and a lower bound leak volume of 7,570 L (2,000 gal).

Figure 4-1. Decreases in Water Table Level with Time at Waste Management Area C, with a Projection to Future Conditions.

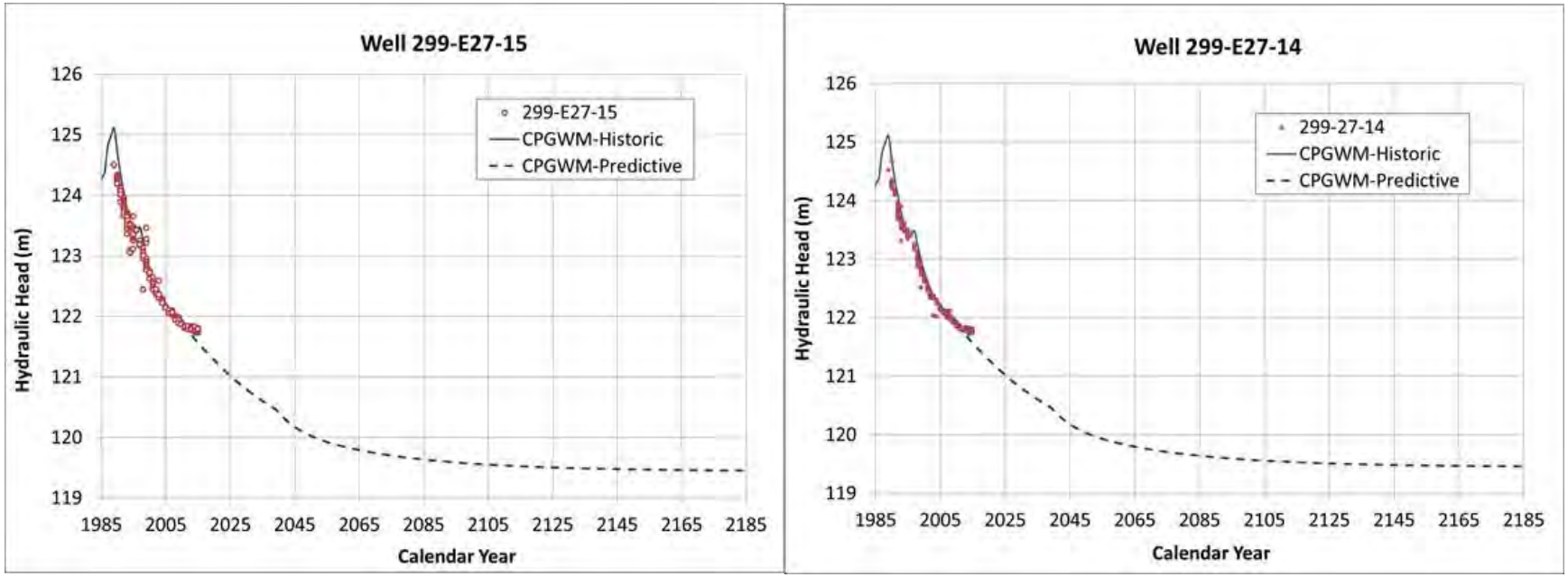

CPGWM = Central Plateau Groundwater Model

References:

RPP-ENV-58782, *Performance Assessment of Waste Management Area C, Hanford Site, Washington*, Appendix C – Technical Basis for Waste Management Area C Unconfined Aquifer Conceptual Model: Field Data and Related Investigations.

CP-47631, *Model Package Report: Central Plateau Groundwater Model Version 6.3.3*.

Figure 4-2. Points of Calculation for the Scoping Analyses.

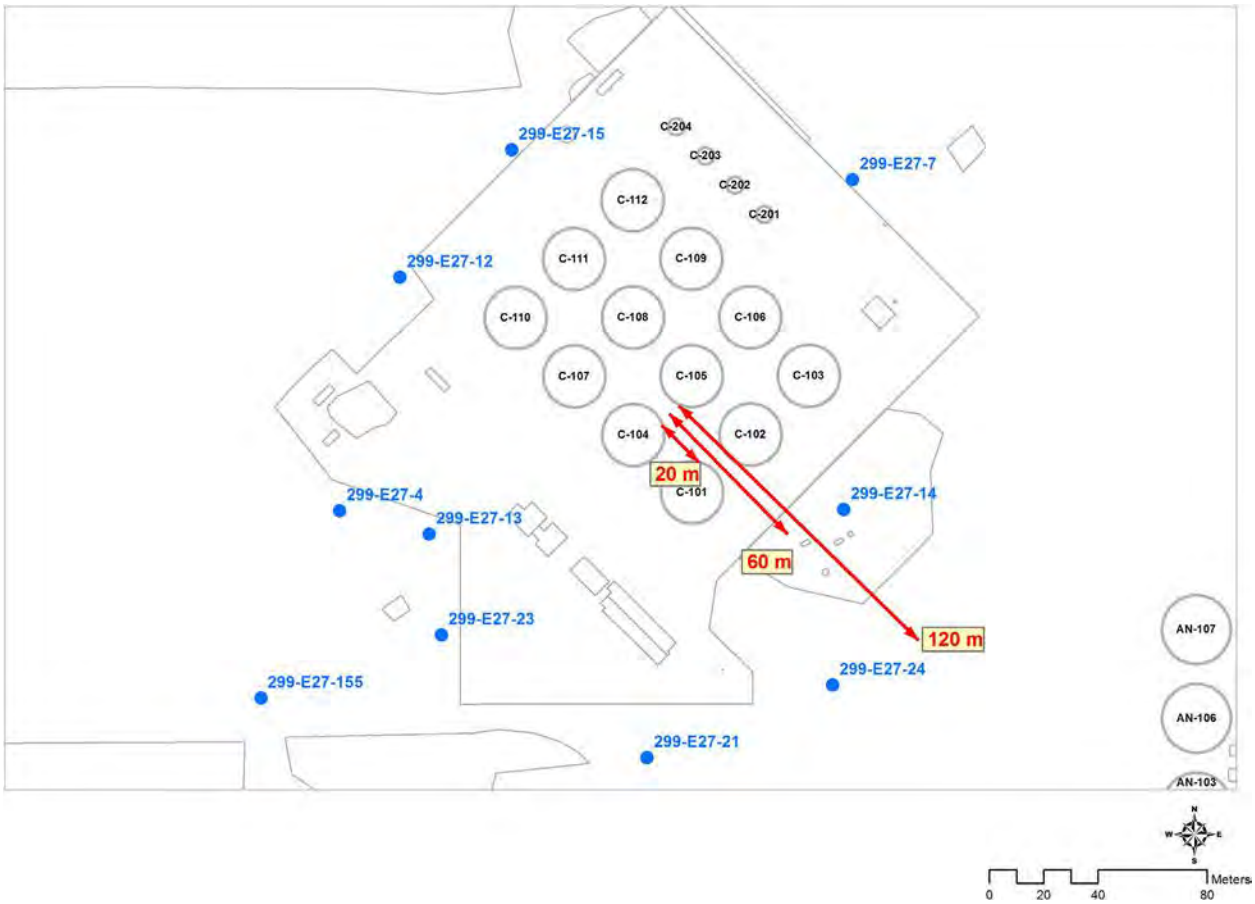

4.1.2 Case Results

Results of Case 1a are shown in Figures 4-3 and 4-4 and summarized at selected PoCals in Table 4-2. A comparison of simulated results with ^{99}Tc concentration levels historically observed at wells 299-E27-14 and 299-E27-23 is also shown in Figure 4-4. The 60-m (197-ft) and 120-m (394-ft) calculated breakthrough curves provide a reasonable match of the first arrival time of the plumes as well as the initial rise in concentration. The calculated curve for 20 m (66 ft) also produces a reasonable match for first arrival of the plume but rises more quickly than the data. The calculation at 20 m (66 ft) provides better match for the peak concentration observed at well 299-E27-23. These observations are important because it means that the model can match time of first arrival without adjustment of input parameters other than the water table elevation correction.

In Figure 4-4, the peak calculated concentrations at 60 m (197 ft) and 120 m (394 ft) are somewhat below the measured peak concentrations. These figures illustrate the drop-off in ^{99}Tc concentration levels with distance from this source and confirm that the peak calculated concentrations occur around 2015 to 2020 followed by falling concentrations. The calculated peak concentrations for Case 1a are in the range 6,000 to 23,000 pCi/L over the downgradient distances evaluated. Owing to the high hydraulic conductivity and associated groundwater flux

used in the model, these results also illustrate how quickly elevated concentrations can migrate in the direction of flow to the WMA C fenceline and other downgradient locations.

In Figure 4-3, the development of the plumes is shown between the year 2000 and the year 2030. The peak concentrations in the aquifer are seen to reach a maximum around the year 2016, after which concentrations are generally seen to fall. The dominant impacts originate for past releases simulated at tank C-105. Impacts at the water table from UPR-86—which is located in an area of slightly lower recharge (63 mm/yr [2.48 in./yr]) than assumed within the tank area (100 mm/yr [3.94 in./yr])—are delayed relative to the impacts from other sources within the tank farm proper.

Results for Case 1b are shown in Figure 4-5 and summarized at selected PoCals in Table 4-2. The timing of the development of the plumes is very similar to Case 1a, but the resulting plume is significantly lower in concentration than Case 1a, and significantly lower than measured groundwater concentrations. As a result of this observation, all other scoping cases were evaluated using the volumes and inventories used in Case 1a. The lower bound inventory and volume for the tank C-105 leak has been judged to be inconsistent with groundwater concentrations in monitoring wells.

4.2 CASE 2: EFFECT OF CHANGES IN GROUNDWATER FLUX RATES

The scoping cases presented in this section represent an attempt to compare alternative modeling assumptions about groundwater flux rates to field data, with a view to identifying modeling assumptions that are either consistent or inconsistent with monitoring data. Monitoring data do not exist prior to 1989, and comparisons of the model with data are only made subsequent to that time. The cases have been run as blind trials; that is, the inputs are best estimates derived as discussed in Sections 2 and 3, and the models run in a forward manner from the time of the leaks to today. There are no fitting parameters in the model, and no adjustments to model inputs have been made to improve the comparisons. The intent is to identify which sets of inputs are contradicted by data, and hence develop improved understanding of the implications of various alternative assumptions on the comparison between the model and data.

As discussed in the introduction to this section, because of the complicating effect of the time-varying water table on monitoring data, it is not appropriate to compare the model results in this section at the location of the monitoring wells. The static gradient applied in the models discussed in this section is not necessarily oriented in the same direction as the real water table at any given time in the analysis. Instead, the model is used primarily for comparison with time of arrival of the plume, and secondarily to calculate concentrations as fixed distances from the releases, and this is used as an indicator of the effect of distance from the leak on groundwater concentrations. Model comparisons with the changing water table are presented in Section 5, along with comparisons with field data.

4.2.1 Case Descriptions

The set of two analysis cases described in this section both make use of the Case 1a analysis with input modifications to allow for examination of the effect of changed groundwater flux rates. In Case 1, the conclusion was reached that the upper bound leak inventory was consistent with data, but the lower bound was not. Case 2 was selected to confirm that judgment by examining another key parameter that could affect concentration. All other parameters remain the same as in Case 1a; as a result, there is no new information provided by this scoping case regarding arrival time.

The parameters that determine the groundwater flux and the amount of dilution that occurs in the aquifer are the hydraulic conductivity and hydraulic gradient. In a natural system, the two parameters offset one another. If the groundwater flux through an aquifer volume remains constant, then in areas with high hydraulic conductivity, the hydraulic gradient will be less, and vice versa. They are considered to be coupled parameters because changes to the flux term caused by changes made to one term are inseparable from changes made to the other term. These parameters act inversely proportional to one another, and the same change in the flux can be made by making the same proportional change to either parameter. Therefore, only one of the parameters needs to be varied to produce the variability in the flux necessary to conduct the sensitivity analysis.

The scoping analysis includes two cases evaluating different values of groundwater flux:

- **Case 2a**: This case assumes the 10th percentile value for aquifer flux (0.11 m/day [0.36 in./day])

- **Case 2b**: This case assumes the 90th percentile value (0.33 m/day [1.08 in./day]).

The underlying distribution of this specific hydraulic property parameter used in these cases was developed as a part of the uncertainty analysis performed to support the DOE O 435.1 WMA C PA (see Section 8.1.3.6 in RPP-ENV-58782).

Figure 4-3. Development of Technetium-99 Plumes over Selected Time Periods for Case 1a (Upper Bound Inventory for the Tank 241-C-105 Leak).

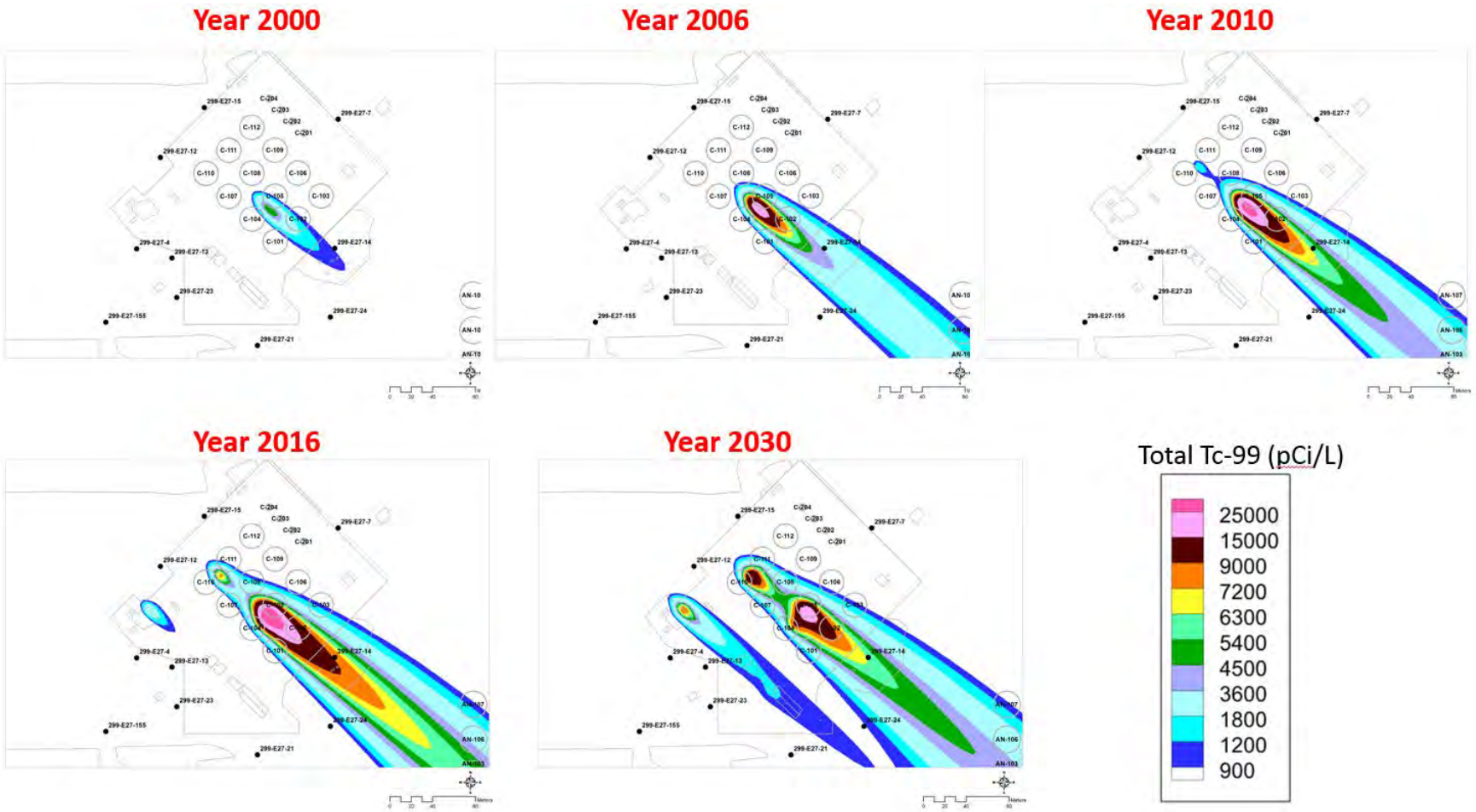

Figure 4-4. Concentrations at the Selected Points of Calculation for Case 1a (Upper Bound Inventory for the Tank 241-C-105 Leak).

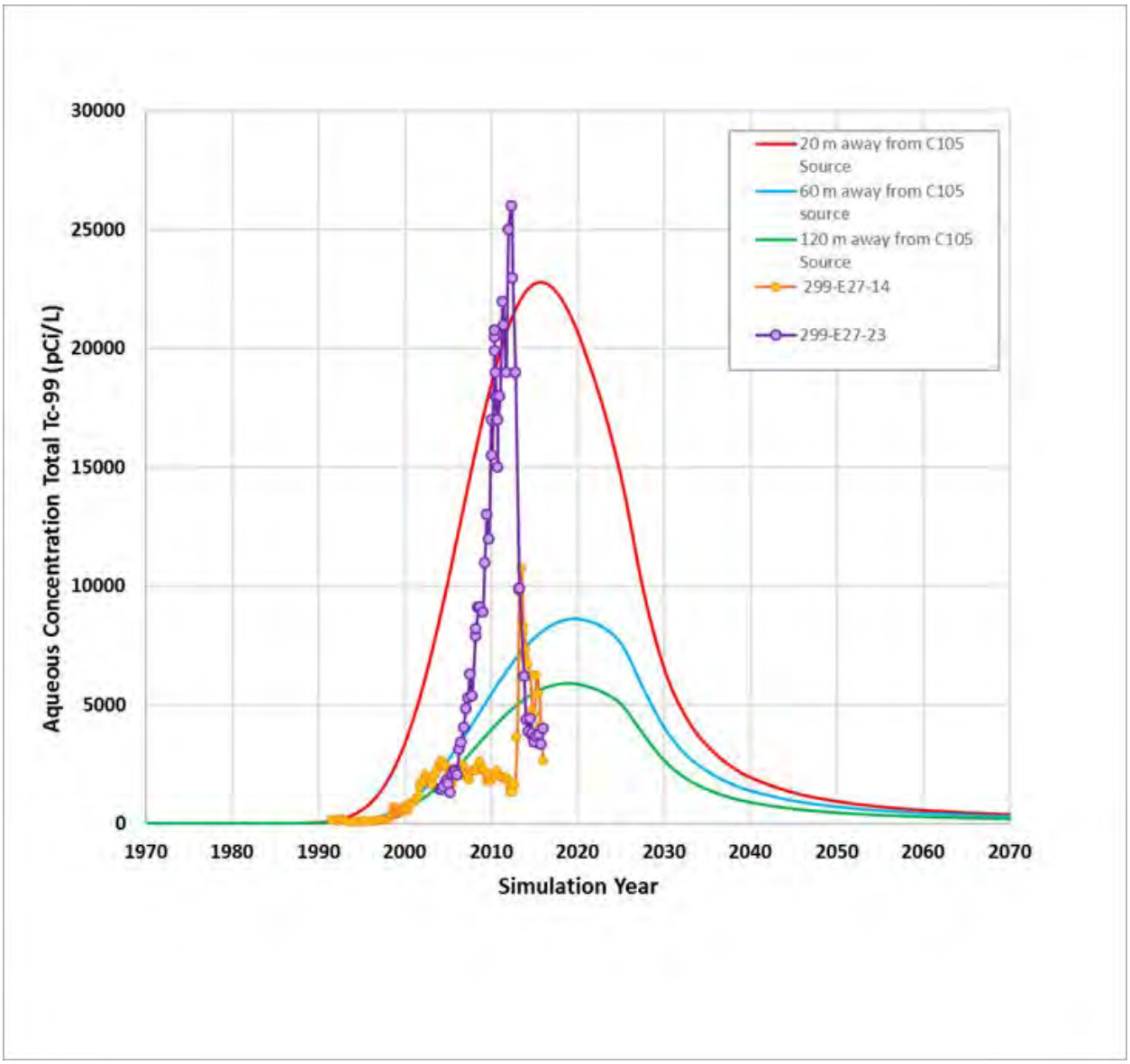

Note: Also shown are measured Technetium-99 concentration data from wells 299 E27-14 and 299-E27-23.

4.2.2 Case Results

Results of Case 2a (10th percentile groundwater flux) are presented in Figure 4-6 and summarized at selected PoCals in Table 4-3. The time of arrival of the plume is identical to Case 1 and provides a reasonable match to the monitoring data. In addition, the peak concentrations at 60 m (197 ft) and 120 m (394 ft) are somewhat below the data from the monitoring wells, and the calculated concentrations at 20 m (66 ft) exceed the measured values. Therefore, the results from Case 2a bracket the data.

Table 4-2. Comparison of the Technetium-99 Concentration Results at Selected Points of Calculation for Scoping Cases 1a and 1b.

	Model Results at 20 Meters Downgradient of Tank 241-C-105 Waste Release Location		Model Results at 60 Meters Downgradient of Tank 241-C-105 Waste Release Location		Model Results at 120 Meters Downgradient of Tank 241-C-105 Waste Release Location	
Case Number	**Time of Maximum Concentration (Calendar Year)**	**Maximum Concentration (pCi/L)**	**Time of Maximum Concentration (Calendar Year)**	**Maximum Concentration (pCi/L)**	**Time of Maximum Concentration (Calendar Year)**	**Maximum Concentration (pCi/L)**
Case 1a[2]	2015	22,800	2017	9,800	2018	5,900
Case 1b	2023	4,200	2023	2,700	2023	1,900

[2] Results from the Alternative case requested by Ecology during the comment resolution process had a peak concentration of 16,900 pCi/L at the WMA C fenceline in about the year 2020. This location is close to the location about 60 m (197 ft) downgradient from tank C-105.

Figure 4-5. Concentrations at the Selected Points of Calculation for Case 1b (Lower Bound Inventory for the Tank 241-C-105 Leak).

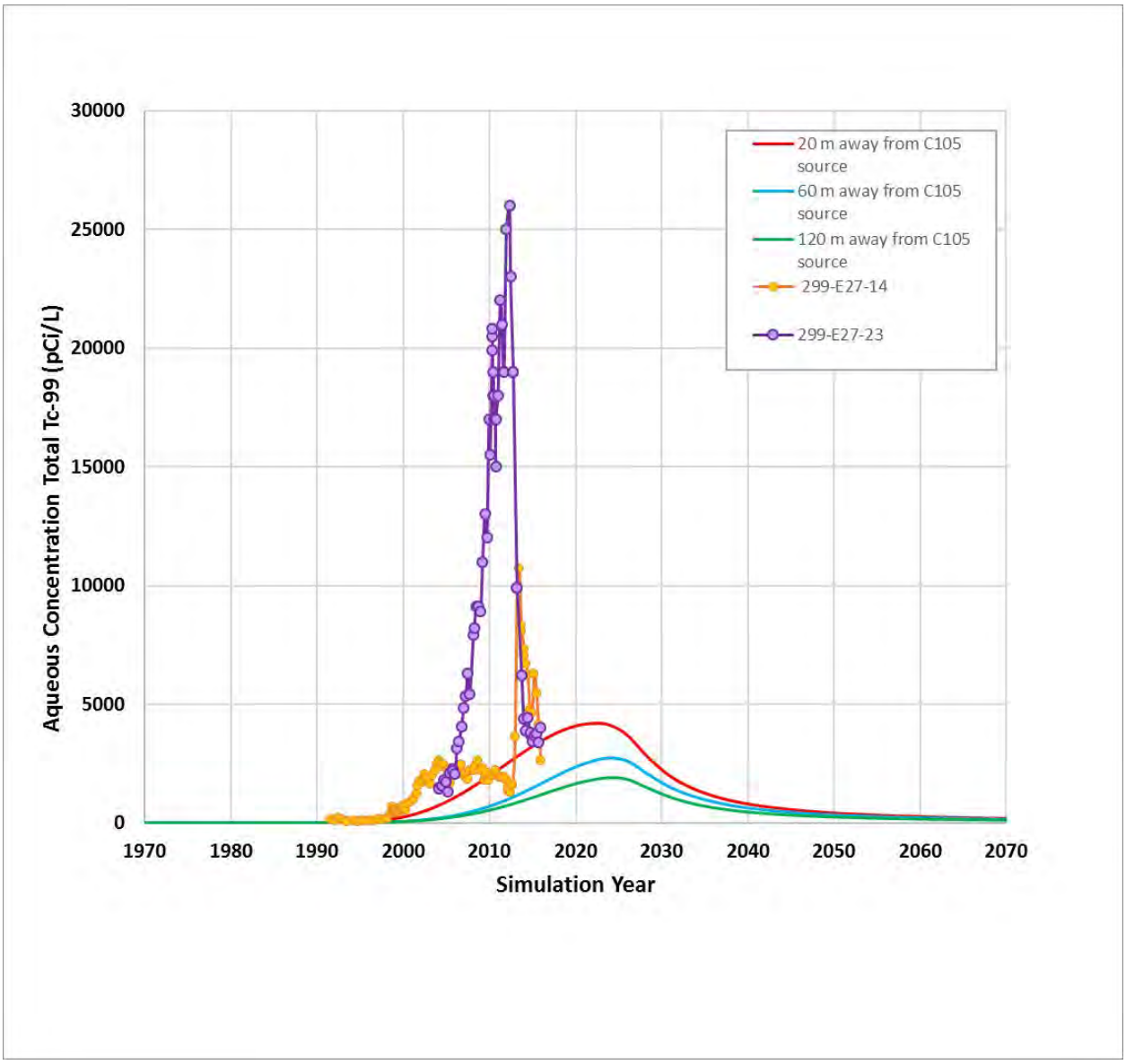

Note: Also shown are measured Technetium-99 concentration data from wells 299-E27-14 and 299-E27-23.

Results of Case 2b (90th percentile groundwater flux) are presented in Figure 4-7 and also summarized at selected PoCals in Table 4-3. The time of arrival of the plume is identical to Case 1 and Case 2a and provides a reasonable match to the first arrival times seen in monitoring data. However, the peak concentrations at 60 m (197 ft) and 120 m (394 ft) are significantly below the monitoring data, and even the calculated 20 m (66 ft) values are less than the measured values.

Figure 4-6. Concentrations at the Selected Points of Calculation for Case 2a (10th Percentile Groundwater Flux).

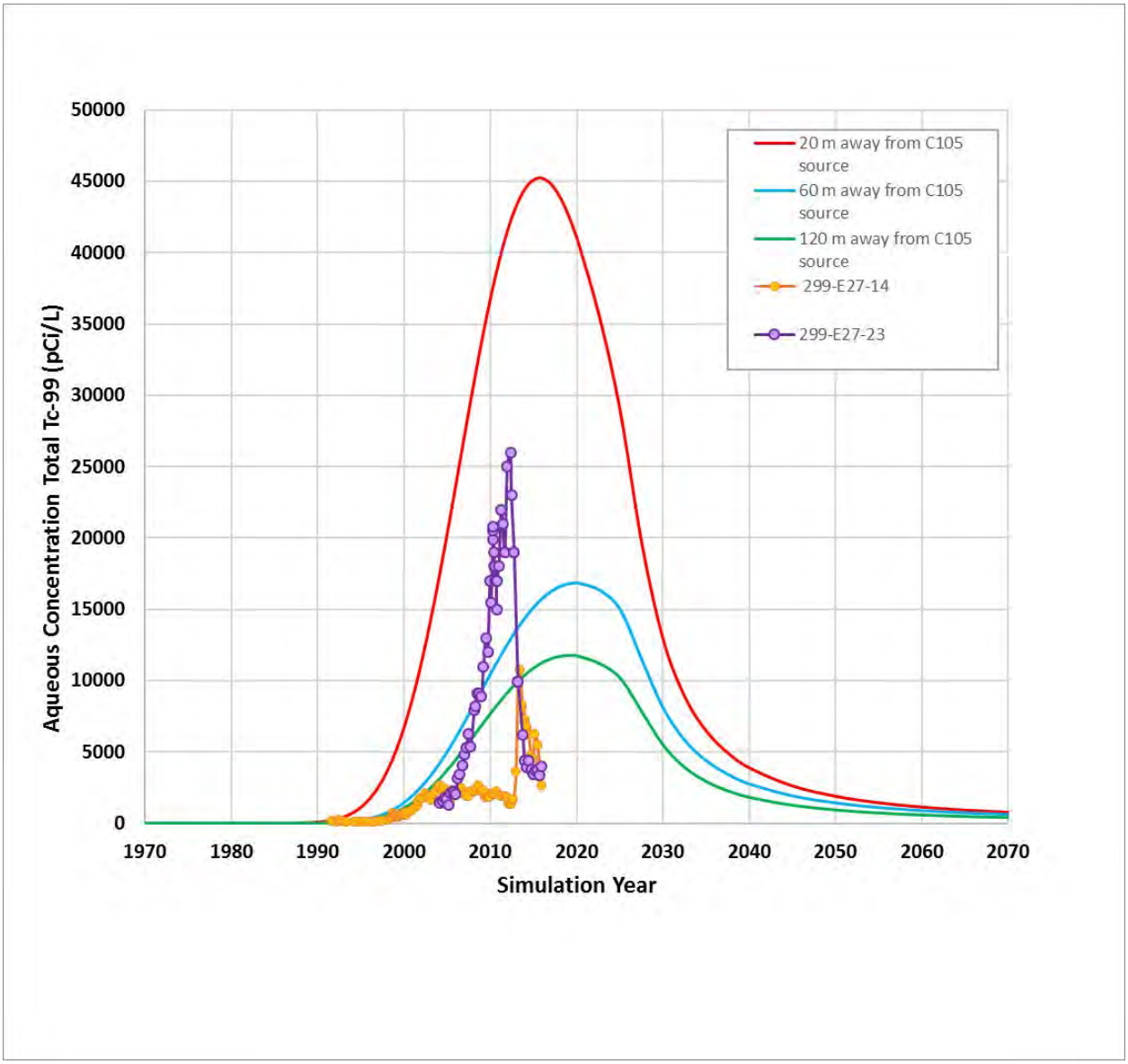

Note: Also shown are measured Technetium-99 concentration data from wells 299 E27-14 and 299-E27-23.

4.3 CASE 3: EFFECT OF CHANGES IN RECHARGE CONDITIONS

The scoping cases presented in this subsection represent an attempt to compare alternative modeling assumptions about recharge conditions to field data, with a view to identifying modeling assumptions that are either consistent or inconsistent with monitoring data. Monitoring data do not exist prior to 1989, and comparisons of the model with data are only made subsequent to that time. The cases have been run as blind trials; that is, the inputs are best estimates derived as discussed in Sections 2 and 3, and the models run in a forward manner from

the time of the leaks to today. There are no fitting parameters in the model, and no adjustments to model inputs have been made to improve the comparisons. The intent is to identify which sets of inputs are contradicted by data, and hence develop improved understanding of the implications of various alternative assumptions on the comparison between the model and data.

As discussed in the introduction of Section 4, because of the complicating effect of the time-varying water table on monitoring data, it is not appropriate to compare the model results in this section at the location of the monitoring wells. The static gradient applied in the models discussed in this section is not necessarily oriented in the same direction as the real water table at any given time in the analysis. Instead, the model is used primarily for comparison with time of arrival of the plume. Secondarily, the model is used to calculate concentrations as fixed distances from the releases, and this is used as an indicator of the effect of distance from the leak on groundwater concentrations. Model comparisons with the changing water table are presented in Section 6, along with comparisons with field data.

4.3.1 Case Descriptions

In this scoping analysis, recharge-related parameters were varied to examine the impact of recharge on the time of arrival of the plume at the water table. This scoping case includes assessment of both the magnitude of the recharge and its spatial variability related to surface conditions that affect recharge. For this analysis, the vadose zone and aquifer hydraulic properties remain unchanged from their base case values.

Three recharge scoping cases were evaluated.

- **Case 3a**: This case assumes higher recharge of 150 mm/yr (5.90 in./yr) everywhere in the vicinity of WMA C where disturbed soil conditions exist (see Figure 4-8) to reflect the effect of increased but uniform anthropogenic recharge during operations on past leak migration inside the tank farm area (see Table 4-4).

- **Case 3b**: This case assumes higher recharge of 100 mm/yr (3.94 in./yr) everywhere in the vicinity of WMA C where disturbed soil conditions exist (see Figure 4-8) to reflect the effect of uniform recharge inside and outside of the farm during operations on past leak migration in the general area of the tank farm (see Table 4-4).

- **Case 3c:** This case examines the effect of gunite caps emplaced at UPR-82, and UPR-86 and local use of water at UPR-81, UPR-82, and UPR-86 to force contamination downward into the vadose zone shortly after identification of waste release.

4.3.2 Case Results

Results of Case 3a (150 mm/y recharge [5.90 in./yr]) are presented in Figure 4-9 and summarized at selected PoCals in Table 4-5. The time of arrival of the plume is earlier than Case 1 and is substantially earlier than the monitoring data. In addition, the peak concentrations at 60 m (197 ft) and 120 m (394 ft) are somewhat lower than the data from the monitoring wells, and only the peak calculated concentrations at 20 m (66 ft) are close to the data for well 299-E27-23. Therefore, the higher recharge rate does not appear to be consistent with data.

Results of Case 3b (100 mm/y recharge [3.94 in./yr]) are presented in Figure 4-10 and summarized at selected PoCals in Table 4-5. The time of arrival, peak concentrations, and shape of the plume are very similar to Case 1, with the arrival time providing a reasonable match to the first arrival of ^{99}Tc in monitoring data. However, peak concentrations are somewhat lower than seen for these other scoping cases.

Results of Case 3c (treatment of UPRs-82 and -86 with a firehose followed by installation of a gunite cap) are presented in Figure 4-11 and also summarized at selected PoCals in Table 4-5. The time of arrival, peak concentrations, and shape of the plume are very similar to Case 1, with the arrival time providing a reasonable match to the monitoring data and the peak concentrations somewhat lower.

Table 4-3. Comparison of the Technetium-99 Concentration Results at Selected Points of Calculation for Scoping Cases 2a and 2b.

	Model Results at 20 Meters Downgradient of Tank 241-C-105 Waste Release Location		Model Results at 60 Meters Downgradient of Tank 241-C-105 Waste Release Location		Model Results at 120 Meters Downgradient of Tank 241-C-105 Waste Release Location	
Case Number	**Time of Maximum Concentration (Calendar Year)**	**Maximum Concentration (pCi/L)**	**Time of Maximum Concentration (Calendar Year)**	**Maximum Concentration (pCi/L)**	**Time of Maximum Concentration (Calendar Year)**	**Maximum Concentration (pCi/L)**
Case 2a	2015	45,200	2019	16,800	2019	11,800
Case 2b	2015	15,200	2019	5,800	2019	3,900

Figure 4-7. Concentrations at the Selected Points of Calculation for Case 2b (90th Percentile Groundwater Flux).

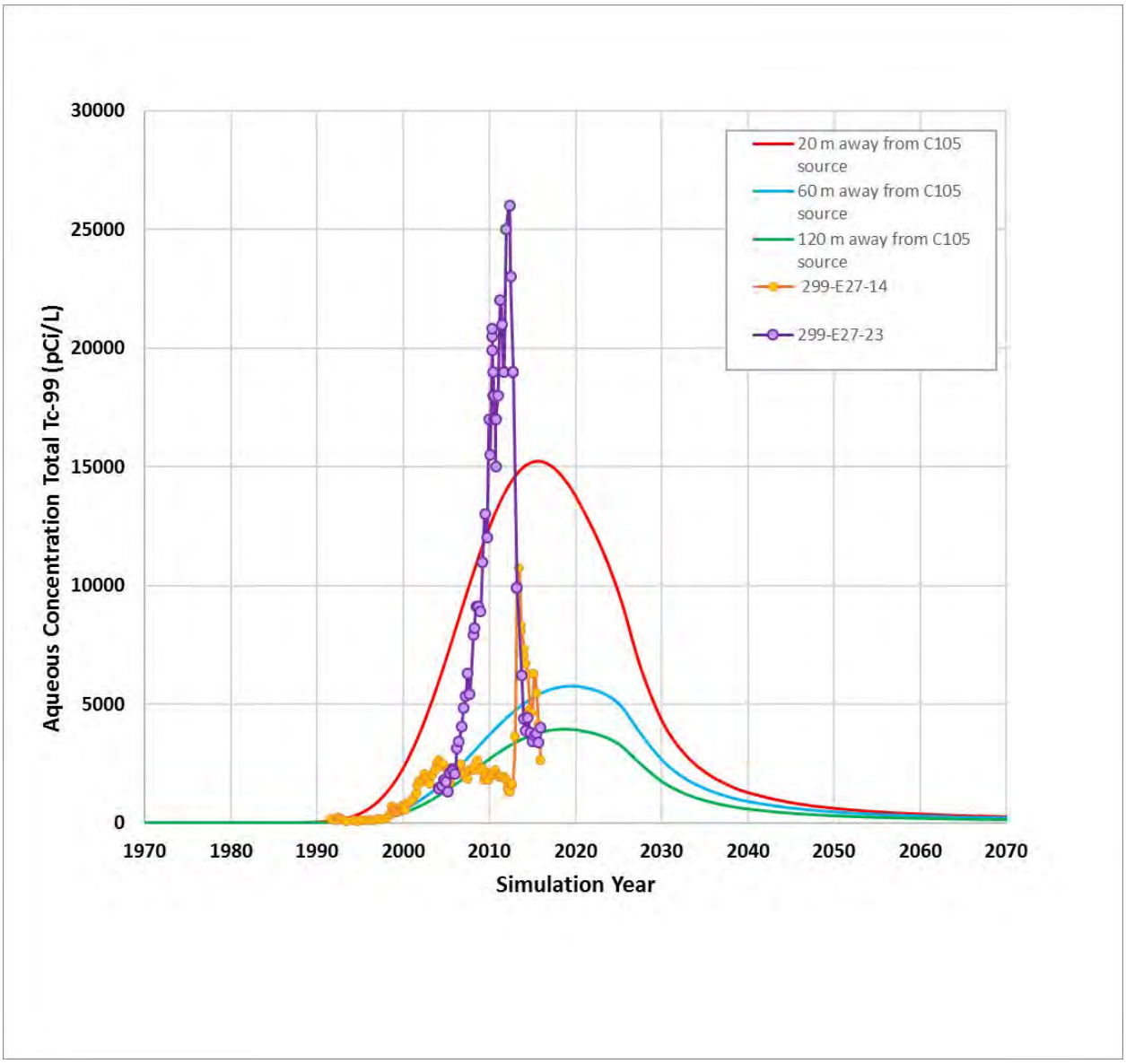

Note: Also shown are measured Technetium-99 concentration data from wells 299 E27-14 and 299-E27-23.

Figure 4-8. Surface Conditions in and Around Waste Management Area C during the Construction and Operations Period.

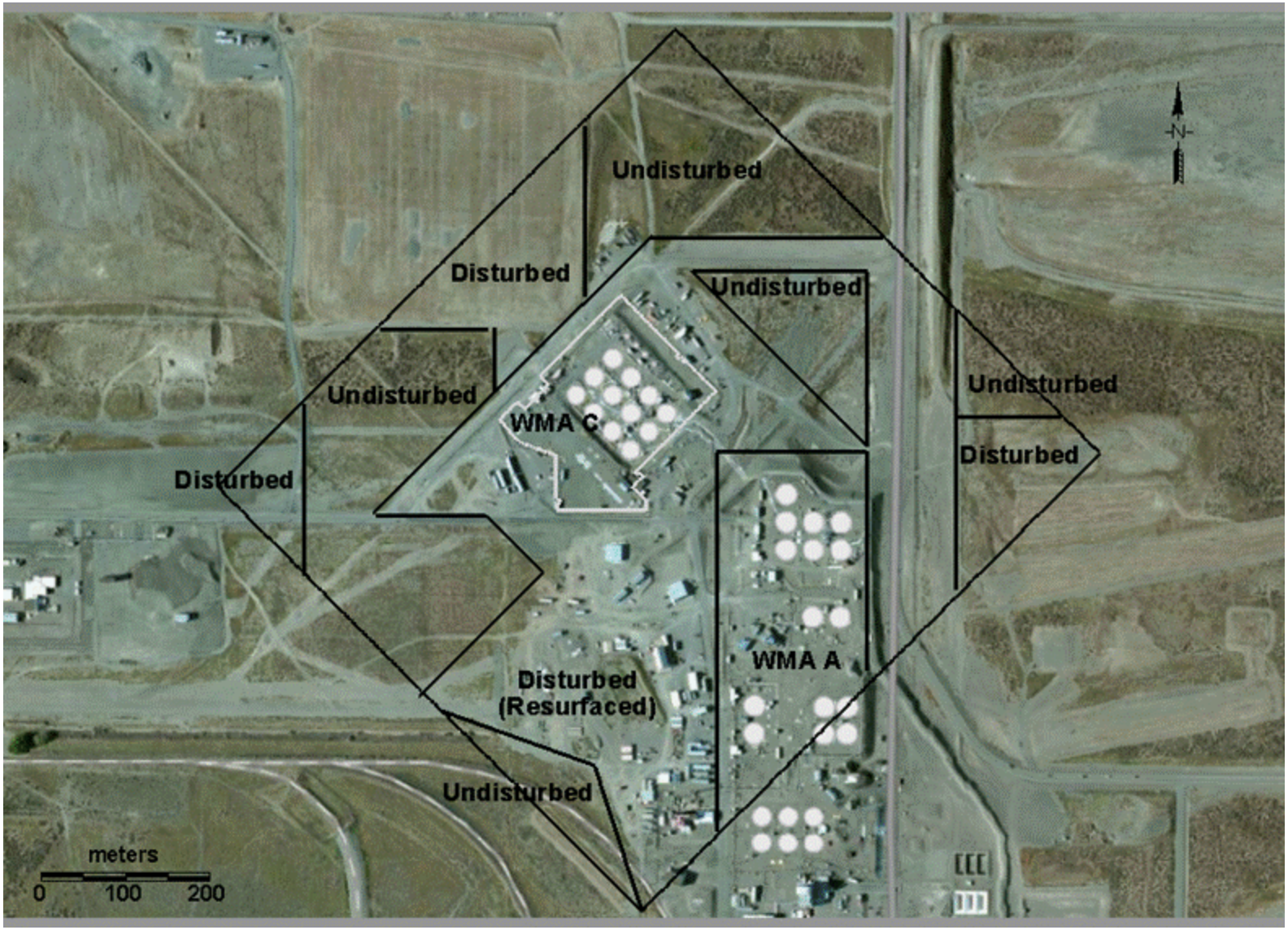

WMA = Waste Management Area

Table 4-4. Assumed Recharge Rates (Net Infiltration) for Surface Conditions during the Pre-Construction, Operational Periods Used in Cases 1a, 1b, 3a, and 3b.

Period	Waste Management Area (WMA) C Region and Surface Condition*	Case 1a and 1b Recharge Rate (mm/yr)	Case 3a	Case 3b
Pre-construction (before 1944)	Undisturbed region (Rupert sand with vegetation)	3.5	3.5	3.5
Operational period (1945 to 2020)	Undisturbed region (Rupert sand with vegetation)	3.5	3.5	3.5
	WMA C Surface region (Gravel without vegetation)	100	150	100
	WMA A Surface region (Gravel without vegetation)	100	150	100
	Disturbed revegetated region (Rupert sand with vegetation)	22	150	100
	Disturbed un-revegetated region (Rupert sand with no vegetation)	63	150	100

* Areas described are shown in Figure 4-8.

4.4 CASE 4: EFFECT OF CHANGING VADOZE ZONE PARAMETERS AND CONCEPTUALIZATION

The scoping cases presented in this subsection represent an attempt to compare alternative modeling assumptions about vadose zone parameters and conceptualizations to field data, with a view to identifying modeling assumptions that are either consistent or inconsistent with monitoring data. Monitoring data do not exist prior to 1989, and comparisons of the model with data are only made subsequent to that time. The cases have been run as blind trials; that is, the inputs are best estimates derived as discussed in Sections 2 and 3, and the models run in a forward manner from the time of the leaks to today. There are no fitting parameters in the model, and no adjustments to model inputs have been made to improve the comparisons. The intent is to identify which sets of inputs are contradicted by data, and hence develop improved understanding of the implications of various alternative assumptions on the comparison between the model and data.

As discussed in the introduction of Section 4, because of the complicating effect of the time-varying water table on monitoring data, it is not appropriate to compare the model results in this section at the location of the monitoring wells. The static gradient applied in the models discussed in this section is not necessarily oriented in the same direction as the real water table at any given time in the analysis. Instead, the model is used primarily for comparison with time of arrival of the plume, and secondarily to calculate concentrations as fixed distances from the releases, and this is used as an indicator of the effect of distance from the leak on groundwater

concentrations. Model comparisons with the changing water table are presented in Section 5, along with comparisons with field data.

4.4.1 Case Description and Model Implementation

The vadose zone evaluation includes a number of different alternative conceptualizations of the geology and vadose parameters.

- **Case 4a**: This case evaluates Alternative Geologic Model II that was developed in the DOE O 435.1 WMA C PA and the RCA effort. This conceptual model considers the Hanford H2 Sand unit to consist of three subunits that each possess different hydraulic characteristics (Figure 4-12). Most of the formation remains identified as H2 Sand and the hydraulic properties for it remain unchanged from the base case analysis. Near the base of the Hanford H2 Sand unit in Alternative Geologic Model II are fine and coarse sand subunits. For this scoping case, these subunits are assigned the Hanford H2 Sand 5th and 95th percentile hydraulic property sets, respectively.

- **Case 4b**: This case evaluates an alternative conceptual model of a heterogeneous representation of the vadose zone that was developed in the DOE O 435.1 WMA C PA and the RCA effort. The development of this model is described in detail in Appendix F of RPP-ENV-58782. A depiction of the numerical implementation is provided in Figure 4-13. Since Case 4b was completed, the results for other alternative representations of subsurface heterogeneity at WMA C have been developed. A summary of these additional developmental efforts and associated modeling results are presented and discussed in Section 5 of this document.

Figure 4-9. Concentrations at Selected Points of Calculation for Case 3a (150 mm/y Recharge).

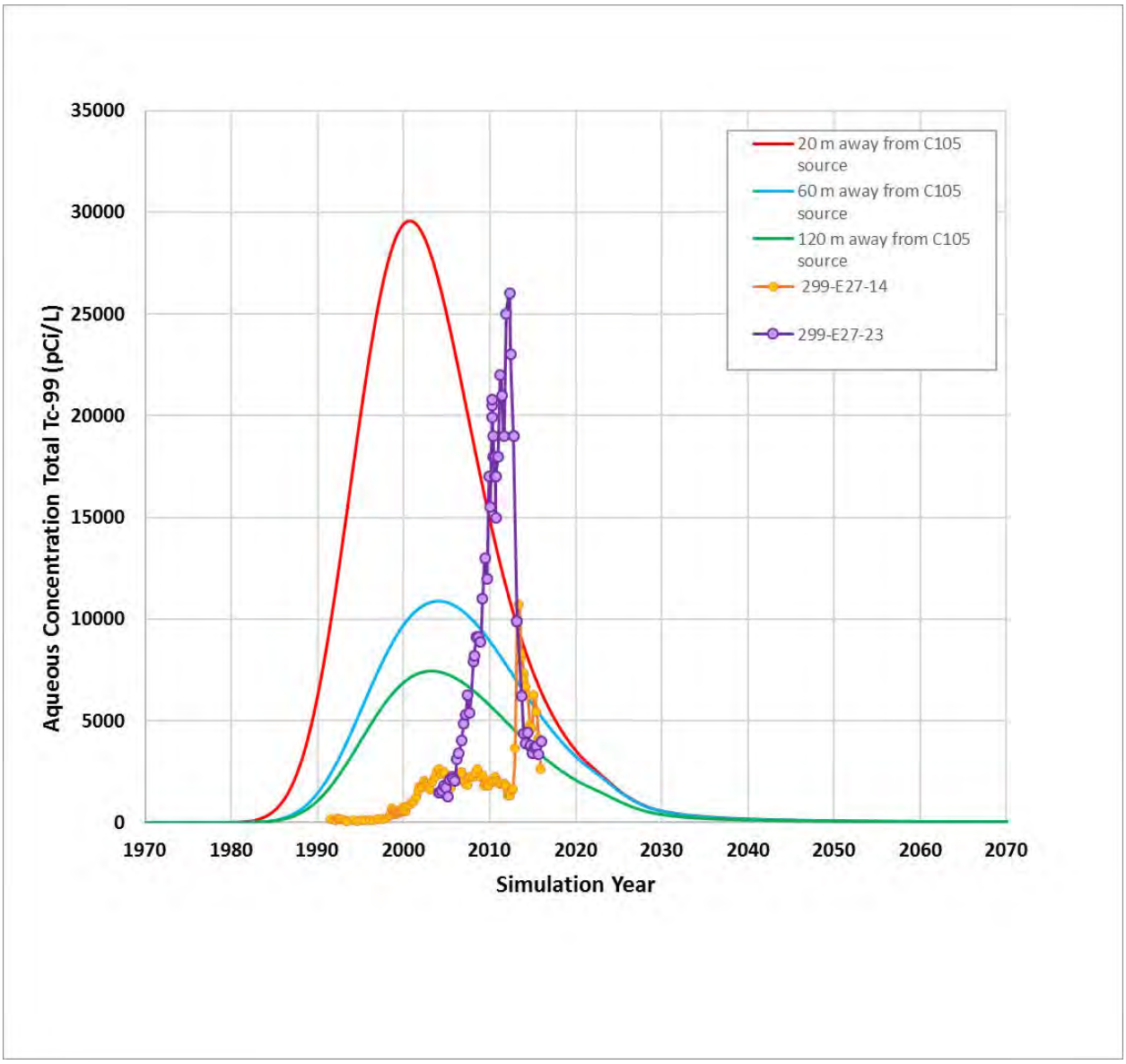

Note: Also shown are measured Technetium-99 concentration data from wells 299 E27-14 and 299-E27-23.

- **<u>Case 4c and 4d:</u>** These two cases evaluate the effect of changing vadose zone hydraulic properties associated with flow and dispersion in the vadose zone. Four vadose zone parameters were varied: van Genuchten α and n (coupled), saturated moisture content (θ_s), residual moisture content (θ_r), and fitted saturated hydraulic conductivity (K_s). The parameters were varied in accordance with the percentile relationships determined in the uncertainty analysis. It is important to note that the percentiles refer to sets of parameter values and not to the properties individually (as discussed in Appendix B of RPP-ENV-58782). Thus, the maximum van Genuchten residual saturation parameter does not necessarily represent the largest value of θ_r, but instead represents the value associated with the fitted unsaturated hydraulic conductivity curve and corresponding set

of hydraulic properties that produces the highest flow velocity at the pre-Hanford Site operations recharge rate. The values of four vadose zone parameters, van Genuchten α and n (coupled), θ_s, θ_r, and fitted saturated hydraulic conductivity (K_s) varied for the median [vzp02], and 95th [vzp03]) percentile sets of parameters are presented in Section 8.1.4 of RPP-ENV-58782 (see Table 4-6). These evaluations used the Case 1 recharge values and time sequence and other model parameters.

- **Case 4e**: This case evaluates one representation of a preferential pathway, a clastic dike, hypothetically located underneath tank C-105. Clastic dikes are discrete polygonal (plan view) features, and typically range in width from 3 cm to 1 m (1.2 in. to 3.3 ft), from 1.5 m to 100 m (4.9 ft to 328 ft) in segment length, and from 2 m (6.6 ft) to greater than 20 m (65.6 ft) in depth (BHI-01103). An especially long clastic dike segment does not appear to exist in the vicinity of WMA C tank area because, if one did, then drywell moisture measurements would reflect localized evidence of a continuous band of high moisture. Localized measurements of relatively high moisture like that have not been observed in drywell moisture logs within WMA C.

  For the scoping case, the length of the dike is assumed to extend for 7.6 m (25 ft), and 3-D model discretization imposes a minimum width of 3.8 m (12 ft) for the dike. Although a width of 3.8 m (12 ft) is more representative of a planar feature than a dike, finer resolution of the model grid is not practicable with the available computational resources (see Figure 4-14). The planar area of the dike is 29 m^2 (312 ft^2), which is comparable to a 1-m (3.3-ft)-wide dike that extends the entire diameter of the tank (23 m^2 [246 ft^2]). Clastic dikes of this size typically occur in sand, silt, and only occasionally in gravel (BHI-01103); therefore, the model representation of the dike extends throughout the depth of the Hanford H2 Sand (Figure 4-14 shows the location of tank C-105; the clastic dike is centered beneath the tank in the Hanford H2 Sand shown in the figure). The hydraulic parameters assigned to the clastic dike material were selected to determine whether the flux conditions exist at WMA C such that the clastic dikes provide a preferential flow path for the residual waste. Thus, the set of clastic dike hydraulic parameters from among the samples listed in PNNL-23711, *Physical, Hydraulic, and Transport Properties of Sediments and Engineered Materials Associated with Hanford Immobilized Low-Activity Waste*, that produced the highest pore water velocity at the undisturbed recharge rate of 3.5 mm/yr (0.14 in./yr) were assigned to the clastic dike material.

- **Case 4f:** This case evaluates another representation of a preferential pathway, which in this case is a poorly sealed or unsealed borehole, hypothetically located adjacent to tank C-105. For this evaluation, the borehole is assumed to be well 299-E27-70 (30-05-02). For the scoping case, the depth of the borehole is assumed to extend in length the extent of the drill depth of well 299-E27-70, 40 m (130 ft), and 3-D model discretization imposes minimum length and width surface dimensions of 3.8 m (12 ft) each for the borehole (see Figure 4-15). Finer resolution of the model grid is not practicable with the available computational resources.

Figure 4-10. Concentrations at Selected Points of Calculation for Case 3b (100 mm/y Recharge).

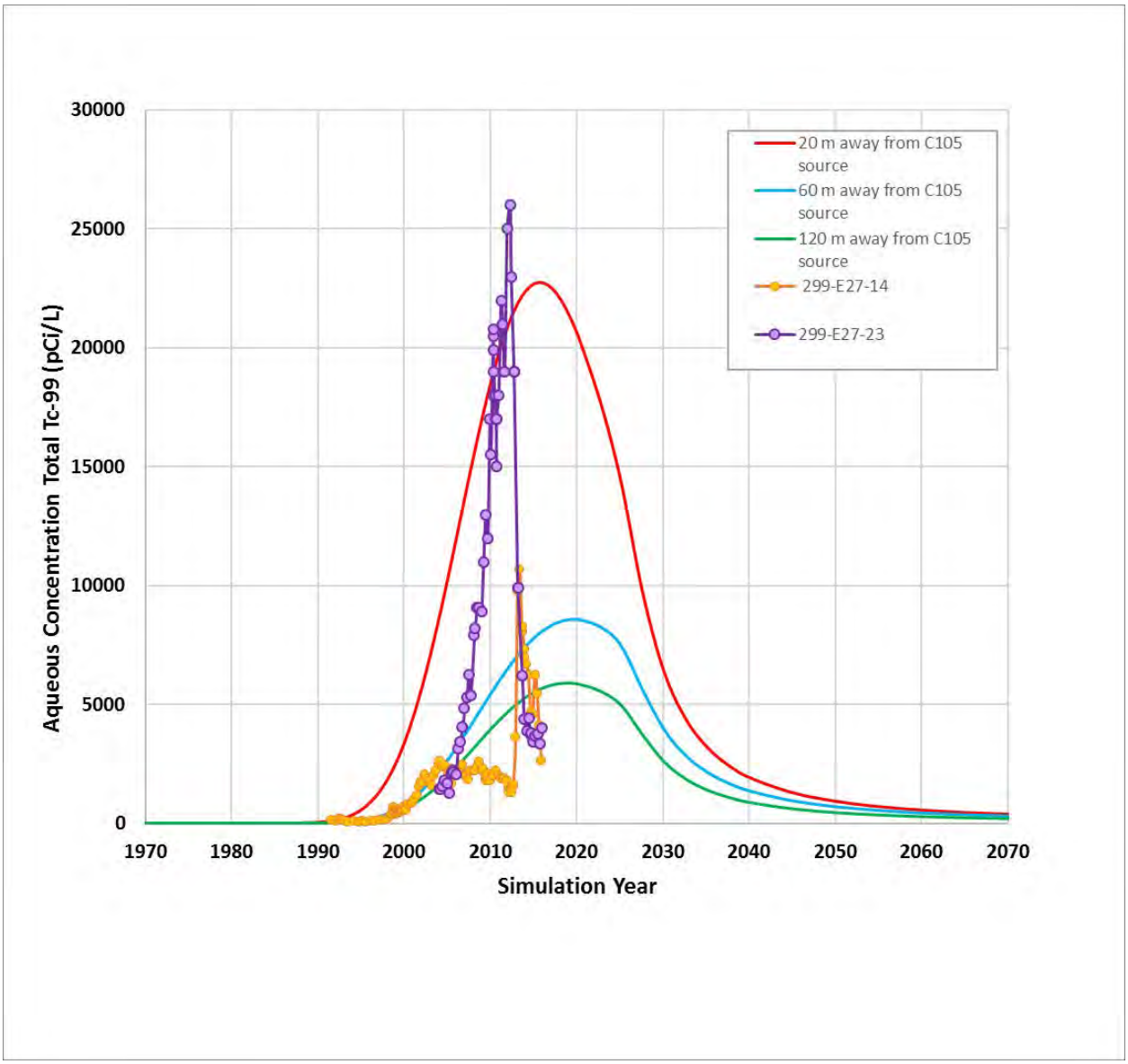

Note: Also shown are measured Technetium-99 concentration data from wells 299 E27-14 and 299-E27-23.

4.4.2 Case Results

Results of Case 4a (Alternative Geologic Model II) are presented in Figure 4-16 and summarized at selected PoCals in Table 4-7. The time of arrival, peak concentrations, and shape of the plume are slightly earlier, but similar to Case 1, with the arrival time providing a reasonable match to the monitoring data and the peak concentrations somewhat lower.

Table 4-5. Comparison of the Technetium-99 Concentration Results at Selected Points of Calculation for Scoping Cases 3a through 3d.

	Model Results at 20 Meters Downgradient of Tank 241-C-105 Waste Release Location		Model Results at 60 Meters Downgradient of Tank 241-C-105 Waste Release Location		Model Results at 120 Meters Downgradient of Tank 241-C-105 Waste Release Location	
Case Number	**Time of Maximum Concentration (Calendar Year)**	**Maximum Concentration (pCi/L)**	**Time of Maximum Concentration (Calendar Year)**	**Maximum Concentration (pCi/L)**	**Time of Maximum Concentration (Calendar Year)**	**Maximum Concentration (pCi/L)**
Case 3a	2000	29,500	2002	12,500	2003	7,500
Case 3b	2015	22,700	2017	9,800	2018	5,900
Case 3c	2015	22,800	2017	9,800	2018	5,900

Figure 4-11. Concentrations at Selected Points of Calculation for Case 3c (Firehose Water Addition followed by Gunite Cover).

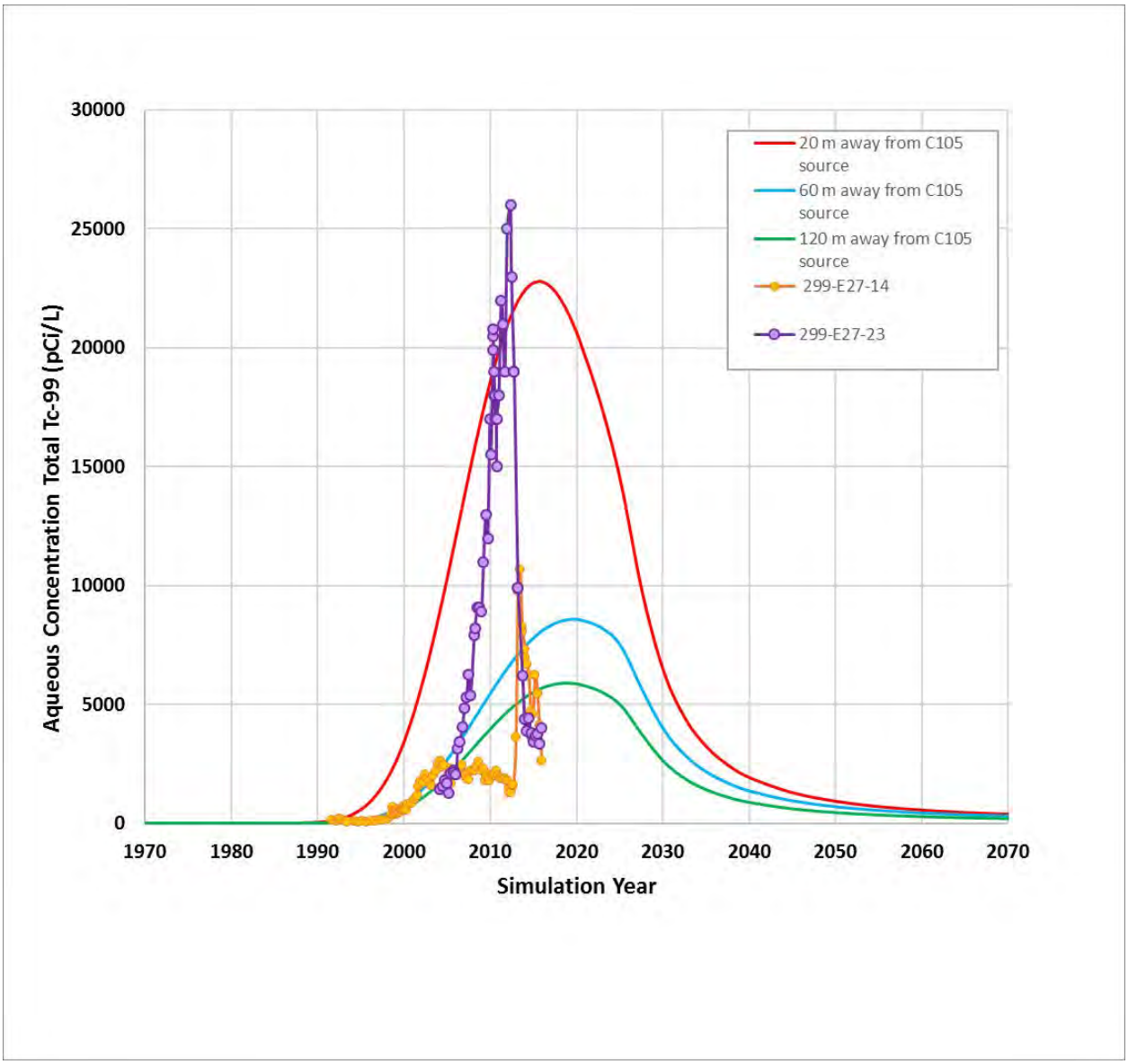

Note: Also shown are measured Technetium-99 concentration data from wells 299 E27-14 and 299-E27-23.

Results of Case 4b (heterogeneous model) are presented in Figure 4-17 and summarized at selected PoCals in Table 4-7. The time of arrival of the plume is earlier than Case 1 and is substantially earlier than indicated by the monitoring data. In addition, the peak concentrations at 60 m (197 ft) and 120 m (394 ft) are somewhat lower than the data from the monitoring wells, and only the peak calculated concentrations at 20 m (66 ft) are close to the data for well 299-E27-23.

Figure 4-12. Depiction of Interpolated Numerical Three-Dimensional Model of Alternative Conceptual Model II for Scoping Case 4a.

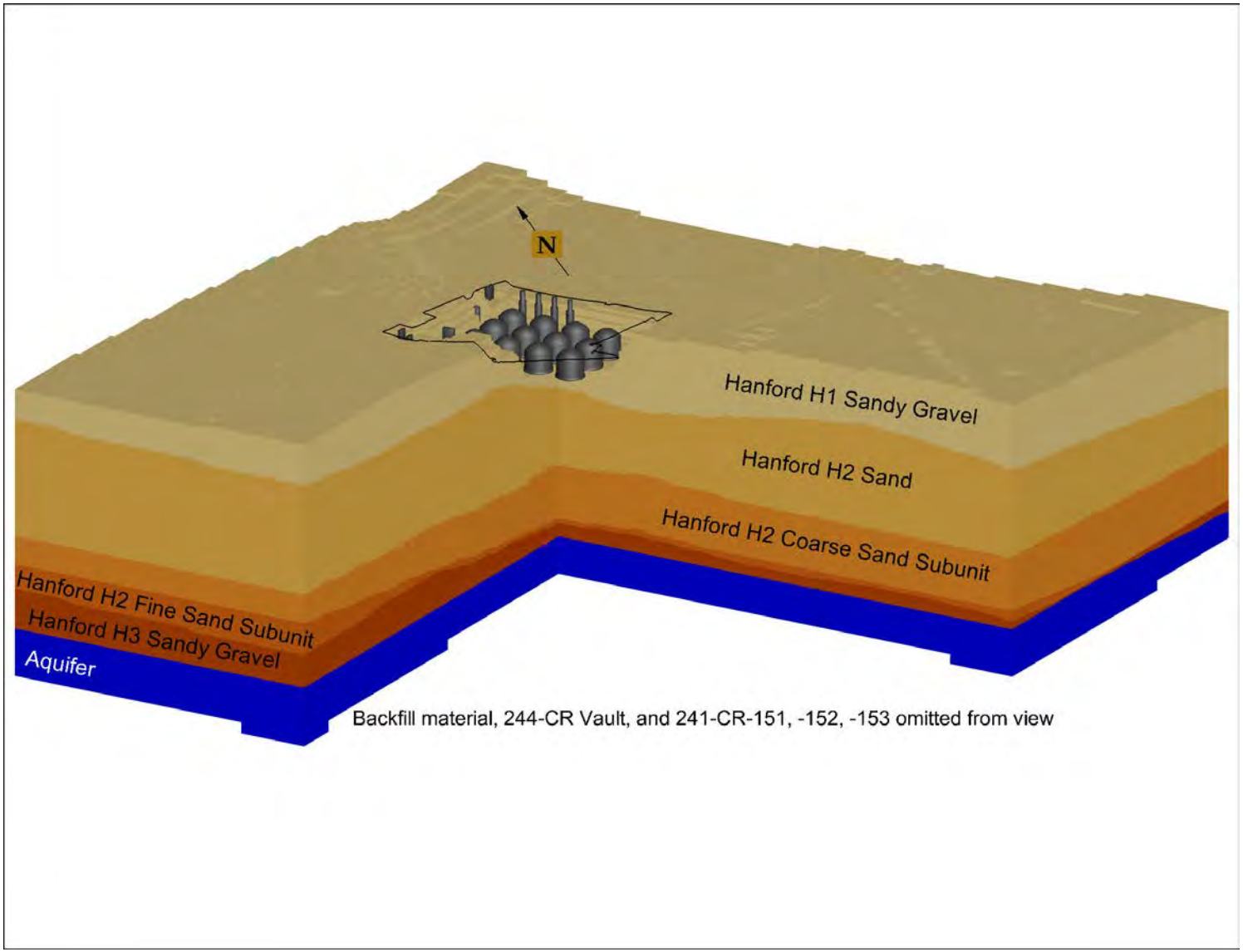

Figure 4-13. Depiction of Interpolated Numerical Three-Dimensional Model of Heterogeneous Alternative Conceptual Model for Scoping Case 4b.

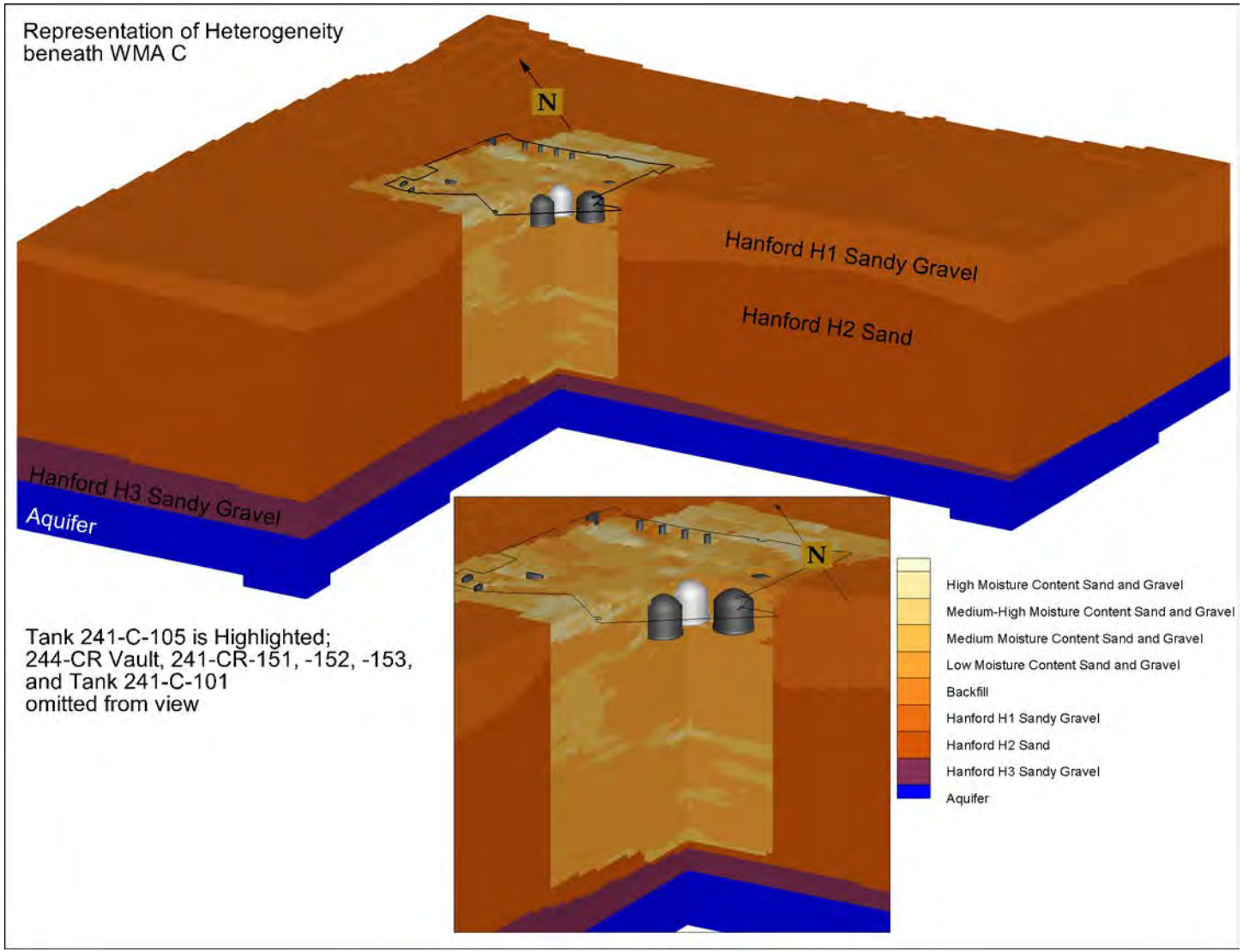

WMA = Waste Management Area

Table 4-6. van Genuchten-Mualem Parameters Corresponding to the Percentiles Selected for Cases 1a, 1b, 4c, and 4d from the Vertical Pore Water Velocity Cumulative Distribution Functions.

Strata (tension)	Percentile	K_s (cm/s)	θ_s	θ_r	α (1/cm)	n
Backfill	5th Percentile	7.91E-06	0.2217	1.23E-02	0.0026	1.441
	25th Percentile	1.08E-05	0.1319	1.57E-02	0.0031	1.310
	Case 4c – 50th Percentile	7.31E-05	0.203	5.94E-03	0.0086	1.577
	75th Percentile	1.98E-04	0.1409	1.42E-02	0.0123	1.470
	Case 4d – 95th Percentile	3.13E-04	0.1287	1.35E-02	0.0298	1.635
	Case 1a and 1b	5.60E-04	0.138	1.10E-02	0.021	1.374
Hanford H1/H3	5th Percentile	7.78E-05	0.2887	3.24E-02	0.0121	1.335
	25th Percentile	5.14E-06	0.2118	2.08E-02	0.0062	1.733
	Case 4c – 50th Percentile	1.49E-04	0.1735	3.06E-02	0.0124	1.603
	75th Percentile	1.58E-03	0.309	7.01E-03	0.0238	1.717
	Case 4d – 95th Percentile	2.99E-04	0.102	1.45E-02	0.0152	1.760
	Case 1a and 1b	7.70E-04	0.171	1.11E-02	0.036	1.491
Hanford H2	5th Percentile	1.79E-03	0.3541	2.89E-02	0.0402	1.633
	25th Percentile	1.15E-03	0.2893	2.99E-02	0.0266	1.971
	Case 4c – 50th Percentile	2.20E-02	0.3304	2.72E-02	0.1253	1.889
	75th Percentile	3.79E-02	0.3474	2.05E-02	0.0966	1.966
	Case 4d – 95th Percentile	1.68E-02	0.2652	2.11E-03	0.1076	1.724
	Case 1a and 1b	4.15E-03	0.315	3.92E-02	0.063	2.047

Table adapted from Table 8-7 in Section 8 of RPP-ENV-58782, *Performance Assessment of Waste Management Area C, Hanford Site, Washington*.

Note: The connectivity parameter ℓ is assumed to be 0.5 for all strata and all percentile values.

Results of Case 4c (median hydraulic properties) are presented in Figure 4-18 and summarized at selected PoCals in Table 4-7. The time of arrival, peak concentrations, and shape of the plume are very similar to Case 1, with the arrival time providing a reasonable match to the monitoring data and the peak concentrations somewhat lower.

Results of Case 4d (95th percentile hydraulic properties) are presented in Figure 4-19 and summarized at selected PoCals in Table 4-7. The time of arrival is substantially earlier than the monitoring data, with peak concentrations similar to Case 1, somewhat lower than the peak concentration in monitoring data.

Figure 4-14. Depiction of Hypothetical Clastic Dike near Tank 241-C-105 Conceptualized for Scoping Case 4e.

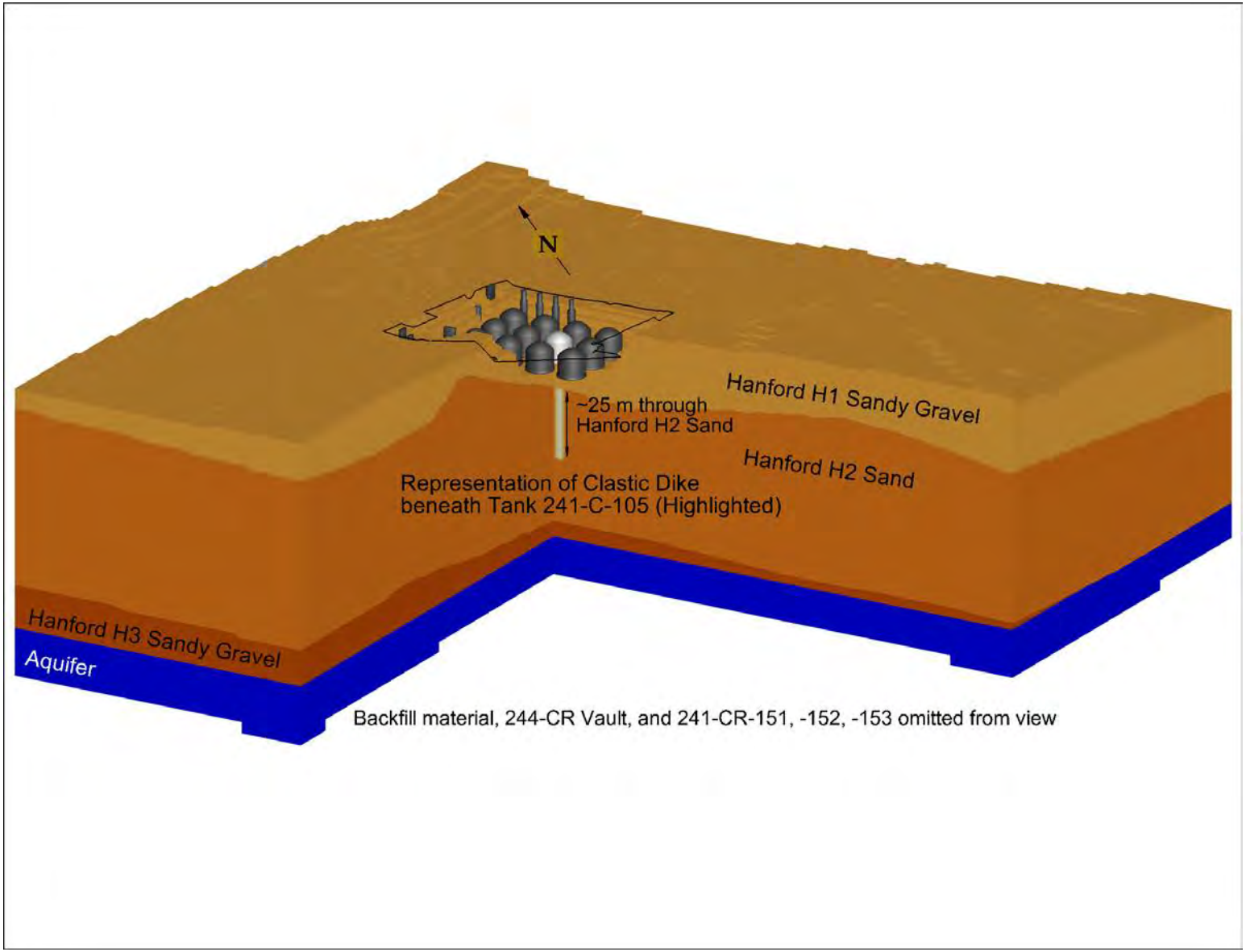

Figure 4-15. Depiction of Hypothetical Unsealed Borehole Near Tank 241-C-105 Conceptualized for Scoping Case 4f.

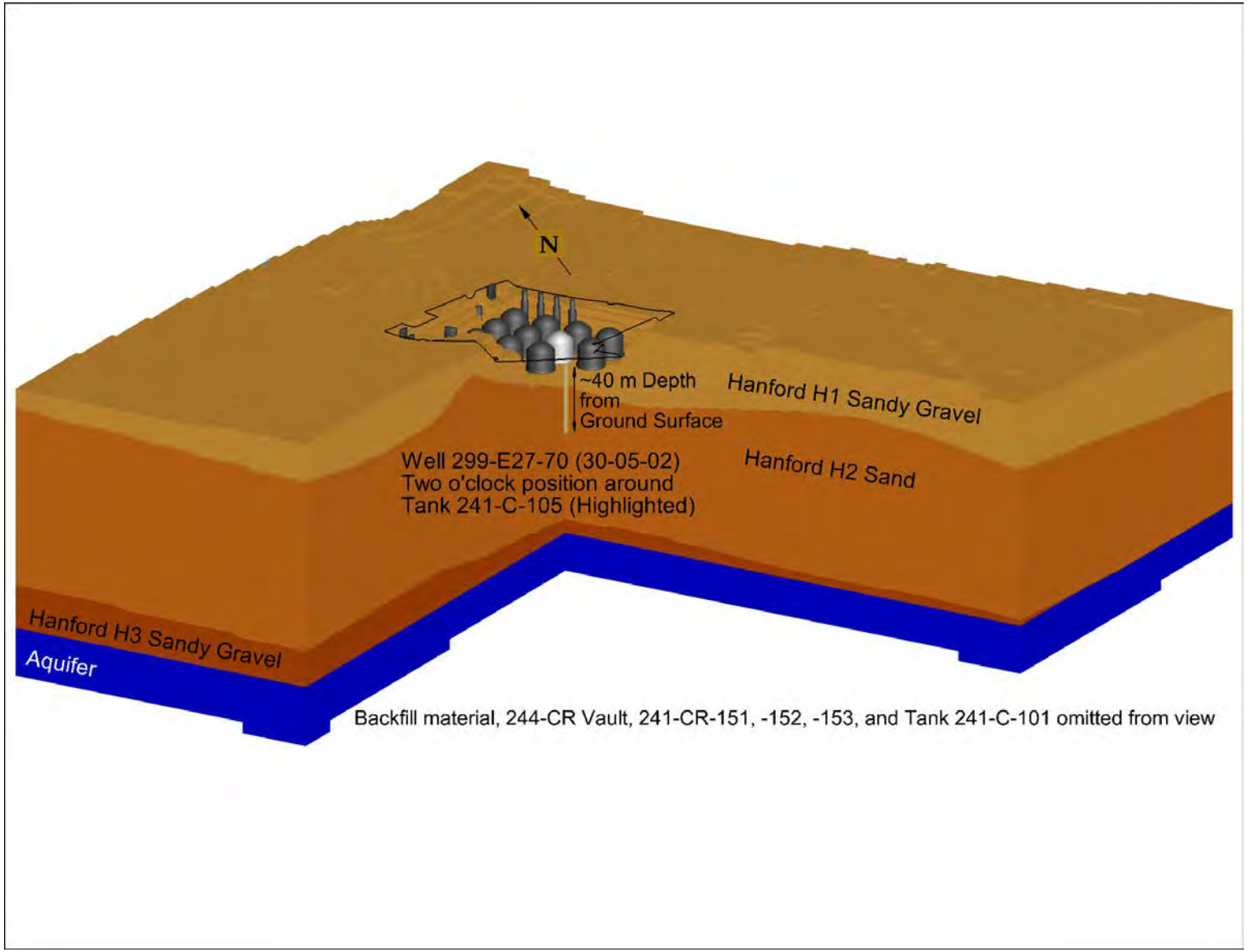

Figure 4-16. Concentrations at Selected Points of Calculation for Case 4a (Alternative Geologic Model II).

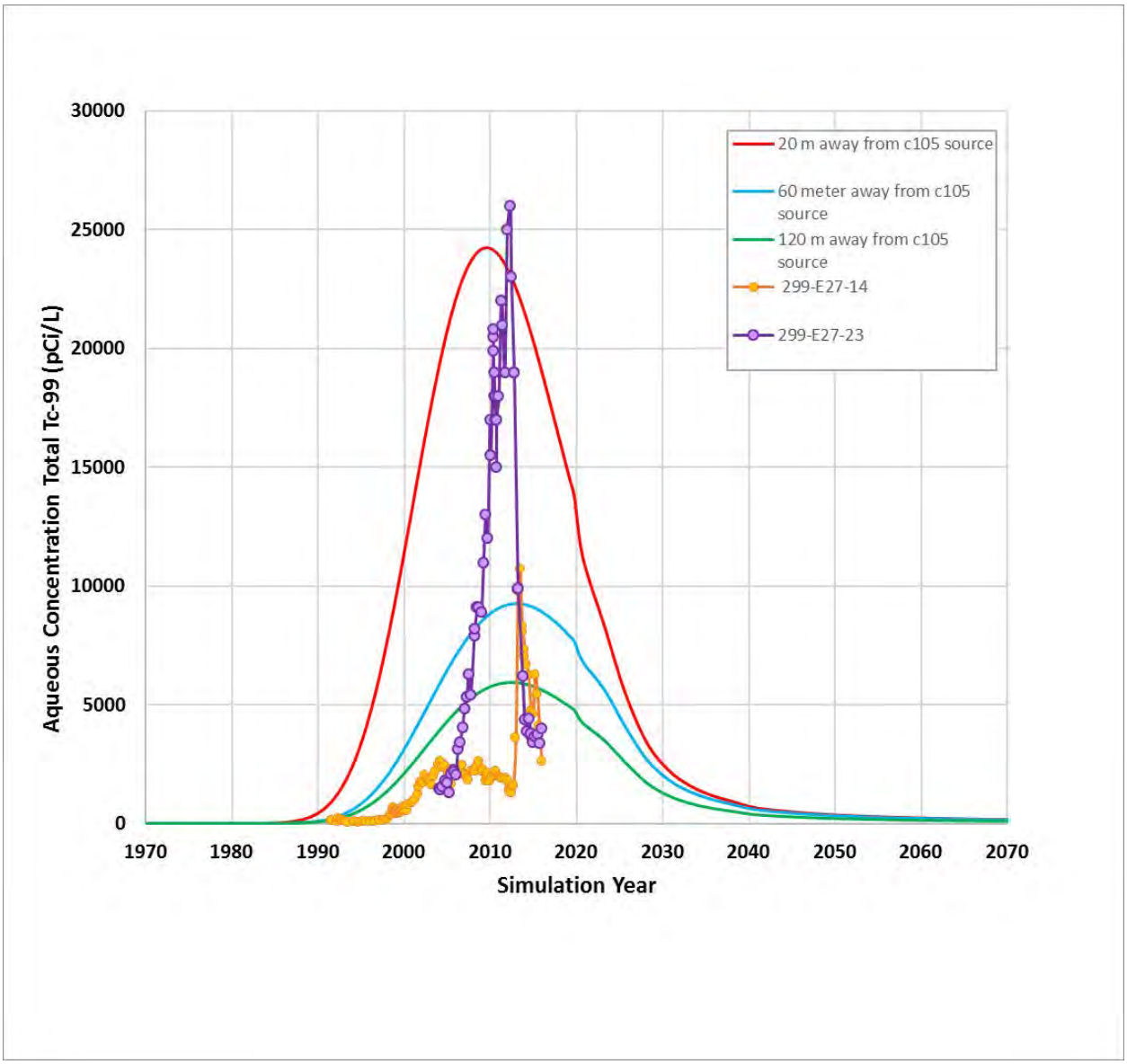

Note: Also shown are measured Technetium-99 concentration data from wells 299 E27-14 and 299-E27-23.

Results of Case 4e (clastic dike) are presented in Figure 4-20 and summarized at selected PoCals in Table 4-7. The peak concentrations and shape of the plume are very similar to Case 1, with the arrival time slightly earlier than Case 1.

Results of Case 4f (borehole preferential pathway) are presented in Figure 4-21. The peak concentrations and shape of the plume are very similar to Case 1, with the arrival time slightly earlier than Case 1.

Table 4-7. Comparison of the Simulated Technetium-99 Concentration Results at Selected Points of Calculation for Scoping Cases 4a through 4f.

	Model Results at 20 Meters Downgradient of Tank 241-C-105 Waste Release Location		Model Results at 60 Meters Downgradient of Tank 241-C-105 Waste Release Location		Model Results at 120 Meters Downgradient of Tank 241-C-105 Waste Release Location	
Case Number	**Time of Maximum Concentration (Calendar Year)**	**Maximum Concentration (pCi/L)**	**Time of Maximum Concentration (Calendar Year)**	**Maximum Concentration (pCi/L)**	**Time of Maximum Concentration (Calendar Year)**	**Maximum Concentration (pCi/L)**
Case 4a	2010	24,200	2011	10,200	2012	5,900
Case 4b	2002	23,700	2004	9,300	2004	6,200
Case 4c	2010	25,300	2013	12,100	2012	7,400
Case 4d	1995	30,700	1998	12,600	1997	7,900
Case 4e	2016	21,000	2018	9,300	2019	5,700
Case 4f	2016	22,400	2018	9,700	2019	5,900

Figure 4-17. Concentrations at Selected Points of Calculation for Case 4b (Alternative Heterogeneous Model).

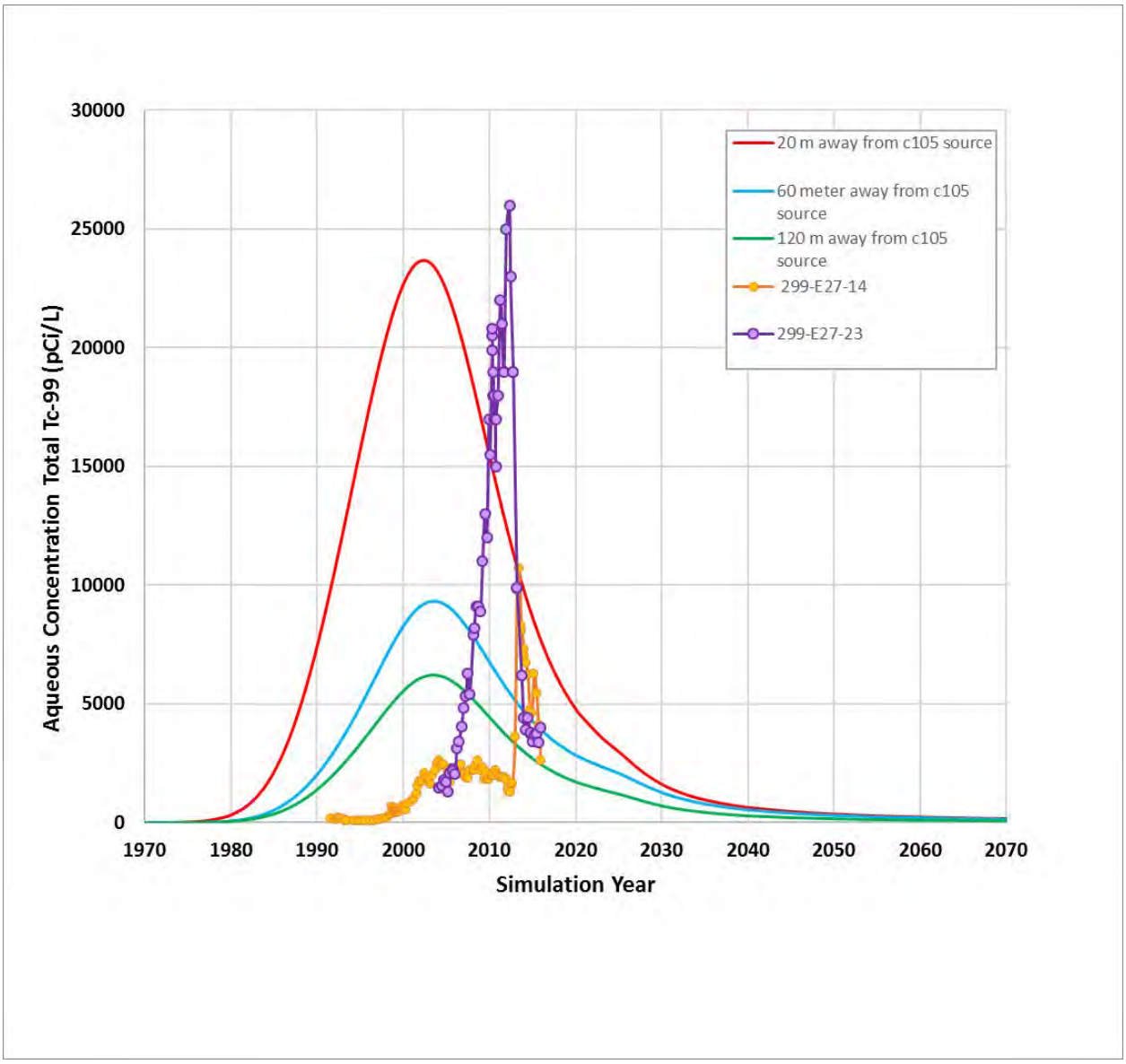

Note: Also shown are measured Technetium-99 concentration data from wells 299 E27-14 and 299-E27-23.

From Scoping Case 4, it can be concluded that the Case 4b (the highly heterogeneous representation) does not appear to be consistent with arrival time data. All of the other cases are indistinguishable from Case 1a, meaning that the alternative conceptual models do not result in a significant change in arrival time of the plume.

4.5 ADDITIONAL INVENTORY SCOPING CASE REQUESTED BY ECOLOGY

As a part of the comment resolution process with Ecology, a request was made by Ecology staff to evaluate an alternative inventory case that examined the groundwater impacts of doubling the release duration, the ^{99}Tc inventory, and the waste volume associated with the tank C-105 leak that were assumed in Case 1a. A complete description of Ecology's requested alternative to Case 1a is provided in Appendix D.

Simulated results for ^{99}Tc concentration levels for the alternative case requested by Ecology during the comment resolution process are summarized in Appendix D. Per agreement with Ecology (See Appendix D), the results of this alternative case were evaluated at the WMA C fence line and 100 m (328 ft) down gradient of WMA C. These locations generally corresponding to the two down gradient location outside of the tank farm evaluated in all of the other scoping cases.

Results from doubling of the duration, the volume, and inventory releases assumed in the alternative case compared to Case 1a (See Figure 4-22) showed the following:

- The first arrival and the timing of peak concentrations of ^{99}Tc remained practically unchanged (about year 2020) when compared to the results for scoping Case 1a (Note: peak concentrations in groundwater at the WMA C fence line [17,000 pCi/l] and 100 m [328 ft] downgradient (~12,000 pCi/yr] occurred about 2 years later (year 2021).

- The maximum concentrations in groundwater were about 80 percent higher at the WMA C fence line when generally compared to the results for the same general locations evaluated in Case 1a (See those comparisons in Appendix D).

- The concentrations at the fence line would compare with concentrations estimated in the other scoping cases at 60 m (197 ft) down gradient of tank C-105.

4.6 SUMMARY OF ANALYSIS CASES AND ASSOCIATED OBSERVATIONS

The analysis cases presented in this subsection have had the goal to match, to the extent possible, the arrival times of the contamination at the water table and the general concentration levels observed in monitoring wells in the vicinity of the tank farms. The intention is to explore the modeling assumptions and input parameter values that are consistent with the observed arrival times and to a lesser extent concentration levels.

Figure 4-18. Concentrations at Selected Points of Calculation for Case 4c (Median Hydraulic Properties).

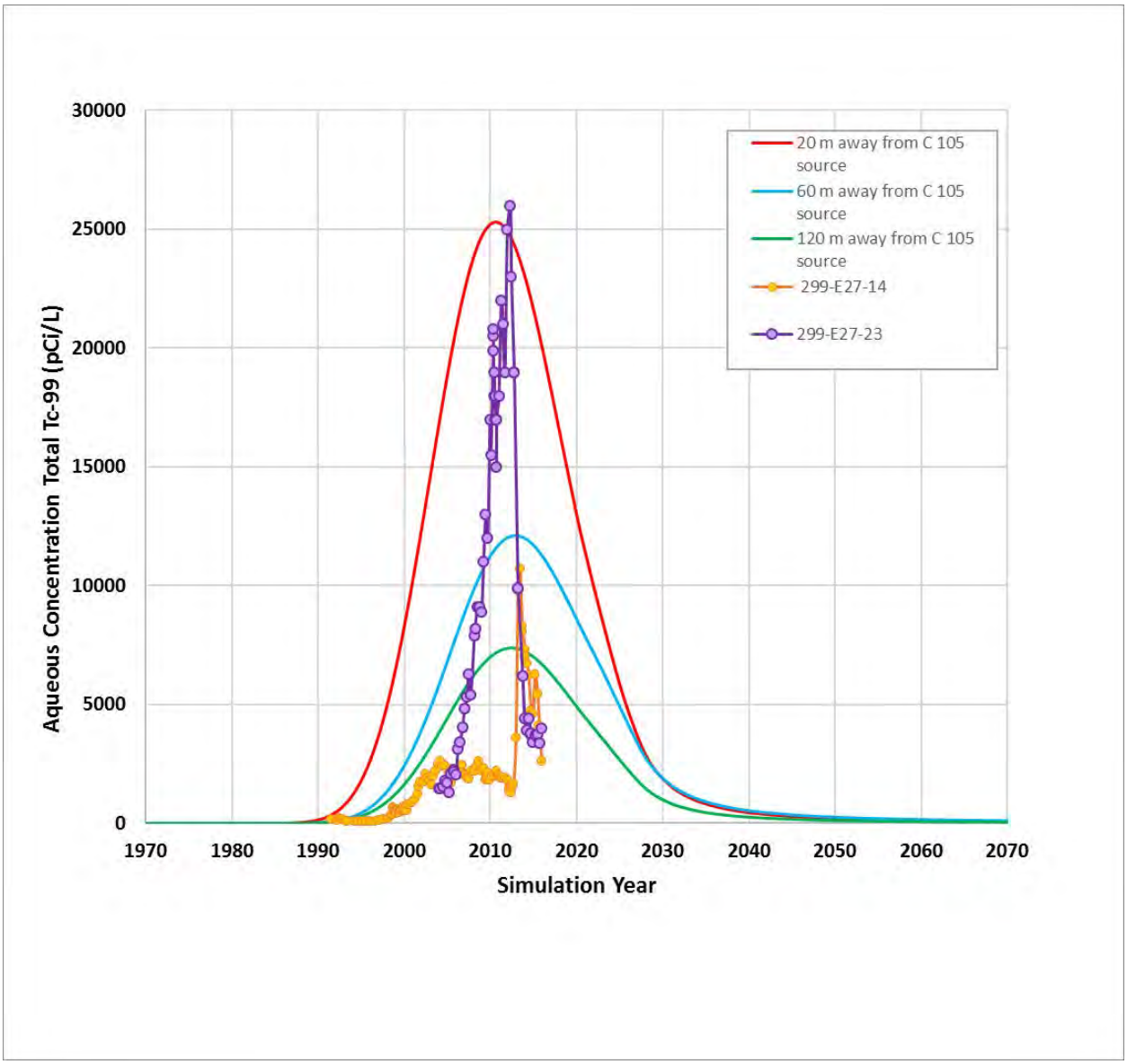

Note: Also shown are measured Technetium-99 concentration data from wells 299 E27-14 and 299-E27-23.

The shapes of the curves presented in this section generally do not provide good matches to the rapid rise and fall of the measured data. This occurs because the data are influenced by the changing orientation of the water table during the period when the plumes arrived at the wells. The steady-state aquifer assumptions implemented in the scoping analyses presented in this section do not represent the changes that lead to the sharp changes in the observed data. This feature of the data is explored in greater depth in Section 6.

Figure 4-19. Concentrations at Selected Points of Calculation for Case 4d (95th Percentile Hydraulic Properties).

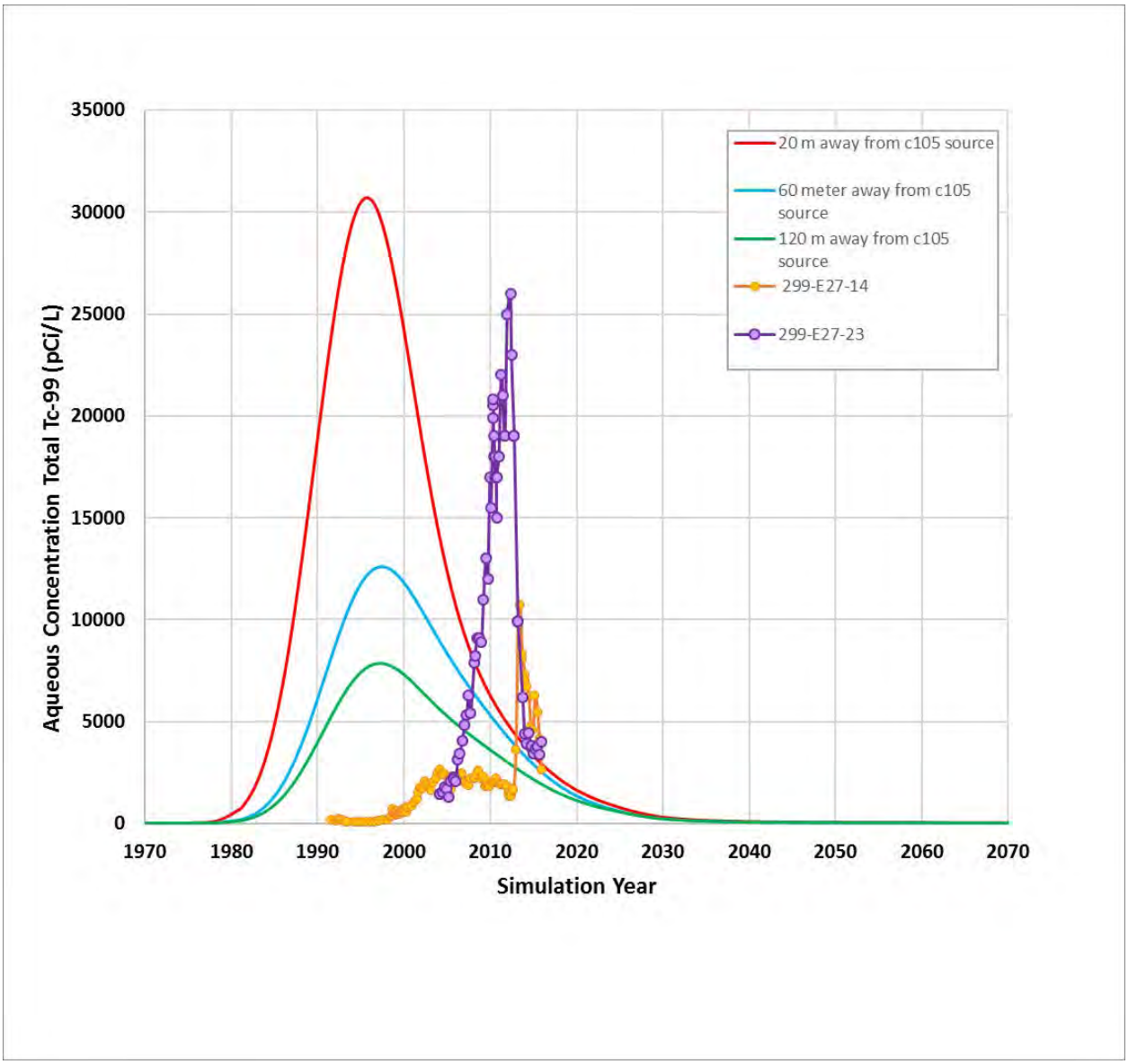

Note: Also shown are measured technetium-99 concentration data from wells 299 E27-14 and 299-E27-23.

A comparison of simulated ^{99}Tc concentrations from all scoping case modeling results at 60 m (197 ft) and at 120 m (394 ft) against ^{99}Tc concentrations observed in wells 299-E27-14 and 299-E27-23 is summarized at selected points of calculation in Table 4-8. A complimentary set of comparisons of simulated ^{99}Tc concentrations from all scoping case modeling results at 60 m (197 ft) and at 120 m (394 ft) with an emphasis on the first arrival of ^{99}Tc concentrations observed in wells 299-E27-14 and 299-E27-23 is also provided in Figures 4-23 and 4-24.

A review of these comparisons show that three scoping analysis cases produced results in which the arrival time of the calculated plume appears to be substantially earlier than the observations in the wells. The specific scoping analysis cases are as follows:

- Case 3a, in which the recharge was increased to 150 mm/yr (5.90 in./yr);
- Case 4b, in which the spatial variability of the vadose zone properties was represented by an alternative heterogeneous representation; and
- Case 4d, in which the flow properties of the vadose zone soil were set to their 95th percentile values.

Case 1 represents a minimal change from the PA/RCA model for residual wastes presented in RPP-ENV-58782 and RPP-ENV-58806, with the level of the water table elevated to represent an appropriate travel distance to the water table for the leaks. Case 1 produced arrival time consistent with monitoring data, without any parameter adjustments other than the water table elevation. This observation provides support that the model provides a reasonable representation of the leaks and vadose zone behavior. Case 1 investigated alternative leak inventories for ^{99}Tc in the tank C-105 leak. It was found that the lower bound estimate of a 1 Ci leak is inconsistent with maximum concentration levels of ^{99}Tc observed in the monitoring data. Using this observation, the inventory for the tank C-105 leak was therefore established at 10 Ci for the other analysis cases.

Case 2 investigated the effect of changing groundwater fluxes on the model results. This case was established to further investigate a potential alternative explanation for the finding of Case 1. This scoping case did not change anything that would affect arrival time. It was found that the higher flux rates led to a greater dilution of plume concentrations at the water table, and it is concluded that the lower groundwater flux rate provides concentration levels of ^{99}Tc that are more consistent with monitoring data.

Case 3 investigated the effect of alternative assumptions about both the magnitude and spatial distribution of recharge. Applying recharge over a broader area at a rate of 100 mm/yr (3.94 in./yr) rather than only over the WMA produced results that were negligibly different. Applying a higher recharge rate of 150 mm/yr (5.90 in./yr) generated earlier arrival times that are not consistent with monitoring data observed in key monitoring well locations. Case 3 also investigated the effect of a localized addition of water using a firehose to mitigate the operational hazard of leaks at UPRs -82 and -86, followed by the addition of gunite caps on the UPRs. The results of the analysis case are very similar to Case 1, indicating that this past practice has had little effect on the waste releases from the three UPRs at WMA C.

Case 4 investigated a number of vadose zone parameters and conceptual models of potential interest, to evaluate the potential for heterogeneities in the vadose zone to affect the plume development migration.

Figure 4-20. Concentrations at Selected Points of Calculation for Case 4e (Clastic Dike).

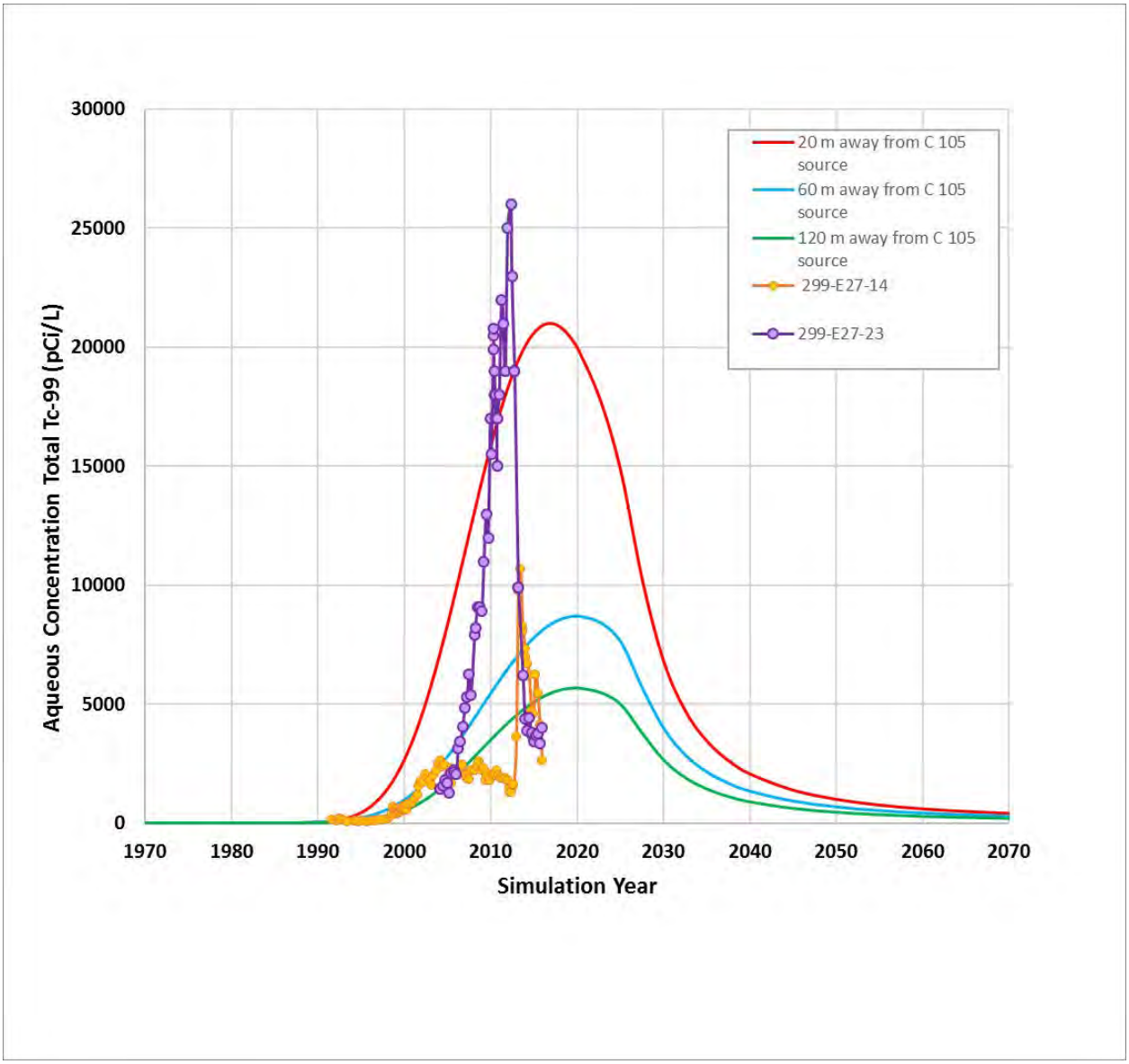

Note: Also shown are measured Technetium-99 concentration data from wells 299 E27-14 and 299-E27-23.

The results of these analysis cases compared to available monitoring data indicate the following:

- The evaluation of ACM-II showed that adding refinement in the Hanford H2 Sand unit does not strongly affect the results of the analysis compared to ACM-I. Neither alternative model is clearly superior to the other in terms of explaining the monitoring well data.

- The evaluation using a heterogeneous representation of the vadose zone showed that adding heterogeneity resulted in an earlier arrival that has been observed in monitoring wells and concentrations levels that were lower than those shown in Case 1. This alternative model appears to be inconsistent with data.

- The evaluation of median values of vadose zone hydraulic properties showed arrival time and concentration results that were not significantly different than those for Case 1. However, the evaluation of 95th percentile values of vadose zone hydraulic properties showed arrival time results that were significantly different than those for Case 1 and the arrival times and concentration levels of ^{99}Tc concentrations from key monitoring wells. Therefore, the use of 95th percentile properties appears to be inconsistent with data.

- The evaluation of a hypothetical clastic dike and a poorly sealed borehole located near the assumed waste release near tank C-105 showed a slightly earlier arrival time at the water and only a small effect of estimated peak concentrations. Since these scoping analysis cases produce results that are similar to cases in which these features are absent, they are not preferred for use in further analyses.

At the outset, it was unclear whether the vadose zone properties, developed for dry post-closure conditions, would be appropriate for the wetter conditions associated with past leaks. Based on the agreement in arrival times between scoping cases that use the dry-calibrated properties and measured data, it is concluded that this is not a significant concern for modeling of the past leaks.

Figure 4-21. Concentrations at Selected Points of Calculation for Case 4f (Borehole Preferential Pathway).

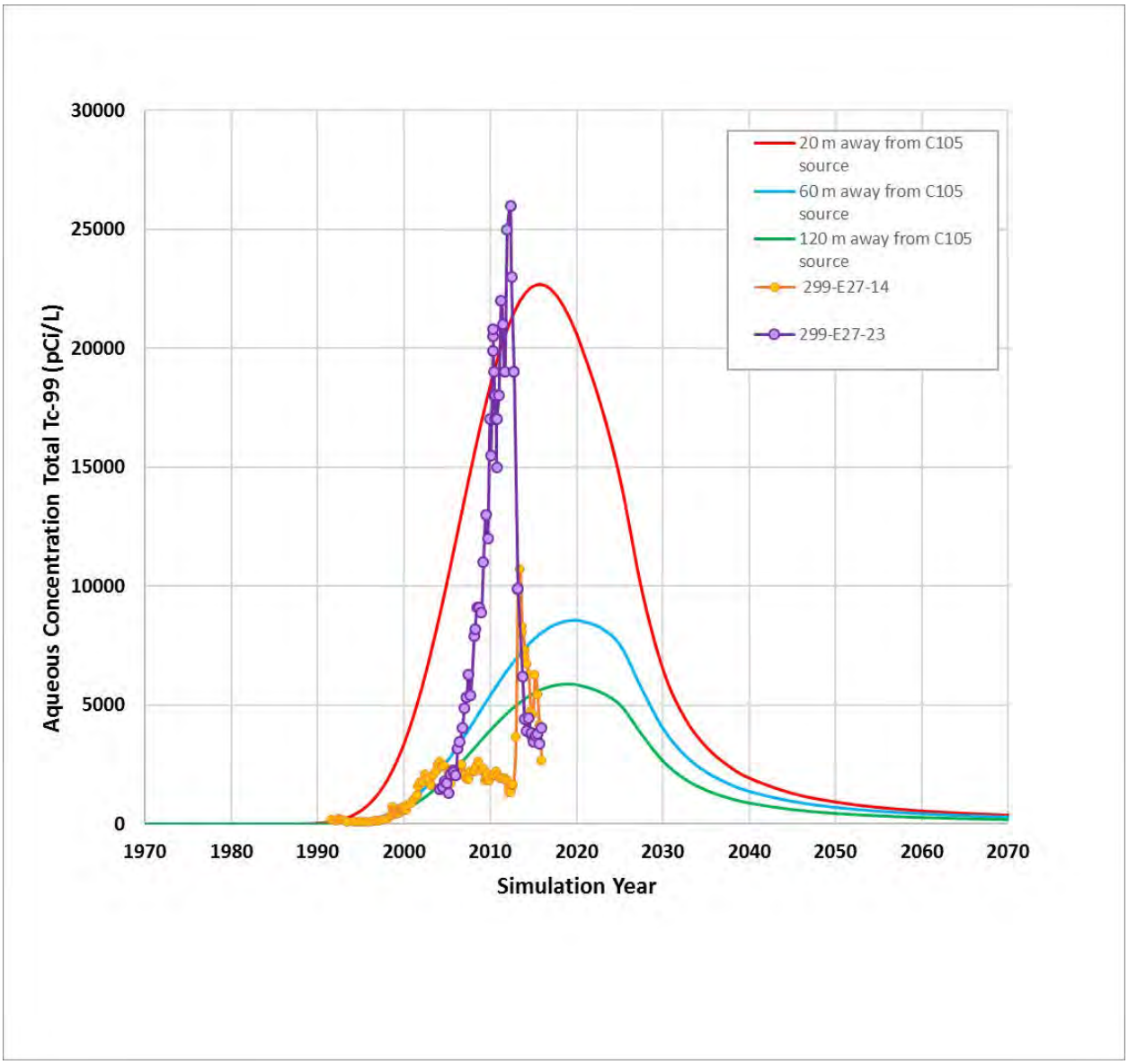

Note: Also shown are measured Technetium-99 concentration data from wells 299 E27-14 and 299-E27-23.

Figure 4-22. Technetium-99 Concentration Results A) at the WMA C Fence line and 100 m down gradient and B) at Fenceline Points of Calculation from Alternative Inventory Case Requested by Ecology.*

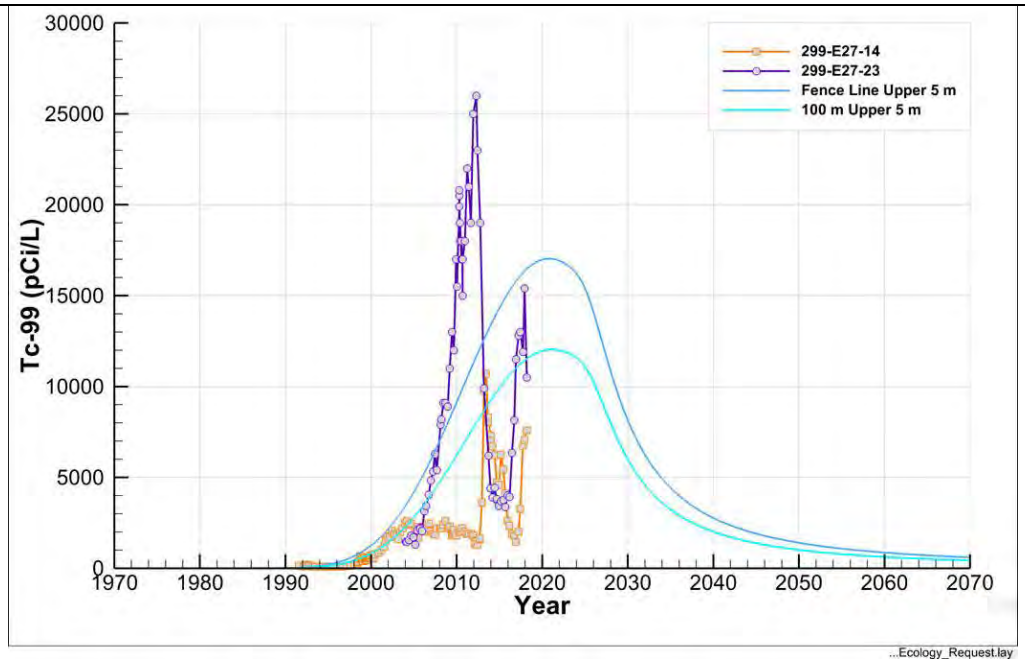

A)

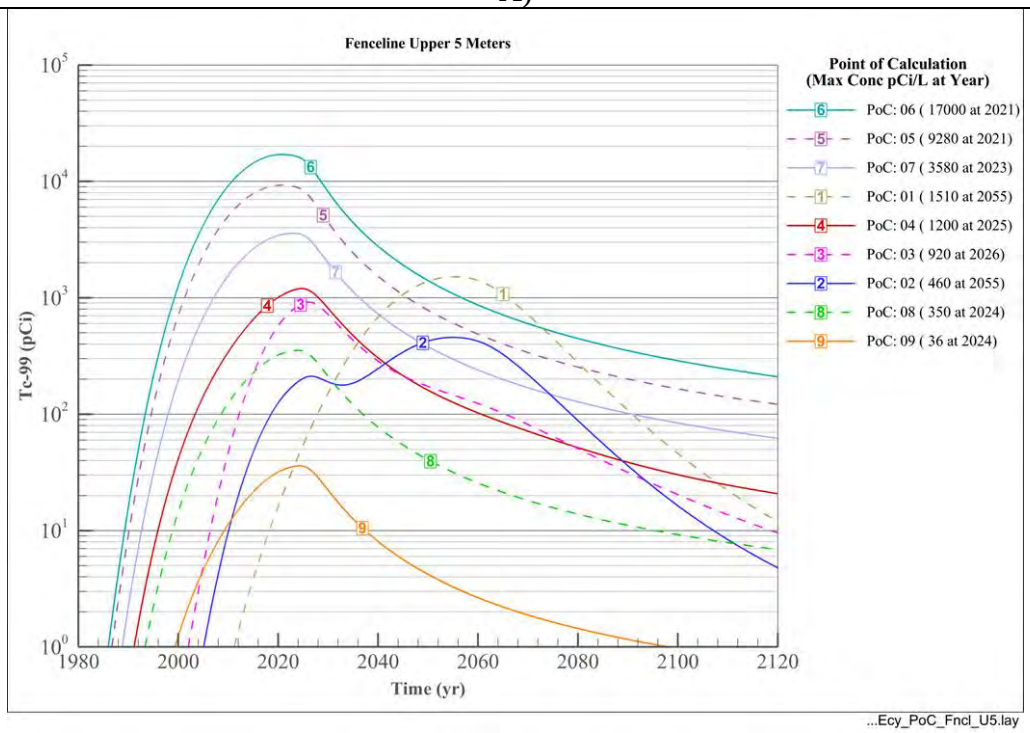

B)

* This case involved doubling the release duration, the Tc-99 inventory, and the waste volume associated with the C-105 tank leak that were assumed in Case 1a.

Table 4-8. Comparison of the Technetium-99 Concentration Results at Selected Points of Calculation for All Scoping Analysis Cases.

	Model Results at 20 Meters Downgradient of Tank 241-C-105 Waste Release Location		Model Results at 60 Meters Downgradient of Tank 241-C-105 Waste Release Location		Model Results at 120 Meters Downgradient of Tank 241-C-105 Waste Release Location	
Case Number	**Time of Maximum Concentration (Calendar Year)**	**Maximum Concentration (pCi/L)**	**Time of Maximum Concentration (Calendar Year)**	**Maximum Concentration (pCi/L)**	**Time of Maximum Concentration (Calendar Year)**	**Maximum Concentration (pCi/L)**
Case 1a[3]	2015	22,800	2017	9,800	2018	5,900
Case 1b	2023	4,200	2023	2,700	2023	1,900
Case 2a	2015	45,200	2019	16,800	2019	11,800
Case 2b	2015	15,200	2019	5,800	2019	3,900
Case 3a	2000	29,500	2002	12,500	2003	7,500
Case 3b	2015	22,700	2017	9,800	2018	5,900
Case 3c	2015	22,800	2017	9,800	2018	5,900
Case 3d	2015	22,800	2017	9,800	2018	5,900
Case 4a	2010	24,200	2011	10,200	2012	5,900
Case 4b	2002	23,700	2004	9,300	2004	6,200
Case 4c	2010	25,300	2013	12,100	2012	7,400
Case 4d	1995	30,700	1998	12,600	1997	7,900
Case 4e	2016	21,000	2018	9,300	2019	5,700
Case 4f	2016	22,400	2018	9,700	2019	5,900

[3] Results from the Alternative Inventory Scoping Case requested by ECY during the comment resolution process, where the leak volume and release time for the past leak at C-tank C-105 in Case 1a was doubled, had a peak concentration of 17,000 pCi/L at the WMA C fence line in about the year 2021. This location is close to the point of calculation about 60 m (197 ft) down gradient from tank C-105.

Figure 4-23 Comparison of Simulated Technetium-99 Concentrations from All Scoping Analysis Cases at 60 Meters Downgradient for the Tank 241-C-105 Past Release Location with a Focus on the First Arrival of Technetium-99 Concentrations Observed at Wells 299-E27-14 and 299-E27-23.

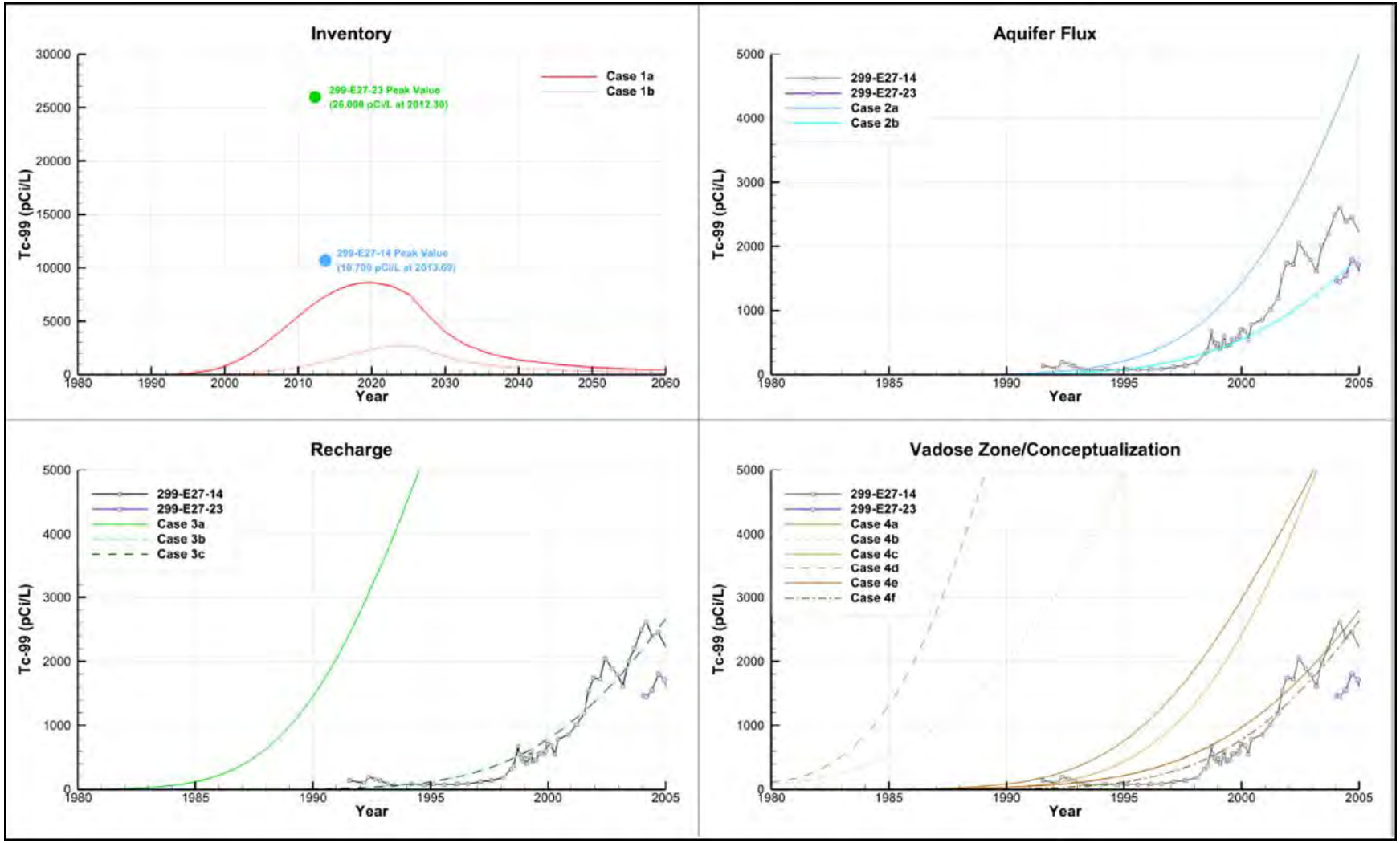

Figure 4-24. Comparison of Simulated Technetium-99 Concentrations from All Scoping Analysis Cases at 120 Meters Downgradient for the Tank 241-C-105 Past Release Location with Focus on First Arrival of Technetium-99 Concentrations Observed at Wells 299-E27-14 and 299-E27-23.

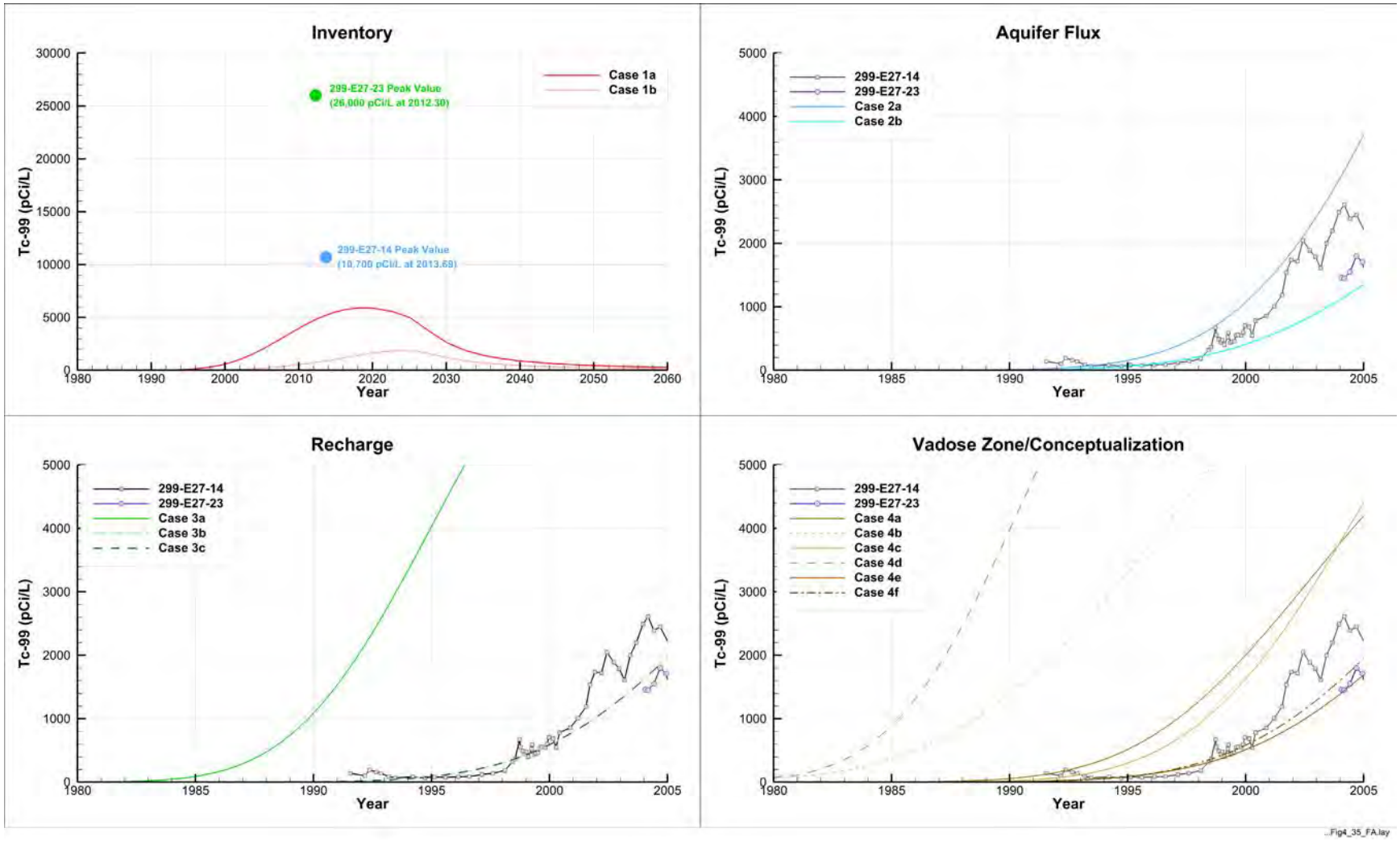

This page intentionally left blank.

5.0 EVALUATIONS OF THE USE OF ALTERNATIVE CONCEPTUAL MODELS TO EVALAUTE THE EFFECTS OF VADOSE HETEROGENEITY ON PLUME TRANSPORT

Conceptual models that explicitly represent vadose zone heterogeneities in major HSUs beneath WMA C have been evaluated more recently than the initial publication of this report. These conceptual models seek to understand the potential effects of heterogeneities on flow and contaminant transport. This section provides summaries of these past efforts at WMA C that includes:

- A summary of previous work by PNNL documented in PNNL-24740, *Alternative Conceptual Models of the Subsurface at WMA C;*

- A summary of previous work by WRPS, PNNL, and INTERA, Inc. (INTERA) that is in the process of being documented in RPP-RPT-61239, *Multiple Lines of Evidence and Modeling Results for Heterogeneous Alternative Conceptual Models of the Subsurface at Waste Management Area C*, in preparation; and

- A summary of recent work by WRPS and INTERA completed at the request of Ecology and documented in Appendix B of this document.

5.1 SUMMARY OF PREVIOUS WORK BY PACIFIC NORTHWEST NATIONAL LABORATORY AS DOCUMENTED IN PNNL-24740

In PNNL-24740, neutron moisture, spectral gamma, and grain-size distribution data were used in conjunction with a geologic framework model to develop alternative conceptual models of the subsurface at WMA C. The development of these models was motivated, in part, by concerns raised during the PA development process about the representation of the subsurface using an EHM approach in the PA base case model. A goal of this work was to evaluate the potential impact of smaller-scale heterogeneities on simulated subsurface flow and transport behavior relative to the EHM-based numerical model being used for WMA C PA calculations.

The spatial distributions and parameters assigned to the smaller-scale heterogeneities were estimated using borehole spectral gamma, neutron moisture, and grain size distribution data. The field-measured moisture content data determined from neutron moisture logging was used as a proxy for sediment texture and associated hydraulic properties in a parameterization method based on similar media scaling. Although application of this parameterization method to WMA C was successful, the effort was complicated by the possible impacts of past tank leaks in and around the tank farms.

Simulations of tank waste residuals and past tank waste releases were performed. The results from this study showed very similar predictions of flow and transport behavior for different

representations of heterogeneity inferred from borehole spectral gamma, neutron moisture, and sediment texture data.

For the tank residual simulations, only the source term for tank C-105 (the largest) was evaluated. The four different models evaluated different approaches to assigning material properties in the vadose zone to address heterogeneity. The models evaluated simulated peak ^{99}Tc concentrations at 100-m (328 ft) downgradient calculation planes used in the analysis that ranged from 18.9 pCi/L at 1,694 years after closure for the Theta001 case to 24.0 pCi/L at 1,315 years after closure for the sensitivity case Facies004, while the PA Base Case had a peak of 19.9 pCi/L at 1,590 years after closure. For simulations of tank waste residual impacts from the four models, the simulated peak concentrations were a factor of 45 or more below the maximum concentration limit for ^{99}Tc (MCL = 900 pCi/L). The small differences in peak concentrations in these models indicates that for the different heterogeneous tank residual models collapse to unit gradient model with recharge being driving factor for long term impacts. However, it should be noted, the differences in timing of the peaks can occur due to different moisture content in the vadose between models.

For the past tank release simulations, the water table was not simulated instead a flux averaged peak ^{99}Tc concentrations were evaluated at flux plane located at the water table. The peak ^{99}Tc concentrations ranged from 1.03E+5 pCi/L in the year 2026 for the Theta001 case to 1.96E+5 pCi/L in the year 2004 for the Facies002 case.

The results of this study suggest that inclusion of smaller scale heterogeneities, inferred here from moisture content and spectral gamma log data, leads to more lateral spreading than would occur otherwise in a homogeneous model. More lateral spreading tends to result in the delayed arrival of contaminants at the water table and reduced peak concentrations. The alternative models developed in PNNL-24740, which attempt to account for smaller scale heterogeneities in the subsurface underlying WMA C, produce results that are similar to and bracket predictions generated by the EHM-based PA model. Additionally, while the results from the various alternative heterogeneous models for both the tank residuals and the past leaks were very similar in their respective magnitude and timing of peak ^{99}Tc concentrations, a better understanding of the range of heterogeneous model predictions could be developed by examining a larger ensemble of realizations.

Finally, the alternative conceptual models discussed in PNNL-24740 did not include an assessment case that contains sloping thin layers that have been suggested in WMA C workshops. While such features may exist, available field-measured moisture content data arguably do not allow thin, continuous sloping layers to be unambiguously identified. Uncertainty exists in the timing, locations, and rates of past releases and therefore detailed inverse modeling or history matching efforts may be of limited value.

5.2 SUMMARY OF PREVIOUS WORK ON ALTERNATIVE HETEROGENEOUS MODELS BEING DOCUMENTED IN RPP-RPT-61239

The work being documented in RPP-RPT-61239 (in preparation) represents a systematic review and analysis of numerous field data sets collected at WMA C to develop alternative geologic conceptual models to incorporate small-scale heterogeneities that may impact contaminant transport. In addition to the field data sets at WMA C, two other 200 East Area sites[1] in which lateral movement of contaminants and/or moisture have been observed are also evaluated for similarities and differences within the vadose zone to WMA C. The primary purpose of this evaluation was to develop multiple lines of evidence which could be used to identify data best suited to provide the basis for the vadose zone conceptual site models to account for any observed geologic heterogeneities. These data sets included the following:

- Geologic logs;
- Particle size data;
- Moisture content data;
- Spectral gamma log data for ^{40}K, ^{238}U, ^{232}Th (K-U-T), and ^{60}Co;
- Geochemical sampling for ^{99}Tc; and
- Comparison of WMA C geology, particle size information, and moisture content to other sites within the 200 East Area showing lateral movement of moisture and/or contaminants. The other sites within the 200 East Area compared include WMA B-BX-BY, and the Vadose Zone Transport Field Study (VZTFS) site.

The geologic logs for the sand-dominated Hanford (H2) unit (the thickest unit underlying WMA C) indicate that the sediment texture is primarily sand, varying from fine to medium to coarse (Figure 5-1) with very little silt. The particle size data are consistent with the geologic logs with almost 500 samples taken from 31 drywells, but with only 0.6 percent of the samples having greater than 15 percent silt (see Figure 5-2). The moisture content directly underneath the SSTs is also consistent with the particle size and lithologic logs. If the assumption is made that higher moisture content is associated with finer-grained sediments, the number of samples greater than 10 (vol %) in the H2 unit was 260 or approximately 1.2 percent of all the measurements (Figure 5-3) and only 61 samples greater than 15 (vol %).

The geologic descriptions and particle size information are also consistent with the evaluation of KUT data. For example, in PNNL-24698, *Geostatistical Realizations of WMA-C Lithofacies*, three primary facies were identified (sand, gravel, and minor mixed facies), none of which was identified as being fine-grained. Together, these data provide multiple lines of evidence that the principal sediment texture underlying the SSTs at WMA C is sand with little evidence for finer-grained layers with strongly contrasting hydraulic properties that would cause lateral flow over large distances.

[1] The unplanned release at SST 241-BX-102 at WMA B-BX-BY and the Vadose Zone Test Field Study site located 1,100 m (3,609 ft) south-southeast of WMA C.

Away from the SSTs, in an area of higher elevations to the southwest, silt layers were identified in the vicinity of the unplanned release site UPR-200-E-82. The silt layers were identified in the direct pushes within the upper, gravel-dominated Hanford (H1) unit. These silt layers have moisture contents much higher (>15 vol %) than those observed in sediments underlying the SSTs (Figure 5-4). These silt layers, which dip toward the northeast, could provide some basis for adding additional heterogeneity beneath the SSTs. However, when projected to the northeast, the upper silt layers would have been destroyed during the excavation for the tank farm. Only the lowermost silt layer could be projected underneath the tanks. However, no evidence of this layer is found in wells to the northeast.

The next line of evidence that was examined is the field sampling for ^{99}Tc in both the vadose zone and groundwater. Soil samples were collected from vertical and slant probe direct push borehole locations throughout WMA C, as well as characterization borehole C4297. Since low concentrations of ^{99}Tc were found in the vadose zone from this sampling (Figure 5-5), the ^{99}Tc is hypothesized to be present at depths exceeding most of the borehole depths in the vadose zone, or the ^{99}Tc released from WMA C already moved through the vadose zone into groundwater. The high mobility of ^{99}Tc is consistent with coarse-grained gravels and sands, and with ^{99}Tc concentrations measured in groundwater beneath WMA C.

Figure 5-1. Analysis of the Geologic Logs for Sediment Texture within Each Hydrostratigraphic Unit.

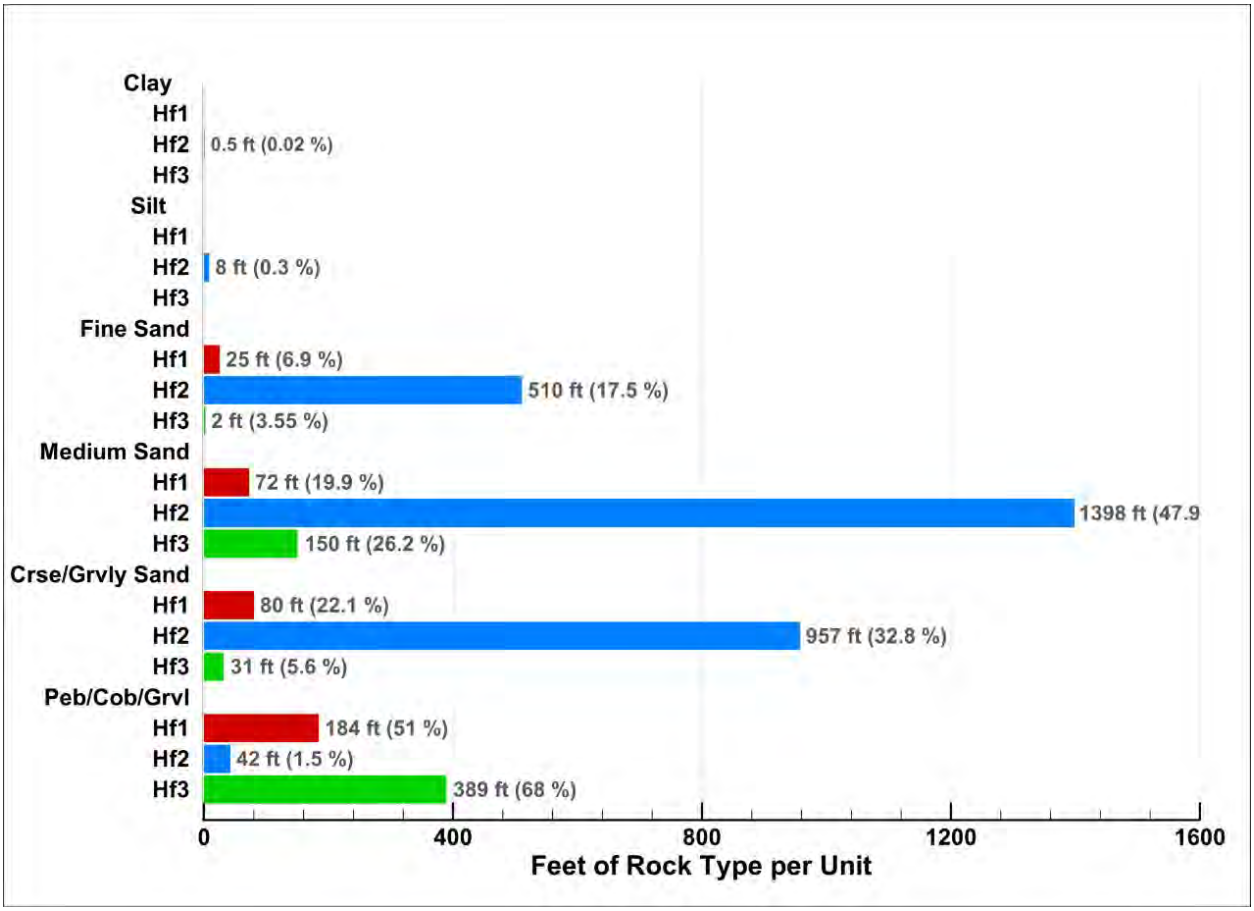

Hf1 = Hanford formation upper gravelly sequence unit
Hf2 = Hanford formation sand sequence unit
Hf3 = Hanford formation lower gravelly sequence unit
Reference: RPP-18290, *241-C Tank Farm Geologic and Stratigraphic Analysis.*

Although ^{60}Co has been reported in the vadose zone in 35 drywells, two groundwater monitoring wells (299-E27-7 and 299-E27-14), and one characterization borehole (C4297) (Figure 5-5), these data were deemed to be less definitive in developing conceptual site models for the following reasons. Cobalt-60 is less definitive in developing conceptual site models because ^{60}Co: 1) is not a dose/risk driver in PA calculations, 2) has a short half-life, 3) has variable transport behavior (PNNL-16663), and 4) does not correlate well with ^{99}Tc at the one location where both were measured (Figure 5-5).

Additionally, to help understand the field data and inform the conceptual site models for WMA C, field data from other sites within the 200 East Area were examined. At the tank 241-BX-102 leak site, widespread lateral movement of contaminants was observed. However, at this site, two supporting observations were made: 1) the particle size information indicates more samples with greater than 15% silt (Table 5-1); and 2) three laterally correlated, fine-grained units with multiple measurements of high moisture content (~7 to 22.36 wt %) were

identified which could cause lateral spreading within the H2 unit. These types of observations have not been made in reviews of similar types of data collected underlying the SSTs at WMA C.

Figure 5-2. Histograms of Silt Particle Size for 31 Drywells at Waste Management Area C.

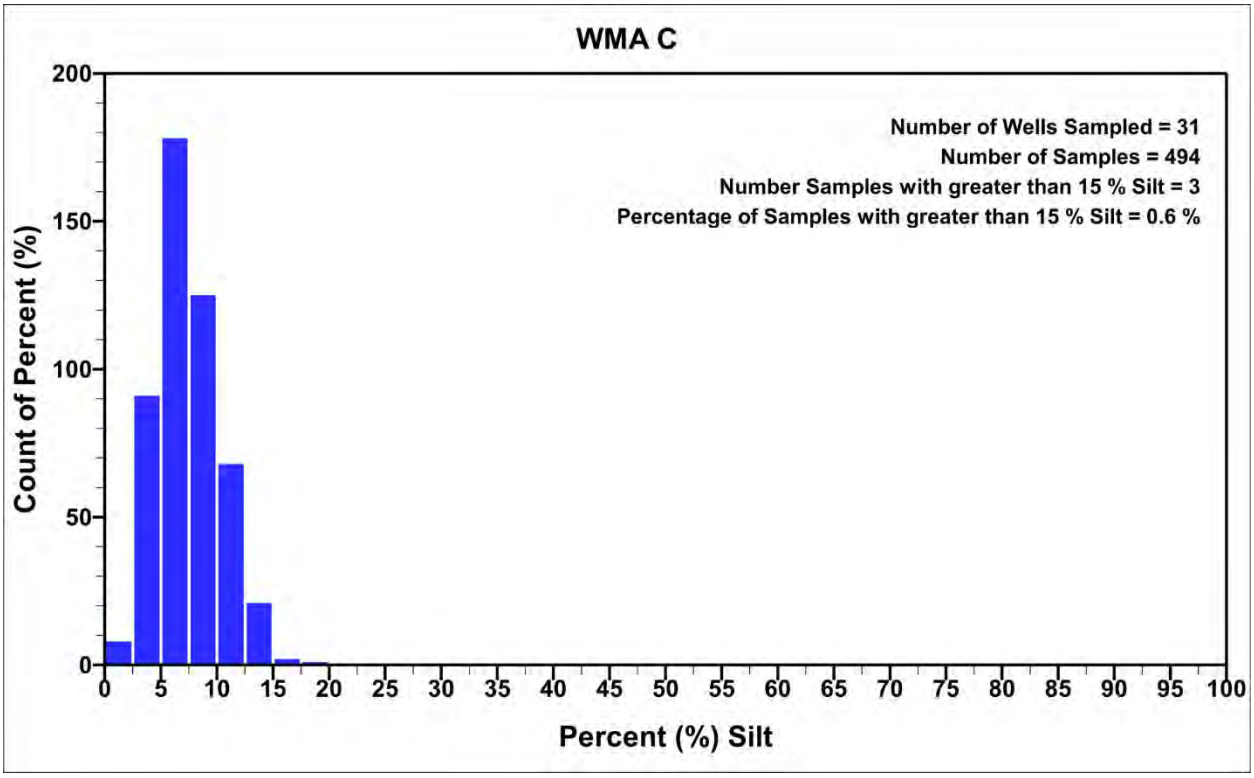

WMA = Waste Management Area

At the Vadose Zone Transport Field Study (VZTFS) site (PNNL-15443, *Vadose Zone Transport Field Study Summary Report*), lithologic logs, moisture measurements and particle size information indicate that there are multiple fine-textured layers. It was further noted in PNNL-15443 that these layers overlie coarse material and the juxtaposition of fine- over coarse-textured sediments may act as a capillary barrier impeding vertical migration of water and solutes.

When comparing these sites to WMA C, it should be noted that no lateral continuous fine-grained units were found within the footprint of the SSTs at WMA C. Outside of the footprint of the SSTs at WMA C, discontinuous fine-grained layers were observed at unplanned release site UPR-E-200-82 and these layers were incorporated into one of the conceptual models.

Based on the analysis of these data sets, four alternative conceptual site models were developed to account for the observed heterogeneities. These alternative conceptual site models are called EHM-Based, Lithofacies [facies]-Based, Moisture Content-Based Model I, and Moisture Content-Based Model II, which are shown in Figure 5-6. Numerical simulations were then performed using these models to identify potential impacts of heterogeneity on the transport of

solutes in the vadose zone where spatial variability and uncertainty in unsaturated hydraulic properties are significant. Grid spacing in the Z-direction was decreased to one foot, which is approximately one-third of what was used in the previous models (RPP-RPT-59197) to allow for thinner units to be accounted for in the models.

Figure 5-3. Histograms of Moisture Content for the H2 Unit at Waste Management Area C.

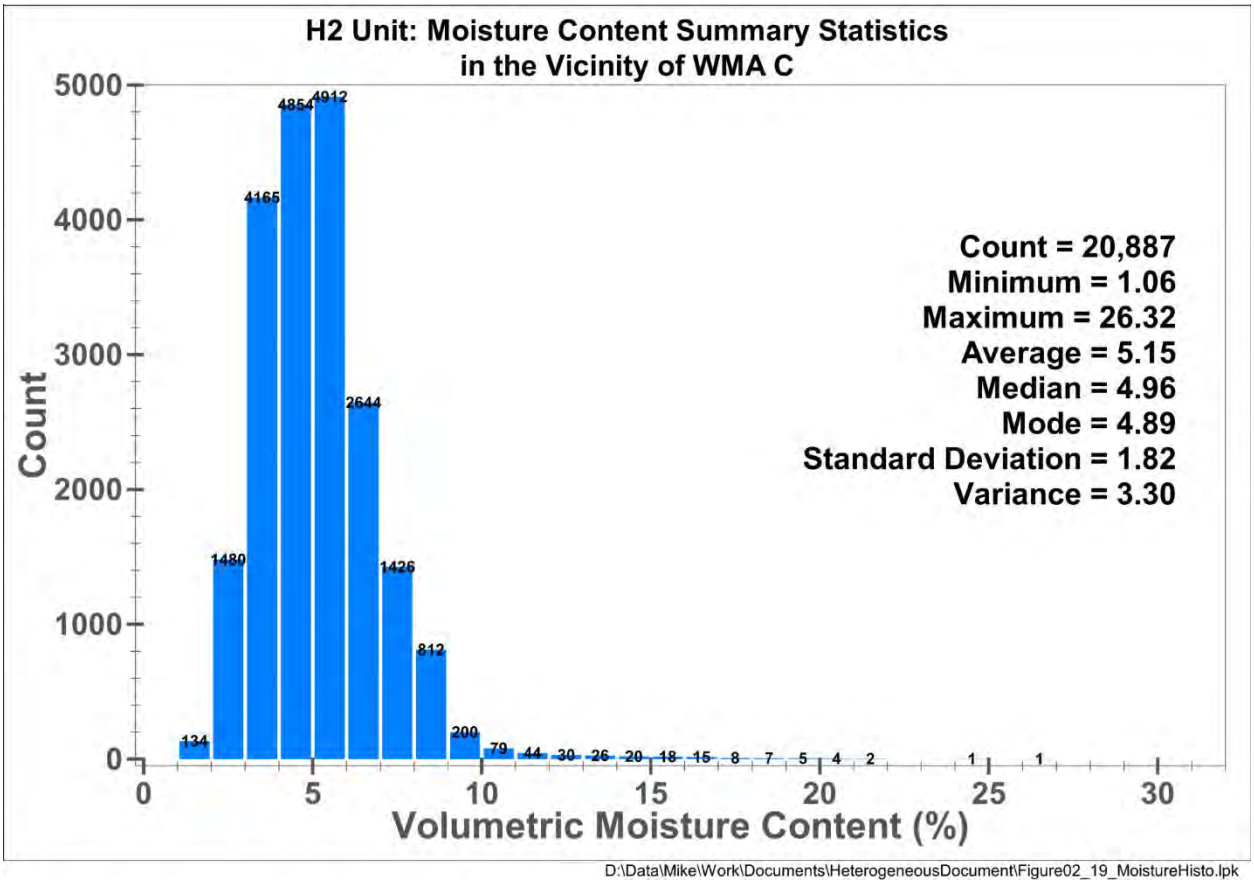

WMA = Waste Management Area

The four conceptual site models were incorporated into numerical models and were used to evaluate flow and transport behavior for unplanned releases at two sites. The intercomparison of results using the alternative models is based on examination of plume footprints and volumes, locations of the center of mass, maximum concentration for each plume, and calculated peak fluxes and arrival times for a conservative solute (i.e., ^{99}Tc) migrating from the vadose zone into the underlying unconfined aquifer.

The four alternative models that evaluated the past unplanned release at tank 241-C-105 (C-105) predicted similar plume footprints, with limited lateral spreading, and with comparable peak fluxes and peak arrival times to the water table (Figure 5-7), in spite of the differences in geologic conceptual models and approaches to parameterizations. In the analysis of the unplanned release at UPR-200-E-82 site, three out of the four modeling approaches produced similar results to those developed for the release at tank C-105. Comparison showing spreading

of the plumes for each alternative model are given in Figure 5-7 (release from tank C-105) for 1995 and Figure 5-8 (release from UPR-200-E-82) for 1990, while the peak flux and arrival times to the water table for each model are shown in Figure 5-9 (release from tank C-105) and Figure 5-10 (release from UPR-200-E-82).

Figure 5-4. Moisture Content Down Dip through Waste Management Area C from UPR-200-E-82.

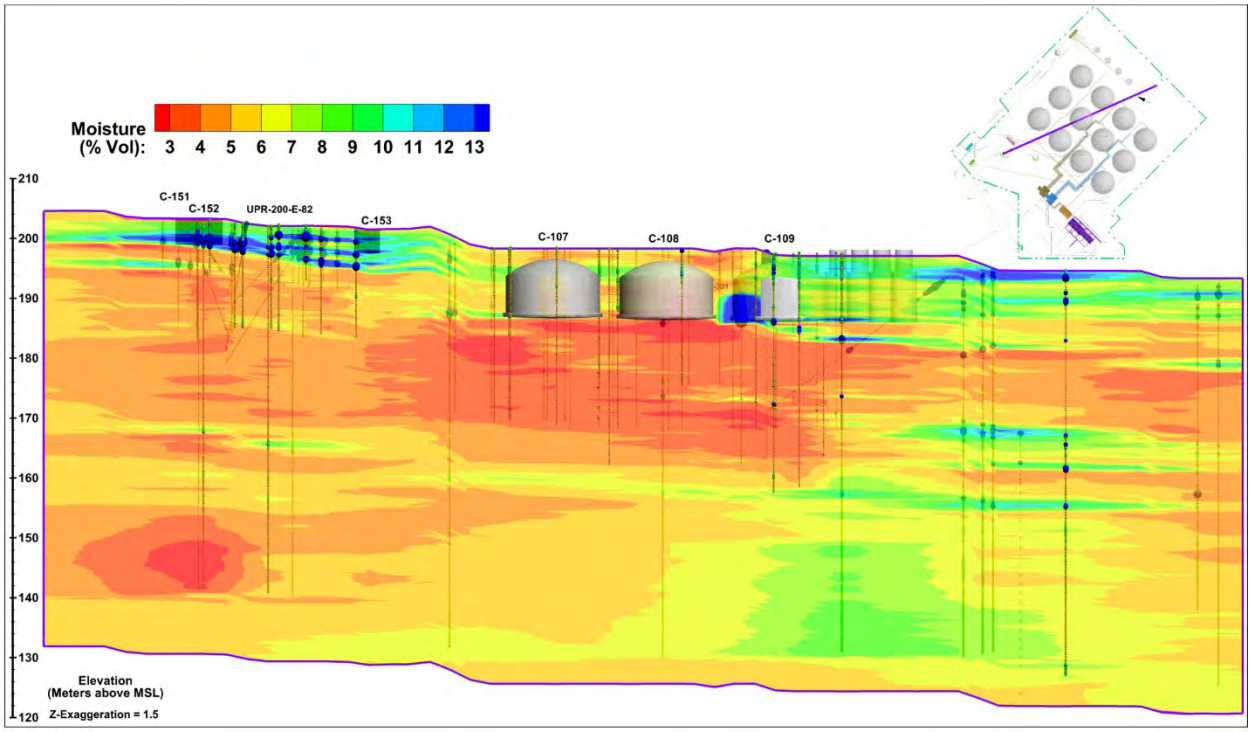

MSL = mean sea level

In one modeling approach (Moisture Content-based Model I), where a fine-grained unit with high volumetric moisture content with strongly-contrasting hydraulic properties was placed below the unplanned release at UPR-200-E-86, the footprint of the plume was greatly expanded relative to the other models. This fine-grained unit was based on the field data (observed in direct pushes that contain silts/muds with a high moisture content at this depth) for this local area and resulted in the volume of sediment affected by the plume being approximately a factor of ten times greater than that produced by the other modeling approaches. This alternative model also had greater lateral movement for both maximum concentration and center of mass; however, the lateral movement of both the maximum concentration and center of mass was still within 20 m (66 ft) of the release location. The arrival times for the peak flux at the water table for this model were earlier due to higher vertical pore water velocities at the edges of the fine-grained unit. The ^{99}Tc flux to the water table for this model is shown in Figure 5-10. The ^{99}Tc flux is dissimilar from the flux of other models in that the flux has three slight increases in flux; this is due to the strongly contrasting hydraulic properties creating three slugs within the plume as shown in Figure 5-8. Furthermore, the spreading of the plume also resulted in the peak fluxes being over a factor of two lower than the EHM-based model, which indicates that the greater the plume spreading in the vadose zone, the lower the peak fluxes will be to the unconfined aquifer.

This observation is also consistent with an observation given in in Section 2.1.2 of PNNL-15443 at the VZTFS site which states the following:

> "Infiltration at the 299-E24-111 test site is 3-D because of multi-scale heterogeneities and anisotropy. Modeling this and similar sites without considering sub-grid features would produce conservative results (enhanced vertical migration), which could lead to the over-engineering of remedial actions."

Figure 5-5. Characterization Data from Borehole C4297 by Single-Shell Tank 241-C-105.

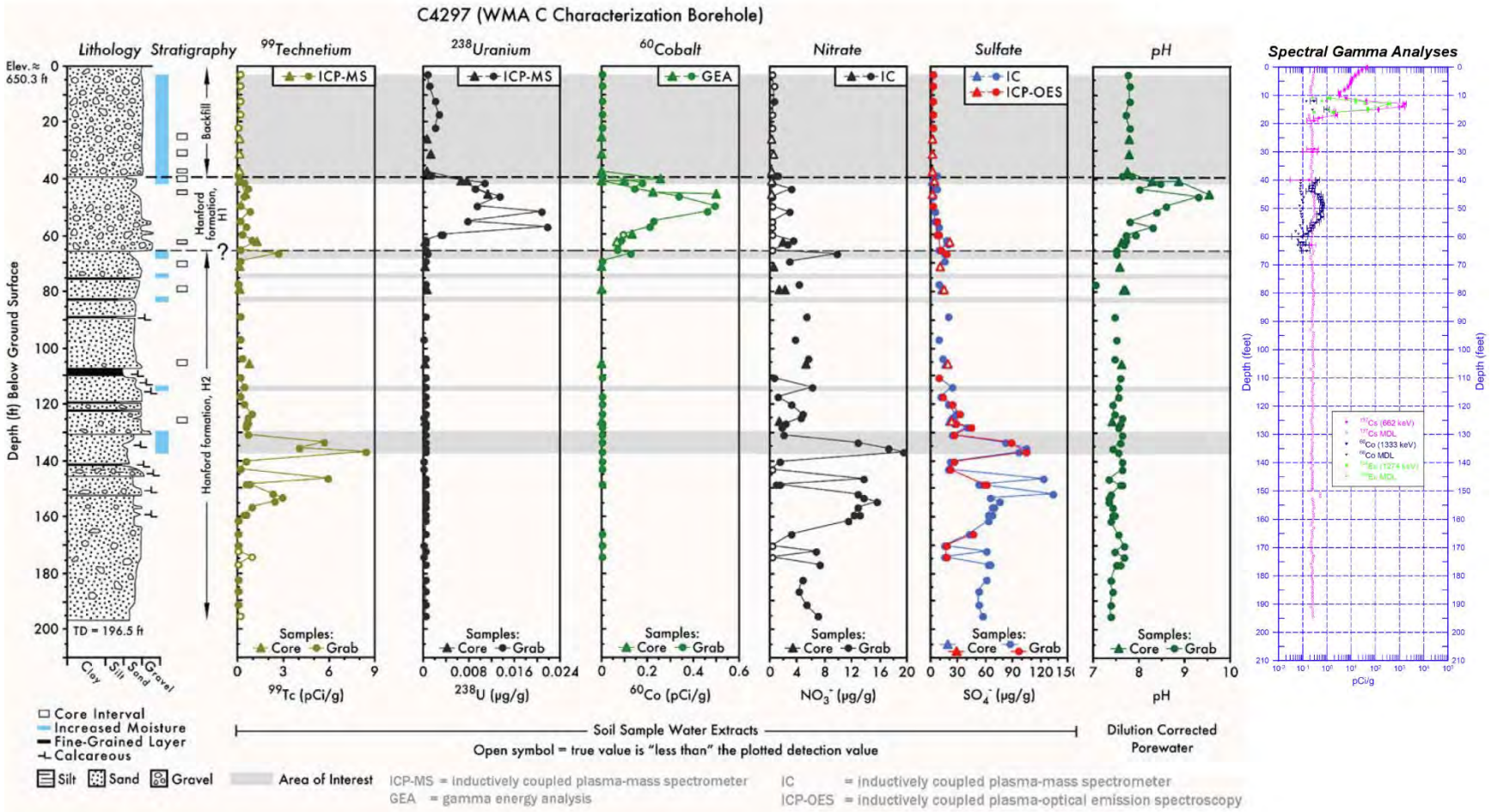

WMA = Waste Management Area

Table 5-1. Summary of Silt Particle Size Collected at Each Waste Management Area and the Vadose Zone Transport Field Study Site.

Location	Area	Number of Wells	Number of Samples	Number of Samples with Greater than 15% Silt	Percentage of Samples with Greater than 15% Silt
WMA A-AX	200 East	51	878	75	8.5%
WMA B-BX-BY	200 East	124	2,809	178	6.3%
WMA C	200 East	31	494	3	0.6%
VZTFS	200 East	6	130	23	17.7%

VZTFS = Vadose Zone Transport Field Study WMA = Waste Management Area

While the ^{99}Tc contamination observed in the groundwater is attributed to source releases at WMA C, the specific source for the observed groundwater contamination has not been identified. Information is lacking to link specific releases within WMA C to contamination at drywells and in groundwater. This lack of information makes the solutions from model calibration non-unique, especially given the uncertainty in the timing, volume, and composition of leaks. Moreover, historical subsurface discharges at the 200 East Area at Hanford resulted in the groundwater table rising on average 14 m (46 ft), which caused groundwater at WMA C to flow to the northwest during operations. In recent years, however, groundwater flow reversal (to the southeast) has occurred due to a cease in the subsurface discharges and subsequent lowering of the water table.

Figure 5-6. Comparison of Material Property Units for each of the Alternative Conceptual Models.

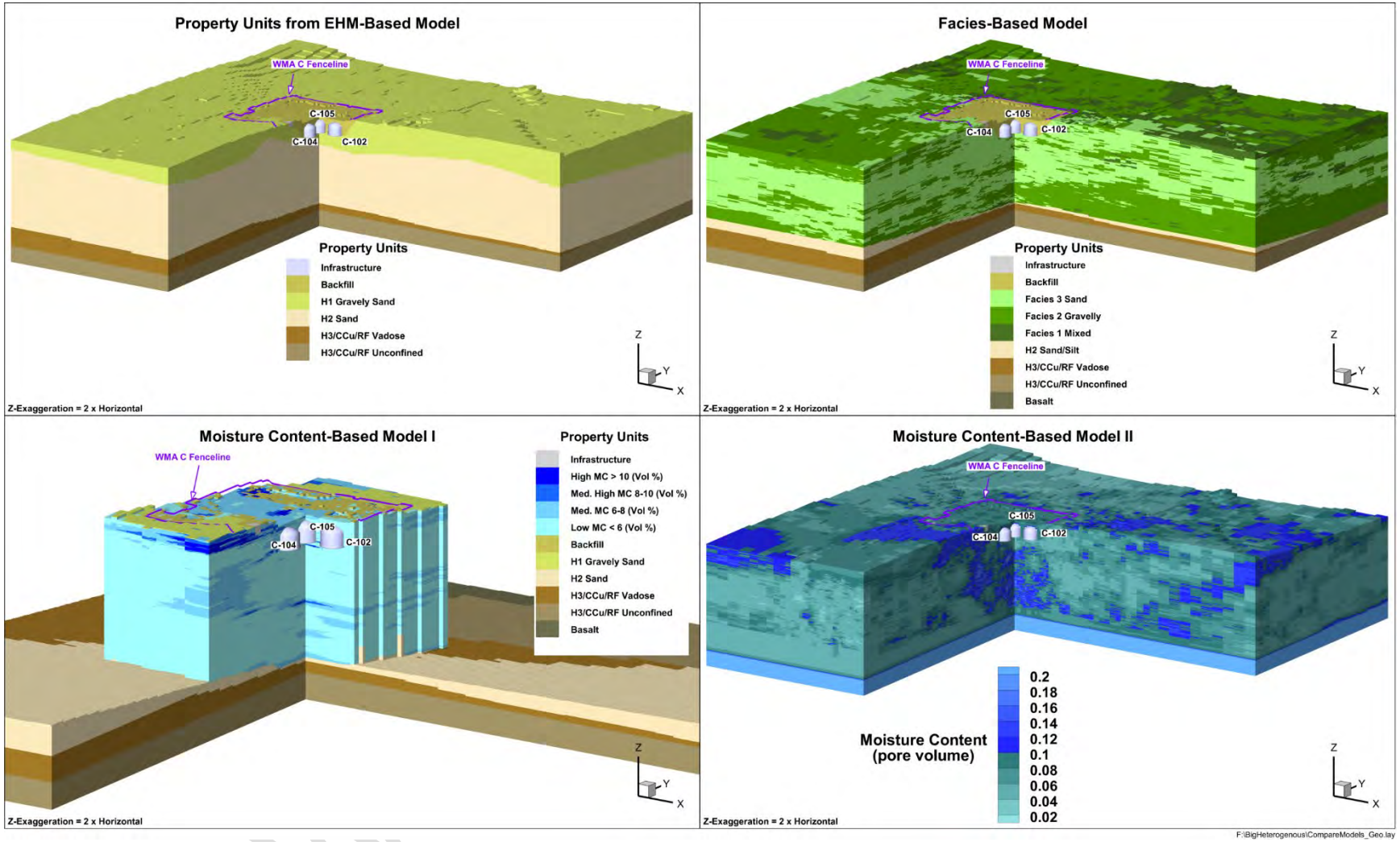

EHM = equivalent homogeneous medium H1 = Hanford formation upper gravelly sequence unit H2 = Hanford formation sand sequence unit
H3/CCu/RF = undifferentiated Hanford formation lower gravelly sequence (H3) unit, Cold Creek Unit and Ringold Formation
MC = moisture content WMA = Waste Management Area Z = vertical

Figure 5-7. Comparison of Plume Spreading in 1995 for the Four Alternative Conceptual Site Models along a Southwest to Northeast Cross-Section at the Location of the Single-Shell Tank 241-C-105 Unplanned Release.

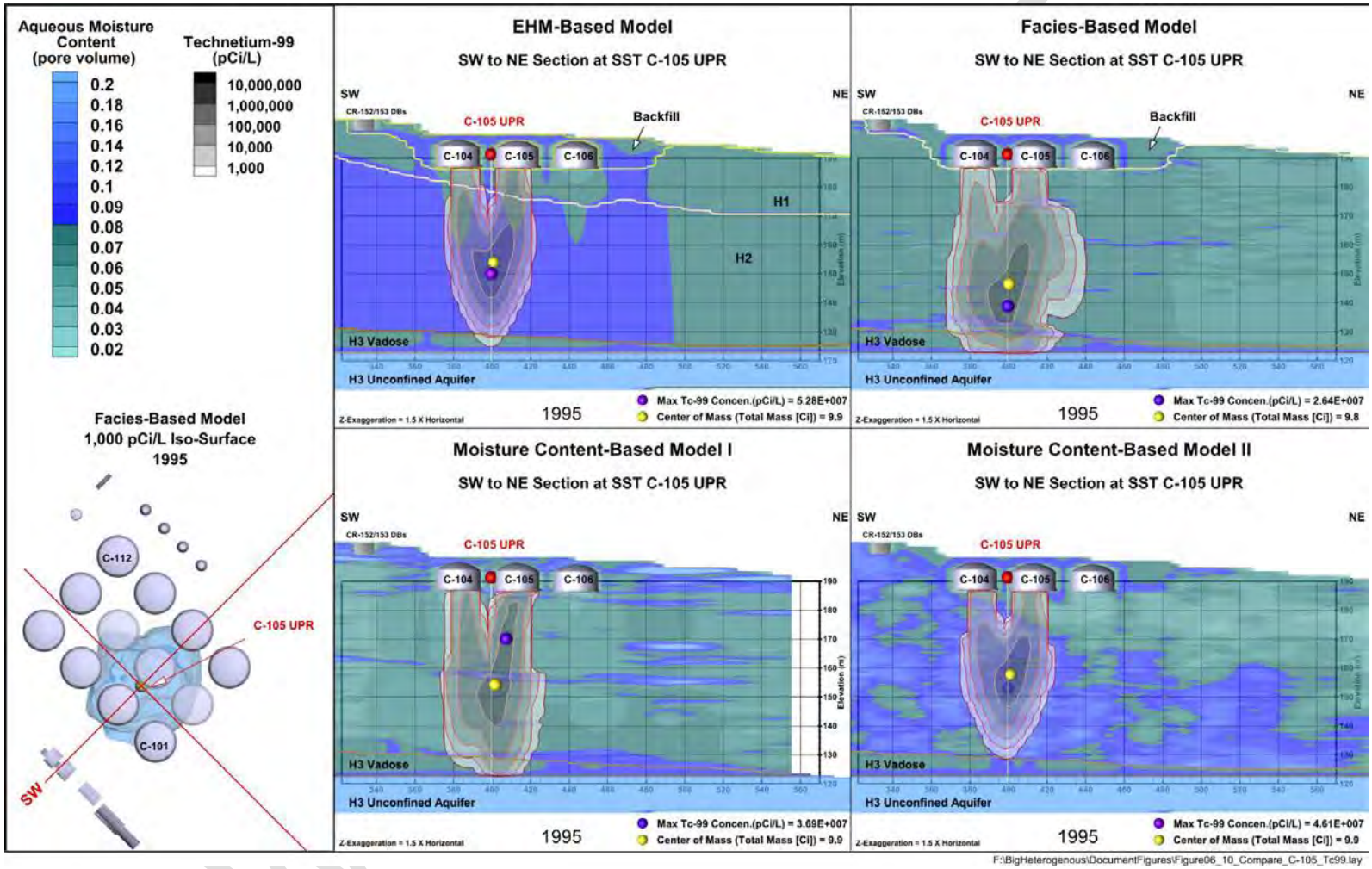

DB = diversion box
EHM = equivalent homogeneous medium
H1 = Hanford formation upper gravelly sequence unit
H2 = Hanford formation sand sequence unit
H3 = Hanford formation lower gravelly sequence unit
NE = northeast
SST = single-shell tank
SW = southwest
UPR = unplanned release
Z = vertical

Figure 5-8. Comparison of Plume Spreading in 1990 for the Four Alternative Conceptual Site Models along a Southwest to Northeast Cross-Section at the Location of the UPR-200-E-82 Pipeline Leak Site.

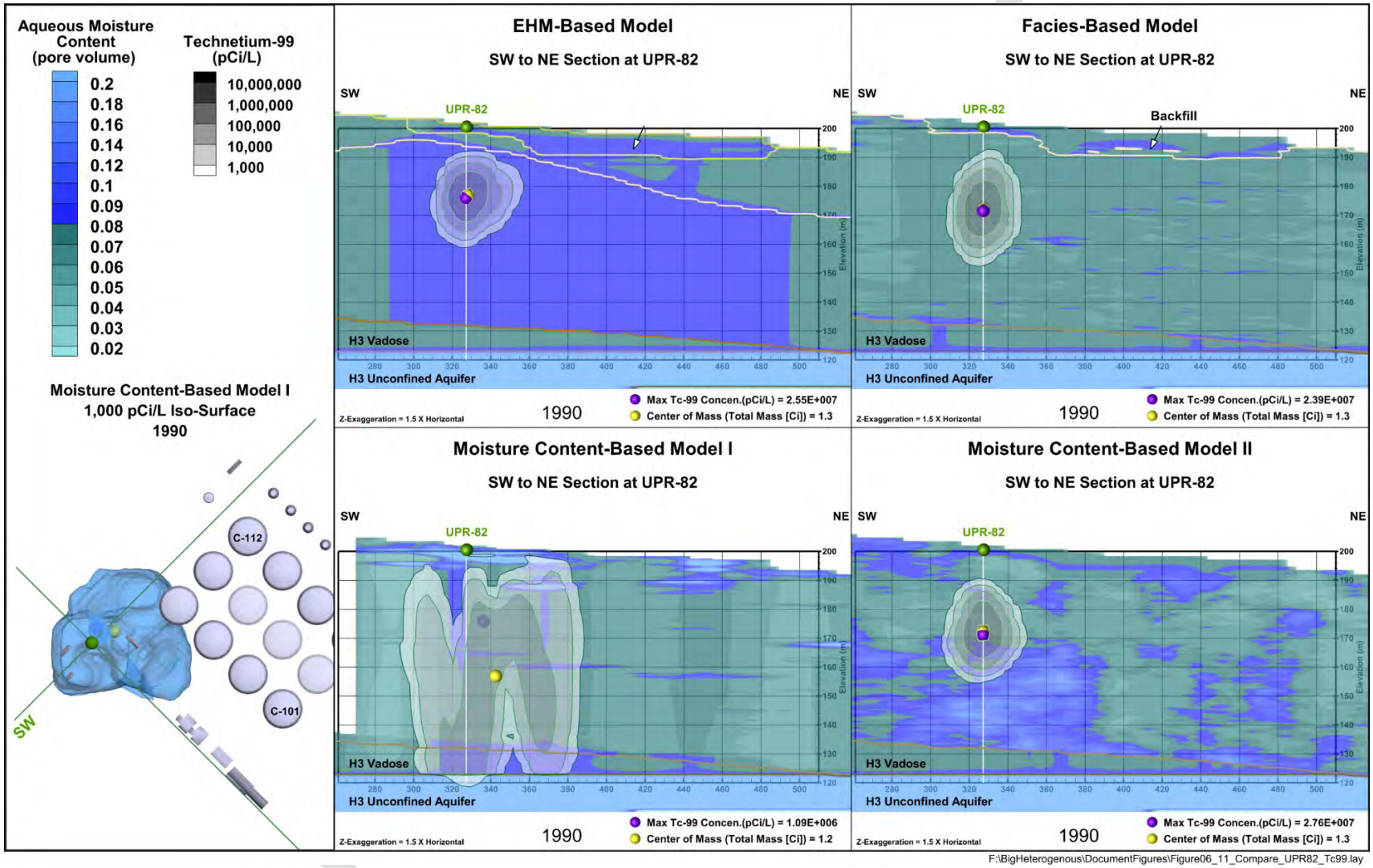

EHM = equivalent homogeneous medium
H3 = Hanford formation lower gravelly sequence unit
NE = northeast
SW = southwest
UPR = unplanned release
Z = vertical

Figure 5-9. Comparison of Instantaneous Technetium-99 Release at the Water Table for Single-Shell Tank 241-C-105 Unplanned Release for All Models.

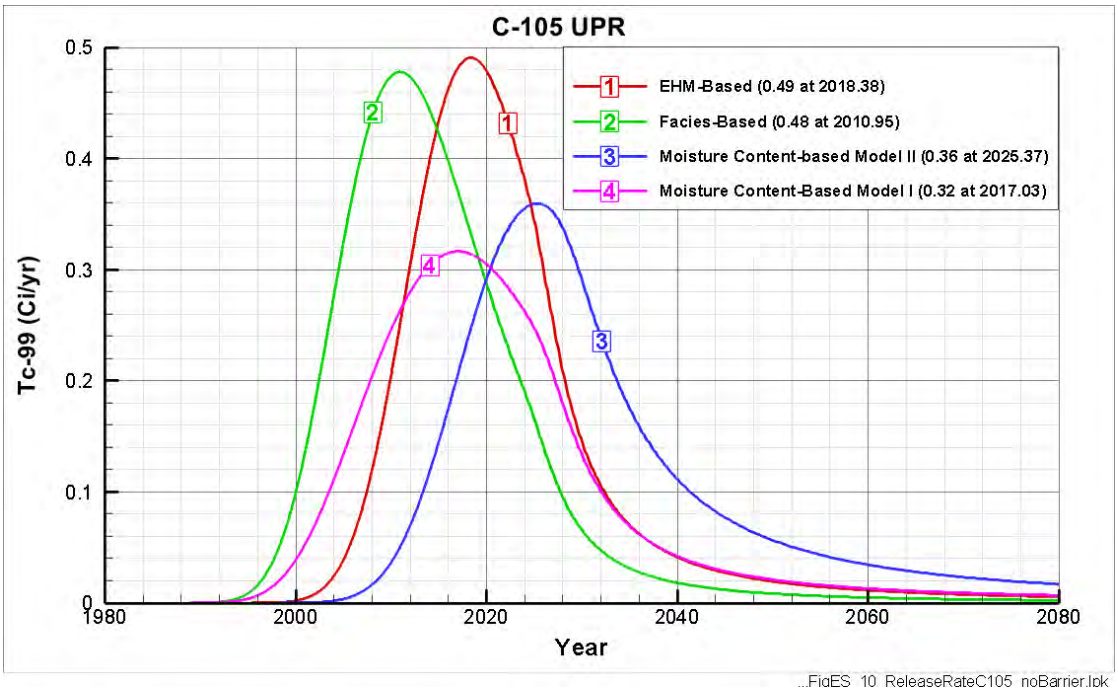

EHM = equivalent homogeneous medium UPR = unplanned release

Figure 5-10. Comparison of Instantaneous Technetium-99 Release at the Water Table for UPR-200-E-82 for All Models.

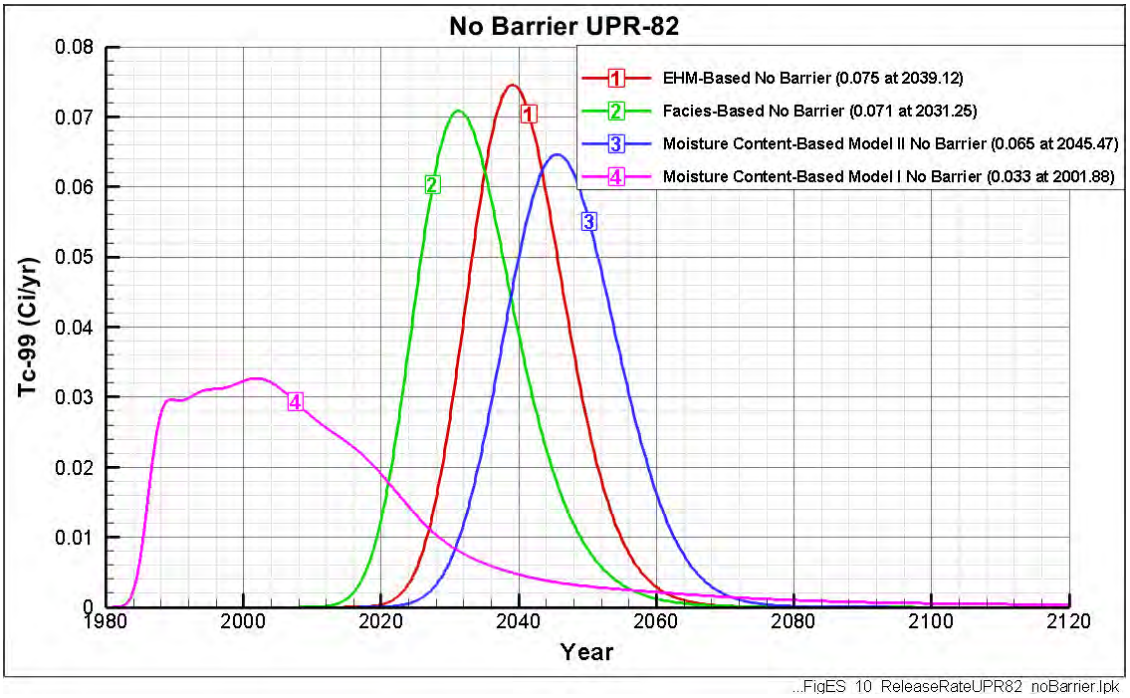

EHM = equivalent homogeneous medium

5.3 SUMMARY OF WORK ON WASHINGTON STATE DEPARTMENT OF ECOLOGY'S ADVOCACY MODELS DOCUMENTED IN APPENDIX B

During the review of this document on the potential impact of local-scale heterogeneity on transport of contaminants from tank leaks and other unplanned releases within the tank farm, Ecology requested that DOE- ORP consider an evaluation of effects of fine-grained thin sediment layers on transport with a separate alternative conceptual model. For this alternative model, Ecology recommended that the model be developed based on the general framework of fine-grained units identified by the Nez Perce in their interpretations of variability in moisture content data collected in the vicinity of WMA C. These interpretations were summarized in an unpublished report by the Nez Perce (EMDT-MO-0031, *WMA C Conceptual Model by Nez Perce*) sent by email to DOE-ORP on Nov. 5, 2014 (e-mail from S. Sobczyk to R. D. Hildebrand and C. J. Kemp, "Alternative Conceptual Model," [Sobczyk, S., 11-05-2014]).

In discussions with DOE-ORP, Ecology acknowledged that the underlying data and interpretations of the occurrence and lateral continuity of the fine-grained thin layers identified by the Nez Perce in their report are uncertain. However, Ecology indicated that this alternative model evaluation based on the Nez Perce framework would provide them with some insight into the transport effects of vadose zone heterogeneities at WMA C.

DOE-ORP agreed to Ecology's request and has provided support for the requested evaluation. The evaluation involved development of an alternative model based on the general framework of the 2014 Nez Perce report (EMDT-MO-0031). The specific model developed in consultation with Ecology is referenced here as "Ecology's Advocacy Model" to differentiate it from other alternative fate and transport models that have been described in this report.

Use of interpretations summarized in the 2014 Nez Perce report (EMDT-MO-0031) as a basis for this requested Ecology's Advocacy Model evaluation of vadose zone heterogeneities at WMA C is limited to the objectives of this analysis. Use of the information in the 2014 Nez Perce report as a basis for this requested evaluation does not constitute any endorsement or agreement by DOE with the Nez Perce interpretation of vadose zone heterogeneities at WMA C.

Because the interpreted results from the 2014 unpublished report (EMDT-MO-0031) by the Nez Perce was only available in the report tables, cross-sections, and maps, it could not be used directly in creating the numerical model. Furthermore, the 2014 Nez Perce report only presented interpretations of the presence of fine-grained units, without identifying the soil characteristics and hydraulic properties that would be associated with those layers. Consequently, the approach was to first develop a digital geologic model to represent the fine-grained thin layers interpreted at different boreholes and direct pushes provided in Table 1 of EMDT-MO-0031. The digital geologic information then was used to create a flow and transport model to represent the tank farm and the fine-grained units interpreted to exist in the vadose zone underlying the WMA C. Finally, it was necessary to assign hydraulic properties to the posited fine-grained layers. This was done by assuming that the layers were composed of fine-grained soils that exist on the Hanford Site, for which measured hydraulic parameters exist. The overall development of the

geologic and flow and transport models along with simulated results are described in detail in Appendix B of this document. A summary level discussion is provided below.

To accommodate the fine discretization requirements for the vadose zone and to reduce the computational demands, the models used in this evaluation were limited to two dimensions. This decision was made in consultation with Ecology and with understanding of the inherent limitations of simulating flow and transport in two dimensions. Given that the primary purpose of the modeling evaluation is to evaluate the effect of the fine-grained units on contaminant transport for a meaningful comparison with the results of the EHM model, a two-dimensional (2-D) version of the EHM model was also developed using the same finer discretization. The 2-D refined-grid cross-sectional model was developed to represent the fine-grained units (up to 15 units) identified in EMDT-MO-0031 is referred as the "FGU cross-sectional model," while the 2-D refined-grid version of the EHM cross-sectional model built for comparison is called the "EHM cross-sectional model." The FGU cross-sectional model is shown in Figure 5-11.

Figure 5-11. Depiction of Numerical Cross-Sectional Model of Fine-Grained Unit Alternative Conceptual Model.

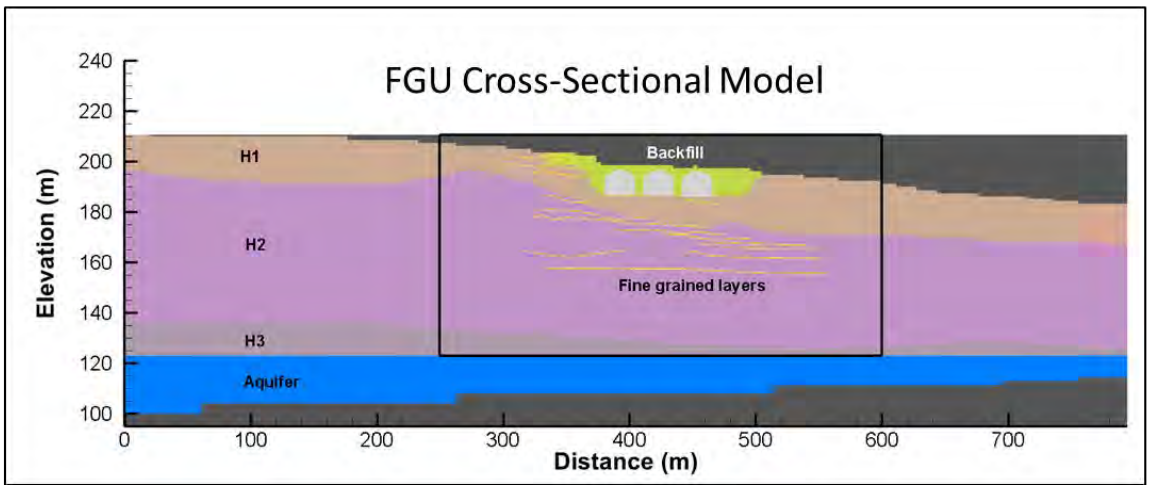

A primary case was defined to evaluate the results of the FGU cross-sectional model with results generated with the EHM cross-sectional model. A general contaminant source was simulated that approximated the timing, the volume, and the inventory of ^{99}Tc estimated for the tank C-105 leak. This specific past leak consisted of a 5-year release from 1963 to 1968 of a 20,500 gal waste volume containing ~10 Ci of ^{99}Tc to the upper part of the vadose zone between the tank 241-C-104 and tank C-105.

Figure 5-12 shows the rate of arrival of ^{99}Tc (mass flux) at the water table (Ci/yr) as a function of time for the EHM cross-sectional model and FGU cross-sectional model (with Hanford sandy silt [Hss] properties for the fine-grained units defined in Table B-1). Compared to the simulated breakthrough curve for the FGU cross-sectional model, the EHM cross-sectional model shows an earlier breakthrough to the water table and a higher peak mass flux. This difference is attributed to the presence of fine-grained units that cause slight delay in vertical movement along with small increase in lateral spreading in comparison to the EHM cross-sectional model. As a result,

contamination arrives later at the water table with a relatively attenuated peak in the FGU cross-sectional model.

Figure 5-13 compares the contaminant distribution in the vadose zone at different times. The relatively slower downward migration and the slight increase in lateral spreading caused by the presence of the fine-grained units in the FGU cross-sectional model can be seen in these plots.

Sensitivity Case 1 is a variation of the primary case where the hydraulic property for the fine-grained units is changed from Hss to sample 31A (see Table B-2 and Figure B-7 for details). Figure 5-14 compares the simulated mass flux at water table for ^{99}Tc. A lower peak flux and delayed arrival is seen for the sensitivity case compared to the primary case. Because of the higher unsaturated hydraulic conductivity of the fine-grained units for the sensitivity case, the ^{99}Tc plume displays more lateral spreading compared to the primary case as shown in Figure 5-15. This effect also results in a double peak in mass flux due to spreading of mass—the first peak is due to mass that moves primarily vertically while the second peak is from arrival of mass that is delayed due to lateral spreading. Figure 5-15 also shows that while the lateral spread of the plume is higher for the sensitivity case, the highest concentration zone has not moved appreciably.

Other sensitivity cases that were performed with these models are described in Appendix B. General observations from the range of simulation cases examined are as follows.

- The movement of the center of mass of the simulated plumes was generally vertically downward below the source for all simulations, including those that incorporated the alternative fine-grained units.

- All simulations that incorporated alternative heterogeneity produced additional plume spreading over what was produced in simulation using the EHM model(s). The spreading resulted in a broadening of the fringes of the plume, resulting in a wider region of low concentration, but lower peak concentrations associated with the center of mass of the plume.

- The EHM representation of the vadose zone generally produced higher peak mass flux and an earlier occurrence of peak fluxes at the water table compared to all analyses incorporating additional alternative interpretation of heterogeneity.

Figure 5-12. Primary Case Results for EHM Cross-Sectional Model and FGU Cross-Sectional Model Comparing Mass Flux Arriving at the Water Table.

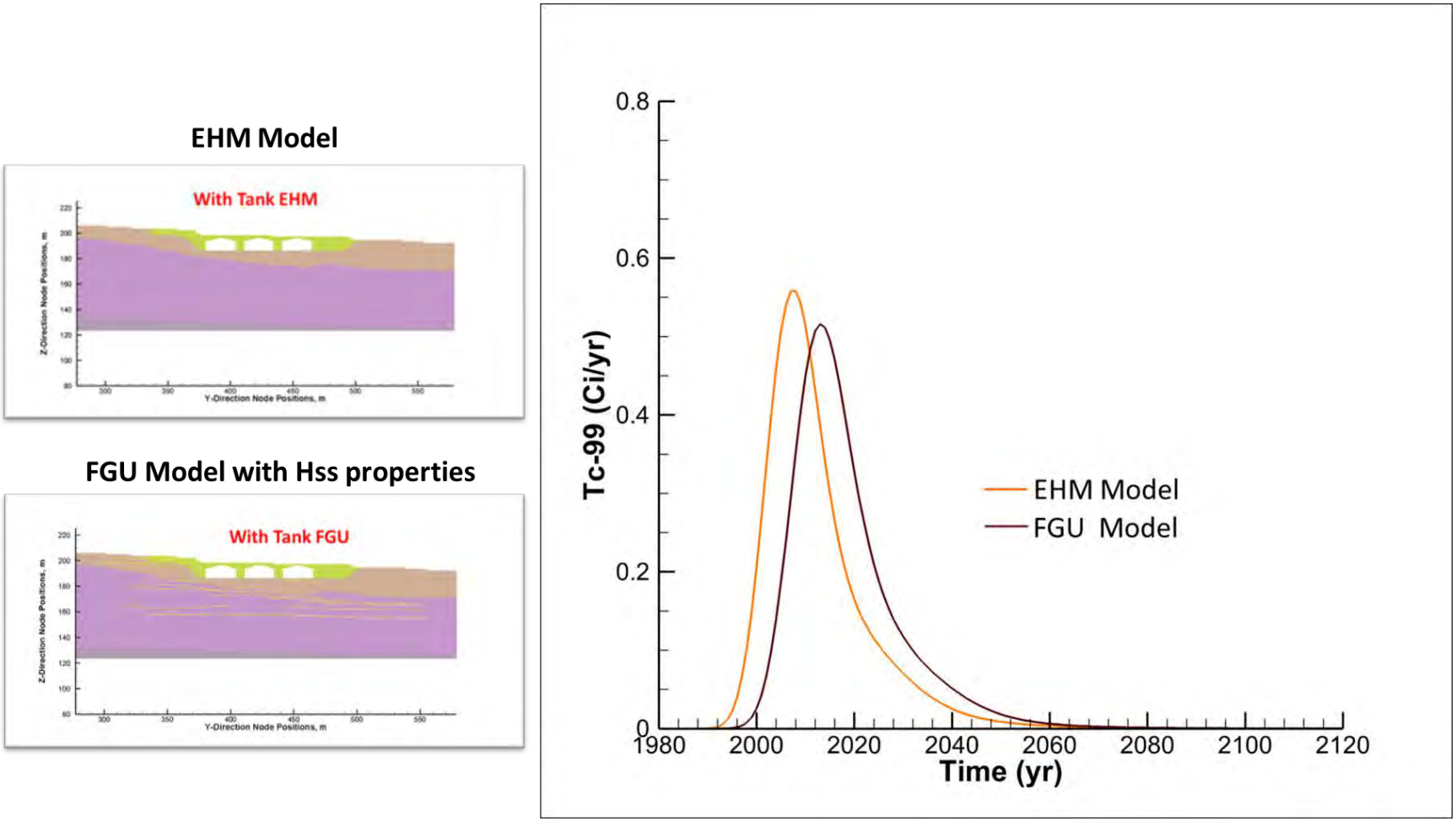

EHM = Equivalent Homogeneous Medium FGU = fine-grained units Hss = Hanford sandy silt (unit)

Figure 5-13. Comparison of Simulated (Primary Case) Technetium-99 Plume in the Vadose Zone in Year 1968 (First Row) and Year 1981 (Second Row) for EHM Cross-Sectional Model and FGU Cross-Sectional Model with Hss Hydraulic Properties for Fine-Grained Units.

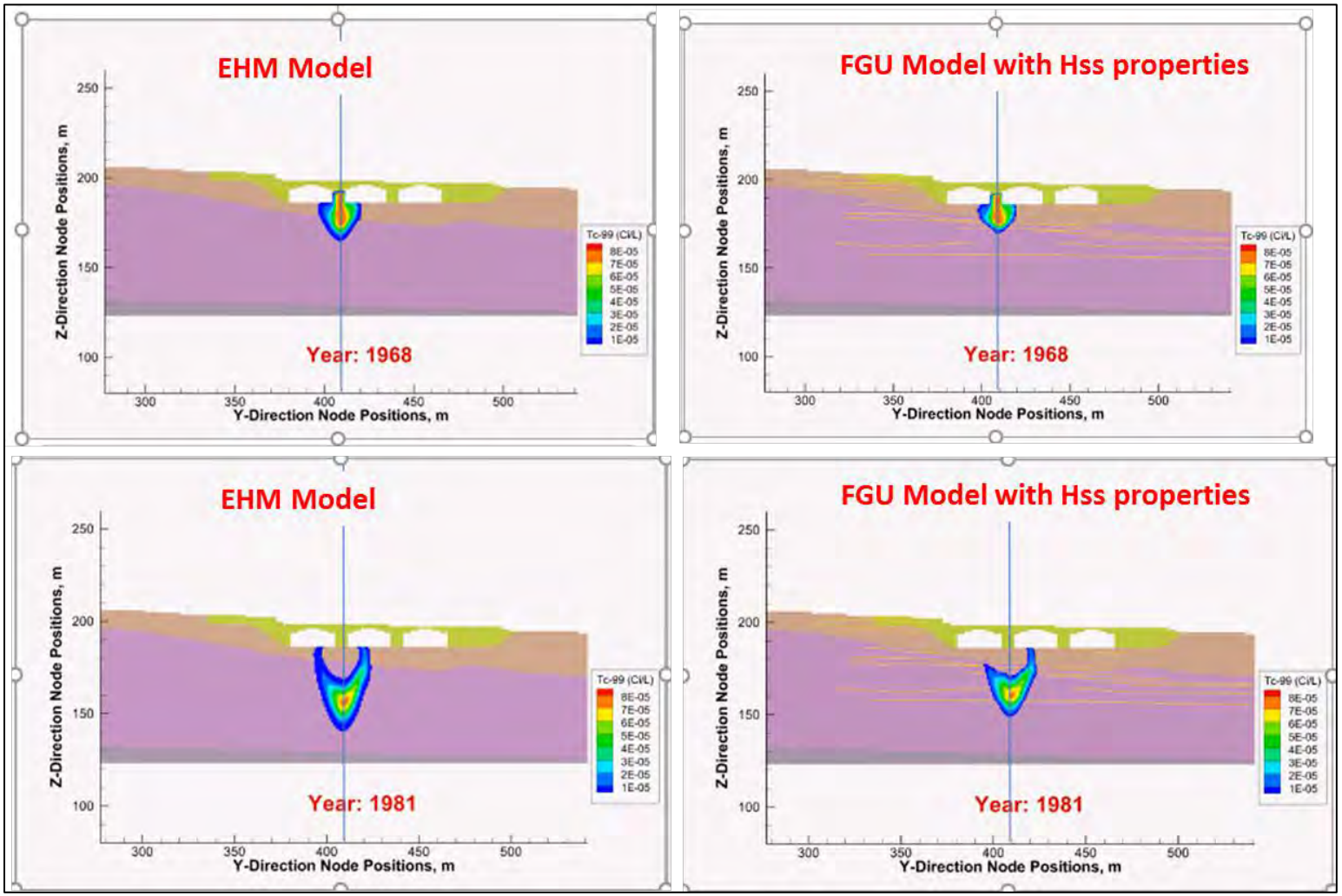

EHM = Equivalent Homogeneous Medium FGU = fine-grained units Hss = Hanford sandy silt (unit)

Figure 5-14. Mass Flux Arriving at Water Table Showing the Effect of Hss and 31A Hydraulic Properties Used for the Fine-Grained Units.

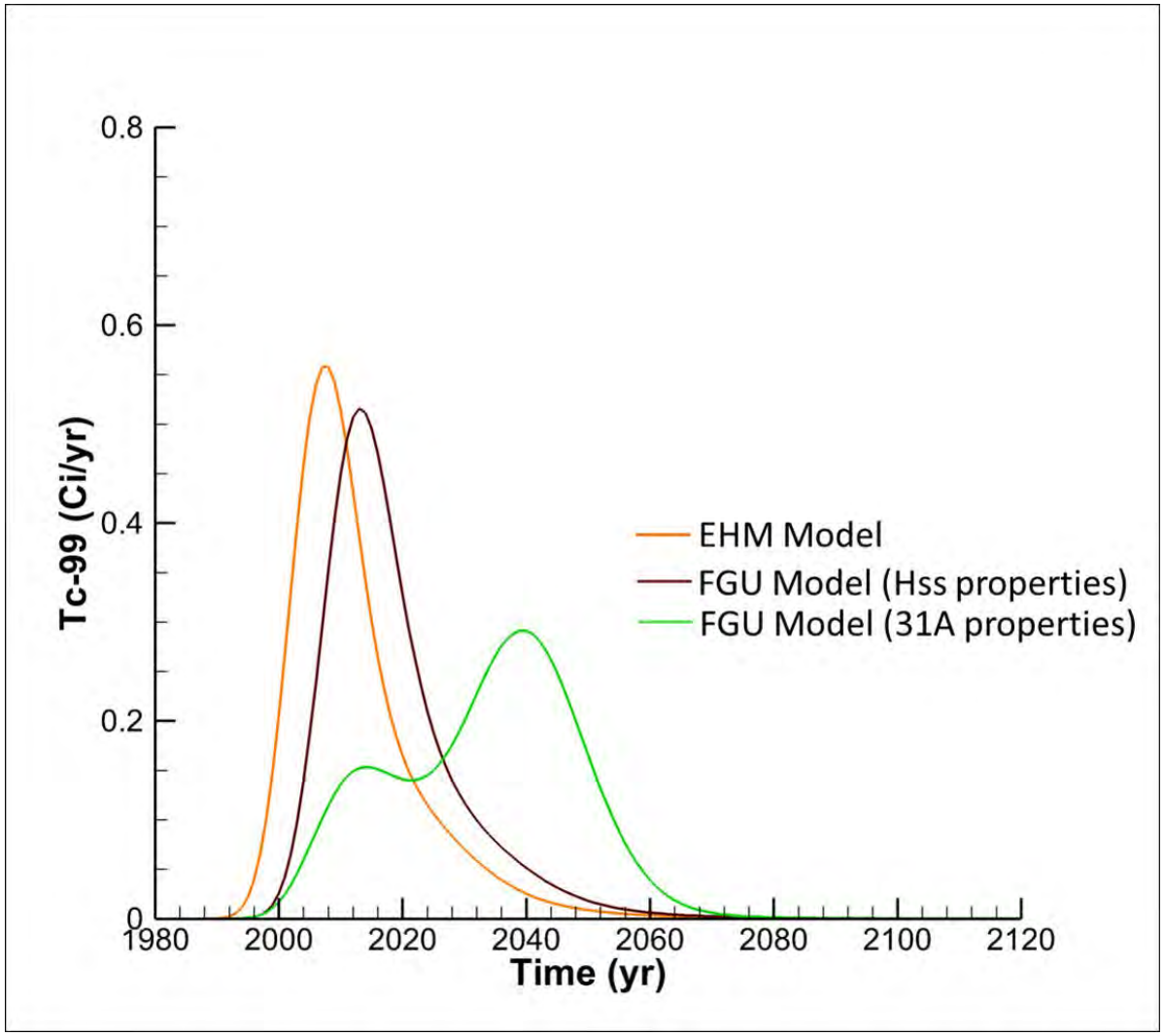

EHM = Equivalent Homogeneous Medium FGU = fine-grained units Hss = Hanford sandy silt (unit)

Figure 5-15. Comparison of Simulated Technetium-99 Plume in the Vadose Zone in Year 1971 (First Row) and Year 2001 (Second Row) using FGU Cross-Sectional Model for the Primary Case (Hss Hydraulic Properties for Fine-Grained Units) and Sensitivity Case 1 (Sample 31A Hydraulic Properties for Fine-Grained Units).

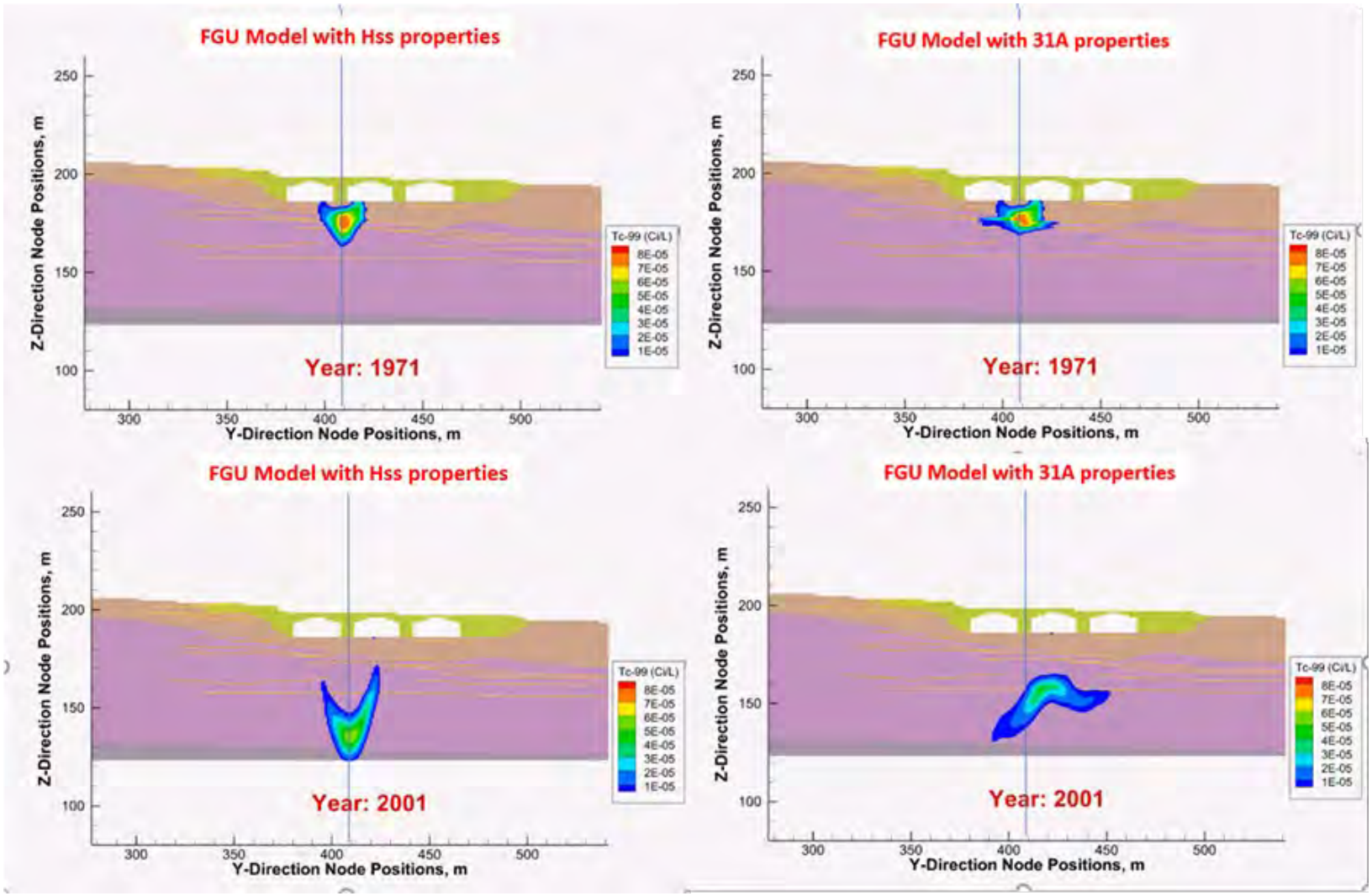

FGU = fine-grained units Hss = Hanford sandy silt (unit)

6.0 EVALUATION OF THE EFFECTS OF TRANSIENT WATER TABLE

In this section, results of a set of transient model cases of past leak behavior are presented. These transient model analysis cases represent the flow conditions in the unconfined aquifer that have existed at WMA C from its construction in 1944 to present day (Figures 2-10 and 2-11). The analysis is intended to provide insight into for the timing, size, and inventory of the past leaks, and the changing hydraulic conditions (i.e., hydraulic gradient [direction and magnitude]) responsible for producing the concentrations observed in the monitoring wells. Existing data do not provide a sufficient basis to determine a complete or definitive description of the orientation and magnitude of the hydraulic gradient during most of the operations period. The gradient appears to have shifted direction several times, and the timing of the shifts is highly uncertain, particularly after discharge to 216-B-3 (B Pond) ceased in 1994. Consequently, the model implements subjective interpretations of the gradient direction and magnitude between 1944 and 2020. The combination of the available but limited field data (especially sparse groundwater monitoring measurements made from 1944 through the early 1990s) and the model results provides a basis for developing model assumptions and determining bounded estimates of model input parameters. The transient evaluation also provides confidence that the model parameters and equations can adequately represent the physical conditions and past events of WMA C. This assurance improves the confidence in the model's ability to evaluate and estimate future impacts from the past leaks and other sources.

Two other clarifications about the analyses in this section:

- The purpose of Section 6 (and any subsection therein) is not to reconstruct the past water table conditions, but to simply evaluate possible conceptual models of past water table conditions as it may have fluctuated/shifted directions.

- A considerable amount of uncertainty in impacts to groundwater exists due to lack of active monitoring at WMA C prior to 1989. There is lack of information prior to 1989 to confirm or refute the extent of impact of past leaks from WMA C on the groundwater.

6.1 TRANSIENT MODEL DESCRIPTION AND IMPLEMENTATION

As discussed in Section 4, monitoring data for groundwater concentrations are believed to be significantly influenced by transient changes in the water table that have occurred between 1944 and today. In the scoping cases presented in Section 4, these transient effects were ignored, to focus on the representation of the leaks and the vadose zone, while avoiding the complications introduced by the changing water table. The model described in this section is intended to address the changing water table, and to produce a model that can be compared directly with the groundwater monitoring data. Other aspects of the model described in previous sections of this document remain the same.

The model is run from 1944 forward in time, with leaks introduced at the times and in the quantities presented in Table 3-1. The representation of the vadose zone is the same as Case 1 in Section 4 and is also run beginning in 1944 to produce the antecedent conditions for the leaks. During the time period between 1944 and 1981, data are unavailable for the groundwater levels at WMA C, and any changes that may have occurred during that time would not affect transport of contaminants in the vadose zone during that time. Although the first documented leak occurred in 1960, the groundwater monitoring results indicate that ^{99}Tc does not reach the water table until after 1981. Therefore, as a simplification and expedient for the model, water table fluctuations before 1981 are omitted from the model, and the period from 1944 to 1981 is simply simulated with the 1981 water table boundary conditions in the aquifer.

STOMP© required an impractical amount of time to solve the flow equations for the 1944 to 1960 time period. This was because of the introduction of the WMA C infrastructure and backfill material in the WMA C, the change in water recharge at the surface, and the variations in the water table boundary conditions. Thus, as a simplification and expedient for the model, the pre-Hanford steady-state conditioning inputs include the tank farm backfill and structures, but the inputs representing the operations period ignore water table fluctuations prior to 1981. Although the first documented leak occurred in 1960, the groundwater monitoring results indicate that ^{99}Tc does not reach the water table until after 1981, so the water table fluctuations before then are irrelevant. Therefore, the period from 1944 to 1981 is simply simulated with the 1981 water table boundary conditions in the aquifer. This assumption to ignore water table fluctuations prior to 1981 is further supported by groundwater monitoring measurements for ^{99}Tc and nitrate. Although both contaminants are reported in low levels in monitoring wells in the early 1990s, rising trends for these contaminants in WMA C wells were not observed until the late 1990s.

6.1.1 Central Plateau Groundwater Model

The initial basis of the flow conditions included in these analysis cases was derived from the CPGWM calibration results (CP-47631, Rev. 0) for the period of interest. The CPGWM provides calibrated output that approximates the water table during the operations period. The CPGWM represents the most recent culmination of understanding of the unconfined aquifer under the Central Plateau and, given the rigorous nature of the development effort, is deemed to be the most suitable for estimating and predicting flow.

The CPGWM represents the best current understanding of groundwater flow conditions under the Central Plateau. The CPGWM represents the product of ongoing development and continued improvement that began in fiscal year 2009 and has undergone several revisions (currently at Revision 6.3.3) to improve its performance with respect to calibration. CPGWM (Revision 6.3.3) takes account of the historical development of understanding of the unconfined aquifer, along with current interpretations of the geology (including the extent of the paleochannel beneath WMA C), and up-to-date measurements of the recovery of the water table from operational discharges (CP-47631). The CPGWM incorporates the large-scale geologic and hydrogeologic features, and provides estimates of water levels, hydraulic gradients, and

groundwater flows throughout the 200 West and 200 East Areas for past, current, and expected future groundwater conditions (CP-47631).

The CPGWM calibration places emphasis on matching water level data from the 1940s, early 1950s, and first decade of the 21st century to estimate hydraulic properties using flow conditions relatively unperturbed by site operations (CP-47631). The observed heads in wells located upgradient and downgradient of the WMA C and corresponding CPGWM-simulated heads, representing a time span of over 20 years, compare well as indicated in Figure 6-1, providing confidence in the estimative and predictive capabilities of the CPGWM.

6.1.2 Application of the Central Plateau Groundwater Model to Waste Management Area C

The CPGWM provides an estimate of the water table on an approximately annual basis for the operations period. The grid spacing of the CPGWM is 100 m by 100 m (328 ft by 328 ft), which is much coarser than the grid spacing used in the WMA C model, but provides adequate output to establish boundary conditions to the WMA C model for the operations period. Hydraulic head values calculated by the CPGWM are interpolated onto the boundary nodes of the WMA C model. Figure 6-2 shows an example of the alignment of the two grids and the values interpolated from the CPGWM representing the year 2000. Each WMA C model node is contained by the triangle formed by the three closest CPGWM nodes, and the value interpolated is the distance-weighted average of those three CPGWM node values. The figure also illustrates the difficulty in evaluating the hydraulic head and gradient in the area around WMA C. The difference between the maximum value (122.791) and minimum value (122.781) across the entire domain of the WMA C model domain is only 10 mm (0.39 in.). The interpolation repeats for each year between 1944 and 2040 that the CPGWM provides hydraulic head values. These boundary conditions provide the basis for the WMA C model's attempt to approximate the flow conditions during the time from 1944 to present day.

The boundary condition type, either prescribed head or prescribed flux, is defined according to the hydraulic head elevation along each boundary. Nine values representing the span of each boundary are averaged, and the average values rounded to three significant digits are ranked highest to lowest. Boundaries ranked 1 or 2 are designated as prescribed flux, and boundaries ranked 3 or 4 are designated as prescribed head. Figure 6-3 shows nodes used to calculate each boundary's average, the average values, and the ranking of the boundaries representing the year 2000. The overall simulation period is broken into discrete segments according to changes in the boundary condition types. Whenever a boundary condition changes from prescribed head to prescribed flux, or vice-versa, the existing segment ends and a new one begins. Table 6-1 shows the rankings segments for the period from 1944 to 2040.

The prescribed head boundary condition values are based on the interpolated values, converted to aqueous pressure. The calculation of the prescribed flux boundary condition values involves some intermediate steps. The flux for a particular node is calculated according to the gradient between the hydraulic head values of that node and the corresponding node on the opposite

boundary. For example, for any node located along the first column of nodes (i.e., i =1, j = 1, …, jmax), the flux is calculated according to the following equation:

$$q_{1,j} = -K_{sat}\left(\frac{h_{imax,j} - h_{1,j}}{737.9\ m}\right) \tag{6-1}$$

where $q_{1,j}$ is the flux at node j along the first column of nodes, K_{sat} is the aquifer hydraulic conductivity (m/yr), $h_{1,j}$ and $h_{max,j}$ are the hydraulic head values (m) at node j along the first and last columns of nodes, respectively, and 737.9 m (2420.9 ft) is the distance across the model domain from the first to the last column of nodes. To calculate flux at node j along the last column of nodes, the equation becomes

$$q_{imax,j} = -K_{sat}\left(\frac{h_{1,j} - h_{imax,j}}{737.9\ m}\right) \tag{6-2}$$

For fluxes along the first or last row of nodes, the equations become, respectively,

$$q_{i,1} = -K_{sat}\left(\frac{h_{i,jmax} - h_{i,1}}{795.3\ m}\right) \quad and \quad q_{i,jmax} = -K_{sat}\left(\frac{h_{i,1} - h_{i,jmax}}{795.3\ m}\right) \tag{6-3}$$

where the distance equals 795.3 m (2609.3 ft). If the flux equals a negative value, then the flux is assigned a value of 0.

Figure 6-1. Central Plateau Groundwater Model Calibration Results in the Vicinity of Waste Management Area C.

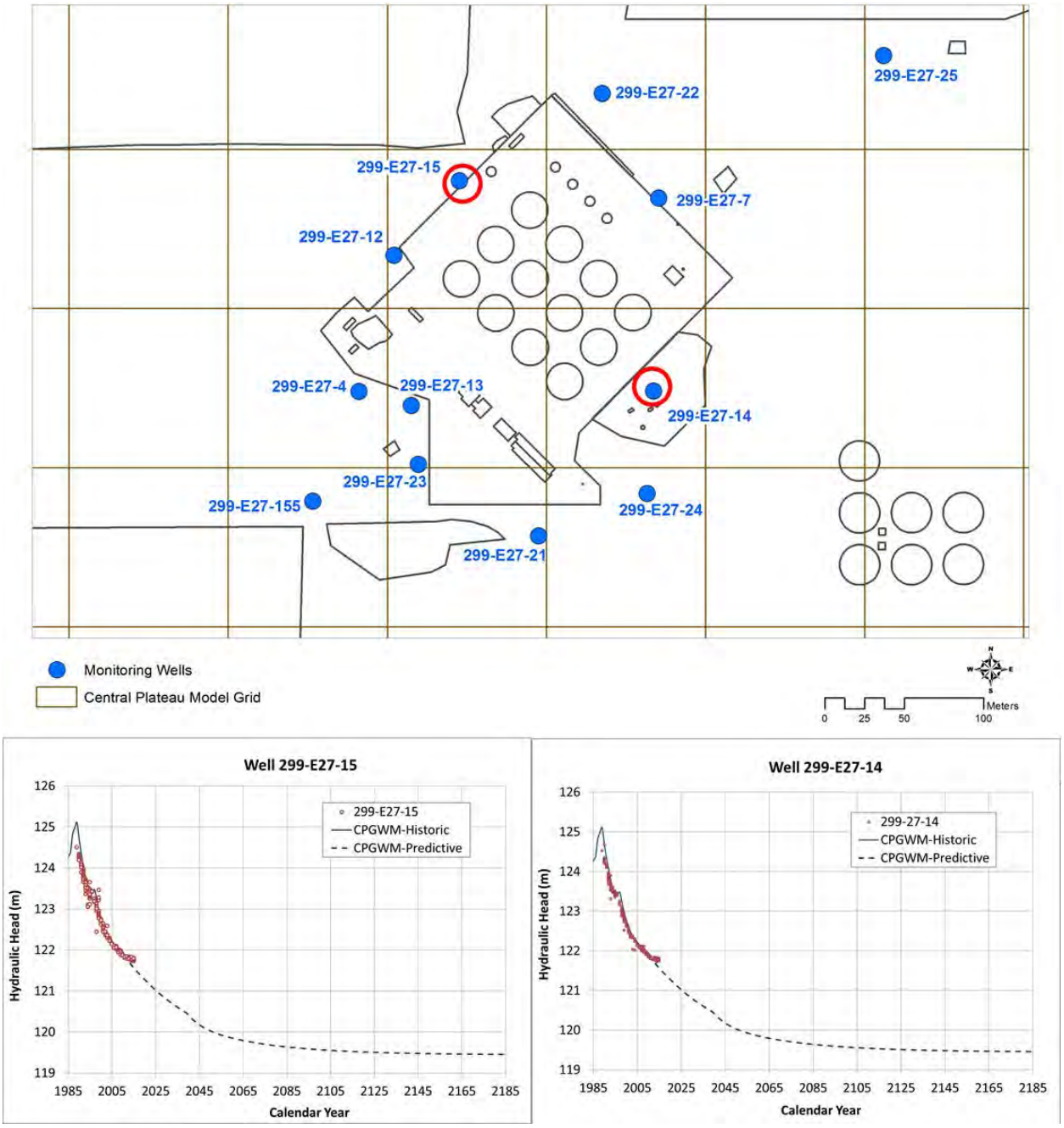

CPGWM = Central Plateau Groundwater Model

Figure 6-2. Alignment of the Central Plateau Groundwater Model and Waste Management Area C Unplanned Release Model Grids and Central Plateau Groundwater Model Hydraulic Head Interpolation Values Representing Calendar Year 2000 on a Triangular Mesh.

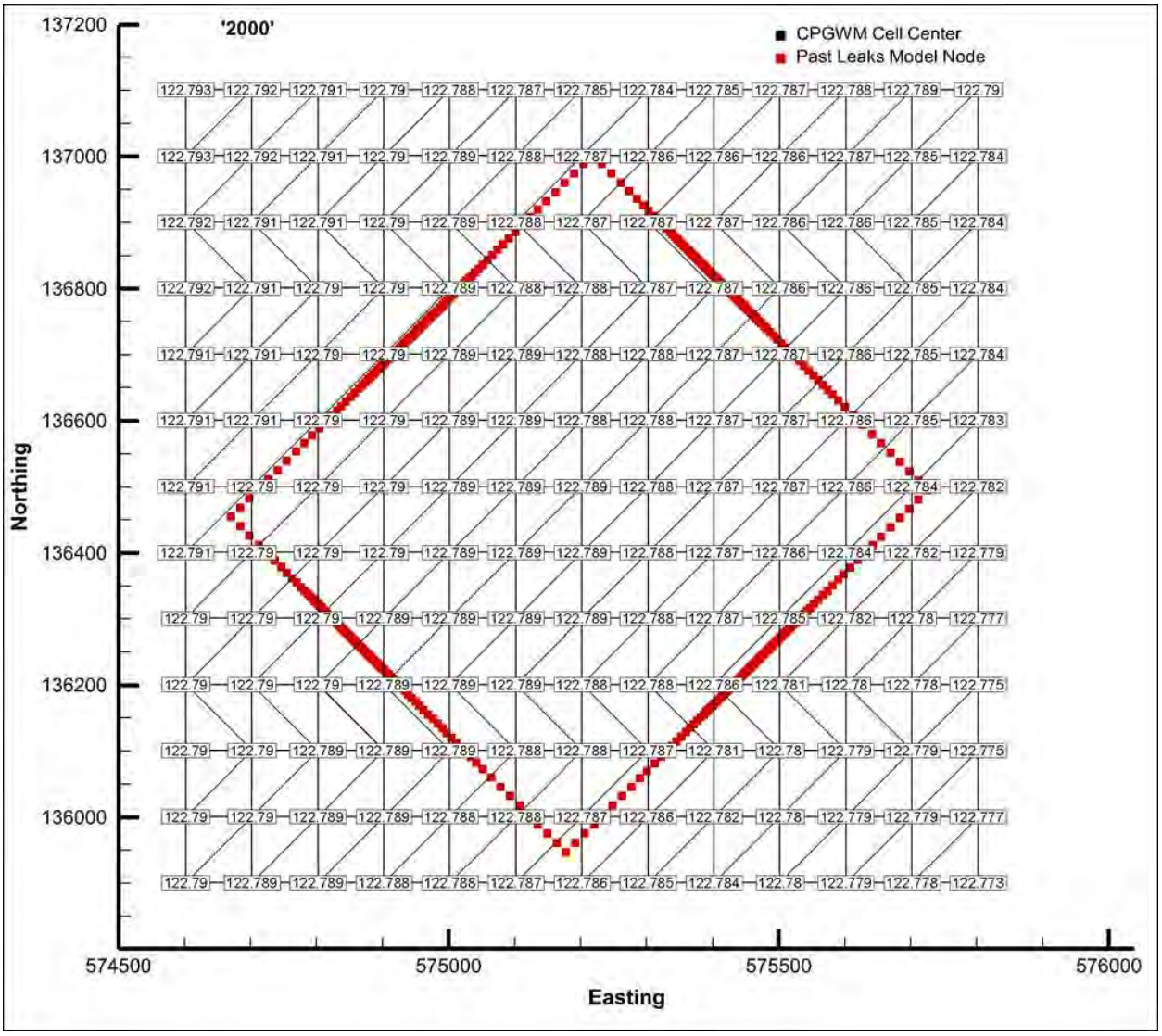

CPGWM = Central Plateau Groundwater Model

6.2 EVALUATION OF THE TRANSIENT WATER TABLE HYDRAULIC GRADIENT

The hydraulic gradient in the 200 East Area is very low and it is very difficult to measure its magnitude and direction accurately. Further compounding the problem of determining the magnitude and direction of the hydraulic gradient in the 200 East Area during the operations period is that the water table increased ~9 m (~30 ft) because of the volume of wastewater disposal occurring in the ponds near the 200 East Area (DOE/RL-2014-32). The presence of the

groundwater mounds also affected the direction of groundwater movement, having caused radial flow to occur from around the discharge areas while those facilities operated (Figure 6-4). Water levels have declined since the cessation of wastewater discharges to 216-B-3 (B Pond) and 216-A-25 (Gable Mountain Pond), but the water table remains ~2 to 3 m (~6.6 to 9.8 ft) the projected steady-state conditions (CP-47631). In the vicinity of WMA C, direction of groundwater flow and magnitude of the hydraulic gradient have been inferred from water-level measurements made around LLWMA-1, which is located ~2,300 m (~ 7,566 ft) northwest of WMA C (SGW-54165, *WMA C Quarterly October Through December 2015 Quarterly Groundwater Monitoring Report*).

Figure 6-3. Waste Management Area C Unplanned Release Model Grid Hydraulic Head Boundary Averaging Values Representing Calendar Year 2000.

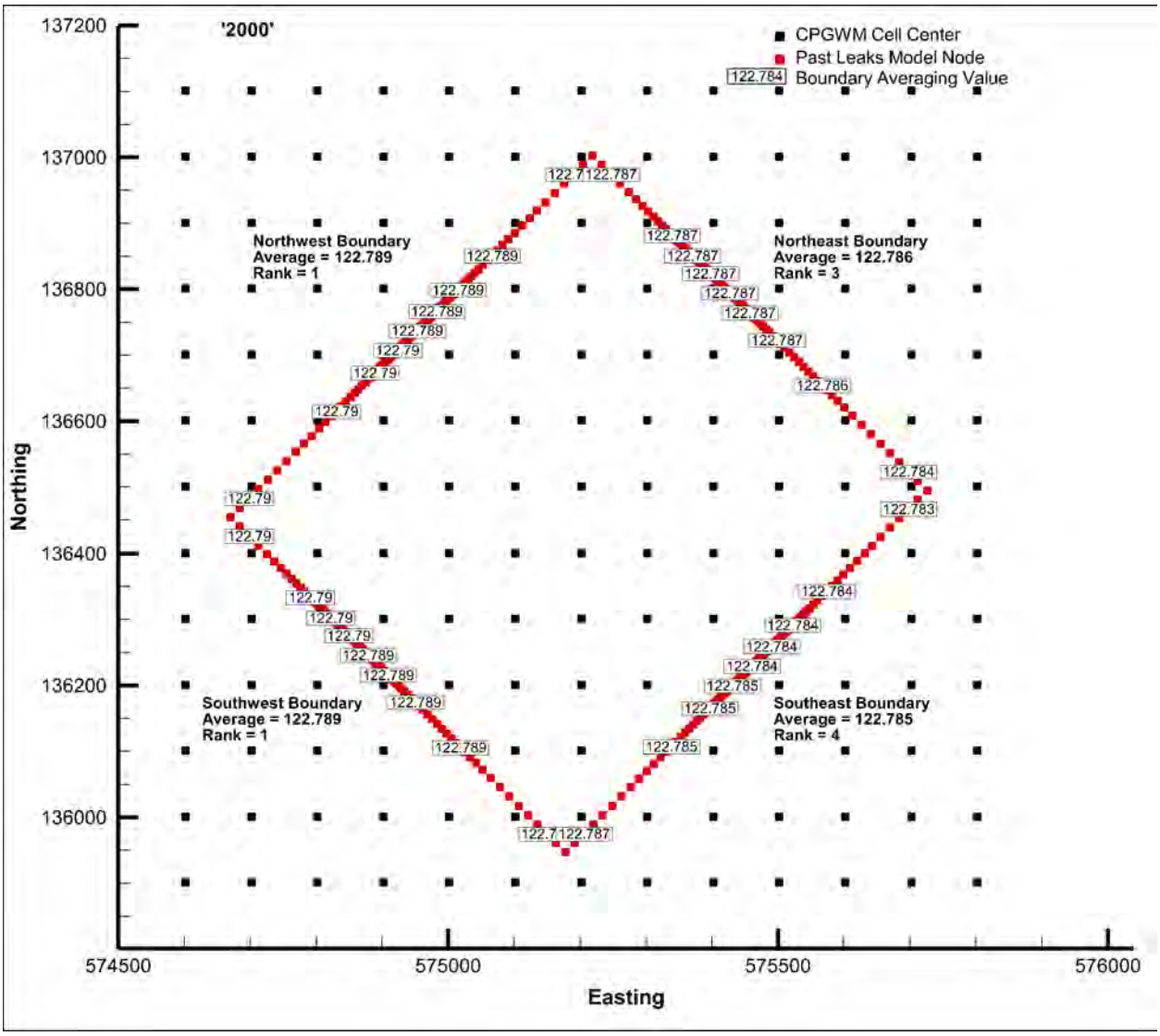

CPGWM = Central Plateau Groundwater Model

Table 6-1. Central Plateau Groundwater Model Hydraulic Head Interpolation Values and Waste Management Area C Unplanned Release Model Grid Boundary Rankings. (3 sheets)

Year	Interpolated Hydraulic Head (m)				Boundary Ranking			
	Southwest	Northwest	Southeast	Northeast	Southwest	Northwest	Southeast	Northeast
1969	125.018	125.026	125.017	125.029	3	2	4	1
1970	124.694	124.695	124.697	124.698	4	3	2	1
1971	124.609	124.615	124.608	124.616	3	2	4	1
1972	124.545	124.549	124.547	124.552	4	2	3	1
1973	124.326	124.326	124.332	124.331	4	3	1	2
1974	124.097	124.096	124.102	124.100	3	4	1	2
1975	123.945	123.946	123.949	123.948	4	3	1	2
1976	123.860	123.861	123.863	123.864	4	3	2	1
1977	123.827	123.830	123.827	123.831	4	2	3	1
1978	123.806	123.809	123.808	123.811	4	2	3	1
1979	123.820	123.822	123.823	123.825	4	3	2	1
1980	123.645	123.643	123.649	123.645	2	4	1	3
1981	123.649	123.650	123.653	123.654	4	3	2	1
1982	123.668	123.666	123.680	123.673	3	4	1	2
1983	123.779	123.783	123.785	123.788	4	3	2	1
1983.5	123.866	123.873	123.864	123.873	3	2	4	1
1984	124.002	124.010	123.998	124.010	3	2	4	1
1985	124.274	124.280	124.274	124.281	3	2	4	1
1986	124.367	124.370	124.368	124.372	4	2	3	1
1987	124.816	124.807	124.858	124.833	3	4	1	2
1988	124.983	124.971	125.029	125.000	3	4	1	2
1989	125.111	125.094	125.169	125.131	3	4	1	2
1990	124.701	124.687	124.738	124.706	3	4	1	2
1991	124.339	124.328	124.361	124.338	2	4	1	3

Table 6-1. Central Plateau Groundwater Model Hydraulic Head Interpolation Values and Waste Management Area C Unplanned Release Model Grid Boundary Rankings. (3 sheets)

Year	Interpolated Hydraulic Head (m)				Boundary Ranking			
	Southwest	Northwest	Southeast	Northeast	Southwest	Northwest	Southeast	Northeast
1992	124.062	124.051	124.082	124.059	2	4	1	3
1993	123.764	123.756	123.775	123.759	2	4	1	3
1994	123.566	123.559	123.574	123.561	2	4	1	3
1995	123.483	123.477	123.494	123.481	2	4	1	3
1996	123.416	123.412	123.424	123.415	2	4	1	3
1997	123.478	123.474	123.493	123.482	3	4	1	2
1998	123.234	123.231	123.239	123.232	2	4	1	3
1999	122.976	122.973	122.974	122.972	1	3	2	4
2000	122.789	122.789	122.785	122.786	2	1	4	3
2001	122.622	122.622	122.617	122.619	1	2	4	3
2002	122.472	122.472	122.466	122.468	2	1	4	3
2003	122.371	122.372	122.365	122.368	2	1	4	3
2004	122.304	122.304	122.298	122.301	2	1	4	3
2005	122.218	122.219	122.212	122.216	2	1	4	3
2006	122.145	122.147	122.138	122.144	2	1	4	3
2007	122.090	122.092	122.083	122.089	2	1	4	3
2008	122.048	122.050	122.040	122.046	2	1	4	3
2009	122.000	122.002	121.992	121.999	2	1	4	3
2010	121.948	121.950	121.940	121.947	2	1	4	3
2011	121.860	121.862	121.852	121.859	2	1	4	3
2012	121.790	121.793	121.781	121.789	2	1	4	3
2013	121.740	121.743	121.730	121.739	2	1	4	3
2015	121.625	121.628	121.614	121.624	2	1	4	3
2016.2	121.549	121.552	121.538	121.548	2	1	4	3

Table 6-1. Central Plateau Groundwater Model Hydraulic Head Interpolation Values and Waste Management Area C Unplanned Release Model Grid Boundary Rankings. (3 sheets)

Year	Interpolated Hydraulic Head (m)				Boundary Ranking			
	Southwest	Northwest	Southeast	Northeast	Southwest	Northwest	Southeast	Northeast
2017.4	121.477	121.481	121.467	121.477	2	1	4	3
2018.7	121.405	121.408	121.394	121.404	2	1	4	3
2020	121.330	121.334	121.320	121.330	2	1	4	3
2021.2	121.267	121.271	121.257	121.267	2	1	4	3
2022.4	121.201	121.205	121.191	121.201	2	1	4	3
2023.7	121.134	121.137	121.124	121.133	2	1	4	3
2025	121.066	121.070	121.056	121.066	2	1	4	3
2026.2	121.010	121.013	121.000	121.009	2	1	4	3
2027.4	120.952	120.955	120.942	120.951	2	1	4	3
2028.7	120.894	120.897	120.884	120.893	2	1	4	3
2030	120.836	120.839	120.826	120.835	2	1	4	3
2031.2	120.787	120.790	120.777	120.786	2	1	4	3
2032.4	120.737	120.740	120.727	120.737	2	1	4	3
2033.7	120.687	120.690	120.677	120.687	2	1	4	3
2035	120.637	120.640	120.627	120.637	2	1	4	3
2036.2	120.595	120.598	120.586	120.595	2	1	4	3
2037.4	120.552	120.555	120.543	120.552	2	1	4	3
2038.7	120.509	120.512	120.499	120.508	2	1	4	3
2040	120.465	120.469	120.456	120.465	2	1	4	3

Figure 6-4. Inferred Direction of Flow During the Operations Period When the High-Volume Discharge Facilities Operated.

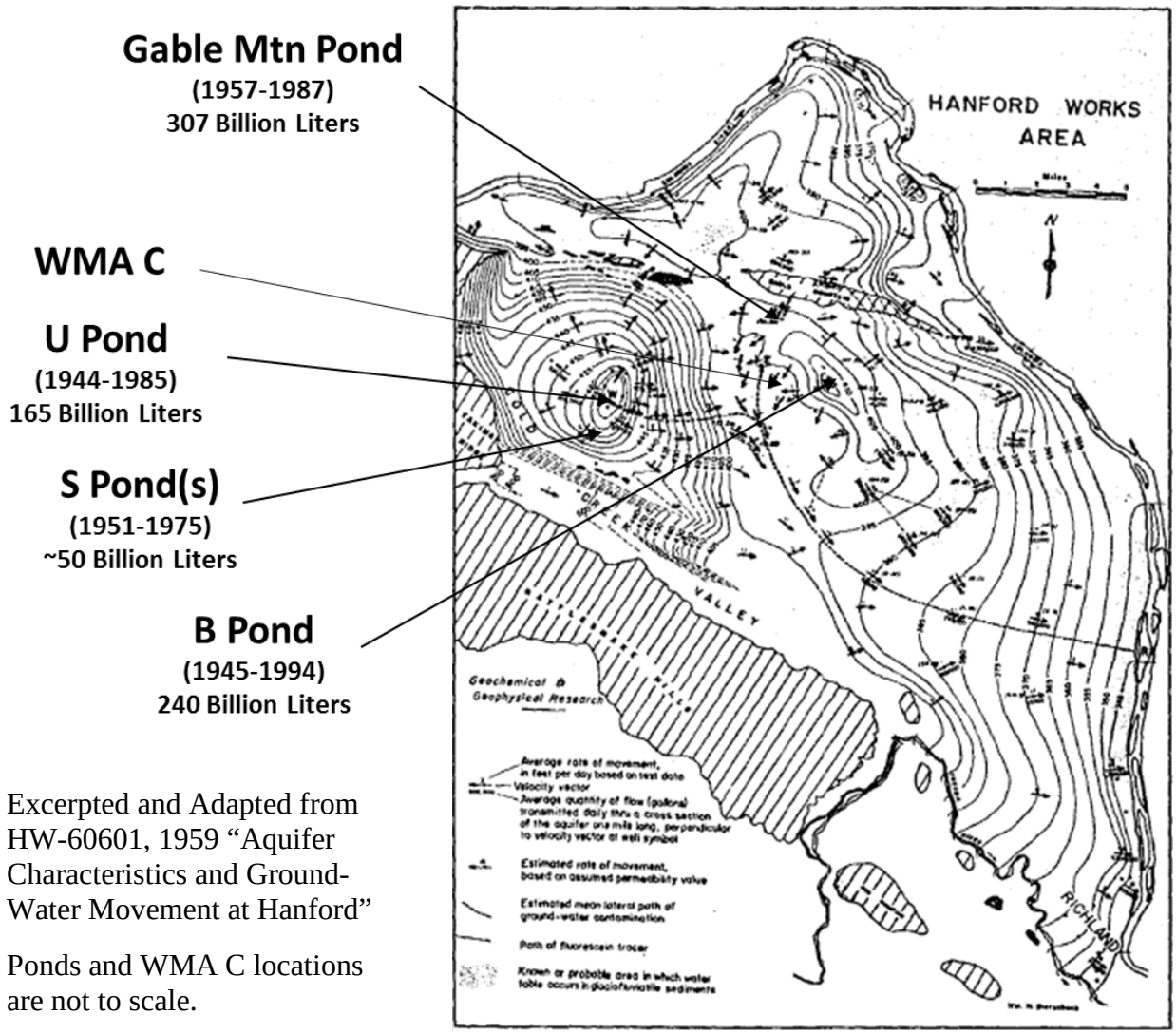

Excerpted and Adapted from HW-60601, 1959 "Aquifer Characteristics and Ground-Water Movement at Hanford"

Ponds and WMA C locations are not to scale.

WMA = Waste Management Area

Large seasonal changes in Columbia River stage and discharges to the TEDF, located 3 km (1.9 mi) east of the 200 East Area, also appear to affect water levels within the highly transmissive paleochannel beneath WMA C (SGW-54165). For example, the hydraulic gradient aligned toward the north-northwest between September 2005 and January 2007, but during August and September 2008 the hydraulic gradient temporarily reversed toward the south, presumably because of the high Columbia River stage during the summer of 2008 (SGW-54165). From October 2008 through June 2011, the hydraulic gradient remained indeterminate, although the flow appeared to reverse slowly back to a north. Beginning in the summer of 2011, the hydraulic gradient direction reversed again and remained toward the south through the end of September 2012 (SGW-54165). During the time between 2005 and 2012, the magnitude of the gradient remained less than 5×10^{-5} m/m. Since 2012, the gradient appears to have acquired a relatively stable south-southeastern direction with a magnitude of ~ 2×10^{-5} m/m.

During the times when the gradient reverses direction, both the magnitude and direction become indeterminate and how the direction reverses, either in a clockwise or counterclockwise manner, is unknown. To address uncertainty in the gradient reversal, the UPR evaluation includes conceptual models of both rotation directions. The boundary conditions adapted directly from the CPGWM (Table 6-1) indicate that the gradient rotates clockwise from the northwest to the southeast. The UPR evaluation implementing a counterclockwise from the northwest to the southeast modifies the boundary conditions by imposing an assumed rotation and magnitude to the gradient between 1999 and 2015 (Table 6-2). The average hydraulic head of the four interpolated boundaries (Figure 6-1) is then projected to the four boundaries according to the assumed gradient, and the new boundary values are ranked (Figure 6-3) from the highest water table elevation (1) to the lowest water table elevation (4). The ranking indicates direction of groundwater flow across WMA C for that particular year.

6.3 RESULTS OF SELECTED TRANSIENT WATER TABLE MODELS

The groundwater monitoring data may be interpreted as being the result of changes in flow direction and magnitude during the operations period. By introducing assumptions into the model that reproduce these trends, the model can produce insights as to the timing, magnitude, and orientation of the flow changes. The results also provide a basis to evaluate the estimates regarding inventory and volumes of past leaks for the purpose of better constraining estimates of the existing contamination. These aspects of the modeling analysis help provide some insight into the events and hydraulic conditions responsible for producing the measured concentrations levels and observed changes in the individual wells (e.g., locations and timing of source releases, the timing of changes in flow direction, and the varying magnitude of the hydraulic gradient during the gradual changes in flow directions).

The results of the modeling provide a basis to evaluate the assumptions and uncertainties associated with the flow direction and magnitude during the operations period. The results also provide a basis to evaluate the estimates regarding inventory and volumes of past leaks for the purpose of better constraining estimates of the existing contamination. These aspects of the modeling analysis help provide some insight into the events and hydraulic conditions responsible for producing the measured concentrations levels and observed changes in the individual wells (e.g., locations and timing of source releases, the timing of changes in flow direction, and the varying magnitude of the hydraulic gradient during the gradual changes in flow directions).

6.3.1 Results of the Assumed Clockwise Rotation of the Transient Hydraulic Gradient Model

The CPGWM boundary conditions (Figure 6-1) and specified inputs with of the clockwise gradient rotation simulation result in the gradient reversing direction rather abruptly between 1998 and 2002, as indicated by the ranking numbers. Figure 6-5 shows the model results of the plume development using the CPGWM boundary conditions and associated changes in groundwater flow conditions as it evolves in the aquifer from 1998 to 2005. According to the figures, the plume appears to be headed in a northwestern direction in 1998, and the direction

rotates clockwise to the southeast by 2002. The model results involving this manner of gradient rotation do not match the observed concentrations of ^{99}Tc in the monitoring wells surrounding WMA C. Although the modeling results of the timing of the peak concentration at well 299-E27-7 coincide with the timing of the peak concentration observed in the monitoring data, the magnitude of the peak concentration values differ by an order of magnitude (Figure 6-6).

The monitoring data indicate that ^{99}Tc arrived southwest of the tank farm in wells 299-E27-4, 299-E27-13, and 299-E27-23 around 2000, first reaching a peak concentration in well 299-E27-4 by 2004, and then reaching peak concentrations in the other two wells around 2011 and 2012. The modeling results representing these wells exhibit little response to the ^{99}Tc releases (Figure 6-6). This lack of response is a likely consequence of the rapid change and almost complete reversal in the direction of the gradient between 1998 and 2000 included in the CPGWM-based boundary conditions (Figure 6-2). According to the CPGWM boundary conditions, the gradient switches direction by almost 180 degrees almost immediately and does not become oriented toward the southwest. None of the results representing the three wells exceeds 150 pCi/L until after 2020 in the simulations. This is almost two orders of magnitude less than the peak concentrations measured in the three wells (Figure 6-6).

The modeling results representing the three wells south and southeast of the tank farm, 299-E27-21, 299-E27-24, and 299-E27-14, do not fit the monitoring data very well. The modeling results indicate that ^{99}Tc arrives in well 299-E27-14 in 2000, and that the concentration jumps to 9,000 pCi/L almost immediately (Figure 6-7). The concentration increases to a peak value of 14,200 pCi/L in 2011 and remains relatively stable at that level thereafter. The monitoring data indicate that the concentration in the well measured around 100 pCi/L as early as 1991 when sampling and analysis for ^{99}Tc began at the well. From 1997 to 2003, the concentration increased from 100 pCi/L to 2,600 pCi/L. The concentration remained relatively stable at that level until 2012 when it began increasing and reached its peak value of 10,700 pCi/L in 2013. The concentration has steadily declined since then, measuring 2,620 pCi/L in 2016. While the peak concentration of the modeling results is comparable to the peak measured value, the trend exhibited by the modeling results does not agree with the trend observed in the monitoring data. The modeling results representing wells 299-E27-21 and 299-E27-24 also do not agree with the monitoring data. Concentrations in excess of 25,000 pCi/L and 5,000 pCi/L have been measured in those wells, but the modeling results for the wells are each more than an order of magnitude less than the measured values. Because sampling did not begin in the wells until 2003 and 2010, respectively, it is difficult to evaluate the timing of arrival. Overall, the comparison of the simulated concentrations at the locations in the model representing the monitoring wells and the data collected from the monitoring wells do not corroborate the clockwise conceptualization of the gradient movement.

Table 6-2. Comparison of Central Plateau Groundwater Model Hydraulic Gradient Results (Magnitude and Direction) and Central Plateau Groundwater Model Results Modified to Rotate the Hydraulic Gradient Counterclockwise at Waste Management Area C.

Year			Interpolated Hydraulic Gradient (m)		
	Central Plateau Groundwater Model		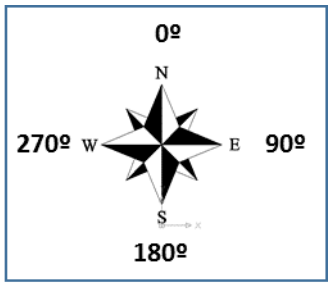	Modified Central Plateau Groundwater Model	
	Magnitude	Degrees Clockwise from North		Magnitude	Degrees Clockwise from North
1996	1.6E-05	319		1.6E-05	319
1997	2.6E-05	304		2.6E-05	304
1998	1.1E-05	328		1.1E-05	328
1999	5.2E-06	30		5.1E-06	33
2000	6.6E-06	100		3.5E-06	31
2001	7.8E-06	106		1.7E-06	29
2002	9.6E-06	103		0	27
2003	1.0E-05	113		0	327
2004	9.0E-06	110		1.7E-06	267
2005	9.8E-06	120		3.5E-06	262
2006	1.2E-05	129		5.2E-06	257
2007	1.2E-05	129		5.1E-06	252
2008	1.4E-05	124		5.1E-06	247
2009	1.4E-05	130		5.3E-06	242
2010	1.4E-05	130		5.1E-06	236
2011	1.4E-05	130		5.2E-06	230
2012	1.6E-05	131		5.3E-06	224
2013	1.8E-05	131		5.2E-06	184
2015	1.9E-05	131		5.1E-06	144

Table 6-3. Central Plateau Groundwater Model Hydraulic Head Interpolation Values Modified to Rotate the Hydraulic Gradient Counterclockwise at Waste Management Area C, and Revised Model Grid Boundary Rankings.

Year	Interpolated Hydraulic Head (m)				Boundary Ranking			
	Southwest	Northwest	Southeast	Northeast	Southwest	Northwest	Southeast	Northeast
1999	122.976	122.973	122.974	122.972	1	3	2	4
2000	122.789	122.787	122.788	122.786	1	3	2	4
2001	122.62	122.62	122.62	122.619	1	3	2	4
2002	122.469	122.469	122.469	122.469	1	1	1	1
2003	122.369	122.369	122.369	122.369	1	1	1	1
2004	122.301	122.301	122.302	122.302	4	3	2	1
2005	122.215	122.216	122.217	122.217	4	3	2	1
2006	122.142	122.143	122.145	122.145	4	3	2	1
2007	122.087	122.088	122.09	122.091	4	3	2	1
2008	122.044	122.045	122.047	122.048	4	3	2	1
2009	121.996	121.998	121.999	122	4	3	2	1
2010	121.944	121.946	121.946	121.948	4	3	2	1
2011	121.856	121.858	121.858	121.86	4	3	2	1
2012	121.786	121.788	121.788	121.79	4	2	3	1
2013	121.736	121.739	121.737	121.739	4	2	3	1
2015	121.622	121.625	121.621	121.623	3	1	4	2

6.3.2 Results of the Assumed Counter-Clockwise Rotation of the Transient Hydraulic Gradient Model

The results of the simulation with the revised boundary conditions indicating gradient changing in a counterclockwise motion corroborate much better with the data collected from the monitoring wells than did the results of the initial simulation. Figure 6-8 shows the model results of the plume as it evolves in the aquifer from 1998 to 2016. The simulated concentrations at the locations in the model representing the monitoring wells appear to coincide reasonably well in both timing and magnitude with data collected from the monitoring wells (Figures 6-9 and 6-10).

The modeling results of the timing of the peak concentration at well 299-E27-7 coincide with the timing of the peak concentration observed in the monitoring data, and the magnitude of the peak concentration values differ by less than a factor of 2 (Figure 6-8). The modeling results representing well 299-E27-15 are more problematic and less consistent with the measured data.

The modeled concentration exhibits three distinct peaks in response to the ^{99}Tc releases, and the modeled peak value exceeds the maximum measured value by approximately an order of magnitude. This well is located upgradient of WMA C relative to the long-term groundwater hydraulic gradient. The imposed rotation appears to include more of an upgradient component than the data indicate existed during the late 1990s and middle 2000s, but this discrepancy appears to be relatively minor compared to the overall performance of the model in representing the data collected from the other monitoring wells.

The modeling results approximate reasonably well the timing of arrival and magnitude of concentration of the ^{99}Tc in groundwater southwest of the tank farm (Figure 6-8). The modeling results indicate a peak concentration occurring in 2006 at well 299-E27-4, where the data reach their peak in 2004. The magnitude of the modeled and measured peak values are nearly identical. The model results indicate the peak concentration occurred in well 299-E27-13 about five years before the data reach their peak in that well, but the magnitude of the modeled and measured peak values differs by less than 50 percent. The magnitude of the modeled and measured peak values of well 299-E27-23 are very comparable, 31,000 pCi/L and 26,000 pCi/L, respectively, with the modeled peak arriving in the well about one year before the data indicate the peak arrived. Similarly, the magnitude of the modeled and measured peak values of well 299-E27-21 are comparable, 19,600 pCi/L and 26,700 pCi/L, respectively, although the concentration present in well 299-E27-21 may not yet have reached a peak. The model indicates that the peak occurred in 2014, but the data continue to increase in concentration from that time to present day.

The modeling results representing the arrival of the peak concentration of ^{99}Tc in wells 299-E27-24 and 299-E27-14 appear to lag the actual peak arrival by a few years (Figure 6-9). The modeling results indicate that ^{99}Tc concentration peaked in well 299-E27-24 in late 2015, whereas the monitoring data peaked in 2013. The modeling results indicate that ^{99}Tc concentration will not peak in well 299-E27-14 until late 2016, but the monitoring data peaked in 2013. The magnitude of the modeled concentration levels and measured peak concentration values observed at these wells differs but are within the same order of magnitude. This difference is less than 50 percent for well 299-E27-14, and the modeled peak value for well 299-E27-24 is within a factor of 3 of the measured peak in that well.

It is useful to put the comparisons between model and data in Figures 6-9 and 6-10 in perspective. The model and its input parameters were developed almost wholly from inputs independent of groundwater data. All these inputs have large amounts of uncertainty in them, with the model implementation containing best estimates from within that uncertainty. These inputs include the structure of the model, the timing and magnitude of the leaks, the stratigraphy of the vadose zone and the parameters needed to represent flow through it. There was no calibration of any of these inputs with the groundwater data; the model was solely run as a forward calculation. To take account of the temporally varying aquifer gradient, reasonable estimates were used for the timing, magnitude, and initial and final orientations of the gradient. The transition of the orientation was represented by a rather simplistic counterclockwise rotation of a flat surface. No attempt was made to optimize these assumptions about the gradient to improve the match between the model and data.

Figure 6-5. Simulated Technetium-99 Plume in Groundwater Calendar Years 1998, 2000, 2002, 2005, 2010 and 2016 and Resulting from Waste Management Area C Unplanned Releases (Clockwise Rotation of the Hydraulic Gradient Based on Central Plateau Groundwater Model Boundary Conditions).

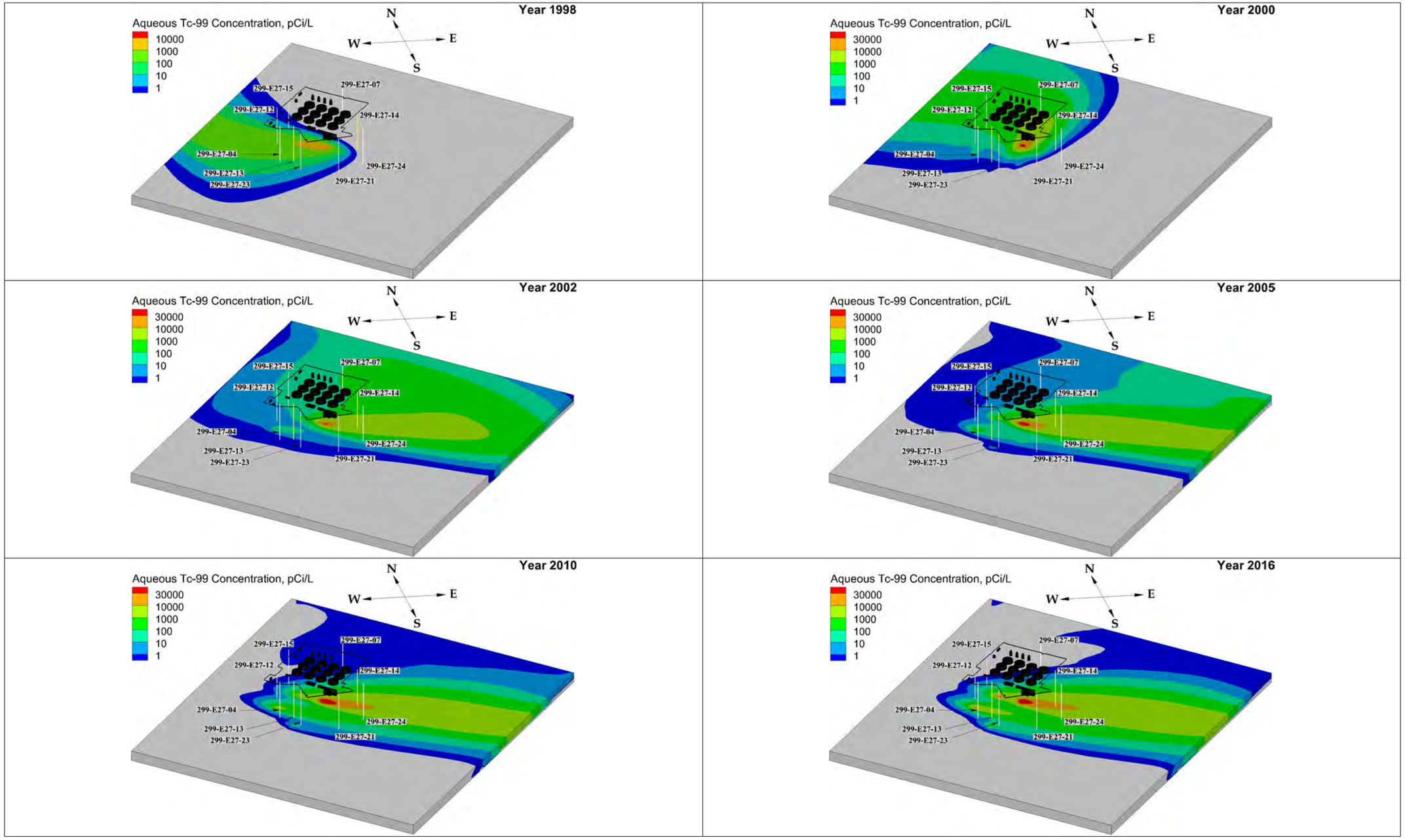

Given these observations about the model, and the amount of uncertainty surrounding many of the inputs, the matches between model and data shown in Figures 6-9 and 6-10 are surprisingly good. The model matched the peak ^{99}Tc concentrations and timing of the peaks in several key wells. Furthermore, from a qualitative perspective, the model reproduced the rapid decline in concentration in well 299-E27-23, and the rapid increase in concentration in well 299-E27-21. As shown in Section 4, these rapid changes in ^{99}Tc concentration were not well described using a static water table. Where the model deviates from data, a likely cause may be found in the many uncertainties about the leaks including leak timing, magnitude, and composition. A second potential cause of deviations between the model and data may be that the aquifer transition may have been considerably more complex than the simplistic rotation used here; such complexity could cause contamination to show up at times and locations not represented in the model.

These observations suggest that the general conceptual model (i.e., the leaks, their transport through the vadose zone, and their subsequent distribution in the aquifer by a temporally changing gradient) is consistent with the groundwater monitoring data. This is not to suggest that this model is the only model that could explain the groundwater monitoring data. However, any alternative conceptual model would need to produce similar or better fidelity relative to the groundwater monitoring data to be considered credible. This is also not to suggest that the fit between the model and groundwater monitoring data is optimized; by modifying some assumptions in the model, it is likely that a better fit could be produced.

Figure 6-6. Comparison of Simulated Technetium-99 Concentrations in Groundwater to Measured Concentrations around the Northeast, Northwest, and Southwest of Waste Management Area C.

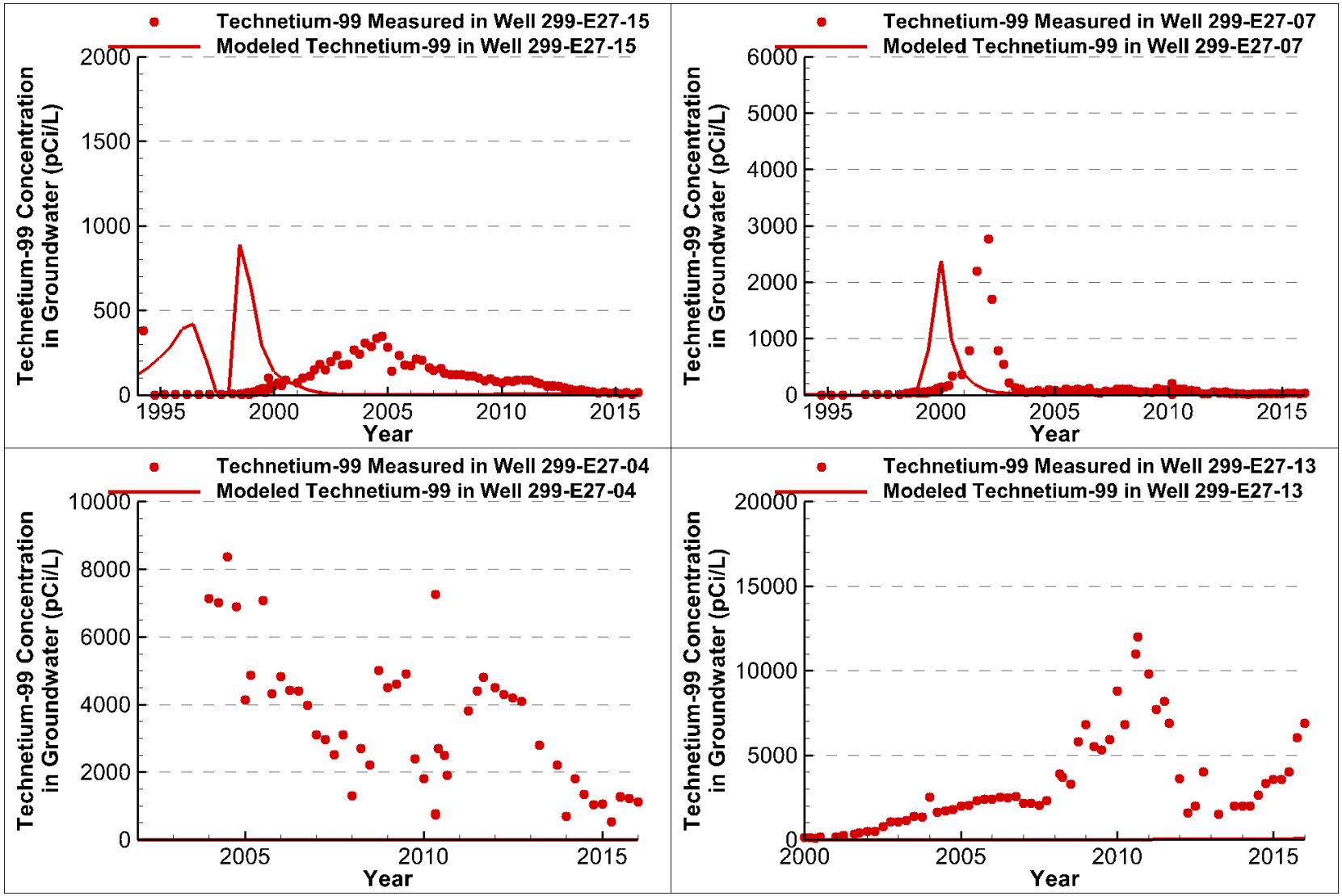

Note: This figure uses the Initial Conceptual Model with Clockwise Rotation of the Hydraulic Gradient.

Figure 6-7. Comparison of Simulated Technetium-99 Concentrations in Groundwater to Measured Concentrations around the Southwest and Southeast of Waste Management Area C.

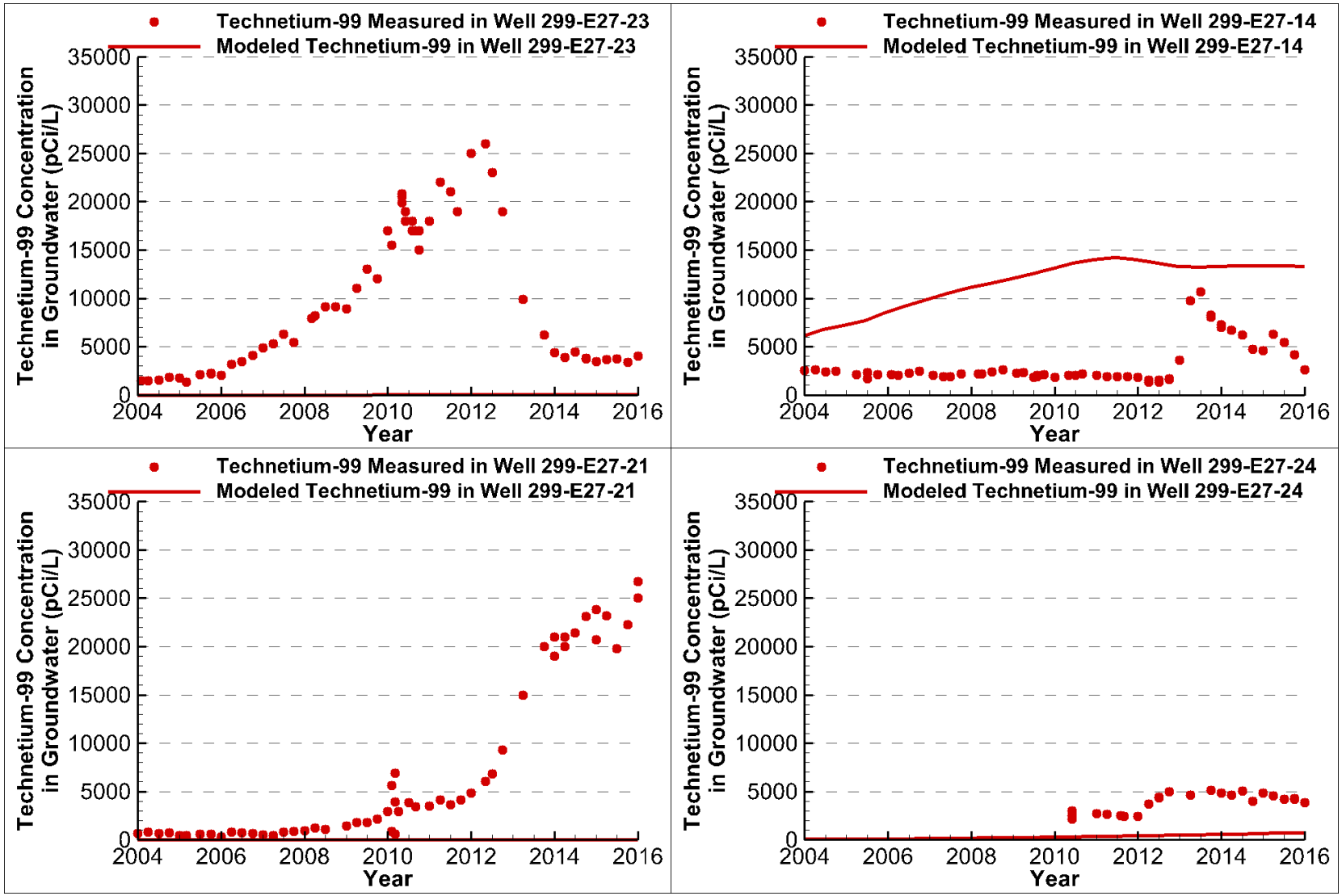

Note: This figure uses the Initial Conceptual Model with Clockwise Rotation of the Hydraulic Gradient.

6-21

RPP-RPT-59197, Rev. 2

This page is intentionally left blank.

Figure 6-8. Simulated Technetium-99 Plume in Groundwater Calendar Years 1998, 2002, 2004, 2008, 2012 and 2016 and Resulting from Waste Management Area C Unplanned Releases (Counterclockwise Rotation of the Hydraulic Gradient).

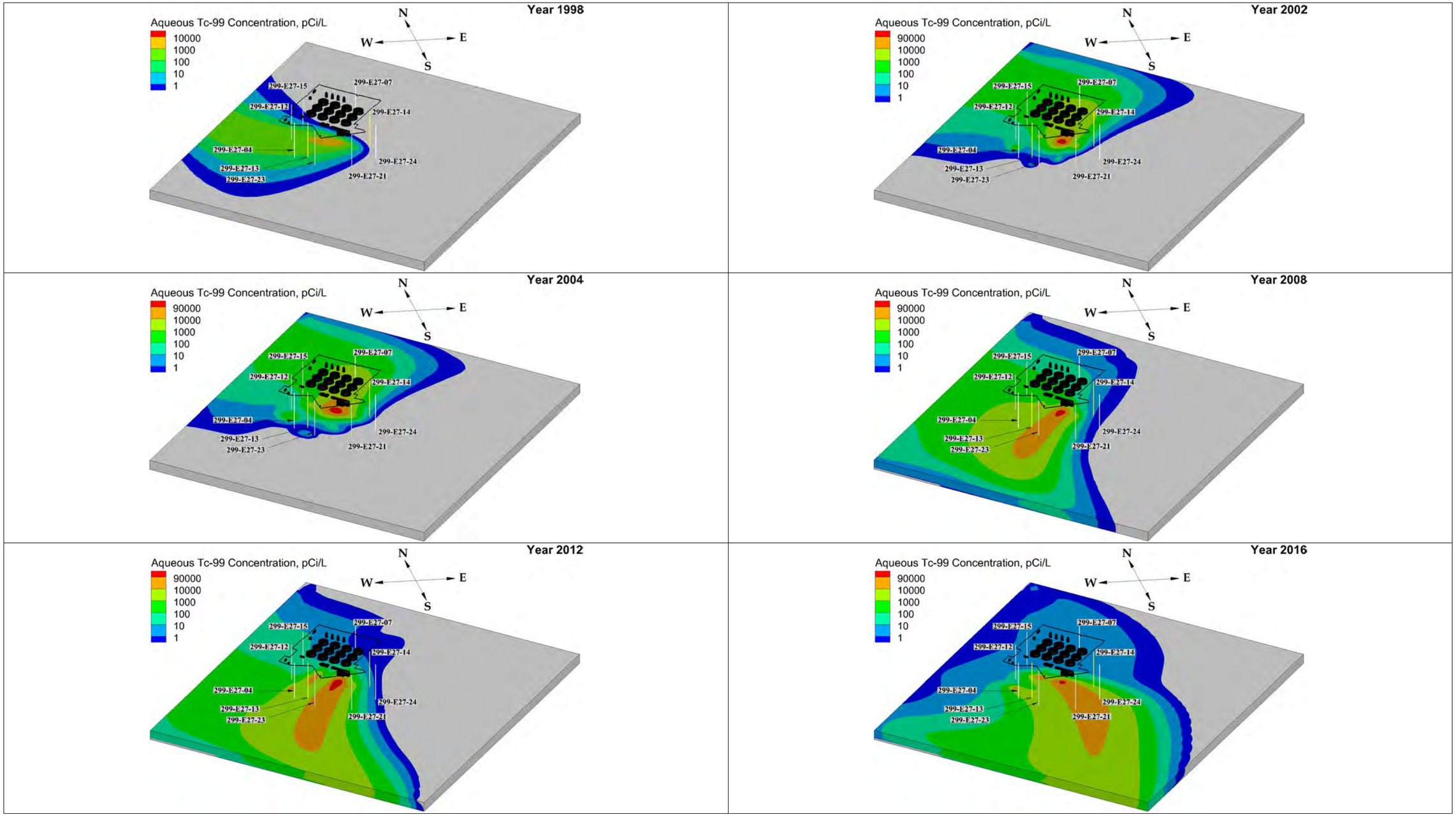

Figure 6-9. Comparison of Simulated Technetium-99 Concentrations in Groundwater to Measured Concentrations around the Northeast, Northwest, and Southwest of Waste Management Area C.

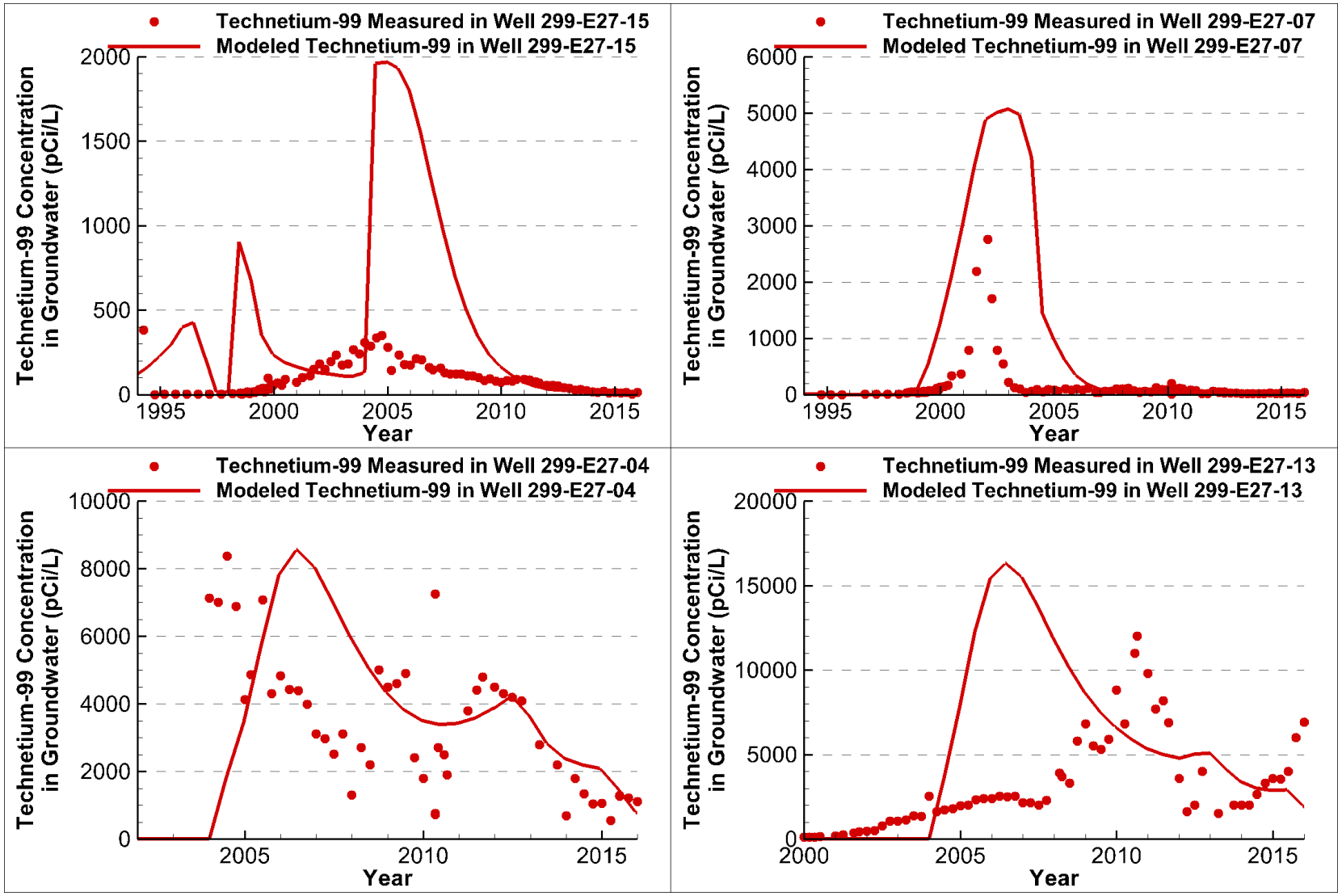

Note: This figure uses the Conceptual Model with Counterclockwise Rotation of the Hydraulic Gradient.

Figure 6-10. Comparison of Simulated Technetium-99 Concentrations in Groundwater to Measured Concentrations around the Southwest and Southeast of Waste Management Area C.

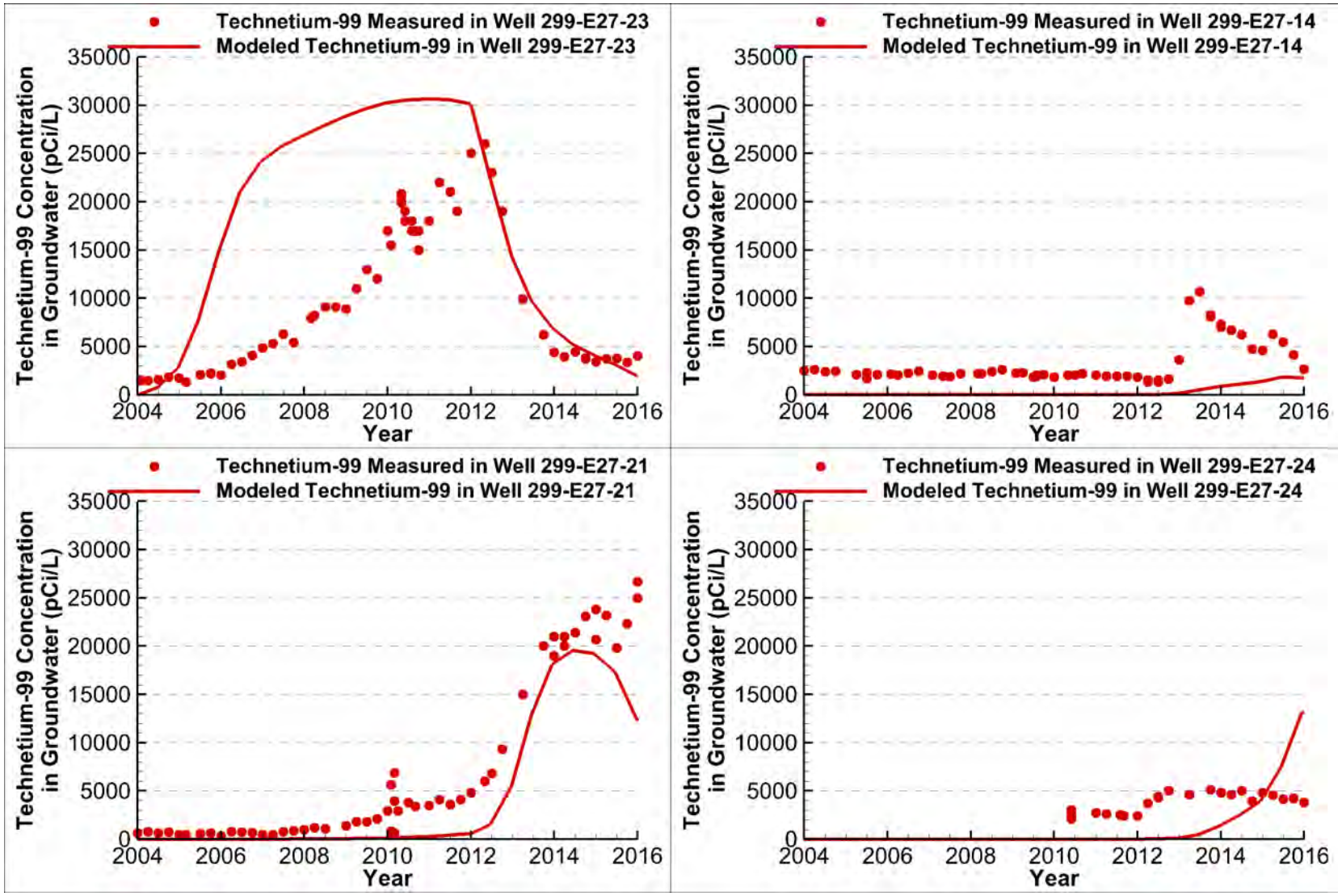

Note: This figure uses the Conceptual Model with Counterclockwise Rotation of the Hydraulic Gradient.

6.3.3 Summary

The conceptual model involving the counterclockwise rotation of the hydraulic gradient from northwest to southeast, and the associated numerical model results, appear capable of approximating observed field data for the time of arrival of ^{99}Tc to groundwater and concentration levels of ^{99}Tc in groundwater. The model results include several assumptions regarding the timing and inventory of the past releases, and direction and magnitude of the hydraulic gradient during the time it could not be measured. Because of these assumptions, it is unknown how accurately the model calculations represent the actual release of ^{99}Tc and its transport in the vadose zone and groundwater. The results do, however, provide some insight into the concentration levels observed in monitoring wells, and the changes in concentration that have occurred in those wells since 2000. The concentration of ^{99}Tc observed in most of the monitoring wells appears to change too abruptly to represent the one-dimensional passing of a contaminant front. The modeling results indicate that the concentration in the wells changes so abruptly because the direction and the magnitude of the groundwater hydraulic gradient changes. The rotation of the gradient continually changes the orientation of the groundwater plumes relative to the wells. The high concentrations measured in wells 299-E27-23 and 299-E27-13 between 2010 and 2012 likely correspond to the time when those wells were located downgradient of the sources. By 2014, the concentration in those two wells dropped markedly, while the concentration in well 299-E27-21 began increasing quickly around that same time. According to the modeling results, this pattern in the data can be explained by, and corresponds to, the further rotation of gradient from the south to the southeast.

The release from tank C-105 that was estimated to occur between 1963 and 1967 (see Table 3-1) appears to be the dominant source of ^{99}Tc observed in groundwater in the monitoring wells. According to the inventory estimates in RPP-RPT-42294, it is the only release large enough and that occurred early enough to bring about the concentration levels observed in the monitoring wells. However, according to the model, most of the ^{99}Tc observed in the monitoring wells located southwest of the farm originated from the tank leaks, and not from the UPRs that occurred away from the tanks. Releases from UPR-81 (an acute release estimated to occur in 1969); UPR-82 (an acute release estimated to occur in 1969) and UPR-86 (an acute release estimated to occur in 1971) and the leak associated with tank C-110 (a continuous release 1971-1972) (See timing of these leaks in Table 3-1) occurred later than the release from tank C-105, and the modeling results exhibit the implications of this. Again, according to the model, the concentration of ^{99}Tc in the wells located nearest the UPRs is dominated by the ^{99}Tc contained in the release from tank C-105. The concentration of ^{99}Tc attributed to the ^{99}Tc contained in three UPRs peaks a few years after the concentration of ^{99}Tc peaks attributed to the tank C-105 release. Based on assumptions about the timing of releases given above, the modeling that was done suggests that the tank C-105 source may be the dominant source and that the ^{99}Tc originating from the UPRs may be secondary sources that has not yet been observed because it has not yet reached the water table. Whether or not the release from tank C-105 is truly the dominant source of ^{99}Tc observed at the monitoring wells is unknown. However, given the uncertainties in the timing and of the UPR releases and the magnitude of the overall ^{99}Tc inventories in two of the three releases (i.e., 1.3 Ci at UPR-82 and 2.7 Ci at UPR-86), the use of other modeling assumptions about the releases at the UPRs relative to the assumed releases at

tank C-105 could lead to different modeling results and conclusions about the relative importance of the UPR releases as major contributing sources to observed contamination to groundwater at WMA C .

6.3.4 Conclusion

The modeling results indicate that as the water table returns to more natural conditions, the rotation of the gradient will continue to alter the primary movement of the plumes from primarily a southerly direction to a more southeasterly direction in the near future. The high concentrations of ^{99}Tc observed in wells 299-E27-23 and 299-E27-21, southwest and south of WMA C, respectively, are likely to be observed in wells 299-E27-24 and 299-E27-14, which are located to the southeast of WMA C.

The combination of the field data and the model results provide a reasonable basis for developing model assumptions and determining bounded estimates of input parameters. The model provides a basis to evaluate the uncertainties in the inventory and volumes of past leaks for the purpose of better constraining estimates of the existing contamination. The transient evaluation also provides an element of confidence that the model parameters and equations can adequately represent the physical conditions and past events of WMA C. This assurance improves the confidence in the model's ability to evaluate and estimate future impacts from the past leaks.

7.0 FUTURE IMPACTS OF PAST WASTE LEAKS AND RELEASES

In this section, the results for a set of forward calculations to evaluate the future consequences of the past waste leaks and releases are presented to evaluate how the groundwater concentrations may change in the future based on the constraints on the scoping modeling analysis cases established in Sections 4 and 5. The results included in this section are as follows:

- The results of a screening analysis used to identify key constituents to evaluate in this analysis; and
- The results of a transport analysis of past waste releases, both before and after the time of assumed site closure in year 2020.

7.1 APPROACH TO THE FORWARD PROJECTION

The scoping analyses presented in Section 4 of this document provides comparisons of the STOMP© model to groundwater monitoring data to evaluate the credibility of alternative assumptions for the migration of the leaks from the time of their assumed occurrence to the current time. As discussed in Section 4.8, several analysis cases were inconsistent with data and additional analysis cases produced comparable results to each other. Of the steady-state aquifer cases that were consistent with the arrival time at the aquifer, none were obviously superior to others in terms of explaining the observed groundwater monitoring well data.

The analysis that showed the best representation of most groundwater monitoring well data was the transient water table analysis presented in Section 6. However, the conditions evaluated in that case are not relevant for projections into the future, as the current water table orientation is expected to be similar to the projected future water table, with only the height and gradient changing as it relaxes to its long-term state.

Scoping Analysis Case 1a (see Table 4-1) was selected to project concentrations into the future. This selection has several advantages. 1) Case 1a has the fewest alterations from the WMA CPA (RPP-ENV-58782) and RCA (RPP-ENV-58806) residual waste model, differing only in the height of the aquifer, allowing the effects of residual wastes and leaks to be considered on a common basis. 2) It approximates the arrival times at the aquifer and aquifer concentrations as that observed in well 299-E27-14 evaluated in the scoping analysis. It therefore has been judged to be the most appropriate analysis case to use for projecting future consequences of the leaks. While Case 1a provides useful insights on projected contaminant concentrations, the results should be interpreted with understanding of uncertainties inherent in evaluating transport processes in the natural system. The effect on arrival times and magnitude of contaminant concentrations resulting from some of these uncertain parameters was evaluated in Section 4 (see Table 4-1). The linear relationship of potential increases or decreases in estimated groundwater

flux to corresponding decreases or increases on predicted concentrations levels is of particular importance.

The concentrations results provided in this section are taken from forward predictions of some key constituents using one of the numerical models that did a reasonable job of matching observed first arrival in groundwater. The idea was not to necessarily predict absolute concentrations but to provide overall temporal trends in groundwater impacts. These trends were meant to provide general information to inform any remediation of groundwater. Assessing the uncertainty in these predictions is well beyond the intended scope of these analyses.

To implement the forward projection, a distinction must be made between the behavior of sorbing and nonsorbing contaminants. The analysis cases presented in Section 4 were established to evaluate nonsorbing contaminants, with ^{99}Tc being the indicator contaminant of concern used in the cases. Nonsorbing contaminants such as ^{99}Tc arrive at the water table during the time period between the occurrence of the leaks and today, as indicated by both monitoring data and model results. During that time, the water table was elevated, as discussed extensively in previous sections, and as a result the scoping analysis cases were implemented with an elevated water table. By contrast, sorbing contaminants are expected to arrive at the water table in the future, in some cases the distant future, when the water table will have recovered its long-term steady level. Appropriate modeling of the arrival at the water table for sorbing contaminants should therefore use the expected future water table level. This assumption is used in the PA/RCA model documented in RPP-ENV-58782 and RPP-ENV-58806.

Therefore, the forward modeling of leaks has been undertaken using slightly different models for the sorbing and nonsorbing contaminants. For sorbing contaminants, the PA/RCA model was used, while for nonsorbing contaminants Case 1a was used. The two models are compared in Figure 7-1. In both cases the leaks were introduced into the model in the same manner as described in Section 4. The inventories of the contaminants considered in the analysis are shown in Table 7-1.

7.2 IDENTIFICATION OF CONTAMINANTS OF POTENTIAL CONCERN

The STOMP© 3-D groundwater flow and transport model was used to identify those COPCs that are not sufficiently mobile to impact groundwater until more than 10,000 years. This step helps to streamline the past release analysis, and to focus attention on the contaminants that may impact the environment within a plausible time frame of evaluation.

The criterion chosen for screening is the first-arrival time of the contaminant. Hydraulic property selection was carried out to yield maximum transport rates. Maximum net infiltration rates were also assumed in this analysis. An incremental range of K_d values was evaluated between 0.25 mL/g and 2.5 mL/g (prior to gravel correction) to determine threshold values that reached the water table in 1,000 and 10,000 years. The use of such approaches is accepted by the EPA, and appropriate methods are outlined in EPA guidance (EPA/540/F-95/041, *Soil Screening Guidance: Fact Sheet*). This approach minimizes the number of contaminants eliminated from analysis. As a result, some contaminants may only arrive at the water table for

particular sensitivity and uncertainty evaluations (i.e., evaluations that minimize the time of transport through the vadose zone). For the conditions of analysis used in many of the scoping analysis cases, a number of the radionuclide contaminants may have no impact on the past leaks analyses results because their transport to the water table requires more than 10,000 years.

Results of the screening analysis are presented in Figure 7-2. The results show that the time of first arrival is a strong linear function of the K_d value. From this relationship, the first-arrival time for any radionuclide can be estimated accurately by using the trend equation shown on the figure. According to the screening model results, the minimum K_d values that produce an impact to groundwater within 1,000 years and 10,000 years are less than 0.5 mL/g (without any gravel correction), and less than 2 mL/g (without any gravel correction), respectively. This screening analysis demonstrates for the setting of WMA C that small changes in K_d values can result in a significant change in the time of arrival at the water table. For example, the difference of assuming a K_d value of 0.5 L/kg to 1.5 L/kg can result in first arrival times increasing from the number of years from just over 1,000 years to between 6,000 and 7,000 years). For slightly sorbed constituents like ^{129}I (i.e., assumed K_d value of 0.2 l/kg) and total uranium and the uranium isotopes (i.e., assumed K_d value of 0.6 l.kg), small changes in assumed K_d values can change the first arrival and timing of peak concentrations in the water table.

Figure 7-1. Case 1a Past Leak Model Used for Nonsorbing Contaminants for the Forward Projection Compared to the Performance Assessment/RCRA Closure Analysis Model Used for the Sorbing Contaminants.

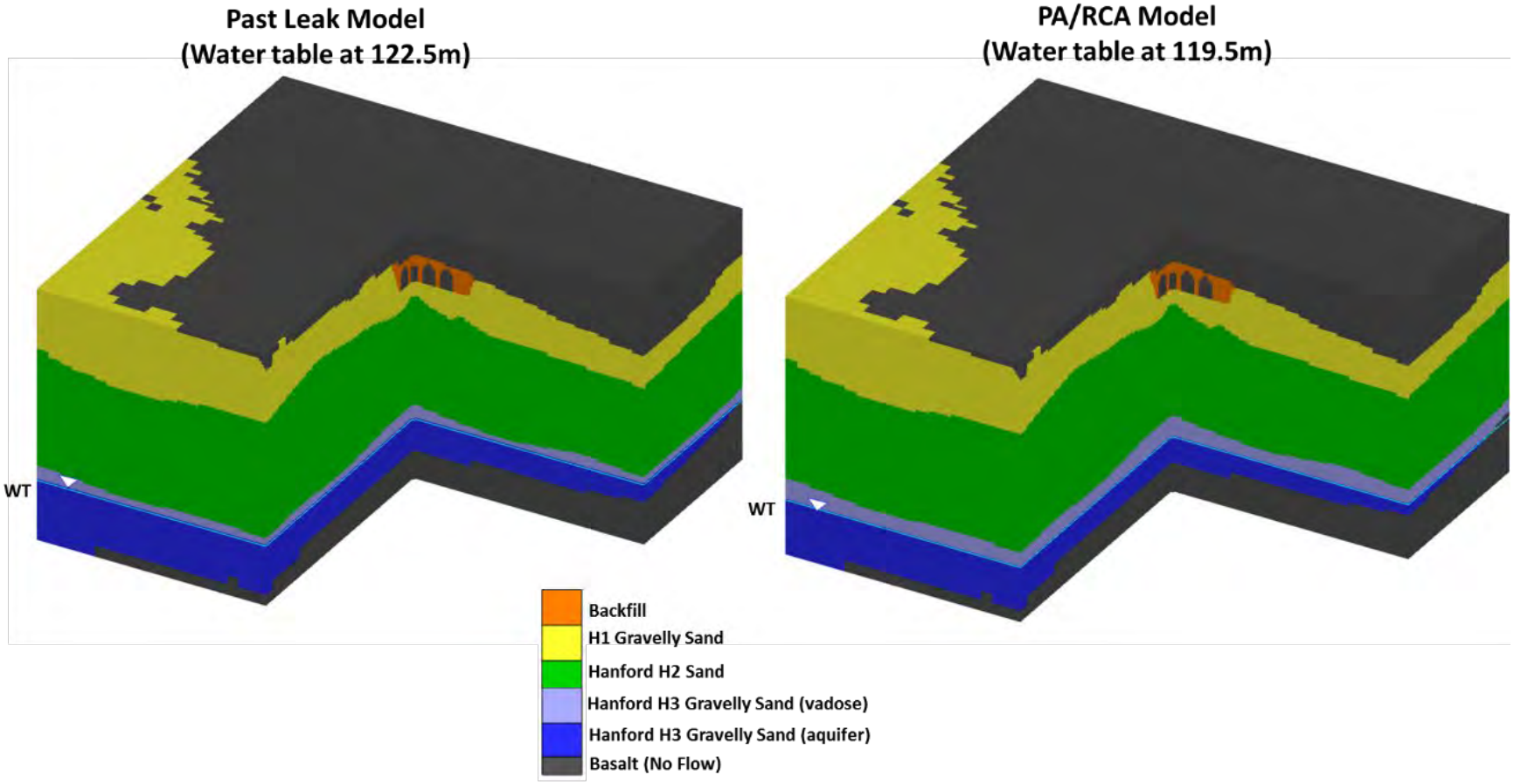

PA = performance assessment
RCA = RCRA Closure Analysis
RCRA = Resource Conservation and Recovery Act of 1976

References:
RPP-ENV-58782, *Performance Assessment of Waste Management Area C, Hanford Site, Washington*.
RPP-ENV-58806, *RCRA Closure Analysis of Tank Waste Residuals Impacts at Waste Management Area C, Hanford Site, Washington*.

The first-arrival times for each of the representative K_d values used in the COPC calculations are summarized in Table 7-2. The results of the COPC analysis indicate that even when using parameter estimates biased to produce the greatest pore water velocity in the vadose zone:
1) contaminants with $K_d > 0.50$ mL/g do not reach groundwater within 1,000 years; and
2) radionuclides with $K_d \geq 2.0$ mL/g do not reach groundwater within 10,000 years (see Table 7-2). While the actual 10,000-year K_d value cutoff is likely only slightly greater than 2.0 mL/g, the COPC evaluation did not include a representative contaminant with a K_d value between 2 mL/g and 2.5 mL/g (see Table 7-2).

Of the list of radionuclides and non-radiological contaminants considered (see Table 7-1), some are modeled as nonsorbing contaminants ($K_d = 0$ mL/g). These are ^{99}Tc, ^{3}H, ^{60}Co, SO_4, NO_3, and Cr. Potential impacts from cyanide are also evaluated (see Appendix A). The remaining contaminants (^{79}Se, ^{129}I, ^{126}Sn, ^{238}U, and total uranium) are modeled with small retardation (K_d values between 0.1 and 0.6 mL/g). Other radionuclides and non-radiological contaminants that are part of the WMA C past release inventory are not included in further groundwater impact analysis due to either larger retardation or small inventories.

7.3 FUTURE PROJECTIONS OF PAST WASTE LEAKS AND RELEASES

This analysis of future impacts of past release includes calculations of the highest calculated concentration, with an allowance for some volume averaging based on projected groundwater use, at the WMA C fenceline. To determine the highest groundwater concentration, the modeling results indicate the average concentration in the aquifer within nine segments along a hypothetical line parallel to the southeast edge of WMA C shown in Figure 7-3. Most of the nine segments are ~30 m (~98 ft) long (Table 7-3), and aligned such that the centerlines of the plumes in the groundwater resulting from the past releases from a single line of 100-series tanks parallel to the direction of groundwater flow (e.g., the centerline of the plumes resulting from the past releases from tanks C-105 and C-108) intersect the fenceline within the same PoCal segment. Two of the three segments substantially different than 30 m (98 ft) long align with the more irregularly spaced centerlines of the plumes resulting from the UPRs that are not associated with a particular tank. The third segment, PoCal 5, represents a gap between adjacent centerlines.

EPA/540/R-95/128, *Soil Screening Guidance: Technical Background Document*, and WAC 173-340-747, "Deriving Soil Concentrations for Groundwater Protection," imply that the aquifer mixing width ought to equal the width of contamination entering the aquifer. Other PAs conducted at the Hanford Site and other DOE facilities have used an aquifer mixing width equal to the width of the facility (e.g., WCH-520, *Performance Assessment for the Environmental Restoration Disposal Facility, Hanford Site, Washington*; and WSRC-MS-2003-00582, *Performance Assessment/Composite Analysis Modeling to Support a Holistic Strategy for the Closure of F Area, a Large Nuclear Complex at the Savannah River Site*). As indicated previously, the width of the PoCal segments is sufficient to intercept the centerline of the plumes resulting from the tank residuals from a single line of 100-series tanks, which appears consistent with the intent of EPA/540/R-95/128 and WAC 173-340-747. The aquifer mixing zone extends into the upper 5 m (16.4 ft) of the aquifer on the basis of the 5 m mixing zone dimension

associated with Equation 747-4 in WAC 173-340-747, "Deriving soil concentrations for groundwater protection." The elevated ^{99}Tc concentrations around WMA C appear to extend throughout the depth of the aquifer, indicating that the plume is well mixed (DOE/RL-2011-01, *Hanford Site Groundwater Monitoring Report for 2010*). Owing to the vertical and lateral dispersivities that are used to represent the contaminant transport through the unconfined aquifer system, the WMA C model groundwater concentration results appear to be relatively constant throughout the depth of the aquifer and there is little difference between the concentrations calculated in the upper 5 meters (16.4 feet) and those calculated through the entire thickness of the aquifer along the flow path.

7.3.1 Results of Groundwater Pathway Evaluation: Time before Assumed Closure of Waste Management Area C in 2020

The results of modeling Case 1a indicate that only contaminants with K_d values less than or equal to 0.1 mL/g arrive in groundwater at the fenceline PoCals within 1,000 years (Table 7-4). Among radionuclides, the only ones producing calculated concentrations that exceed zero in groundwater at the WMA C fenceline before closure are ^{99}Tc, tritium, ^{60}Co, and ^{79}Se. The concentrations in groundwater of ^{99}Tc, tritium, and ^{60}Co reach a peak during this period. The maximum concentration of ^{99}Tc in groundwater at the fenceline during this period is 9,400 pCi/L in 2018, which is over a factor of 10 greater than its Drinking Water Standard (DWS) of 900 pCi/L (Figure 7-4). The maximum concentration decreases to 6,700 pCi/L after traveling 100 m (328 ft) through the aquifer (Figure 7-5). The predicted maximum concentration of tritium in groundwater at the WMA C fenceline during this period is about 22,000 pCi/L in 2012, which is slightly over its DWS of 20,000 pCi/L (Figure 7-6). The tritium concentrations predicted at the 100-m (328-ft) downgradient location (Figure 7-7) undergo comparable decrease as ^{99}Tc does between the fenceline and the 100-m (328-ft) downgradient location. The predicted peak concentration of ^{60}Co at the 100 m (328 ft) is about 860 pCi/L that occurs in 2009 (Figure 7-8) and exceeds the DWS of 100 pCi/L by a factor of 8. Selenium-79 arrives at the WMA C fenceline and 100 m (328 ft) downgradient of it shortly before closure; however, the maximum concentration at any of the PoCals is less than 0.001 pCi/L (Figure 7-9). The peak concentrations for ^{79}Se occur much later (Table 7-4).

The predicted high concentrations of tritium are inconsistent with the observed concentrations in groundwater wells around WMA C, which have remained significantly below the predicted values throughout the monitoring record. Recent concentrations of tritium in wells in the vicinity of WMA C are generally found to be between 1,000 and 2,000 pCi/L. The current results are conservative in that they do not account for the fact that tritium partitions into the vapor phase and a significant mass depletion can occur in the vadose zone from vapor phase transport towards the surface. This mass depletion is conservatively ignored in the transport model, where all of the mass is assumed to remain within the aqueous phase and transported for evaluating the groundwater impacts. Therefore, groundwater impacts estimated with this specific flow and transport model of tritium releases was not considered to be credible as a part of the future projections of the impacts in this section of the document.

The predicted high concentrations of ^{60}Co are also inconsistent with the observed concentrations in groundwater wells around WMA C. Concentrations of ^{60}Co have remained significantly below the predicted values throughout the monitoring record. Recent concentrations of ^{60}Co in wells in the vicinity of WMA C have been below detection limits for a number of years.

For ^{60}Co, the choice of applying a K_d value of 0 mL/g throughout the vadose zone and saturated zone leads to an overestimation of ^{60}Co concentrations in the groundwater. The sorption characteristics of ^{60}Co can vary widely and are discussed in Appendix A of PNNL-16663, *Geochemical Processes Data Package for the Vadose Zone in the Single-Shell Tank Waste Management Areas at the Hanford Site*. Based on review of literature in PNNL-16663 and available data for adsorption of cobalt on Hanford Site sediments, the following conclusions can be drawn: (a) Co(II) is the stable valence state in water under oxidizing and moderately reducing conditions; (b) Co(II) is highly immobile (K_d > 1,000 mL/g) for typical Hanford groundwater and vadose zone conditions in the absence of organic chelating agents such as EDTA (ethylenediaminetetraacetic acid); and (c) moderate-to-high concentrations of CN^- and EDTA reduce Co(II) adsorption on sediments. Co-EDTA anionic complexes can undergo dissociation via a complex series of reactions with iron and aluminum oxides in the sediments forming a suite of adsorbates: Co2+, CoIIEDTA2-, FeEDTA, and AlEDTA- that compete for the EDTA and surface adsorption sites. The sorbed Co(II) is then oxidized to the extremely stable but weakly reactive CoIIIEDTA-. In the case of Mn(IV) minerals, such as pyrolusite, the adsorption and subsequent oxidation of CoIIEDTA2- to produce CoIIIEDTA- results in the reduction of Mn(IV) to Mn(III) and the formation of a layer of α-Mn2IIIO2 on the pyrolusite, which eventually limits the production of CoIIIEDTA-. The adsorption behavior of cobalt therefore varies greatly and is a function of pH, oxidation state, sediment interactions, and environmental availability of organic complexants (PNNL-16663). Based on this information, it is conceptualized that near the source locations of past leaks and UPRs, the mobility of Co(II) could be high due to possible availability of chelating agents and organic complexants in the waste stream. But with increasing transport distance away from the source location and with increasing dissolution-exchange reactions with the sediments in the vadose zone, the sorption behavior will change towards a gradually increasing K_d value. PNNL-17154, *Geochemical Characterization Data Package for the Vadose Zone in the Single-Shell Tank Waste Management Areas at the Hanford Site*, recommends a best-estimate K_d value of 0 mL/g for ^{60}Co (II, III) for high and intermediate impact zones influenced by waste streams and a best-estimate K_d value of 10 mL/g for minimally impacted zones. Since the exact depths of these impact zones are not available within WMA C, it is not possible to precisely apply the variable K_d values. Thus, groundwater impacts estimated with the specific transport model of ^{60}Co releases using a K_d value of 0 was not considered to be credible as a part of the future projections of groundwater impacts in this section of the document. Instead, a uniform small K_d value is considered for ^{60}Co in the transport model to evaluate the impact of imposing minor retardation along the transport pathway.

To evaluate the sensitivity to minor amounts of retardation, an additional simulation was made with a selected K_d value of 0.1 mL/g. The results of this simulation on peak flux of ^{60}Co at the water table indicate that by just considering a small change in sorption behavior, the flux of ^{60}Co is reduced dramatically. With its short half-life (5.27 years) and the small amount of assumed adsorption which delays the arrival of ^{60}Co at the water table, the ^{60}Co inventory associated with the simulated leaks decays away during its transport through the vadose zone and no impacts are seen at the water table during the period of analysis. The transport modeling results based on the

use of a small K_d value (e.g., 0.1 mL/g) are consistent with the observations of non-detects in the recent monitoring record of groundwater wells surrounding WMA C.

The only non-radiological contaminants arriving in groundwater at the WMA C fenceline before closure are nitrate, sulfate, and hexavalent chromium. The concentrations in groundwater of nitrate, sulfate, and hexavalent chromium (if all chromium is assumed to be hexavalent) reach a peak during this period. None of these exceed a regulatory standard unless all of the chromium is assumed to be hexavalent. The maximum concentration of nitrate in groundwater at any of the PoCals during this period is 9 mg/L in 2017 at PoCal 6 (Figure 7-10). The concentration of nitrate reaches a peak during this period at PoCal 6 but is still increasing at PoCal 3 in year 2020. The sulfate reaches a peak concentration of 0.6 mg/L in 2018 at PoCal 6 (Figure 7-11). The maximum concentration of chromium is 0.06 mg/L at PoCal 6 in year 2019. If all chromium is assumed to be hexavalent (Figure 7-12) these concentration levels would exceed the MTCA Method B groundwater CUL of 48 µg/L. Any of the hexavalent chromium that reduces to trivalent chromium fails to reach the water table within 10,000 years because the K_d value of trivalent chromium exceeds the K_d value screening criterion.

Appendix A provides an estimate of the inventory and potential impacts from past releases of cyanide at WMA C. Inventory estimates from past releases in WMA C tank farm, for the majority of analytes that are tracked in the Best-Basis Inventory, are based on supernatant composition derived from Hanford Defined Waste (HDW) model (RPP-19822, *Hanford Defined Waste Model – Revision 5.0*). This approach is described in Section 2.1 of this document. The predominant supernatant waste types assumed to have been released from tanks and ancillary equipment in WMA C tank farm are a combination of Plutonium Uranium Extraction Plant high-level waste (P1 [1956-1962], P2 [1963-1967]) and aluminum fuel cladding waste (CWP1 [1956-1960], CWP2 [1961-1972]), B Plant cesium recovery waste (CSR), and Sr-Cs Rec (P2) stack drain waste streams. The average compositions for these waste streams in the HDW model are presented in Table 2-2 of this document. The concentration of ferrocyanide [$Fe(CN)_6^{-4}$] for these waste stream supernates was assumed to be zero within the HDW model based on assumption that all of the ferrocyanide would be in the precipitated phase (sludge). However, ferrocyanide degradation and dissolution are <u>not</u> accounted for by the HDW model, and therefore the HDW model estimates for ferrocyanide concentrations are considered unreliable (see Section 7.2.11 of RPP-19822).

Discharged inventory estimates from past releases at WMA C are summarized in Table 2-3 of this report for selected analytes. The ferrocyanide inventory was estimated to be zero as the supernatant compositions were taken from the HDW model (see footnote in Table 2-3 of Section 2). However, this assumption about the ferrocyanide inventory may be inconsistent with the observations of cyanide in the groundwater monitoring well network for WMA C. The occurrence of low levels of cyanide in groundwater wells has been attributed to past releases from WMA C (see discussion in Section 2.3.3.3 for further details).

To estimate the supernatant concentration of ferrocyanide with the primary purpose of developing inventory estimates for past discharges at WMA C, a two-staged approach was adopted and is described in Appendix A. The first stage involved conducting a Hanford Site-specific literature search related to the solubility and dissolution potential of precipitated nickel ferrocyanide within the tanks. The second stage involved searching the Tank Waste Information

Network System (TWINS) for historical records related to sampling data for cyanide for WMA C tanks. The results from both evaluations are summarized in Section A2.2 of Appendix A.

Taking the leak volume estimates for various tanks that were used during the scavenging process (or in later transfers), the released inventory of free cyanide (referred to as cyanide henceforth) is estimated in Table A-2 of Appendix A. The cyanide concentrations are based on the average of sampled data from Table A-1 in Appendix A (for tanks 241-C-104 and 241-C-110) and an average concentration of 1.58 g/L (for tanks C-108 and C-112). Of the total released cyanide inventory of about 151 kg, about 108 kg is estimated to have been released from tank C-108 (See Table A2.2 in Appendix A).

Estimates on the cyanide inventories discharged at different possible release locations can be combined with information from contaminant transport modeling of past releases documented in in this section to examine whether releases of these probable cyanide inventories can yield groundwater impacts that are consistent with past observations of cyanide concentrations in groundwater.

Figure 6-10 in this section provides modeling-based concentration of nitrate in groundwater at the points of calculation located 100 m (328 ft) from the WMA C fenceline. Cyanide and nitrate anions have similar transport characteristics, so the modeled results for nitrate can be used to estimate the impact of cyanide on groundwater[1]. The peak nitrate concentrations for each source type is predicted at point of calculation. For the tank C-108 leak, the peak nitrate concentration is calculated to be 1.54 mg/L as shown in Figure A-4 of Appendix A (same as information in Figure 6-10 of this section). The model predictions are based on a released nitrate inventory of 2,900 kg for a leak volume of 18,000 gallons (68,130 L) in calendar year 1965.

Normalizing the simulated concentration of nitrate with its released inventory results is shown in Figure A-5 of Appendix A. The normalized peak concentration is 5.3×10^{-4} mg/L (per kg of nitrate inventory) or 0.53 µg/L (per kg of nitrate inventory). This value can be used to determine the peak concentration for cyanide from tank C-108. Considering 108 kg of cyanide inventory, the peak concentration is calculated to be about 57 µg/L. This peak concentration matches reasonably with the observed maximum groundwater concentrations, which vary between 40 and 50 µg/L (Figure A-3). Given that the simulated high concentrations occur approximately within calendar years 2010 and 2025, the current observed concentrations in the groundwater monitoring wells are likely to be near their peak values. The impact of additional inventory from tank C-112 could increase the simulated peak concentration by as much as 22 µg/L, but only if the plumes coincide. However, since groundwater flow paths for tanks C-108 and C-112 are believed to be parallel into the future as the aquifer enters a long-term stable direction toward the southwest, limited overlap is expected and the two leaks are not expected to be additive. Therefore, based on the assumption that groundwater flow paths remain unchanged and do not overlap, the calculated peak groundwater concentration of cyanide of 57 µg/L based on tank C-108 leak inventory is deemed to be a reasonable estimate of the peak concentration in groundwater.

[1] This is supported by the observation of cyanide to nitrate concentration ratio trend for well 299-E27-14 as shown in Figure 2-29. The concentration ratio from calendar years 2006 to 2012 has remained within approximately 0.1 to 0.2 (µg/L of cyanide to mg/L of nitrate) with minor short-term fluctuations outside this tight range.

An inverse calculation to determine leaked inventory and waste stream concentration can also be performed using the nitrate normalized concentration relationship outlined above. Given that observed peak cyanide concentration in groundwater is about 45 µg/L, the discharged inventory is estimated to be about 85 kg (45 µg/L divided by 0.53 µg/L per kg of cyanide). Assuming this inventory is released in 18,000 gallons (68,130 L) of supernatant fluid from tank C-108, the concentration of cyanide in the leak is estimated to be 1.24 g/L, which provides a reasonable match with the measured average liquid concentration of 1.58 g/L.

Consistent with the simulated nitrate concentrations, the cyanide concentrations are also projected to decline over time from the present-day values. The model suggests that in about a decade the concentrations could be appreciably lower than current observed values.

Concentration contours of ^{99}Tc and nitrate in the vadose zone corresponding to years 2000 and 2016 are shown in Figures 7-13 through 7-16, respectively. Technetium-99 and nitrate contained in the past leaks have reached the water table by 2000, but the center of the ^{99}Tc and nitrate mass remains above the water table. By 2016, the center of the ^{99}Tc mass has reached the water table, while the center of the nitrate mass remains just above the water table. Table 7-4 provides a summary of results for those radionuclides and non-radiological contaminants arriving in groundwater at the WMA C fenceline before closure.

Table 7-1. Leak Inventories of Contaminants of Concern Used in the Forward Projection Analyses.

Leak Site	Tank 241-C-101	Tank 241-C-104	Tank 241-C-105 (high estimate)	Tank 241-C-108	Tank 241-C-110	Tank 241-C-112	UPR-81	UPR-82	UPR-86	Surface Contamination	French Drain 216-C-8
Estimated Leak Time	**Late 1965 through 1969**	**~1965**	**Multiple releases between 1963 and 1967; another possible in first quarter of 1968**	**~1965**	**Sometime between 1971 and 1972**	**Sometime between 1946 and 1974**	**October, 1969**	**December, 1969**	**December, 1969 (discovered)**	**Unknown (Assumed to be 1965)**	**January 1960 through March 1965**
Modeled Leak Beginning Time	**1965**	**1965**	**1963**	**1965**	**1971**	**1965**	**1969**	**1969**	**1971**	**1965**	**1960**
Leak Volume (gal)*	37,000	28,000	20,500	18,000	2,000	7,000	36,000	2,600	17,000	1,000	32,000
Tc-99 (Ci)	2.49E-01	3.01E-02	9.84E+00	1.94E-02	3.36E+00	7.53E-03	1.10E-01	1.25E+00	2.68E+00	1.08E-03	0
I-129 (Ci)	3.84E-02	2.97E-02	5.91E-04	1.91E-02	1.99E-03	7.42E-03	9.53E-02	7.49E-05	1.61E-04	1.06E-03	0
Co-60 (Ci)	1.96E+02	1.48E+02	2.06E+02	9.52E+01	2.91E+01	3.70E+01	7.60E+02	1.19E+01	1.96E+01	5.29E+00	0
H-3 (Ci)	1.74E+02	1.34E+02	5.81E+00	8.62E+01	2.50E+00	3.35E+01	5.55E+02	5.26E-01	1.01E+00	4.79E+00	0
U-238 (Ci)	1.45E-03	1.10E-03	6.00E-04	7.05E-04	2.42E-04	2.74E-04	5.64E-03	7.61E-05	1.64E-04	3.92E-05	2.00E-05
Se-79 (Ci)	7.59E-04	6.91E-05	3.15E-02	4.44E-05	1.05E-02	1.73E-05	2.64E-04	3.99E-03	8.59E-03	2.47E-06	0
Sn-126 (Ci)	3.14E-03	2.85E-04	1.31E-01	1.83E-04	4.39E-02	7.11E-05	1.09E-03	1.67E-02	3.58E-02	1.02E-05	0
NO3 (kg)	5.90E+03	4.53E+03	4.32E+02	2.91E+03	1.82E+03	1.13E+03	2.32E+04	5.48E+01	1.18E+02	1.62E+02	1.46E-01
SO4 (kg)	1.29E+02	9.03E+01	6.91E+02	5.81E+01	2.12E+02	2.26E+01	3.53E+02	8.76E+01	1.88E+02	3.23E+00	1.37E-01
Cr (kg)	2.32E+01	1.70E+01	2.46E+01	1.09E+01	3.86E+01	4.25E+00	8.68E+01	3.12E+00	6.70E+00	6.07E-01	0
Utot (kg)	4.34E+00	3.29E+00	1.80E+00	2.11E+00	7.27E-01	8.21E-01	1.69E+01	2.28E-01	4.90E-01	1.17E-01	6.00E-05

Reference: RPP-RPT-42294, *Hanford Waste Management Area C Soil Contamination Inventory Estimates*, Rev. 2.
Note: The inventory estimates have been radioactive decay corrected to the beginning of the leak or unplanned release modeled year.
Isotopes of Uranium are not explicitly modeled as its concentration in groundwater can be predicted based on U-238 concentrations and scaling by the U-234/U-238 ratios in the inventory.

*Conversion 1 gallon = 3.78541 liters

1

2

Leak time sources	
Tank C-101	Section 4.1.3.3 “Timing of the Release”, RPP-ENV-33418, *Hanford C-Farm Leak Inventory Assessments Report*, Rev. 4
Tank C-104	Section 4.7.2 “Leak Assessment Considerations”, Section 4.7.3.3 “Timing of the Release”, RPP-ENV-33418, Rev. 4
Tank C-105 (low estimate)	
Tank C-105 (high estimate)	Section 4.2.3.1 “Release type”, Section 4.2.1 “Leak Status of Tank 241-C-105”, and Section 4.2.3.3 “Timing of the Release”, RPP-ENV-33418, Rev. 4
Tank C-108	Section 4.8.2 “Leak Assessment Considerations” and Section 4.8.3.3 “Timing of the Release”, RPP-ENV-33418, Rev. 4
Tank C-110	Section 4.3.2 “Leak Assessment Considerations”, and Section 4.3.3.3 “Timing of the Release”, RPP-ENV-33418, Rev. 4.
Tank C-112	Section 4.9.2 “Leak Assessment Considerations”, and Section 4.9.3.3 “Timing of the Release”, RPP-ENV-33418, Rev. 4
UPR-81	Section 5.2.3.3 “Timing of Release” and Table 5-1, Section 5.2.1 “UPR-200-E-81 Data and information”, RPP-ENV-33418, Rev. 4
UPR-82	Section 5.3.3.3 “Timing of Release” and Table 5-1, Section 5.3.1 “UPR-200-E-82 Data and information”, RPP-ENV-33418, Rev. 4
UPR-86	Section 5.4.3.3 “Timing of Release” and Section 5.4.3.1, and Table 5-1, RPP-ENV-33418, Rev. 4
Surface	RPP-RPT-42294, *Hanford Waste Management Area C Soil Contamination Inventory Estimates*, Rev. 2
French Drain 216-C-8	Section 6.4 “216-C-8 French Drain”, RPP-ENV-33418, Rev. 4. Not cited, but also a good source of information is RPP-RPT-42294, Rev. 2

3

Figure 7-2. First-Arrival Time (in Calendar Year) of Radionuclides for Various K_d Values Based on Screening Analysis Using Subsurface Transport Over Multiple Phases.

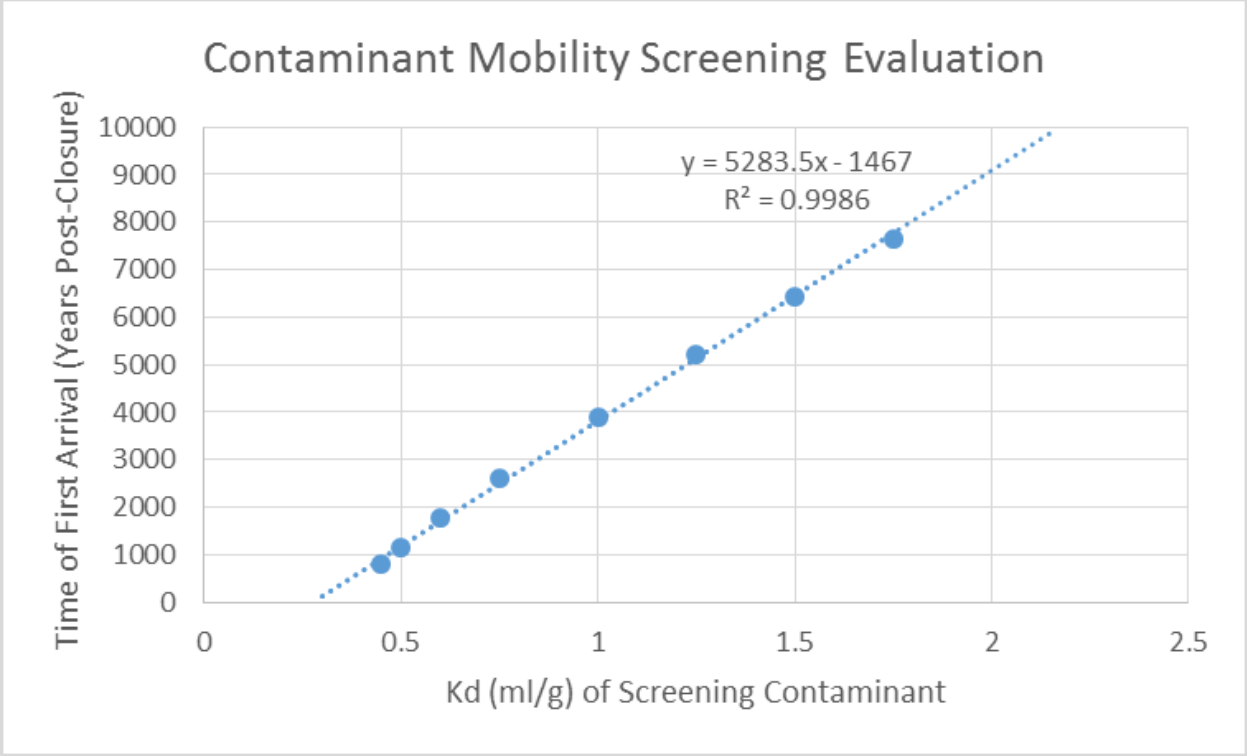

Table 7-2. First-Arrival Time (in Calendar Year) of Radionuclides for Various K_d Values Based on Screening Analysis Using Subsurface Transport Over Multiple Phases.

Contaminant K_d (Material < 2 mm) (mL/g)	Calendar Year of First Arrival at Water Table	Time of Arrival, Post-Closure (Closure Occurring in 2020) Years
0.25	1997	-23
0.3	2006	-14
0.45	2842.5	822.5
0.5	3170	1,150
0.6	3815	1,795
0.75	4640	2,620
1	5930	3,910
1.25	7240	5,220
1.5	8460	6,440
1.75	9670	7,650
2	> 12020	> 10,000

Figure 7-3. Points of Calculation 100 Meters Downgradient of Waste Management Area C.

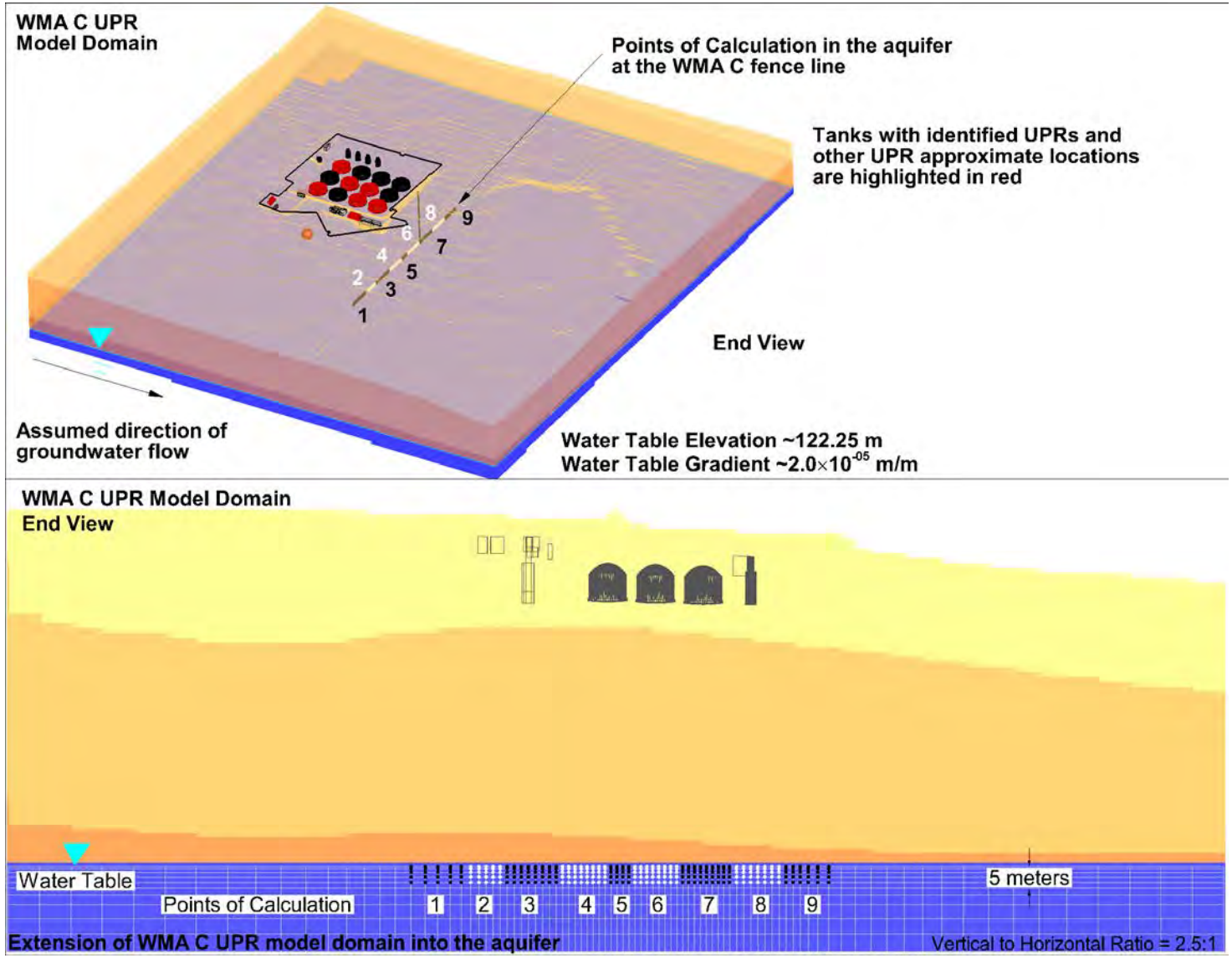

PA = Performance Assessment WMA = Waste Management Area

Table 7-3. Width of the Nine Points of Calculation at the Waste Management Area C Fenceline.

Points of Calculation								
1	2	3	4	5	6	7	8	9
Width (m)	Width (m)	Width (m)	Width (m)	Width (m)	Width (m)	Width (m)	Width (m)	Width (m)
40	24	35.5	31	15.3	30.4	34.1	31.5	33.5

7.3.2 Results of Groundwater Pathway Evaluation: Time after Assumed Closure of Waste Management Area C in 2020

Except for nitrate, the concentration all of the radionuclides and non-radiological contaminants with a K_d of 0 mL/g decreases markedly 100 m (328 ft) downgradient of the fenceline after the assumed closure of WMA C in 2020. The concentration of nitrate at PoCal 3 reaches a peak value of about 7 mg/L in 2030 and then begins to decline steadily and reaches a value of less than 1 mg/L by 2120 (refer to Figure 7-10). General trends of cyanide impacts for tanks C-108 and C-112, which are the tanks with the largest inventories estimated for cyanide, are expected to be very similar to the impacts estimated for nitrate for these tanks.

The concentrations in groundwater of ^{99}Tc, sulfate, and hexavalent chromium, if all chromium is assumed to be hexavalent, also (refer to Figures 7-4, 7-11, and 7-12, respectively) decline steadily from the peak value reached during the period before the assumed closure of WMA C in 2020. By 2120, the maximum concentrations of ^{99}Tc, sulfate, and hexavalent chromium 100 m (328 ft) downgradient of the WMA C fenceline decrease to less than 100 pCi/L, 10 µg/L, and 1 µg/L, respectively. The concentration of ^{79}Se increases after 2020 and reaches a peak value of about 0.5 pCi/L in year 4040 (refer to Figure 7-8). The concentration decreases after that until reaching an effective zero value by year 9000. There is no MCL for ^{79}Se, and it is not considered a significant risk driver due to its low inventory. The concentration of ^{129}I at the WMA C fenceline reaches a peak value of slightly greater than 1pCi/L in year 5920 at PoCal 6, with a second relative peak value of about 1.0 pCi/L occurring at PoCal 3 in year 8380 (Figure 7-17). The former value slightly exceeds the MCL for ^{129}I, which is 1 pCi/L, and the latter value is slightly less than the MCL. The maximum concentration values at the two aforementioned PoCals are about 0.8 and 0.6 pCi/L, respectively (Figure 7-18) at 100 m (328 ft) downgradient of the fenceline. The concentration of ^{129}I decreases from the peak values but persists at the PoCals through the end of the simulation period. The maximum concentration for PoCal 3 at 100 m (328 ft) downgradient of the WMA C fenceline in year 12020 is less than about 0.02 pCi/L.

Table 7-4. Summary Results of Radionuclides and Non-Radiological Contaminants that Arrive in Groundwater at the Waste Management Area C Fenceline before Closure. (3 sheets)

	Cobalt-60				Hydrogen-3 (Tritium)			
	Fenceline		100 Meters Downgradient		Fenceline		100 Meters Downgradient	
	Year of Peak	Peak Concentration (pCi/L)	Year of Peak	Peak Concentration (pCi/L)	Year of Peak	Peak Concentration (pCi/L)	Year of Peak	Peak Concentration (pCi/L)
PoCal 1	2036	0.6	2025	1	2030	11	2028	66
PoCal 2	2024	24	2024	34	2028	1,300	2028	1,700
PoCal 3	2024	200	2024	120	2027	10,000	2028	6,000
PoCal 4	2010	59	2011	97	2016	1,300	2025	2,500
PoCal 5	2009	990	2009	490	2013	20,000	2013	9,600
PoCal 6	2008	1,200	2009	860	2012	22,000	2013	16,000
PoCal 7	2009	200	2009	420	2013	3,800	2013	7,600
PoCal 8	2010	33	2010	92	2015	890	2014	2,000
PoCal 9	2011	5	2011	18	2015	140	2015	490
	Selenium-79				Technetium-99			
	Fenceline		100 Meters Downgradient		Fenceline		100 Meters Downgradient	
Year of Peak	Year of Peak	Peak Concentration (pCi/L)	Year of Peak	Peak Concentration (pCi/L)	Year of Peak	Peak Concentration (pCi/L)	Year of Peak	Peak Concentration (pCi/L)
PoCal 1	4515	0.1	4520	0.06	2055	1,500	2056	980
PoCal 2	4575	0.04	4555	0.06	2055	450	2055	720
PoCal 3	4910	0.04	4830	0.04	2026	910	2026	740
PoCal 4	4640	0.05	4605	0.05	2025	880	2025	1,100
PoCal 5	4045	0.3	4080	0.2	2019	5,000	2020	3,300
PoCal 6	4040	0.7	4045	0.5	2019	9,400	2019	6,600

Table 7-4. Summary Results of Radionuclides and Non-Radiological Contaminants that Arrive in Groundwater at the Waste Management Area C Fenceline before Closure. (3 sheets)

Selenium-79 (continued)					Technetium-99 (continued)			
	Fenceline		100 Meters Downgradient		Fenceline		100 Meters Downgradient	
Year of Peak	Year of Peak	Peak Concentration (pCi/L)	Year of Peak	Peak Concentration (pCi/L)	Year of Peak	Peak Concentration (pCi/L)	Year of Peak	Peak Concentration (pCi/L)
PoCal 7	4090	0.2	4065	0.4	2022	2,200	2021	4,100
PoCal 8	4100	0.05	4085	0.2	2024	240	2023	920
PoCal 9	4100	0.008	4095	0.04	2024	26	2024	150
Hexavalent Chromium					**Nitrate**			
	Fenceline		100 Meters Downgradient		Fenceline		100 Meters Downgradient	
	Year of Peak	Peak Concentration (mg/L)	Year of Peak	Peak Concentration (mg/L)	Year of Peak	Peak Concentration (mg/L)	Year of Peak	Peak Concentration (mg/L)
PoCal 1	2055	0.004	2055	0.003	2055	0.07	2052	0.1
PoCal 2	2032	0.006	2031	0.009	2032	2	2031	2
PoCal 3	2030	0.05	2030	0.03	2030	13	2031	7
PoCal 4	2026	0.008	2027	0.01	2026	1	2029	3
PoCal 5	2019	0.06	2020	0.03	2018	11	2018	6
PoCal 6	2020	0.08	2020	0.06	2017	12	2018	9
PoCal 7	2023	0.02	2022	0.03	2019	3	2019	5
PoCal 8	2023	0.004	2023	0.009	2020	0.6	2020	1
PoCal 9	2023	0.0005	2023	0.002	2020	0.1	2021	0.3

Table 7-4. Summary Results of Radionuclides and Non-Radiological Contaminants that Arrive in Groundwater at the Waste Management Area C Fenceline before Closure. (3 sheets)

Sulfate				
	Fenceline		100 Meters Downgradient	
	Year of Peak	Peak Concentration (mg/L)	Year of Peak	Peak Concentration (mg/L)
PoCal 1	2055	0.1	2056	0.07
PoCal 2	2054	0.05	2054	0.07
PoCal 3	2029	0.2	2029	0.2
PoCal 4	2025	0.08	2026	0.1
PoCal 5	2018	0.6	2019	0.3
PoCal 6	2018	0.9	2018	0.6
PoCal 7	2021	0.2	2020	0.4
PoCal 8	2022	0.03	2021	0.08
PoCal 9	2022	0.003	2022	0.02

Figure 7-4. Concentration of Technetium-99 in Groundwater in the Points of Calculation at the Fenceline.

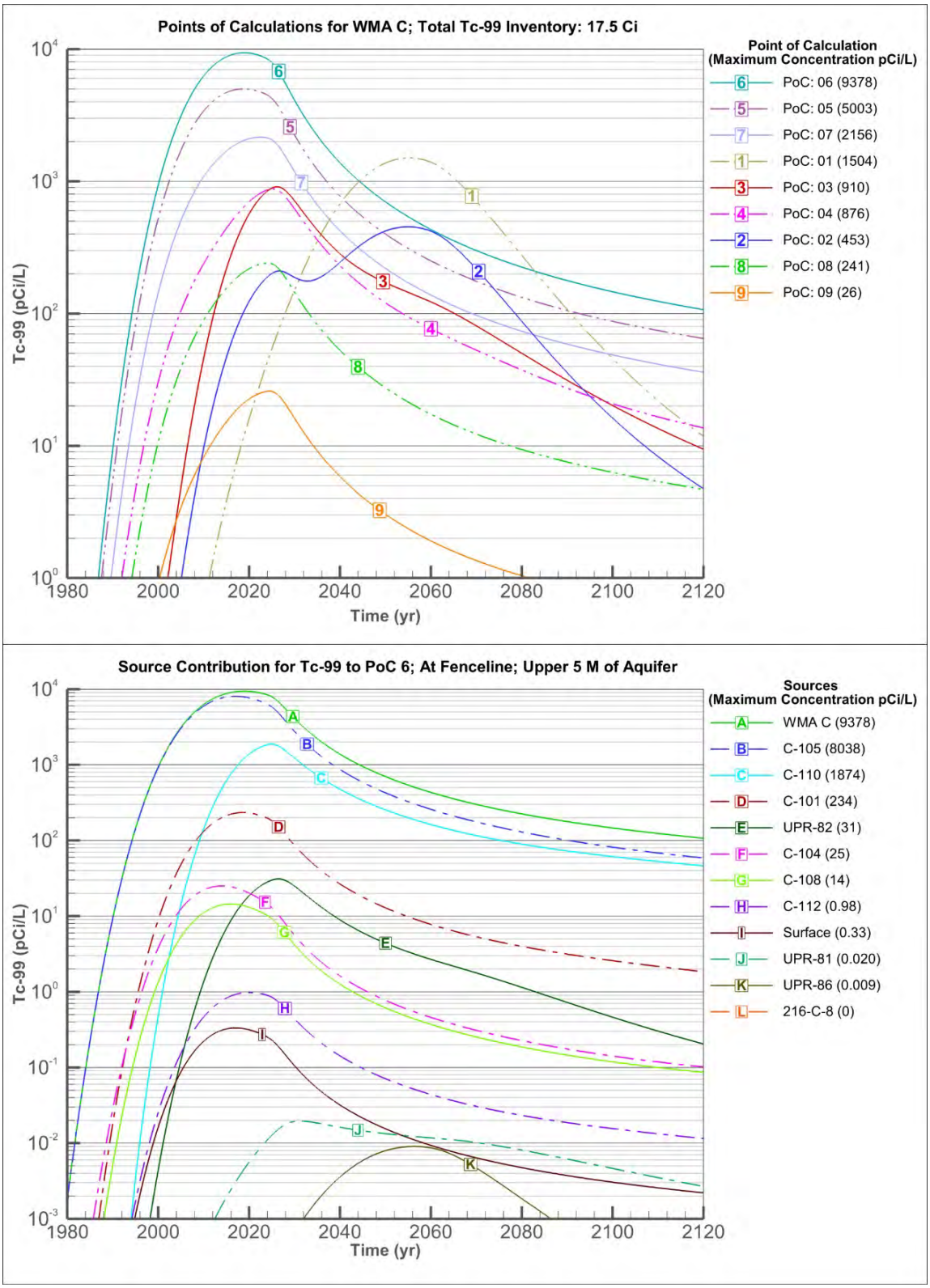

PoC = point of calculation WMA = Waste Management Area

Figure 7-5. Concentration of Technetium-99 in Groundwater in the Points of Calculation 100 Meters Downgradient of the Fenceline.

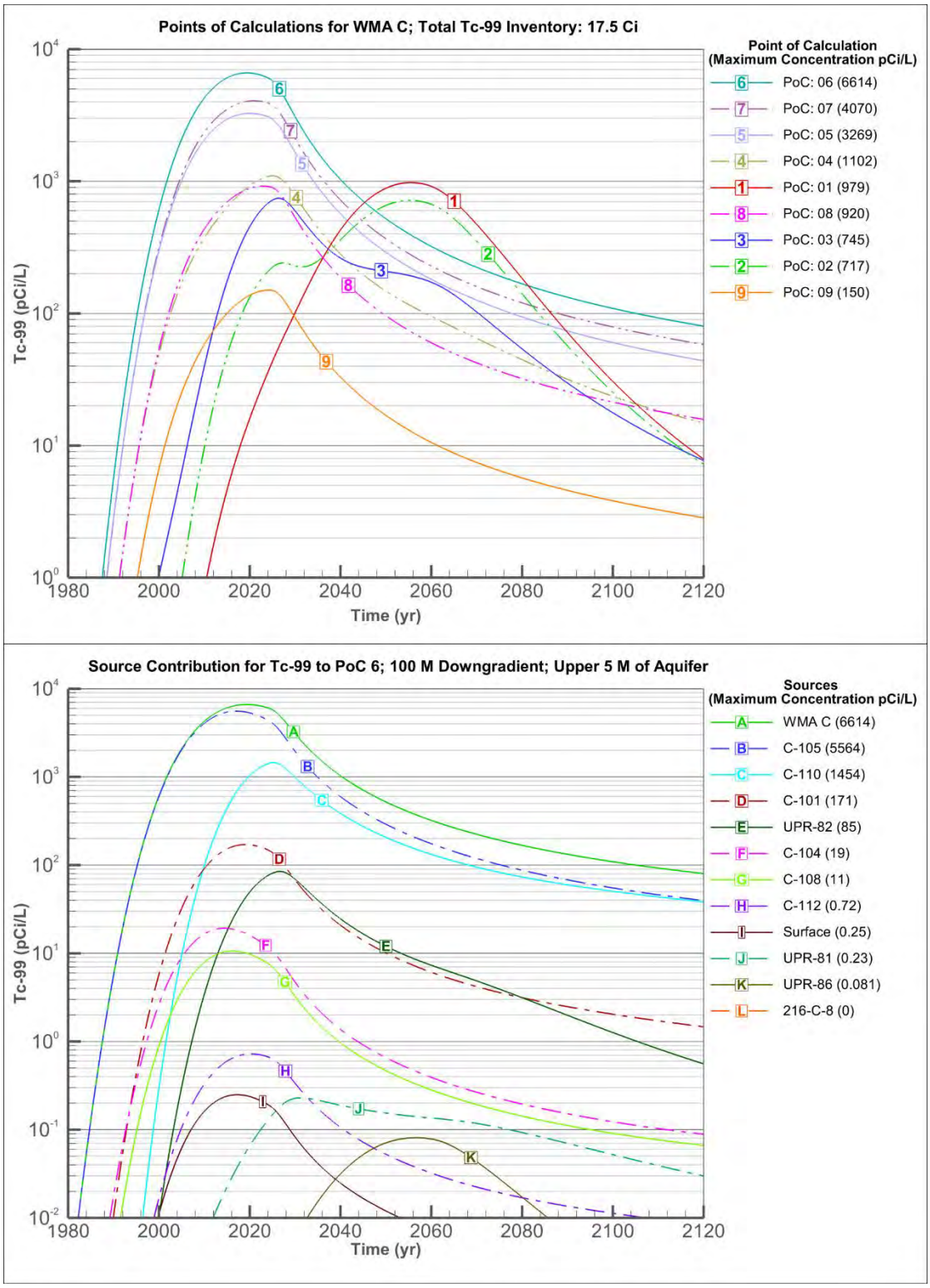

PoC = point of calculation WMA = Waste Management Area

Figure 7-6. Concentration of Tritium in Groundwater in the Points of Calculation at the Fenceline.

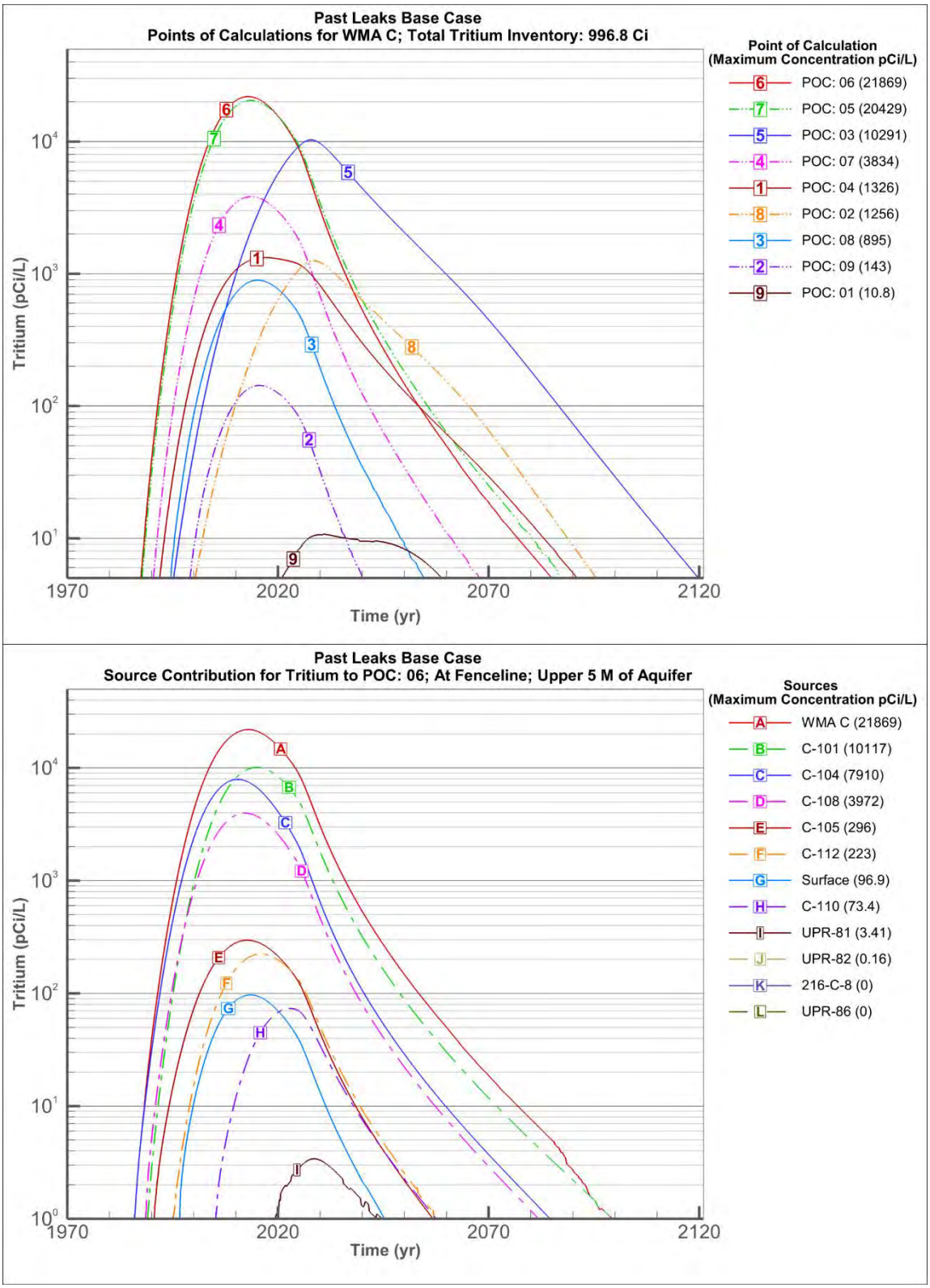

PoC = point of calculation WMA = Waste Management Area

Figure 7-7. Concentration of Tritium in Groundwater in the Points of Calculation 100 Meters Downgradient of the Fenceline.

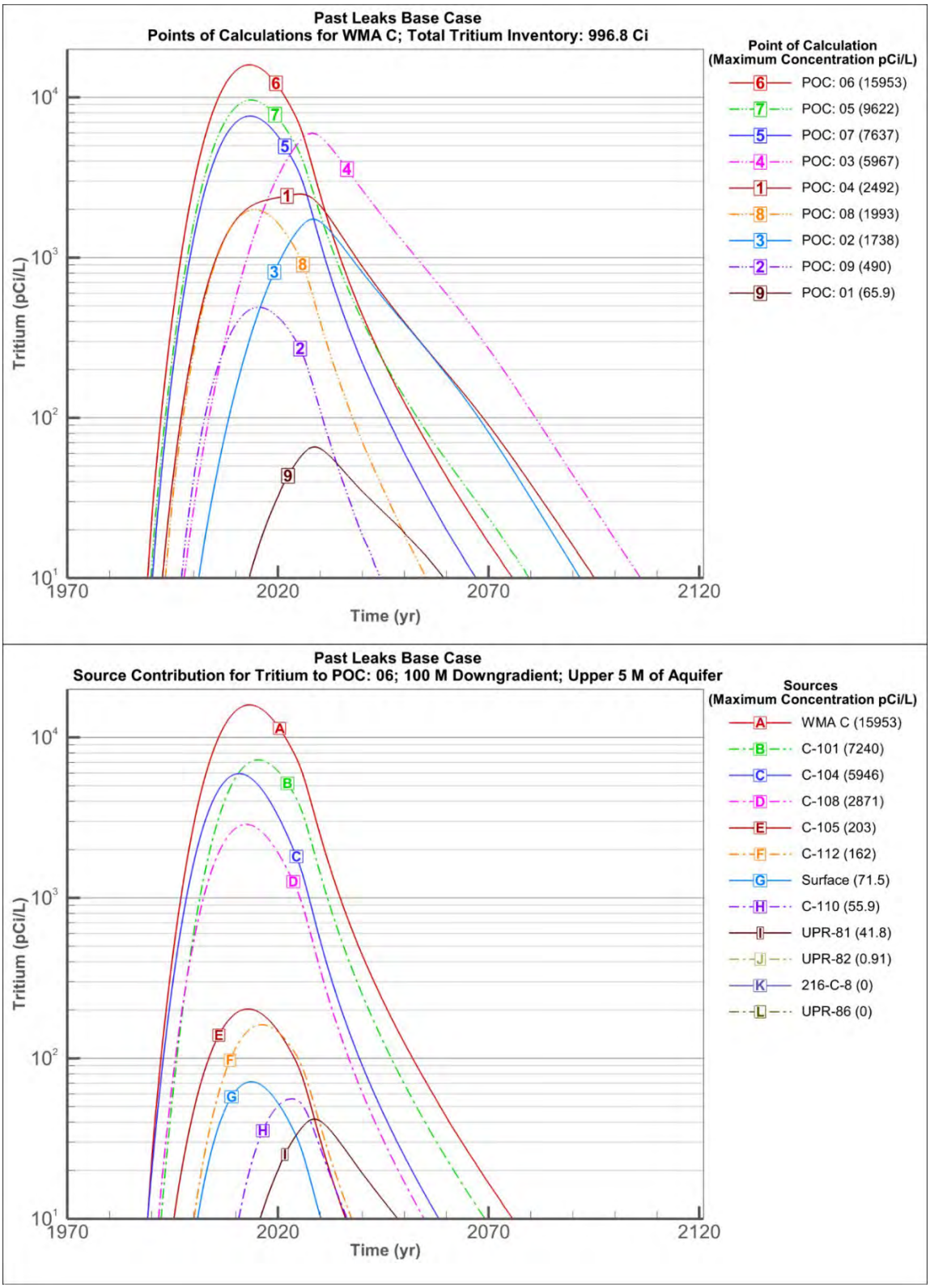

PoC = point of calculation WMA = Waste Management Area

Figure 7-8. Concentration of Cobalt-60 in Groundwater in the Points of Calculation 100 Meters Downgradient of the Fenceline.

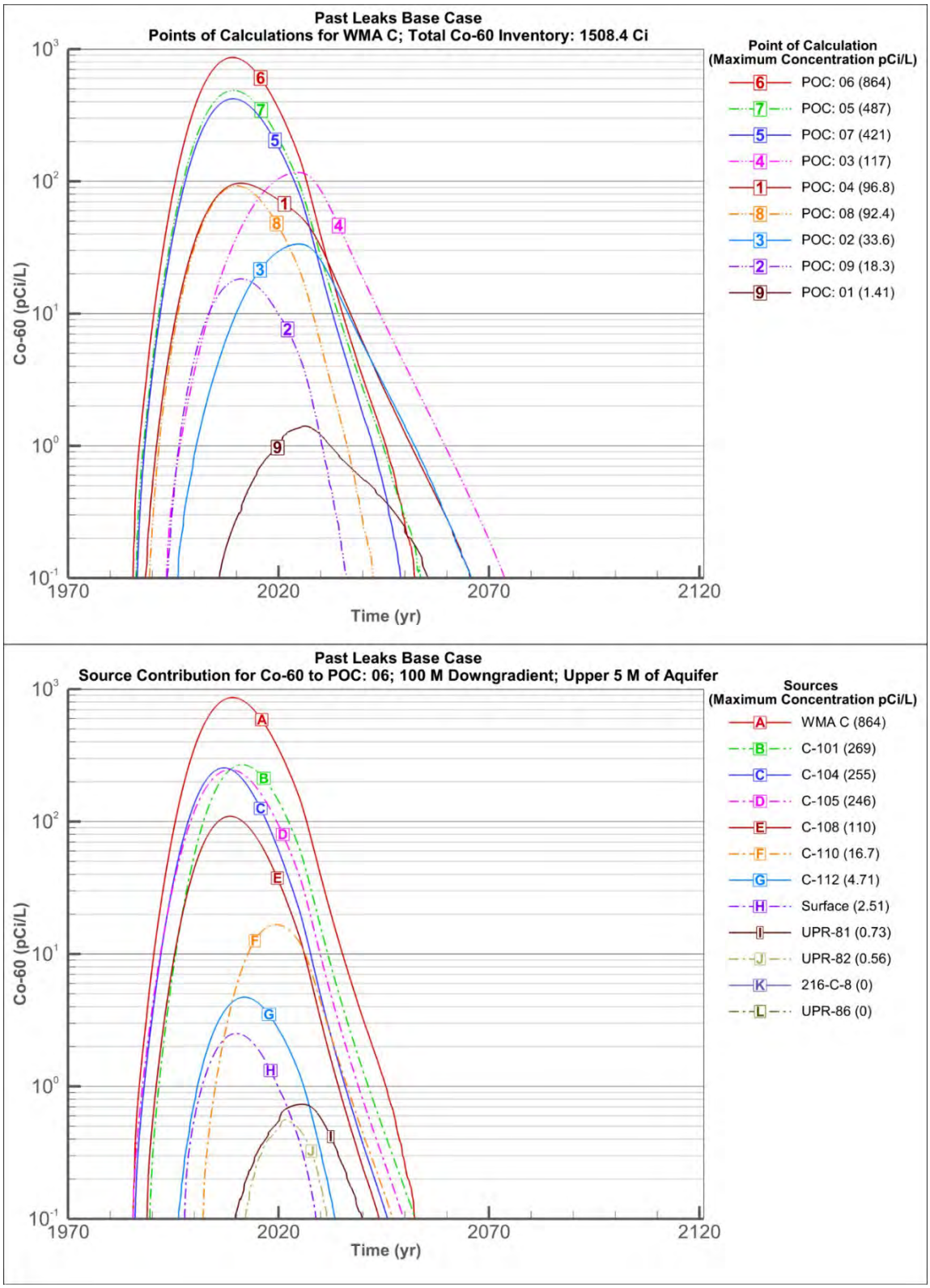

PoC = point of calculation WMA = Waste Management Area

Figure 7-9. Concentration of Selenium-79 in Groundwater in the Points of Calculation 100 Meters Downgradient of the Fenceline.

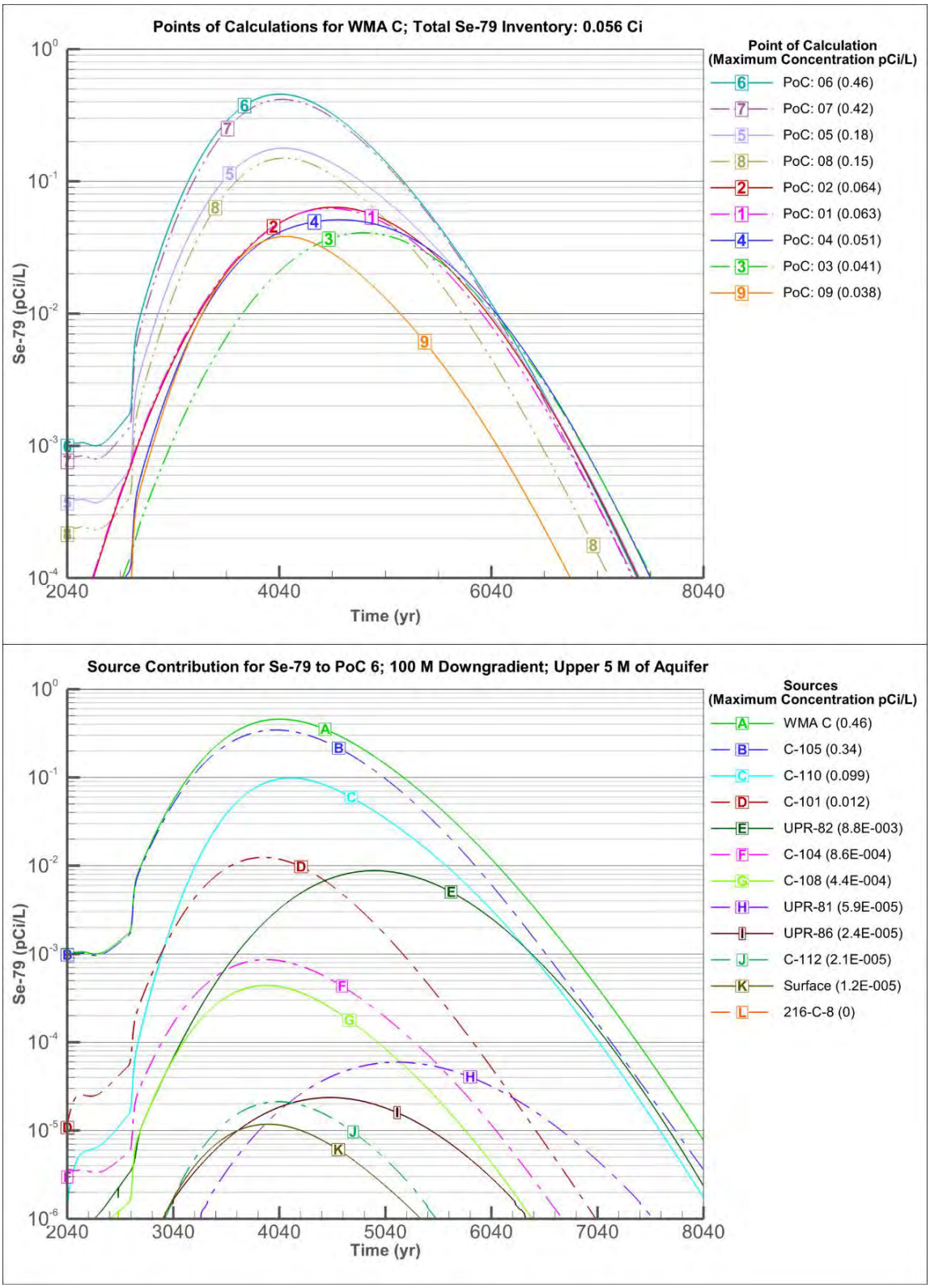

PoC = point of calculation WMA = Waste Management Area

Figure 7-10. Concentration of Nitrate in Groundwater in the Points of Calculation 100 Meters Downgradient of the Fenceline.

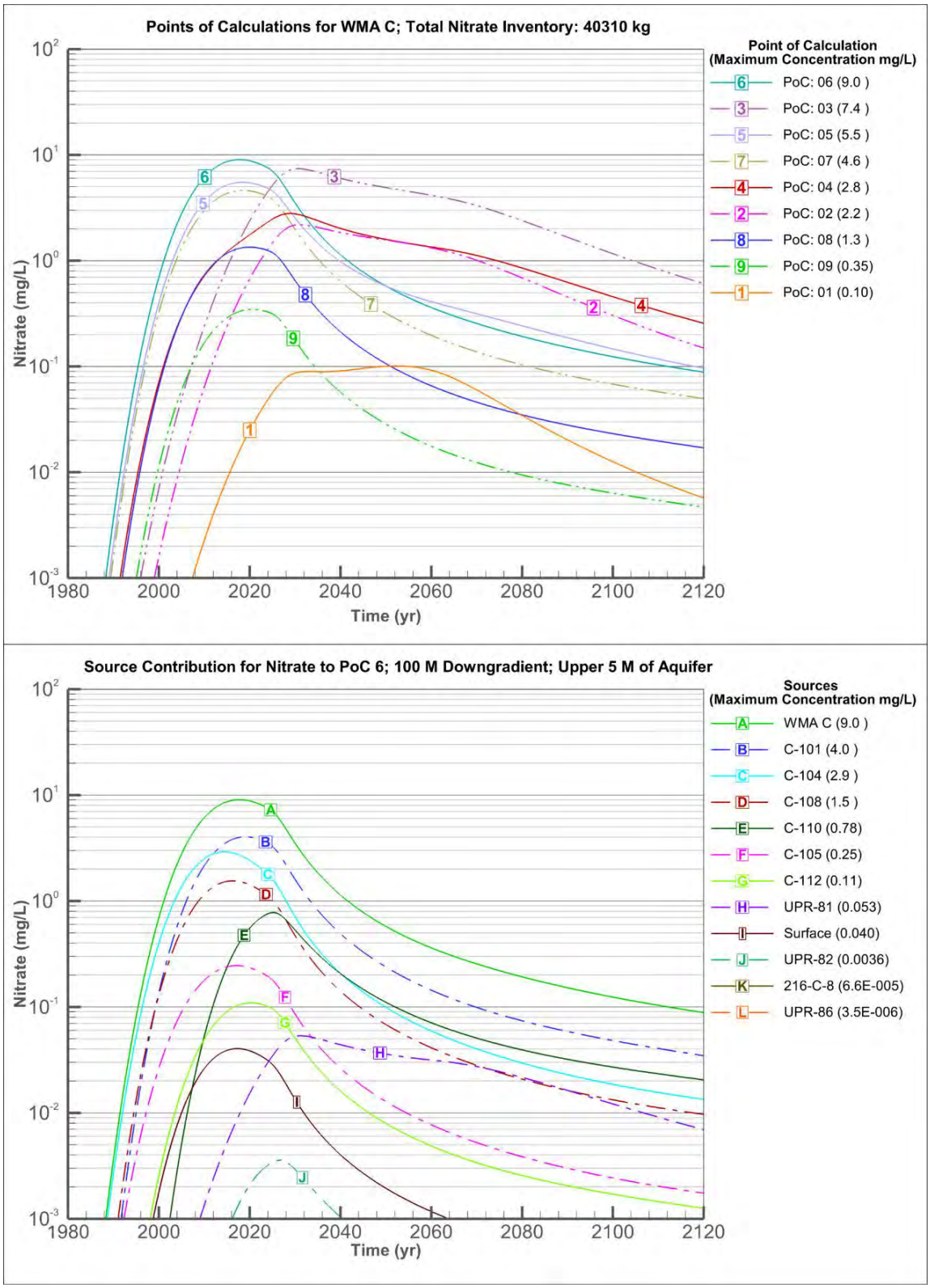

PoC = point of calculation WMA = Waste Management Area

Figure 7-11. Concentration of Sulfate in Groundwater in the Points of Calculation 100 Meters Downgradient of the Fenceline.

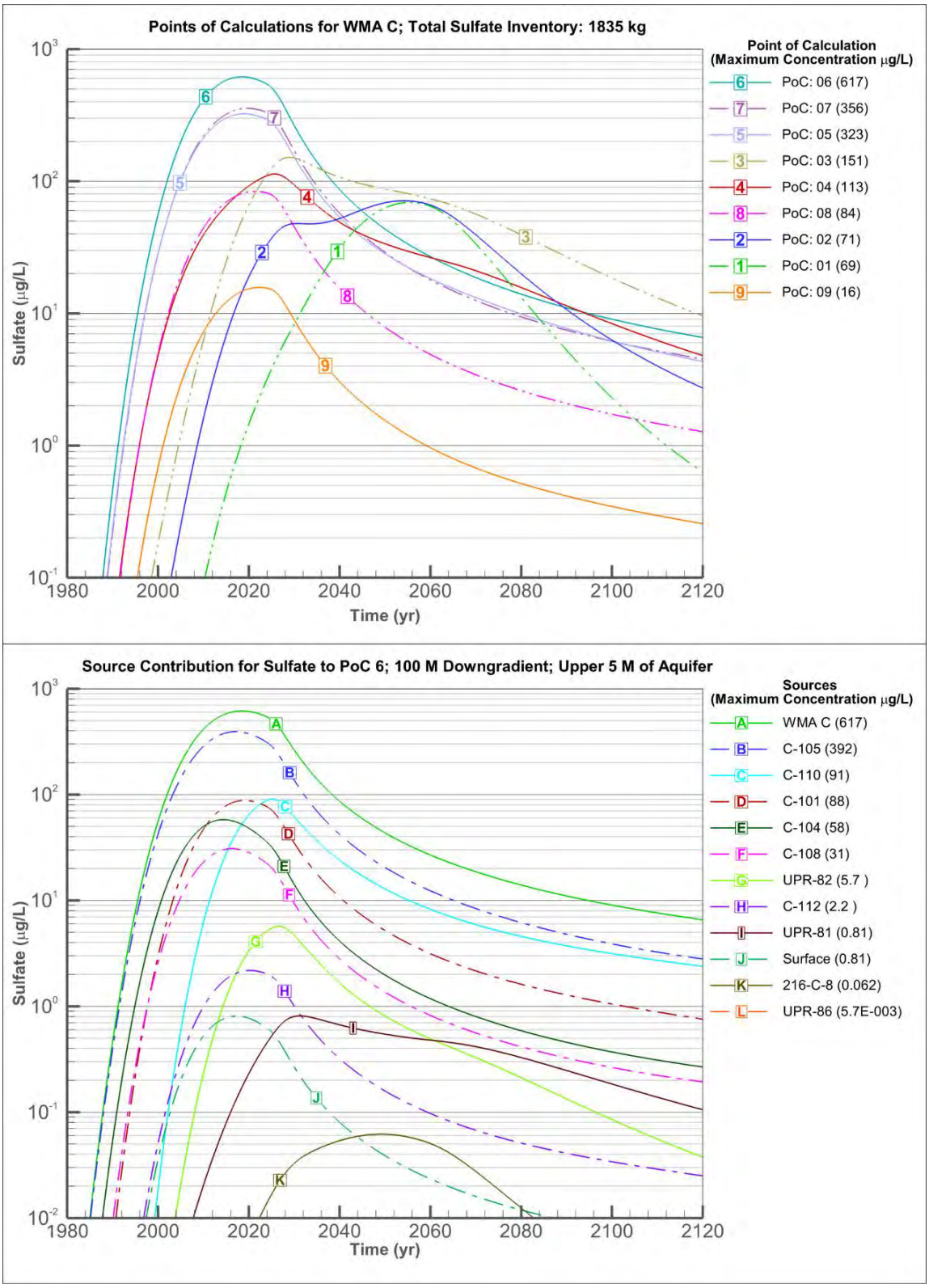

PoC = point of calculation WMA = Waste Management Area

Figure 7-12. Concentration of Chromium (as Cr^{+6}) in Groundwater in the Points of Calculation 100 Meters Downgradient of the Fenceline.

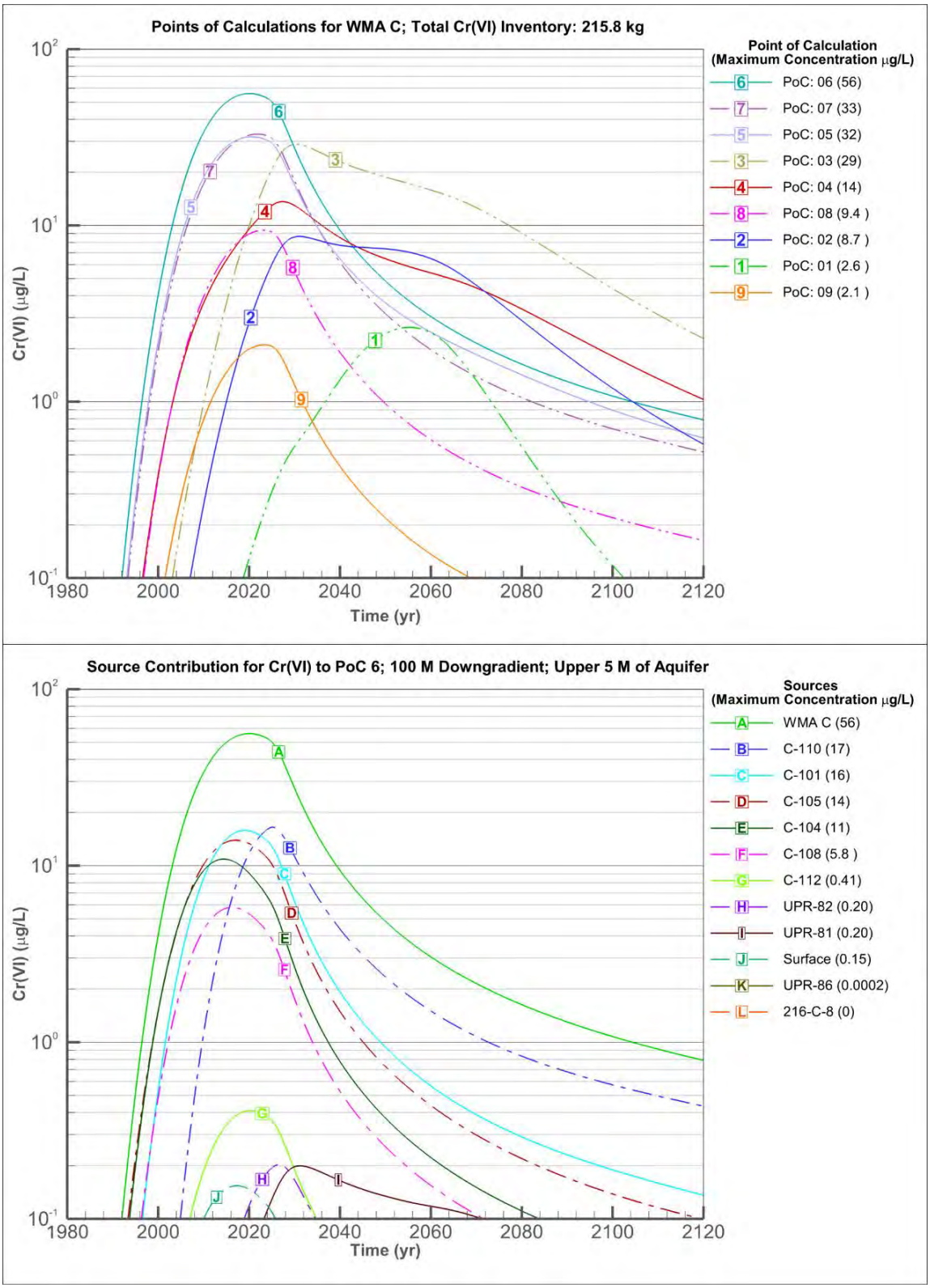

PoC = point of calculation WMA = Waste Management Area

Figure 7-13. Concentration Contours of Technetium-99 along Cross-Section Planes through Unplanned Releases 200-E-81 and 200-E-82 and Tank Row 241-C-110, 241-C-107, 241-C-104 and 241-C-101 Corresponding to Year 2000.

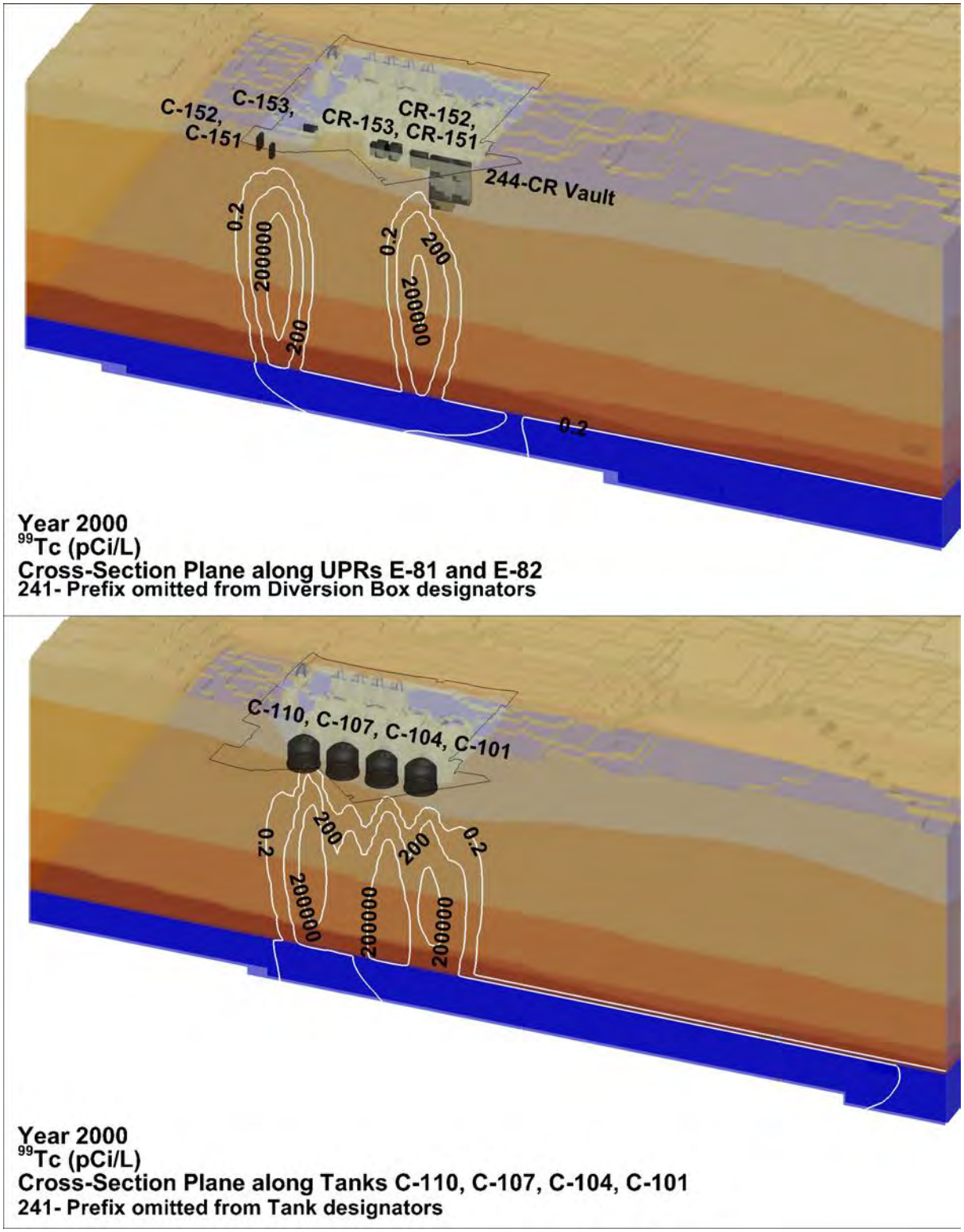

UPR = unplanned release

Figure 7-14. Concentration Contours of Technetium-99 along Cross-Section Planes through Unplanned Releases 200-E-81 and 200-E-82 and Tank Row 241-C-110, 241-C-107, 241-C-104 and 241-C-101 Corresponding to Year 2016.

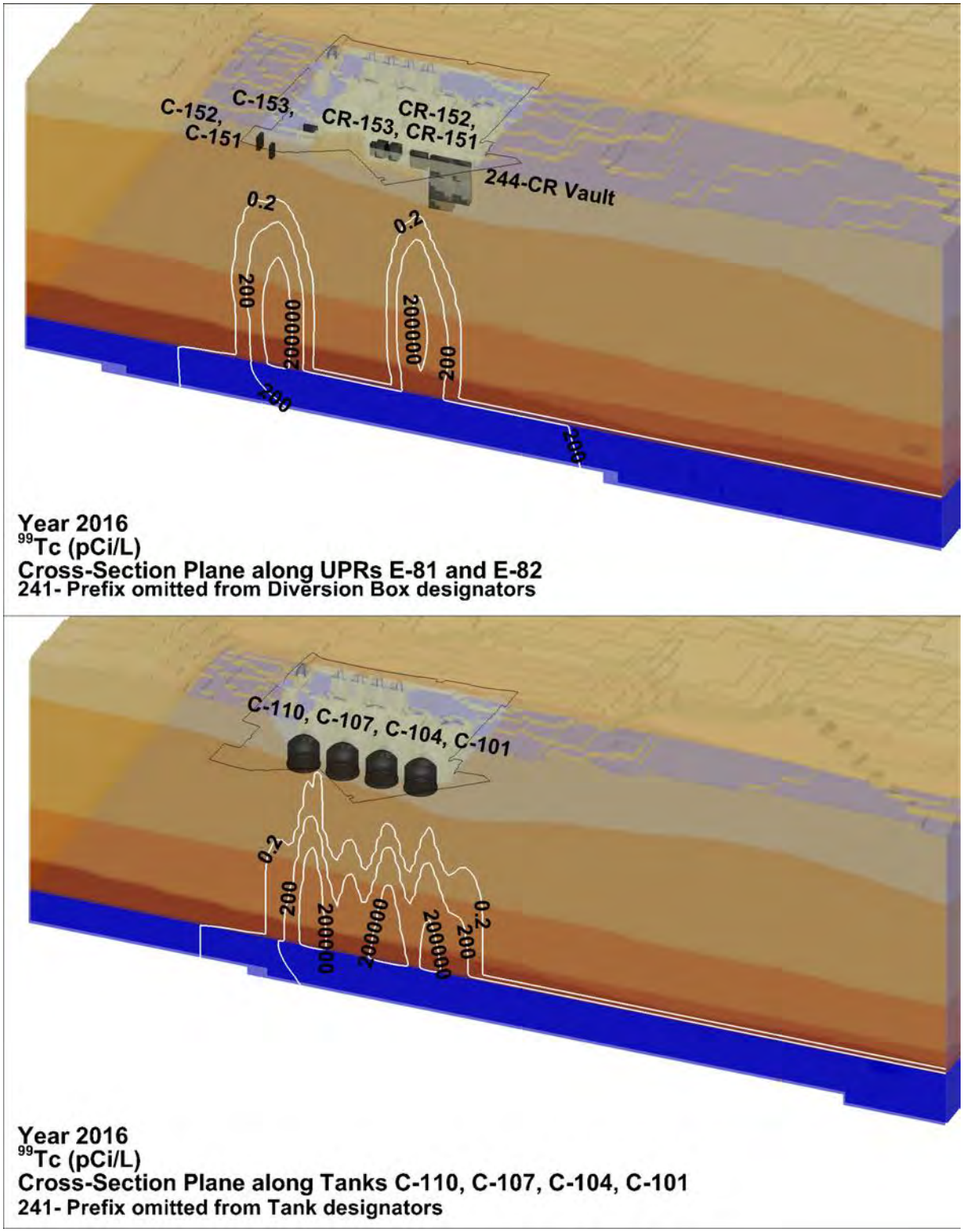

UPR = unplanned release

Figure 7-15. Concentration Contours of Nitrate along Cross-Section Planes through Unplanned Releases 200-E-81 and 200-E-82 and Tank Row 241-C-110, 241-C-107, 241-C-104 and 241-C-101 Corresponding to Year 2000.

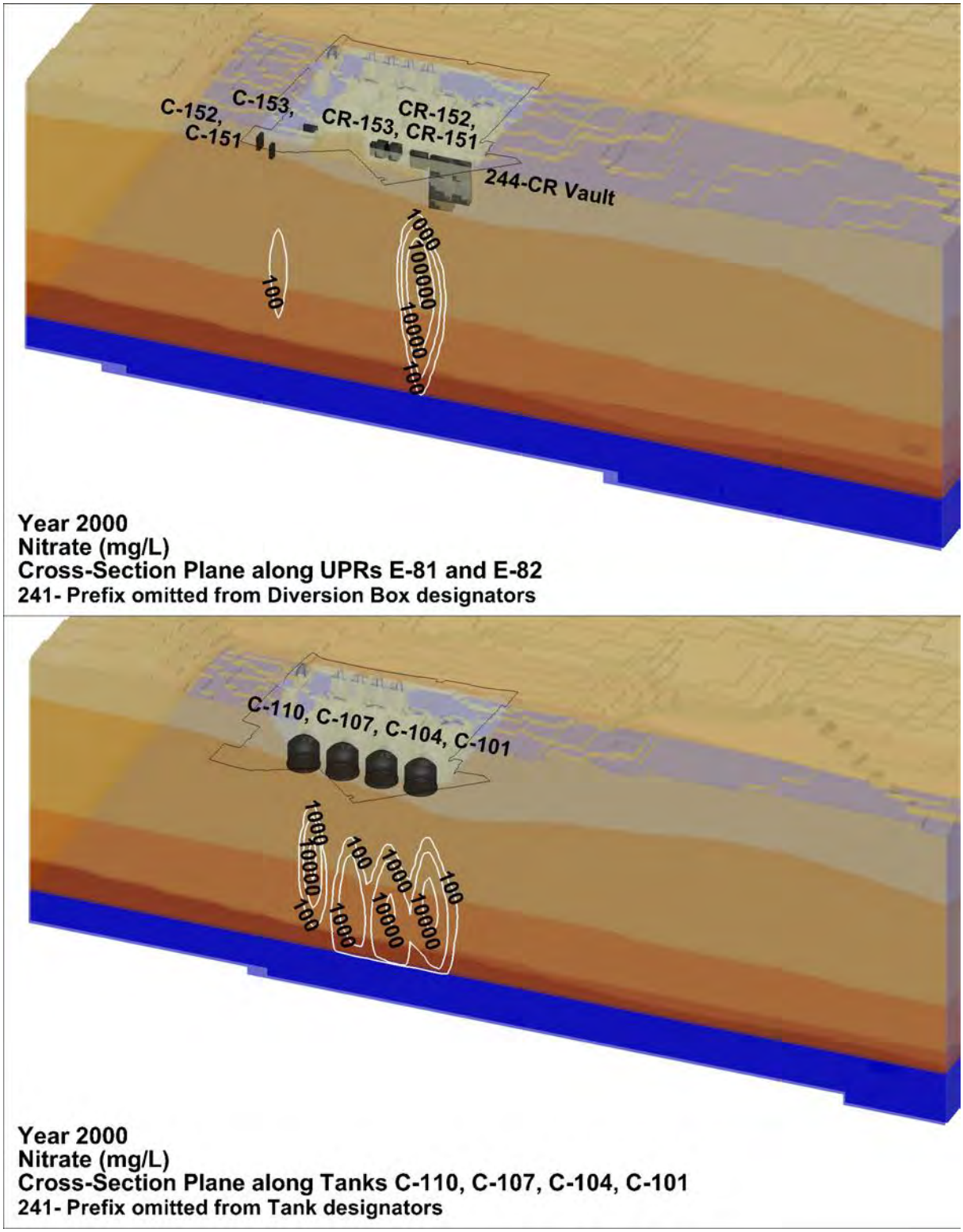

UPR = unplanned release

Figure 7-16. Concentration Contours of Nitrate along Cross-Section Planes through Unplanned Releases 200-E-81 and 200-E-82 and Tank Row 241-C-110, 241-C-107, 241-C-104 and 241-C-101 Corresponding to Year 2016.

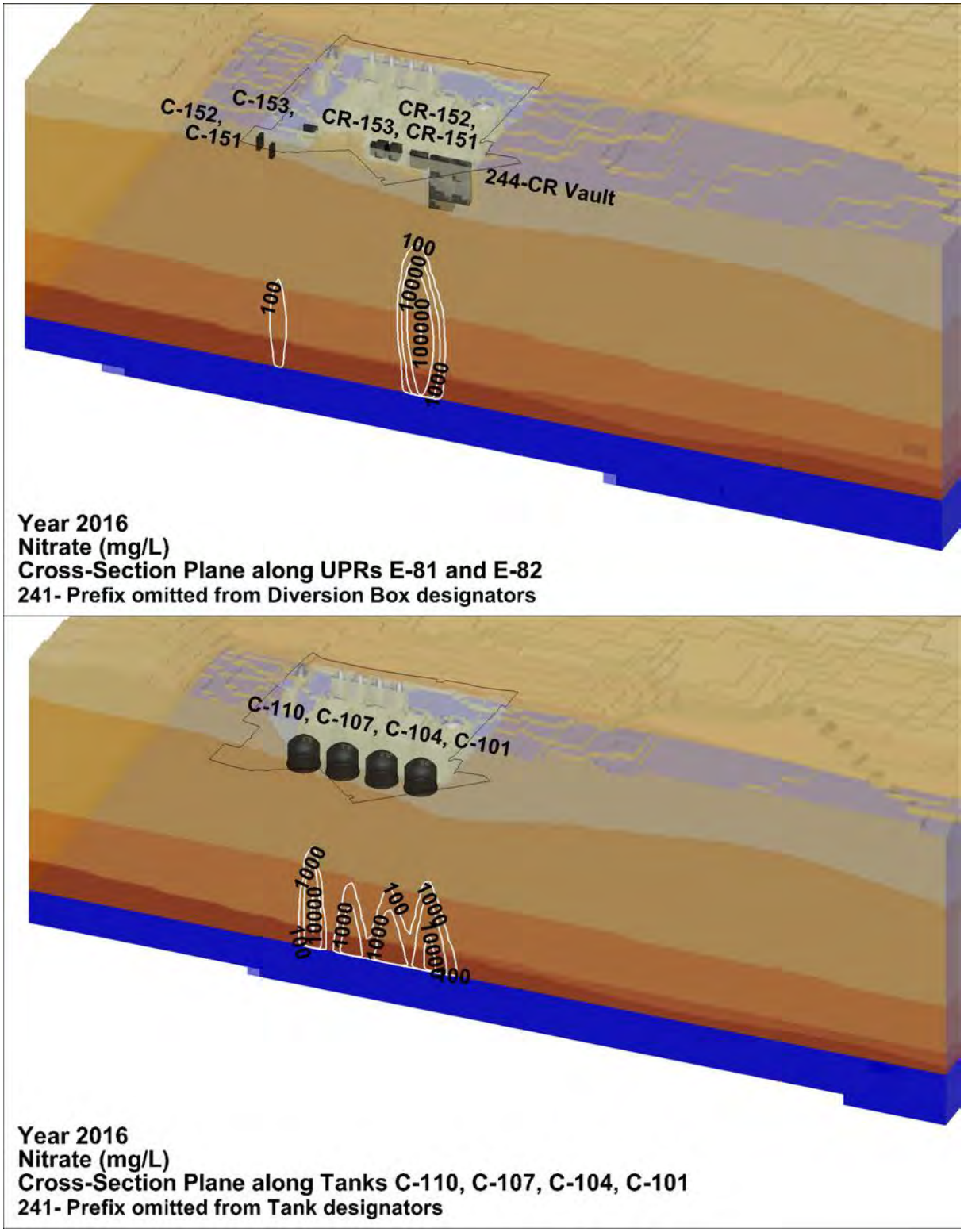

UPR = unplanned release

Figure 7-17. Concentration of Iodine-129 in Groundwater in the Points of Calculation at the Fenceline.

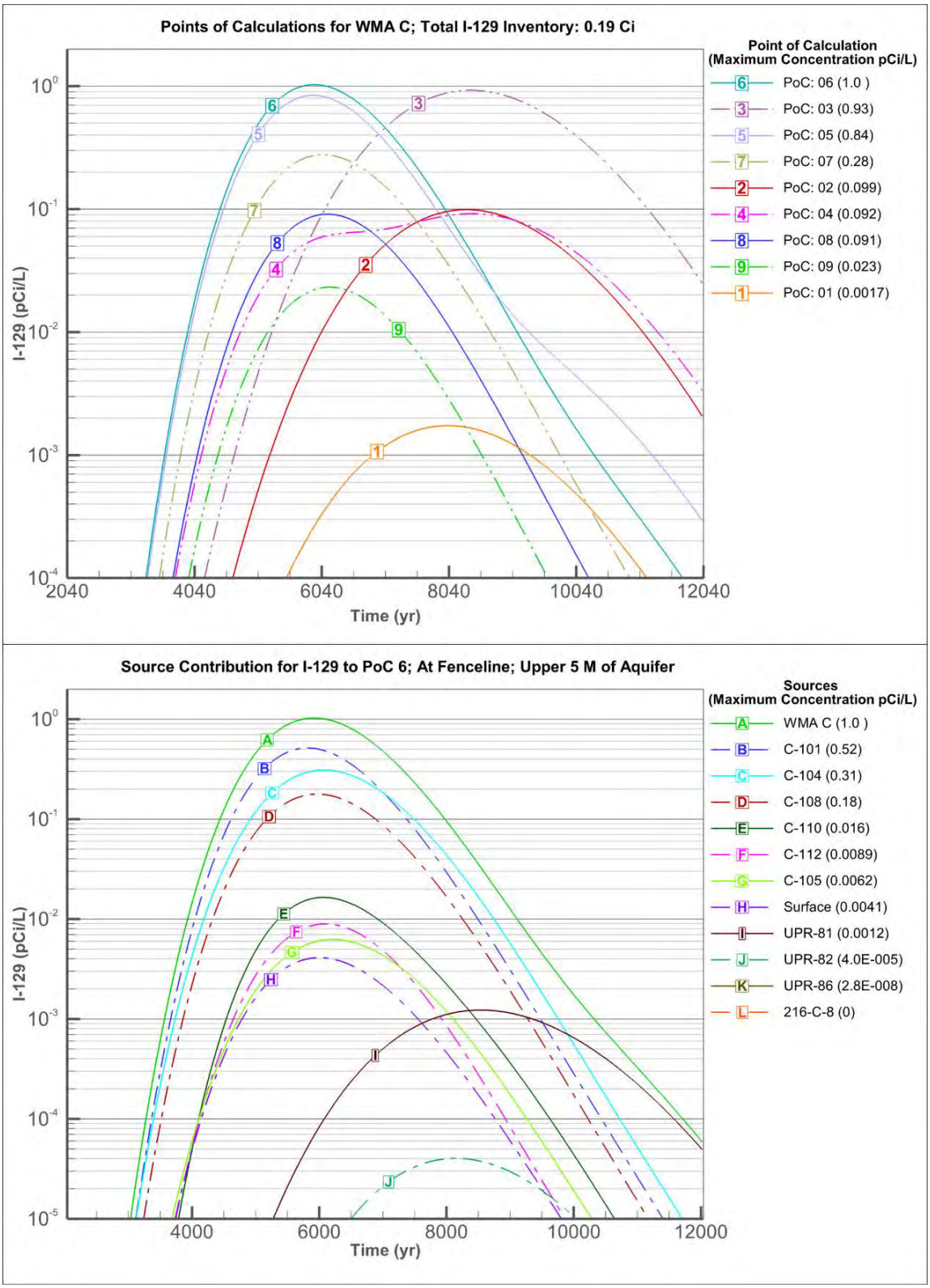

PoC = point of calculation WMA = Waste Management Area

Figure 7-18. Concentration of Iodine-129 in Groundwater in the Points of Calculation 100 Meters Downgradient of the Fenceline.

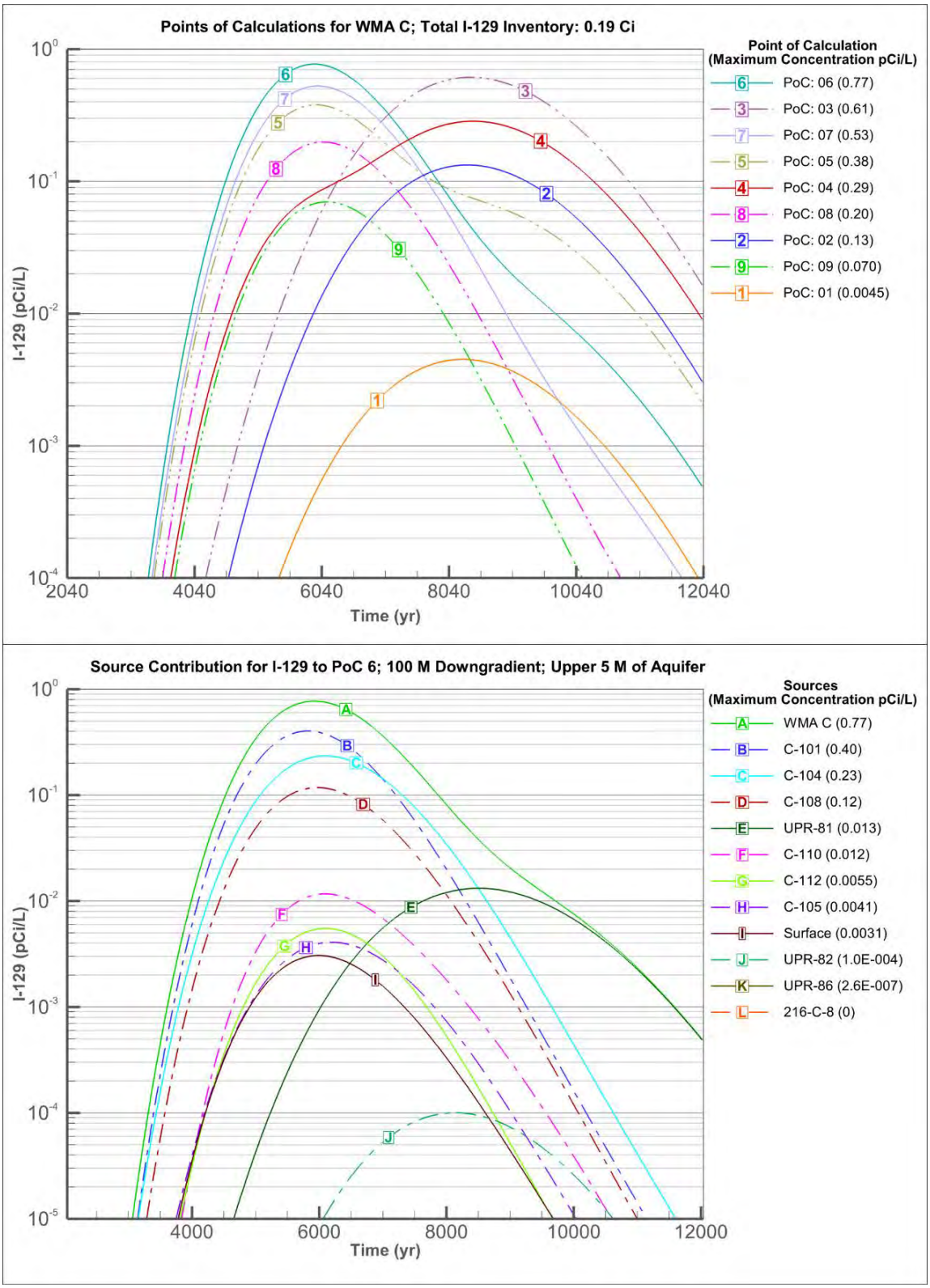

PoC = point of calculation WMA = Waste Management Area

The calculated concentration of ^{126}Sn reaches a peak 10,000 years after the assumed closure of WMA C in year 2020. The maximum concentration 100 m (328 ft) downgradient of the WMA C fenceline at this time is 0.5 pCi/L at PoCal 6 (Figure 7-19). Neither the concentration of ^{238}U or total uranium reach a peak within 10,000 years after the assumed closure of WMA C. Both of the trends are increasing at the end of the evaluation period. The maximum concentration of ^{238}U remains less than 0.01 pCi/L (Figure 7-20), and the concentration of total uranium reaches a maximum value of ~0.02 µg/L (Figure 7-21). Similar to ^{99}Tc and other nonsorbing radionuclides and non-radiological contaminants, the maximum concentration of ^{238}U and total uranium at 100 m (328 ft) downgradient of the WMA C fenceline represent an approximate 25 percent reduction in concentration from the fenceline values (Figures 7-22 and 7-23, respectively). Table 7-5 provides a summary of results for those radionuclides and non-radiological contaminants that arrive in groundwater at the WMA C fenceline after the assumed date of closure in year 2020.

7.3.3 Results of Groundwater Pathway Evaluation: Contaminant Flux to Groundwater

Neither the concentration of ^{238}U nor total uranium reach a peak within 10,000 years after the assumed closure of WMA C. Both of the trends are increasing at the end of the evaluation period. The maximum concentration of ^{238}U remains less than 0.01 pCi/L (Figure 6-20), and the concentration of total uranium reaches a maximum value of ~0.02 µg/L (Figure 6-21). For purposes of this analysis, the simulations were only performed up to 10,000 years after the assumed closure of WMA C. However, results of impacts from release of uranium from tank residuals done in RPP-ENV-58782 would suggest that peak concentrations for ^{238}U (and other uranium isotopes) and total uranium from the past leak releases would likely occur between 14,000 and 15,000 years post-closure at levels well below the DWS of 30 ug/l.

Figures 7-24 through 7-27 show the calculated fluxes of ^{99}Tc, NO_3, ^{79}Se, and ^{238}U from the vadose zone entering groundwater. The source of ^{99}Tc associated with tank C-105 dominates the ^{99}Tc flux to groundwater, especially during the time that the peak concentrations occur in groundwater at PoCal 6 (Figure 7-24). The source associated with tank C-110 provides the second largest flux and is the second largest component of the absolute peak concentration of ^{99}Tc that occurs at PoCal 6 (refer to Figures 7-4 and 7-5). Although the sources of ^{99}Tc associated with UPRs E-86 and E-82 provide the third and fourth largest fluxes, respectively, the plumes in groundwater resulting from the UPRs are offset from PoCal 6 and do not contribute substantially to the concentration calculated there. Tank C-101 is better aligned with PoCal 6 than the UPRs, thus although the flux of ^{99}Tc associated with that tank is less than either of those two UPRs, it is the third largest contributor to the peak concentration of ^{99}Tc that occurs at PoCal 6. The arrival of the ^{99}Tc fluxes at the water table from the three UPRs not ascribed to a particular tank (i.e., UPRs E-81, E-82, and E-86) lags the arrival of the flux from tank C-105 because the three UPRs occur after the tank C-105 release and begin at shallower depths in the vadose zone. In addition, UPR E-86 is located outside the tank farm, where the ground is described as resurfaced and the net infiltration (63 mm/yr [2.47 in./yr]) is less than the amount in the tank farm gravel (100 mm/yr [3.94 in./yr]).

As indicated back in Figure 7-10, the concentration of nitrate reaches its absolute peak value at PoCal 6 in 2017. The sources of nitrate associated with the six tank-ascribed UPRs are the

six largest contributors to the peak concentration, even though the source and flux associated with UPR-81 is larger than any of those associated with the tanks (Figure 7-25). The proximity of the tank-ascribed UPRs to one another and their alignment with PoCal 6 result in comingling of the sources and fluxes. The relative peak that occurs later in year 2030 at PoCal 3 is almost solely a consequence of the source associated with UPR-81, and the nitrate flux associated with UPR-81 is almost entirely responsible for producing the concentration calculated at PoCal 3.

Based in information provided in Appendix A, the overall trends in flux of cyanide from tanks C-108 and C-112, which are the tanks with the largest estimated cyanide inventories, from the vadose zone to groundwater would be similar to trends in fluxes for nitrate from the vadose zone to groundwater for the same tanks (see results provided in Figure 7-25).

The source of ^{79}Se associated with tank C-105 dominates the ^{79}Se fluxes to groundwater, especially during the time that the peak concentrations occur in groundwater at PoCals 6 and 7 (Figure 7-26). The ^{79}Se breakthrough curves for PoCals 6 and 7 are nearly identical (refer to Figure 7-9). The source associated with tank C-110 provides the second largest flux and is the second largest component of the absolute peak concentration of ^{99}Tc that occurs at both PoCal 6 and PoCal 7. The flux of ^{79}Se associated with tank C-105 is responsible for about 75 percent of the total flux and resulting concentration at PoCals 6 and 7. Together, the sources of ^{79}Se associated with tanks C-105 and C-110 provide more than 95 percent of the total flux and resulting concentration at PoCals 6 and 7.

As indicated back in Figure 7-20, the concentration of ^{238}U does not reach its maximum value at any of the PoCals until the end of the simulation period 10,000 years after the assumed closure date of WMA C. The absolute peak concentration likely occurs after this time. Similarly, the flux of ^{238}U to groundwater does not reach its maximum value until the end of the simulation period (Figure 7-27). The source of ^{238}U associated with tank C-101 is the largest component of the flux of ^{238}U to groundwater, and by itself is responsible for approximately half of the ^{238}U that enters groundwater. The next two largest fluxes indicated by Figure 7-27 result from the UPRs associated with tanks C-104 and C-108, but the magnitude of these flux values is approximately one-third that of the maximum flux resulting from the tank C-101 UPR.

Figure 7-19. Concentration of Tin-126 in Groundwater in the Points of Calculation 100 Meters Downgradient of the Fenceline.

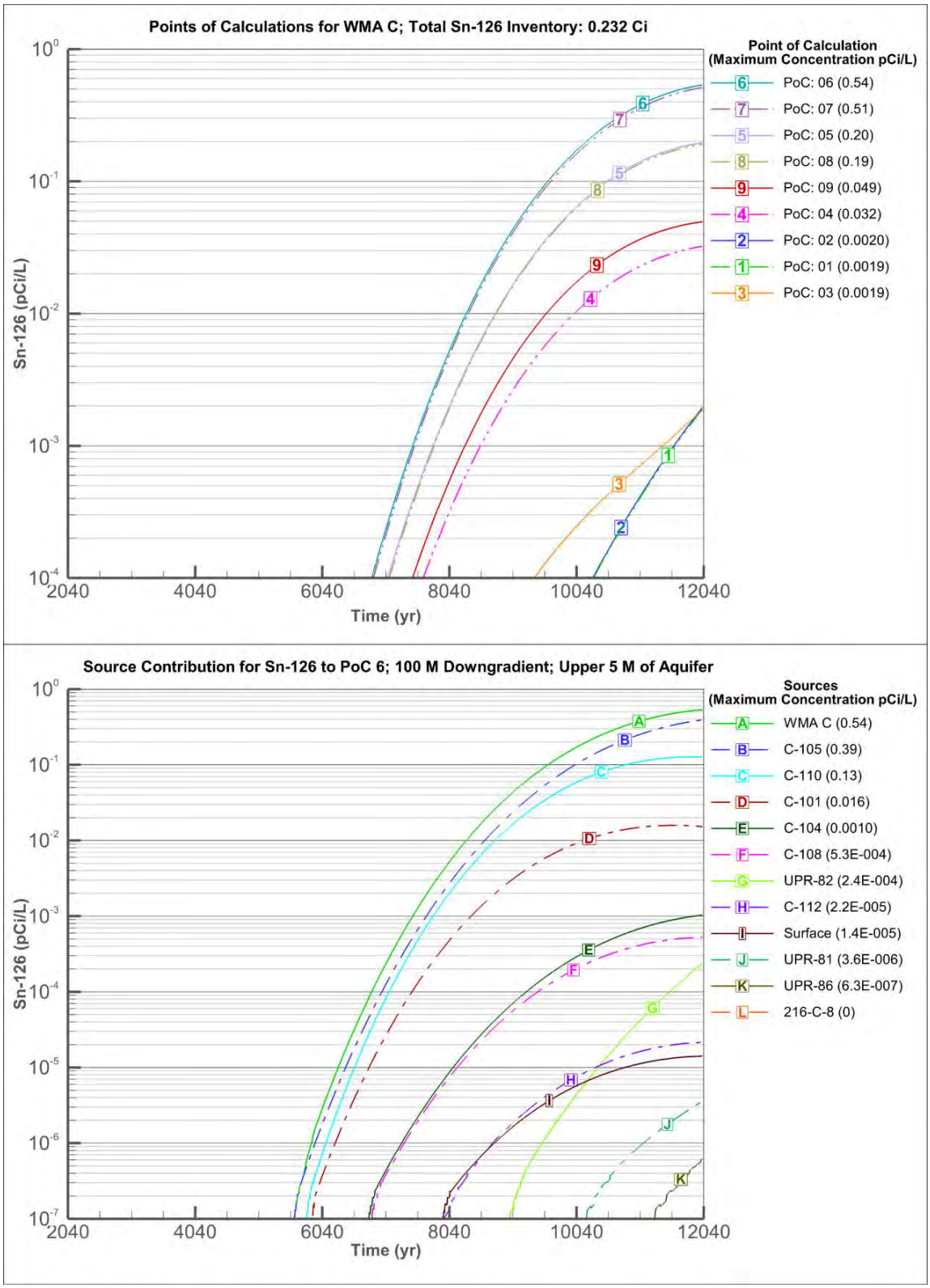

PoC = point of calculation WMA = Waste Management Area

Figure 7-20. Concentration of Uranium-238 in Groundwater in the Points of Calculation 100 Meters Downgradient of the Fenceline.

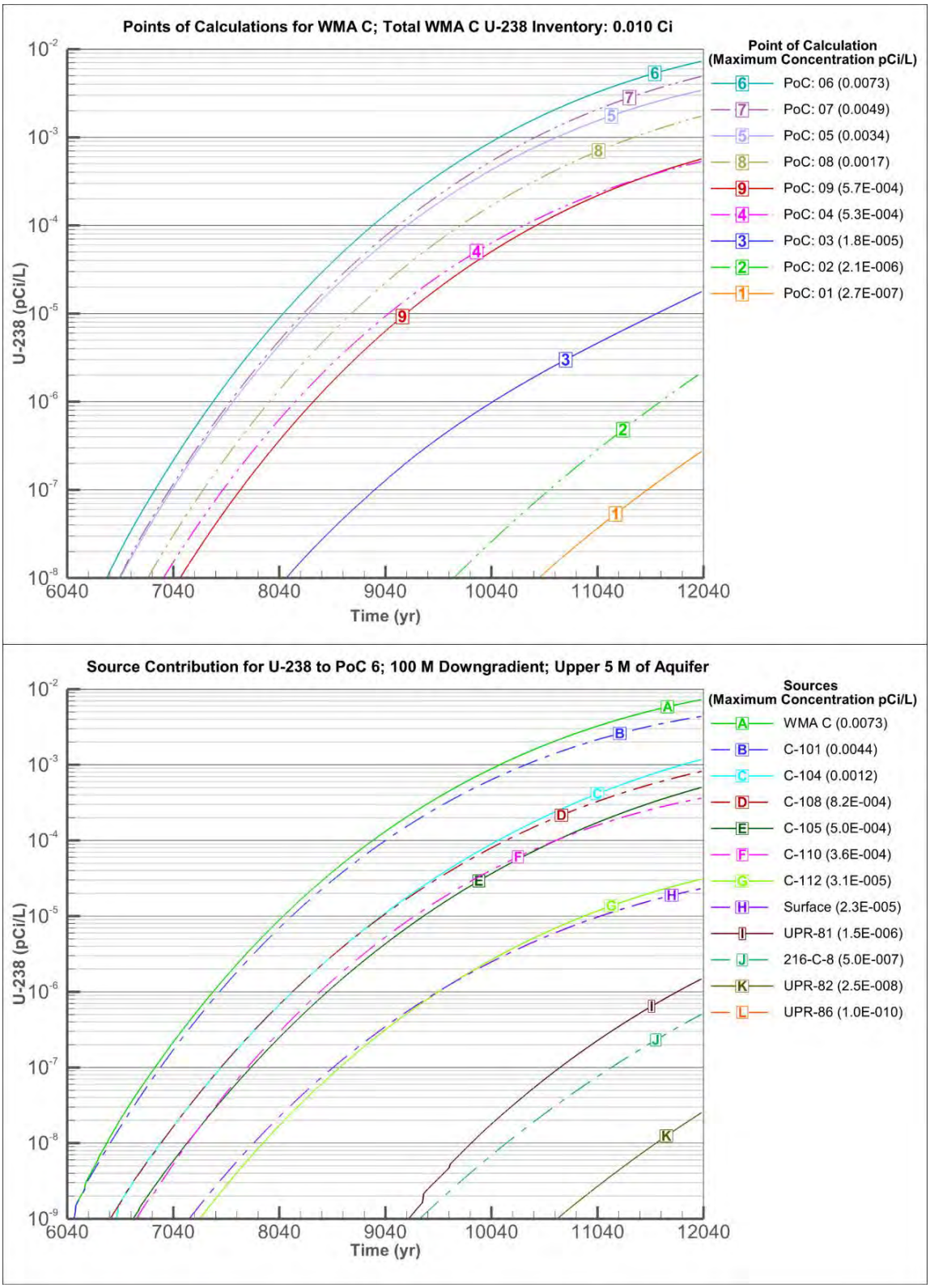

PoC = point of calculation WMA = Waste Management Area

Figure 7-21. Concentration of Total Uranium in Groundwater in the Points of Calculation 100 Meters Downgradient of the Fenceline.

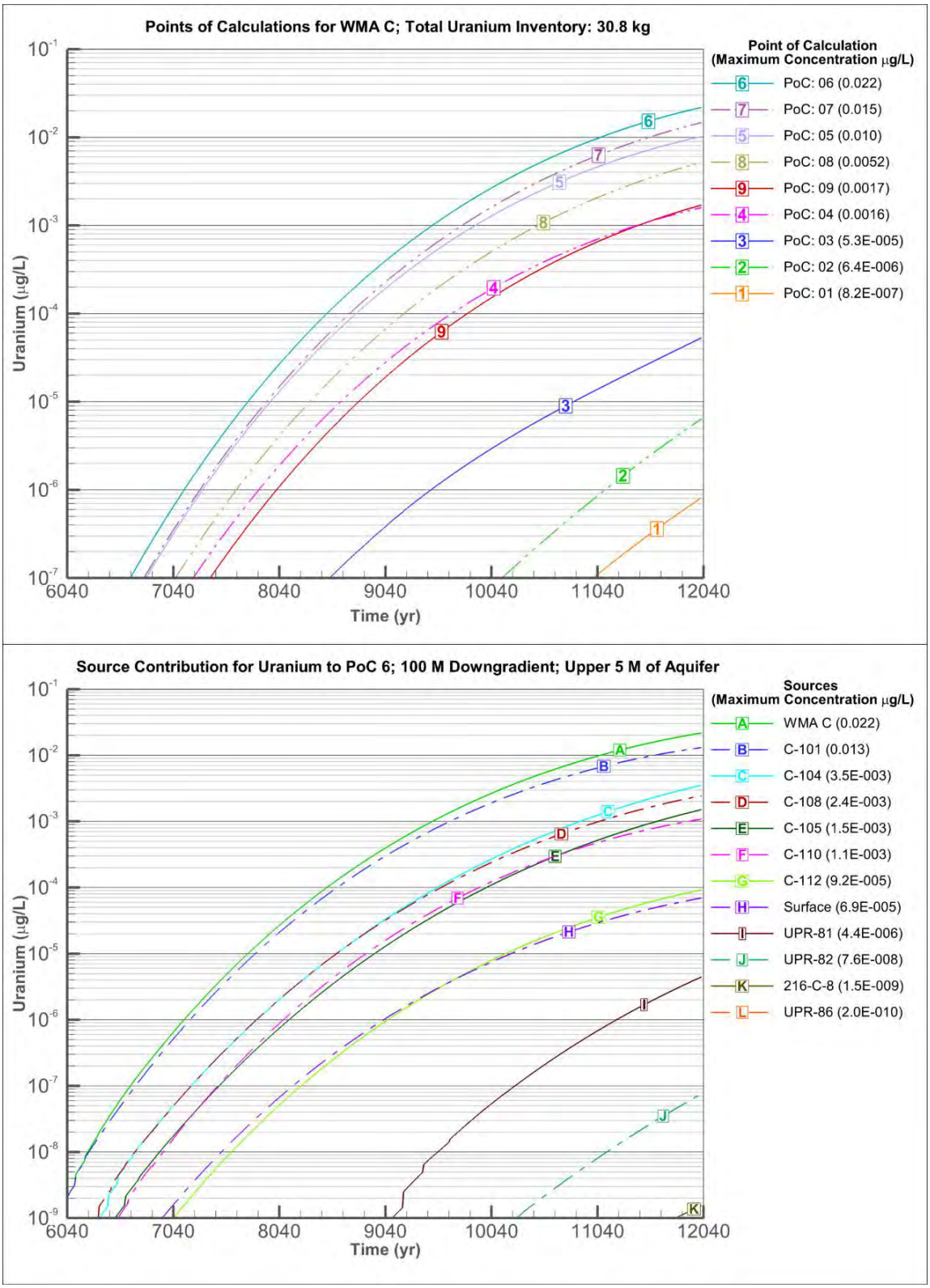

PoC = point of calculation WMA = Waste Management Area

Figure 7-22. Concentration of Uranium-238 in Groundwater in the Points of Calculation at the Fenceline.

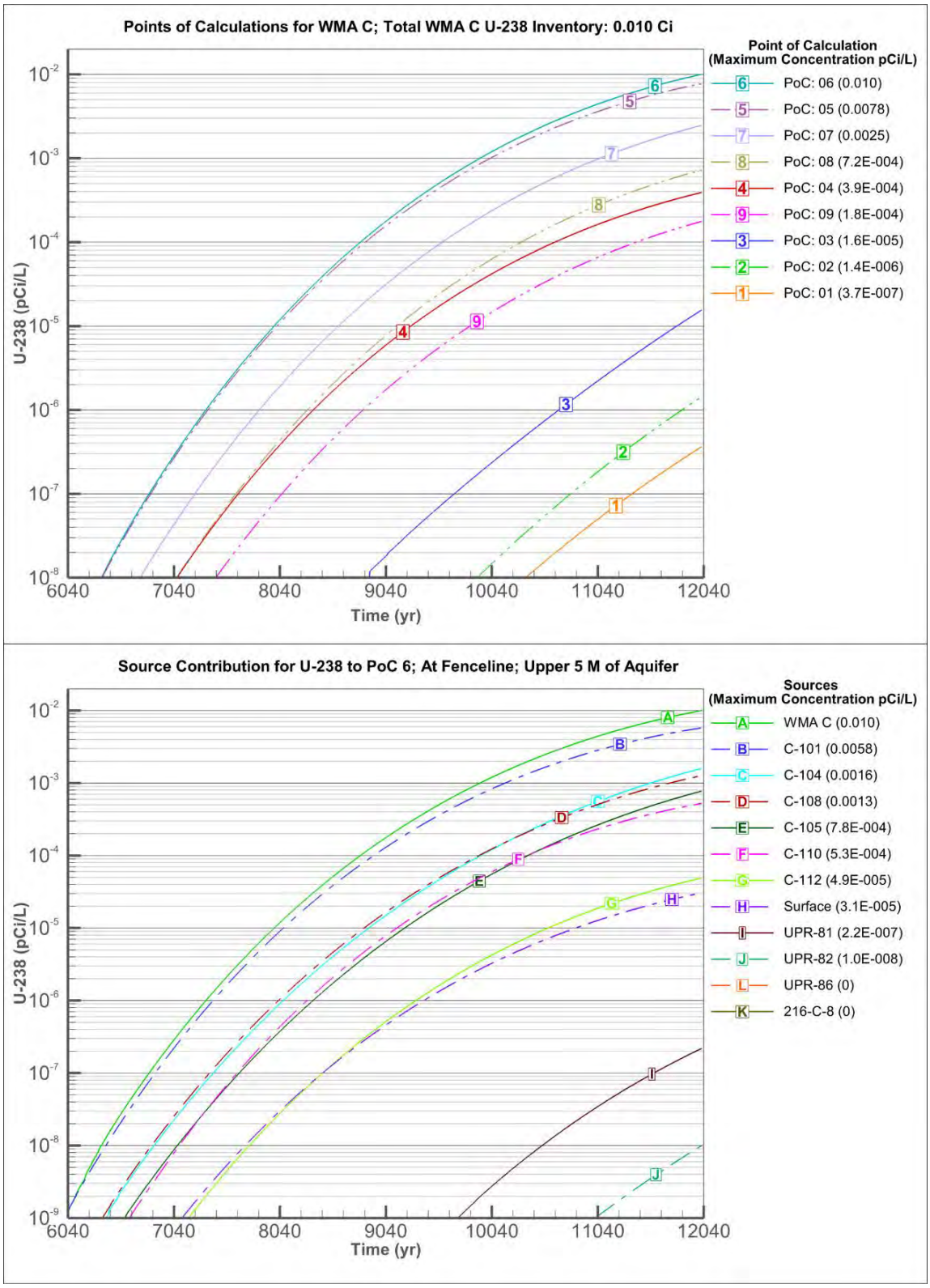

PoC = point of calculation WMA = Waste Management Area

Figure 7-23. Concentration of Total Uranium in Groundwater in the Points of Calculation at the Fenceline.

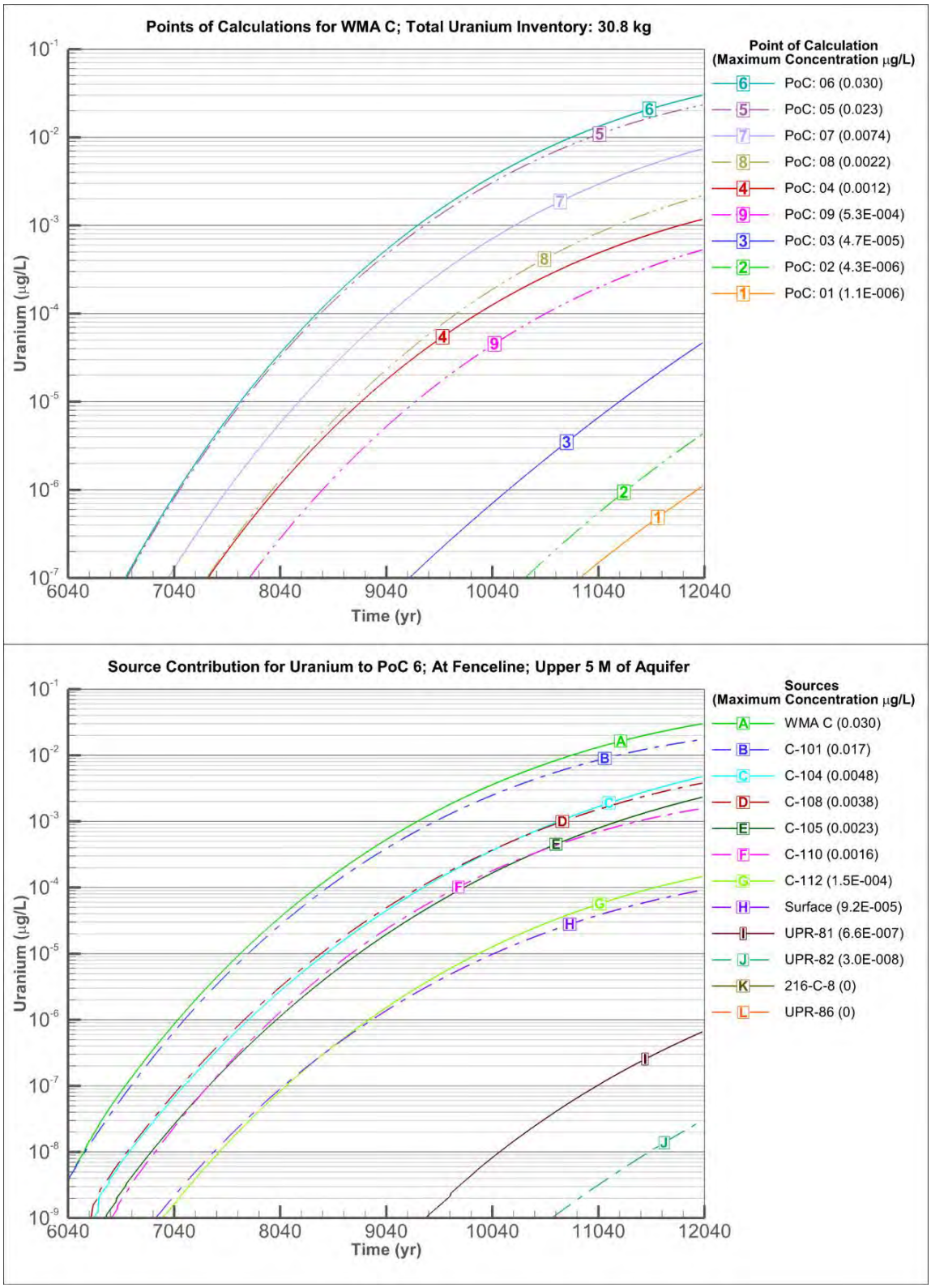

PoC = point of calculation WMA = Waste Management Area

Table 7-5. Summary Results of Radionuclides and Non-Radiological Contaminants that Arrive in Groundwater at the Waste Management Area C Fenceline after Closure.

	Iodine-129				Tin-126			
	Fenceline		100 Meters Downgradient		Fenceline		100 Meters Downgradient	
	Year of Peak	Peak Concentration (pCi/L)	Year of Peak	Peak Concentration (pCi/L)	Year of Peak	Peak Concentration (pCi/L)	Year of Peak	Peak Concentration (pCi/L)
PoCal 1	8020	0.002	8260	0.005	12020	0.003	12020	0.002
PoCal 2	8310	0.1	8330	0.1	12020	0.001	12020	0.002
PoCal 3	8380	0.9	8380	0.6	12020	0.001	12020	0.002
PoCal 4	8400	0.09	8420	0.3	12020	0.03	12020	0.03
PoCal 5	5910	0.8	5950	0.4	12020	0.3	12020	0.2
PoCal 6	5920	1	5920	0.8	12020	0.8	12020	0.5
PoCal 7	6060	0.3	5980	0.5	12020	0.3	12020	0.5
PoCal 8	6130	0.09	6060	0.2	12020	0.06	12020	0.2
PoCal 9	6160	0.02	6120	0.07	12020	0.01	12020	0.05
	Uranium-238				Total Uranium			
	Fenceline		100 Meters Downgradient		Fenceline		100 Meters Downgradient	
Year of Peak	Year of Peak	Peak Concentration (pCi/L)	Year of Peak	Peak Concentration (pCi/L)	Year of Peak	Peak Concentration (ug/L)	Year of Peak	Peak Concentration (ug/L)
PoCal 1	12020	0.0000004	12020	0.0000003	12020	0.000001	12020	0.0000008
PoCal 2	12020	0.000001	12020	0.000002	12020	0.000004	12020	0.000006
PoCal 3	12020	0.00002	12020	0.00002	12020	0.00005	12020	0.00005
PoCal 4	12020	0.0004	12020	0.0005	12020	0.001	12020	0.002
PoCal 5	12020	0.008	12020	0.003	12020	0.02	12020	0.01
PoCal 6	12020	0.01	12020	0.007	12020	0.03	12020	0.02
PoCal 7	12020	0.002	12020	0.005	12020	0.007	12020	0.01
PoCal 8	12020	0.0007	12020	0.002	12020	0.002	12020	0.005
PoCal 9	12020	0.0002	12020	0.0006	12020	0.0005	12020	0.002

Figure 7-24. Flux of Technetium-99 from the Vadose Zone that Enters Groundwater.

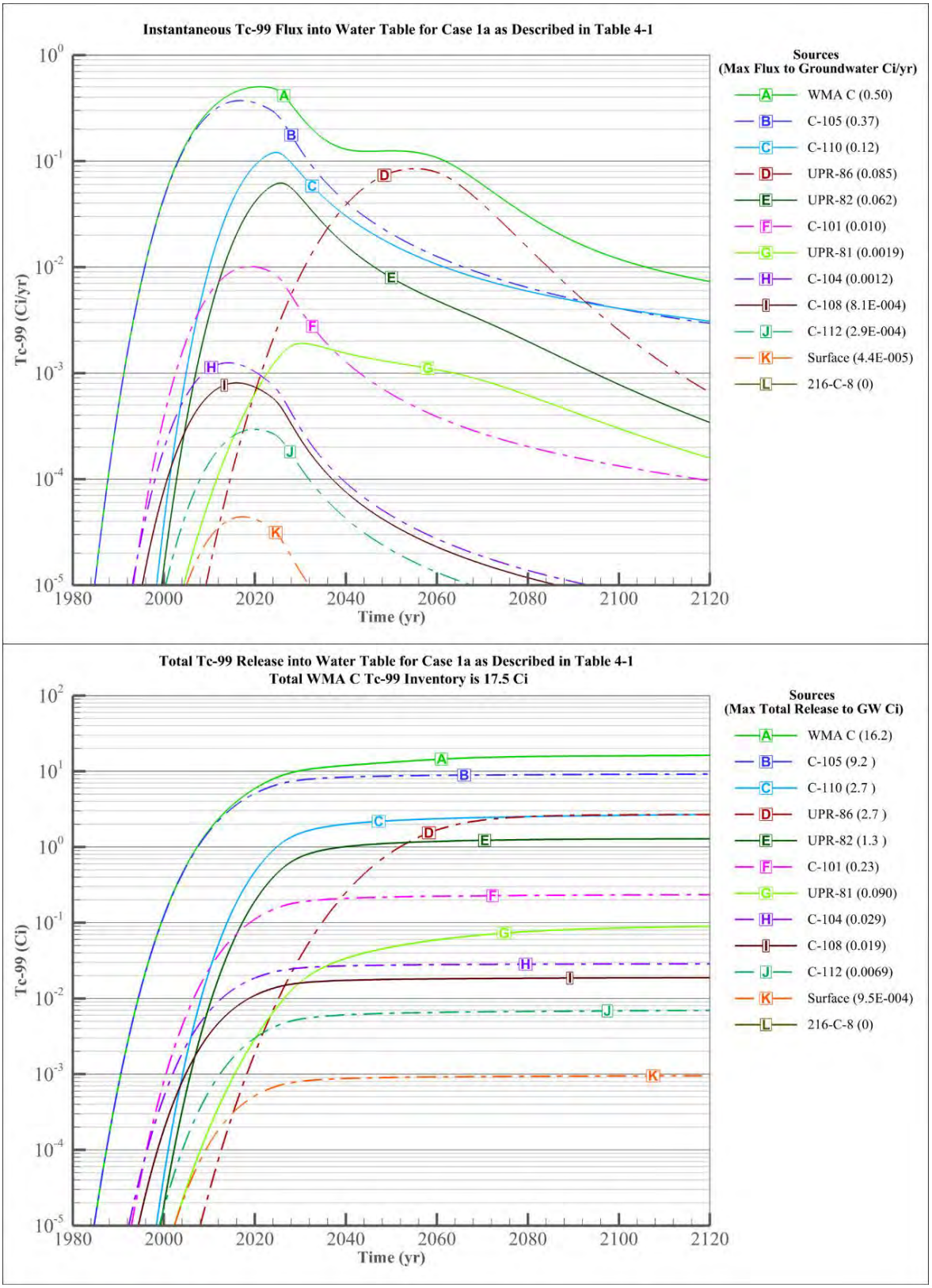

WMA = Waste Management Area

Figure 7-25. Flux of Nitrate from the Vadose Zone that Enters Groundwater.

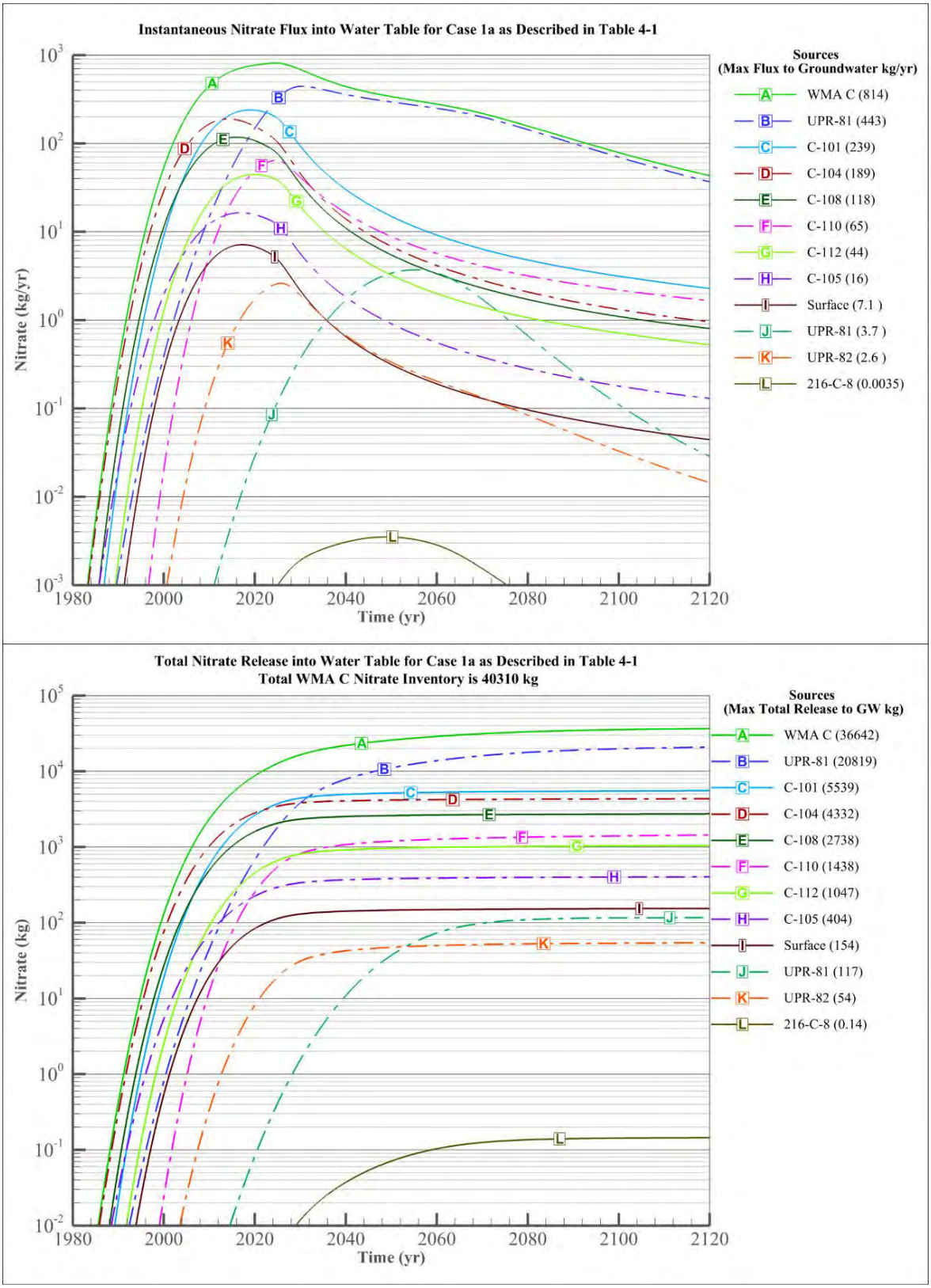

WMA = Waste Management Area

Figure 7-26. Flux of Selenium-79 from the Vadose Zone that Enters Groundwater.

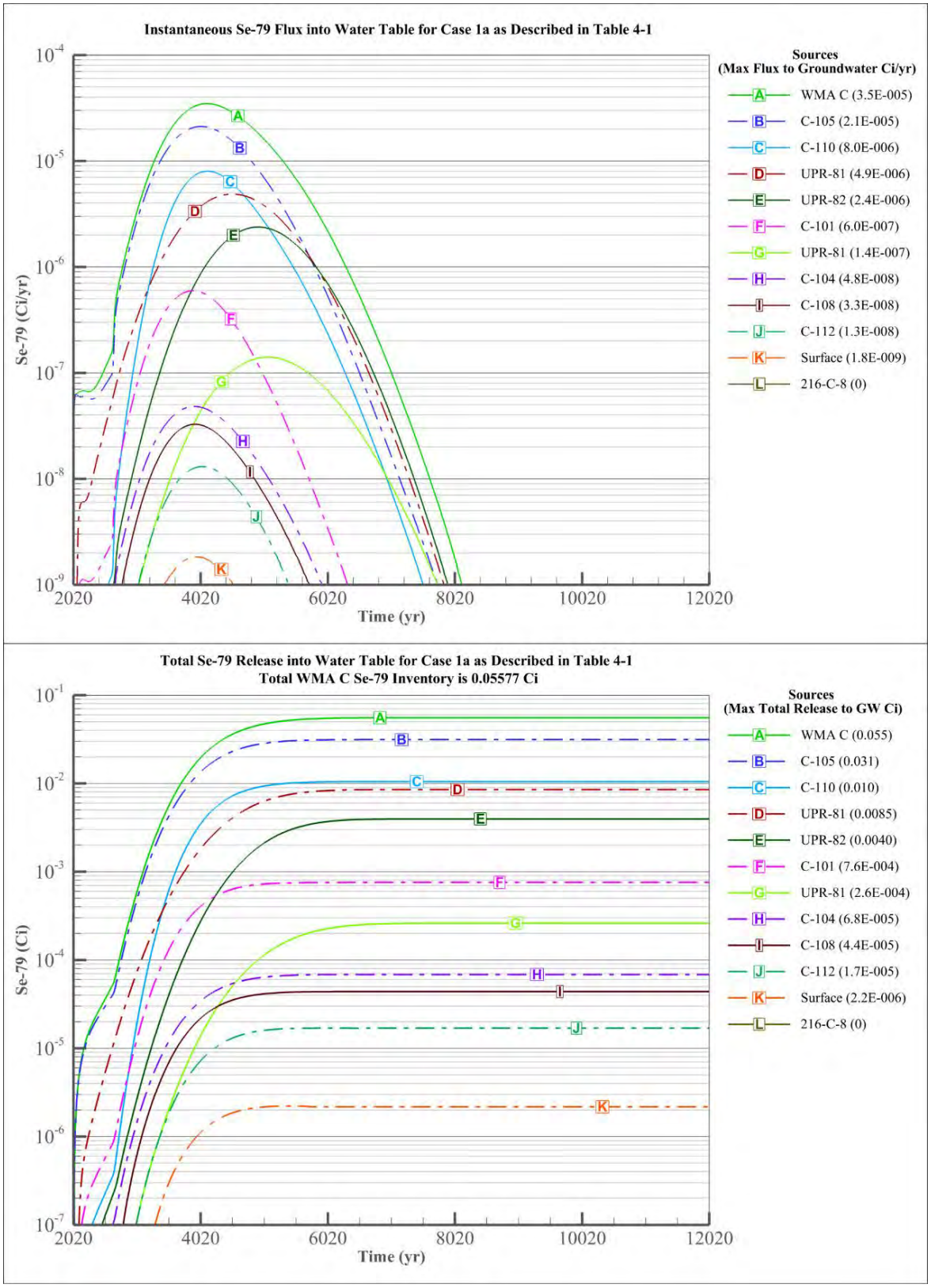

WMA = Waste Management Area

Figure 7-27. Flux of Uranium-238 from the Vadose Zone that Enters Groundwater.

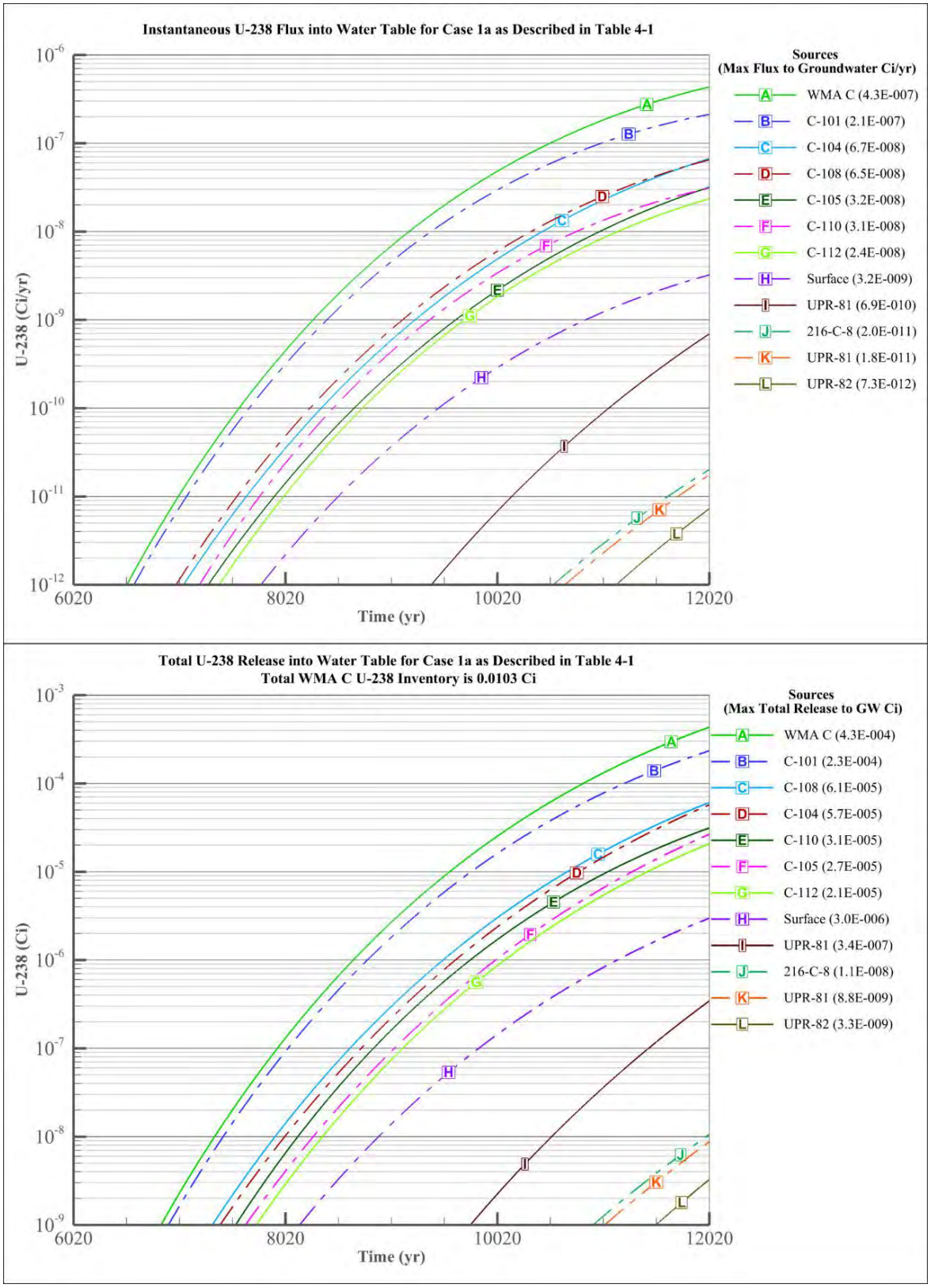

WMA = Waste Management Area

7.4 DISCUSSION OF MONITORING RESULTS WITH PROJECTED MODELING RESULTS FOR NITRATE, SULFATE, CHROMIUM, AND CYANIDE

The main objective of the set of forward calculations presented in this section is to evaluate the future consequences of the past waste leaks and releases. This would include a general evaluation of the persistence of elevated concentrations of certain constituents such as ^{99}Tc already observed in groundwater monitoring wells. The evaluation of the modeling results needs to bear in mind that the simulations projecting into the future assume a steady state water table as a basis for groundwater conditions. This situation differs from the one that produced concentrations measured in individual wells over past few decades. Given the large uncertainties in the timing, volumes and inventories of past releases and the historical changes in the direction and rate of groundwater during the periods when plumes developed in the unconfined aquifer, it is anticipated that many discrepancies in modeling results when compared with past specific concentration levels and trends in individual wells would exist. In spite of the shortcomings, the projected modeling results do provide some useful insights on projected contaminant concentration trends into the future but the results should be interpreted with understanding of uncertainties inherent in evaluating transport processes in the natural system. In general, what the modeling of ^{99}Tc has shown is the following: 1) The model reasonably approximates the time of first arrival at the aquifer (see Section 4), which means that the model provides a consistent representation of processes in the vadose zone. The location and amount of contamination in the vadose zone is key to understanding the persistence of contamination in the future. 2) The model shows ^{99}Tc concentration levels well above the DWS. When the model was corrected for the temporally varying water table (see Section 6), good agreement was produced with the magnitude of concentrations at the wells. 3) Without implementation of any corrective measures at WMA C tank farm, ^{99}Tc concentration levels projected by the modeling will continue to be well above the DWS in the near term and will likely remain at levels above the DWS for decades. 4) The primary contributors to the highest concentration levels seen at the WMA C fence line and downgradient are from those plumes that have opportunity to superimpose with one another both temporally and spatially. For the assumed northwest to southeast flow conditions evaluated, the key sources were found to be releases from tanks C-101, C-105, and C-110. Secondary sources included releases at UPR-82, tank C-104, and tank C-108.

Nitrate and sulfate plumes existed in the groundwater around WMA C prior to when the WMA C past releases are estimated to have reached the water table. The nitrate and sulfate contamination in the aquifer likely stem from the regional plume that has many sources away from WMA C. Nitrate and sulfate concentrations measured between 1990 and 1997 (data available from prior to 1990 are sparse) in regional wells where impacts from WMA C are unlikely (e.g., wells 299-E26-8, 299-E24-8, and 299-E27-9, range between 5 and 10 mg/L, and 40 and 96 mg/L, respectively). Because of the apparent regional sources of nitrate and sulfate, it is difficult to quantify the nitrate and sulfate impacts caused by the past releases at WMA C or distinguish them from those originating elsewhere.

According to the monitoring data and the modeling results, nitrate and sulfate contained in the past releases from WMA C do not appear to have reached the water table until after 1997. Trends in the nitrate and sulfate concentrations remain relatively stable until the late 1990s when

they begin to increase markedly. Technetium-99 appears to be a distinct signature contaminant in groundwater associated with the WMA C past releases because there are no other known nearby sources of ^{99}Tc. Groundwater monitoring results collected from wells surrounding WMA C (e.g., wells 299-E27-7, 299-E27-12, 299-E27-13, 299-E27-14, and 299-E27-15) indicate that ^{99}Tc did not arrive at the water table in substantial quantity until after 1997.

Around WMA C, increases in the nitrate and sulfate concentrations coincide with increases in ^{99}Tc concentrations. However, in most wells the nitrate and sulfate concentrations do not decrease when ^{99}Tc concentrations do, or concentrations remain at relatively elevated levels compared to where they started prior to the arrival of ^{99}Tc. Although the shifting hydraulic gradient may have directed a different portion of the pre-existing plume toward the monitoring wells, the sustained elevated concentrations of nitrate and sulfate appear to be more indicative of the arrival of a different plume. This different plume appears to have arrived in the area about the same time as when the WMA C past releases initially reached the water table and consists of relatively high concentrations of nitrate and sulfate with a relatively low concentration of ^{99}Tc.

The arrival at the water table of the source originating from UPR-200-E-81, and its co-mingling with ^{99}Tc associated with releases from the 100-series tanks, provides an explanation of the nitrate concentrations that have been observed in wells to the south and southwest of WMA C (e.g., wells 299-E27-13 and 299-E27-23). UPR-200-E-81 is estimated to contain a relatively small quantity of ^{99}Tc and a relatively large quantity of nitrate (RPP-RPT-42294). According to the modeling results, the groundwater concentration of ^{99}Tc that released from the 100-series tanks peaks around year 2019, but the concentration of nitrate that released in UPR-200-E-81 peaks around year 2030. The initial increase in nitrate concentration observed in the monitoring wells surrounding WMA C appears to be attributable to the releases from the 100-series tanks, with the later elevated concentrations sustained by the nitrate contained in UPR-200-E-81. Similar to the ^{99}Tc modeling results, the application of the long-term steady-state gradient appears to cause the magnitude of the modeled nitrate concentrations at the WMA C fenceline (~12 to 13 mg/L) to underestimate the observed concentrations by factors that range from approximately a factor of 2 in well 299-E27-13) to factor of 8 in well 299-E27-14. The uncertainty in the magnitude and direction of the hydraulic gradient during the decline of the 216-B-3 Pond hydraulic mound is essentially impossible to quantify with the data that are available from that time. The text is intended to provide an explanation for why the model results that use a steady-state gradient appear to underestimate the observed concentrations. The actual hydraulic gradient during 216-B-3 Pond operations reversed, and is in the process of reversing back, which indicates that the magnitude of the gradient must have at times decreased from the steady-state value. Measurements made during 2005 through 2011 provides some insights into the variability in the magnitude of the hydraulic gradient that occurred, and indicate that at times the gradient measured less than one half of the estimated steady-state value while reestablishing a south or southeasterly direction. As the gradient provides a proportional indicator of the groundwater flux, and the concentration of contaminants in groundwater is generally inversely proportional to the flux. Therefore, the application of the estimated steady-state gradient in the model likely contributes to the underestimation of contaminant concentrations in the modeling results compared to the observed values.

The trends in the sulfate concentrations measured in the monitoring wells around WMA C tend to track very closely with the trends in the nitrate data. The consistency of the correlation between the sulfate and nitrate concentration data almost certainly indicates common sources of those contaminants. The difference between the magnitude of the modeled sulfate concentrations at the WMA C fenceline (< 1 mg/L) are orders of magnitude less than the increases observed in the measured data between 2000 and 2010. During this time, for example, the concentration of sulfate increases from ~20 mg/L to 120 mg/L in well 299-E27-13, from ~60 mg/L to 180 mg/L in well 299-E27-21, and from ~70 mg/L to 300 mg/L in well 299-E27-14.

The trends in the chromium concentrations measured in the monitoring wells around WMA C do not track very closely with the trends in the nitrate, sulfate, or ^{99}Tc concentration data. Most wells do show an increase in chromium concentration around year 2010 relative to the years around it, but the chromium monitoring data present no discernable trend or correlation with the nitrate, sulfate, or ^{99}Tc data. Compared to the years preceding 2010, the chromium concentration in year 2010 is approximately 8 to 10 µg/L greater in wells 299-E27-13, 299-E27-21, 299-E27-23, and 299-E27-14. According to the modeling results, chromium concentrations would be expected to increase by ~76 µg/L, and that is without factoring in the underestimation observed in the concentrations of nitrate and ^{99}Tc. The disparity between the model results and the monitoring data may be attributed to the modeling assumption that all chromium inventory is and remains hexavalent chromium. Not all of the chromium inventory in the tanks was hexavalent, and much of the hexavalent chromium that may have been released would have reacted with the oxides of iron, aluminum, and manganese due to waste fluid-sediment interactions and become either relatively immobilized or partially reduced to trivalent chromium. Some surface adsorption is also likely due to formation of reactive surfaces from mineral reactions that would occur during neutralization of the waste stream. Trivalent chromium is relatively immobile in the environment; estimates of its distribution coefficient (K_d) typically exceed the 10,000-year screening threshold value established in Section 4 [Washington State Department of Ecology Cleanup Levels and Risk Calculation (CLARC), Queried 08/30/2016, [CLARC Data Tables – July 2015, Chemical Parameters], https://fortress.wa.gov/ecy/clarc/FocusSheets/CLARC%20Parameters.pdf]. Thus, it appears unlikely that chromium contained in the past releases is responsible for the chromium contamination that exists in groundwater.

A general comparison of potential impacts of cyanide with monitoring data from groundwater (see Section A4.0) are provided in Section A5.0 of Appendix A. The overall concentration impacts estimated for cyanide in Appendix A (see Section A.5.0) are in general of the same order of magnitude as the observed values of cyanide in groundwater (See Section A4.0).

8.0 OTHER SOURCES OF CONTAMINATION AT WASTE MANAGEMENT AREA C

In this section, the forward projections of groundwater concentrations from past leaks are compared to two additional sources that have the potential to impact groundwater under WMA C. These potential sources of contamination are tank residual waste that will be left in tanks and ancillary equipment at a landfill closed WMA C, as discussed in RPP-ENV-58782 and RPP-ENV-58806; and sources of contamination upgradient to WMA C that are contributing to current groundwater contamination in the general vicinity and could impact groundwater at WMA C in the future. This section is intended to put the forward projections of past leaks in context of the broader groundwater contamination conditions now and into the future at WMA C.

8.1 CONTRIBUTION OF CONTAMINATION ASSOCIATED WITH UPGRADIENT SOURCES

In this section, future projections are discussed of the contribution to contamination under WMA C from upgradient sources. It is emphasized that existing evaluations of upgradient contamination assume that there will be no remedial activities undertaken at B Complex. They therefore likely provide significant overestimations of future contamination discharges. Therefore, the results in this section should only be regarded as a qualitative indication of the relative importance of various sources of contamination at WMA C.

The current understanding of groundwater contamination in the vicinity of WMA C has been described in the RI for the 200-BP-5 Groundwater OU (DOE/RL-2009-127, *Remedial Investigation Report for the 200-BP-5 Groundwater Operable Unit, Draft A*). The 200-BP-5 OU extends north-northwest from the 200 East Area, across the Hanford Site, to the Columbia River, and includes WMA C (Figure 2-3). The observed groundwater contamination in the 200-BP-5 OU resulted largely from liquid waste generated during the operational period of B Plant and associated facilities within the northern portion of the 200 East Area (DOE/RL-2009-127 Draft A).

The most recent interpretation (2013) of the groundwater plumes in the 200-BP-5 OU is shown in Figure 8-1. The figure shows the regions in which the plumes exceed their drinking water standard; lower levels of contamination exist in wider regions than shown on the map. The groundwater plumes and data were further implemented (DOE/RL-2009-127) in a groundwater transport model designated as the Plateau to River (P2R) model, which allows the evaluation of the time dependence of plumes arriving at WMA C. A complete description of the P2R model is provided in CP-57037, *Model Package Report: Plateau to River Groundwater Transport Model Version 7.1*, and its application to simulate contaminant fate and transport for the scenarios is detailed in ECF-Hanford-13-0031, *Fate and Transport Modeling for Baseline Conditions for*

Remedial Investigation/Feasibility Studies of the 200-BP-5 and 200-PO-1 Groundwater Operable Units. A summary of the model and its results are presented in DOE/RL-2009-127.

Results of the P2R model have been used to provide estimates of the contribution of upgradient sources at WMA C. The basis for this discussion is the remedial evaluation case described in ECF-Hanford-18-0023, *Evaluation of Contaminant Transport for the 200-BP-5 and 200-PO-1 Operable Units Feasibility Study Evaluation of Remedial Alternatives*, Draft A. The remedial evaluation case provides a baseline set of simulation results that can be used to compare subsequent simulations in order to assess treatment effectiveness. Key features of the remedial evaluation case for the 200 East Feasibility Study include (ECF-Hanford-18-0023):

- Initial contaminant concentration distributions are based on the average concentrations from the annual report plumes within the boundary of each computational cell;
- No continuing source is considered for any contaminant plumes; and
- Discharge from TEDF is assumed to occur.[1]

Results of the remedial evaluation case for contaminants of concern are presented in Figures 8-2 to 8-12. The peak values of these curves are summarized in Table 8-1. Depictions of the calculated future plumes from upgradient sources are presented in Appendix B of ECF-Hanford-18-0023.

The results of the work associated with the selection of remedial options at the B-complex is not work that was done by WRPS. It represents work that is being cited to examine the potential baseline impacts of upgradient sources at WMA C using some alternative cases of no remediation. This case provides a baseline for assessing the effectiveness of the pump and treat (P&T) scenarios. We acknowledge that the specific remedial evaluation case applies assumptions about continuing sources for selected contaminants that may underestimate their impacts. The basis for these assumptions and the development of P2R model used in the analysis are provided in DOE/RL-2009-127. Active remediation of perched water in the B-complex area is ongoing and interim action plans related to active remediation of groundwater plumes in the B-complex area are also in the process of being developed. Implementation of a pump & treat system to expedite the remediation of groundwater contaminant plumes at WMA C tank farm is also under way under the 200 BR-5 OU RI/FS process. The design of this pump and treat system is using continuing sources of a number of contaminants developed under the past leaks analysis.

[1] Based on interpretations made from monitoring information during the last couple of years (DOE/RL-2016-67, *2016 100 Areas Pump and Treat Report: August 2017*), large operational discharges at TEDF combine with other changes in this stage in the Columbia River to the northwest of the gable gap area generally can have a subtle, but noticeable effect on reducing the overall hydraulic gradient of the water table in 200 East area.

8.1.1 Technetium-99

The P2R model (DOE/RL-2009-127 Draft A) was used to simulate the evolution of the ^{99}Tc plume forward in time, beginning at year 2015. The results of the analysis are shown in Figures 8-2 to 8-5. The figures show a high concentration plume of ^{99}Tc under B Complex at the beginning of the simulation, part of which moves in the direction of WMA C, while part discharges through Gable Gap. A second source of ^{99}Tc in the analysis is that associated with leaks from WMA C. Over the next ~20 years the plume moves with groundwater past WMA C, leading to a period of high ^{99}Tc concentrations beginning in about year 2020 and lasting until about year 2035. Following that time, the concentrations decrease continuously in time.

The time dependence of the ^{99}Tc contamination from upstream sources is shown in Figure 8-6. The peak concentration of about 1,400 pCi/L is at the present day or the near future with a second lower peak around year 2060.

8.1.2 Nitrate

The P2R model was used to simulate the evolution of the nitrate plume forward in time, beginning at year 2015. The results of the analysis are shown in Figures 8-7 to 8-10. The figures show a high concentration plume of nitrate under B Complex at the beginning of the simulation, part of which moves in the direction of WMA C, while part discharges through Gable Gap. Over the next ~20 years the plume moves with groundwater past WMA C, leading to a period of high nitrate concentrations beginning in about year 2020 and lasting until about year 2035. Following that time, the nitrate concentrations decrease continuously in time.

The time dependence of nitrate contamination from upstream sources is shown in Figure 8-11. The peak concentration of about 130 mg/L is at the present day or the near future.

Figure 8-1. 2013 200-BP-5 Operable Unit Consolidated Plume Map.

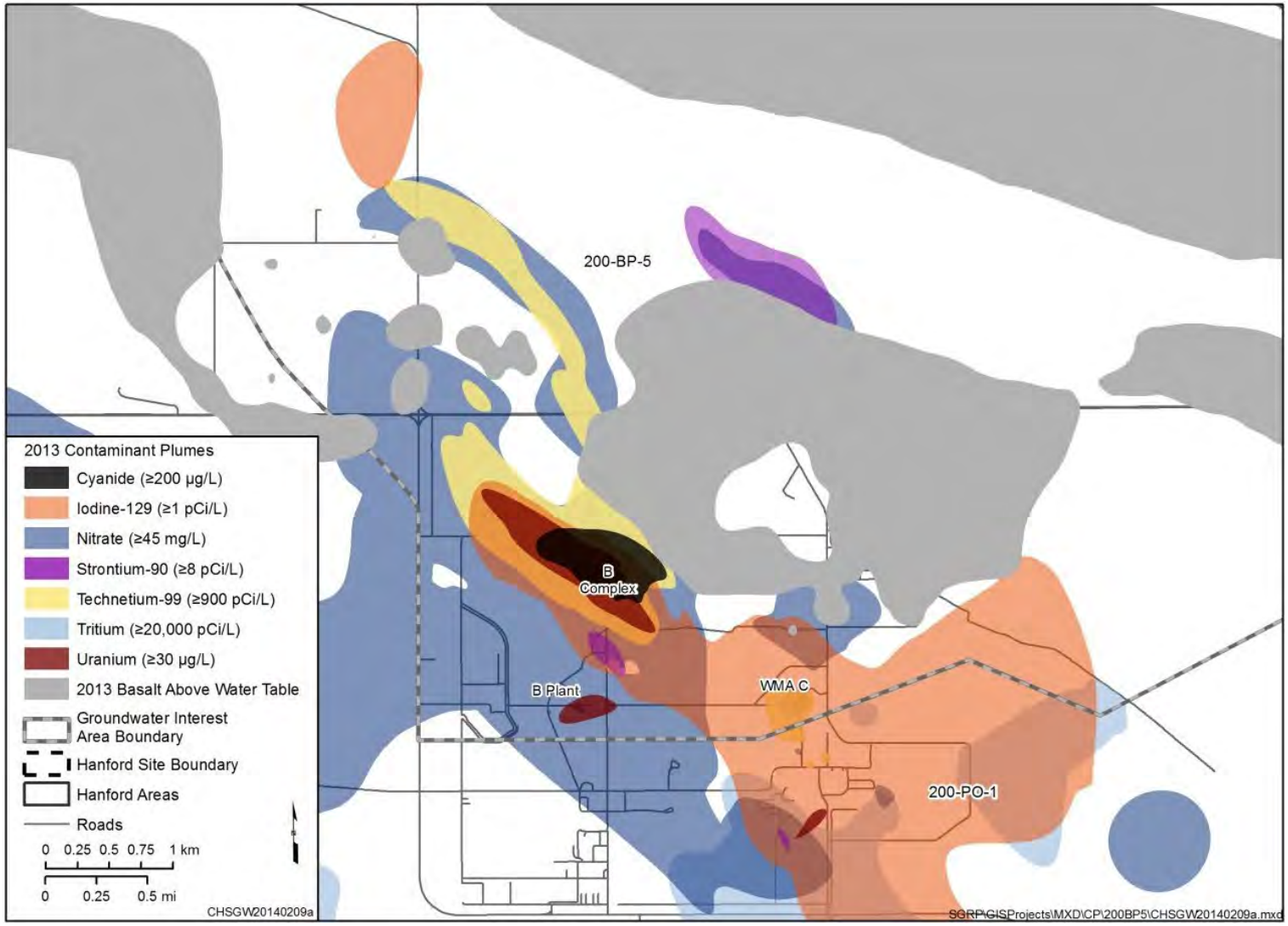

WMA = Waste Management Area

Reference: DOE/RL-2009-127, *Remedial Investigation Report for the 200-BP-5 Groundwater Operable Unit*, Draft A.

Figure 8-2. The Technetium-99 Plume at Year 2015 (Year 0 of the Simulation) for the Remedial Evaluation Case of 200-BP-5.

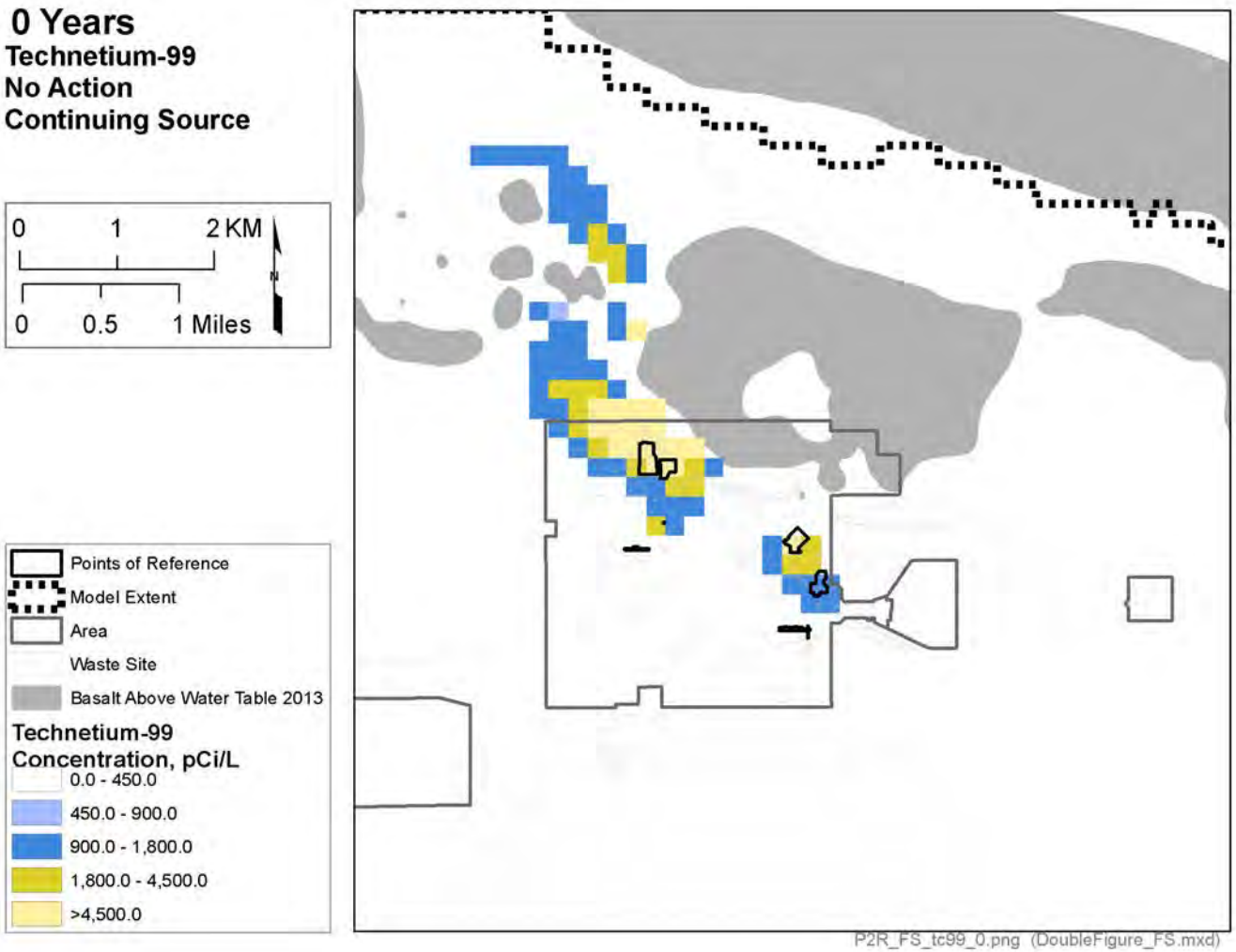

OU = operable unit

Note: The higher concentrations (yellow contours) are both upgradient from Waste Management Area C in the B Complex area and under Waste Management Area C.

Figure 8-3. The Technetium-99 Plume at Year 2020 (Year 5 of the Simulation) for the Remedial Evaluation Case of 200-BP-5.

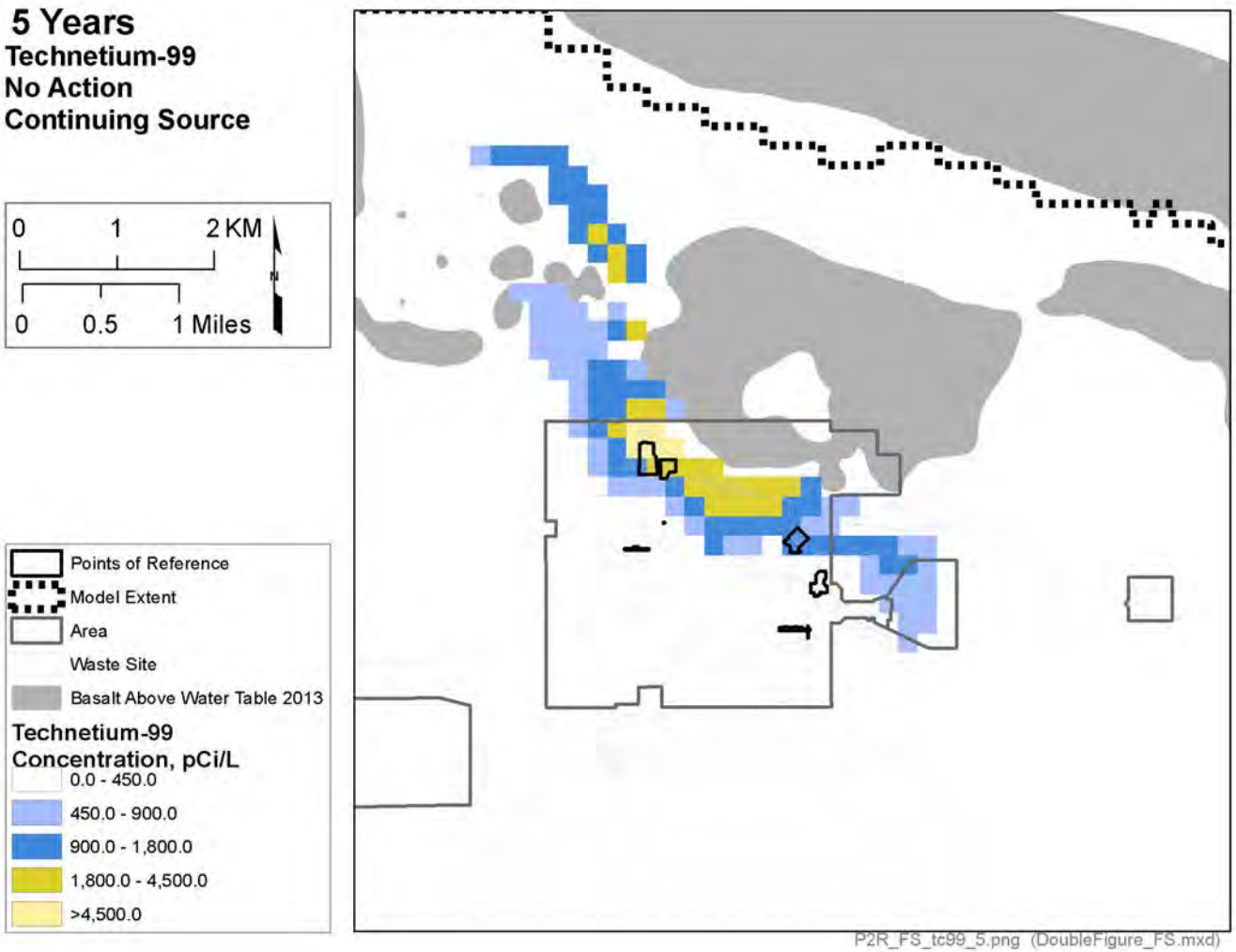

OU = operable unit

Note: The higher concentrations (yellow contours) from B Complex have moved significantly toward Waste Management Area C.

Figure 8-4. The Technetium-99 Plume at Year 2025 (Year 10 of the Simulation) for the Remedial Evaluation Case of 200-BP-5.

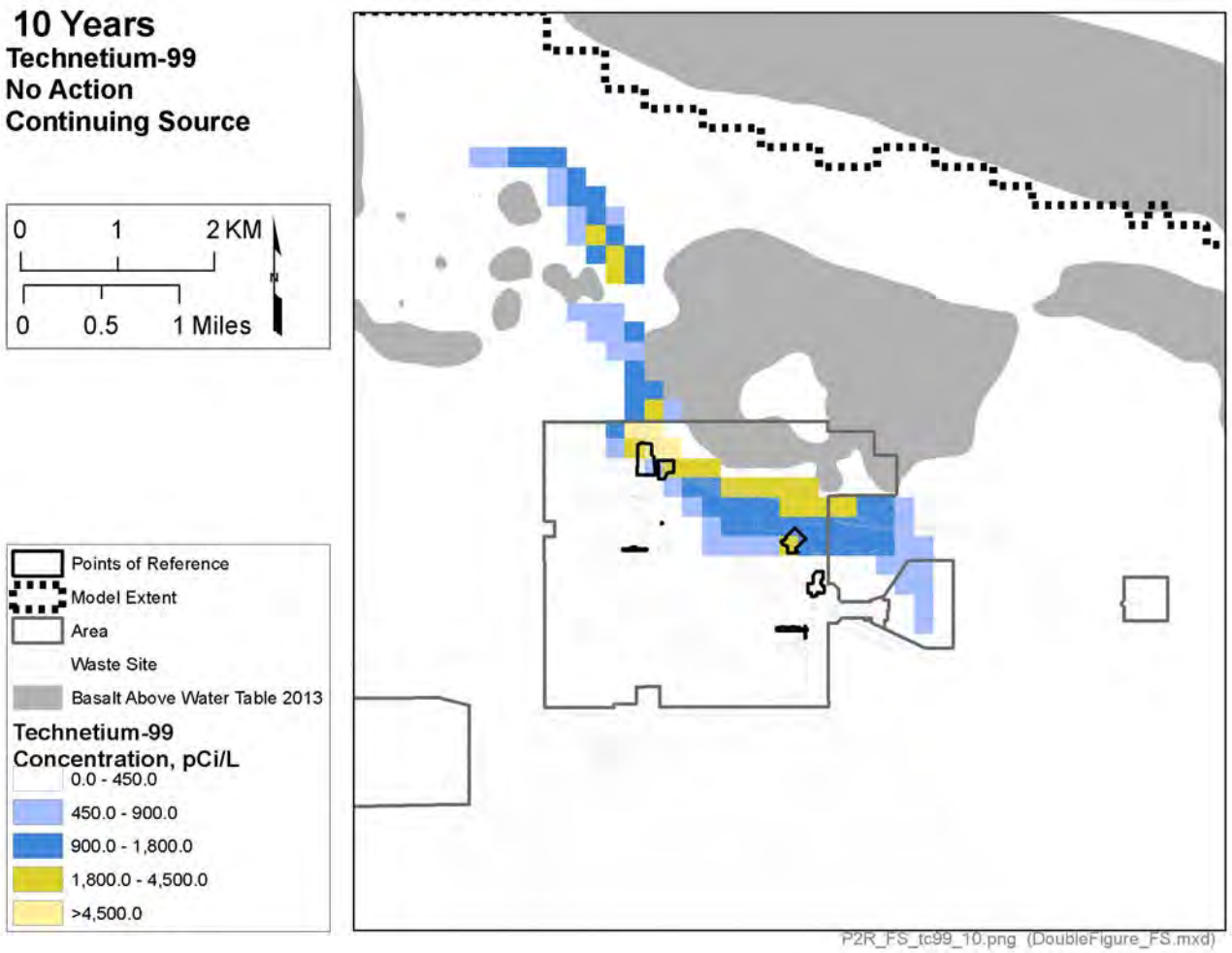

OU = operable unit

Note: Yellow higher concentration contour has moved to the vicinity of Waste Management Area C, but has remained slightly north of Waste Management Area C.

Figure 8-5. The Technetium-99 Plume at Year 2035 (Year 20 of the Simulation) for the Remedial Evaluation Case of 200-BP-5.

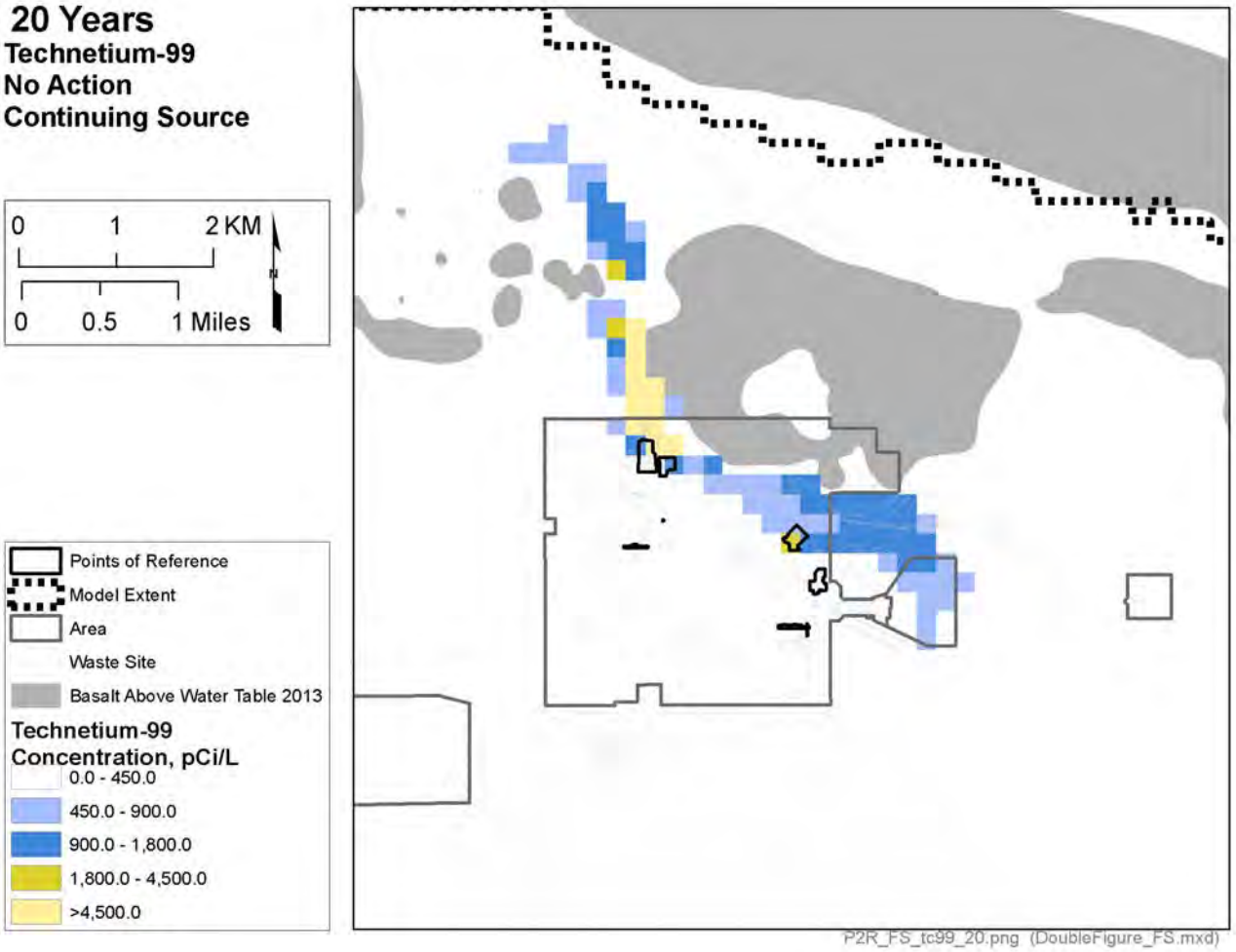

OU = operable unit

Note: The center of mass of the higher concentration contour has moved downgradient from Waste Management Area C and has significantly dispersed to the extent that it no longer shows up as a yellow contour.

Figure 8-6. Remedial Evaluation Case Technetium-99 Concentrations at Waste Management Area C as a Function of Time.

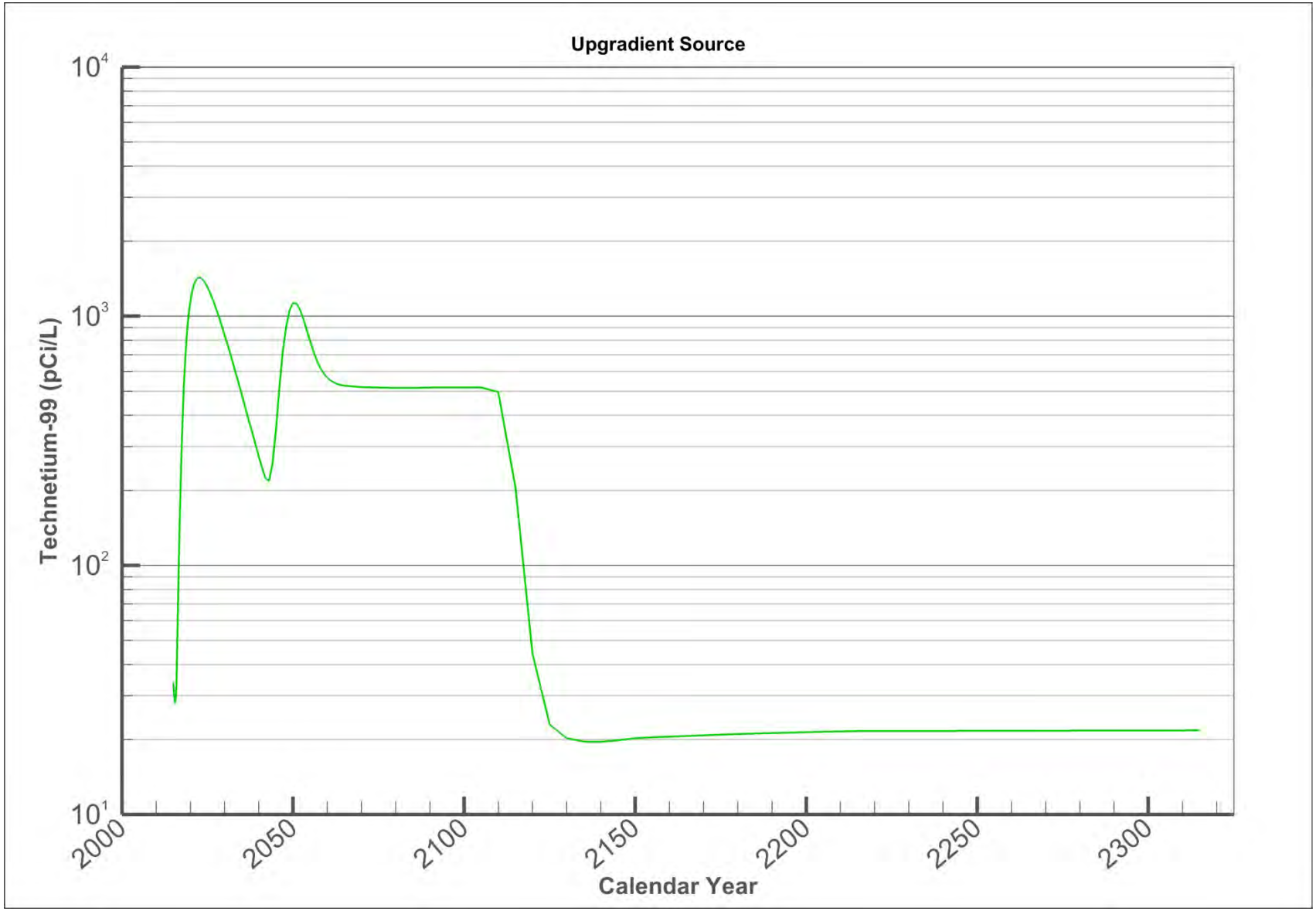

Figure 8-7. The Nitrate Plume at Year 2015 (Year 0 of the Simulation) for the Remedial Evaluation Case of 200-BP-5.

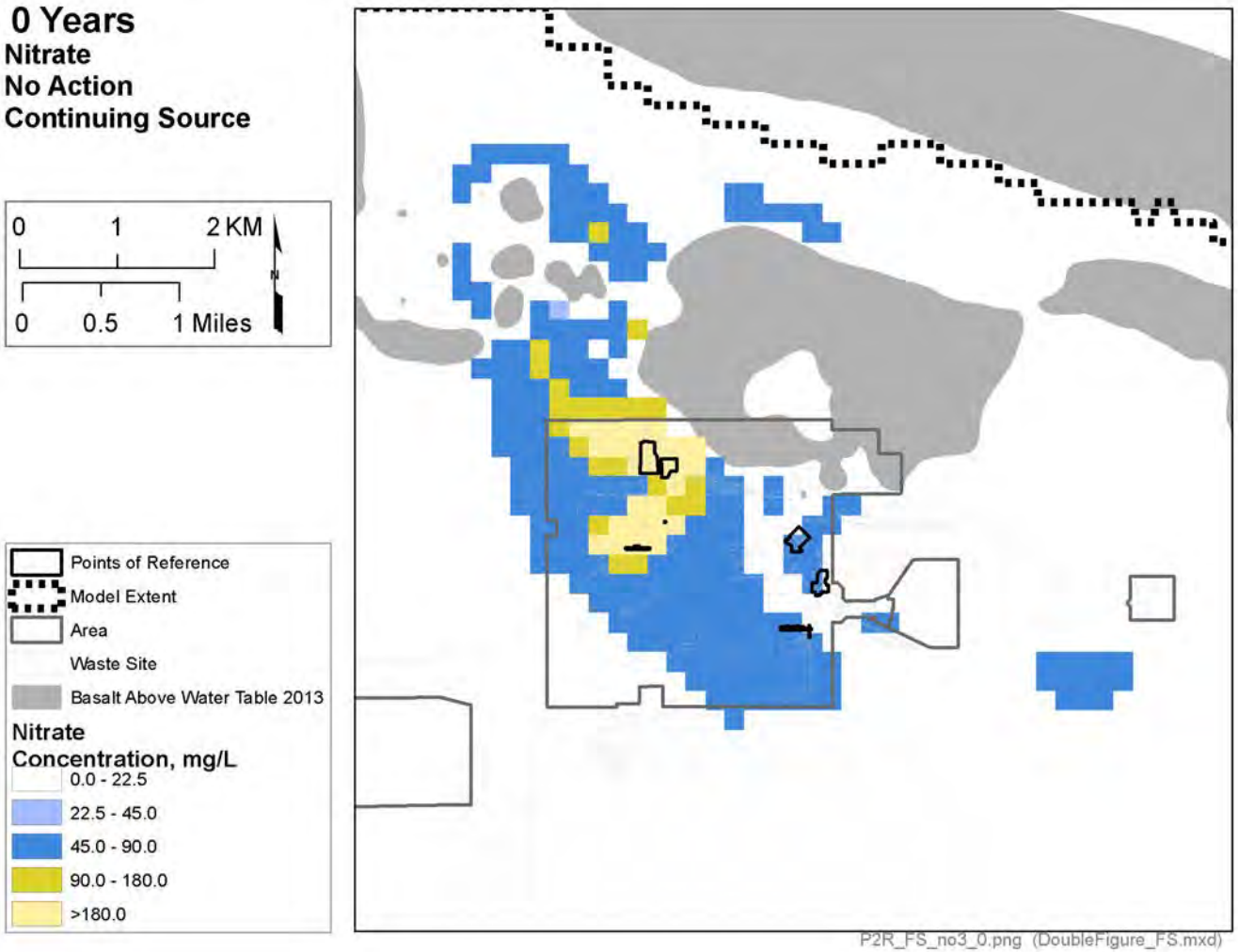

OU = operable unit

Note: The higher concentrations (yellow contours) are entirely upgradient from Waste Management Area C in the B Complex area.

Figure 8-8. The Nitrate Plume at Year 2025 (Year 10 of the Simulation) for the Remedial Evaluation Case of 200-BP-5.

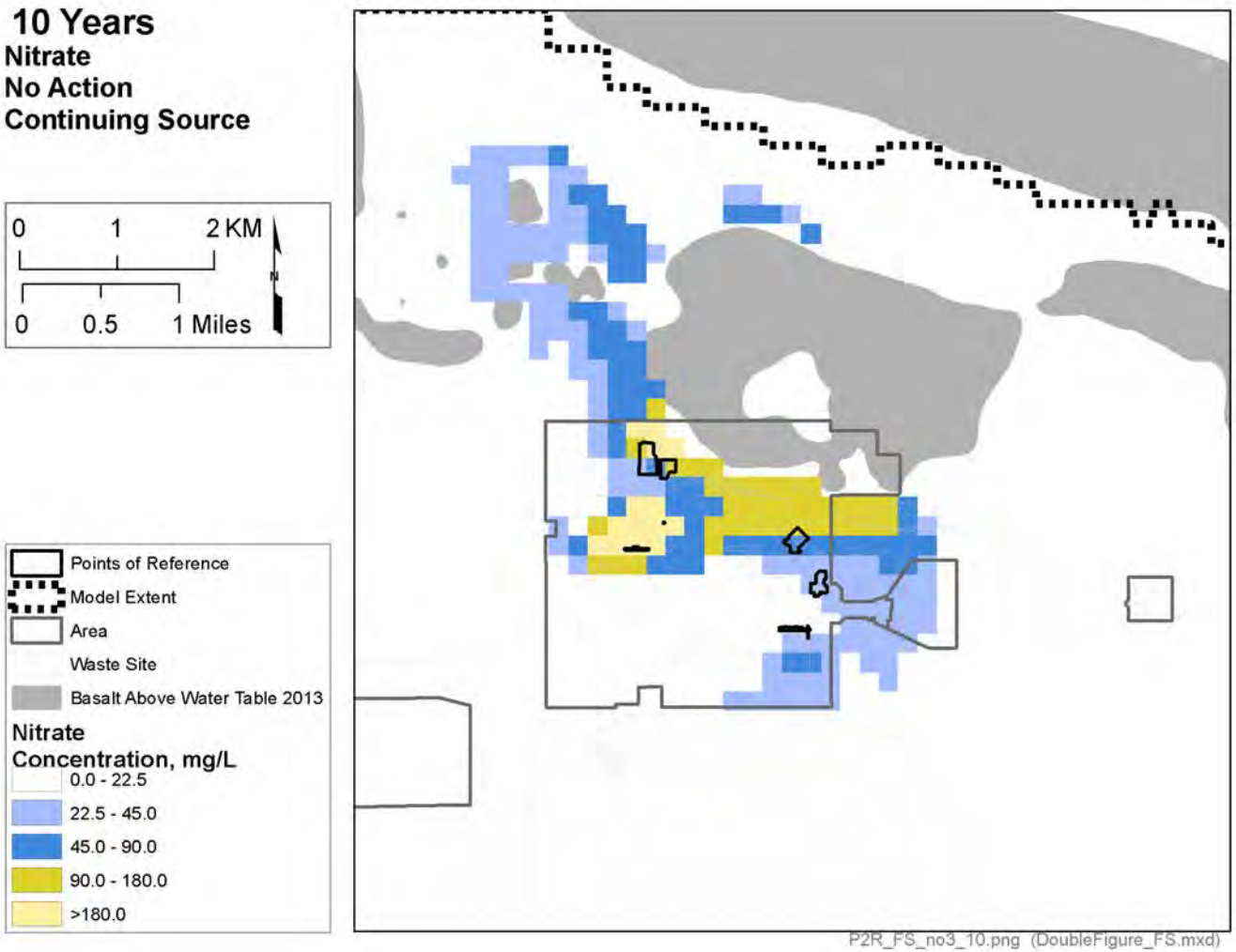

OU = operable unit

Note: The yellow higher concentration contour has moved to the vicinity of Waste Management Area C.

Figure 8-9. The Nitrate Plume at Year 2030 (Year 15 of the Simulation) for the Remedial Evaluation Case of 200-BP-5.

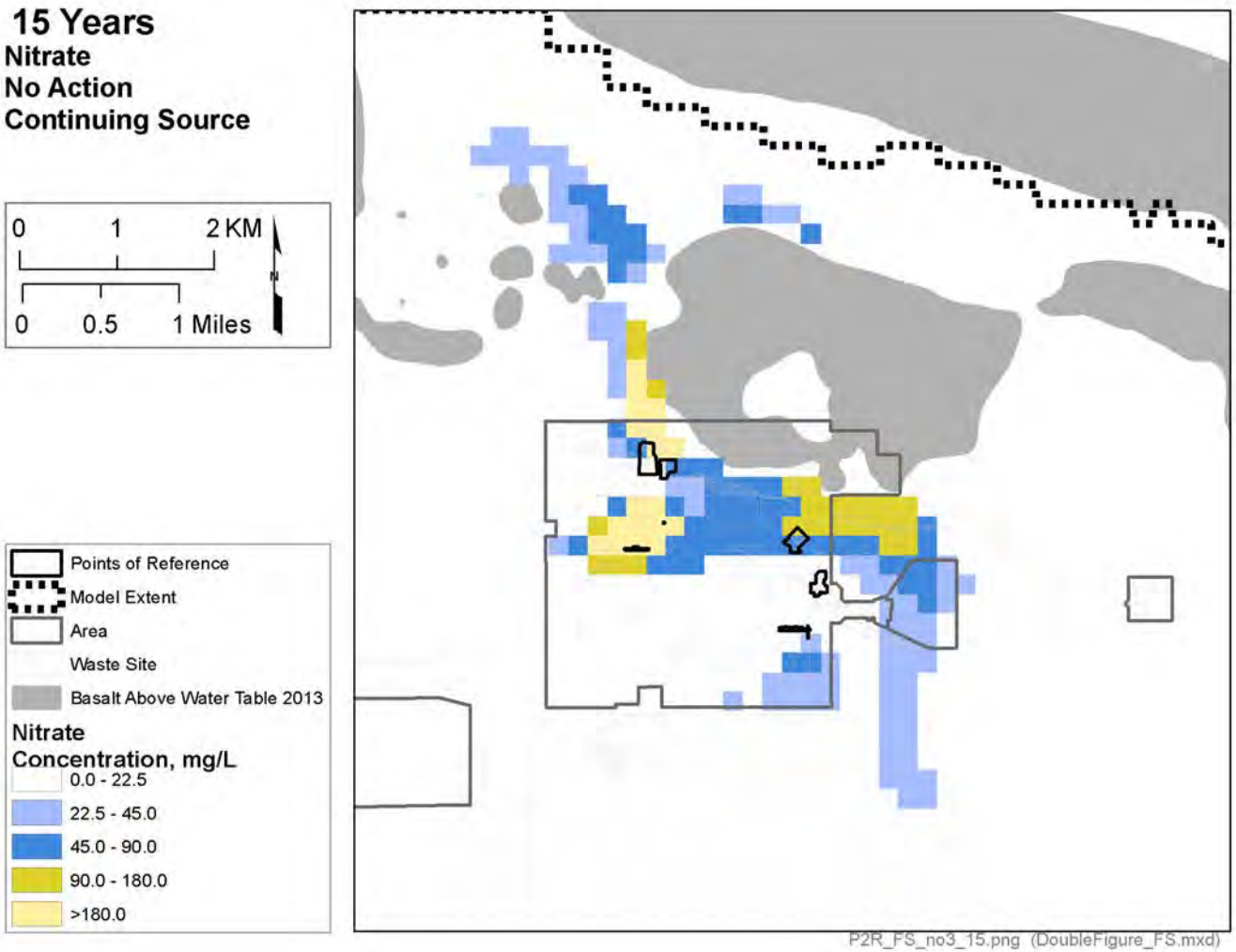

OU = operable unit

Note: The yellow higher concentration contour is predominantly downgradient from Waste Management Area C.

Figure 8-10. The Nitrate Plume at Year 2035 (Year 20 of the Simulation) for the Remedial Evaluation Case of 200-BP-5.

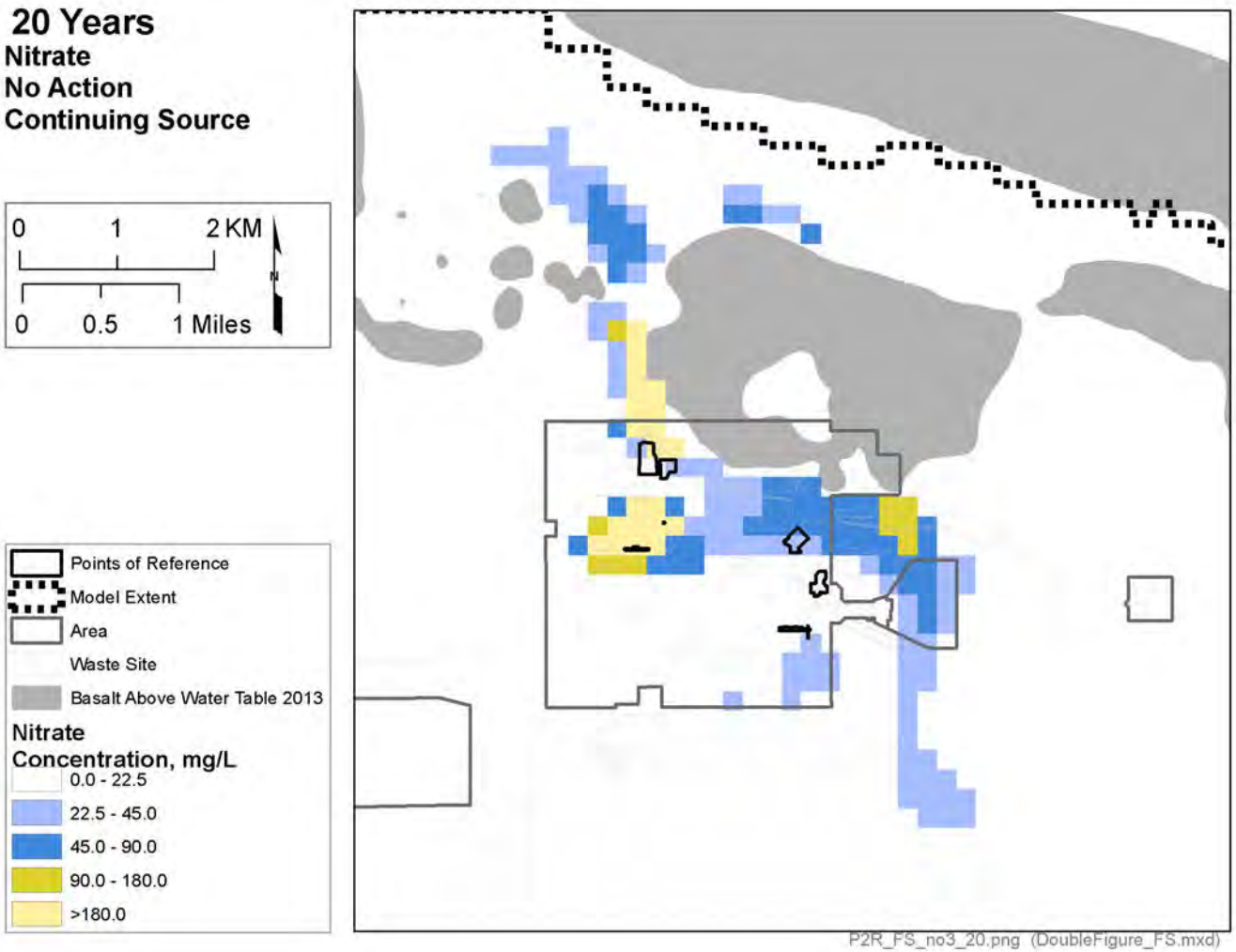

OU = operable unit

Note: The center of mass of the yellow higher concentration contour has moved downgradient from Waste Management Area C and has significantly dispersed.

Figure 8-11. Remedial Evaluation Case Nitrate Concentrations at Waste Management Area C as a Function of Time.

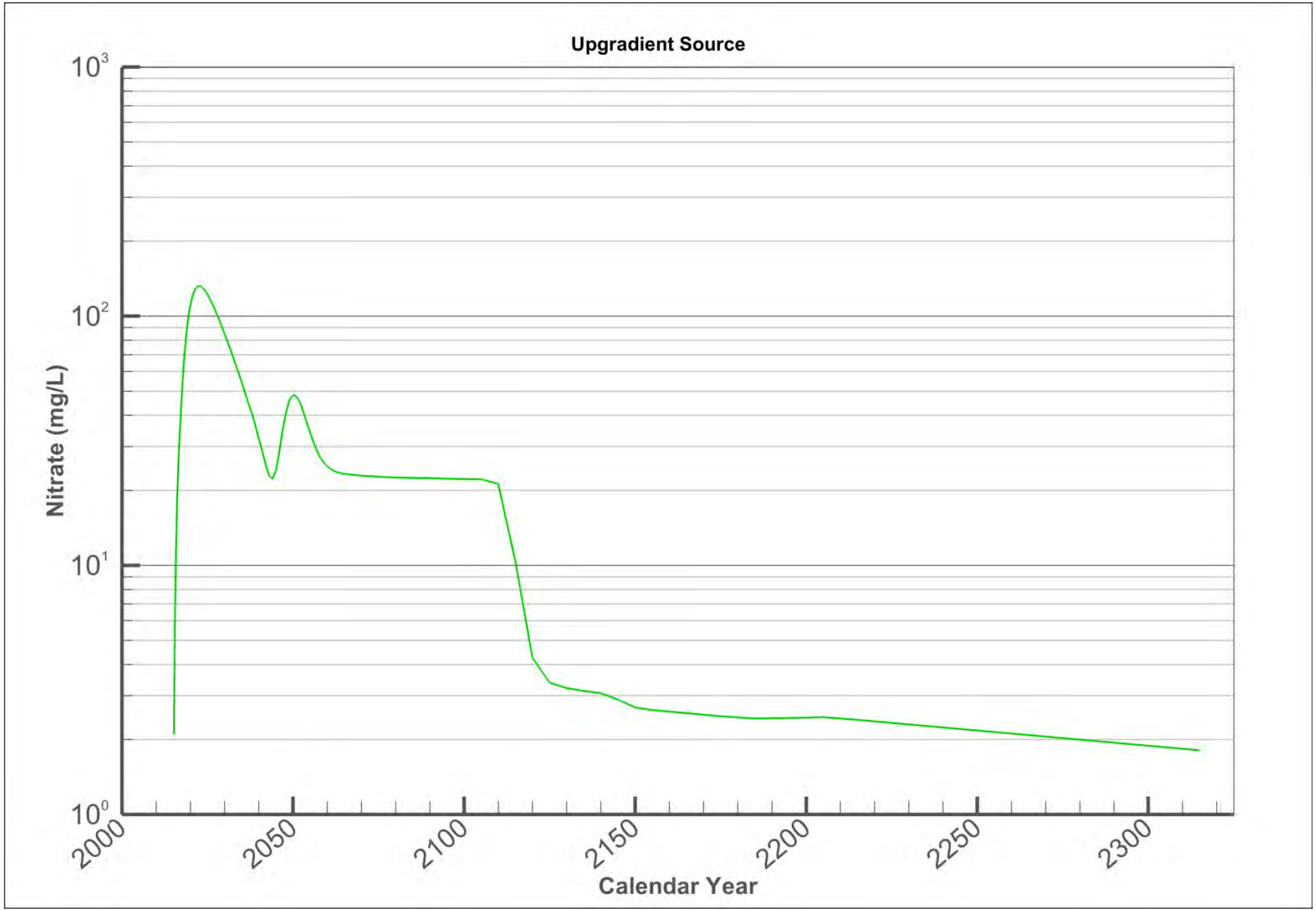

Figure 8-12. The Cyanide Plume at Year 2015 (Year 0 of the Simulation) for the Remedial Evaluation Case of 200-BP-5.

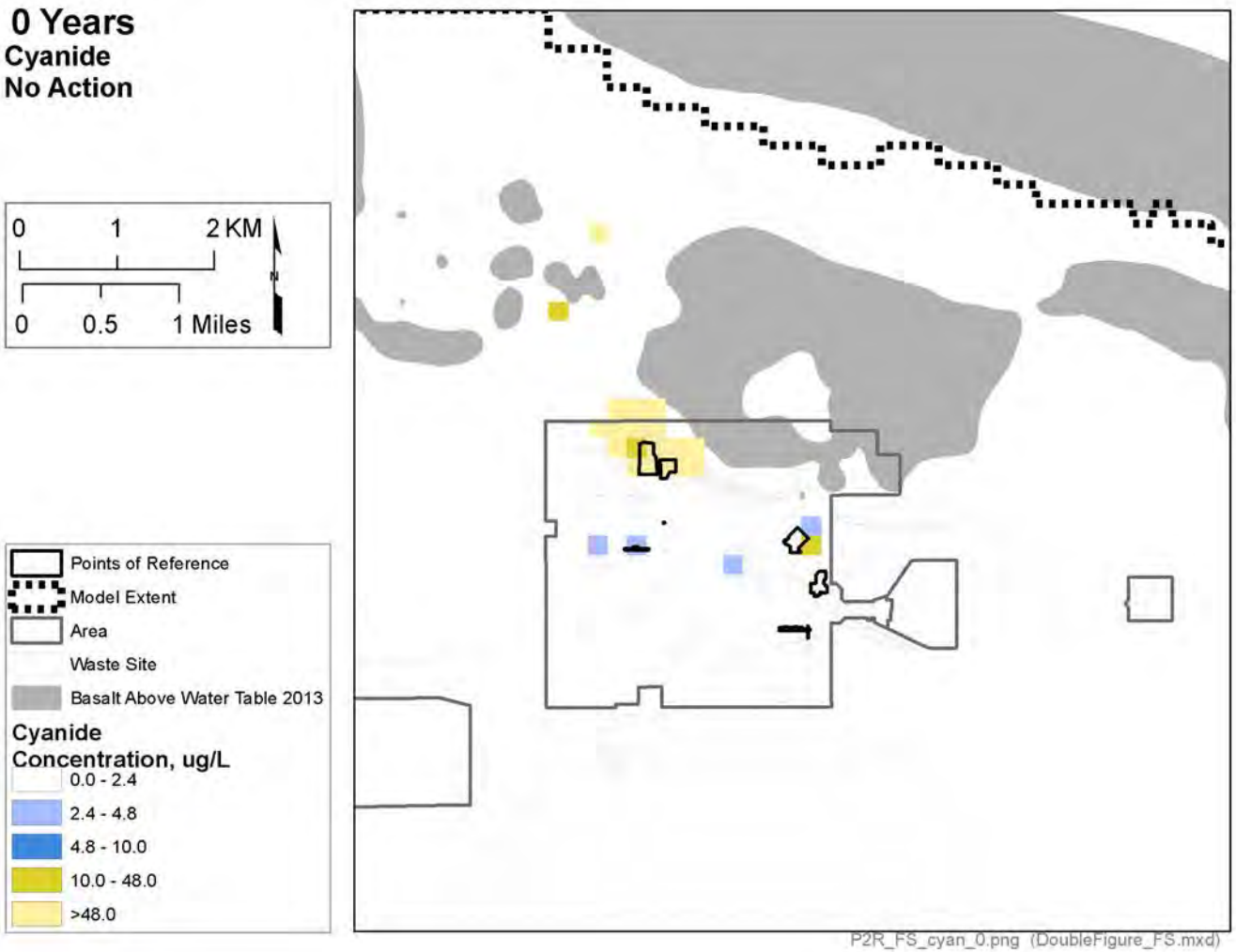

OU = operable unit

Note: The predominant source in the 200-BP-5 Operable Unit is shown under B Complex.

Table 8-1. Peak Concentrations and Time of Peak of Arrival at Waste Management Area C from the Calculated Remedial Evaluation Case for Upgradient Sources.

Contaminant of Concern	Peak Calculated Concentration	Calculated Year of Peak
Tc-99	1,430 pCi/L	2023
NO3	130 mg/L	2022
Uranium	38 µg/L	2059
I-129	4.3 pCi/L	2015
CN	39 µg/L	2023

8.1.3 Cyanide

The P2R model (DOE/RL-2009-127 Draft A) was used to simulate the evolution of the cyanide plume forward in time, beginning at year 2015. Cyanide is not a key contaminant of concern in the WMA C residual waste analyses (RPP-ENV-58806), but is discussed in detail in Appendix A of this document. The results of the P2R analysis are shown in Figures 8-12 to 8-15. The figures show elevated concentrations of cyanide in the vicinity of B Complex. By about year 2020, the plume has begun to arrive at WMA C. By year 2025, the center of mass of the plume is in the vicinity of WMA C. By year 2035, the plume has moved downgradient from WMA C.

The time dependence of the cyanide contamination from upstream sources is shown in Figure 8-16. The peak concentration of about 38 µg/L is at the present day or the near future.

8.1.4 Iodine-129

The P2R model (DOE/RL-2009-127 Draft A) was used to simulate the evolution of the ^{129}I plume forward in time, beginning at year 2015. The results of the analysis are shown in Figures 8-17 to 8-20. The figures show a ubiquitous plume of ^{129}I throughout the 200-BP-5 OU. The concentrations near WMA C remain in the higher concentration (dark blue) contour for the first 10 years. By year 2035 the concentration has begun to decrease (light blue contour), and by year 2045 the area under WMA C shows minimal ^{129}I concentration.

The time dependence of ^{129}I contamination from upstream sources is shown in Figure 8-21. The peak concentration of about 4 pCi/L is at the present day or the near future.

8.1.5 Uranium

The P2R model (DOE/RL-2009-127 Draft A) was used to simulate the evolution of the total uranium plume forward in time, beginning at year 2015. The results of the analysis are shown in Figures 8-22 to 8-25. The figures show a high concentration plume of ^{238}U under B Complex at the beginning of the simulation, which predominantly moves toward WMA C. The uranium

plume moves more slowly than ^{99}Tc or nitrate, and over the next ~130 years the plume moves with groundwater past WMA C, leading to a period of higher ^{238}U concentration beginning in about year 2050 and lasting until about year 2150.

Figure 8-13. The Cyanide Plume at Year 2020 (Year 5 of the Simulation) for the Remedial Evaluation Case of 200-BP-5.

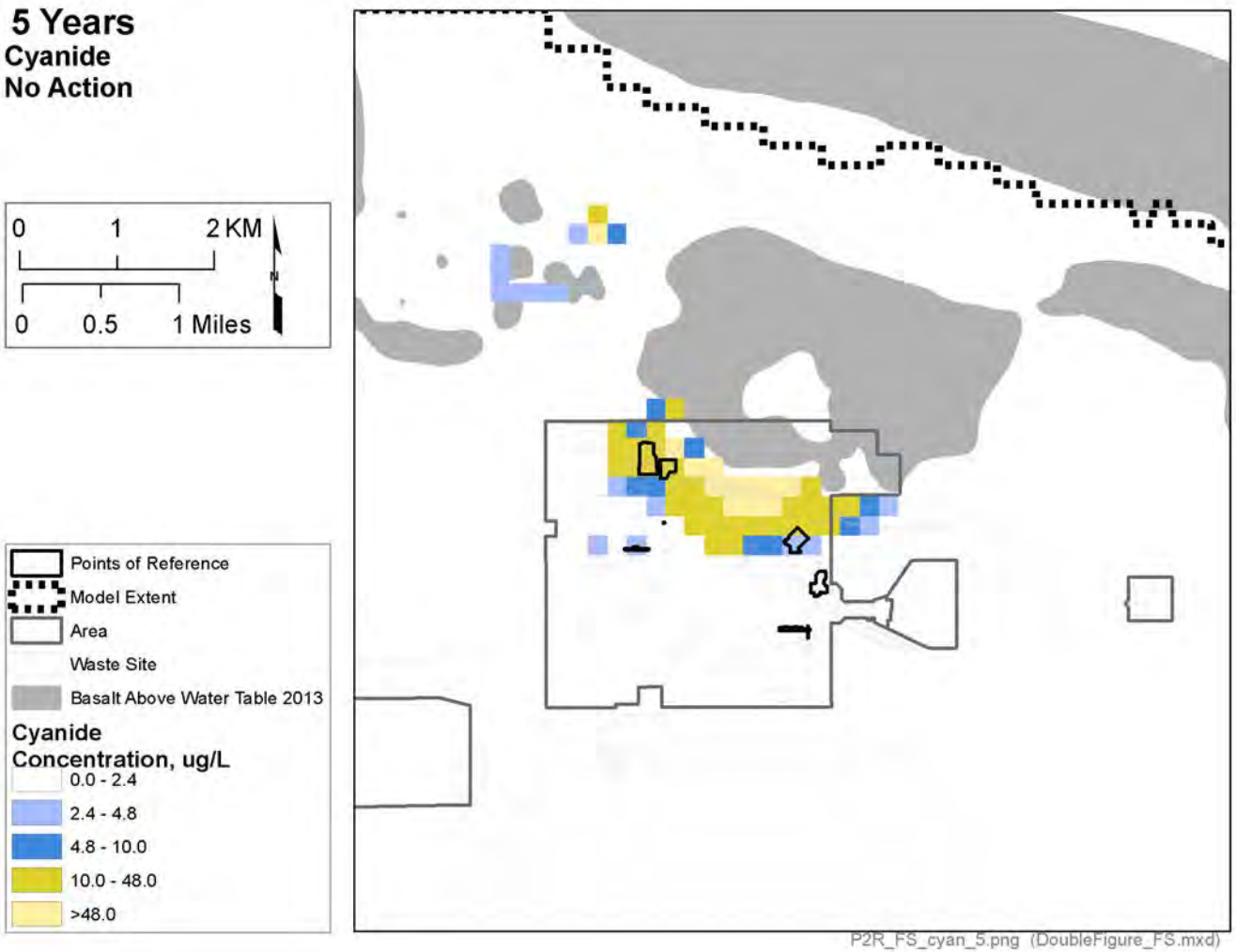

OU = operable unit

Note: The predominant source originating under B Complex has begun to arrive at Waste Management Area C.

Figure 8-14. The Cyanide Plume at Year 2025 (Year 10 of the Simulation) for the Remedial Evaluation Case of 200-BP-5.

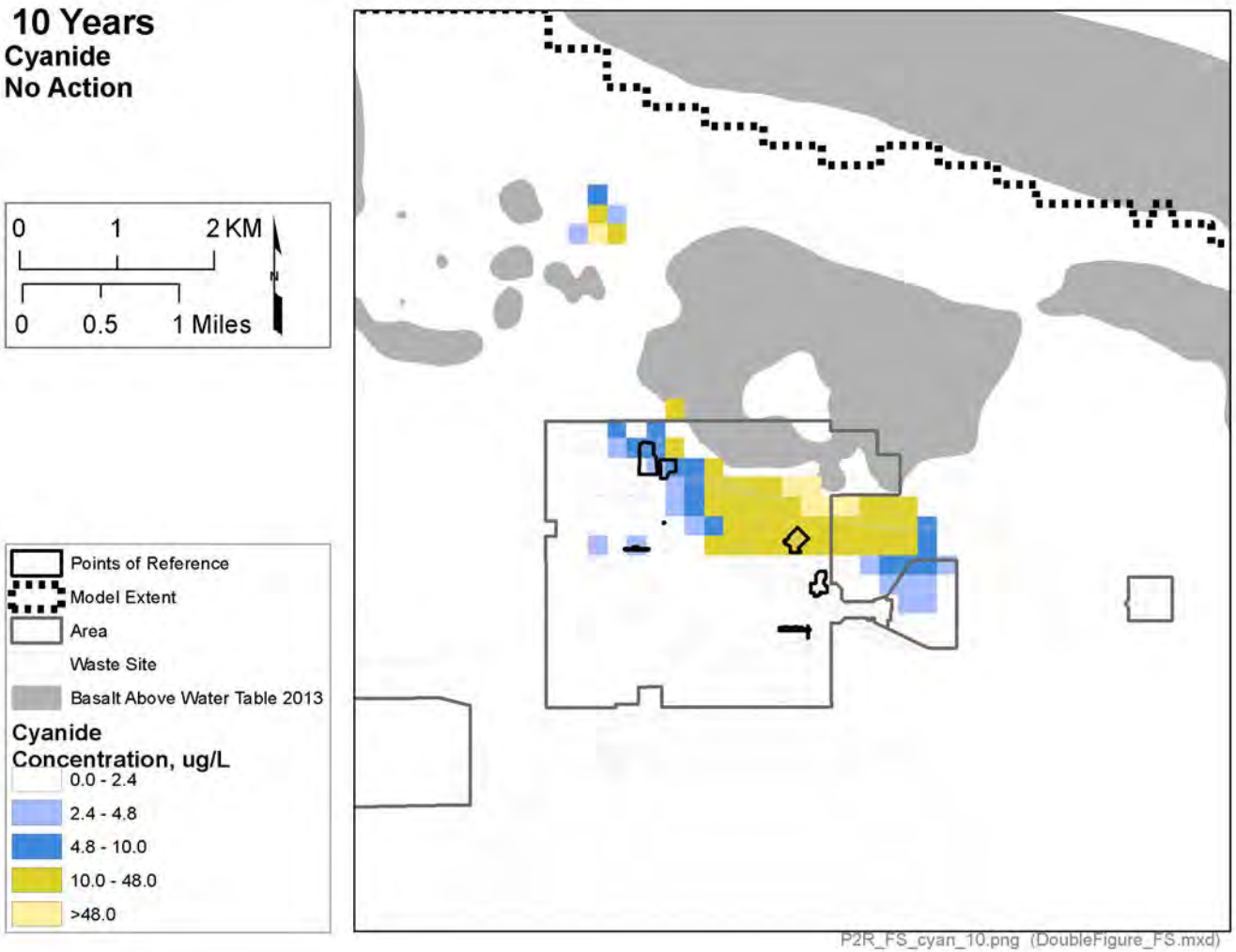

OU = operable unit

Note: The center of mass of the plume is in the vicinity of Waste Management Area C.

Figure 8-15. The Cyanide Plume at Year 2025 (Year 20 of the Simulation) for the Remedial Evaluation Case of 200-BP-5.

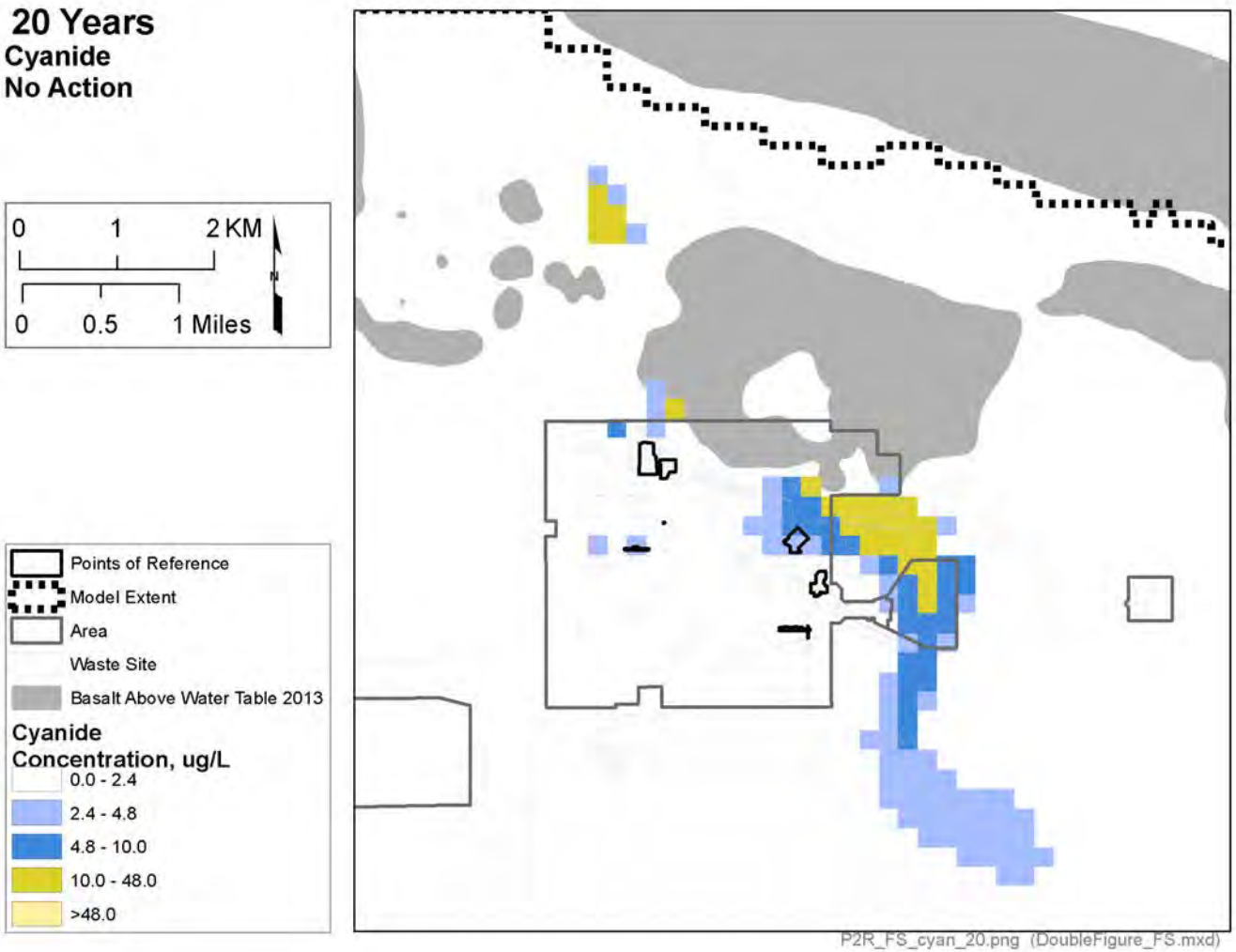

OU = operable unit

Note: The center of mass of the plume has moved downgradient from Waste Management Area C.

Figure 8-16. Remedial Evaluation Case Cyanide Concentrations at Waste Management Area C as a Function of Time.

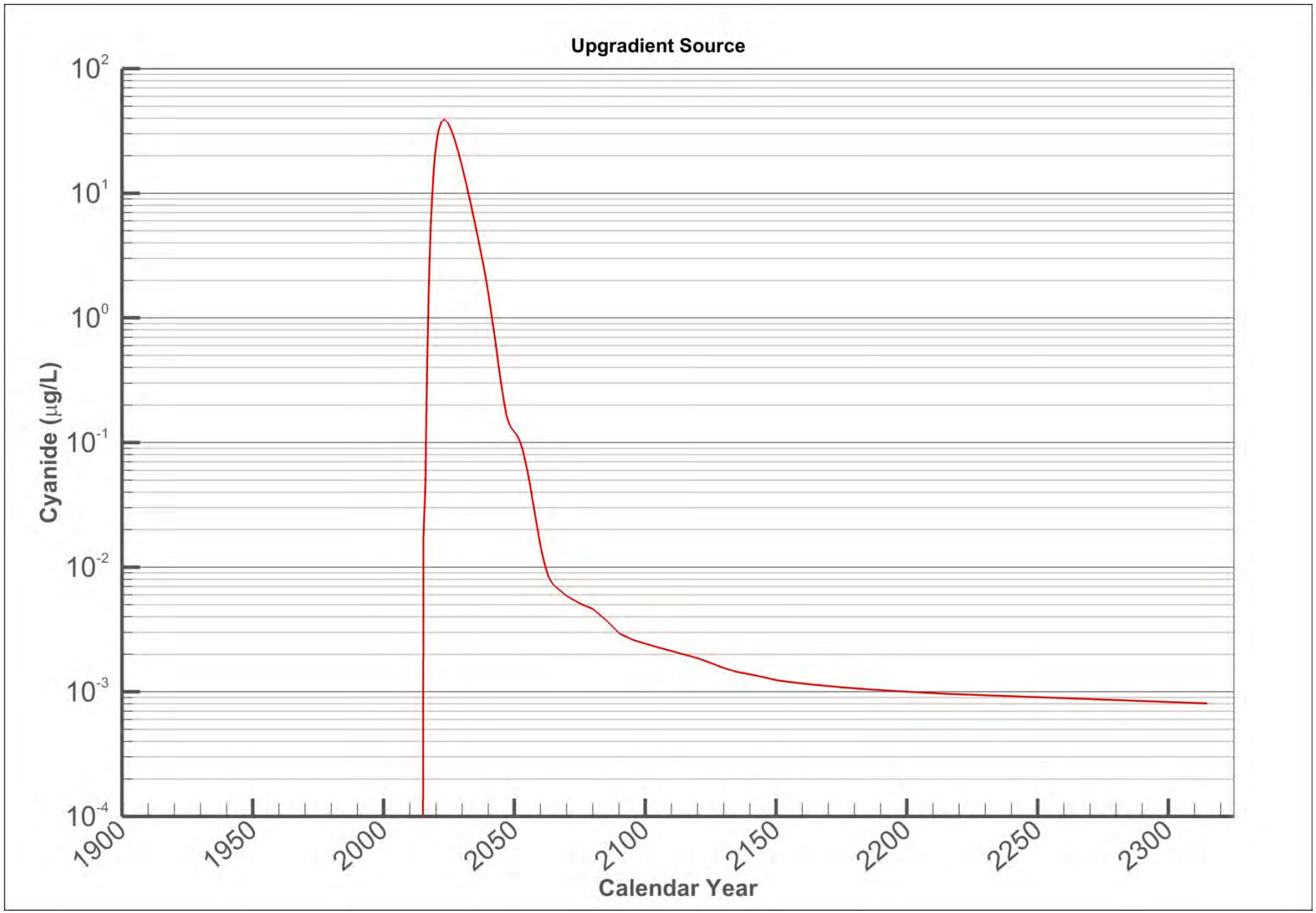

Figure 8-17. The Iodine-129 Plume at Year 2015 (Year 0 of the Simulation) for the Remedial Evaluation Case of 200-BP-5.

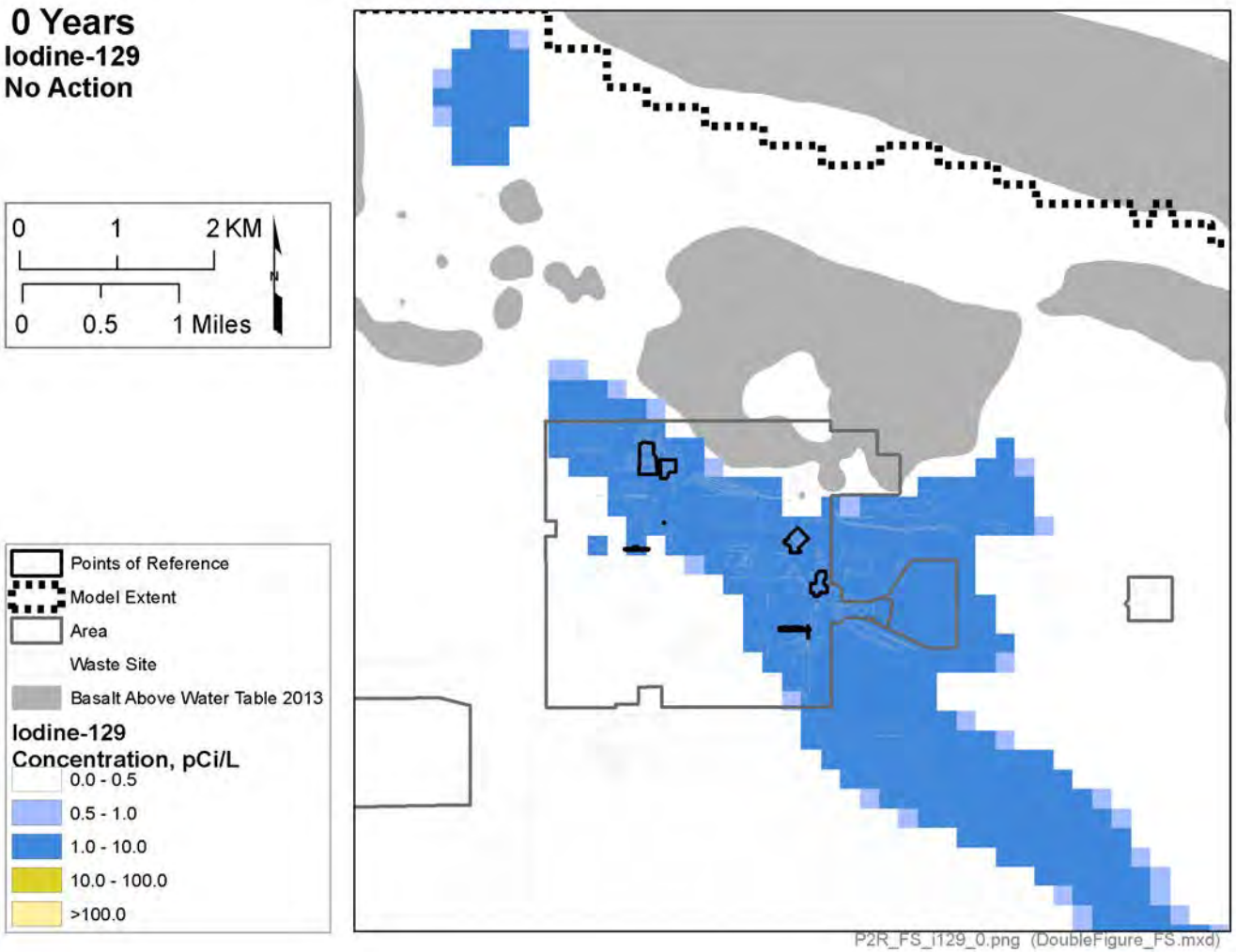

OU = operable unit

Note: The higher concentrations (dark blue contours) are widely distributed in the 200-BP-5 Operable Unit including under Waste Management Area C.

Figure 8-18. The Iodine-129 Plume at Year 2025 (Year 10 of the Simulation) for the Remedial Evaluation Case of 200-BP-5.

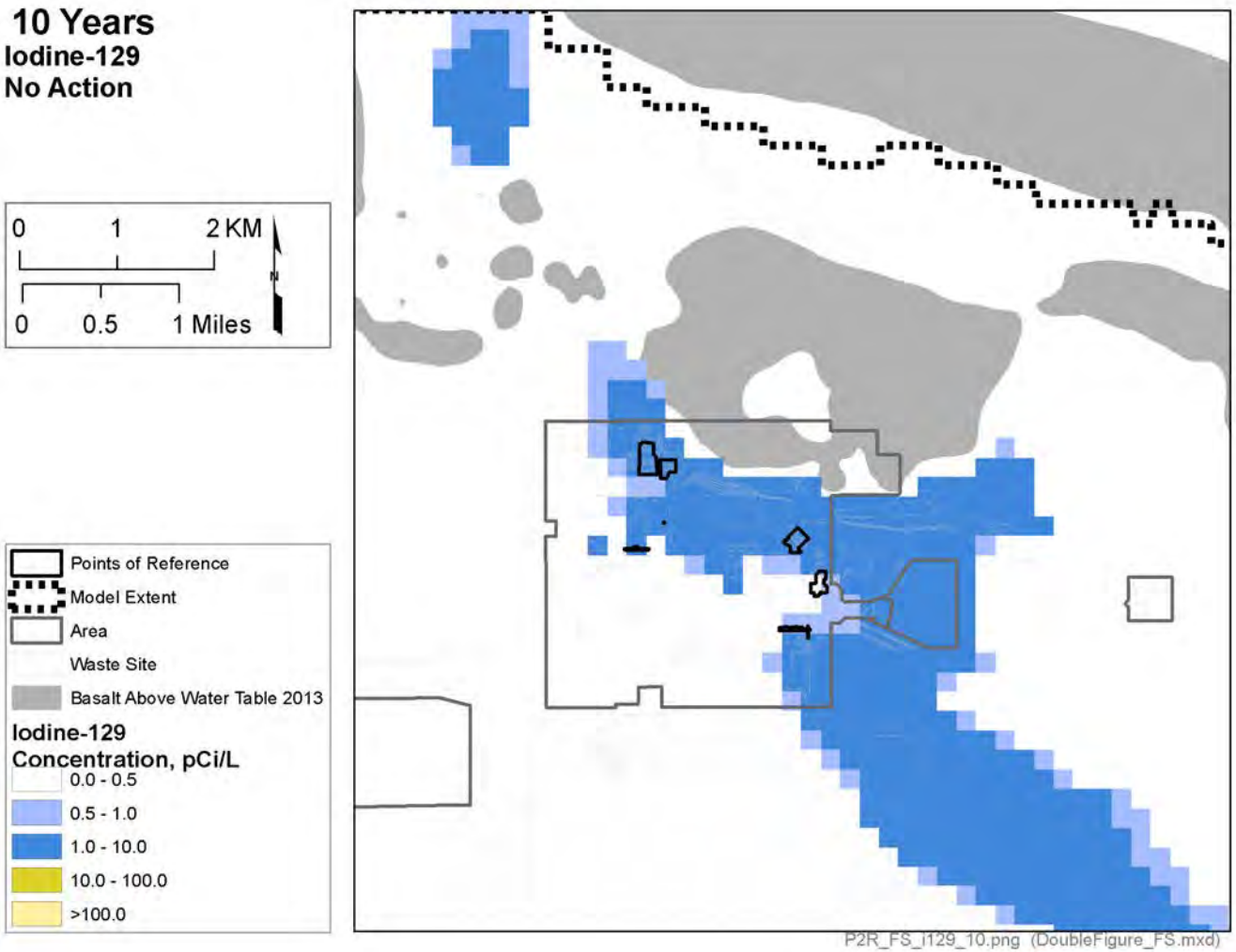

OU = operable unit

Note: The higher concentrations (dark blue contours) remain widely distributed in the 200-BP-5 Operable Unit and near Waste Management Area C.

Figure 8-19. The Iodine-129 Plume at Year 2035 (Year 20 of the Simulation) for the Remedial Evaluation Case of 200-BP-5.

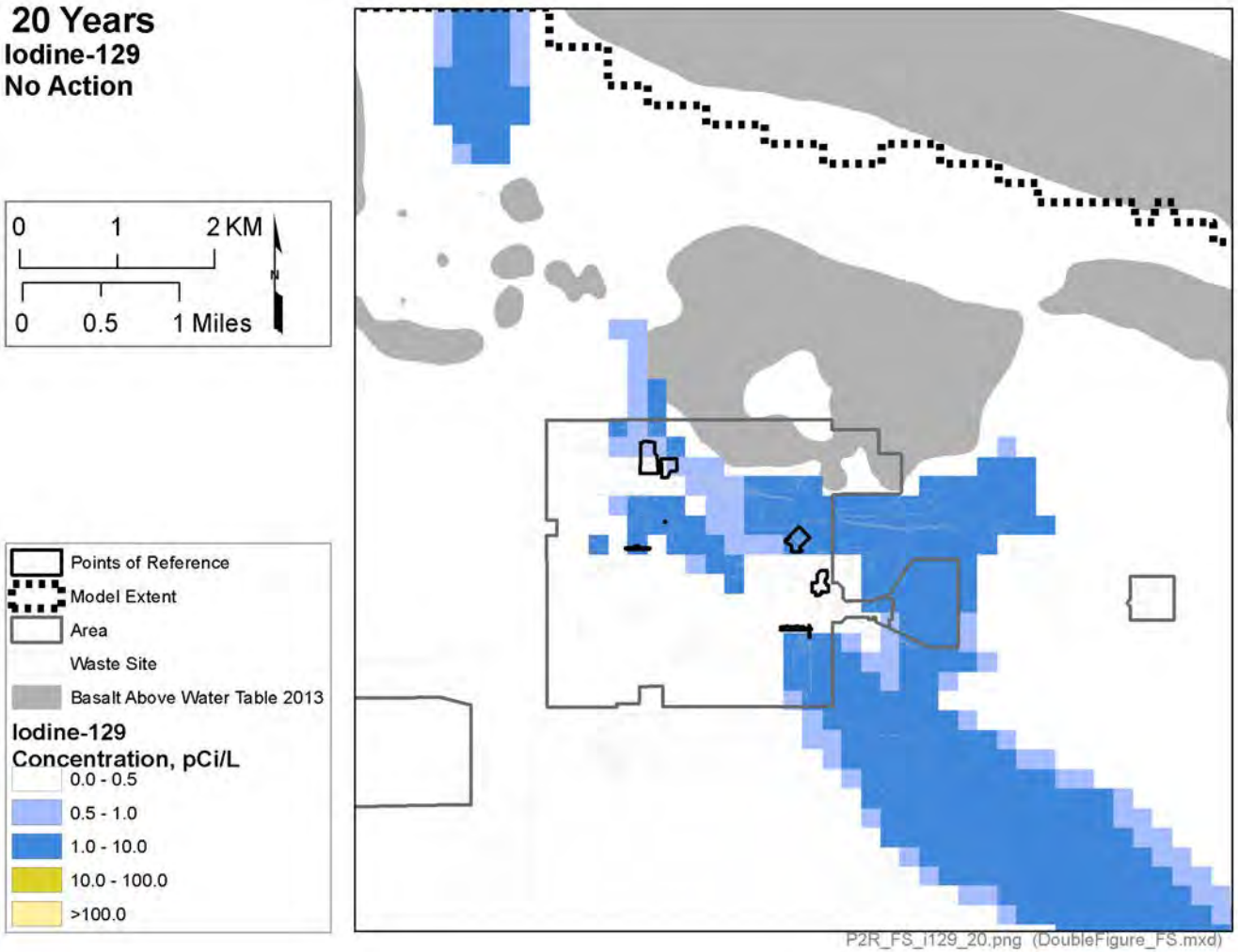

OU = operable unit

Note: The higher concentrations (dark blue contours) remain widely distributed in the 200-BP-5 Operable Unit, but have begun to move downgradient from Waste Management Area C.

Figure 8-20. The Iodine-129 Plume at Year 2045 (Year 30 of the Simulation) for the Remedial Evaluation Case of 200-BP-5.

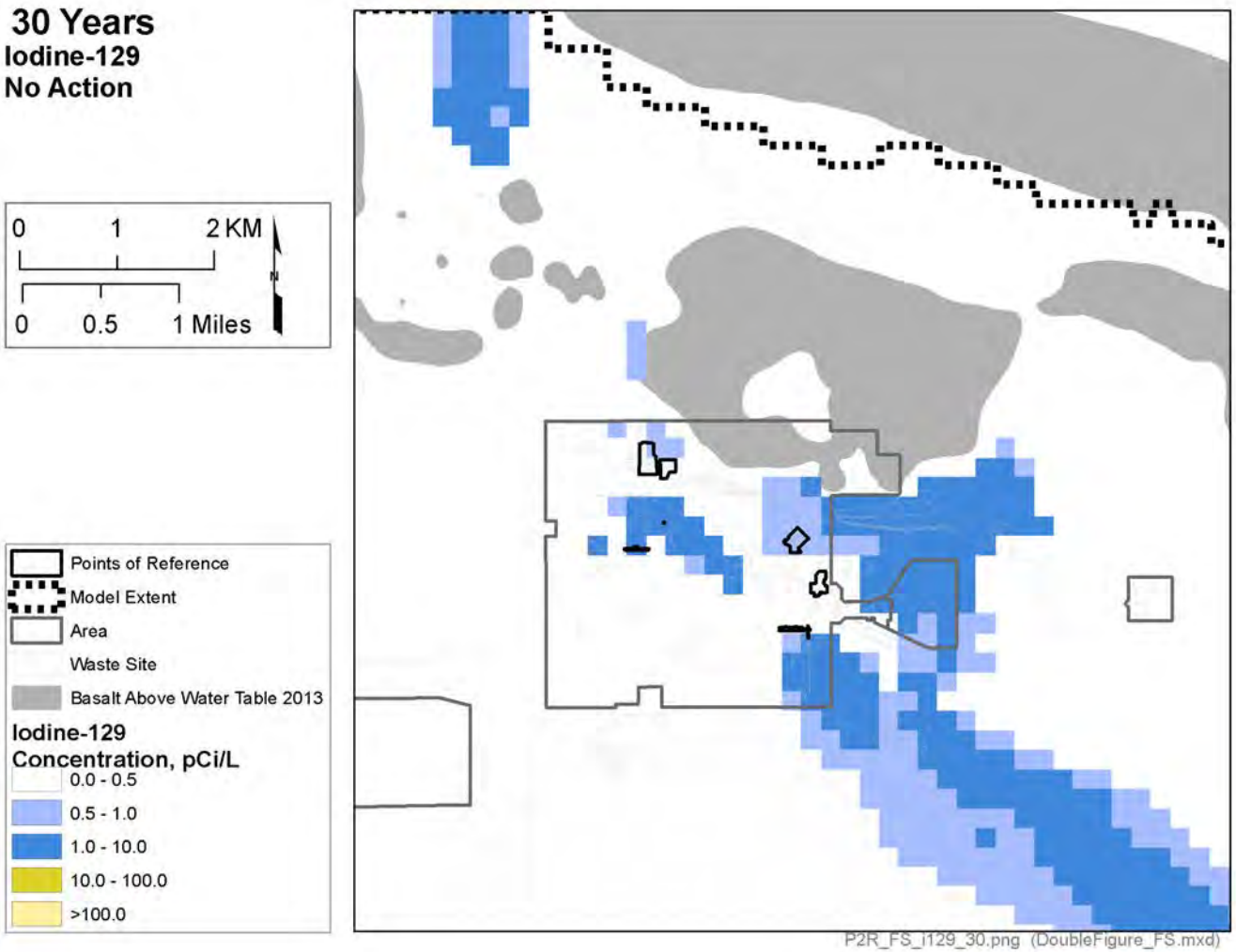

OU = operable unit

Note: Both the higher concentrations (dark blue contours) and lower concentration (light blue contours) have moved downgradient from Waste Management Area C.

Figure 8-21. Remedial Evaluation Case Iodine-129 Concentrations at Waste Management Area C as a Function of Time.

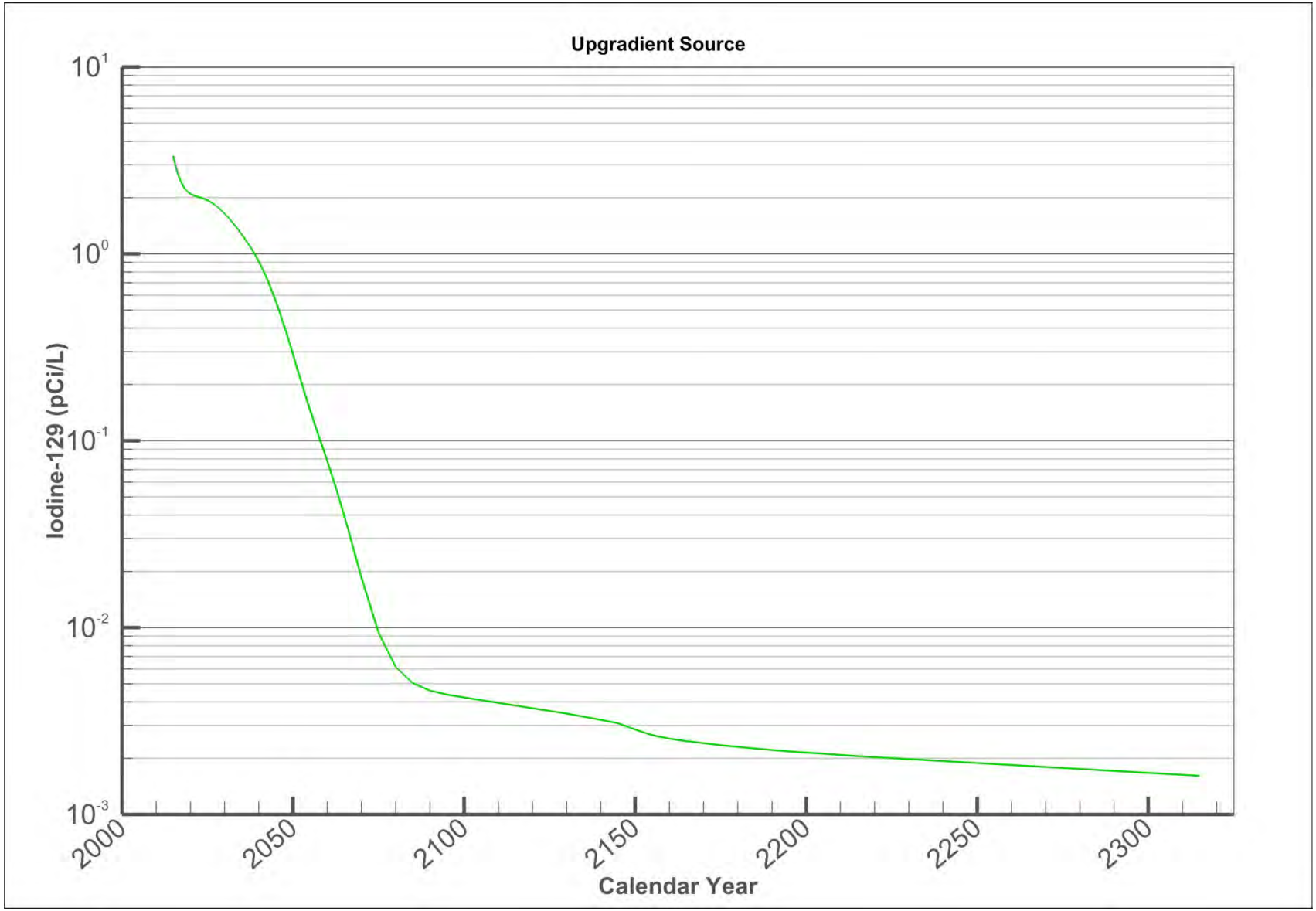

Figure 8-22. The Uranium Plume at Year 2015 (Year 0 of the Simulation) for the Remedial Evaluation Case of 200-BP-5.

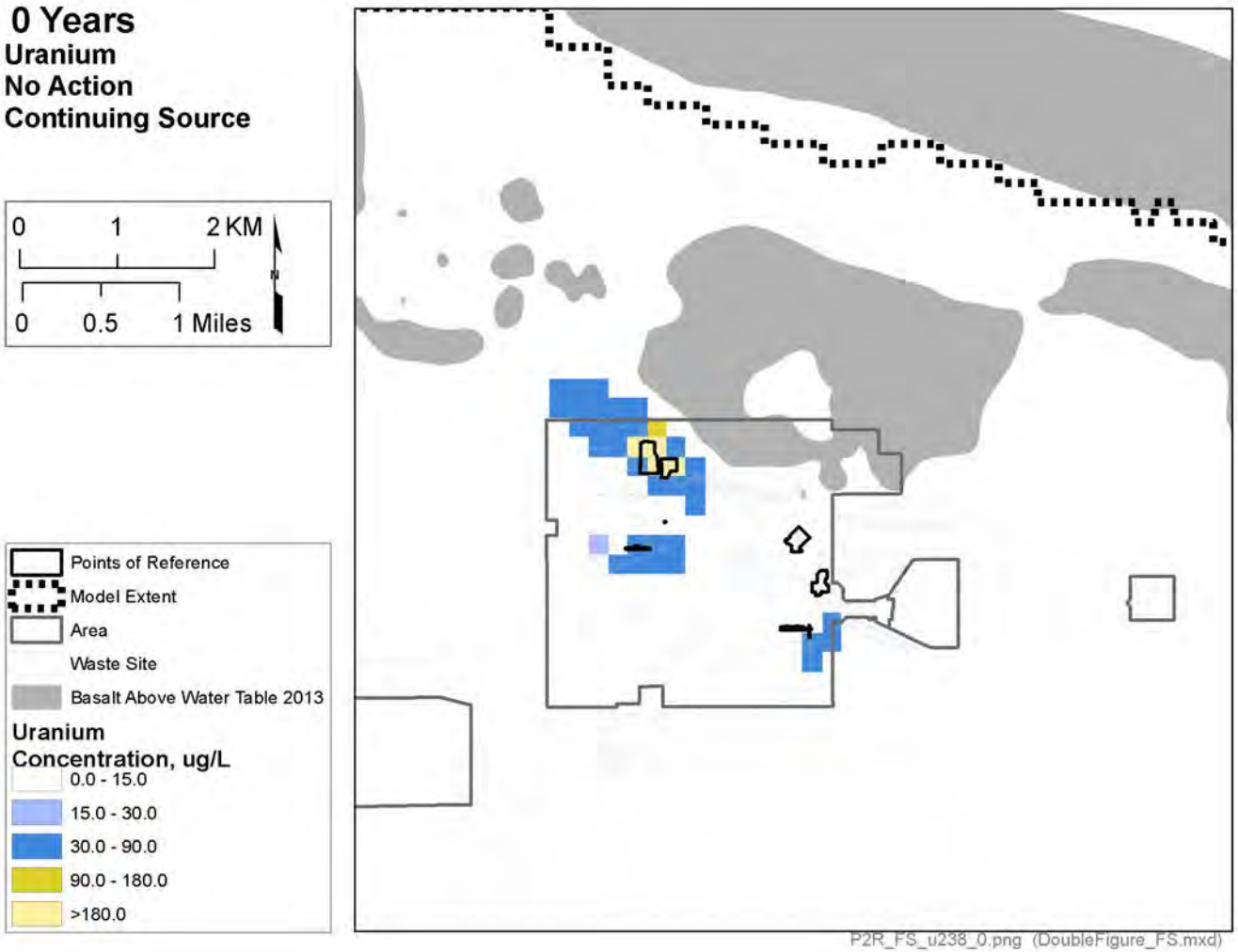

OU = operable unit

Note: Note that the higher concentrations (yellow contours are entirely upgradient from Waste Management Area C in the B Complex area.

Figure 8-23. The Uranium Plume at Year 2035 (Year 20 of the Simulation) for the Remedial Evaluation Case of 200-BP-5.

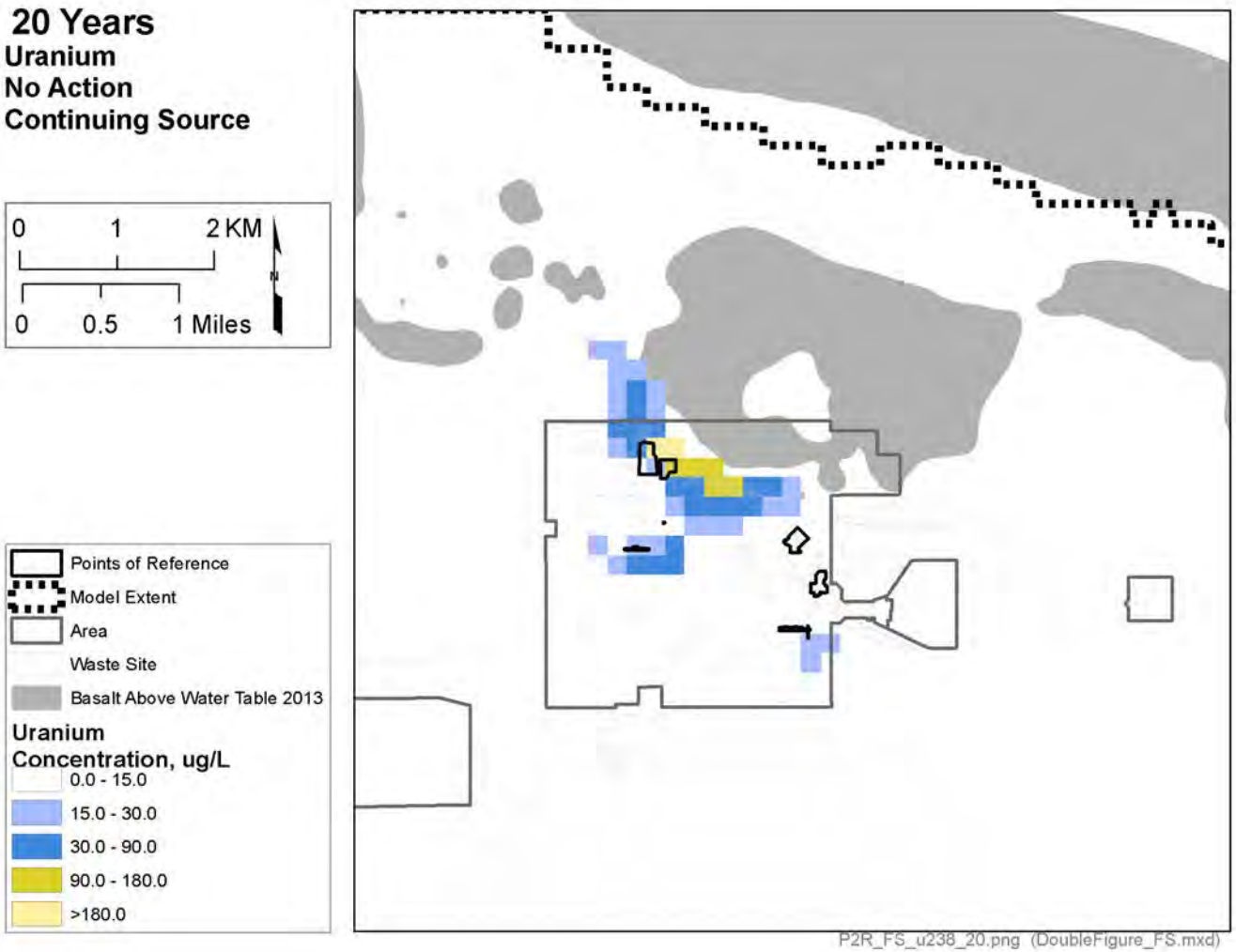

OU = operable unit

Note: The higher concentrations (yellow contours) have moved in the direction of Waste Management Area C but have not yet arrived. At this point in time the conservative species ^{99}Tc and nitrate have already passed Waste Management Area C.

Figure 8-24. The Uranium Plume at Year 2045 (Year 30 of the Simulation) for the Remedial Evaluation Case of 200-BP-5.

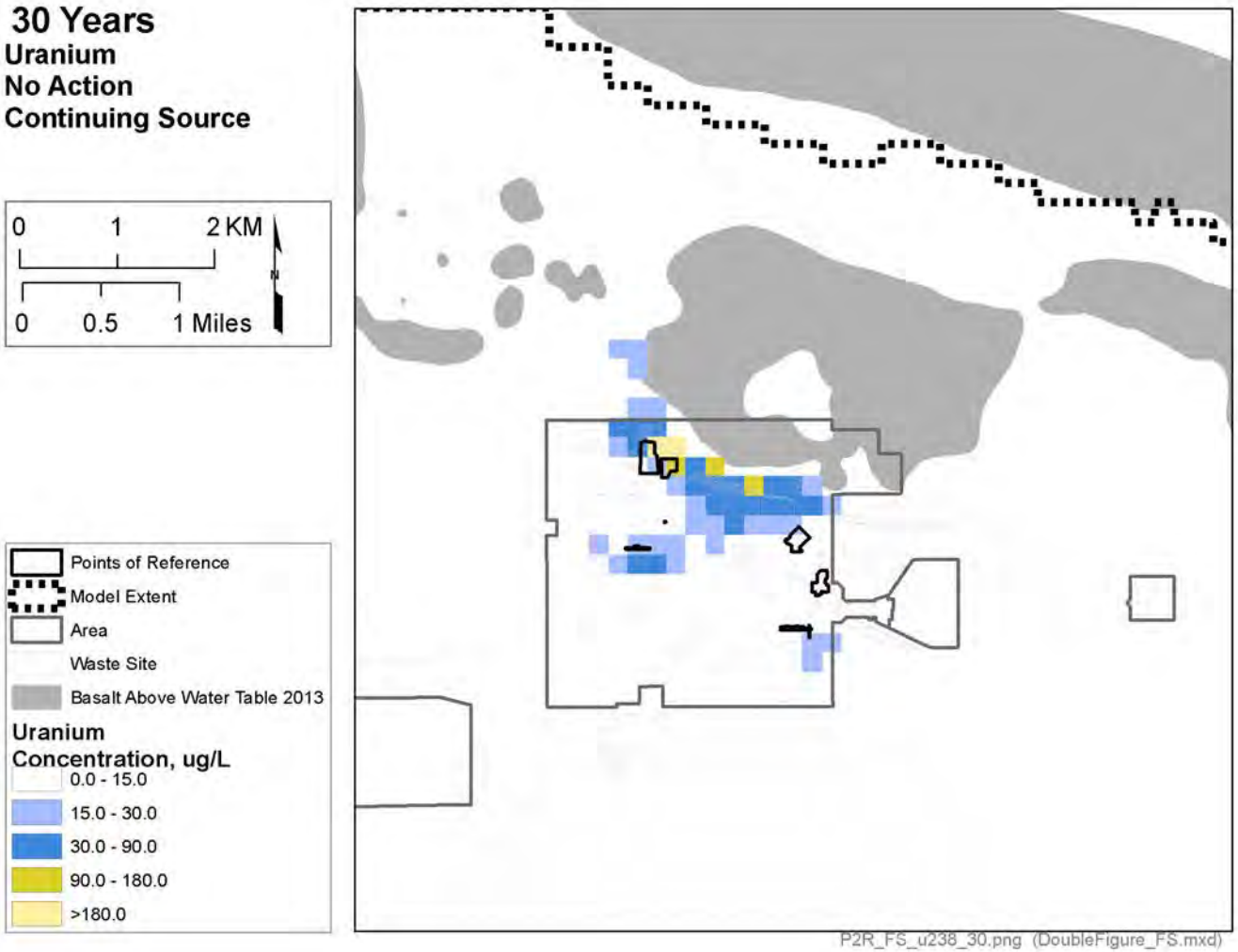

OU = operable unit

Note: Somewhat elevated ^{238}U concentrations have begun to arrive at Waste Management Area C.

Figure 8-25. The Uranium Plume at Year 2065 (Year 50 of the Simulation) for the Remedial Evaluation Case of 200-BP-5.

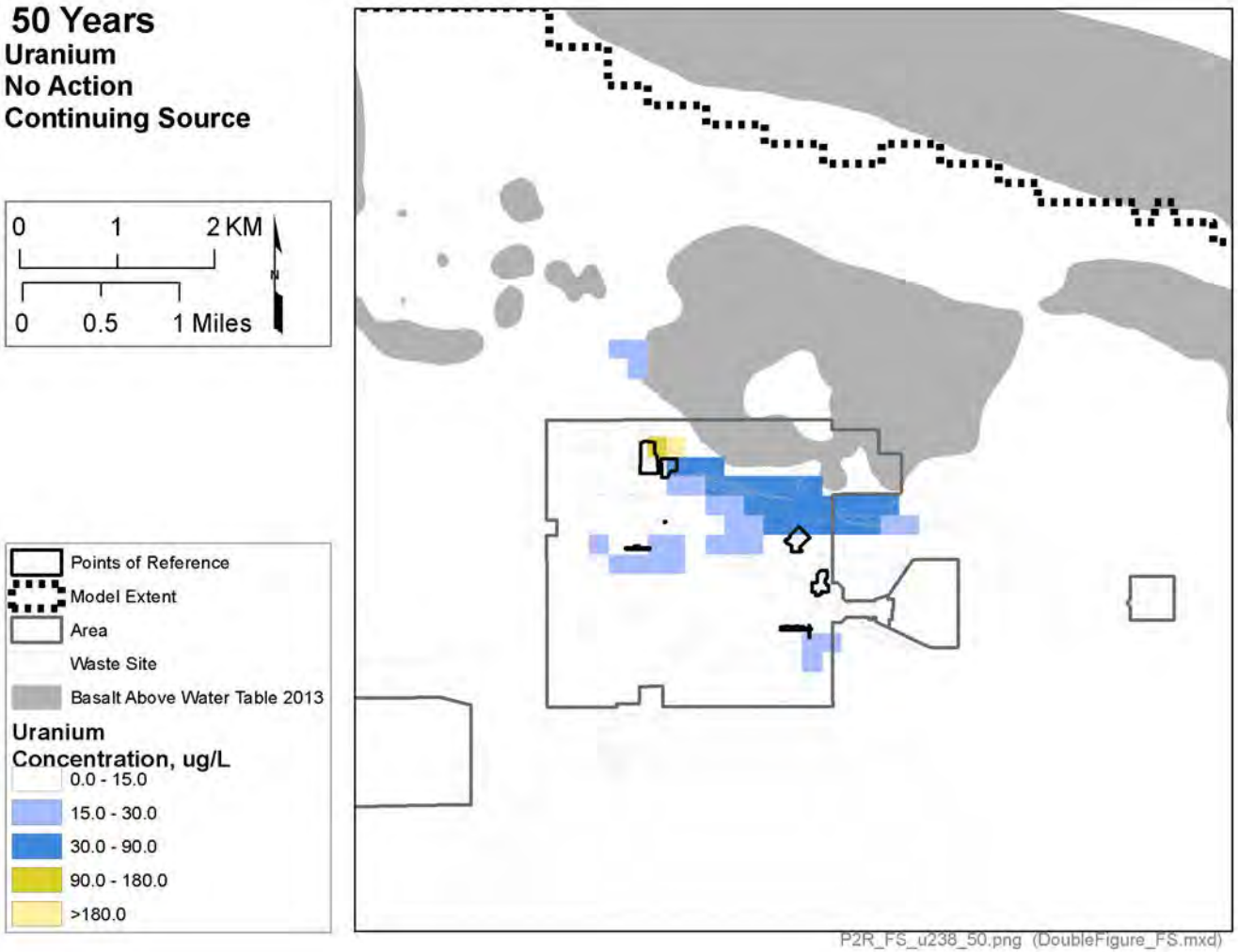

OU = operable unit

Note: The center of mass of the elevated uranium concentrations is in the vicinity of Waste Management Area C, remaining slightly to the north.

The time dependence of uranium contamination from upstream sources is shown in Figure 8-26. The peak concentration of ~38 µg/L occurs around year 2060.

8.2 CONTRIBUTION OF RESIDUAL WASTES

In this section, future projections of the contributions of groundwater impacts from landfill closure of residual wastes in tanks and ancillary equipment at WMA C are summarized. The details of the analyses and approaches that produced these results are presented in the PA report (RPP-ENV-58782) and RCA report (RPP-ENV-58806).

In each of the sections below, concentrations are reported at a distance 100 m (328 ft) from the boundary of the facility. To find the peak concentration in groundwater at this distance, a set of nine PoCals are used to evaluate the local concentration. Since the points of concentration are affected by different sources in WMA C, they have different peak concentrations. The results presented in this section represent the PoCal with the highest peak concentration, which may differ between contaminants. Results presented in this section are the "base case" results of the PA and RCA; both the PA and the RCA present extensive discussions of sensitivity and uncertainties in the analyses, and the base case results are understood as indicators of performance in the context of the broader treatment of uncertainties presented in RPP-ENV-58782 and RPP-ENV-58806.

8.2.1 Technetium-99

Technetium-99 is a key dose contributor in the residual waste performance assessment (RPP-ENV-58782). It is a mobile contaminant (K_d=0) and is not significantly retained in the residual wastes over performance assessment time scales. Calculated concentrations of ^{99}Tc at the highest point of calculation are presented in Figure 8-27. The peak concentration is 30 pCi/L at 1,570 years after closure. The spatial distribution of ^{99}Tc at the time of the peak concentration is shown in Figure 8-28. The MCL for ^{99}Tc is 900 pCi/L. More information about the groundwater impacts of ^{99}Tc found in residual wastes can be found in Section 7.2.1.2.2 of RPP-ENV-58782.

8.2.2 Nitrate

Nitrate is a key contaminant of concern in the RCA (RPP-ENV-58806). It is a mobile contaminant (K_d=0.0). Calculated concentrations of nitrate at the PoCals are presented in Figure 8-29. The peak concentration within 10,000 years is 0.3 mg/L at 1,375 years after closure. The spatial distribution of nitrate at the time of the peak concentration is shown in Figure 8-30. The current MCL for nitrate is 45 mg/L.

8.2.3 Cyanide

Cyanide is a contaminant evaluated in the RCA (RPP-ENV-58806). This analysis assumed that it is a mobile contaminant (K_d=0.0). Calculated peak concentration of cyanide at the PoCals downgradient of WMA C within a 10,000-year period of analysis is 0.01 ug/L at ~1500 years after closure. The DWS for cyanide is 200 µg/L. The current WAC 173-340-720 Method B groundwater cleanup level for cyanide (hazard quotient = 1) is 9.6 µg/L for CN^- and 4.8 µg/L for HCN.

8.2.4 Iodine-129

Iodine-129 is a key contaminant of concern in the PA (RPP-ENV-58782). It is a slightly sorbed contaminant (K_d=0.2). Calculated concentrations of ^{129}I at the PoCals are presented in Figure 8-31. The peak concentration within 10,000 years is 0.004 pCi/L at 6,200 years after closure. The current MCL for ^{129}I is 1 pCi/L. More information about the ground water impacts of ^{129}I found in residual wastes can be found in Section 7.2.1.2.2 of RPP-ENV-58782.

Figure 8-26. Remedial Evaluation Case Total Uranium Concentrations at Waste Management Area C as a Function of Time.

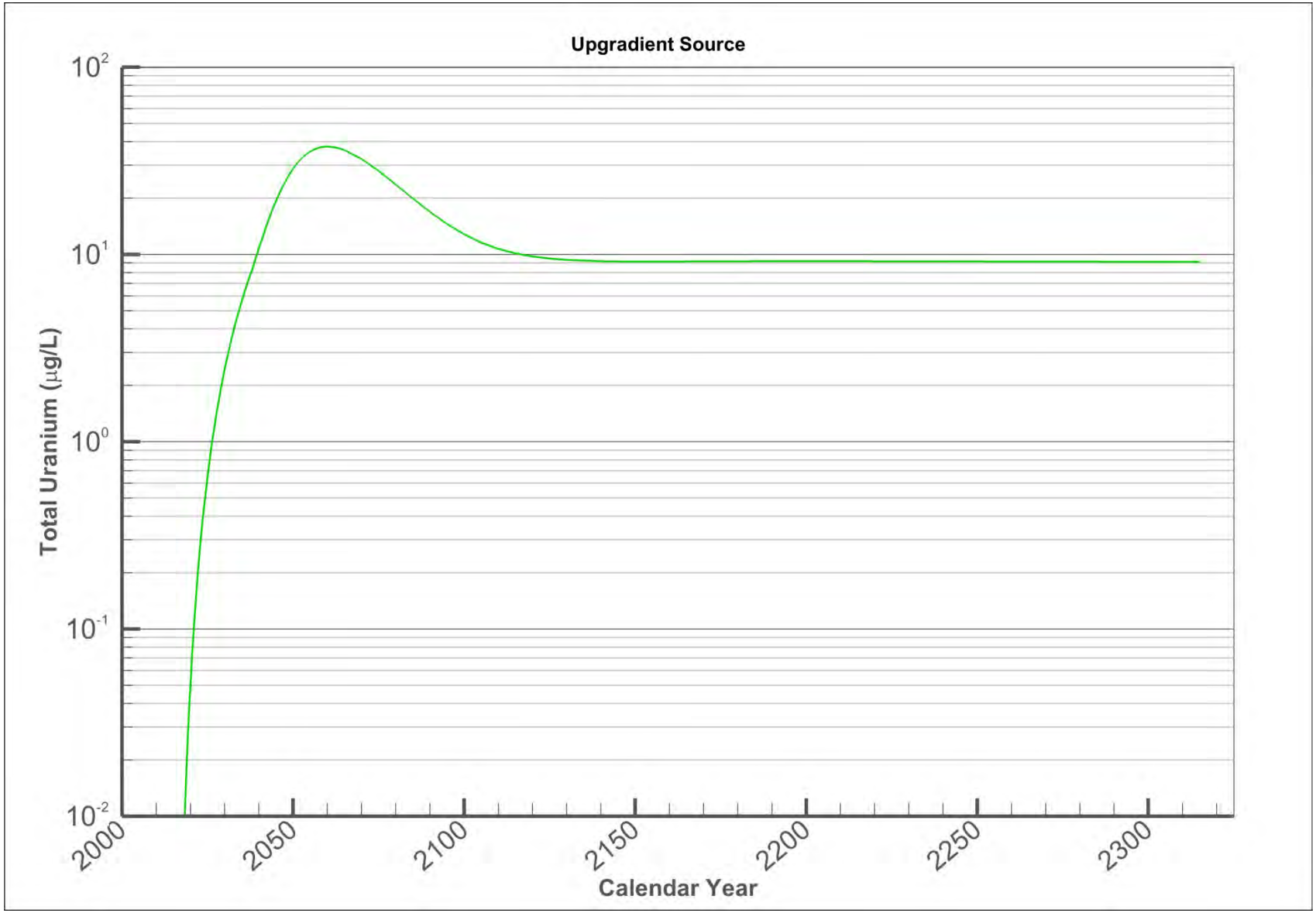

Figure 8-27. Groundwater Concentration of Technetium-99 at the Highest Point of Calculation 100 Meters Downgradient from Waste Management Area C.

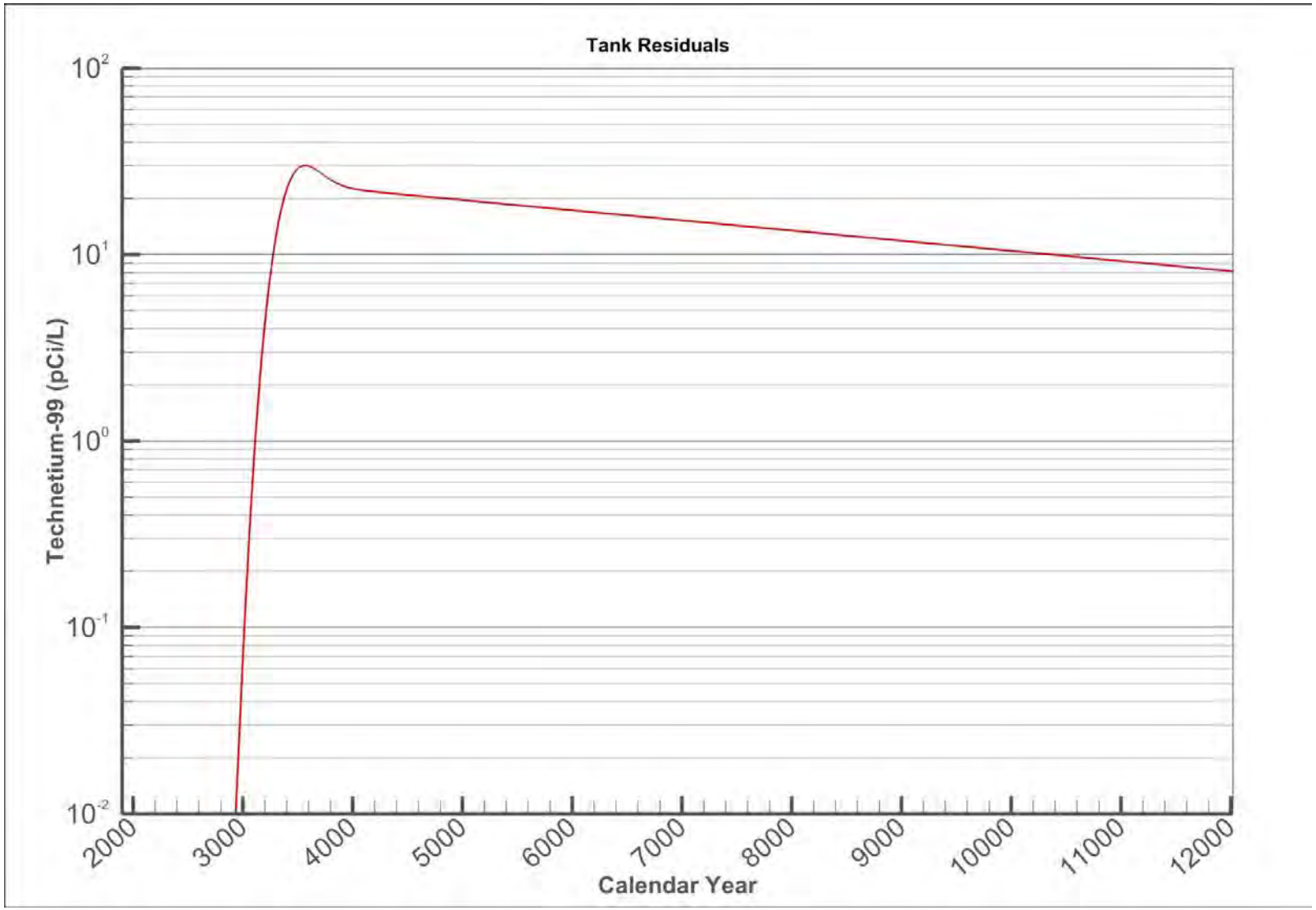

Reference: RPP-ENV-58782, *Performance Assessment of Waste Management Area C, Hanford Site, Washington*.

Figure 8-28. Extent of Technetium-99 Plume in Groundwater 1,570 Years after Closure at the Time of the Maximum Concentration at the Point of Compliance.

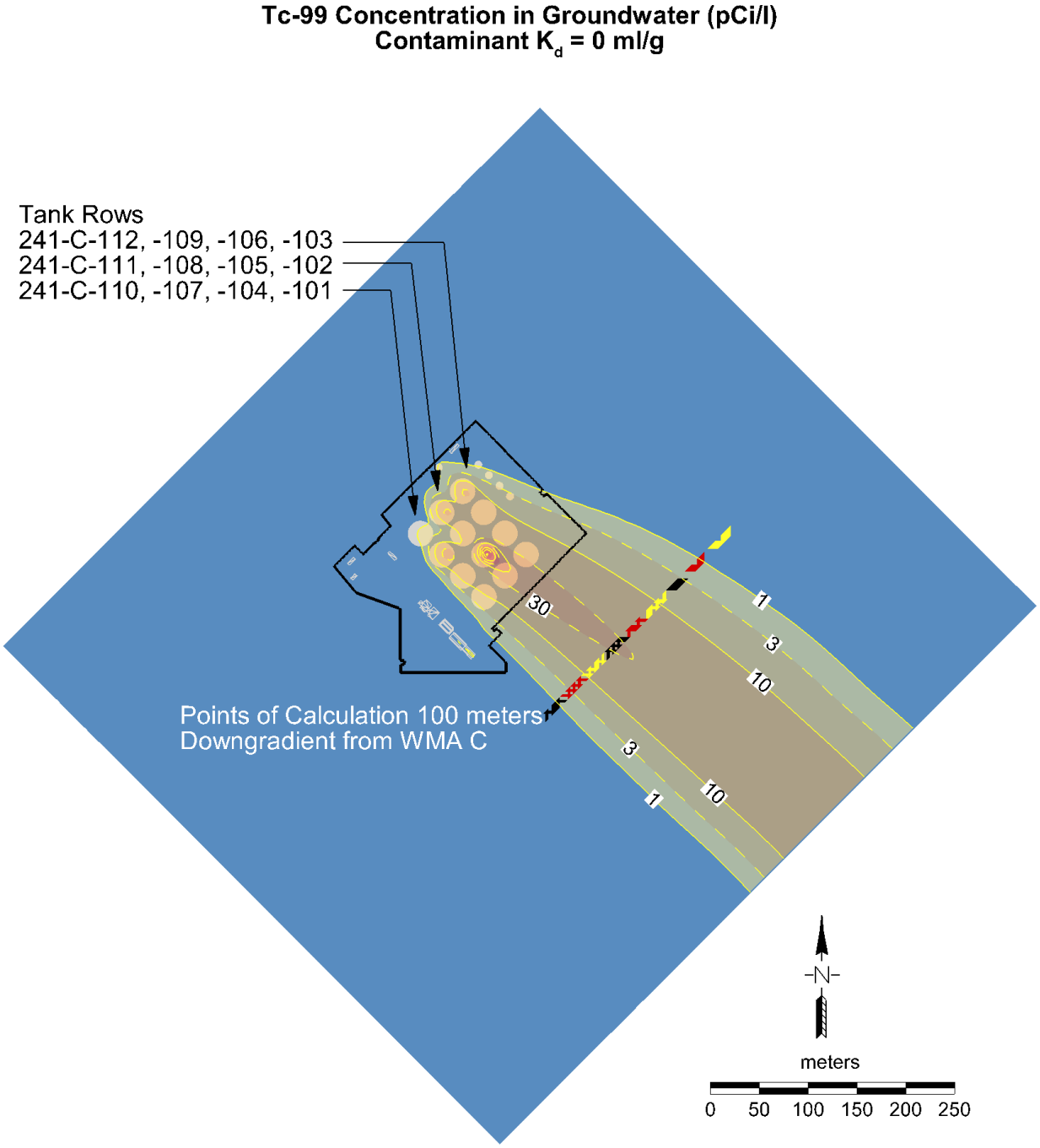

Approximate time of peak concentration at point of calculation

WMA = Waste Management Area

Reference: RPP-ENV-58782, *Performance Assessment of Waste Management Area C, Hanford Site, Washington*.

Figure 8-29. Maximum Predicted Groundwater Concentration of Nitrate (K_d = 0 mL/g) at All Points of Calculation 100 Meters Downgradient from Waste Management Area C from Residual Wastes.

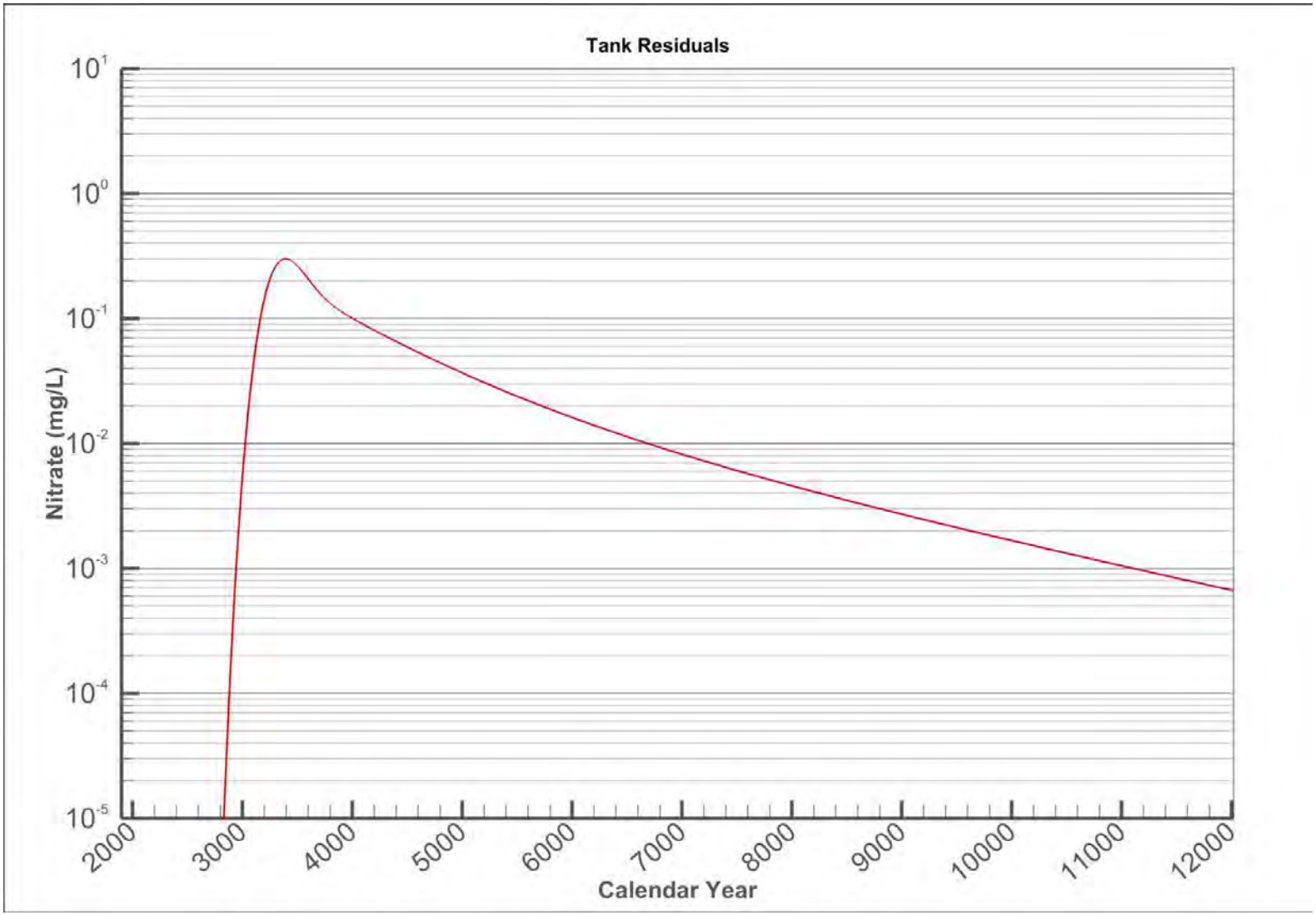

Reference: RPP-ENV-58806, *Analysis of Post-Closure Groundwater Impacts from Hazardous Chemicals in Residual Wastes in Tanks and Ancillary Equipment at Waste Management Area C at the Hanford Site, Southeast Washington, Washington*.

Figure 8-30. Extent of Nitrate Plume in Groundwater 1,375 Years after Closure at the Time of the Maximum Concentration at the 100-meter Point of Calculation.

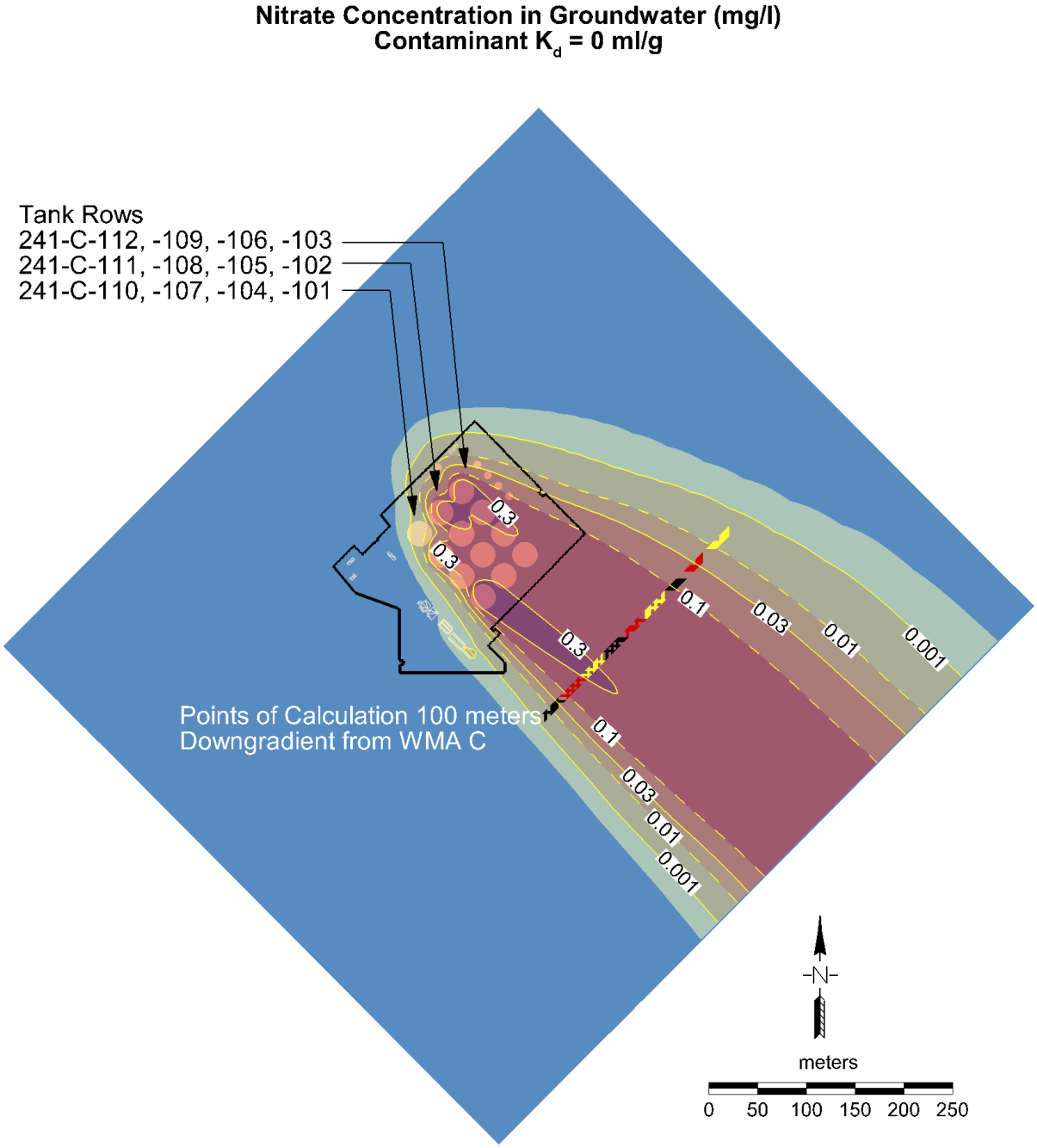

Approximate time of peak concentration at point of calculation

WMA = Waste Management Area

Reference: RPP-ENV-58806, *Analysis of Post-Closure Groundwater Impacts from Hazardous Chemicals in Residual Wastes in Tanks and Ancillary Equipment at Waste Management Area C at the Hanford Site, Southeast Washington, Washington.*

Figure 8-31. Groundwater Concentration of Iodine-129 at All Points of Calculation 100 Meters Downgradient from Waste Management Area C from Residual Wastes.

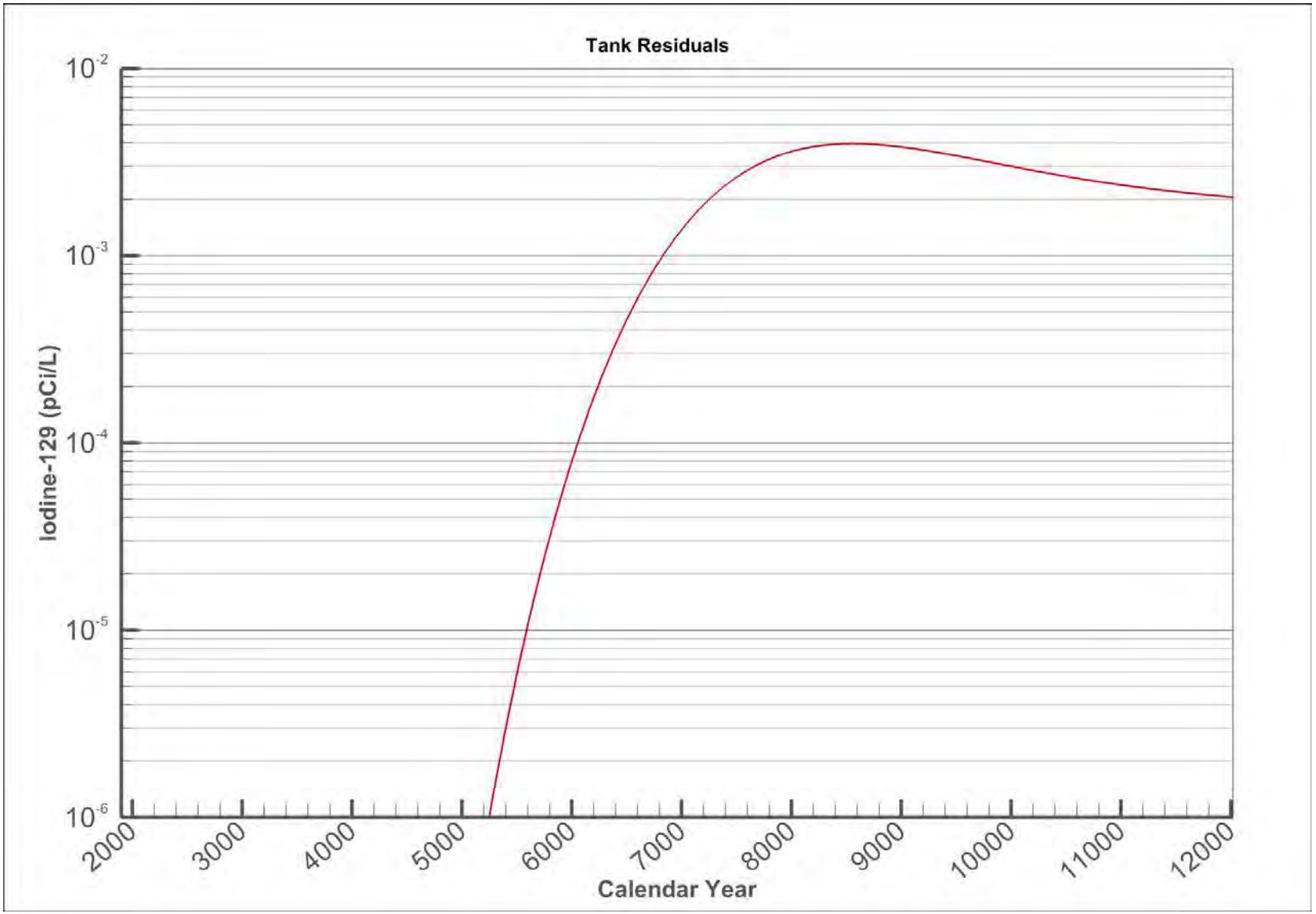

8.2.5 Uranium-238/Total Uranium

Uranium-238 is not a key dose contributor in the residual waste PA (RPP-ENV-58782), but uranium is of broad concern as a contaminant in the Central Plateau, and concentrations of total uranium are presented in the RCA (RPP-ENV-58806). It is a semi-mobile contaminant (K_d=0.6). Calculated concentrations of ^{238}U at the highest point of calculation are presented in Figure 8-32a, and total uranium in Figure 8-32b. The peak concentration for ^{238}U within 10,000 years is 0.02 pCi/L at 10,000 years after closure. The peak concentration for total uranium within 10,000 years is 0.05 µg/L at 10,000 years after closure. The concentrations are still increasing at 10,000 years. The current MCL for total uranium is 30 µg/L. More information about the groundwater impacts of ^{238}U, as surrogate for total uranium, found in residual wastes can be found in Section 7.2.1.2.2 and 8.28 of RPP-ENV-58782. These results show that concentrations from uranium released in ancillary equipment peaks sometime around 15,000 years after closure.

8.3 COMPARISON OF UPGRADIENT SOURCES, RESIDUAL WASTES, AND PAST LEAKS

In this section, a qualitative comparison is provided between projected concentrations from past leaks, residual wastes, and upgradient sources. Caution must be used in drawing too strong conclusions from this comparison because the purpose and intent of each is different, and the underlying assumptions differ. Key assumptions in the analyses include the following.

- The projected concentrations for upgradient sources are based on an assumption that no remedial activities will be conducted. Currently, the planned remedial actions will likely reduce these concentrations.

- The concentrations calculated for residual wastes are intended for regulatory compliance, and are calculated at a distance 100 m (328 ft) downgradient from WMA C. This location does not correspond to the location of the results presented in Section 4.

Consequently, results for the past leaks analysis were calculated at the 100 m (328 ft) PoCals, allowing direct comparisons of results from the assessment of leaks and of residual wastes. Results for the upgradient sources represent the upgradient locations presented in Section 8.1, so caution must be exercised in the comparison with the WMA C sources.

8.3.1 Technetium-99

A comparison of results for ^{99}Tc is presented in Figure 7-33, along with results from the residual waste PA and upgradient sources. The calculation of concentrations from leaks and residual wastes coincide at the same line of analysis at 100 m (328 ft) downgradient, but the upgradient source concentrations are at the PoCals from the P2R model discussed in Section 7.1. Owing to differences in grid spacing used between the P2R model and the local-scale model of WMA C,

results from the P2R model for the comparison of impacts from upgradient sources to other source were extracted at a PoCal that most closely corresponded to the upgradient boundary the WMA C fenceline.

The peak concentration of ^{99}Tc associated with the past leaks is approximately two orders of magnitude higher than for residual wastes, and about a factor of five higher than upgradient sources. Caution should be used in interpreting these results. As the results are generated by two different models with differing spatial discretizations and hydraulic parameters, the concentrations from past leaks analysis and upgradient sources cannot be simply combined in a strict sense, but rather should be evaluated in a qualitative manner.

Figure 8-32a. Predicted Groundwater Concentration of Uranium-238 at the Highest Point of Calculation 100 Meters Downgradient from Waste Management Area C.

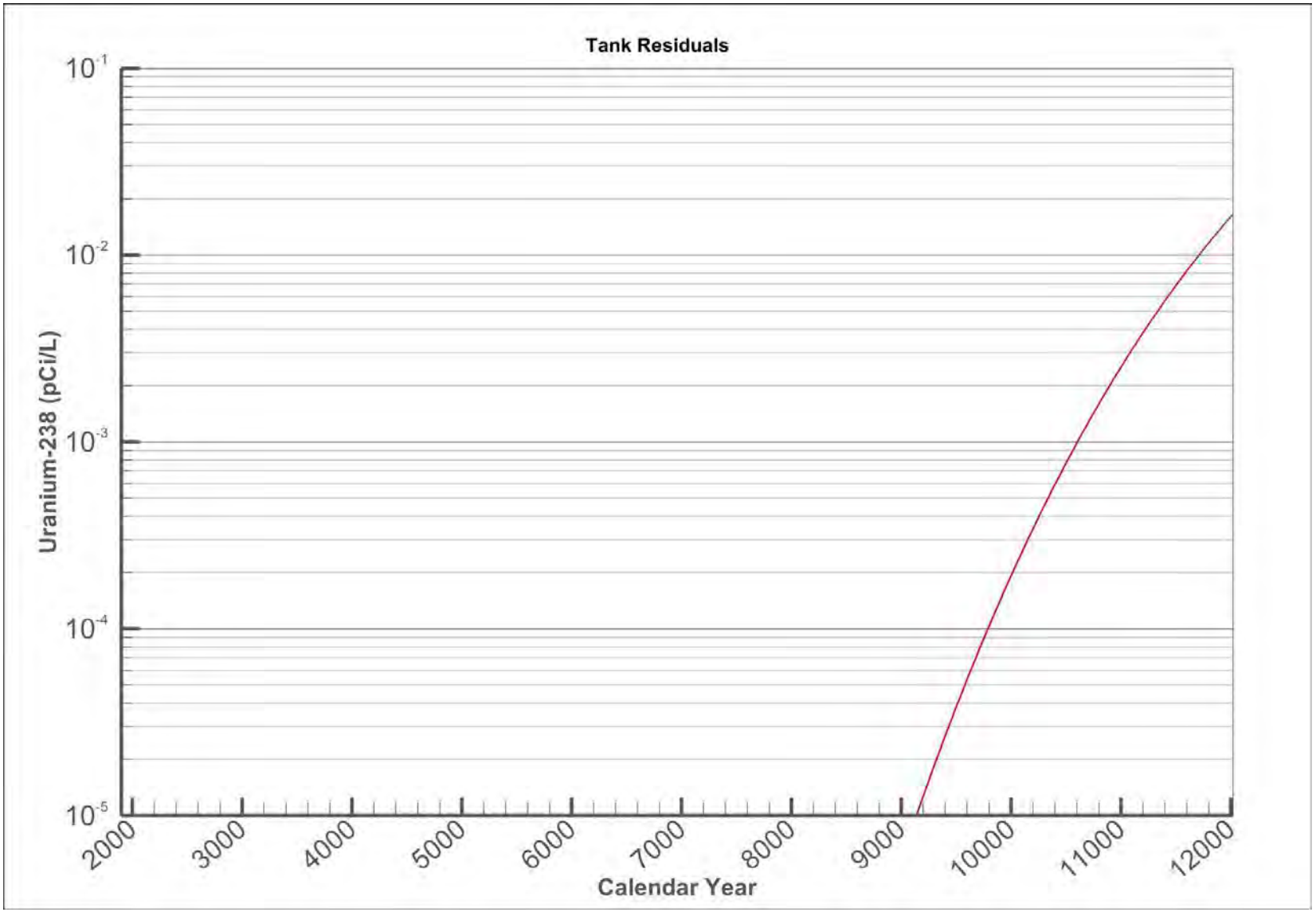

Figure 8-32b. Predicted Groundwater Concentration of Total Uranium at the Highest Point of Calculation 100 Meters Downgradient from Waste Management Area C.

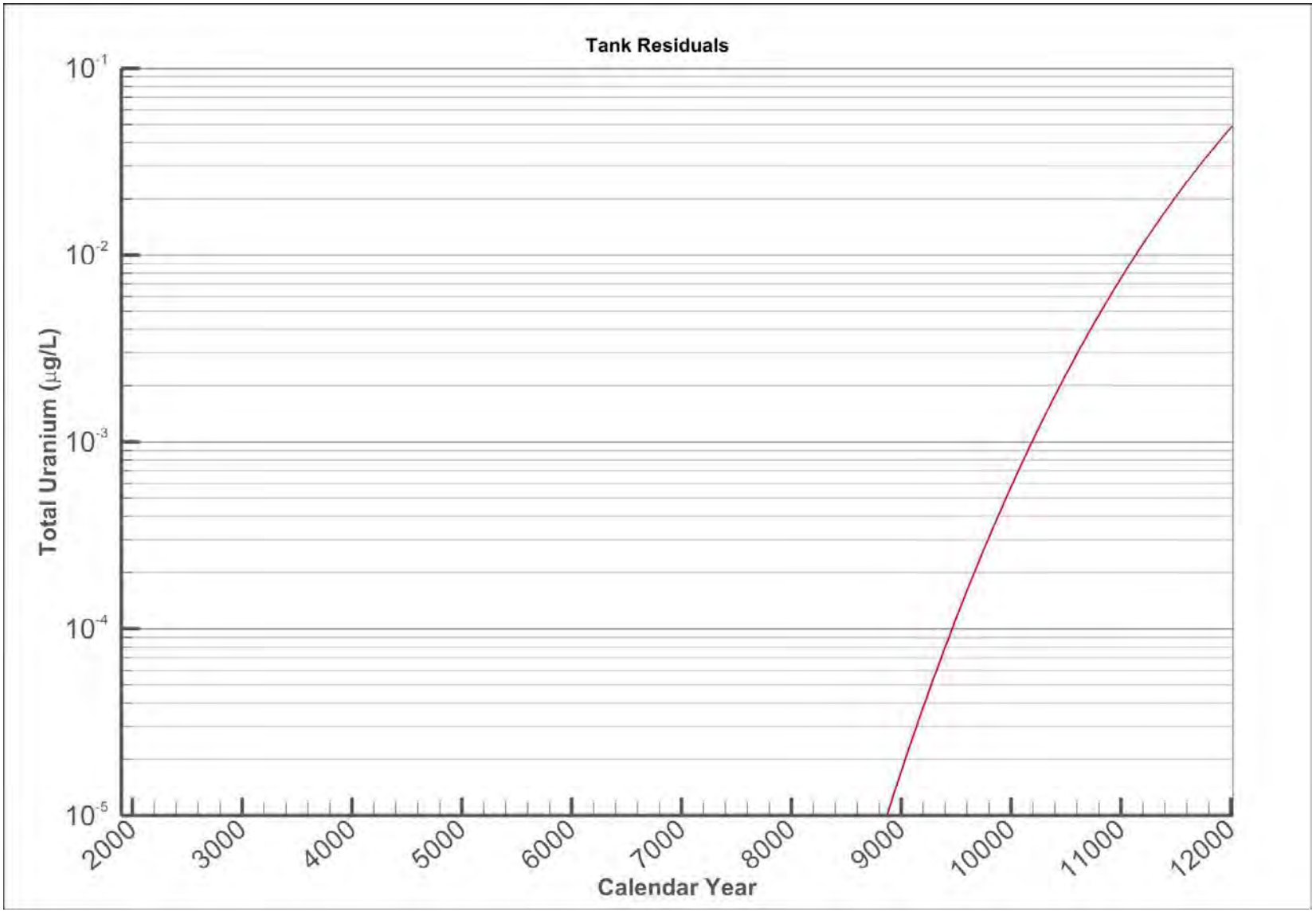

Figure 8-33. Results of the Past Leak Analysis for Technetium-99 at Points of Calculation 100 Meters Downgradient, Compared to Results from the Residual Waste Analysis and Upgradient Sources.

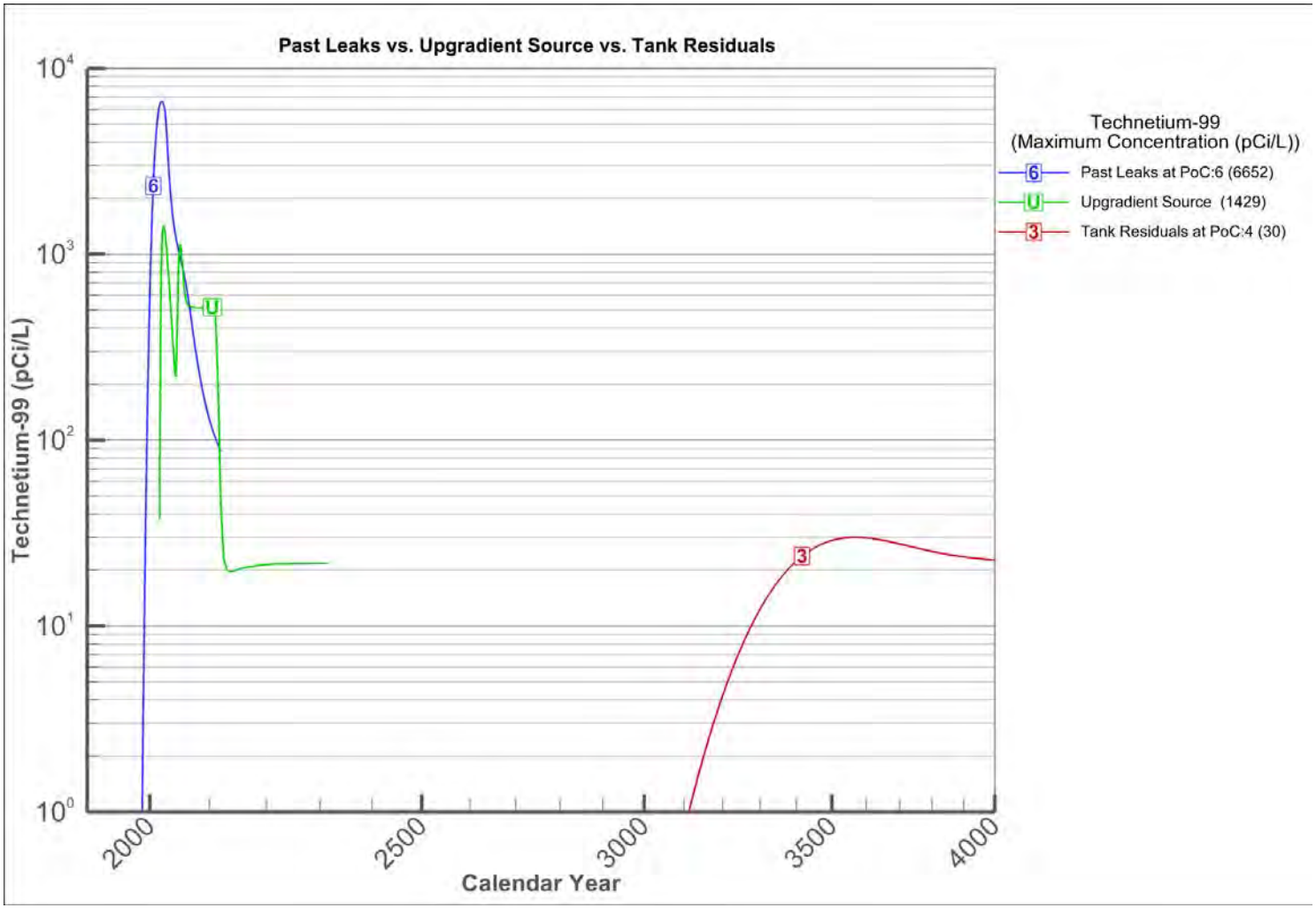

PoC = point of calculation

Note: The peak concentration for each curve is shown in parenthesis in the legend. The plots are on log-log scale to allow comparison of curves at different scales.

8.3.2 Nitrate

Results for nitrate are presented in Figure 8-34, compared with results from the residual waste PA and upgradient sources. The calculation of concentrations from leaks and residual wastes coincide at the same line of analysis at 100 m (328 ft) downgradient, but the upgradient source concentrations are at the PoCals from the P2R model discussed in Section 7.1. The concentration of nitrate from upgradient sources is approximately two orders of magnitude higher than nitrate concentration results from residual wastes. The peak concentration for past leaks is now or the near future, whereas the peak concentration from residual wastes is approximately 1,400 years in the future. Upgradient sources are more than an order of magnitude higher than the peak concentration from past leaks at WMA C.

8.3.3 Cyanide

A comparison of the peak concentration results for cyanide from past leaks, upgradient sources and residual wastes is presented in Table 8.3. The calculation of concentrations from past leaks and residual wastes coincide at the same line of analysis at 100 m (328 ft) downgradient, but the upgradient source concentrations are at the PoCals from the P2R model discussed in Section 8.1.

Model results show estimated peak concentrations from past leaks and upgradient sources occur well before estimated peak concentrations of cyanide for residual wastes. The peak concentrations of cyanide from past leaks and upgradient sources without remediation were estimated to be well below the DWS for cyanide of 200 ug/l but above current WAC 173-340-720 Method B groundwater cleanup level for cyanide (hazard quotient = 1) is 9.6 µg/L for CN- and 4.8 µg/L for HCN. Peak concentrations of cyanide from residual wastes were estimated to be well below both standards.

Table 8.3. Comparison of Results for Cyanide from Past Leaks, Upgradient Sources, and Tank Waste Residual.

Sources of Cyanide	Estimated Peak Concentration (ug/l)	Timing of Peak Concentration
Past Leaks*	57	~Year 2017
Upgradient Sources**	39	~Year 2023
Tank Waste Residual***	0.01	~Year 3520

* See discussion of these results in Section 7
** See discussion of these results in Section 8.1.3
*** See discussion of these results in Section 8.2.3

8.3.4 Iodine-129

Results for ^{129}I are presented in Figure 8-35, and compared with results from the residual waste PA and upgradient sources. The calculation of concentrations from leaks and residual wastes coincide at the same line of analysis at 100 m (328 ft) downgradient, but the upgradient source concentrations are at the points of calculation from the P2R model discussed in Section 7.1. The

concentration of ^{129}I associated with the past leaks is more than two orders of magnitude higher than for residual wastes; both peaks occur thousands of years in the future. The peak concentration associated with upgradient sources is the highest among the three, is occurring now or the near future, and does not overlap substantially with the ^{129}I from either source in WMA C.

8.3.5 Total Uranium

Results for total uranium are presented in Figure 8-36, and compared with results from the residual waste PA and upgradient sources. The calculation of concentrations from leaks and residual wastes coincide at the same line of analysis at 100 m (328 ft) downgradient, but the upgradient source concentrations are at the PoCals from the P2R model discussed in Section 8.1. The concentrations of uranium associated with the past leaks and residual wastes are about the same and occur at the end of the simulation period (10,000 years). The peak uranium concentration from upgradient sources that originate in the B-Complex area is approximate three orders of magnitude higher than WMA C sources and occurs in the near future.

8.4 SUMMARY OF PEAK CONCENTRATIONS OF SELECTED CONTAMINANTS OF POTENTIAL CONCERN

A comparison of the peak concentrations and time of the peaks is shown in Table 8-2. Calculated concentrations from upgradient sources are significantly higher than peak concentrations for all contaminants except ^{99}Tc. [Note: the results presented here reflect peak concentration of results for the remedial evaluation case discussed in Section 7.1]. However, as discussed in Section 8.3, the evaluations of upgradient contamination assume that there will be no remedial activities undertaken at B Complex. They therefore likely provide significant overestimations of future contamination discharges. Therefore, the results in this section should only be regarded as a qualitative indication of the relative importance of various sources of contamination at WMA C.

As stated earlier in the beginning of Section 8.3, evaluation of these results need to consider that this summary represents a qualitative comparison between projected concentrations from past leaks, residual wastes, and upgradient sources to give an overview of overall trends from these sources. Given the potential uncertainties in these estimates, caution must be used in drawing too strong a set of conclusions from this comparison, because the purpose and intent of each of the estimates is different, and the underlying assumptions differ.

Figure 8-34. Results of the Past Leak Analysis for Nitrate at Points of Calculation 100 Meters Downgradient, Compared to Results from the Residual Waste Analysis and Upgradient Sources.

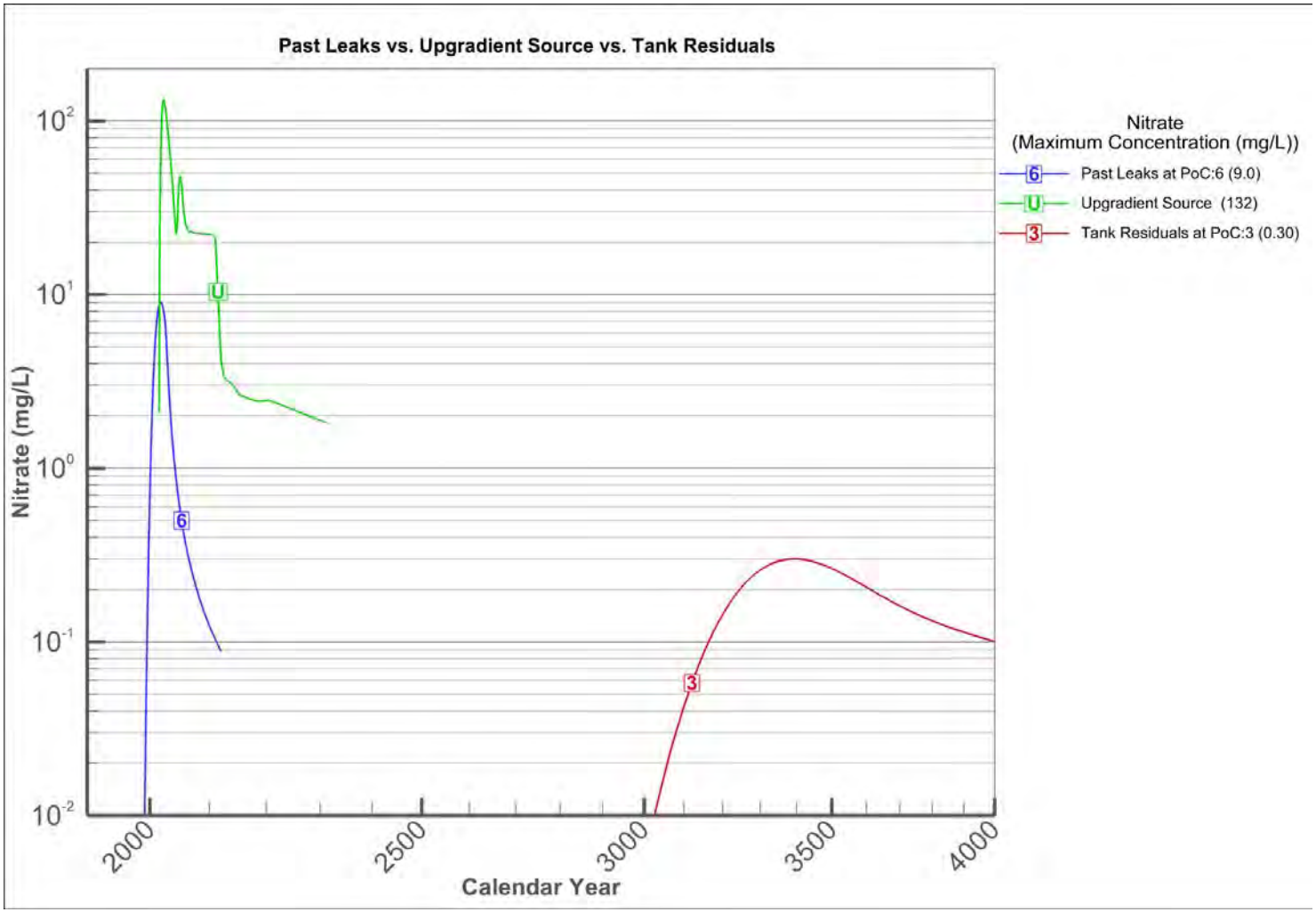

PoC = point of calculation

Note: The peak concentration for each curve is shown in parenthesis in the legend. The plots are on log-log scale to allow comparison of curves at different scales.

Figure 8-35. Results of the Past Leak Analysis for Iodine-129 at Points of Calculation 100 Meters Downgradient, Compared to Results from the Residual Waste Analysis and Upgradient Sources.

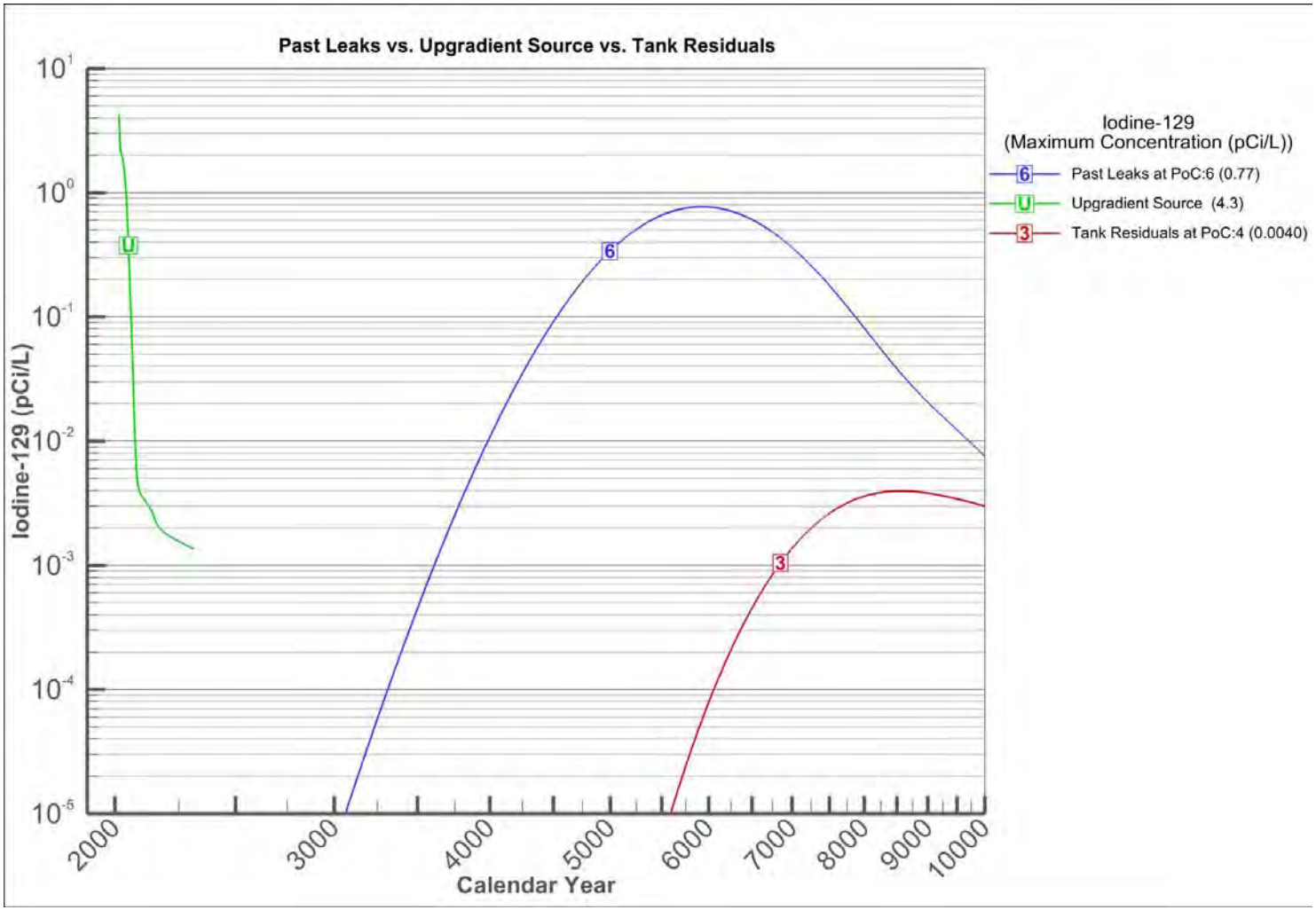

PoC = point of calculation

Note: The peak concentration for each curve is shown in parenthesis in the legend. The plots are on log-log scale to allow comparison of curves at different scales.

Figure 8-36. Results of the Past Leak Analysis for Total Uranium at Points of Calculation 100 Meters Downgradient, Compared to Results from the Residual Waste Analysis and Upgradient Sources.

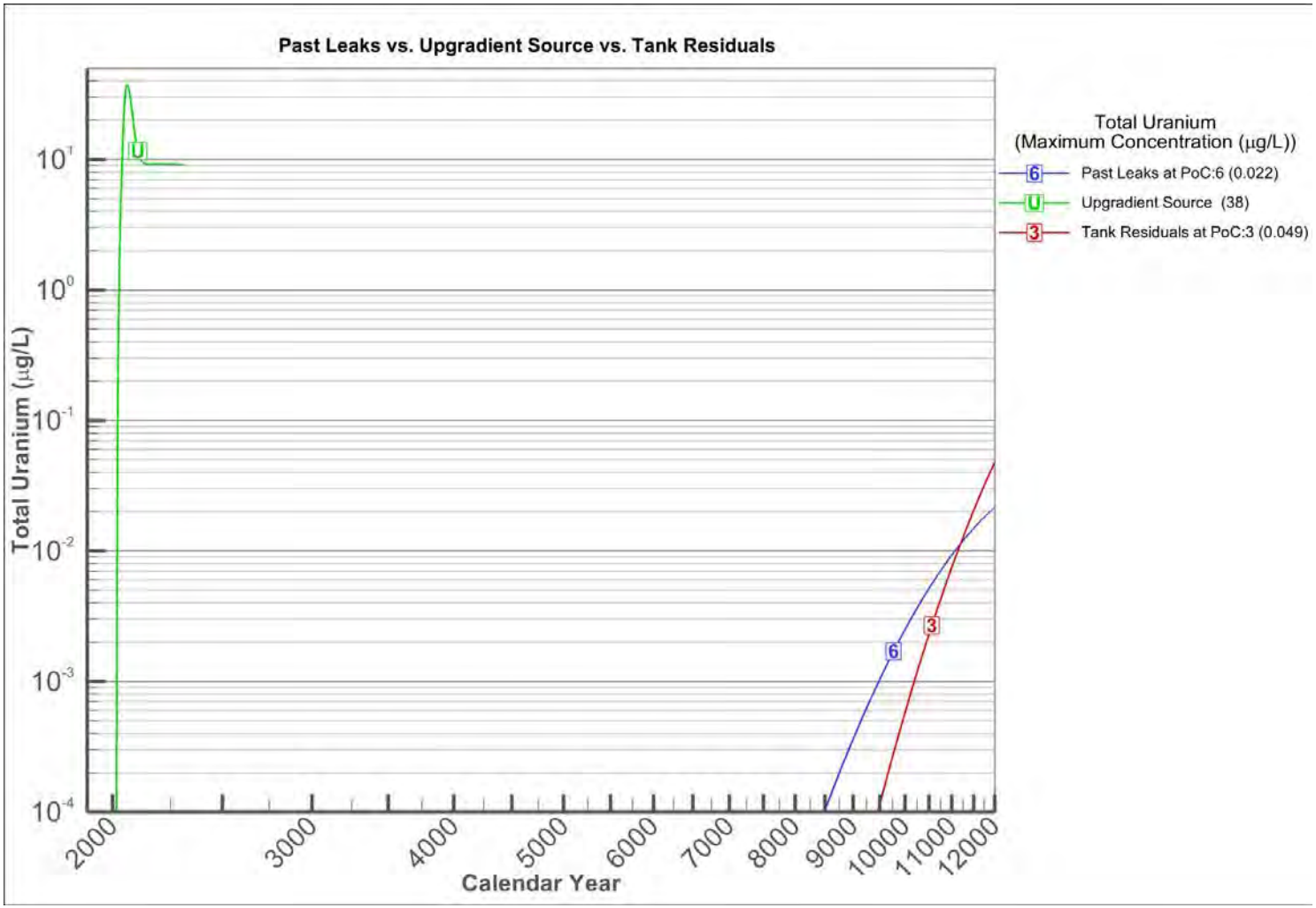

PoC = point of calculation

Note: The peak concentration for each curve is shown in parenthesis in the legend. The plots are on log-log scale to allow comparison of curves at different scales.

Table 8-2. Comparison of Peak Concentrations and Approximate Calendar Year of the Occurrence of the Peak.

Contaminant	Past Leaks		Residual Wastes		Upgradient Sources	
	Year of Peak	Peak Concentration	Year of Peak	Peak Concentration	Year of Peak	Peak Concentration
^{99}Tc	2020	6,650 pCi/L	3500	30 pCi/L	2020	1,430 pCi/L
Total uranium	12000	0.02 µg/L	12000	0.05 µg/L	2020	38 µg/L
Nitrate	2020	9.0 mg/L	3500	0.3 mg/L	2020	130 mg/L
^{129}I	6000	0.8 pCi/L	8500	0.004 pCi/L	2020	4.3 pCi/L

Note: Values have been rounded.

This page intentionally left blank.

9.0 SUMMARY AND OBSERVATIONS

The analysis of past leaks has been structured to meet several goals. First, the analysis is intended to be responsive to ideas and concerns expressed in the 2009 – 2011 PA scoping sessions (see Section 1.1.1), in which specific features of WMA C were identified as requiring particular attention because of their potential to influence the migration of contaminants from WMA C. Second, the analysis is intended to be consistent, to the extent possible, with the PA (RPP-ENV-58782) and RCA (RPP-ENV-58806) for disposal of residual wastes in WMA C. Third, the goal is to provide an understanding of the key features and processes discussed in Sections 1 and 2 that influence the migration of contaminants. Fourth, the goal is to use the understanding gained by the analysis to provide a projection of the future evolution of the contamination beneath WMA C.

The scoping analyses presented in Section 4 of this document provides comparisons of alternative conceptual and numerical models of WMA C based on groundwater monitoring data to evaluate the credibility of alternative assumptions for the migration of the leaks from the time of occurrence to today. The alternative models evaluated different assumptions about leak volumes and inventories, groundwater flux, recharge, and vadose zone conceptual models. Changes in the modeling inputs for each of the scoping cases is summarized in Table 4-1 in Section 4.

The comparisons associated with scoping cases from Section 4 are primarily focused on evaluating the arrival times of the ^{99}Tc contamination at the water table and general concentration of ^{99}Tc levels observed in monitoring wells. These two indicators are regarded as the most reliable and reproducible aspects of the groundwater monitoring data. Given the uncertainties in the estimates and timing of past leaks and complexities of the behavior of the site, it is unrealistic to hope to achieve exact matches with data. Instead, the goal is to provide a reasonable match with groundwater data, in a way that provides information and insight into the processes and parameter values that are consistent with observed contamination in monitoring wells at WMA C. The general shapes of the breakthrough curves observed in data (sharp rises and falls in concentration) are believed to be associated with shifts in the direction of the groundwater flow. This aspect of the breakthrough curves is not well represented by the scoping cases presented in this section (see Section 4), since they all assume a constant groundwater flow rate and direction. The scoping case in Section 6 addresses the changing water table and produces much better comparisons with data. Given the transient conditions under which the observed concentrations in wells have developed, it is believed that evaluation of the additional criteria, such as the time of disappearance, peak amplitude, skewness, kurtosis, and area under the curve would have limited value for the limited objectives of the scoping analysis.

Scoping Case 1 represents a minimal change from the PA/RCA model for residual wastes presented in RPP-ENV-58782 and RPP-ENV-58806, with the level of the water table elevated to represent an appropriate travel distance to the water table for the leaks. Case 1a uses upper bound leak inventories and volumes based on an assumed upper bound inventory for the tank C-

105 waste loss of 9.8 Ci and an upper bound leak volume of 75,600 L (20,500 gal). Case 1b uses the lower bound leak inventories and volumes based on assumed lower bound ^{99}Tc inventory for the tank C-105 waste loss of 1.0 Ci and a lower bound leak volume of 7,570 L (2,000 gal).

Scoping analysis for Case 1b produced concentrations substantially below observed concentrations for ^{99}Tc in observation wells. It was concluded that the lower bound estimate is inconsistent with data, and the upper bound estimate of 10 Ci ^{99}Tc in the tank C-105 leak waste was used for all other analyses. The upper bound estimate, when evaluated with the 10th percentile aquifer flux and in the transient water table boundary analysis, produces modeled concentration results comparable to the highest values measured in the monitoring wells around WMA C.

Scoping Case 2 investigated the effect of changing groundwater fluxes on the model results. It was found that the higher flux rates (i.e., 90th percentile groundwater flux of 0.33 m/day [1.08 ft/day]) led to a greater dilution of plume concentrations at the water table, and it is concluded that the lower groundwater flux rate (i.e., 10th percentile groundwater flux of 0.11 m/day [.36 ft/day]) provides concentration levels of ^{99}Tc that are more consistent with monitoring data observed in key monitoring well locations (see Figures 4-34 and 4-35). It is important to note here that the historical decline in water table conditions, the associated changing direction of groundwater, and related changes in the overall hydraulic gradient have undoubtedly had a significant effect of historical observations of contaminant concentrations found in groundwater at WMA C. However, the actual historical changes in these overall groundwater conditions that have created observed concentrations of selected contaminants at WMA C are uncertain and cannot be reasonably replicated for current monitoring information.

Scoping Case 3 investigated the general effect of a higher effective recharge rate than used in the other scoping analysis cases. Generally, it was found that the higher recharge rates led to early arrival of the contaminant at the water table. At a rate of 100 mm/yr (3.9 in./yr) used both within and in the immediate vicinity of the tank farms (Case 3b), the difference in first arrival at contaminants at the water table (See Figure 4-15) resulted in an earlier first arrival and peak concentration when compared to the Case 1a results (See Figure 4-4). where the 100 mm/yr (3.9 in./yr) was only used within the tank farm area. For the enhanced recharge rate of 150 mm/yr (5.9 in./yr)(Case 3a) the higher recharge rate generated earlier arrival times that are not consistent with monitoring data observed in key monitoring well locations (see Figures 4-34 and 4-35). Case 3c investigated the effect of a localized addition of water using a firehose to mitigate the operational hazard of leaks at UPRs -82 and -86, followed by the addition of gunite caps on the UPRs. The results of the analysis case are very similar to Scoping Case 1, indicating that this past practice had little effect on the downward migration of waste releases from the three UPRs to groundwater at WMA C (see Figures 4-34 and 4-35).

Scoping Case 4 investigated a number of vadose zone parameters and conceptual models of potential interest, to evaluate the potential for variations in the vadose zone properties to affect the plume development migration. The results of these analysis cases compared to available monitoring data (see Figures 4-34 and 4-35) indicate the following:

- The evaluation of ACM-II in Case 4a showed that adding refinement in the Hanford H2 Sand unit did not strongly affect the results of the analysis. Neither alternative model represented in Case 4a and Case 1a was found to be clearly superior to the other in terms of explaining the monitoring well data.

The evaluation in Case 4b of ACM using a heterogeneous representation of the vadose zone in Case 4b showed that adding heterogeneity resulted in an earlier arrival time of contamination at the water table than has been observed in monitoring wells and concentrations levels that were slightly higher than concentration levels resulting from Case 1a. Because of the inconsistency of the results from this alternative scoping model with monitoring well data, this case was not identified as a preferred case for further analyses of the projected impacts of plumes into the future.

The evaluation of median values of vadose zone hydraulic properties in Case 4c showed slightly faster transport and earlier arrival time of contaminants and concentration results when compared to arrival time and concentration results simulated for Case 1a. However, the evaluation of 95th percentile values of vadose zone hydraulic properties in Case 4d showed transport and arrival time results that were significantly faster and earlier when compared to the arrival times and levels of ^{99}Tc concentrations from key monitoring wells. These results showed faster transport and earlier arrival of contaminants at the water table when evaluated against comparable results for Case 1a. Therefore, the use of 95th percentile properties as implemented in Case 4d was not identified as a preferred case for use in further analyses of projected impacts of plumes into the future.

The evaluation of a hypothetical clastic dike and a poorly sealed borehole located near the assumed waste release near tank C-105 in Cases 4e and 4f showed a slightly earlier arrival time at the water table and only a small effect of estimated peak concentrations. Since these scoping analysis cases produce results that are similar to cases in which these features are absent, they are not preferred to use in further analyses.

As discussed in Section 4.8, three scoping analysis cases produced results in which the arrival time of the calculated plume appears to be substantially earlier than the observations in the wells. These scoping analysis cases are:

- Case 3a, in which the recharge was increased to 150 mm/yr (5.9 in/yr);

- Case 4b, in which the spatial variability of the vadose zone properties was represented by an alternative heterogeneous representation; and

- Case 4d, in which the flow properties of the vadose zone soil were set to their 95th percentile values.

The remaining scoping analysis cases evaluated in Section 4 produced comparable results to each other in terms of first arrival of contaminants at the water table and none were obviously superior to each other in terms of explaining the arrival of contaminants at the water table

observed in monitoring wells. The specific cases that generally had similar results for first arrival of contaminants at the water table include:

- Case 1a, in which a 9.8 Ci inventory of ^{99}Tc and 20,500 gal. (77,601 L) was applied for tank C-105.
- Case 1b, in which a 1.0 Ci inventory of ^{99}Tc and a volume of 10,000 gal. (37,854 L) was applied was applied for tank C-105.
- Case 2a, in which a 10th percentile groundwater flux of 0.11 m/day (1.08 ft/day) was applied.
- Case 2b, in which a 90th percentile groundwater flux of 0.33 m/day (0.36 ft/day) was applied.
- Case 3b, in which an enhanced recharge rate of 100 mm/yr (3.94 in./yr) was applied in all areas of the WMA C modeling domain.
- Case 3c, in which enhanced localized recharge (i.e., 72,000 gal. [272,550 L] over 4 hours) was applied at three unplanned releases locations (i.e., UPR-81, UPR-82, and UPR 86) just after initial releases at these UPRs were detected.
- Case 4a, in which alternative conceptual model II, where the effect of a finer alternative treatment of major hydrogeologic units in the vadose zone, was implemented.
- Case 4c, in which a 50th percentile set of hydraulic properties was applied to the vadose zone.
- Case 4e, in which a hypothetical clastic dike placed below past leak tank C-105 was considered.
- Case 4f, in which an inadequately sealed borehole located near past leak tank C-105 was considered.

When uncertainties in groundwater fluxes were considered, the full range of these scoping analyses cases were each found to be capable of producing both arrival times and concentrations consistent with observed groundwater monitoring well data for ^{99}Tc. One of the uncertainties is the general lack of groundwater monitoring data prior to the late 1980s.

The analysis in Section 4 showed that the best representation of the observed groundwater monitoring well data was modeled with the transient water table analysis presented in Section 6. However, it was necessary to make alterations to the boundary conditions to achieve the good agreement with data. These alterations are speculative but serve to provide insight into the evolution of the groundwater monitoring well data.

The model analysis of transient flow conditions provided in Section 6 showed that the conceptual model involving the counterclockwise rotation of the hydraulic gradient from northwest to southeast provided the best representation of observed groundwater conditions in monitoring wells near WMA C. The associated numerical model is capable of approximating observed field data for the time of arrival of ^{99}Tc to groundwater and concentration levels of ^{99}Tc in groundwater. The model results include several assumptions regarding the timing and inventory of the past releases, and direction and magnitude of the hydraulic gradient during the time it could not be measured. Because of these assumptions, it is unknown how accurately the model calculations represent the actual release of ^{99}Tc and its transport in the vadose zone and groundwater. The modeling results do, however, provide some insight into the concentration levels observed in the groundwater monitoring wells, and the changes in contaminant concentrations that have occurred in those wells since 2000. The concentration of ^{99}Tc observed in most of the groundwater monitoring wells appears to change too abruptly to represent the one-dimensional passing of a contaminant front. The modeling results indicate that the ^{99}Tc concentration in the wells changes so abruptly because of the direction and the magnitude of the groundwater hydraulic gradient changes. The rotation of the gradient continually changes the orientation of the groundwater plumes relative to the wells. The high ^{99}Tc concentrations measured in wells 299-E27-23 and 299-E27-13 between 2010 and 2012 likely correspond to the time when those wells were located downgradient of the sources. By 2014, the ^{99}Tc concentration in those two wells dropped markedly, while the concentration in well 299-E27-21 began increasing quickly around that same time. According to the modeling results, this pattern in the data can be explained by, and corresponds to, the further rotation of gradient from the south to the southeast.

The release from tank C-105 appears to be the dominant source of ^{99}Tc observed in groundwater in the monitoring wells. According to the inventory estimates in RPP-RPT-42294, it is the only release large enough and that occurred early enough to bring about the concentration levels observed in the monitoring wells. Whether or not the release from tank C-105 is truly the dominant source of ^{99}Tc observed at the monitoring wells is unknown. However, the modeling results do indicate that most of the ^{99}Tc observed in the monitoring wells located southwest of the farm originated from the sources inside the farm, and not from the UPRs that occurred away from the tanks. These three UPRs occurred later than the release from tank C-105, and the modeling results exhibit the implications of this. The concentration of ^{99}Tc in the wells located nearest the UPRs is dominated by the ^{99}Tc contained in the release from tank C-105. The concentration of ^{99}Tc attributed to the ^{99}Tc contained in the three UPRs peaks a few years after the concentration of ^{99}Tc peaks because of the tank C-105 release. This is later than the observed groundwater monitoring well data indicates that the peaks occurred in the wells.

The modeling results indicate that as the water table returns to more natural conditions, the rotation of the gradient will continue to alter the primary movement of the plumes from primarily a southerly direction to a more southeasterly direction in the near future. The very high concentration levels of ^{99}Tc observed in wells 299-E27-23 and 299-E27-21, southwest and south of WMA C, respectively, are likely to be observed in wells 299-E27-24 and 299-E27-14, which are located to the southeast of WMA C.

In the assessment of the impacts of past waste releases into the future, sorbing and nonsorbing contaminants were treated differently because of the anticipated difference in the height of the water table now and in the future. As a result of this difference, the forward modeling of leaks has been undertaken using models with different water table heights for the sorbing and nonsorbing contaminants. For sorbing contaminants, the PA/RCA model was used, while for nonsorbing contaminants, Case 1a was used.

The forward projection results lead to several observations, as follows.

- Model results indicate that current high concentrations of ^{99}Tc below WMA C are expected to decline over the next several decades as the contamination in the vadose zone is depleted.

- Contaminated groundwater, which is now impacted by releases from past waste leaks and losses at WMA C and, in the future, by upgradient sources in the B Complex area, will continue to migrate downgradient and will impact groundwater in local areas contained within the 200-PO-1 groundwater OU such as the A Complex area.

- There are not significant overlaps between releases from residual wastes in a closed WMA C and the releases from leaks.

- Compared to the releases from WMA C past leaks or residual wastes, the releases from upgradient sources produce more significant groundwater concentrations for all contaminants other than ^{99}Tc. For ^{99}Tc, the concentrations associated with past leaks are the most significant.

10.0 REFERENCES

04-TPD-083, 2004, "Agreement on Content of Tank Waste Retrieval Work Plans" (external letter from R. J. Schepens to M. A. Wilson, Nuclear Waste Program, State of Washington Department of Ecology, August 20), U.S. Department of Energy, Office of River Protection, Richland, Washington.

7G420-MEJ-06-007, 2006, "Waste Discharged to the 216-C-8 Crib" (interoffice memo from M. E. Johnson to J. F. Kristofzski, November 28), CH2M HILL Hanford Group, Inc., Richland, Washington.

18-NWP-088, 2018, "Department of Ecology's (Ecology) Comments on the United States Department of Energy (USDOE) Submittal of the Phase 2 RCRA Facility Investigation Report for Waste Management Area C (RFI), RPP-RPT-58339, Revision 0, and Waste Management Area C Phase 2 Corrective Measures Study Report (CMS), RPP-RPT-59379, Revision 0" (external letter from J.J. Lyon to J. Bovier, Office of River Protection, U.S. Department of Energy, June 11), Nuclear Waste Program, State of Washington Department of Ecology, Richland, WA.

40 CFR 141, "National Primary Drinking Water Regulations," *Code of Federal Regulations*, as amended.

ARH-1945, 1971, *B Plant Ion Exchange Feed Line Leak*, Atlantic Richfield Hanford Company, Richland, Washington.

Atomic Energy Act of 1954, 42 USC 2011, et seq.

BHI-00169, 1995, *Environmental Restoration Disposal Facility Performance Assessment*, Revision 00, Bechtel Hanford, Inc., Richland, Washington.

BHI-01103, 1999, *Clastic Injection Dikes of the Pasco Basin and Vicinity – Geologic Atlas Series*, Rev. 0, Bechtel Hanford, Inc., Richland, Washington.

BNWL-B-360, 1974, *Selected Water Table Contour Maps and Well Hydrographs for the Hanford Reservation, 1944-1973*, Pacific Northwest Laboratory, Richland, Washington.

CHPRC-00269, 2013, *STOMP Requirements Traceability Matrix CHPRC Build 4*, Rev. 3, CH2M HILL Plateau Remediation Company, Richland, Washington.

CP-47631, 2011, *Model Package Report: Central Plateau Groundwater Model Version 3.3*, Rev. 0, CH2M HILL Plateau Remediation Company, Richland, Washington.

CP-47631, 2015, *Model Package Report: Central Plateau Groundwater Model Version 6.3.3*, Rev. 2, INTERA, Inc., Richland, Washington.

CP-57037, 2015, *Model Package Report: Plateau to River Groundwater Transport Model Version 7.1*, Rev. 0, CH2M HILL Plateau Remediation Company, Richland, Washington.

DOE/EIS-0391, 2012, *Final Tank Closure and Waste Management Environmental Impact Statement for the Hanford Site, Richland, Washington*, U.S. Department of Energy, Washington, D.C.

DOE O 435.1, 2001, *Radioactive Waste Management*, U.S. Department of Energy, Washington, D.C.

DOE/ORP-2000-24, 2001, *Hanford Immobilized Low-Activity Waste Performance Assessment: 2001 Version*, Rev. 0, U.S. Department of Energy, Office of River Protection, Richland, Washington.

DOE/ORP-2005-01, 2006, *Initial Single-Shell Tank System Performance Assessment for the Hanford Site*, Rev. 0, U.S. Department of Energy, Office of River Protection, Richland, Washington.

DOE/ORP-2008-01, 2010, *RCRA Facility Investigation Report for Hanford Single-Shell Tank Waste Management Areas*, Rev. 1, U.S. Department of Energy, Office of River Protection, Richland, Washington.

DOE/RL-88-30, 2015, *Hanford Site Waste Management Units Report*, Rev. 24, U.S. Department of Energy, Richland Operations Office, Richland, Washington.

DOE/RL-92-04, 1993, *PUREX Source Aggregate Area Management Report*, Rev.0, U.S. Department of Energy, Richland Operations Office, Richland, Washington.

DOE/RL-93-33, 1996, *Focused Feasibility Study of Engineered Barriers for Waste Management Units in the 200 Areas*, Rev. 1, U.S. Department of Energy, Richland Operations Office, Richland, Washington.

DOE/RL-2002-39, 2002, *Standardized Stratigraphic Nomenclature for Port Ringold Formation Sediments Within the Central Pasco Basin*, Rev. 0, U.S. Department of Energy, Richland Operations Office, Richland, Washington.

DOE/RL-2008-01, 2008, *Hanford Site Groundwater Monitoring for Fiscal Year 2007*, Rev. 0, U.S. Department of Energy, Richland Operations Office, Richland, Washington.

DOE/RL-2008-66, 2009, *Hanford Site Groundwater Monitoring for Fiscal Year 2008*, Rev. 0, U.S. Department of Energy, Richland Operations Office, Richland, Washington.

DOE/RL-2009-77, 2010, *Groundwater Quality Assessment Plan for the Single-Shell Tank Waste Management Area C*, Rev. 0, U.S. Department of Energy, Richland Operations Office, Richland, Washington.

DOE/RL-2009-127, 2015, *Remedial Investigation Report for the 200-BP-5 Groundwater Operable Unit, Draft A*, U.S. Department of Energy, Richland Operations Office, Richland, Washington.

DOE/RL-2010-11, 2010, *Hanford Site Groundwater Monitoring and Performance Report for 2009 Volumes 1 and 2*, Rev. 1, U.S. Department of Energy, Richland Operations Office, Richland, Washington.

DOE/RL-2011-01, 2011, *Hanford Site Groundwater Monitoring Report for 2010*, Rev. 0, U.S. Department of Energy, Richland Operations Office, Richland, Washington.

DOE/RL-2011-50, 2012, *Regulatory Basis and Implementation of a Graded Approach to Evaluation of Groundwater Protection*, Rev. 1, U.S. Department of Energy, Richland Operations Office, Richland, Washington.

DOE/RL-2011-118, 2012, *Hanford Site Groundwater Monitoring for 2011*, Rev. 0, U.S. Department of Energy, Richland Operations Office, Richland, Washington.

DOE/RL-2013-22, 2013, *Hanford Site Groundwater Monitoring Report For 2012*, Rev. 0, U.S. Department of Energy, Richland Operations Office, Richland, Washington.

DOE/RL-2014-32, 2014, *Hanford Site Groundwater Monitoring Report for 2013*, Rev. 0, U.S. Department of Energy, Richland Operations Office, Richland, Washington.

DOE/RL-2015-07, 2015, *Hanford Site Groundwater Monitoring Report for 2014*, Rev. 0, U.S. Department of Energy, Richland Operations Office, Richland, Washington.

DOE/RL-2016-66, 2017, *Hanford Site RCRA Groundwater Monitoring Report for 2016*, Rev. 0, U.S. Department of Energy, Richland Operations Office, Richland, Washington.

DOE/RL-2016-67, 2017, *Hanford Site Groundwater Monitoring Report for 2016*, Rev. 0, U.S. Department of Energy, Richland Operations Office, Richland, Washington.

ECF-Hanford-13-0031, 2015, Fate and Transport Modeling for Baseline Conditions for Remedial Investigation/Feasibility Studies of the 200-BP-5 and 200-PO-1 Groundwater Operable Units, Rev. 0, CH2M HILL Plateau Remediation Company, Richland, Washington.

ECF-Hanford-13-0037, 2015, *Development of Source Terms for Inclusion in Fate and Transport Modeling for Remedial Investigation/Feasibility Studies of the 200-BP-5 and 200-PO-1 Groundwater Operable Units*, Rev. 0, INTERA, Inc., Richland, Washington.

ECF-Hanford-18-0023, 2018, *Evaluation of Contaminant Transport for the 200-BP-5 and 200-PO-1 Operable Units Feasibility Study Evaluation of Remedial Alternatives*, Rev. 0, INTERA, Inc., Richland, Washington.

Ecology, EPA, and DOE, 1989, *Hanford Federal Facility Agreement and Consent Order – Tri-Party Agreement*, 2 vols., as amended, State of Washington Department of Ecology, U.S. Environmental Protection Agency, and U.S. Department of Energy, Olympia, Washington.

EMDT-MO-0031, 2019, Environmental Modeling Data Transmittal of an unpublished report entitled, "WMA C Conceptual Model" sent to DOE by the Nez Perce Tribe by email on Wednesday, Nov. 5, 2014 at 2:31 pm PST.

EPA/540/F-95/041, 1996, *Soil Screening Guidance: Fact Sheet, Publication 9355.4-14FSA*, U.S. Environmental Protection Agency, Office of Solid Waste and Emergency Response, Washington, D.C.

EPA/540/R-95/128, 1996, *Soil Screening Guidance: Technical Background Document, Second Edition*, U.S. Environmental Protection Agency, Washington, D.C.

EPA/600/2-91/065, 1991, *The RETC Code for Quantifying the Hydraulic Functions of Unsaturated Soils*, Office of Research and Development, U.S. Environmental Protection Agency, Washington, D.C.

ERDA-1538, 1975, *Final Environmental Impact Statement, Waste Management Operations, Hanford Reservation, Richland, Washington*, U.S. Energy Research and Development Administration, Richland, Washington.

Fayer, M. J., and G. W. Gee, 2006, "Multiple-Year Water Balance of Soil Covers in a Semiarid Setting," Journal of Environmental Quality, Vol. 35, No. 2, pp. 366–377.

GJO-98-39-TAR/GJO-HAN-18, 1998, *Hanford Tank Farms Vadose Zone: C Tank Farm Report*, U.S. Department of Energy, Grand Junction Office, Grand Junction, Colorado.

GJO-98-39-TARA/GJO-HAN-18, 2000, *Hanford Tank Farms Vadose Zone: Addendum to the C Tank Farm Report*, U.S. Department of Energy, Grand Junction Office, Grand Junction, Colorado.

HNF-EP-0182, 2013, *Waste Tank Summary Report for Month Ending September 30, 2013*, Rev. 306, Washington River Protection Solutions, LLC, Richland, Washington.

HNF-EP-0182, 2015, *Waste Tank Summary Report for Month Ending February 28, 2015*, Rev. 326, Washington River Protection Solutions, LLC, Richland, Washington.

HW-60601, 1959, *Aquifer Characteristics and Ground-Water Movement at Hanford*, General Electric Company, Richland, Washington.

HW-67459, 1960, *Chemical Processing Department Monthly Report for November, 1960*, Hanford Atomic Products Operation, Hanford, Washington.

ITRC, 2010, "Use and Measurement of Mass Flux and Mass Discharge," Interstate Technology & Regulatory Council, Washington, DC.

Jury, W. A., W. R. Gardner, and W. H. Gardner, 1991, Soil Physics, 5th edition, Wiley and Sons, Inc., New York, New York.

Jury, W. A. and R. Horton, 2004, Soil Physics, 6th edition, Wiley and Sons, Inc., New York, New York.

Khaleel, R., J. F. Relyea, and J. L. Conca, 1995, "Evaluation of van Genuchten-Mualem Relationships to Estimate Unsaturated Hydraulic Conductivity at Low Water Contents," Water Resources Research, Vol. 31, Issue 11, pp. 2659–2668.

Millington, R. J. and J. P. Quirk, 1961, "Permeability of Porous Solids," Transactions of the Faraday Society, Vol. 57, pp. 1200–1207.

Mualem, Y., 1976, "A New Model for Predicting the Hydraulic Conductivity of Unsaturated Porous Media," Water Resources Research, Vol. 12, No. 3, pp. 513–522.

Murray, C. J., A. L. Ward, and J. L. Wilson, 2007, "Influence of Clastic Dikes on Vertical Migration of Contaminants at the Hanford Site," Vadose Zone Journal, Vol. 6, No. 4, pp. 959–970.

NOAA Manual NOS NGS 5, 1990, State Plane Coordinate System of 1983, National Geodetic Survey, U.S. Department of Commerce, National Oceanic and Atmospheric Administration, Rockville, Maryland.

NUREG/CR-6767, 2002, *Evaluation of Hydrologic Uncertainty Assessments for Decommissioning Sites Using Complex and Simplified Models*, Pacific Northwest Laboratory, Richland, Washington.

Pacific Northwest National Laboratory, Queried 12/18/2015, *[STOMP User Guide]*, http://stomp.pnnl.gov/user_guide/STOMP_guide.stm.

PNL-6464, 1988, *Environmental Monitoring at Hanford for 1987*, Pacific Northwest Laboratory, Richland, Washington.

PNL-10886, 1995, *Development of a Three-Dimensional Ground-Water Model of the Hanford Site Unconfined Aquifer System: FY 1995 Status Report*, Pacific Northwest National Laboratory, Richland, Washington.

PNNL-11216, 1997, *STOMP Subsurface Transport Over Multiple Phases Application Guide*, Pacific Northwest National Laboratory, Richland, Washington.

PNNL-12030, 2000, *STOMP Subsurface Transport Over Multiple Phases Version 2.0 Theory Guide*, Pacific Northwest National Laboratory, Richland, Washington.

PNNL-12261, 2000, *Revised Hydrogeology for the Suprabasalt Aquifer System, 200-East Area and Vicinity, Hanford Site, Washington*, Pacific Northwest National Laboratory, Richland, Washington.

PNNL-13024, 2001, *RCRA Groundwater Monitoring Plan for Single-Shell Tank Waste Management Area C at the Hanford Site*, as amended, Pacific Northwest National Laboratory, Richland, Washington.

PNNL-13033, 1999, *Recharge Data Package for the Immobilized Low-Activity Waste 2001 Performance Assessment*, Pacific Northwest National Laboratory, Richland, Washington.

PNNL-13641, 2001, *Uncertainty Analysis Framework – Hanford Site-Wide Groundwater Flow and Transport Model*, Pacific Northwest National Laboratory, Richland, Washington.

PNNL-14224, 2003, *Influence of Clastic Dikes on Vertical Migration of Contaminants in the Vadose Zone at Hanford*, Pacific Northwest National Laboratory, Richland, Washington.

PNNL-14398, 2003, *Transient Inverse Calibration of the Site-Wide Groundwater Flow Model (ACM-2): FY 2003 Progress Report*, Pacific Northwest National Laboratory, Richland, Washington.

PNNL-14548, 2004, *Hanford Site Groundwater Monitoring for Fiscal Year 2003*, Pacific Northwest National Laboratory, Richland, Washington.

PNNL-14753, 2006, *Groundwater Data Package for Hanford Assessments*, Rev. 1, Pacific Northwest National Laboratory, Richland, Washington.

PNNL-15443, 2006, *Vadose Zone Transport Field Study Summary Report*, Pacific Northwest National Laboratory, Richland, Washington.

PNNL-15670, 2006, *Hanford Site Groundwater Monitoring for Fiscal Year 2005*, Pacific Northwest National Laboratory, Richland, Washington.

PNNL-16346, 2006, *Hanford Site Groundwater Monitoring for Fiscal Year 2006*, Pacific Northwest National Laboratory, Richland, Washington.

PNNL-16663, 2007, *Geochemical Processes Data Package for the Vadose Zone in the Single-Shell Tank Waste Management Areas at the Hanford Site*, Pacific Northwest National Laboratory, Richland, Washington.

PNNL-16688, 2007, *Recharge Data Package for Hanford Single-Shell Tank Waste Management Areas*, Pacific Northwest National Laboratory, Richland, Washington.

PNNL-17154, 2008, *Geochemical Characterization Data Package for the Vadose Zone in the Single-Shell Tank Waste Management Areas at the Hanford Site*, Pacific Northwest National Laboratory, Richland, Washington.

PNNL-17176, 2007, *200-BP-1 Prototype Hanford Barrier Annual Monitoring Report for Fiscal Years 2005 Through 2007*, Pacific Northwest National Laboratory, Richland, Washington.

PNNL-19702, 2010, *Hydrogeologic Model for the Gable Gap Area, Hanford Site*, Pacific Northwest National Laboratory, Richland, Washington.

PNNL-23711, 2015, *Physical, Hydraulic, and Transport Properties of Sediments and Engineered Materials Associated with Hanford Immobilized Low-Activity Waste*, RPT-IGTP-004, Rev. 0, Pacific Northwest National Laboratory, Richland, Washington.

PNNL-24698, 2015, *Geostatistical Realizations of WMA-C Lithofacies*, Pacific Northwest National Laboratory, Richland, Washington.

PNNL-24740, 2017, *Alternative Conceptual Models of the Subsurface at WMA C*, Rev. 1, Pacific Northwest National Laboratory, Richland, Washington.

Polmann, D. J., 1990, "Application of Stochastic Methods to Transient Flow and Transport in Heterogeneous Unsaturated Soils," Ph.D. Thesis, Massachusetts Institute of Technology, Cambridge, Massachusetts.

Resource Conservation and Recovery Act of 1976, 42 USC 6901, et seq.

RHO-CD-673, 1979, *Handbook 200 Areas Waste Sites*, Rockwell Hanford Operations, Richland, Washington.

Rovey, C. W. II and D. S. Cherkauer, 1995, "Scale Dependency of Hydraulic Conductivity Measurements," Ground Water Vol. 33, No. 5, pp. 769–780.

RPP-18290, 2004, *241-C Tank Farm Geologic and Stratigraphic Analysis*, Rev. 1, CH2M HILL Hanford Group, Inc., Richland, Washington.

RPP-19822, 2005, *Hanford Defined Waste Model – Revision 5.0*, Rev. 0-A, CH2M HILL Hanford Group, Inc./Technical Resources International, Inc., Richland, Washington.

RPP-26744, 2005, *Hanford Soil Inventory Model, Rev. 1*, Rev. 0, CH2M HILL Hanford Group, Inc., Richland, Washington.

RPP-32681, 2013, *Process to Assess Tank Farm Leaks in Support of Retrieval and Closure Planning*, Rev. 2, Washington River Protection Solutions, LLC, Richland, Washington.

RPP-35484, 2008, "*Field Investigation Report for Waste Management Areas C and A-AX*, Rev. 1, CH2M HILL Hanford Group, Inc., Richland, Washington.

RPP-ASMT-38219, 2008, *Tank 241-C-110 Leak Assessment Report*, Rev. 0, CH2M HILL Hanford Group, Inc., Richland, Washington.

RPP-ASMT-39155, 2008, *Tank 241-C-111 Leak Assessment Report*, Rev. 0, CH2M HILL Hanford Group, Inc., Richland, Washington.

RPP-ASMT-46452, 2010, *Tank 241-C-105 Leak Assessment Completion Report*, Rev. 0, Washington River Protection Solutions, LLC, Richland, Washington.

RPP-ENV-33418, 2016, *Hanford C-Farm Leak Inventory Assessments Report*, Rev. 4, Washington River Protection Solutions, LLC, Richland, Washington.

RPP-ENV-58782, 2016, *Performance Assessment of Waste Management Area C, Hanford Site, Washington*, Rev. 0, Washington River Protection Solutions, LLC, Richland, Washington.

RPP-ENV-58806, 2016, *Analysis of Post-Closure Groundwater Impacts from Hazardous Chemicals in Residual Wastes in Tanks and Ancillary Equipment at Waste Management Area C at the Hanford Site, Southeast Washington, Washington*, Rev. 0, Washington River Protection Solutions, LLC, Richland, Washington.

RPP-PLAN-39114, 2012, *Phase 2 RCRA Facility Investigation/Corrective Measures Study Work Plan for Waste Management Area C*, Rev. 2, Washington River Protection Solutions, LLC, Richland, Washington.

RPP-RPT-29191, 2006, *Supplemental Information Hanford Tank Waste Leaks*, Rev. 0, CH2M HILL Hanford Group Inc., Richland, Washington.

RPP-RPT-38152, 2008, *Data Quality Objectives Report Phase 2 Characterization for Waste Management Area C RCRA Field Investigation/Corrective Measures Study*, Rev. 0, Washington River Protection Solutions, LLC, Richland, Washington.

RPP-RPT-41918, 2010, *Assessment Context for Performance Assessment for Waste in C Tank Farm Facilities after Closure*, Rev. 0, Washington River Protection Solutions, LLC, Richland, Washington.

RPP-RPT-42294, 2016, *Hanford Waste Management Area C Soil Contamination Inventory Estimates*, Rev. 2, Washington River Protection Solutions, LLC, Richland, Washington.

RPP-RPT-42323, 2015, *Hanford C-Farm Tank and Ancillary Equipment Residual Waste Inventory Estimates*, Rev. 3, Washington River Protection Solutions, LLC, Richland, Washington.

RPP-RPT-44042, 2010, *Recharge and Waste Release within Engineered System in Waste Management Area C*, Rev. 0, Washington River Protection Solutions, LLC, Richland, Washington.

RPP-RPT-46088, 2010, *Flow and Transport in the Natural System at Waste Management Area C*, Rev. 1, Washington River Protection Solutions, LLC/GSI Water Solutions, Inc., Richland, Washington.

RPP-RPT-46879, 2011, *Corrosion and Structural Degradation within Engineered System in Waste Management Area C*, Rev. 2, Washington River Protection Solutions, LLC, Richland, Washington.

RPP-RPT-47479, 2011, *Exposure Scenarios for the Waste Management Area C Performance Assessment*, Rev. 1, Washington River Protection Solutions, LLC, Richland, Washington.

RPP-RPT-48490, 2011, *Technical Approach and Scope for Flow and Contaminant Transport Analysis in the Initial Performance Assessment of Waste Management Area C*, Washington River Protection Solutions, LLC, Richland, Washington.

RPP-RPT-49425, 2011, *Ecological Risk Assessment Approach for Hanford Waste Management Area C*, Rev. 1, Washington River Protection Solutions, LLC, Richland, Washington.

RPP-RPT-56356, 2014, *Development of Alternative Digital Geologic Models of Waste Management Area C*, Rev. 0, Freestone Environmental Services Inc./Washington River Protection Solutions, LLC, Richland, Washington.

RPP-RPT-58297, 2014, *Screening-Level Evaluation of Groundwater Monitoring Data Collected in Vicinity of WMA C*, Rev. 0, INTERA, Inc./Washington River Protection Solutions, LLC, Richland, Washington.

RPP-RPT-58329, 2014, *Risk Assessment of Contaminated Soils and Vadose Zone Sediments Waste Management Area C at the Hanford Site, Southeast Washington*, Rev. 0, INTERA, Inc./Washington River Protection Solutions, LLC, Richland, Washington.

RPP-RPT-58339, 2014, *Phase 2 RCRA Facility Investigation Report for Waste Management Area C*, Draft A, Washington River Protection Solutions, LLC, Richland, Washington.

RPP-RPT-59197, 2016, Analysis of Past Tank Waste Leaks and Losses in the Vicinity of Waste Management Area C at the Hanford Site, Southeast Washington, Rev. 1, Washington River Protection Solutions, LLC, Richland, Washington.

RPP-RPT-61239, in process, *Multiple Lines of Evidence and Modeling Results for Heterogeneous Alternative Conceptual Models of the Subsurface at Waste Management Area C*, Rev. 0, TecGeo, Inc./Pacific Northwest National Laboratory/INTERA, Inc./ CH2M HILL Plateau Remediation Company/Washington River Protection Solutions, LLC, Richland, Washington.

Schulze-Makuch, D., D. A. Carlson, D. S. Cherkauer, P. Malik, 1999, "Scale Dependency of Hydraulic Conductivity in Heterogeneous Media," Ground Water, Vol. 37, No. 6, pp. 904–919.

SGW-54165, 2014, *Evaluation of the Unconfined Aquifer Hydraulic Gradient Beneath the 200 East Area, Hanford Site*, Rev. 0, CH2M HILL Plateau Remediation Company, Richland, Washington.

SGW-58561, 2015, *WMA C Quarterly October through December 2014 Quarterly Groundwater Monitoring Report*, Rev. 0, CH2M HILL Plateau Remediation Company, Richland, Washington.

SGW-59669, 2016, *WMA C Quarterly October Through December 2015 Quarterly Groundwater Monitoring Report*, Rev. 0, CH2M HILL Plateau Remediation Company, Richland, Washington.

Sobczyk, S., 11-05-2014, "Alternative Conceptual Model," (e mail to R. D. Hildebrand [U.S. Department of Energy-Richland Operations Office] and C. J. Kemp [U.S. Department of Energy-Office of River Protection], Nez Perce Tribe, Lapwai, Idaho.

van Genuchten, M. Th., 1980, "A Closed-form Equation for Predicting the Hydraulic Conductivity of Unsaturated Soils," Soil Science Society of America Journal, Vol. 44, No. 5, pp. 892–898.

WAC 173-303-610, "Closure and Post-Closure," Washington Administrative Code, as amended.

WAC 173-340-747, "Deriving Soil Concentrations for Groundwater Protection," Washington Administrative Code, as amended.

Washington State Department of Ecology Cleanup Levels and Risk Calculation (CLARC), Queried 08/30/2016, [CLARC Data Tables – July 2015, Chemical Parameters], https://fortress.wa.gov/ecy/clarc/FocusSheets/CLARC%20Parameters.pdf.

WCH-520, 2013, *Performance Assessment for the Environmental Restoration Disposal Facility, Hanford Site, Washington*, Rev. 1, Washington Closure Hanford, Richland, Washington.

WHC-EP-0645, 1995, *Performance Assessment for the Disposal of Low-Level Waste in the 200 West Area Burial Grounds*, Westinghouse Hanford Company, Richland, Washington.

WHC-EP-0707, 1994, *216-U-10 Pond and 216-Z-19 Ditch Characterization Studies*, Rev. 0 (formerly RHO-ST-45), Westinghouse Hanford Company, Richland, Washington.

WHC-EP-0815, 1995, *Groundwater Impact Assessment Report for the 216-T-4-2 Ditch*, Westinghouse Hanford Company, Richland, Washington.

WHC-SD-EN-AP-012, 1991, *Interim-Status Groundwater Monitoring Plan for the Single-Shell Tanks*, Rev. 1, Westinghouse Hanford Company, Richland, Washington.

WHC-SD-ER-TI-003, 1991, *Geology and Hydrology of the Hanford Site: A Standardized Text for Use in Westinghouse Hanford Company Documents and Reports*, Rev. 0, Westinghouse Hanford Company, Richland, Washington.

WHC-SD-WM-EE-004, 1995, *Performance Assessment of Grouted Double-Shell Tank Waste Disposal at Hanford*, Rev. 1, Westinghouse Hanford Company, Richland, Washington.

WHC-SD-WM-TI-730, 1996, *Performance Assessment for the Disposal of Low-Level Waste in the 200 East Area Burial Grounds*, Rev. 0, Westinghouse Hanford Company, Richland, Washington.

WHC-SD-WM-TI-731, 1996, *Predominant Radionuclides in Hanford Site Waste Tanks*, Rev. 0, Westinghouse Hanford Company, Richland, Washington.

WSRC-MS-2003-00582, 2004, *Performance Assessment/Composite Analysis Modeling to Support a Holistic Strategy for the Closure of F Area, a Large Nuclear Complex at the Savannah River Site*, Rev. 1, Savannah River Technology Center, Aiken, South Carolina.

Ye, M., R. Khaleel, T. J. Yeh, 2005, “Stochastic analysis of moisture plume dynamics of a field injection experiment,” Water Resources Research, Vol. 41, W03013.

Yeh, T.-C. J., M. Ye, R. Khaleel, 2005, “Estimation of effective unsaturated hydraulic conductivity tensor using spatial moments of observed moisture plume,” Water Resources Research, Vol. 41, W03014.

This page intentionally left blank.

APPENDIX A

ESTIMATION OF POTENTIAL IMPACTS FROM PAST RELEASES OF CYANIDE AT WASTE MANAGEMENT AREA C

This page intentionally left blank.

TABLE OF CONTENTS

A1.0 INTRODUCTION A-1

A2.0 INVENTORY ESTIMATES OF CYANIDE IN PAST RELEASES FROM WASTE MANAGEMENT AREA C A-3

A2.1 CYANIDE INVENTORY ESTIMATION PROCESS A-3
A2.2 ESTIMATION OF CYANIDE INVENTORY IN PAST RELEASES AT WASTE MANAGEMENT AREA C A-6

A3.0 PHASE 2 CHARACTERIZATION RESULTS FOR CYANIDE IN VADOSE ZONE BENEATH WASTE MANAGEMENT AREA C A-7

A4.0 GROUNDWATER MONITORING RESULTS FOR CYANIDE SINCE 2000 ..... A-8

A5.0 EVALUATION OF POTENTIAL IMPACTS TO GROUNDWATER FROM PAST RELEASES OF CYANIDE A-17

A6.0 REFERENCES A-20

LIST OF FIGURES

Figure A-1. Temperature Dependence of Ferrocyanide Concentrations When 1F-1B Dissolves in 2M NaOH. A-5
Figure A-2. Total Cyanide Concentrations in Groundwater Monitoring Wells around Waste Management Area C. A-12
Figure A-3. Cyanide Concentrations in Waste Management Area C Wells from January 2006 through December 2017. ..... A-13
Figure A-4. Simulated Nitrate Concentration in Groundwater from Tank 241-C-108 Source 100 meters Downgradient of the Fenceline. A-18
Figure A-5. Nitrate Concentrations Normalized with Respect to Inventory for Tank 241-C-108 Source. A-19

LIST OF TABLES

Table A-1. Historical Sampling Data for Free Cyanide in 241-C Farm Tanks (based on Tank Waste Information Network System record). A-9
Table A-2. Estimated Cyanide Inventory in Past Releases at 241-C Farm Tanks. A-11
Table A-3. Analytical Results of Total Cyanide, Amenable Cyanide, and Free Cyanide from Sampling of Groundwater Monitoring Wells at Waste Management Area C for Calendar Year 2017. ..... A-14

LIST OF TERMS

CSR	B Plant cesium recovery waste
CWP1	Plutonium Uranium Extraction Plant aluminum fuel cladding waste (1956-1960)
CWP2	Plutonium Uranium Extraction Plant aluminum fuel cladding waste (1961-1972)
HDW	Hanford Defined Waste
MCL	Maximum Contaminant Level
MDL	method detection limit
MTCA	Model Toxics Control Act
P1	Plutonium Uranium Extraction Plant high-level waste (1956-1962)
P2	Plutonium Uranium Extraction Plant high-level waste (1963-1967)
PQL	practical quantitation limit
TWINS	Tank Waste Information Network System
WMA	Waste Management Area
WHC	Westinghouse Hanford Company

A1.0 INTRODUCTION

During the 1950s, a process to remove (scavenge) ^{137}Cs through precipitation was developed to create additional waste storage space in the underground storage tanks. Sodium ferrocyanide, followed by nickel sulfate, was added to the waste to create a nickel ferrocyanide [$Na_2NiFe(CN)_6$] precipitate that would bind with ^{137}Cs. Generally, the waste was taken out of the tanks and sent to the treatment facility where it was mixed with sodium (or potassium) ferrocyanide and then with nickel sulfate. Once the chemicals were added to the waste, the slurry containing the solids was transferred to certain single-shell tanks and settling was allowed to occur over a 7- to 10-day period after which the supernate was decanted and discharged to the ground via cribs and trenches. This scavenging process lasted from 1953 until early 1958 and used approximately 140 metric tons of ferrocyanide that ended up in 18 tanks (HNF-SA-3126-FP, *Resolution of the Hanford Site Ferrocyanide Safety Issue*). The ferrocyanide was added in excess and resulted mostly in precipitate of sodium nickel ferrocyanide. By one estimate (HW-43066, "*Metal Recovery Waste Scavenging Process*") approximately 8.4×10^4 m^3 (2.2×10^7 gal) of waste were scavenged and 6.1×10^4 m^3 (1.6×10^7 gal) of waste were sent to the cribs during the period from September 1954 to May 1956.

The 18 tanks that were used in the scavenging process were from 241-BY Tank Farm (241-BY-103, 241-BY-104, 241-BY-105, 241-BY-106, 241-BY-107, 241-BY-108, 241-BY-110, 241-BY-111, and 241-BY-112), 241-C Tank Farm (C Farm) (241-C-108 [C-108], 241-C-109 [C-109], 241-C-111 [C-111], and 241-C-112 [C-112]), 241-T-107, 241-TX-118, and 241-TY Tank Farm (241-TY-101, 241-TY-103, and 241-TY-104). Based on the flowsheet data and process records the amount of $Na_2NiFe(CN)_6$ that was added to the waste varied from 2 to 25 wt% on dry-weight sample basis (20,000 to 250,000 µg/g of the mixed slurry), with the highest concentrations used for C Farm (9 to 25 wt% on dry weight basis). The nominal ferrocyanide concentration used at Hanford was 0.005 M (~1.06 g/L of $Fe(CN)_6^{4-}$), but some variations occurred during the scavenging campaigns ("Chemical Reactivity of Potential Ferrocyanide Precipitates in Hanford Tanks with Nitrates and Nitrites" [Scheele et al. 1992]).

Based on the flowsheet records, it is evident that C Farm tanks (tanks C-108, C-109, C-111, and C-112) received waste with the highest concentration of ferrocyanide. However, it is estimated that over 90% of ferrocyanide would have undergone aging by thermal or radiolytic degradation by the mid-1990s while stored in the tank over a 40-year time period (HNF-SA-3126-FP). Since the rate of degradation (aging) is a strong function of temperature, the majority of the aging would have occurred in the late 1950s and 1960s. Three of the four C Farm tanks have recorded temperatures in the mid-70 to 80 °C range during the 1960s. The temperatures show a constant decline following scavenging operations (for example, for tank C-109, the temperatures were 77 °C in January 1963 and 27 °C in January 1983).

For safety evaluations that were conducted in the 1990s, analyte concentrations were determined from all four C-Farm tank samples as part of the Ferrocyanide Data Quality Objectives

(WHC-SD-WM-DQO-007, *Data Requirements for the Ferrocyanide Safety Issue Developed Through the Data Quality Objectives Process*, Rev. 2). The measurements conducted in the mid-1990s indicated that average $Na_2NiFe(CN)_6$ varied from 0.02 to 1.6 wt% (approximately 200 to 16,000 µg/g) on dry-weight sample basis. These values are significantly lower than the original concentrations calculated from the process flowsheets (22 to 25 wt%, dry) (HNF-SA-3126-FP).

While sodium nickel ferrocyanide is largely insoluble, it undergoes some dissolution in a caustic solution containing 0.01 M or higher hydroxide ions as shown below leading to soluble ferrocyanide and nickel hydroxide precipitate:

$$Na_2NiFe(CN)_6\ (s) + 2\ OH \leftrightarrow Fe(CN)_6^{-4} + 2\ Na^+ + Ni(OH)_2\ (s)$$

Under the tank waste conditions, the ferrocyanide complex, $Fe(CN)_6^{-4}$, is expected to slowly hydrolyze to formate ($HCOO^-$), ferric oxide (Fe_3O_4), and ammonia (NH_3) due to thermal or radiolytic degradation.

Although ferrocyanide was added to only tanks C-108, C-109, C-111, and C-112 in 1957 and 1958, some waste was transferred to tanks 241-C-103 and 241-C-104 from tanks C-111 and C-112. Unplanned releases from these tanks occurred between 1963 and 1974 (RPP-ENV-33418, *Hanford C-Farm Leak Inventory Assessments Report*), which could have released ferrocyanide in solution into the ground.

A2.0 INVENTORY ESTIMATES OF CYANIDE IN PAST RELEASES FROM WASTE MANAGEMENT AREA C

Inventory estimates from past releases in C Farm, for the majority of analytes that are tracked in the Best-Basis Inventory, are based on supernatant composition derived from Hanford Defined Waste (HDW) model (RPP-19822, *Hanford Defined Waste Model – Revision 5.0*). This approach is described in Section 2.1 of this document. The predominant supernatant waste types assumed to have been released from tanks and ancillary equipment in C Farm are a combination of Plutonium Uranium Extraction Plant high-level waste (P1 [1956-1962], P2 [1963-1967]) and aluminum fuel cladding waste (CWP1 [1956-1960], CWP2 [1961-1972]), B Plant cesium recovery waste (CSR), and Sr-Cs Rec (P2) stack drain waste streams. The average compositions for these waste streams in the HDW model are presented in Table 2-2 of this report. The concentration of ferrocyanide [$Fe(CN)_6^{-4}$] for these waste stream supernates was assumed to be zero within the HDW model based on assumption that all of the ferrocyanide would be in the precipitated phase (sludge). However, ferrocyanide degradation and dissolution are <u>not</u> accounted for by the HDW model, and therefore the HDW model estimates for ferrocyanide concentrations are considered unreliable (see Section 7.2.11 of RPP-19822).

Discharged inventory estimates from past releases at Waste Management Area (WMA) C are summarized in Table 2-3 of this report for selected analytes. The ferrocyanide inventory was estimated to be zero as the supernatant compositions were taken from the HDW model (see footnote in Table 2-3). However, this assumption about the ferrocyanide inventory appears to be inconsistent with the observations of cyanide in the groundwater monitoring well network for WMA C. The occurrence of low levels of cyanide in groundwater wells has been attributed to past releases from WMA C (see discussion in Section 2.3.3.3 of this report for further details).

A2.1 CYANIDE INVENTORY ESTIMATION PROCESS

To estimate the supernatant concentration of ferrocyanide with the primary purpose of developing inventory estimates for past discharges at WMA C, a two-staged approach was adopted. The first stage involved conducting a Hanford-specific literature search related to the solubility and dissolution potential of precipitated nickel ferrocyanide within the tanks. The second stage involved searching the Tank Waste Information Network System (TWINS) for historical records related to sampling data for cyanide for C Farm tanks. The results from both evaluations are presented here.

Based on the literature review, the most detailed and relevant information was found to be in PNNL-11211, *Ferrocyanide Safety Project: Ferrocyanide Aging Studies – Final Report*. The goal of this study was to evaluate the long-term chemical and radiolytic decomposition ("aging") of ferrocyanide materials under conditions found in the single-shell tanks at Hanford. The aging studies investigated possible reactions between the caustic waste and the precipitated ferrocyanide waste in a radiation field. The dissolution studies were performed on three types of

alkali metal nickel ferrocyanide-containing materials that had varying cesium content. The results indicate that the cesium to ferrocyanide ratio exerts a strong control on dissolution due to hydrolysis. As the Cs/Fe (cesium to iron) ratio increased, the extent of dissolution decreased appreciably under variable pH conditions. This indicates that the cesium-containing ferrocyanide phase [e.g., $CsNaNiFe(CN)_6$ or $Cs_2NiFe(CN)_6$] remains relatively insoluble compared to the pure sodium nickel ferrocyanide phase [$Na_2NiFe(CN)_6$].

This has large implications for tank waste operations, as ^{137}Cs would undergo ion exchange with ferrocyanide while dissolution of the pure ferrocyanide phase is occurring under alkaline conditions. Thus, the sorption of ^{137}Cs (a scavenging process) would be dependent on the interplay of ion exchange versus dissolution kinetics. As cesium accumulation increases at the particle surface, the composition of the phase would have increasing Cs/Fe ratio leading to lower dissolution rates and solubility. Note that the actual scavenging process involved precipitating ferrocyanides by adding nickel sulfate followed by removal of the supernate and then adding highly caustic waste on top of the precipitated cesium-ferrocyanide layer. From this process, there would have been a constant competition between dissolution of the precipitated solid, release of ^{137}Cs, and re-sorption via ion exchange. Laboratory studies conducted to evaluate these processes indicate that cesium becomes concentrated at the particle surface to form an insoluble cesium-rich phase, inhibiting dissolution of otherwise soluble $Na_2NiFe(CN)_6$.

Detailed hydrolysis-based dissolution experiments were conducted on solid material from the Westinghouse Hanford Company (WHC)-prepared flowsheet ferrocyanide material for the bottom layer (IF-1B flowsheet)[1], with a starting Cs/Fe molar ratio of 0.02. The extent of dissolution as a function of temperature was determined under 2 M NaOH solutions and the ferrocyanide (total Fe) concentrations are presented in Figure A-1 (taken from Figure 2.1 of PNNL-11211).

[1] In-Farm-1B, Rev. 7, WHC-prepared flowsheet ferrocyanide material.

Figure A-1. Temperature Dependence of Ferrocyanide Concentrations When 1F-1B Dissolves in 2M NaOH.

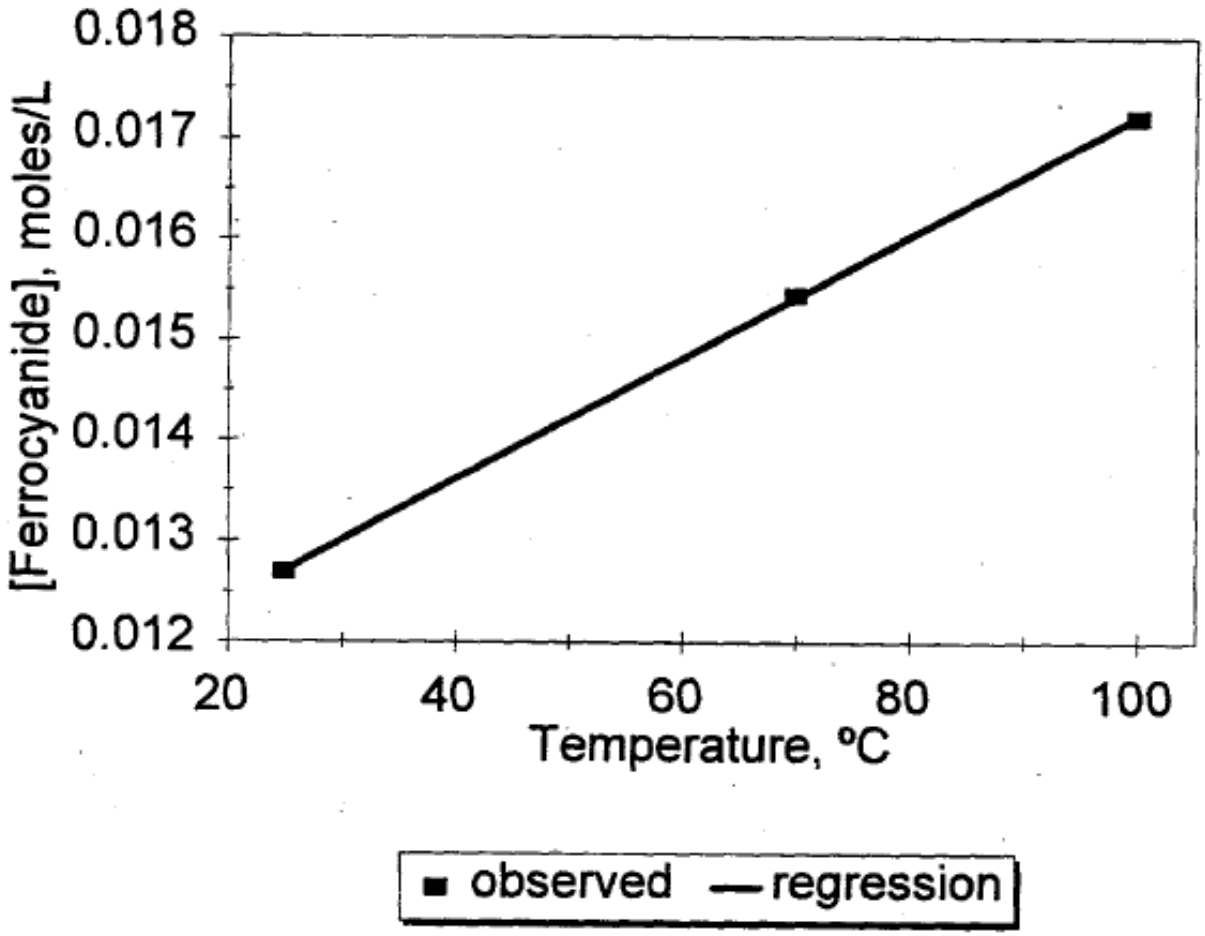

Source: PNNL-11211, *Ferrocyanide Safety Project Ferrocyanide Aging Studies – Final Report*, Figure 2.1.

During the time of past releases (1963 through 1974) the temperature conditions within the C Farm tanks were in the range of 25 to 80 °C. In this range of temperatures in Figure A-1, the ferrocyanide [$Fe(CN)_6^{-4}$] concentration is likely to vary from 0.0125 to 0.016 moles/L. This corresponds to dissolved concentrations of 2.6 to 3.4 g/L. These are likely to be bounding concentrations since increased incorporation of ^{137}Cs in the precipitates would have led to reduced dissolution (increasing Cs/Fe ratio). A dissolution experiment conducted on ferrocyanide material containing cesium showed over 50% reduction in dissolved mass compared to the ferrocyanide material that did not initially contain any cesium (see Figure 2.19 of PNNL-11211). Based on this information, a more realistic concentration range for the C Farm tanks could be about 1.3 to 2 g/L.

In the second stage of the evaluation, the information in TWINS (and underlying reports) were queried (query date 2/5/2018) to find historical cyanide sampling data from C Farm tanks. The sampling years ranged from 1992 to 1999 for the various tanks; results of this sampling are presented in Table A-1. Among the primary C Farm tanks that received ferrocyanide, sample results are only available for tanks C-109 and C-112. The cyanide concentrations reported are

"free cyanide" (as CN^- or HCN) based on the analytical method/procedure (WHC-SD-WM-DP-026, *Single Shell Tank Waste Characterization Project and Safety Analysis Project Core 34, 35 and 36 Data Report Tank 241-C-112*, Addendum 2, Rev. 0). Because the purpose of this evaluation is to estimate the cyanide concentration in the supernate (leak volume), the reported concentration for liquid composite water leach analysis or drainable liquid water analysis is particularly relevant, as the drainable liquids were filtered, and then the supernate was analyzed using ion chromatography. From the information presented in Table A-1, the reported concentrations of 1,350 and 1,320 µg/g (for tank C-109) and concentrations of 1,550, 1,020, 1,640, and 1,030 µg/g (for tank C-112) are therefore considered representative supernatant concentrations[2]. Since these concentrations are reported per unit weight of liquid, in order to convert them to volumetric units, an average liquid density of 1.2 g/mL has been used based on information in WHC-SD-WM-DP-026, Addendum 2, Rev. 0 and TWINS. Converting into liquid concentrations, the cyanide values range from 1.22 to 1.97 g/L, with an average concentration of 1.58 g/L.

Although this concentration is reportedly for free cyanide (CN^- or HCN), the test method likely also detects anionic cyanide complexes of the transition metals (from dissociation of simple and weak metal-cyanide complex) through anion exchange (ion chromatography). While the ferrocyanide ion is characterized as a strong-acid dissociable cyanide, no information is available on total cyanide, and therefore it is not possible to differentiate it from the reported free cyanide concentration. For this study, the reported free cyanide concentration is considered to be inclusive of simple cyanide, amenable cyanide (cyanide amenable to chlorination), and weak metal-cyanide complex. The average concentration of 1.58 g/L (for tanks C-109 and C-112) falls within the expected concentration of ^{137}Cs complexed ferrocyanide based on the dissolution experiments. Due to the slow degradation expected at lower temperatures, the concentration of cyanide from the 1990s may not have changed much over the decades since the unplanned releases. Given the lack of sample-based cyanide concentrations at the time of the leaks, a reasonable approximation of the cyanide concentration released to the soils is to use the tank concentration from sampling in the 1990s.

A2.2 ESTIMATION OF CYANIDE INVENTORY IN PAST RELEASES AT WASTE MANAGEMENT AREA C

Taking the leak volume estimates for various tanks that were used during the scavenging process (or in later transfers), the released inventory of free cyanide (referred to as cyanide henceforth) is estimated in Table A-2. The cyanide concentrations are based on the average of sampled data from Table A-1 (for tanks 241-C-104 and 241-C-110) and an average concentration of 1.58 g/L (for tanks C-108 and C-112). Of the total released cyanide inventory of about 151 kg, about 108 kg is estimated to have been released from tank C-108.

[2] The reported values of 0.315 and 0.316 wt% (3,150 and 3,160 µg/g) for tank C-109 presented in Table A-1 represent total cyanide calculated using a separate method (see "Description" field in Table A-1).

A3.0 PHASE 2 CHARACTERIZATION RESULTS FOR CYANIDE IN VADOSE ZONE BENEATH WASTE MANAGEMENT AREA C

As part of the Phase 2 Characterization for WMA C *Resource Conservation and Recovery Act of 1976* (RCRA) Field Investigation/Corrective Measures Study (RPP-RPT-38152, *Data Quality Objectives Report Phase 2 Characterization for Waste Management Area C RCRA Field Investigation/Corrective Measures Study*; RPP-PLAN-39114, *Phase 2 RCRA Facility Investigation/Corrective Measures Study Work Plan for Waste Management Area C*), 147 soil samples were collected from 13 judgment sampling locations (A, B, C, E, F, G, H, I, J, L1/L2, P, R, and U) and analyzed for cyanide at WMA C. Cyanide was not detected (below detection limit) at all locations. All sample results were set equal to their corresponding reporting limits that ranged from 0.2 to 5.6 mg/kg. It should be noted that Model Toxics Control Act (*Revised Code of Washington* 70.105D, "Hazardous Waste Cleanup — Model Toxics Control Act") (MTCA) Method B and MTCA Method C soil cleanup levels for cyanide are 48 and 2,100 mg/kg, respectively.

A4.0 GROUNDWATER MONITORING RESULTS FOR CYANIDE SINCE 2000

Cyanide has been detected in monitoring wells around WMA C since about calendar year 2000. The trend plots for various monitoring wells along with their relative locations are shown in Figure A-2. Cyanide is regulated as Free Cyanide with Federal Drinking Water Maximum Contaminant Level (MCL) of 200 µg/L for Cyanide (as free cyanide) [Table in Title 40 *Code of Federal Regulations*, Part 141, "National Primary Drinking Water Regulations" (40 CFR 141), Subpart G—National Primary Drinking Water Regulations: Maximum Contaminant Levels and Maximum Residual Disinfectant Levels, § 141.62 Maximum contaminant levels for inorganic contaminants, section (b)]. The U.S. Environmental Protection Agency has regulated free cyanide as cyanides amenable to chlorination. Cyanides amenable to chlorination provides a conservative estimate of toxicity because, in addition to free cyanide, it recovers some weak acid dissociable metal cyanide complexes that may or may not actually release free cyanide in the environment. For the State of Washington, the cleanup value for free cyanide is 4.8 µg/L based on MTCA Method B (*Washington Administrative Code* 173-340, "Model Toxics Control Act—Cleanup" Method B).

Table A-1. Historical Sampling Data for Free Cyanide in 241-C Farm Tanks (based on Tank Waste Information Network System record).

Tank Name	Sampling Year	Aggregation Level	Data Status	Result Type	Reported Value	Reported Units	Standard Value	Standard Units	Description	Referenced Document
241-C-103	1994	Drainable Liquid	Pre-Transfer	DUPLICATE_RESULT	27.2	µg/mL	27	µg/mL	C-103 Core 63, Segment 4 Drainable Liquid (Analysis Method Group: Spectrophotometer – 580 mm; Analysis Method ID: 403)	WHC-SD-WM-DP-099, Rev. 0A
241-C-103	1994	Drainable Liquid	Pre-Transfer	PRIMARY_RESULT	26.6	µg/mL	27	µg/mL	C-103 Core 63, Segment 4 Drainable Liquid (Analysis Method Group: Spectrophotometer – 580 mm; Analysis Method ID: 403)	WHC-SD-WM-DP-099, Rev. 0A
241-C-104	1999	Tank Composite	Pre-Transfer	DUPLICATE_RESULT	8.5	µg/mL	9	µg/mL	C-104 Cores 248 & 249 Composite, Supernatant Liquid, Distillation (Analysis Method Group: CN; Analysis Method ID: 787)	PNNL-13364/WTP-RPT-007, Rev. 0
241-C-104	1999	Tank Composite	Pre-Transfer	PRIMARY_RESULT	7.4	µg/mL	7	µg/mL	C-104 Cores 248 & 249 Composite, Supernatant Liquid, Distillation (Analysis Method Group: CN; Analysis Method ID: 787)	PNNL-13364/WTP-RPT-007, Rev. 0
241-C-109	1993	Tank Composite	Pre-Transfer	DUPLICATE_RESULT	1,350	µg/g	1,350	µg/g	C-109 Cores 47 & 49 Liquid Composite, Water Leach (Analysis Method Group: IC:W; Analysis Method ID: 301)	WHC-SD-WM-DP-036, Rev. 0
241-C-109	1993	Tank Composite	Pre-Transfer	DUPLICATE_RESULT	0.316	wt%	3,160	µg/g	C-109 Cores 47 & 49 Liquid Composite (Analysis Method Group: CN; Analysis Method ID: 624)	WHC-SD-WM-DP-036, Addendum 2A, Rev. 0
241-C-109	1993	Tank Composite	Pre-Transfer	PRIMARY_RESULT	1,320	µg/g	1,320	µg/g	C-109 Cores 47 & 49 Liquid Composite, Water Leach (Analysis Method Group: IC:W; Analysis Method ID: 301)	WHC-SD-WM-DP-036, Rev. 0
241-C-109	1993	Tank Composite	Pre-Transfer	PRIMARY_RESULT	0.315	wt%	3,150	µg/g	C-109 Cores 47 & 49 Liquid Composite (Analysis Method Group: CN; Analysis Method ID: 624)	WHC-SD-WM-DP-036, Addendum 2A, Rev. 0
241-C-110	1993	DL Tank Composite	Utilized/ Pre-Transfer	DUPLICATE_RESULT	2.6	µg/mL	3	µg/mL	C-110 Drainable Liquid Tank Composite (Analysis Method Group: Spectrophotometer – 580 mm; Analysis Method ID: 403)	WHC-SD-WM-DP-027, Addendum 4, Rev. 0A
241-C-110	1993	DL Tank Composite	Utilized/ Pre-Transfer	PRIMARY_RESULT	2.65	µg/mL	3	µg/mL	C-110 Drainable Liquid Tank Composite (Analysis Method Group: Spectrophotometer – 580 mm; Analysis Method ID: 403)	WHC-SD-WM-DP-027, Addendum 4, Rev. 0A
241-C-112	1992	DL Core Composite	current	DUPLICATE_RESULT	1,550	µg/g	1,550	µg/g	C-112 Core 34 Core Composite Drainable Liquid Water (Analysis Method Group: IC:W; Analysis Method ID: 304)	WHC-SD-WM-DP-026, Addendum 2, Rev. 0
241-C-112	1992	DL Core Composite	current	DUPLICATE_RESULT	1,020	µg/g	1,020	µg/g	C-112 Core 35 Core Composite Drainable Liquid Water (Analysis Method Group: IC:W; Analysis Method ID: 304)	WHC-SD-WM-DP-026, Addendum 2, Rev. 0
241-C-112	1992	DL Core Composite	current	PRIMARY_RESULT	1,640	µg/g	1,640	µg/g	C-112 Core 34 Core Composite Drainable Liquid Water (Analysis Method Group: IC:W; Analysis Method ID: 304)	WHC-SD-WM-DP-026, Addendum 2, Rev. 0
241-C-112	1992	DL Core Composite	current	PRIMARY_RESULT	1,030	µg/g	1,030	µg/g	C-112 Core 35 Core Composite Drainable Liquid Water (Analysis Method Group: IC:W; Analysis Method ID: 304)	WHC-SD-WM-DP-026, Addendum 2, Rev. 0

Tank Waste Information Network System (TWINS) sample data. Downloaded 2/5/2018.

DL = Drainable Liquid

References:
PNNL-13364/WTP-RPT-007, "*Inorganic and Radiochemical Analysis of 241-C-104 Tank Waste*."
WHC-SD-WM-DP-026, *Single Shell Tank Waste Characterization Project and Safety Analysis Project Core 34, 35 and 36 Data Report Tank 241-C-112*, Rev. 0, Addendum 2.
WHC-SD-WM-DP-027, *222-S Laboratories Single Shell Tank Waste Characterization, Tank C-110, Cores 37, 38, and 39*, Rev. 0A, Addendum 4.
WHC-SD-WM-DP-036, *PNL 325 Laboratories Single Shell Tank Waste Characterization for Tank C-109, Cores 47, 48, and 49*.
WHC-SD-WM-DP-036, Addendum 2A
WHC-SD-WM-DP-099, *Final Report for Tank 241-C-103, Push Mode Sample Cores 63 and 66*.

Table A-2. Estimated Cyanide Inventory in Past Releases at 241-C Farm Tanks.

Waste Release (Tank)	Leak Volume (gal) (RPP-RPT-59197, Rev. 1)	Time of Release (RPP-RPT-59197, Rev. 1)	Cyanide Concentration (g/L) (Estimated from Table A-1)	Estimated Cyanide Inventory in Leak Volume (kg)
241-C-101	37,000	1965	0	0
241-C-104	28,000	1965	0.008	0.85
241-C-105	2,000 to 20,500	1963	0	0
241-C-108	18,000	1965	1.58	108
241-C-110	2,000	1971	0.003	0.02
241-C-112	7,000	1965	1.58	42
Total				151

Reference: RPP-RPT-59197, "*Analysis of Past Tank Waste Leaks and Losses in the Vicinity of Waste Management Area C at the Hanford Site, Southeast Washington*," Rev. 1.

Remnant levels of low cyanide concentrations appear to be present sporadically beneath the eastern and western portions of the C Farm facility, while more persistent concentrations exist to the southeast (wells 299-E27-14 and 299-E27-24) as can be seen in Figure A-3. As discussed in DOE/RL-2009-77, *Groundwater Quality Assessment Plan for the Single-Shell Tank Waste Management Area C*, the source is likely be related to past releases from WMA C, but a specific tank/leak source within WMA C has not been identified. Cyanide was detected at four WMA C wells in December 2014 at concentrations far below the 200 µg/L drinking water standard. A possible reason for the increased number of wells with detectable cyanide between June and December 2014 is that the detection limit for cyanide decreased from 4 to 1.67 µg/L. In December of 2015, two wells (299-E27-14 and 299-E27-24) had concentrations approaching 15 µg/L, while two wells (299-E27-4 and 299-E27-23) had concentrations at or below 5 µg/L (Figure A-2). The other well (299-E27-7) had historically the highest value (40.7 µg/L) in 2009, but levels had fallen in that well to less than 5 µg/L by 2012. Concentrations at well 299-E27-4 are generally near the detection level but were higher in December of 2009, 2011, and 2014 (10.4, 7.98, and 7.9 µg/L, respectively).

Due to recent concerns about cyanide treatment requirements at the 200 West Pump & Treat facility, more detailed analyses of groundwater were conducted for 200-BP-5 groundwater operable units, which includes monitoring wells from WMA C. In addition to total cyanide, free cyanide and amenable cyanide was analyzed separately. The results from sampling in calendar year 2017 are presented in Table A-3. The method detection limits (MDLs) and practical quantitation limits (PQLs) for total cyanide are 1.67 and 5 µg/L, respectively, while for free cyanide they are 3 and 10 µg/L, respectively. Where total cyanide concentrations are found to be below detection limits, the same concentration is applied to amenable cyanide.

Figure A-2. Total Cyanide Concentrations in Groundwater Monitoring Wells around Waste Management Area C.

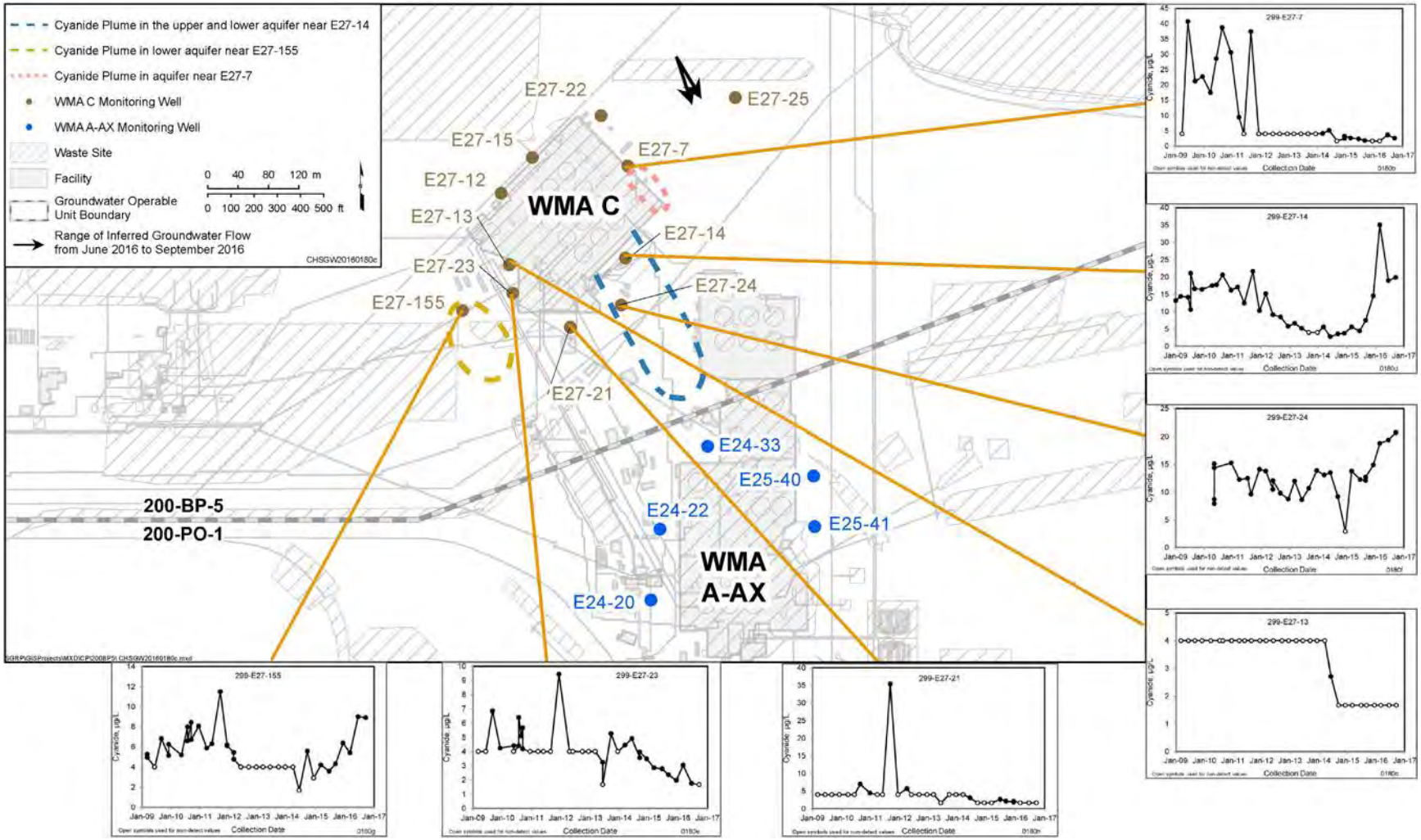

WMA = Waste Management Area

Figure A-3. Cyanide Concentrations in Waste Management Area C Wells from January 2006 through December 2017.

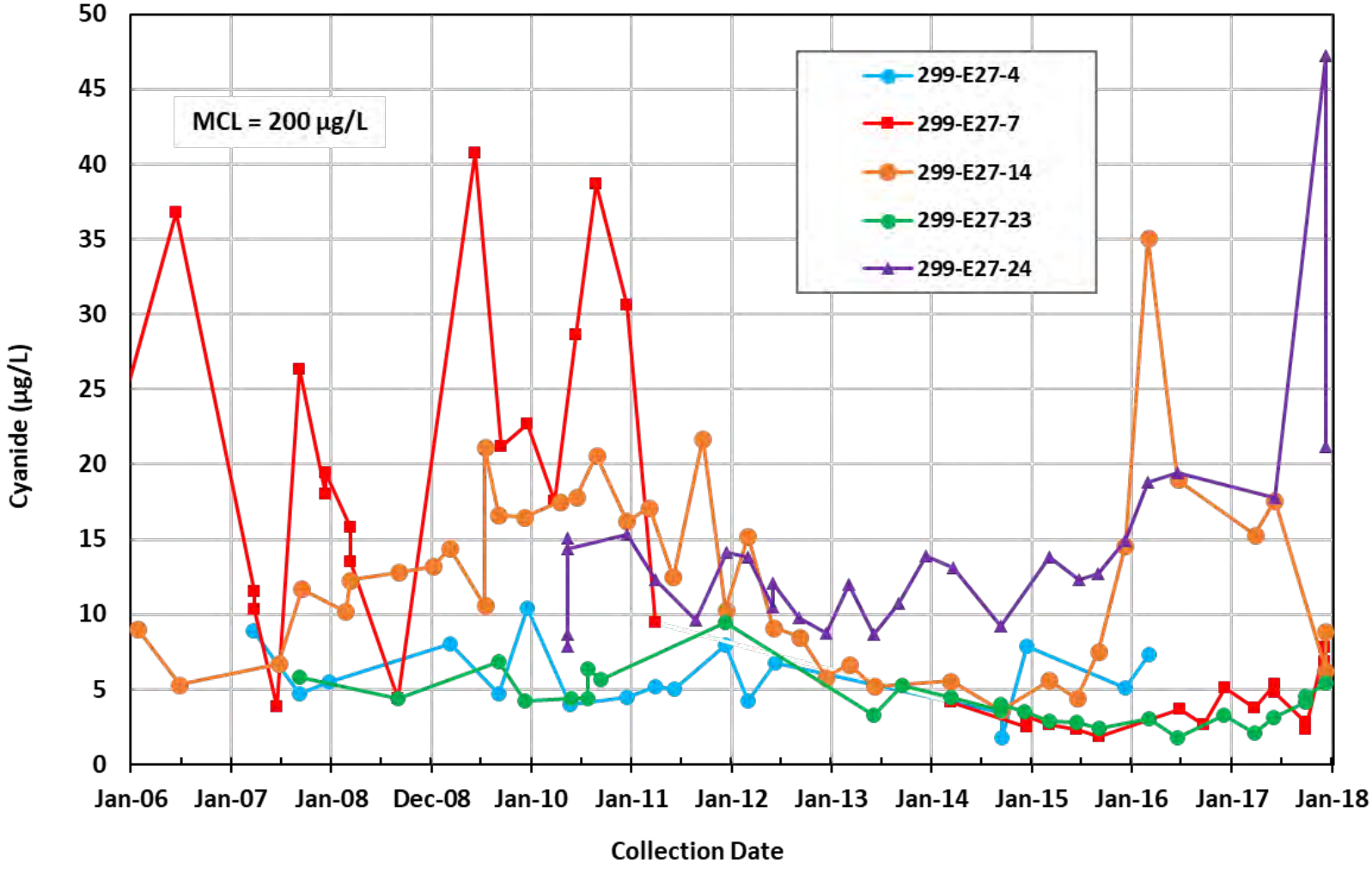

Note: Data that are flagged except for "B" flag (for lab qualified) and "G" flag (for review qualified) were removed

MCL = maximum contaminant level

Table A-3. Analytical Results of Total Cyanide, Amenable Cyanide, and Free Cyanide from Sampling of Groundwater Monitoring Wells at Waste Management Area C for Calendar Year 2017. (2 sheets)

Waste Management Area C 2017: Total Cyanide Quarterly Results (µg/L)				
Well Name	**March**	**June**	**September (Filtered/Unfiltered)**	**December (Filtered/Unfiltered)**
299-E27-12	<1.67	<3.1	<1.67/<1.67	<5.0/<5.0
299-E27-13	<1.67	<1.67	<1.67/<1.67	<1.67/<1.67
299-E27-14	15.3	17.6	7.44/8.07	8.86/6.25
299-E27-15	<1.67	<1.67	<1.67/<1.67	<5.0/<5.0
299-E27-155	16.2	18.7	30.2/30.6	38.8/38.1
299-E27-21	<1.67	<1.67	<1.67/2.08	<5.0/<5.0
299-E27-22	<1.67	<3.1	3.06[a] /3.19[a]	4.54[a] /5.05
299-E27-23	2.06[a]	3.16[a]	4.56[a] /4.16[a]	5.42/<5
299-E27-24	18.4	17.8	20.8/20.6	21.2/47.2
299-E27-25	<1.67	<1.67	<1.67/<1.67	<1.67/<1.67
299-E27-26	9.12	10.1	8.5/8.64	12.8/14.3
299-E27-7	3.79[a]	5.35	2.32[a] /2.84[a]	7.78/6.87

Waste Management Area C March 2017: Total, Amenable, and Free Cyanide Results (µg/L)				
Well Name	**Date Sampled**	**Total Cyanide (Filtered/Unfiltered)**	**Cyanide Amenable to Chlorination (Filtered/Unfiltered)**	**Free Cyanide (Filtered/Unfiltered)**
299-E27-12	3/29/2017	<1.67	<1.67	<3
299-E27-13	3/24/2017	<1.67	<1.67	<3
299-E27-14	3/27/2017	15.3	4.7[a]	3.63[a]
299-E27-15	3/29/2017	<1.67	<1.67	<3
299-E27-155	3/24/2017	16.2	4[a]	<3
299-E27-21	3/24/2017	<1.67	<1.67	<3
299-E27-22	3/27/2017	<1.67	<1.67	<3
299-E27-23	3/24/2017	2.06	2.06[a]	<3
299-E27-24	3/29/2017	18.4	5.6	<3
299-E27-25	3/27/2017	<1.67	<1.67	<3
299-E27-26	3/27/2017	9.12	<1.67	<3
299-E27-7	3/27/2017	3.79	1.82[a]	<3

Table A-3. Analytical Results of Total Cyanide, Amenable Cyanide, and Free Cyanide from Sampling of Groundwater Monitoring Wells at Waste Management Area C for Calendar Year 2017. (2 sheets)

Waste Management Area C September 2017: Total, Amenable, and Free Cyanide Results (µg/L)				
Well Name	**Date Sampled**	**Total Cyanide (Filtered/Unfiltered)**	**Cyanide Amenable to Chlorination (Filtered/Unfiltered)**	**Free Cyanide (Filtered/Unfiltered)**
299-E27-12	9/29/2017	<1.67/<1.67	<1.67/<1.67	<3/<3
299-E27-13	9/29/2017	<1.67/<1.67	<1.67/<1.67	<3/<3
299-E27-14	9/28/2017	7.44/8.07	3.42[a] /4.32[a]	<3/<3
299-E27-15	9/29/2017	<1.67/<1.67	<1.67/<1.67	<3/<3
299-E27-155	9/29/2017	30.2/30.6	30.2/5.4	7.36[a] /4.97[a]
299-E27-21	9/29/2017	<1.67/2.08	<1.67/2.08[a]	<3/<3
299-E27-22	9/28/2017	3.06/3.19	<1.67/<1.67	6.71[a] /<3
299-E27-23	9/29/2017	4.56/4.16	4.56[a] /<1.67	3.44[a] /5.62[a]
299-E27-24	9/28/2017	20.8/20.6	6.2/6.7	6.27[a] /6.27[a]
299-E27-25	9/29/2017	<1.67/<1.67	<1.67/<1.67	<3/<3
299-E27-26	9/28/2017	8.5/8.64	2.53[a] /<l.67	<3/5.19[a]
299-E27-7	9/29/2017	2.32/2.84	2.32[a] /2.84[a]	<3/<3
Waste Management Area C December 2017: Total, Amenable, and Free Cyanide Results (µg/L)				
Well Name	**Date Sampled**	**Total Cyanide (Filtered/Unfiltered)**	**Cyanide Amenable to Chlorination (Filtered/Unfiltered)**	**Free Cyanide (Filtered/Unfiltered)**
299-E27-12	12/8/2017	<5.0/<5.0	<5/<5	<5/<5
299-E27-13	12/8/2017	<1.67/<1.67	<l.67/<1.67	<3/<3
299-E27-14	12/8/2017	8.86/6.25	8.86/6.25	<5/5.28
299-E27-15	12/6/2017	<5.0/<5.0	<5/<5	<5/<5
299-E27-155	12/8/2017	38.8/38.1	5.4/4.0[a]	<3/<3
299-E27-21	12/8/2017	<5.0/<5.0	<5/<5	<5/<5
299-E27-22	12/6/2017	4.54/5.05	<l.67/<l.67	<3/<3
299-E27-23	12/8/2017	5.42/<5	5.42/<5	<5/<5
299-E27-24	12/8/2017	21.2/47.2	21.2/37.1	<5/<5
299-E27-25	12/6/2017	<1.67/<1.67	<1.67/<1.67	<3/<3
299-E27-26	12/6/2017	12.8/14.3	3.08[a] /3.2[a]	<3/<3
299-E27-7	12/6/2017	7.78/6.87	7.78/6.87	<5/<5

Only maximum values reported where duplicates were collected.
< = less than detection limit
a = sample detected above Method Detection Limit, but below Required Detection Limit.

The results indicate that the free cyanide and amenable cyanide concentrations are generally below the MDL. Where the concentrations are greater than the MDL, they usually are much lower than the total cyanide concentration indicating that the remaining fraction is strong acid dissociable cyanide [perhaps $Fe(CN)_6$]. The concentrations in monitoring wells located on the east side of WMA C (299-E27-14, E27-24, E27-26, and E27-7) are higher, with some concentrations above 4.8 µg/L MTCA Method B limit indicating a likely source from tank C-108 (or tank C-112); however, no clear trends are observed. On the west side of WMA C, only well 299-E27-155 shows concentrations that are above the MDL and above the 4.8 µg/L MTCA Method B.

A5.0 EVALUATION OF POTENTIAL IMPACTS TO GROUNDWATER FROM PAST RELEASES OF CYANIDE

Estimates on the cyanide inventories discharged at different possible release locations can be combined with information from contaminant transport modeling of past releases documented in RPP-RPT-59197, *Analysis of Past Tank Waste Leaks and Losses in the Vicinity of Waste Management Area C at the Hanford Site, Southeast Washington*, to examine whether releases of these probable cyanide inventories can yield groundwater impacts that are consistent with past observations of cyanide concentrations in groundwater.

Figure 6-10 in RPP-RPT-59197 provides modeling-based concentration of nitrate in groundwater at the points of calculation located 100 m (328 ft) from the WMA C fenceline. Cyanide and nitrate anions have similar transport characteristics, so the modeled results for nitrate can be used to estimate the impact of cyanide on groundwater[3]. The peak nitrate concentrations for each source type is predicted at point of calculation 6. For the tank C-108 leak, the peak nitrate concentration is calculated to be 1.54 mg/L as shown in Figure A-4 (same as information in Figure 6-10 of RPP-RPT-59197). The model predictions are based on a released nitrate inventory of 2,900 kg for a leak volume of 18,000 gallons (68,130 L) in calendar year 1965.

Normalizing the simulated concentration of nitrate with its released inventory results is shown in Figure A-5. The normalized peak concentration is 5.3×10^{-4} mg/L (per kg of nitrate inventory) or 0.53 µg/L (per kg of nitrate inventory). This value can be used to determine the peak concentration for cyanide from tank C-108. Considering 108 kg of cyanide inventory, the peak concentration is calculated to be about 57 µg/L. This peak concentration matches reasonably with the observed maximum groundwater concentrations, which vary between 40 and 50 µg/L (Figure A-3). Given that the simulated high concentrations occur approximately within calendar years 2010 and 2025, the current observed concentrations in the groundwater monitoring wells are likely to be near their peak values. The impact of additional inventory from tank C-112 could increase the simulated peak concentration by as much as 22 µg/L, but only if the plumes coincide. However, since groundwater flow paths for tanks C-108 and C-112 are believed to be parallel as the aquifer enters a long-term stable direction toward the southwest, limited overlap is expected and the two leaks are not expected to be additive. Therefore, the calculated peak groundwater concentration of cyanide of 57 µg/L based on tank C-108 leak inventory is deemed to be a reasonable estimate of the peak concentration in groundwater.

[3] This is supported by the observation of cyanide to nitrate concentration ratio trend for well 299-E27-14 as shown in Figure 2-29. The concentration ratio from calendar years 2006 to 2012 has remained within approximately 0.1 to 0.2 (µg/L of cyanide to mg/L of nitrate) with minor short-term fluctuations outside this tight range.

Figure A-4. Simulated Nitrate Concentration in Groundwater from Tank 241-C-108 Source 100 meters Downgradient of the Fenceline.

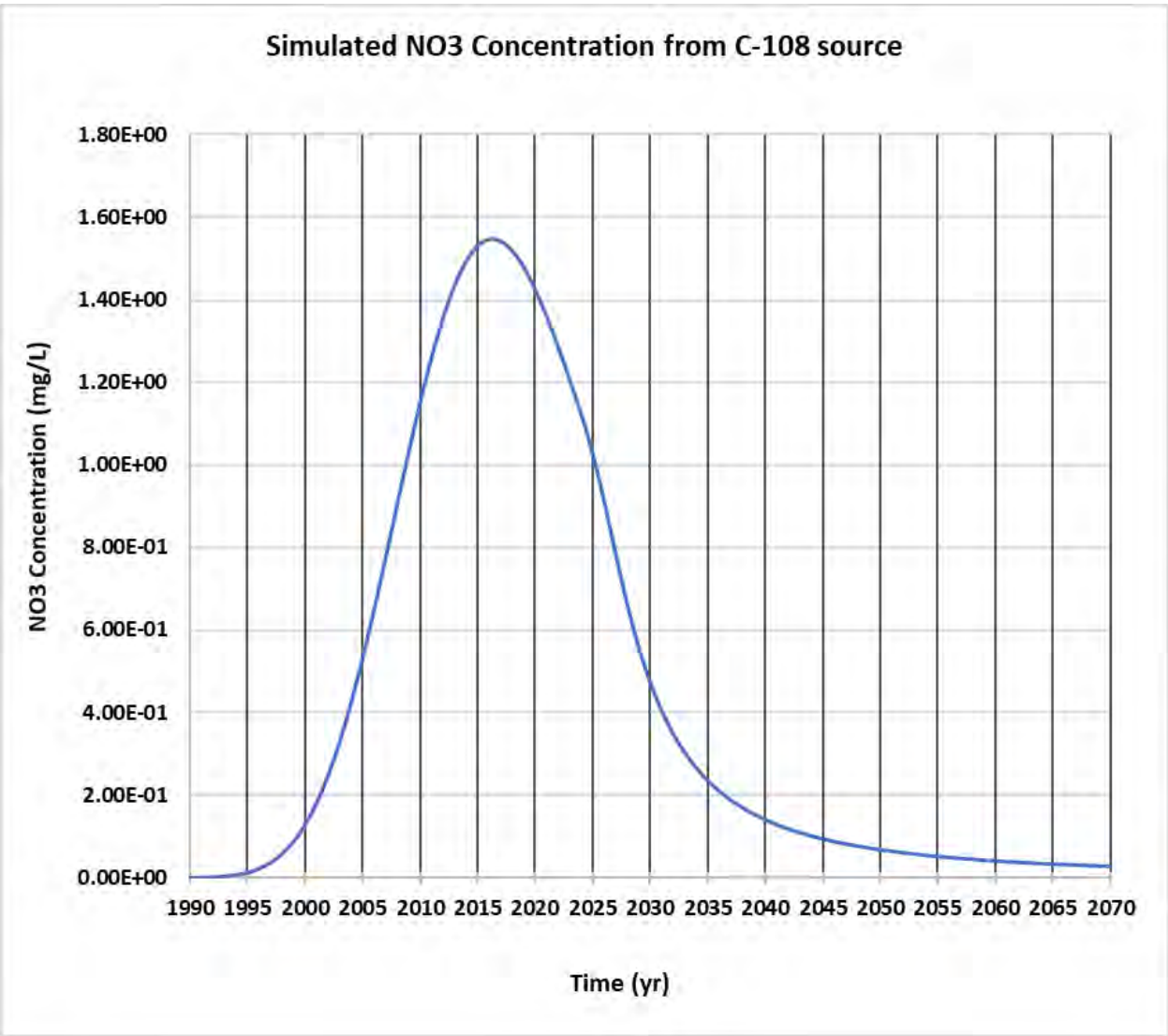

An inverse calculation to determine leaked inventory and waste stream concentration can also be performed using the nitrate normalized concentration relationship outlined above. Given that observed peak cyanide concentration in groundwater is about 45 µg/L, the discharged inventory is estimated to be about 85 kg (45 µg/L divided by 0.53 µg/L per kg of cyanide). Assuming this inventory is released in 18,000 gallons (68,130 L) of supernatant fluid from tank C-108, the concentration of cyanide in the leak is estimated to be 1.24 g/L, which provides a reasonable match with the measured average liquid concentration of 1.58 g/L.

Figure A-5. Nitrate Concentrations Normalized with Respect to Inventory for Tank 241-C-108 Source.

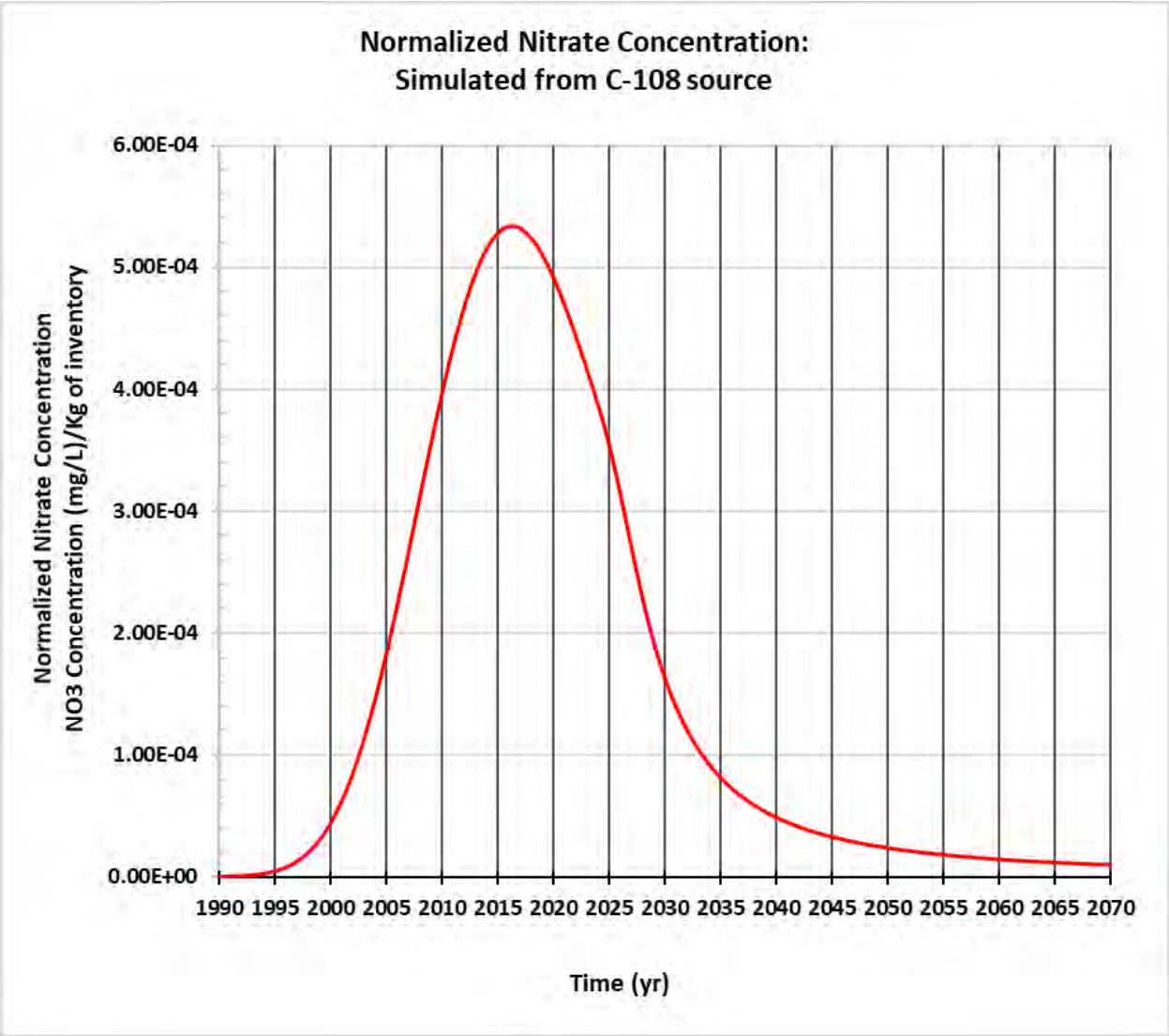

Consistent with the simulated nitrate concentrations, the cyanide concentrations are also projected to decline over time from the present-day values. The model suggests that in about a decade the concentrations could be appreciably lower than current observed values.

A6.0 REFERENCES

40 CFR 141, "National Primary Drinking Water Regulations," Subpart G—National Primary Drinking Water Regulations: Maximum Contaminant Levels and Maximum Residual Disinfectant Levels, § 141.62 Maximum contaminant levels for inorganic contaminants, *Code of Federal Regulations*, as amended.

DOE/RL-2009-77, 2010, *Groundwater Quality Assessment Plan for the Single-Shell Tank Waste Management Area C*, Rev. 0, U.S. Department of Energy, Richland Operations Office, Richland, Washington.

HNF-SA-3126-FP, 1997, *Resolution of the Hanford Site Ferrocyanide Safety Issue*, DE&S Hanford, Inc./Pacific Northwest National Laboratory/Babad Technical Services, Richland, Washington.

HW-43066, 1956, *Metal Recovery Waste Scavenging Process*, Hanford Atomic Products Operation, Richland, Washington.

PNNL-11211, 1996, *Ferrocyanide Safety Project Ferrocyanide Aging Studies – Final Report*, Pacific Northwest National Laboratory, Richland, Washington.

PNNL-13364/WTP-RPT-007, 2000, *Inorganic and Radiochemical Analysis of 241-C-104 Tank Waste*, Rev. 0, Pacific Northwest National Laboratory, Richland, Washington.

RCW 70.105D, "Hazardous Waste Cleanup — Model Toxics Control Act," *Revised Code of Washington*, as amended.

Resource Conservation and Recovery Act of 1976, 42 USC 6901, et seq.

RPP-19822, 2005, *Hanford Defined Waste Model – Revision 5.0*, Rev. 0-A, CH2M HILL Hanford Group, Inc./Technical Resources International, Inc., Richland, Washington.

RPP-ENV-33418, 2016, *Hanford C-Farm Leak Inventory Assessments Report*, Rev. 4, Washington River Protection Solutions, LLC, Inc., Richland, Washington.

RPP-PLAN-39114, 2012, *Phase 2 RCRA Facility Investigation/Corrective Measures Study Work Plan for Waste Management Area C*, Rev. 2, Washington River Protection Solutions, LLC, Richland, Washington.

RPP-RPT-38152, 2008, *Data Quality Objectives Report Phase 2 Characterization for Waste Management Area C RCRA Field Investigation/Corrective Measures Study*, Rev. 0, Cenibark International, Inc., Richland, Washington.

RPP-RPT-59197, 2016, *Analysis of Past Tank Waste Leaks and Losses in the Vicinity of Waste Management Area C at the Hanford Site, Southeast Washington*, Rev. 1, Washington River Protection Solutions, LLC, Richland, Washington.

Scheele, R. D., L. L. Burger, J. M. Tingey, R. T. Hallen, and M. A. Lilga, 1992, "Chemical Reactivity of Potential Ferrocyanide Precipitates in Hanford Tanks with Nitrates and Nitrites," *Proceedings of the Symposium on Waste Management at Tucson, Arizona, March 1-5, 1992*, Vol. 1, pp. 835–842.

WAC 173-340, "Model Toxics Control Act – Cleanup," *Washington Administrative Code*, as amended.

WHC-SD-WM-DP-026, 1993, *Single Shell Tank Waste Characterization Project and Safety Analysis Project Core 34, 35 and 36 Data Report Tank 241-C-112*, Addendum 2, Rev. 0, Westinghouse Hanford Company, Richland, Washington.

WHC-SD-WM-DP-027, 1993, *222-S Laboratories Single Shell Tank Waste Characterization, Tank C-110, Cores 37, 38, and 39*, Addendum 4, Rev. 0A, Westinghouse Hanford Company, Richland, Washington.

WHC-SD-WM-DP-036, 1994, *PNL 325 Laboratories Single Shell Tank Waste Characterization for Tank C-109, Cores 47, 48, and 49*, Rev. 0, Westinghouse Hanford Company, Richland, Washington.

WHC-SD-WM-DP-036, 1994, *PNL 325 Laboratories Single Shell Tank Waste Characterization for Tank C-109, Cores 47, 48, and 49*, Rev. 0, Addendum 2A, Westinghouse Hanford Company, Richland, Washington.

WHC-SD-WM-DP-099, 1995, *Final Report for Tank 241-C-103, Push Mode Sample Cores 63 and 66*, Rev. 0A, Westinghouse Hanford Company, Richland, Washington.

WHC-SD-WM-DQO-007, 1995, *Data Requirements for the Ferrocyanide Safety Issue Developed Through the Data Quality Objectives Process*, Rev. 2, Westinghouse Hanford Company/Pacific Northwest Laboratory, Richland, Washington.

This page intentionally left blank.

APPENDIX B

EVALUATION OF IMPACTS OF VADOSE ZONE HETEROGENEITIES ON CONTAMINANT TRANSPORT AT WMA C USING WASHINGTON STATE DEPARTMENT OF ECOLOGY'S ADVOCACY MODEL

This page intentionally left blank.

TABLE OF CONTENTS

B1.0 INTRODUCTION B-1

B2.0 PURPOSE B-2

B3.0 GEOLOGIC FRAMEWORK MODEL DEVELOPMENT B-3

B4.0 FLOW AND TRANSPORT MODEL DEVELOPMENT B-6

B4.1 EHM CROSS-SECTIONAL MODEL B-9

B4.2 FGU CROSS-SECTIONAL MODEL B-9

B4.3 MODEL INPUTS B-12

B4.3.1 Simulation Time Periods B-12

B4.3.2 Initial Conditions B-12

B4.3.3 Boundary Conditions B-12

B4.3.4 Contaminant Source B-14

B4.3.5 Hydraulic Properties B-14

B4.3.6 Transport Properties B-14

B4.4 SIMULATION CASES B-15

B4.4.1 Primary Case B-15

B4.4.2 Sensitivity Cases B-15

B4.5 KEY ASSUMPTIONS/LIMITATIONS OF THE MODEL B-18

B5.0 EVALUATION OF RESULTS B-19

B5.1 PRIMARY CASE: EFFECT OF FINE-GRAINED UNITS B-19

B5.1.1 Sensitivity Case 1: Effect of Changing Hydraulic Property of the Fine-Grained Units B-22

B5.1.2 Sensitivity Case 2: Effect of Leak Volume B-22

B5.1.3 Sensitivity Case 3: Effect of Tank Structure B-22

B6.0 SUMMARY AND CONCLUSIONS B-28

B7.0 REFERENCES B-30

LIST OF FIGURES

Figure B-1. Wells, Boreholes, and Cross-Section Lines Presented in Figure 2 of the 2014 Nez Perce Report. B-4

Figure B-2. Top Elevation and Lateral Extent of Fine-Grained Unit Layer B Presented in Figure 15 of 2014 Nez Perce Report (Left) and that Generated from Geologic Model Developed Using Kingdom® Software (Right) Interpolated Over the Extent of the Model Domain. B-7

Figure B-3. Comparison of C-C' Cross-Section from Figure 6 of the 2014 Nez Perce Report (Top) with that Generated from Geologic Model Developed Using Kingdom® Software (Bottom). B-8

Figure B-4. Comparison of Geology as Represented in 3-D Coarse Grid EHM Model (left) and EHM Cross-Sectional Model (right). B-10

Figure B-5. Construction Details of FGU Cross-Sectional Model. B-11

Figure B-6. Boundary Conditions Applied in the Flow and Transport Models. B-13

Figure B-7. Comparison of Hydraulic Properties Used for H2 Unit in the EHM Cross-Sectional Model and the Hss and 31A Hydraulic Properties Used for Fine-Grained Units in the FGU Cross-Sectional Model: Unsaturated Hydraulic Conductivity Versus Matric Potential (Left) and Volumetric Moisture Content Versus Matric Potential (Right). B-17

Figure B-8. Primary Case Results for EHM Cross-Sectional Model and FGU Cross-Sectional Model Comparing Mass Flux Arriving at the Water Table. B-20

Figure B-9. Comparison of Simulated (Primary Case) Technetium-99 Plume in the Vadose Zone in Year 1968 (First Row) and Year 1981 (Second Row) for EHM Cross-Sectional Model and FGU Cross-Sectional Model with Hss Hydraulic Properties for Fine-Grained Units. B-21

Figure B-10. Mass Flux Arriving at Water Table Showing the Effect of Hss and 31A Hydraulic Properties Used for the Fine-Grained Units. B-23

Figure B-11. Comparison of Simulated Technetium-99 Plume in the Vadose Zone in Year 1971 (First Row) and Year 2001 (Second Row) using FGU Cross-Sectional Model for the Primary Case (Hss Hydraulic Properties for Fine-Grained Units) and Sensitivity Case 1 (Sample 31A Hydraulic Properties for Fine-Grained Units). B-24

Figure B-12. Comparison of Simulated Water Saturation (Background Color) and Technetium-99 Plume (Foreground Color) in Year 1971 using FGU Cross-Sectional Model for the Primary Case (Hss Hydraulic Properties for Fine-Grained Units) and Sensitivity Case 1 (Sample 31A Hydraulic Properties for Fine-Grained Units). B-25

Figure B-13. Mass Flux Arriving at Water Table Showing the Effect of Leak Volume in Source. B-26

Figure B-14. Mass Flux Arriving at Water Table Showing the Effect of Tank Structure..... B-27

LIST OF TABLES

Table B-1. Statistical Mean Values for Site-Wide Samples…….....B-12
Table B-2. Comparison of Hydraulic Properties. B-16

LIST OF TERMS

2-D	two-dimensional
3-D	three-dimensional
DOE	U.S. Department of Energy
Ecology	Washington State Department of Ecology
EHM	Equivalent Homogeneous Medium
FGU	fine-grained units (report)
H1	Hanford formation upper gravelly sequence unit
H2	Hanford formation sand sequence unit
H3	Hanford formation lower gravelly sequence unit
HISI	Hanford Information System Inventory
Hss	Hanford sandy silt (unit)
HSU	hydrostratigraphic unit
Kingdom®	Kingdom® Geology modeling software
ORP	DOE-Office of River Protection
STOMP©	Subsurface Transport Over Multiple Phases
WMA	Waste Management Area
WMA C	Waste Management Area C

B1.0 INTRODUCTION

During the comment resolution discussions on the potential impact of local-scale heterogeneity on transport of contaminants from tank leaks and other unplanned releases within the tank farm in this document, Washington State Department of Ecology (Ecology) requested that U.S. Department of Energy (DOE)-Office of River Protection (ORP) consider an evaluation of effects of fine-grained thin sediment layers on transport with a separate alternative conceptual model. For this alternative model, Ecology recommended that the model be developed based on the general framework of fine-grained units identified by the Nez Perce Tribe in their interpretations of variability in moisture content data collected in the vicinity of Waste Management Area (WMA) C. These interpretations were summarized in an unpublished report by the Nez Perce Tribe sent by email to DOE-ORP on Nov. 5, 2014 (EMDT-MO-0031).

In discussions with DOE-ORP, Ecology acknowledged that the underlying data and interpretations of the occurrence and lateral continuity of the fine-grained thin layers identified by the Nez Perce Tribe in the 2014 unpublished report (EMDT-MO-0031) are uncertain. However, Ecology indicated that this alternative model evaluation based on the Nez Perce Tribe framework would provide them with some insight into the transport effects of vadose zone heterogeneities at WMA C.

DOE-ORP agreed to Ecology's request and has provided support for the requested evaluation that involved development of an alternative model based on the general framework of EMDT-MP-0031. This appendix documents the basis for its development and the evaluation of modeling results from its implementation. The specific model developed in consultation with Ecology is referenced here as "Ecology's Advocacy Model" to differentiate it from other alternative fate and transport models that have been described in this document.

Use of interpretations summarized in the 2014 Nez Perce Tribe unpublished report (EMDT-MO-0031) as a basis for this requested Ecology's Advocacy Model evaluation of vadose zone heterogeneities at WMA C is limited to the objectives of this analysis. DOE considers this evaluation to be an alternative evaluation of vadose zone heterogeneities at WMA C. Use of the information in EMDT-MO-0031 as a basis for this requested evaluation does not constitute any endorsement or agreement by DOE with the Nez Perce Tribe interpretation of vadose zone heterogeneities at WMA C.

DOE has supported and stands by its own evaluations of vadose zone heterogeneities at WMA C using the same moisture content data used by the Nez Perce Tribe that are in the process of being documented (see RPP-RPT-61239, *Multiple Lines of Evidence and Modeling Results for Heterogeneous Alternative Conceptual Models of the Subsurface at Waste Management Area C*, in preparation).

B2.0 PURPOSE

This appendix is focused on documenting the development of Ecology's Advocacy Model based on the information presented in the 2014 Nez Perce Tribe unpublished report (EMDT-MO-0031) regarding the interpreted extent of the fine-grained units based on volumetric moisture contents from neutron-moisture logs collected at WMA C. Because the interpreted results from the 2014 unpublished report by the Nez Perce Tribe, EMDT-MO-0031, was only available in the report tables, cross-sections, and maps, it could not be used directly in creating the numerical model. Furthermore, the unpublished 2014 Nez Perce Tribe report (EMDT-MO-0031) only presented interpretations of the presence of fine-grained units, without identifying the soil characteristics and hydraulic properties that would be associated with those layers.

As a consequence, the approach was to first develop a digital geologic model to represent the fine-grained thin layers interpreted at different boreholes and direct pushes provided in Table 1 of the 2014 Nez Perce Tribe unpublished report (EMDT-MO-0031). The digital geologic information then was used to create a flow and transport model based on the STOMP©[1] code to represent the tank farm and the fine-grained units interpreted to exist in the vadose zone underlying the WMA C. Finally, it was necessary to assign hydraulic properties to the posited fine-grained layers. This was done by assuming that the layers were composed of fine-grained soils that exist on the Hanford Site, for which measured hydraulic parameters exist. It is noted that there is no evidence that these soil types exist at WMA C; they are used solely as surrogates for the hypothesized fine-grained soil layers.

Section B3.0 of this appendix provides information on how the geologic data in the 2014 Nez Perce Tribe unpublished report (EMDT-MO-0031) were processed to develop the digital geologic model. Section B4.0 provides the details on the development of a flow and transport model from this geologic framework and other assumed model boundary conditions, contaminant source information, and parameter inputs. Section B5.0 provides the results from running the primary case and a set of sensitivity cases agreed with Ecology with the numerical model implementation. Section B6.0 provides a summary and conclusions of the implementation of Ecology's Advocacy Model and the potential effects of heterogeneity on contaminant transport in the vadose zone at WMA C.

[1] Subsurface Transport Over Multiple Phases (STOMP)© is copyrighted by Battelle Memorial Institute, 1996.

B3.0 GEOLOGIC FRAMEWORK MODEL DEVELOPMENT

The 2014 Nez Perce unpublished report (EMDT-MO-0031 provides an evaluation of moisture content data collected from various wells and boreholes in the vicinity of WMA C. This evaluation provided the basis for development of a geologic framework that identified 15 separate fine-grained units distributed vertically with variable but generally continuous lateral extent in the vadose zone beneath WMA C (Figure B-1). The elevations for the identified fine-grained units for each of the boreholes and direct push holes used in the evaluation are presented in Table 1 within the 2014 Nez Perce Tribe unpublished report (EMDT-MO-0031. These interpretations of fine-grained units provide the starting point for development of the geologic model used in the Ecology's Advocacy Model development. Not all 15 fine-grained units are present in any given borehole and direct-push hole. To build the geologic model, these units were assumed to be 1.5 ft (0.46 m) in thickness and somewhat laterally continuous; the implementation of continuity of these layers is described below. These data were imported into the Kingdom®[2] Geology modeling software (Hanford Information System Inventory [HISI] Identification Number 3899; CHPRC-02937, *Kingdom-Geology Software Management Plan*) used for developing the geologic framework model. No additional interpretations or modifications were performed on Nez Perce Tribe intepretations during the development of this geologic model.

[2] Kingdom® is a registered trademark of IHS Markit, London, United Kingdom.

Figure B-1. Wells, Boreholes, and Cross-Section Lines Presented in Figure 2 of the 2014 Nez Perce Report.

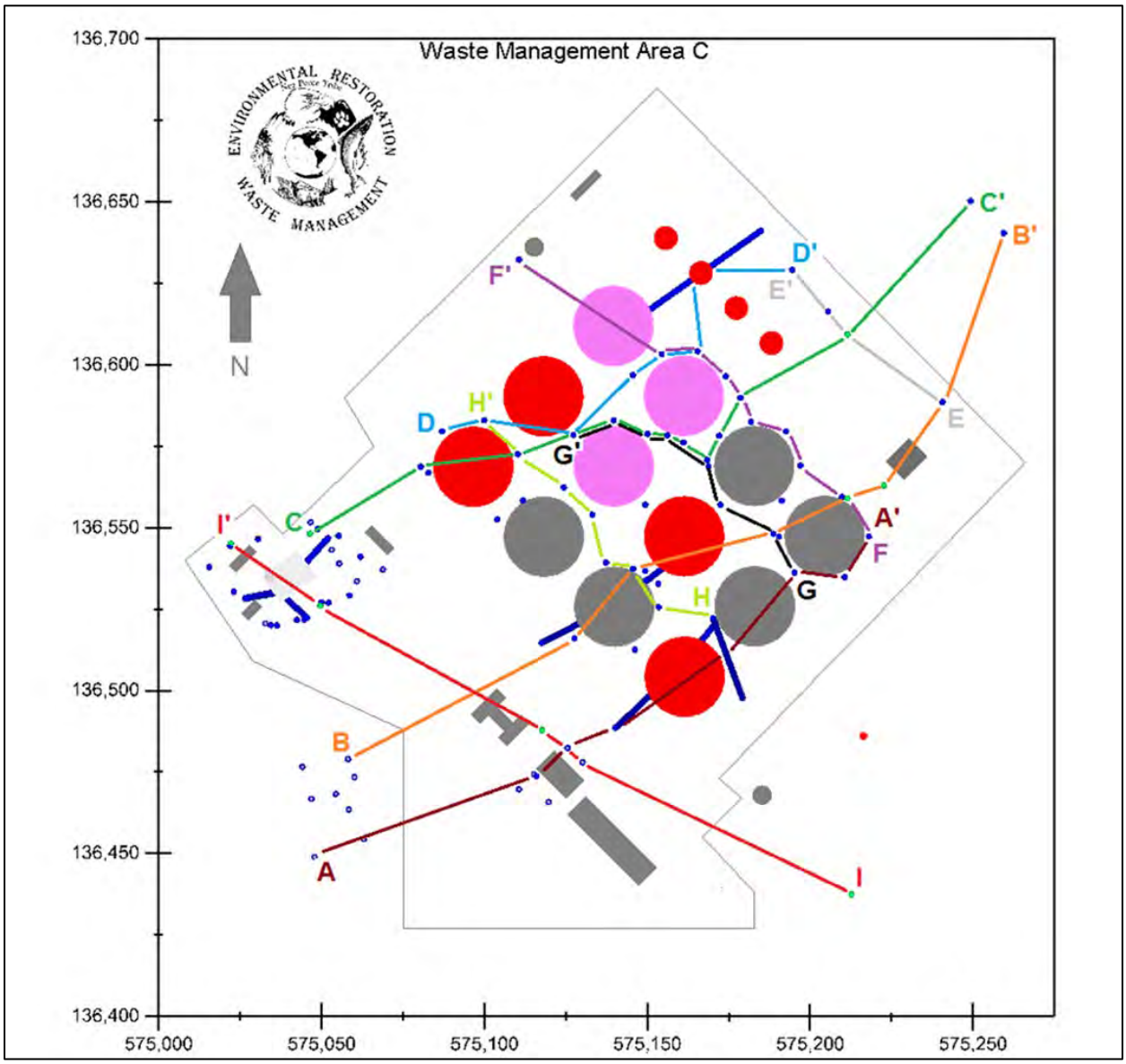

Reference: EMDT-MO-0031, Environmental Modeling Data Transmittal of an unpublished report entitled, "WMA C Conceptual Model" sent to DOE by the Nez Perce Tribe by email on Wednesday, Nov. 5, 2014 at 2:31 pm PST.

The Kingdom® Geology modeling software (Kingdom®) was used for spatial interpolation, gridding, and visualization. The Hanford Site geospatial data that is included within the Kingdom® well database was used to associate the well identification numbers with their spatial locations and surface elevations. The fine-grained unit information was imported by matching the well name in the table to the existing Kingdom® well database and adding the fine-grained unit layer name as a formation top property at the appropriate elevation. Once the fine-grained units table was imported, each of the 15 fine-grained unit layers was then run through the Kingdom® software's gridding algorithm using 1-m (3.3-ft) grid node spacing and a 5-m (16-ft) buffer to limit the grid extrapolation. The 5-m (16-ft) outside buffer allows the Kingdom® grids

to approximate the lateral extent of the gridded file representation of individual fine-grained units produced in the 2014 Nez Perce Tribe unpublished report (EMDT-MO-0031). While the original gridding method was not mentioned in EMDT-MO-0031, all grids produced using Kingdom® were visually compared with the figures in EMDT-MO-0031 to maintain a general consistency with the Nez Perce Tribe geologic framework. An example comparison of the top elevation and lateral extent for the fine-grained unit Layer B provided in EMDT-MO-0031 and that generated with Kingdom® software is shown in Figure B-2.

With visually accurate gridded surfaces and extents for all 15 fine-grained unit surfaces, a further comparison was made by reproducing two of the cross sections mentioned in EMDT-MO-0031 (cross-sections B-B' and C-C'). These two cross-sections are also roughly aligned with the flow and transport model orientation described in the next section. The comparison of C-C' cross-section from EMDT-MO-0031 to that from the geologic model built using Kingdom® software is shown in Figure B-3.

B4.0 FLOW AND TRANSPORT MODEL DEVELOPMENT

Section B3.0 describes the process for transforming the geologic framework model of 15 fine-grained units summarized in the 2014 Nez Perce Tribe unpublished report (EMDT- MO-0031) into a digital format. These digitally transformed fine-grained units were used to construct a flow and transport model using STOMP© code. According to the 2014 Nez Perce Tribe unpublished report (EMDT-MO-0031), these fine-grained units are conceived to be generally less than 0.45 m (1.5 ft) thick. To include the 0.45 m (1.5 ft) thick fine-grained units explicitly, the original STOMP© model that was built for evaluation of past leaks (Section 3.6.3.1) had to be refined appreciably. This is because the original Equivalent Homogeneous Medium (EHM) model had a coarser vertical discretization that varied between 1 to 1.5 m (3.3 to 4.9 ft).

Figure B-2. Top Elevation and Lateral Extent of Fine-Grained Unit Layer B Presented in Figure 15 of 2014 Nez Perce Report (Left) and that Generated from Geologic Model Developed Using Kingdom® Software (Right) Interpolated Over the Extent of the Model Domain.

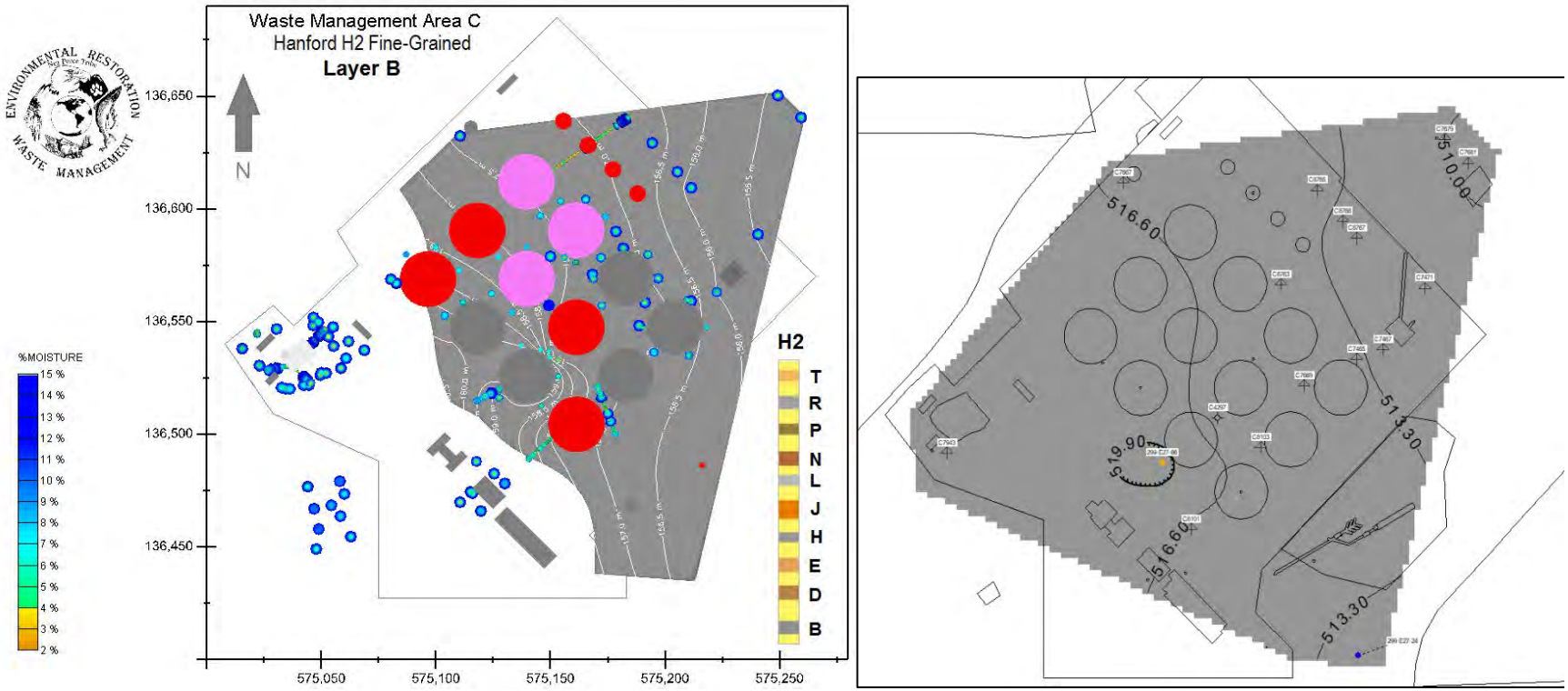

H2 = Hanford formation sand sequence unit

Kingdom® is a registered trademark of IHS Markit, London, United Kingdom.

Figure B-3. Comparison of C-C' Cross-Section from Figure 6 of the 2014 Nez Perce Tribe Report (Top) with that Generated from Geologic Model Developed Using Kingdom® Software (Bottom).

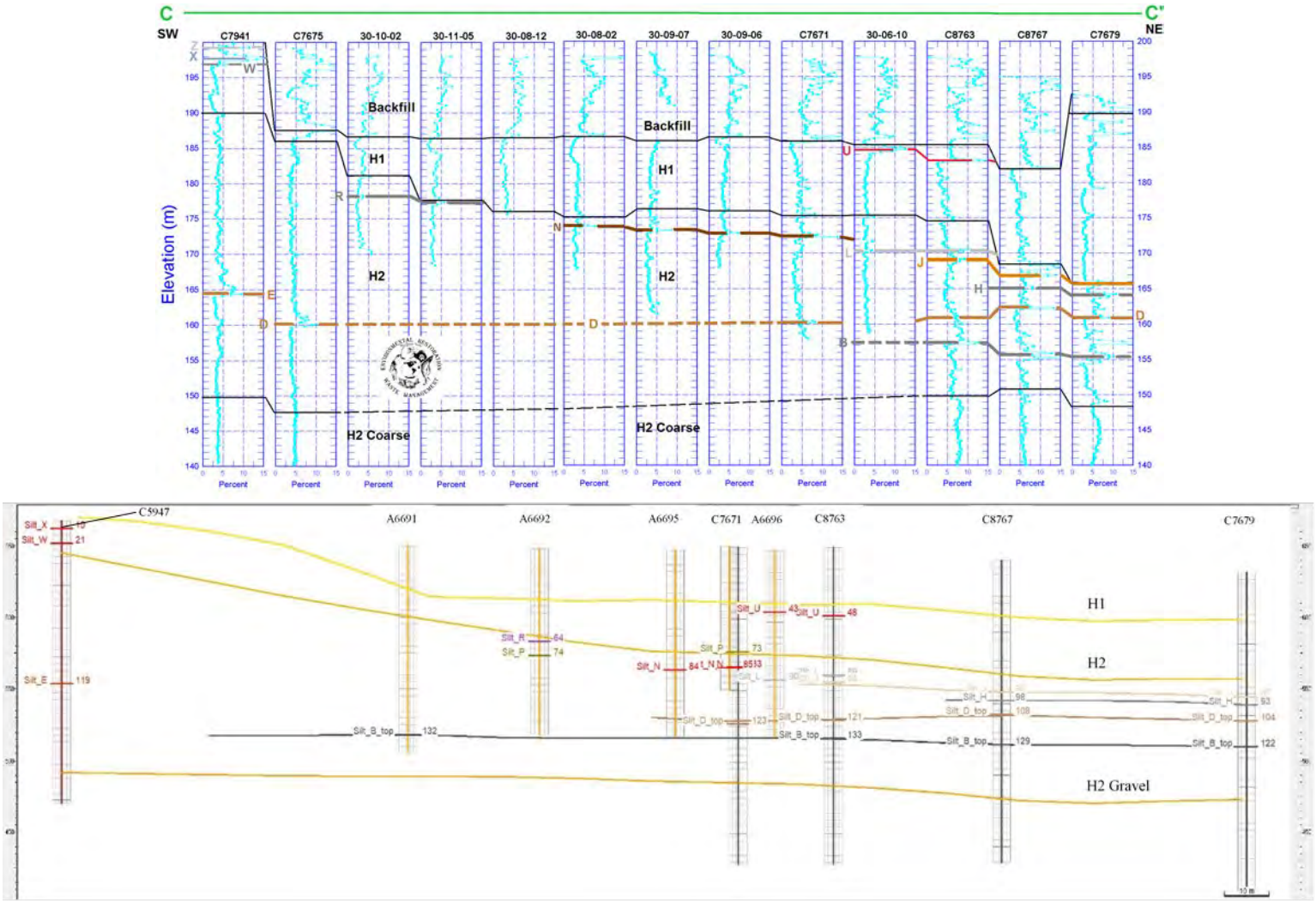

H1 = Hanford formation upper gravelly sequence unit H2 = Hanford formation sand sequence unit NE = northeast SW = southwest

Kingdom® is a registered trademark of IHS Markit, London, United Kingdom.

To accommodate the fine discretization requirements for the vadose zone and to reduce the computational demands, the models used in this evaluation were limited to two dimensions. This choice was made in consultation with Ecology and with understanding the inherent limitations of simulating flow and transport in two dimensions. Given that the primary purpose of the modeling evaluation is to evaluate the effect of the fine-grained units on contaminant transport for a meaningful comparison with the results of the EHM model, a two-dimensional (2-D) version of the EHM model was also developed using the same finer discretization. Further details are presented below.

For purpose of discussions that follow, the 2-D refined-grid cross-sectional model developed to represent the fine-grained units (up to 15 units) identified in EMDT-MO-0031 is referred as the "FGU cross-sectional model" while the 2-D refined-grid version of the EHM cross-sectional model built for comparison is called the "EHM cross-sectional model." The original three-dimensional (3-D) EHM model that is used to evaluate the past leaks (Section 3.6.3.1) is referred to as the "3-D coarse grid EHM model."

B4.1 EHM CROSS-SECTIONAL MODEL

A 2-D slice along the direction of the apparent dip (southwest-northeast) was extracted from the 3-D coarse grid EHM model (Figure B-4). Then a refined grid with 1-m (3.3-ft) lateral spacing and 0.15 m (0.5 ft) vertical spacing was developed (referred as EHM cross-sectional model) and different material zones from the coarse grid EHM model were populated. The tank structure was also included in the EHM cross-sectional model. Special attention was made in this process so that the contact between different hydrostratigraphic units (HSUs) remain the same as the coarse grid model. Figure B-4 shows the comparison of the geology as represented by the 3-D coarse grid EHM model and the EHM cross-sectional model.

B4.2 FGU CROSS-SECTIONAL MODEL

The FGU cross-sectional model was created by merging the digitally transformed 15 fine-grained units into the EHM cross-sectional model. First, the digitally transformed 15 fine-grained units were obtained from the Kingdom®-based model in 3-D scatter points format. The location of the fine-grained units was used to identify the corresponding grid nodes in the cross-sectional model. The HSUs of the EHM cross-sectional model in the identified grid nodes were replaced by the fine-grained units to obtain the FGU cross-sectional model. The mapping process is shown in Figure B-5.

Figure B-4. Comparison of Geology as Represented in 3-D Coarse Grid EHM Model (left) and EHM Cross-Sectional Model (right).

WMA C Past Leak 3-D EHM Model
Variable grid spacing
(3.8m x 3.8m x 1m in tank farm area)

EHM Cross-Sectional Model
Uniform grid spacing
1m x 0.15m (lateral x vertical)

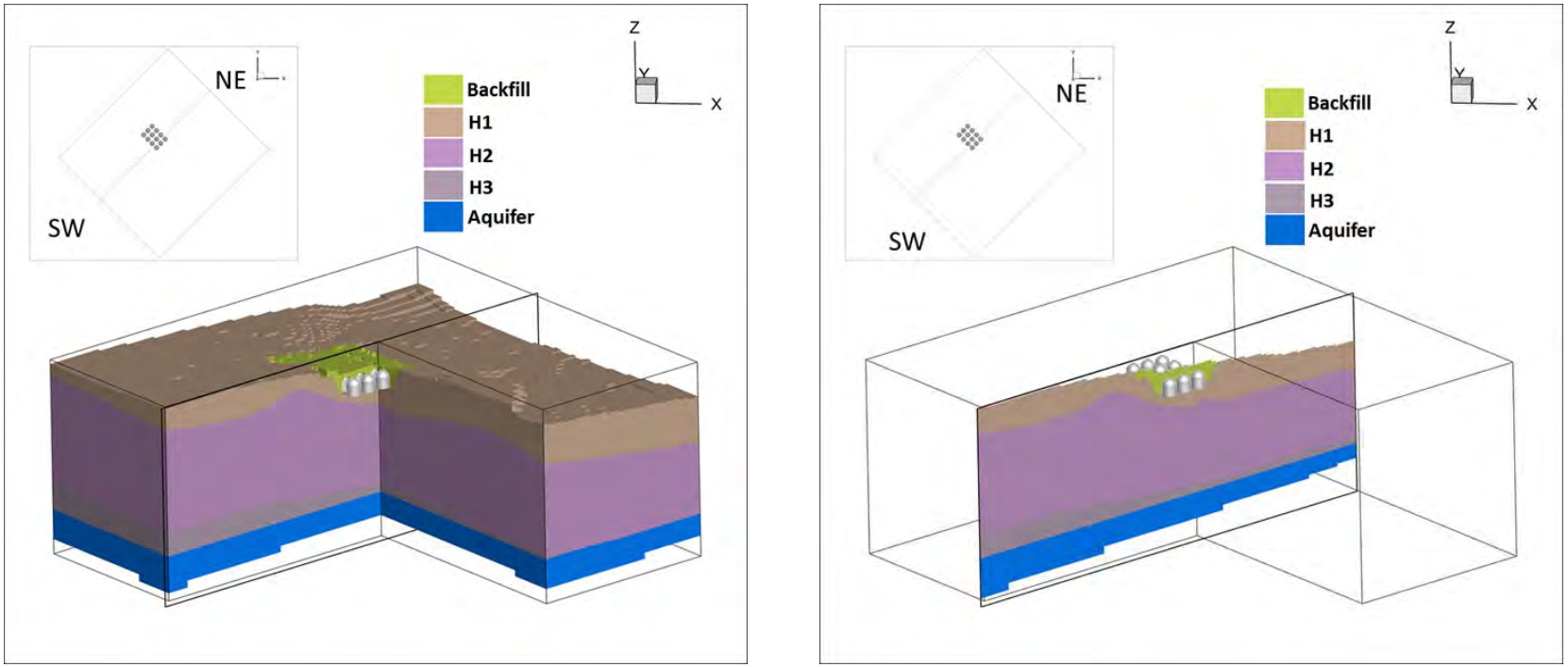

3-D = three-dimensional
EHM = Equivalent Homogeneous Medium
H1 = Hanford formation upper gravelly sequence unit
H2 = Hanford formation sand sequence unit
H3 = Hanford formation lower gravelly sequence unit
NE = northeast
SW = southwest
WMA = Waste Management Area

Figure B-5. Construction Details of FGU Cross-Sectional Model.

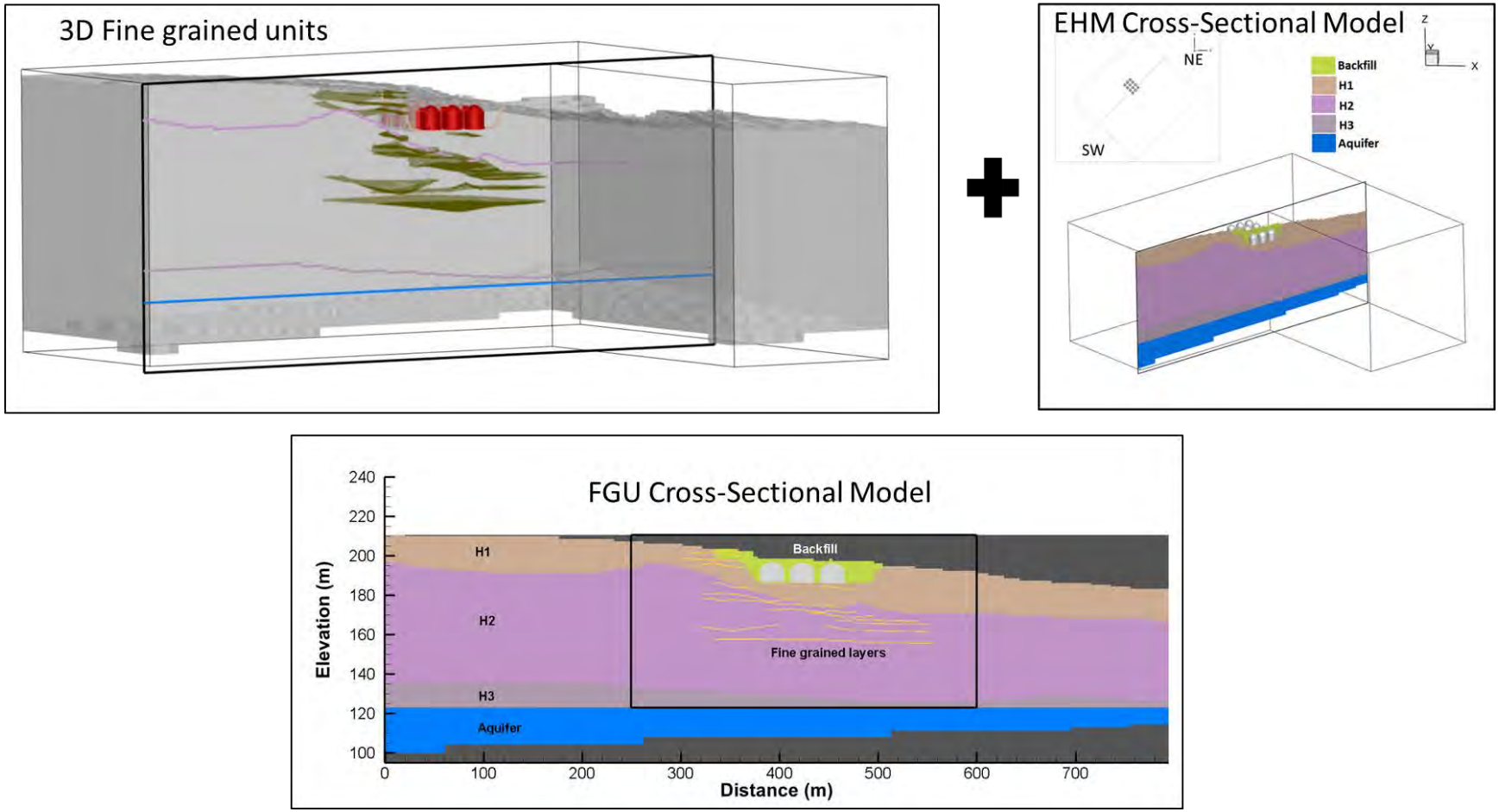

3-D = three-dimensional
EHM = Equivalent Homogeneous Medium
FGU = fine-grained units (report)
H1 = Hanford formation upper gravelly sequence unit
H2 = Hanford formation sand sequence unit
H3 = Hanford formation lower gravelly sequence unit
NE = northeast
SW = southwest

Three vertical grid nodes (each 0.15 m [0.5 ft] thick) were used to represent the 0.45-m (1.5-ft) thick fine-grained units. All 15 fine-grained units that were identified in the 2014 Nez Perce Tribe unpublished report (EMDT-MO-0031) were mapped into the FGU cross-sectional model. To reduce the computational burden, the lateral extent of the model was limited to the interpreted lateral extents of the fine-grained units plus some buffer areas to reduce the effect of lateral boundary conditions. The base of the model (bottom boundary) was limited to the top of the water table. The model domain used for the flow and transport simulations is shown by the black rectangle in the bottom figure within Figure B-5.

B4.3 MODEL INPUTS

All aspects of model inputs used in this evaluation as outlined below were selected in consultation with Ecology.

B4.3.1 Simulation Time Periods

All flow and transport model simulations used in this evaluation were run starting in calendar year 1944 and ending in calendar year 2120. The time period was selected to accommodate the establishment of hydraulic conditions in the vadose zone prior to the introduction of the selected contaminant source release between 1963 and 1968 and to allow sufficient time (i.e., ~150 years after the end of the source release) to capture the peak mass flux from the source release at the water table.

B4.3.2 Initial Conditions

A long-term simulation using pre-Hanford average recharge rates of 3.5 mm/yr (0.14 in./yr) was used to establish the hydraulic conditions at the beginning of each simulation in 1944. By simulating a sufficiently long time with unchanging boundary conditions (primarily the recharge rate at the top boundary), the pressures and saturations in the model domain stabilize under near steady-state conditions. The initial contaminant concentrations were zero.

B4.3.3 Boundary Conditions

All flow and transport model simulations used in this evaluation used a specified-flux boundary condition at the top surface with a constant net infiltration rate (recharge rate). A constant recharge rate of 3.5 mm/yr (0.14 in./yr) was applied for pre-Hanford Site conditions (before 1944). From 1944, a constant recharge rate of 100 mm/yr (3.9 in./yr) was applied inside of the tank farm area and 63 mm/yr (2.48 in./yr) was applied outside the tank farm area and continued through the end of the simulation. The bottom boundary of the model is set to atmospheric pressure to represent the water table. Boundary conditions at the sides of the model domain were assigned to be no flow. The applied boundary conditions are shown schematically in Figure B-6.

Figure B-6. Boundary Conditions Applied in the Flow and Transport Models.

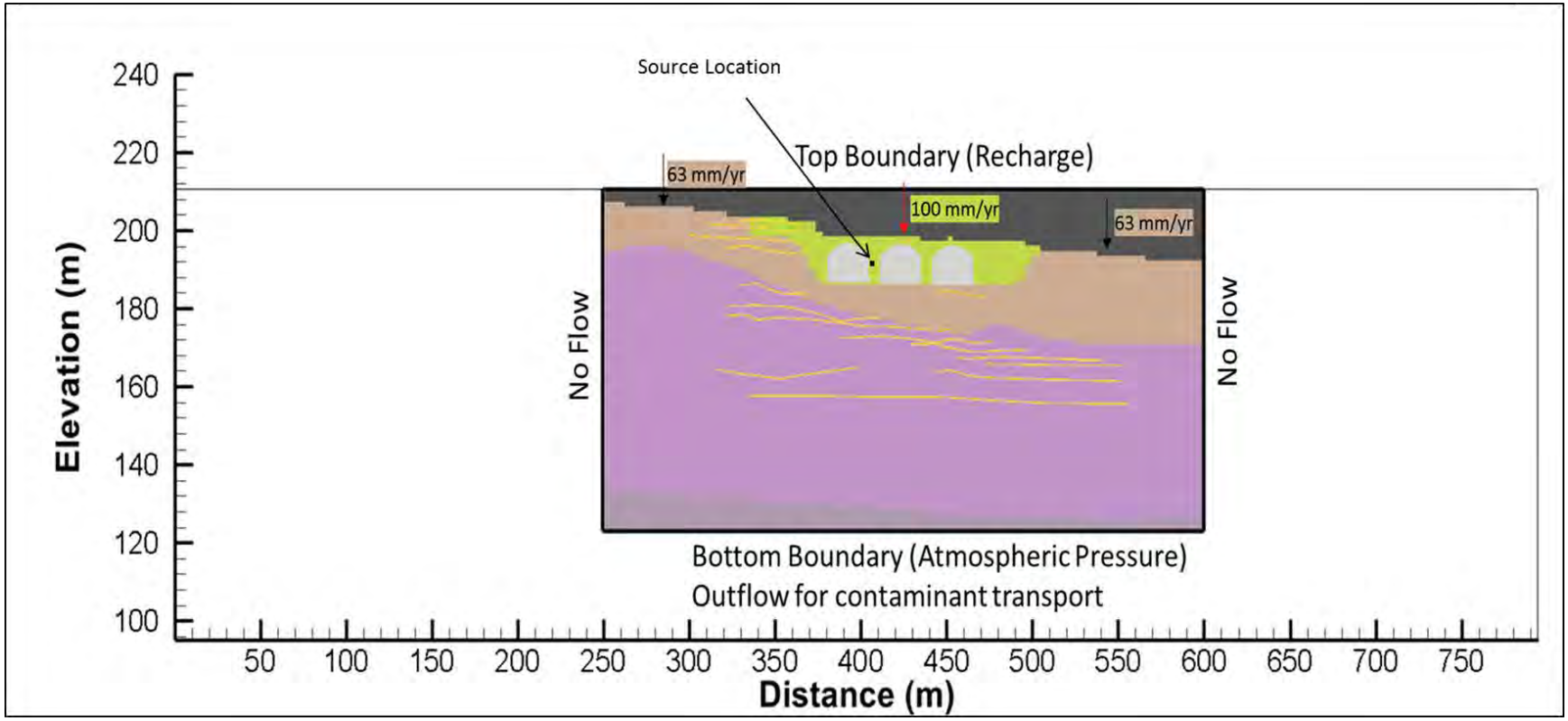

B4.3.4 Contaminant Source

All flow and transport model cases simulated in this evaluation used a general contaminant source that approximated the timing, the volume, and the inventory of ^{99}Tc estimated for the tank 241-C-105 leak. This specific past leak consisted of a 5-year release from 1963 to 1968 of a 20,500 gal waste volume containing ~10 Ci of ^{99}Tc to the upper part of the vadose zone between the tanks 241-C-104 and 241-C-105. The source release location is shown in Figure B-6.

B4.3.5 Hydraulic Properties

The hydraulic properties of HSU in the 3-D coarse grid EHM model (see Section 3.6.3.4 of RPP-RPT-59197) were used in the EHM and FGU cross-sectional models. For the fine-grained units in the FGU cross-sectional model, Ecology recommended that the average hydraulic properties developed for a "Hanford silty sand (Hss)" unit in Table 4.5 of PNNL-14702, *Vadose Zone Hydrogeology Data Package for Hanford Assessments* shown below will be used. All fine-grained units were assigned the same Hss set of hydraulic properties. Table B-1 summarizes the average (mean) hydraulic properties for various soils classes based on samples collected site-wide at the Hanford Site.

Table B-1. Statistical Mean Values for Site-Wide Samples

Soil Class	Count	α (1/cm)	n	θR (cm3/cm3)	θs (cm3/cm3)	Ks (cm/sec)	Sr	% gravel	Bulk Density (g/cm3)
Bf	6	0.019	1.400	0.030	0.262	5.98E-04	0.103	33.5	1.94
Hss	38	0.008	1.915	0.072	0.445	8.58E-05	0.162	0.2	1.61
Hfs	36	0.027	2.168	0.032	0.379	3.74E-04	0.086	0.6	1.60
Hcs	81	0.061	2.031	0.027	0.349	2.27E-03	0.080	2.6	1.67
Hgs	16	0.014	2.120	0.033	0.238	6.65E-04	0.140	25.8	1.94
Hg	28	0.017	1.725	0.022	0.167	3.30E-04	0.134	51.4	1.93
Hrg	40	0.007	1.831	0.020	0.102	1.46E-03	0.200	67.6	1.97
PPlz	9	0.005	2.249	0.040	0.419	5.57E-05	0.097	0.4	1.68
PPlc	14	0.011	1.740	0.054	0.281	8.45E-04	0.185	16.7	1.72
Rg	18	0.008	1.660	0.026	0.177	4.13E-04	0.135	46.1	1.90

B4.3.6 Transport Properties

The transport properties of HSUs in the 3-D coarse grid EHM model (see Section 3.6.3.4 of this document) were also used for equivalent HSUs identified in the EHM and FGU cross-sectional

models. For the fine-grained units in the FGU cross-sectional model, dispersivity values of 5 cm (2 in.) longitudinal and 0.5 cm (0.2 in.) transverse were used.

All other transport-related input parameters between the EHM cross-sectional model and the FGU cross-sectional model were kept the same. In other words, the only difference between the two models for any simulation cases is the presence of fine-grained units in the FGU cross-sectional model.

B4.4 SIMULATION CASES

For evaluating the effect of fine-grained units on flow and transport behavior, DOE and Ecology worked together to define a range of different simulations for consideration in this evaluation. A primary case was defined to evaluate the results of the FGU cross-sectional model that was advocated by Ecology to compare with results generated with the EHM cross-sectional model. Other simulation cases evaluated include sensitivity cases examining the effects of change in hydraulic properties, the leak volumes, and tank structure. These sensitivity cases were developed with modifications of the primary case. These cases are described below.

B4.4.1 Primary Case

This case is the comparison of results between the EHM cross-sectional model with the FGU cross-sectional model. As discussed earlier, the hydraulic properties for the Hanford sandy silt (Hss) unit, taken from PNNL-14702, as recommended by Ecology, are assigned to all fine-grained units used in the FGU cross-sectional model.

B4.4.2 Sensitivity Cases

In the following sensitivity cases, only one specific aspect was changed in the primary case simulated with the FGU cross-sectional model. All the other input parameters are kept the same as the primary case.

B4.4.2.1 Sensitivity Case 1: Effect of Hydraulic Property of the Fine-grained Units. This sensitivity case was evaluated to examine the effect of changing the hydraulic properties of the fine-grained units used in the FGU cross-sectional model to a different set of properties. Instead of assigning the hydraulic property of the Hss unit, the hydraulic property assigned to the high moisture zone greater than 10 percent volumetric moisture content) from the 3-D past leak heterogeneous model Case 4b (documented in Section 4.0 of this document) was chosen. Note that in Case 4b, the hydraulic properties used to represent the high moisture zone were based on sample 31A from the hydraulic properties database comprised of 44 Integrated Disposal Facility borehole samples from the H2 unit (see Appendix B and F of the RPP-ENV-58782, *Performance Assessment of Waste Management Area C, Hanford Site, Washington*; RPP-20621, *Far-Field Hydrology Data Package for the Integrated Disposal Facility Performance Assessment*). The

hydraulic property of sample 31A tends to bound the variability in hydraulic properties associated with the H2 unit. A comparison of hydraulic properties of the H2 unit (applied to the EHM model) with the hydraulic properties of the Hss unit (applied to the fine-grained units in the primary case) and hydraulic properties of sample 31A (applied to the fine-grained units in this sensitivity case) is presented in Table B-1 and Figure B-7.

Table B-2. Comparison of Hydraulic Properties.

Soil Class	Ks (cm/s)	θ_s (cm^3/cm^3)	θ_r (cm^3/cm^3)	α (1/cm)	n
H2	4.15E-03	0.315	0.039	0.063	2.000
Hss	8.58E-05	0.445	0.072	0.008	1.915
31A	8.21E-04	0.418	0.044	0.006	2.012

B4.4.2.2 Sensitivity Case 2: Effect of Leak Volume. This sensitivity case was evaluated to examine the effect of leak volume on the contaminant transport results. In this case, the 20,500-gal (77,600 L) leak volume assumed in the primary case was set to zero volume but the timing, location, and 5-year release period of 10 Ci of ^{99}Tc inventory was maintained.

B4.4.2.3 Sensitivity Case 3: Effect of Tank Structure. This sensitivity case was evaluated to examine the effect of the presence of the tanks on contaminant transport results. In the primary case, the tank structure was modeled as an inactive region (no flow through the tank). In this sensitivity case, the tank structures were removed, and the inactive regions were activated as the surrounding material (backfill).

Figure B-7. Comparison of Hydraulic Properties Used for H2 Unit in the EHM Cross-Sectional Model and the Hss and 31A Hydraulic Properties Used for Fine-Grained Units in the FGU Cross-Sectional Model: Unsaturated Hydraulic Conductivity Versus Matric Potential (Left) and Volumetric Moisture Content Versus Matric Potential (Right).

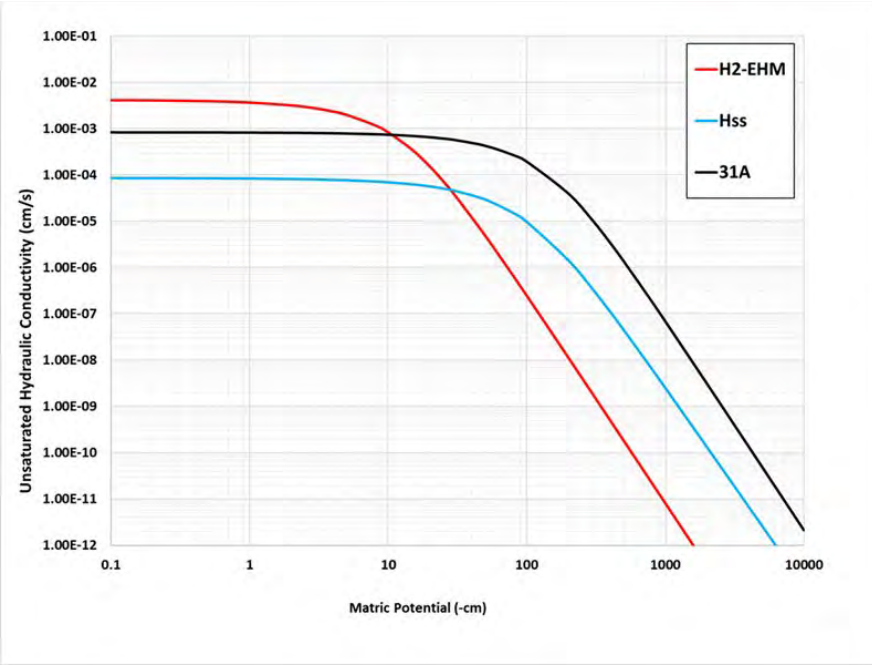

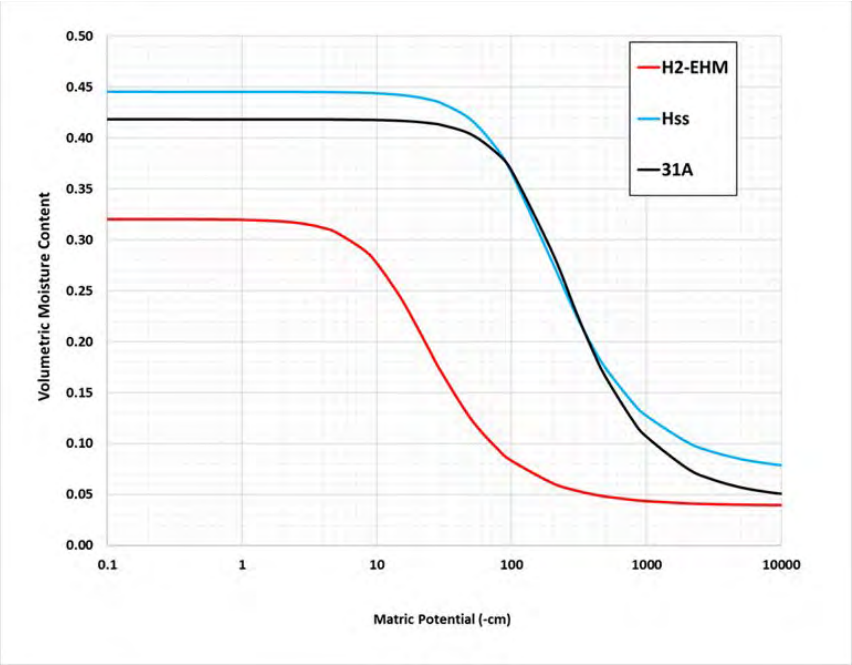

EHM = Equivalent Homogeneous Medium FGU = fine-grained units H2 = Hanford formation sand sequence unit Hss = Hanford sandy silt (unit)

B4.5 KEY ASSUMPTIONS/LIMITATIONS OF THE MODEL

The key assumptions and model limitations that provide the basis for the models used in this inter-model comparison are summarized below. These models are advocated by Ecology.

- The continuity of fine-grained units in the FGU cross-sectional model are maintained to generally match the interpretations in the 2014 Nez Perce Tribe unpublished report (EMDT- MO-0031) even though observations of fine-grained units are limited to a few boreholes.

- All fine-grained units in the FGU cross-sectional model are assumed to have the same thickness of ~ 1.5 ft (~0.5 m).

- All fine-grained units in the FGU cross-sectional model are assigned the same hydraulic property.

- The injected waste liquid volume and contaminants used in all the cross-sectional models evaluated in the primary and sensitivity cases can spread only in two directions (vertical and along the cross section) and therefore the results cannot be directly compared with the 3-D model results.

B5.0 EVALUATION OF RESULTS

This section provides an overview of the primary case and the range of sensitivity cases examined in the evaluation of the effects of vadose zone heterogeneities on contaminant transport at WMA C.

B5.1 PRIMARY CASE: EFFECT OF FINE-GRAINED UNITS

Figure B-8 shows the rate of arrival of ^{99}Tc (mass flux) at the water table (Ci/yr) as a function of time for the EHM cross-sectional model and FGU cross-sectional model (with Hss properties for the fine-grained units). Compared to the simulated breakthrough curve for the FGU cross-sectional model, the EHM cross-sectional model shows an earlier breakthrough to the water table and a higher peak mass flux. This difference is attributed to the presence of fine-grained units that cause slight delay in vertical movement along with small increase in lateral spreading in comparison to the EHM cross-sectional model. As a result, contaminant arrives later at the water table with a relatively attenuated peak in the FGU cross-sectional model.

Figure B-9 compares the contaminant distribution in the vadose zone at different times. The relatively slower downward migration and the slight increase in lateral spreading caused by the presence of the fine-grained units in the FGU cross-sectional model can be seen in these plots.

Figure B-8. Primary Case Results for EHM Cross-Sectional Model and FGU Cross-Sectional Model Comparing Mass Flux Arriving at the Water Table.

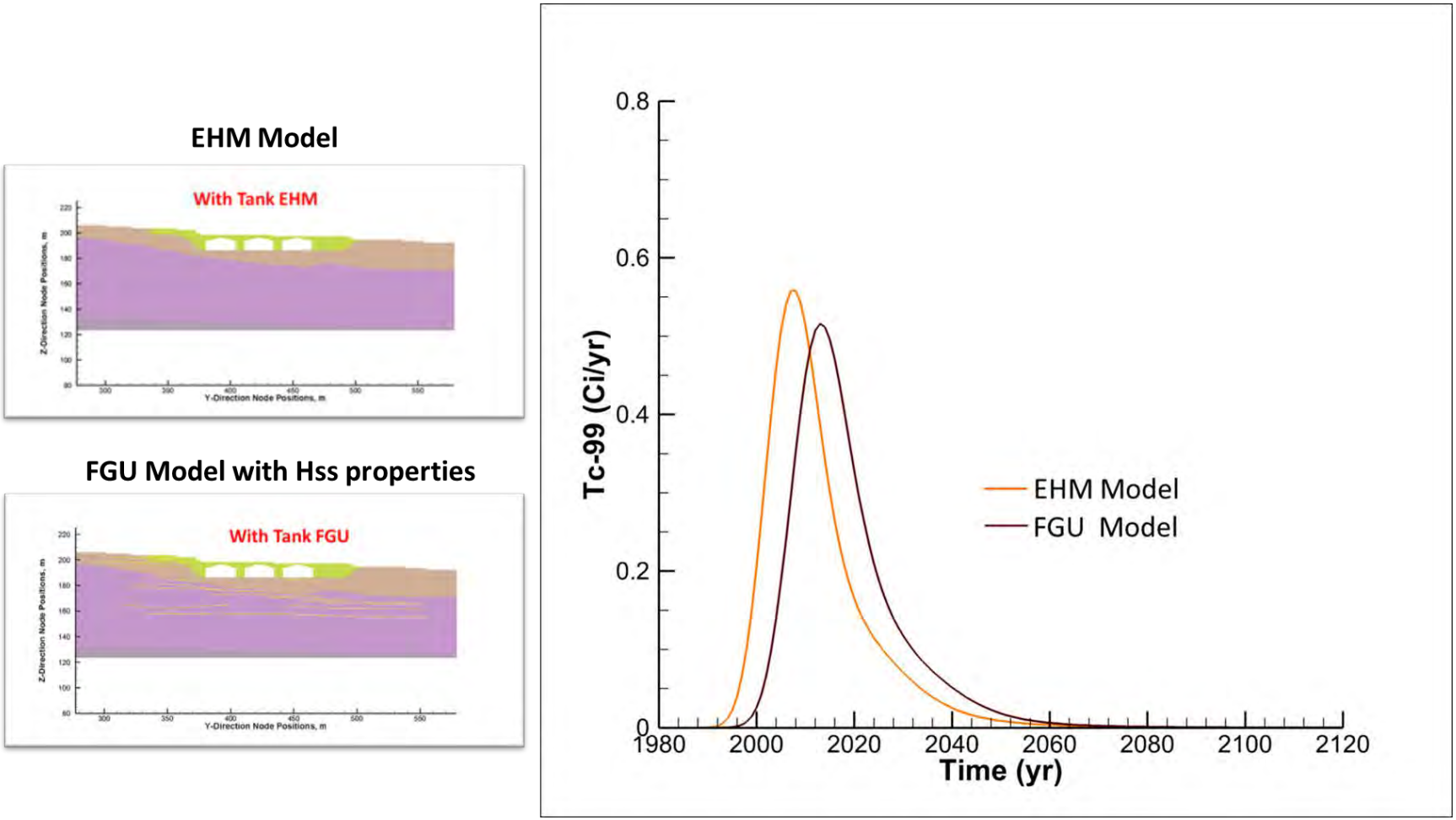

EHM = Equivalent Homogeneous Medium FGU = fine-grained units Hss = Hanford sandy silt (unit)

Figure B-9. Comparison of Simulated (Primary Case) Technetium-99 Plume in the Vadose Zone in Year 1968 (First Row) and Year 1981 (Second Row) for EHM Cross-Sectional Model and FGU Cross-Sectional Model with Hss Hydraulic Properties for Fine-Grained Units.

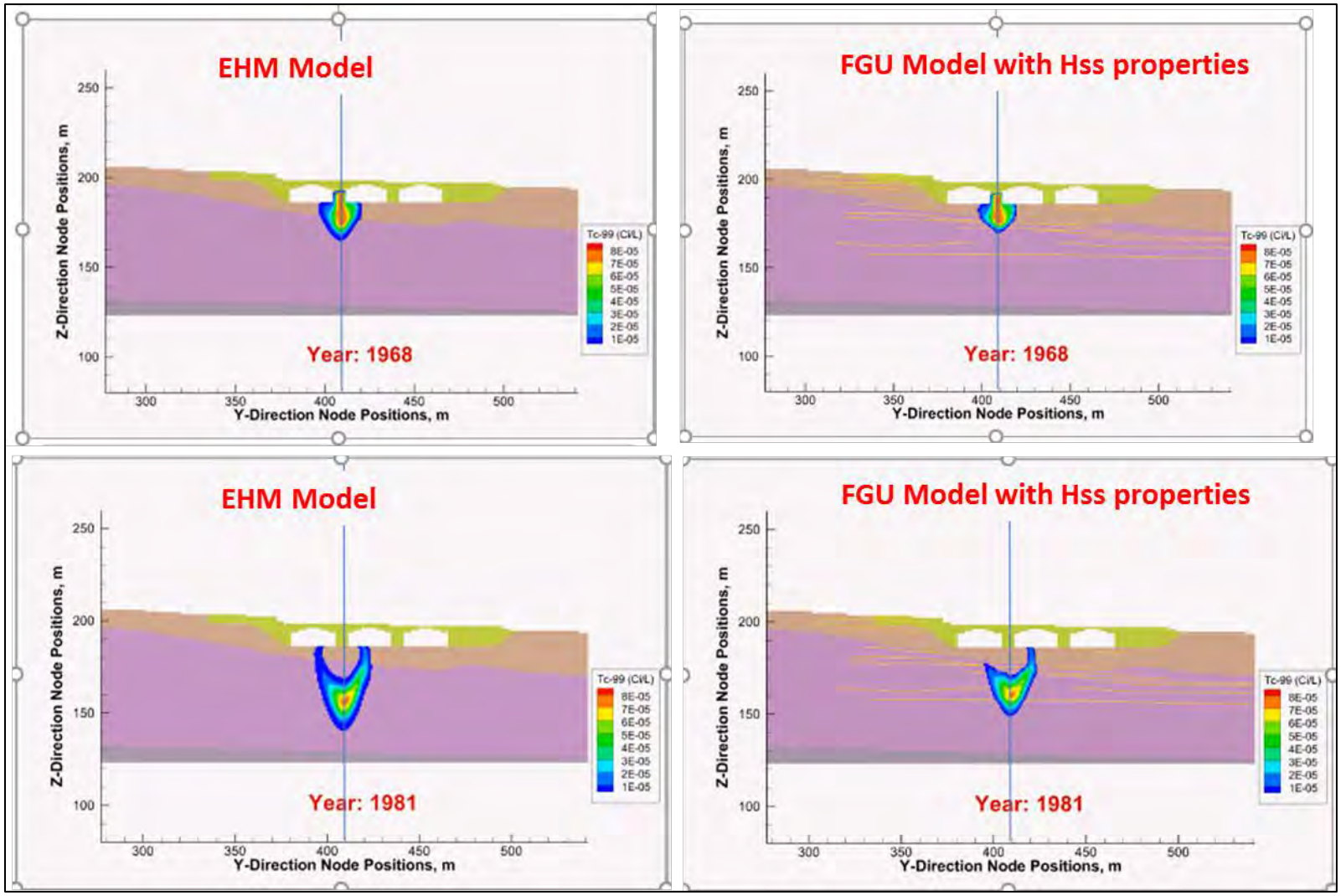

EHM = Equivalent Homogeneous Medium FGU = fine-grained units Hss = Hanford sandy silt (unit)

B5.1.1 Sensitivity Case 1: Effect of Changing Hydraulic Property of the Fine-Grained Units

Sensitivity Case 1 is a variation of the primary case where the hydraulic property for the fine-grained units is changed from Hss to sample 31A. As illustrated in Figure B-7, the moisture retention characteristics between Hss and sample 31a are similar; however, for the simulated matric potential, the unsaturated hydraulic conductivity is about one order of magnitude larger for sample 31A compared to that for Hss.

Figure B-10 compares the simulated mass flux at water table for ^{99}Tc. A lower peak flux and delayed arrival is seen for the sensitivity case compared to the primary case. Because of the higher unsaturated hydraulic conductivity of the fine-grained units for the sensitivity case, the ^{99}Tc plume displays more lateral spreading compared to the primary case as shown in Figure B-11. This effect also results in a double peak in mass flux due to spreading of mass—the first peak is due to mass that moves primarily vertically while the second peak is from arrival of mass that is delayed due to lateral spreading. Figure B-11 also shows that while the lateral spread of the plume is higher for the sensitivity case, the highest concentration zone has not moved appreciably.

Figure B-12 compares the water saturations (background color) and ^{99}Tc concentrations (foreground color) between the two cases at a given time. The water saturations are very similar between the two cases with near full saturation of the fine-grained units, but the lateral spreading of the ^{99}Tc plume is significantly different between the two cases resulting from differences in unsaturated hydraulic conductivity.

B5.1.2 Sensitivity Case 2: Effect of Leak Volume

Sensitivity Case 2 evaluates the effect of leak volume in hydraulically driving the contamination using the FGU cross-sectional model. This case simulates the release of 10 Ci of ^{99}Tc at tank 241-C-105 leak location but without the leak volume of 20,500 gal (77,600 L) (applied over the 5-year period).

Figure B-13 shows a comparison of the mass flux at the water table for the primary case (with leak volume in source) and the sensitivity case (without leak volume in source). The simulated mass flux for ^{99}Tc without the leak volume has a slightly higher peak flux due to less dilution at the source and the first arrival time at the water table is slightly later because of removal of the downward driving force caused by the leak volume.

B5.1.3 Sensitivity Case 3: Effect of Tank Structure

Compared to the primary case, Sensitivity Case 3 does not include the presence of the tank structure. The simulated release corresponds to a release into the backfill sediments without any flow diversion around the tanks. Other aspects of this sensitivity case are identical to those of the primary case. The refined-grid FGU model was used for this sensitivity case.

Figure B-10. Mass Flux Arriving at Water Table Showing the Effect of Hss and 31A Hydraulic Properties Used for the Fine-Grained Units.

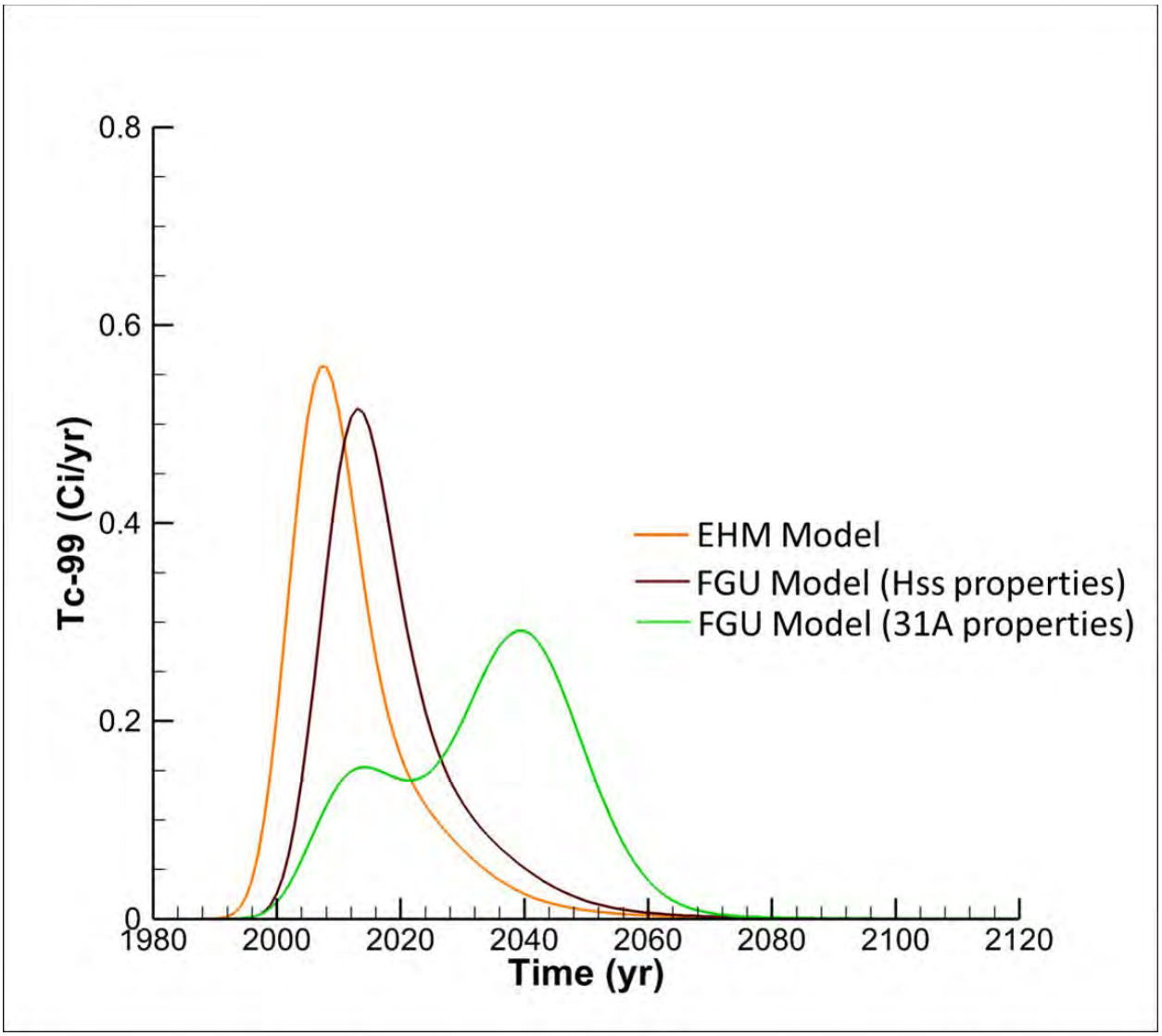

EHM = Equivalent Homogeneous Medium FGU = fine-grained units Hss = Hanford sandy silt (unit)

Figure B-11. Comparison of Simulated Technetium-99 Plume in the Vadose Zone in Year 1971 (First Row) and Year 2001 (Second Row) using FGU Cross-Sectional Model for the Primary Case (Hss Hydraulic Properties for Fine-Grained Units) and Sensitivity Case 1 (Sample 31A Hydraulic Properties for Fine-Grained Units).

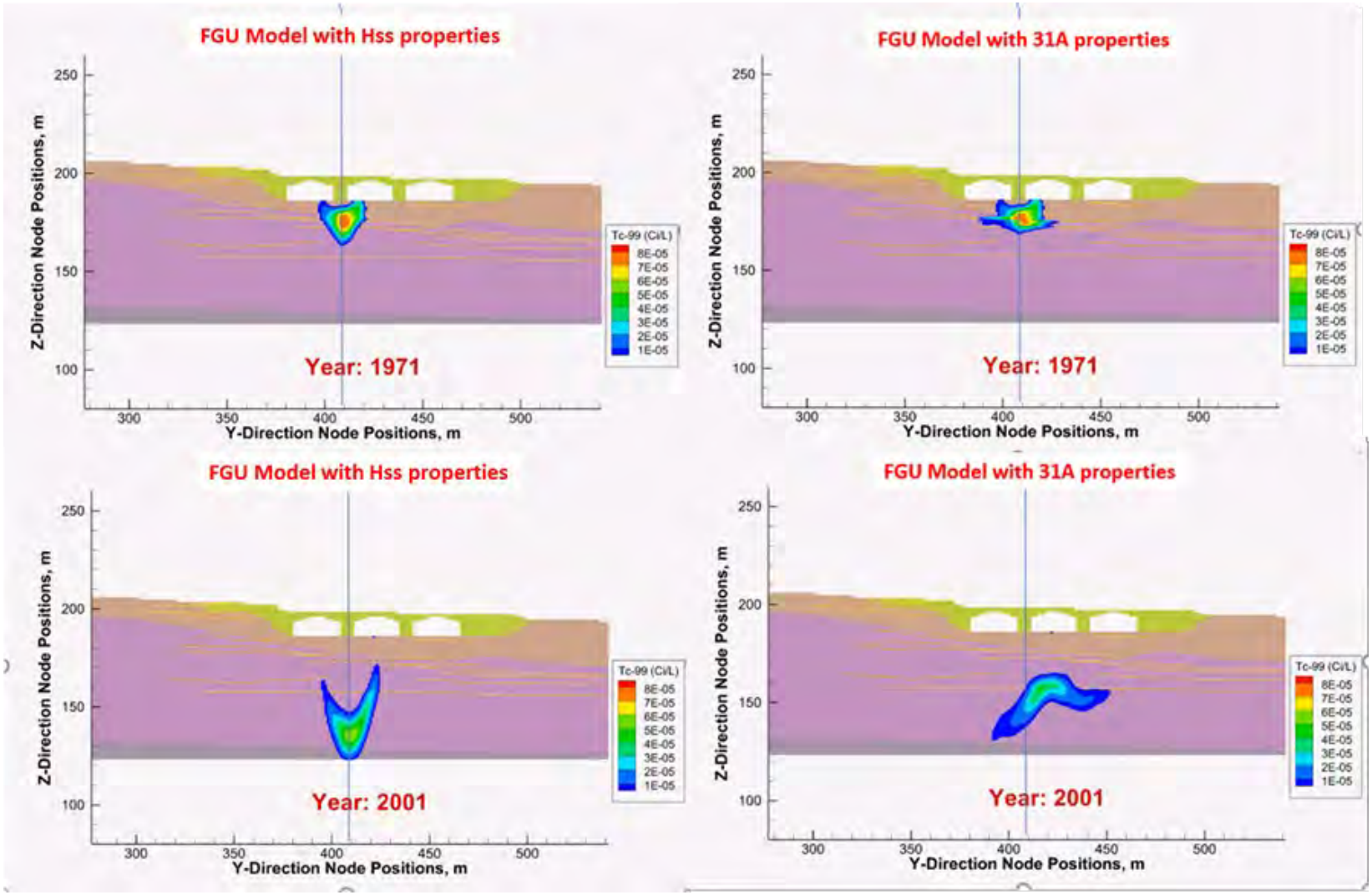

FGU = fine-grained units

Hss = Hanford sandy silt (unit)

Figure B-12. Comparison of Simulated Water Saturation (Background Color) and Technetium-99 Plume (Foreground Color) in Year 1971 using FGU Cross-Sectional Model for the Primary Case (Hss Hydraulic Properties for Fine-Grained Units) and Sensitivity Case 1 (Sample 31A Hydraulic Properties for Fine-Grained Units).

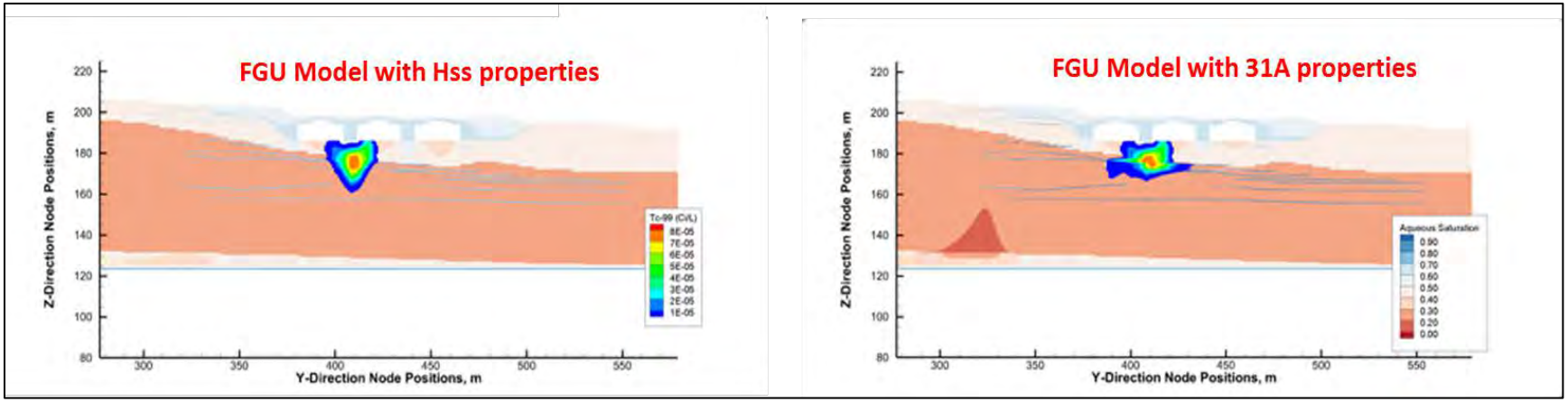

FGU = fine-grained units Hss = Hanford sandy silt (unit)

Figure B-13. Mass Flux Arriving at Water Table Showing the Effect of Leak Volume in Source.

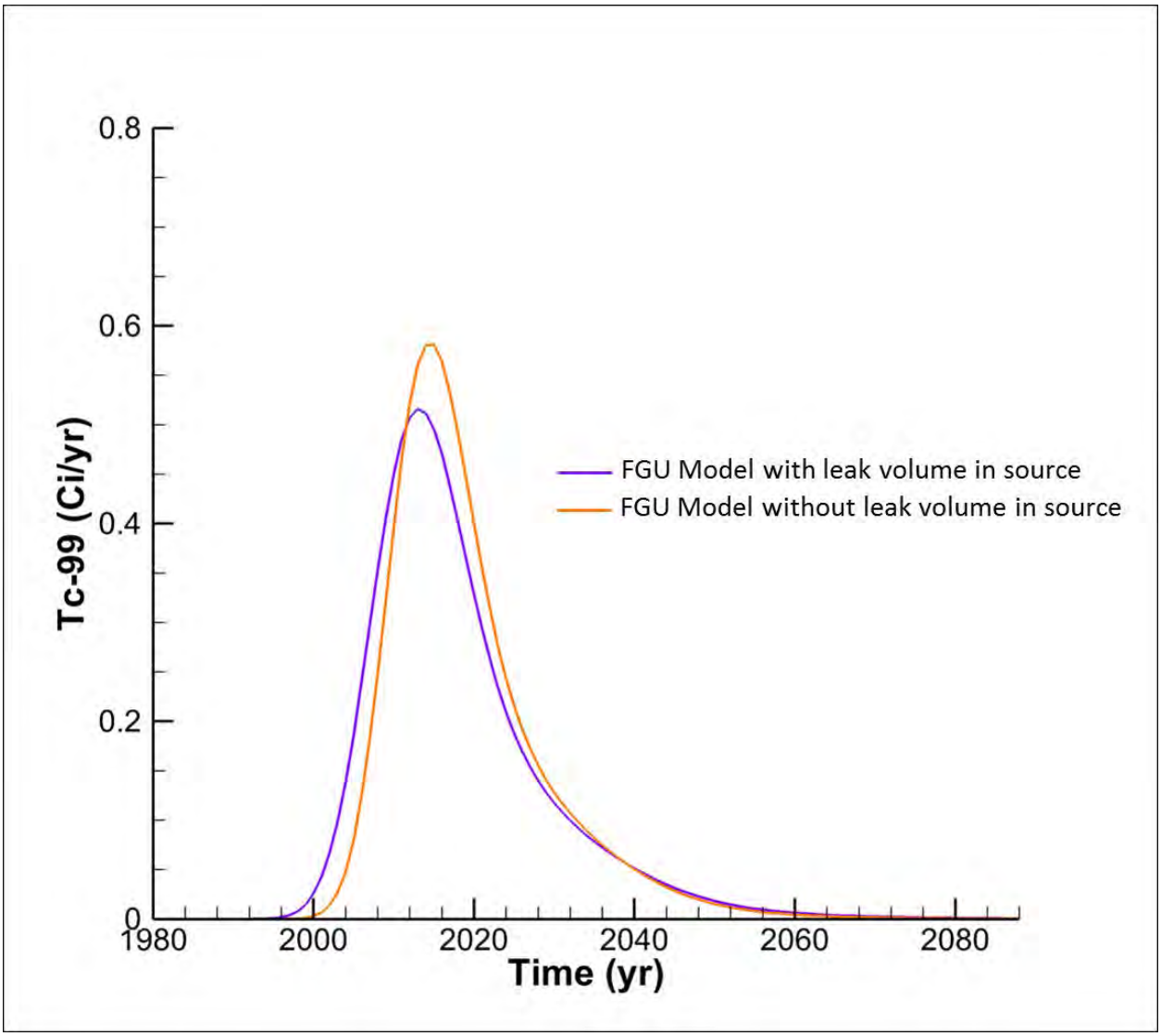

Note: Simulations Performed with the FGU Cross-Sectional Model with Hss Hydraulic Properties for Fine-Grained Units.

FGU = fine-grained units Hss = Hanford sandy silt (unit)

Figure B-14 shows a comparison of the mass flux at the water table with and without consideration of tank structures. The simulated mass flux for ^{99}Tc without the tank structure results in a higher peak with some delay compared to the primary case (with the tanks). This effect results from the tank structure that acts as an umbrella for the infiltrating water and focuses the infiltration in the backfill region between the tanks. This not only increases the water flux between the tanks but also dilutes the source concentration. Without the tank structure, the source is not diluted from increased flow but also there is less driving force that results in delayed breakthrough. The presence of tanks also dries out sediments directly below the tanks, which causes movement of both water and contaminants via capillarity into the drier sediments beneath the tank. This effect is not observed after removal of the tank structure.

Figure B-14. Mass Flux Arriving at Water Table Showing the Effect of Tank Structure.

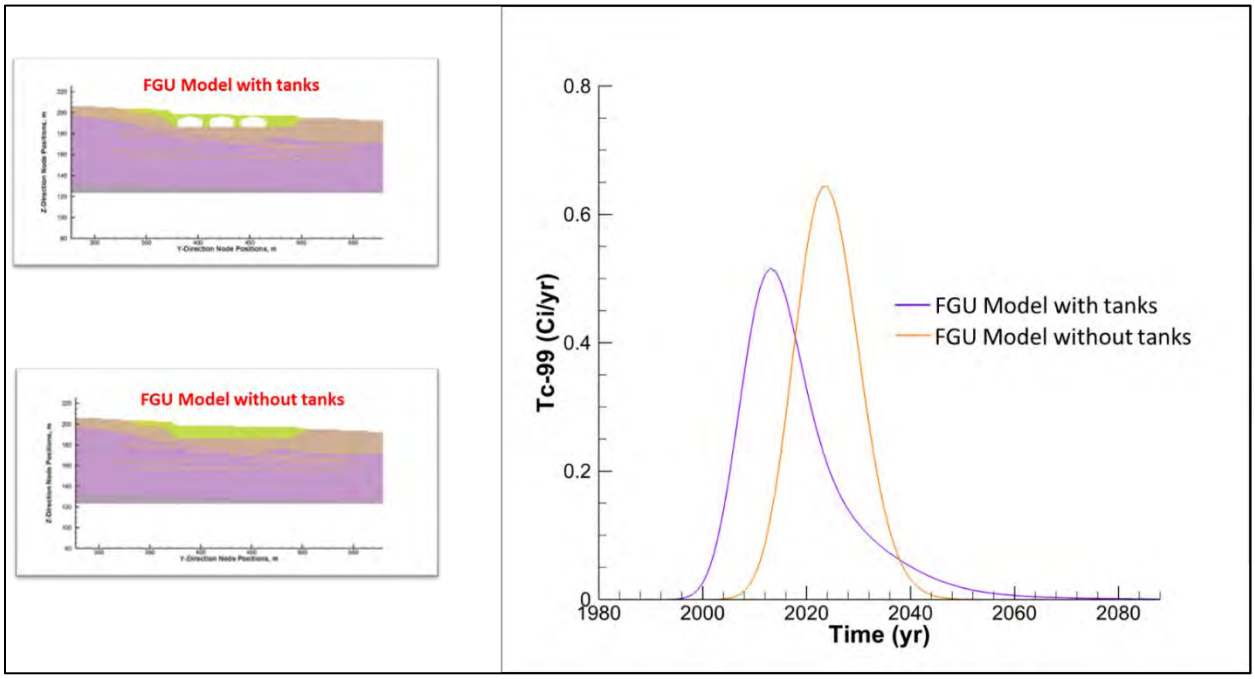

Note: Simulation Performed with the FGU Cross-Sectional Model with Hss Hydraulic Properties for Fine-Grained Units.

FGU = fine-grained units Hss = Hanford sandy silt (unit)

B6.0 SUMMARY AND CONCLUSIONS

General observations from the range of simulation cases examined in the evaluation of the effects of alternative vadose zone heterogeneities at WMA C are as follows.

- The movement of the center of mass of the simulated plumes was generally vertically downward below the source for all simulations, including those that incorporated the alternative interpretation of fine-grained units.

- All simulations that incorporated alternative interpretations of heterogeneity produced additional plume spreading over what was produced in simulation using the EHM model(s). The spreading resulted in a broadening of the fringes of the plume, resulting in a wider region of low concentration, but lower peak concentrations associated with the center of mass of the plume.

- Simulations that used the Hss (silty-sand) hydraulic properties, suggested by Ecology for the alternative interpretations of fine-grained units, generally produced similar spreading and slightly lower peak mass flux at the water table when compared to the EHM modeling results.

- Simulations that used the Hss (silty-sand) hydraulic properties, suggested by Ecology for the alternative interpretations of fine-grained units, generally produced less spreading and an earlier arrival of mass flux at the water table when compared to the use of hydraulic properties from sample 31A.

- The EHM representation of the vadose zone generally produced higher peak mass flux and an earlier occurrence of peak fluxes at the water table compared to all analyses incorporating additional alternative interpretations of heterogeneity.

Other secondary observations from the range of simulation cases examined at WMA C are as follows.

- The effect of leak volumes was evaluated with model simulations that used dry mass releases (i.e., removing liquid volume). These simulations resulted in slightly higher and slightly delayed arrival of peak mass flux at the water table. These effects are attributed to the reduced level of dilution and downward driving force of contaminants with the leak volume removed.

- The effect of the presence of tanks was evaluated with model simulations that removed the tanks from the backfill sediments. The presence of tanks resulted in a dilution of contaminant concentrations in the source release area due to flow focusing between the tanks. Removal of the tank structures leads to an increased mass flux but delayed arrival

at the water table. These effects are attributed to the reduced fluid flow in the contaminant source area.

B7.0 REFERENCES

CHPRC-02937, 2017, *Kingdom-Geology Software Management Plan*, Rev. 0, CH2M HILL Plateau Remediation Company, Richland, Washington.

EMDT-MO-0031. 2019, Environmental Modeling Data Transmittal of an unpublished report entitled, "WMA C Conceptual Model" sent to DOE by the Nez Perce Tribe by email on Wednesday, Nov. 5, 2014 at 2:31 pm PST.

PNNL-14702, 2016, *Vadose Zone Hydrogeology Data Package for Hanford Assessments*, Rev. 1, Pacific Northwest National Laboratory, Richland, Washington.

RPP-20621, 2004, *Far-Field Hydrology Data Package for the Integrated Disposal Facility Performance Assessment*, Rev. 0, CH2M HILL Hanford Group, Inc., Richland, Washington.

RPP-ENV-58782, 2016, *Performance Assessment of Waste Management Area C, Hanford Site, Washington*, Rev. 0, Washington River Protection Solutions, LLC, Richland, Washington.

RPP-RPT-61239, in process, *Multiple Lines of Evidence and Modeling Results for Heterogeneous Alternative Conceptual Models of the Subsurface at Waste Management Area C*, Rev. 0, Washington River Protection Solutions, LLC, Richland, Washington.

APPENDIX C

REVIEW COMMENT RECORD
RPP-RPT-59197, ANALYSIS OF PAST TANK WASTE LEAKS AND LOSSES IN THE VICINITY OF WASTE MANAGEMENT AREA C AT THE HANFORD SITE, SOUTHEAST WASHINGTON, REV. 1

This page intentionally left blank.

TABLE OF CONTENTS

C1.0 INTRODUCTION C-1

C2.0 REFERENCES C-47

LIST OF TABLES

Table C-1. Crosswalk of Report Organization Changes between Revision 1 and 2 of RPP-RPT-59197 Resulting from Ecology's Review of this Documentation. C-2
Table C-2. Review Comment Record From Washington State Department of Ecology from Review of RPP-RPT-59197, *Analysis of Past Leaks and Losses at Waste Management Area C at the Hanford Site, Washington*, Rev. 1..... C-5

LIST OF TERMS

3-D	three-dimensional
ACM	alternative conceptual model
bgs	below ground surface
BRA	Baseline Risk Assessment
C Farm	WMA C Tank Farm
CalEPA	California Environmental Protection Agency
CERCLA	*Comprehensive Environmental Response, Compensation, and Liability Act of 1980*
CFR	Code of Federal Regulations
CMS	corrective measures study
CN	cyanide
COC	chemical of concern
COPC	constituent of potential concern
CPGWM	Central Plateau Groundwater Model
CUL	cleanup level
DOE	U.S. Department of Energy
DOE-RL	U.S. Department of Energy, Richland Operations Office
DQO	data quality objective
DW	Dangerous Waste
DWS	drinking water standard
Ecology	State of Washington Department of Ecology
EDTA	ethylenediaminetetraacetic acid
EHM	equivalent homogeneous media

EIS	Environmental Impact Statement
EPA	U.S. Environmental Protection Agency
FLTF	Field Lysimeter Test Facility
FS	Feasibility Study
gpm	gallons per minute
GW	groundwater
GWP	groundwater protection
H1 unit	Hanford formation – upper gravelly sequence
H2 unit	Hanford formation – sand sequence
H3 /CC_n/RF	undifferentiated Hanford formation (H3), Cold Creek unit and Ringold Formation
HDW	Hanford Defined Waste (Model)
HFFACO	*Hanford Federal Facility Agreement and Consent Order*
HI	hazard index
HSU	hydrostratigraphic unit
IAMIT	Interagency Management Integration Team
ID	identification (no.)
IDF	Integrated Disposal Facility
INTERA	INTERA, Inc.
IPA	Appendix I Performance Assessment
MCL	maximum contaminant level
MTCA	Model Toxics Control Act
NRC	U.S. Nuclear Regulatory Commission
ORP	(U.S. Department of Energy,) Office of River Protection

OU	operable unit
P2R	Plateau to River (model)
PA	performance assessment
PNNL	Pacific Northwest National Laboratory
POC	point of compliance
PoCal	point of calculation (also referred to as “PoC”)
PUREX	Plutonium Uranium Extraction (facility)
RCA	RCRA Closure Analysis
RCRA	*Resource Conservation and Recovery Act of 1976*
RETC	RETention Curve (code)
RFI	RCRA facility investigation
ROD	Record of Decision
SAP	Sampling Analysis Plan
SST	single-shell tank
STOMP	Subsurface Transport Over Multiple Phases (computer code)
TBP	tributyl phosphate
TC&WM EIS	Tank Closure and Waste Management Environmental Impact Statement
TEDF	Treated Effluent Disposal Facility
TPA	Tri-Party Agreement (Hanford Federal Facility Agreement and Consent Order)
TSD	treatment, storage or disposal
TWINS	Tank Waste Information Network System
UPR	unplanned release
WAC	Washington Administrative Code

WIDS	Waste Information Data System
WFM	water flux meter
WMA	Waste Management Area
WRPS	Washington River Protection Solutions, LLC

C1.0 INTRODUCTION

This appendix provides a review comment record for comments received from Washington State Department Ecology during their review of RPP-RPT-59197, Rev. 1, Analysis of Past Tank Waste Leaks and Losses in the Vicinity of Waste Management Area C at the Hanford Site, Southeast Washington.

This report (i.e., RPP-RPT-59197) along with other related HFFACO Appendix I analyses and documentation were provided to Ecology in October of 2016. To facilitate Ecology's review, DOE provided a briefing to Ecology staff on an overview of the HFFACO Appendix I analyses and documentation and a second briefing of this specific analysis and document on November 22, 2016.

On July 17, 2017, Ecology provided DOE comments on all of the HFFACO Appendix I analyses and documentation to DOE (Letter 17-NWP-085, "Re: Department of Ecology's (Ecology) Review and Comments of Appendix 1 Performance Assessment for Waste Management Area C (WMA C) Documents"). In October of 2017, ORP entered into a comment resolution process with Ecology staff to address on all of the analyses and related documents. This process involved well over 100 individual meetings with Ecology staff that continued until August of 2020. ORP provided a response to each comment provided by Ecology and was able to reach agreement of a large majority of the comments. Although secondary documents are normally not subject to dispute resolution, ORP worked closely and in good faith with Ecology to reach agreements on some key technical issues that were resolved with documented IAMIT determinations.

The resolution of Ecology's comments resulted in some changes to RPP-RPT-59197, Rev. 0 that are summarized in the following Table C-1, a crosswalk showing report organization changes between RPP-RPT-59197, Rev. 1 and Rev. 2. The changes included the addition of Section 5.0 and four new Appendices **highlighted in bold below** in Table C-1.

Table C-1. Crosswalk of Report Organization Changes between Revision 1 and 2 of RPP-RPT-59197 Resulting from Ecology's Review of this Documentation.

RPP-RPT-59197, Rev. 1		**RPP-RPT-59197, Rev. 2**	
Section or Appendix	**Titles**	**Section or Appendix**	**Titles**
1	INTRODUCTION	1	INTRODUCTION
2	BACKGROUND	2	BACKGROUND
3	FEATURES FOR ANALYSIS	3	FEATURES FOR ANALYSIS
4	SCOPING ANALYSES OF PAST WASTE RELEASES	4	SCOPING ANALYSES OF PAST WASTE RELEASES
5	EVALUATION OF THE EFFECTS OF TRANSIENT WATER TABLE	**5**	**EVALUATIONS OF THE USE OF ALTERNATIVE CONCEPTUAL MODELS TO EVALAUTE THE EFFECTS OF VADOSE HETEROGENEITY ON PLUME TRANSPORT**
6	FUTURE IMPACTS OF PAST WASTE LEAKS AND RELEASES	6	EVALUATION OF THE EFFECTS OF TRANSIENT WATER TABLE
7	OTHER SOURCES OF CONTAMINATION AT WASTE MANAGEMENT AREA C	7	FUTURE IMPACTS OF PAST WASTE LEAKS AND RELEASES
8	SUMMARY AND OBSERVATIONS	8	OTHER SOURCES OF CONTAMINATION AT WASTE MANAGEMENT AREA C
9	REFERENCES	9	SUMMARY AND OBSERVATIONS
		10	REFERENCES
		Appendix A	**ESTIMATION OF POTENTIAL IMPACTS FROM PAST RELEASES OF CYANIDE AT WASTE MANAGEMENT AREA C**
		Appendix B	**EVALUATION OF IMPACTS OF VADOSE ZONE HETEROGENEITIES ON CONTAMINANT TRANSPORT AT WMA C USING WASHINGTON STATE DEPARTMENT OF ECOLOGY'S ADVOCACY MODEL**
		Appendix C	**REVIEW COMMENT RECORD - RPP-RPT-59197, *ANALYSIS OF PAST LEAKS AND***

			***LOSSES AT WASTE MANAGEMENT AREA C AT THE HANFORD SITE, WASHINGTON*, REV. 1**
		Appendix D	**TOC-PRES-19-0068-VA, RESULTS OF ADDITIONAL SCOPING CASE RELATED TO PAST LEAKS ANALYSIS PROPOSED BY ECOLOGY, REVISION 0**

This page was intentionally left blank.

Table C-2. Review Comment Record From Washington State Department of Ecology from Review of RPP-RPT-59197, *Analysis of Past Leaks and Losses at Waste Management Area C at the Hanford Site, Washington*, Rev. 1.

TOC - REVIEW COMMENT RECORD (RCR)	1. Date: 08/26/2020	2. Review No.:
	3. Project No.:	Page 1 of 1

5. Document Number(s)/Title(s):	6. Program/Project/Building Number:	7. Reviewer:	8. Organization/Group:	9. Location/Phone:
RPP-ENV-59197, Rev. 1 - Analysis of Impacts from Past Leaks and Losses at Waste Management C at the Hanford Site, Washington	Waste Management Area C HFFACO Appendix I Performance Assessment	Lead Reviewer - Elizabeth Rochette	Washington State Department of Ecology	Richland, WA (509-372-7922

10. Agreement with Indicated Comment Disposition(s):

Reviewer/Point of Contact: Author/Originator:

Print First and Last Name *Print First and Last Name*

Signature *Date* *Signature* *Date*

11. CLOSED:

Reviewer/Point of Contact: Author/Originator:

Print First and Last Name *Print First and Last Name*

Signature *Date* *Signature* *Date*

17. Comment Submittal Approval::

Organization Manager *(Optional)*:

Print First and Last Name *Signature* *Date*

12. Item	13a. Comments	13b. Basis/Category	13c. Recommendation	14. Reviewer Concurrence		15. Disposition *(provide justification if **NOT** accepted)*	16. Status
				Yes	No		
				○	○		

A-6005-747 (REV 4)

Comment No.	Location	Comment	Basis	Recommendation	Final Disposition
PLG1	General	The Title: Title of the Document: From the content of the document, it is more appropriate to change the title to “impact of past leaks in soil and groundwater in the C Tank farm Area”. It is basically the analysis of impacts on soil and groundwater.	Analysis of past leaks usually entails the rate of leak, type of leak, nature of leaks, inventory analysis. This document is not about all of these. It is mainly on the impact of the leaks.	Revise the title.	Proposed Title Change, "Analysis of Impacts of Past Tank Waste Leaks and Losses in the Vicinity of Waste Management Area C at the Hanford Site, Southeast Washington"
PLG2	General	Scoping of the document: The scoping of the document needs to expand to better understand the uncertainties and various expected scenarios using sensitivity analysis or similar approaches (e.g. multiple realizations using stochastic approaches, etc.).	For example, for the past few years, some of the groundwater data show sharp differences in trends compared to past decades. From the analysis of all the well data and the historical information/behavior, the upward trend observed may go down as assumed in the conceptual model. A few wells are still showing upward trends in concentrations. There are a number of uncertainties and unknowns (e.g. inventory, release rate, lack of data directly under the facility, geological heterogeneities, etc.). One of the conceptual assumptions is that the current trend will continue at least for some time. The concept of dilution and dispersion used for the future decline of concentration of Tc-99 does not adequately fit the basic conceptual model for a number of reasons (e.g. almost flat gradient, the current trend of the decrease of water level/table is significantly lower than the past, etc.) and the associated uncertainties.	In order to make the assessment complete, provide a discussion of these variances and inconsistencies these aspects need to be discussed adequately.	See responses to comment PLG3 and PLG4
PLG3	General	Inventory estimate: Although the inventory of Tc-99 varies from 0.8 ci to ~10 Ci and the field observation was the principal driver to use the inventory of ~ 10 Ci, it is to be noted that this observation assumed that the entire 10 Ci will be depleted from the vadose zone in a few years from now. This assumption is one of the conceptual models. It is unusual to expect the entire inventory of Tc-99 will simply discharge from the vadose zone as a slug within a short period of time.		In order to have a better bounding analysis, one option is to have multiple realization(s) covering these aspects. Another scenario should be to extrapolate the current trend at least for a decade (that seems to be the maximum increase trend so far) and not to assume sudden decrease after that (following the same trend of increase or use some statistical analysis, etc.) and calculate the inventory based on that.	On Wednesday, March 28, WRPS staff met with the commenter and other Ecology staff and came up a proposal from Ecology for another scoping case that help address this comment. The requested case was somewhat similar to Scoping Case 1a. [Note: Case 1a models the release of current estimates of leak Tc-99 inventories and volumes for all sources defined in Table 2.3 and includes an estimate of the upper bound inventory of about 10 Ci (i.e. 9.8 Ci) and volume 77,600 L (20,500 gals) developed for tank 241-C-105 (C-105). In the case, the leak volume and inventory for C-105 is released uniformly at the tank into the vadose zone over a period of 5 years starting in 1963 through the end of 1967.] In the additional requested scoping case, Case 1a would be modified such that the C-105 tank release will continue for additional 5 years. In doing so, the resulting Tc-99 inventory released to the vadose zone would be about 20 Ci (i.e. 19.6 Ci) and 155,200 L (41,000 gals) and the release time would be 10 years (i.e. 1963 through 1972). A description and results of this case has been added to the current discussion of scoping cases in Sections 4.1 and 4.5 as needed. We have also add text on p. 3-2 that will discuss why rigorous model calibration of the WMA C is not very feasible given the limited knowledge about the tank farm history and range of uncertainties associated with historical observations and information on the vadose zone and groundwater impacts.

Comment No.	Location	Comment	Basis	Recommendation	Final Disposition
PLG4	General	Alternative conceptual model using concentration profile calibration and other field data: recent field observations of groundwater were used to estimate Tc-99 inventories and modeling assumptions.	USDOE has used the recent concentration data (~2013 onward). We have data much earlier than 2013.	An alternative scenario of the vadose zone needs to be developed and analyzed based on the calibration of concentration profiles and other field evidence. Use the entire profile data available and see its result (e.g. inventory and expected future trend)	On pp 3-1 and 3-2, an overview of uncertainties associated with past leaks and releases at WMA C are delineated that point to the difficulties in performing any historical analysis of past leaks and releases. These include uncertainties in 1) the timing, inventory, and volumes of leaks; 2) the past actions taken to mitigate the surface manifestations of past leaks and release; 3) the interpretation of impacts from groundwater monitoring and characterization data on current contamination levels that could be attributable to specific past leaks and releases at WMA C; 4) the hydrogeological representation of the stratigraphy below WMA C; 5) the effective values of parameters used in modeling groundwater flow and contaminant transport; and 6) the detailed understanding of evolution of the groundwater system at WMA over the past several decades during the time when the leaks and releases occurred. Given the range and magnitude of uncertainties presented above, it is ORP's position that calibration and use of history matching of modeling results to past observations at WMA C is not a feasible option. In lieu of model calibration, the strategy for this analysis of leaks and releases at WMA C is to define and analyze a suite of scoping cases representing a range of alternative conceptual models with different alternative conceptual modeling assumptions to identify general ACMs that produce modeling results that are consistent with general observations of historical impacts in groundwater.
PLG5	General	Small scale heterogeneity impact: Current scope vs. future PNNL study: The aspects of small scale heterogeneities and their impacts are not clear. It was stated that another analysis by PNNL is on the way to address much of the small scale heterogeneity issues.		This document should be clear about what has been done so far and what else is expected in future studies/ documents.	The work that has been done by PNNL on alternative conceptual models of heterogeneity with some intercomparion of selected modeling simulation results taken from the PA effort has been documented in PNNL-24740. A more detailed presentation of the intercomparison for modeling results between PNNL and PA related models was provided in the webinar conducted on March 29, 2017. Updates to the IPA documentation provide more information on these additional alternative models and modeling results.
PLG6	General	Conceptual model and the uncertainty analysis: Based on the above comments, alternative conceptual model(s) to address uncertainty/concepts/assumptions as outlined above need to be analyzed in the form of multiple realizations/sensitivity analysis.		See comment.	See dispositions associated with comments PLG-3 and PL-G4 dated 04/03/2018.
PLG7	General	The only artificial recharge mentioned is that applied to “wash down” contamination to make the site safe for workers, and B Pond. Other artificial recharge sources (e.g., testing of fire hydrants, hydro-excavating, dust control, chronically leaking pipes and pipe/pipeline failures) appear to be ignored. Please indicate how these other sources of artificial recharge are addressed in attempting to match modeling runs with reality.	From RPP-RPT-44042: "Simulations investigating water line leaks demonstrated the highest peak concentrations occurred for all cases. The leak at 1 gpm over 20 years case had a more significant impact on mobilizing the contaminants than the case of a 200,000-gal leak over 5 days. This effect is due to the larger volume of water (525,960 gal) released in the leak at 1 gpm over 20 years case. A significant effect is on the mobilization of relatively immobile U-238. The peak U-238 concentrations in the leak at 1 gpm over 20 years case were not only the highest and earliest of all simulated cases, but they were also at least an order of magnitude higher than the case that examined the effect of lowering the value of the partitioning coefficient from 0.6 to 0.1 mL/g."	If artificial recharge is not addressed in this manner, state when it will be.	During the review of this document by Ecology, it was suggested that two water line modeling leak cases (Case 3 and 4) that were evaluated in RPP-23752 at the WMA T and WMA TX-TY areas be considered as a part of this scoping analysis. The two waterline leak cases that were discussed in RPP-RPT-44042 involved introducing 1) 1 gpm over 20 years (Case 3) and 2) 200,000 gallons over 5 days (Case 4). These particular cases were compared to base case (Case 1) that involved no water line leak. Previous simulations of these cases produced results inconsistent with the moisture content or monitoring well data that were available at the time they were evaluated. In the former case, the results indicate that approximately one-third to one-half of the vadose zone below the leak area would be at least 90% saturated after 20 years (Figure E-9 in RPP-23752), and in the latter case, the results indicate that a substantial volume of soil extending approximately 10 meters below the base of the tanks would be nearly saturated almost immediately after the leak (Figure E-11 in RPP-23752). A 1 gpm leak amounts to approximately 10,520,000 gallons after 20 years, and a leak of that magnitude does not appear to be consistent with any of the moisture content data that have been collected at the tank farm. The moisture content data are also not consistent with the extent of saturation that a sudden release of 200,000 gallons would cause, as indicated in Figure E-11 in RPP-23752. The results of the 20-year 1 gpm leak (Case 3) indicate that the peak concentrations of Tc-99 arrives between 13 and 21 years for a T-farm cross section and 23 to 31 years for a TX-farm cross-section sooner than if no leak occurs (Case 1), depending on the proximity of the leak to the contamination in the vadose zone. The peak concentrations of the conservative solutes (i.e. Tc-99, NO3, and Cr) increased 284 to 537% for the T cross-section and 94 to 679% for the TX cross-section. Due to the leaked water, the uranium-238 inventory beneath the leak position was flushed into the groundwater. The results of the sudden 200,000 gallon leak (i.e. Case 4) are not substantially different than the base case (i.e. Case 1) results: peak concentrations arrive about 0 to 5 years sooner, and peak concentration values of the conservative solutes (i.e., Tc-99, NO3, and Cr) were reduced 6.7 to 15.7% for the T-farm cross-section but increased 3.9 to 32.7% for the TX cross-section, depending on the proximity of the leak to the contamination in the vadose zone. In spite of the large

Comment No.	Location	Comment	Basis	Recommendation	Final Disposition
					leak volume, very little uranium-238 inventory was flushed into the groundwater. Primarily because of the general inconsistencies of modeled results for these leak cases, performed as a part of RPP-23752, with field measurements of moisture conditions in the vadose available at the WMA T and WMA TX-TY areas, the decision was made not to consider these specific cases in the scoping analysis done to support this leak analysis.
PLG8	General	The term “groundwater flux” is used throughout this document, but not clearly defined as to whether you mean movement of contaminants from the vadose zone to groundwater or something else.		Please clarify throughout these four volumes.	In three of the four IPA documents (RPP-RPT-59197, RPP-ENV-58806, and RPP-ENV-58782), the term "groundwater flux" is only used when discussing modeling cases that evaluated the impact of changing the amount of groundwater flow in the aquifer system beneath the WMA C on predicted concentrations in the aquifer downgradient of the facility. This "groundwater flux" term is not associated with vadose zone but rather with the aquifer beneath WMA C and is calculated on the basis of the hydraulic properties assigned to the aquifer system, and the assumed hydraulic gradient beneath the site projected to exist in the future. This term is not used in RPP-RPT-58329.
PLG9	General	Years of operation took place without groundwater monitoring that might have detected a release.	A compliant groundwater monitoring network was not established until 1989 long after C Farm tanks stopped receiving waste. The first well constructed at C Farm was E27-7 which was built in 1982.	Please address.	Although it is possible that Tc-99 from the past leaks arrived in groundwater prior to the installation of well 299-E27-7 in 1982 and the RCRA groundwater monitoring well network in 1989, the concentration trends of Tc-99 currently observed in those monitoring wells appear to be consistent with the available information regarding the timing, size, and inventory of the leaks. This text has been added as introductory material in discussion of the main body of the report in Section 2.3.3.3, Groundwater Contamination.
PLES1	Exec Summary, p. ES-1, lines 44-45	The document states "This part of the analysis will represent an input to additional analyses for the Appendix I PA." This is vague and does not give the reader an idea about how this document fits in with the other documents, and why this analysis was separated from the others. It is also not clear what relationship this document has with the WMA C RFI.	The document does not have a regulatory context or an obvious purpose.	Provide the context of this document and its relationship with others. The ES would be the best place for this but it could also be included in Section 1. The applicable portions of WAC 173-303 that are addressed by this document, in a general way, should be cited.	Updated text is added to Section 1,2,1 , "First, the conceptual model developed for the PA of residual contamination has been implemented to evaluate how well it explains observed field data for the time of arrival of contaminants to groundwater, concentrations of contaminants in groundwater, and the distribution of contaminants in the vadose zone. Second, the combination of the field data and model have been used to determine bounds on input assumptions that are consistent with groundwater and soil monitoring data from past leaks. In particular, a range of models has been used to evaluate the uncertainties in the inventory and volumes of past leaks, to better constrain estimates of the existing contamination. Third, the constrained model has been used to project future impacts from selected radiological and hazardous chemicals and dangerous waste contaminants associated with past leaks and losses at WMA C. This part of the analysis will represent an input to additional analyses for the Appendix I PA. This analysis of future impacts of past leaks is intended to provide supporting information that could be relevant to the selection and specific implementation of groundwater mitigation measures being undertaken as a part of the CERCLA RI/FS effort in 200-BP-5-OU." Updated text added in PREFACE “This document is volume one of four volumes being written to support the performance assessment (PA) required under Section 2.5 of the Hanford Federal Facility Agreement and Consent Order (Ecology et al. 1989, hereinafter referred to as HFFACO) Appendix I for closure of Hanford Tank Farms. The first single-shell tank (SST) farm being closed is Waste Management Area (WMA) C. This particular volume contains an evaluation of potential future impacts from selected radiological and hazardous chemicals and dangerous waste contaminants associated with past leaks and losses at WMA C. This specific analysis of past leaks is intended to provide supporting information that could be relevant to the selection and specific implementation of groundwater mitigation measures being undertaken as a part of the CERCLA RI/FS effort in 200-BP-5-OU.
PLES1, continued					PLES 1 response continued. As a follow on to the groundwater protection evaluation, site-specific model analyses were performed to gain additional understanding and insight into the potential spatial and temporal impacts to groundwater that would be realized from selected non-radiological and radiological constituents associated with past waste leaks and losses from WMA C. These analyses are intended to provide information that could be relevant to the selection and specific implementation of potential groundwater mitigation measures as a part of the CERCLA RI/FS effort in 200-BP-5-OU. As stated in Ecology Letter 18-NWP-088 dated June 11, 2018: • Ecology approves the RFI and has determined there is a need to capture and remove contaminants of concern from the groundwater in WMA C.

Comment No.	Location	Comment	Basis	Recommendation	Final Disposition
					• Ecology acknowledges that groundwater remediation will be managed through the 200-BP-5 and 200-PO-1 *Comprehensive Environmental Response, Compensation, and Liability Act* (CERCLA) Groundwater Operable Units. The proposed Feasibility Study for Interim Action will cite capture and removal of Tc-99 as the preferred alternative, with Tc-99 cited as a primary contaminant of concern for WMA C. A number of co-contaminants have also been identified for WMA C, including but not limited to cyanide, iodine-129, nitrate, and sulfate. Ecology expects that the co-contaminants identified in the Feasibility Study for Interim Action will be addressed incidentally with the CERCLA remediation. As a part of these analyses, the groundwater concentrations estimated with site-specific modeling down gradient of WMA C were compared against Federal maximum contaminant levels or MTCA groundwater cleanup levels to identify constituents that have or could impact groundwater in the future. For contaminants that impacted the groundwater, the evaluation also identified the year of which the peak concentrations would potentially occur and would examine how long concentrations that exceed Federal maximum contaminant levels or MTCA groundwater cleanup levels might persist. These latter evaluations associated with past waste leaks and losses are presented in this document (RPP-RPT-59197). This information is needed to support the overall closure of WMA C single shell tanks per Washington Administrative Code (WAC) 173-303-610, "Closure and Post-Closure."
PLES2	Exec Summary, p. ES-4, lines 32-37	There was no site specific groundwater monitoring conducted during the operating years of this facility. The first well was not constructed until 1982 (E27-7) and a groundwater monitoring network was not in place until 1989. Furthermore, Tc-99 was not specifically analyzed as an isotope at Hanford until the mid-1980s.		Please explain how you used Tc-99 groundwater data to test modeling results.	Revision added to Executive Summary: Model results have been compared to Tc-99 concentrations observed in groundwater monitoring wells around WMA C because Tc-99 is a key risk driver, and the contamination levels observed there are considered to be distinctly the result of WMA C past leaks. The Tc-99 concentration data collected from groundwater monitoring wells have been used to evaluate and constrain the model inputs and assumptions that produce results that are consistent with the arrival times and concentration levels of Tc-99 observed historically in the vicinity of WMA C. Although it is possible that Tc-99 from the past leaks arrived in groundwater prior to the installation of well 299-E27-7 in 1982 and the RCRA groundwater monitoring well network in 1989, the concentration trends of Tc-99 currently observed in those monitoring wells appear to be consistent with the available information regarding the timing, size, and inventory of the leaks. Revision added to Section 1.2.1 Purpose: First, the conceptual model developed for the performance assessment of residual contamination has been implemented to evaluate how well it explains observed field data for the time of arrival of contaminants to groundwater, concentrations of contaminants in groundwater, and the distribution of contaminants in the vadose zone. Although it is possible that contamination from the past leaks arrived in groundwater prior to the installation of well 299-E27-7 in 1982 and the RCRA groundwater monitoring well network in 1989, the concentration trends of Tc-99 currently observed in those monitoring wells appear to be consistent with the available information regarding the timing, size, and inventory of the leaks. Second, the combination of the field data and model have been used to determine bounds on input assumptions that are consistent with groundwater and soil monitoring data from past leaks. Proposed revision to Section 3.1 OVERVIEW OF ANALYSIS: • Uncertainties exist in interpreting the groundwater monitoring and vadose zone characterization data on current contamination levels resulting from the past leaks since data represent specific locations, and little groundwater monitoring occurred around WMA C prior to the installation of the RCRA groundwater monitoring well network in 1989. The model has been initially compared to Tc-99 concentrations in groundwater, since because Tc-99 is a key risk driver and the contamination levels observed in groundwater monitoring wells are considered to be distinctly the result of WMA C past leaks. The Tc-99 concentration data observed in groundwater monitoring wells have been used to evaluate the input conditions that are consistent with the arrival times and concentration levels of Tc-99 observed historically in the vicinity of WMA C. The resulting constrained model is then also compared with other contaminant data as appropriate. Although it is possible that Tc-99 from the past leaks arrived in groundwater prior to the installation of well

Comment No.	Location	Comment	Basis	Recommendation	Final Disposition
					299-E27-7 in 1982 and the RCRA groundwater monitoring well network in 1989, the concentration trends of Tc-99 currently observed in those monitoring wells appear to be consistent with the available information regarding the timing, size, and inventory of the leaks. For example, assuming that a major leak occurred in 1965, the distance from the release to groundwater was approximately ~70 m, and recharge and moisture content averaged 100 mm/yr and 0.05, respectively, then the travel time of the peak would be expected to be ~70 m / (0.1 m/yr / 0.05) = ~35 years. Year 1965 + ~35 years = ~Year 2000, which coincides rather well with the concentration trend peak at 299-E27-7, which is the earliest a peak is observed in any of the WMA C monitoring wells.
PLES3	Exec Summary, p. ES-4, lines 32-37	Not all groundwater monitoring wells in the WMA C network are screened at the water table. Furthermore, screen lengths vary, so a full and accurate vertical contaminant profile is not known in detail. How did these facts influence your analyses?		Please elaborate.	This analysis did not specifically consider the influence of well screen lengths. The depth and length of the monitoring well screens does not appear to be consequential to the past leaks evaluation of Tc-99 in the aquifer around WMA C. The elevated Tc-99 concentrations around WMA C appear to extend throughout the depth of the aquifer, indicating that the plume is well mixed. The peak Tc-99 activity (20,800 pCi/L) was determined at a depth of about 9 m below the water table in well 299-E27-23 during depth discrete sampling, although the activity was relatively constant at each depth measured in the well (i.e., 19,900 pCi/L and 20,500 pCi/L at depths of 3 m and 6 m, respectively) (DOE/RL-2011-01, *Hanford Site Groundwater Monitoring Report for 2010*). Depth discrete samples collected at wells 299-E27-4, 299-E27-7, and 299-E27-21 further indicate that Tc-99 activity increases with depth and that the Tc-99 is not contained in the upper part of the aquifer. For example, well 299-E27-4 had activity measurements of 727 and 761 pCi/L in the first two intervals but 7,260 pCi/L in the lowest sample interval (DOE/RL-2011-01). Thus, elevated concentrations of Tc-99 in the aquifer appear to be distributed throughout the depth of the aquifer, and the particular depths and lengths of the individual well screens appear to be sufficient to measure the concentration reliably.
PLES4	Exec Summary, p. ES-5, Table ES-2 (Case 2)	The terms “aquifer flux” and “aquifer flow” are used. What do you mean by “aquifer flux”? Is this the flux of contaminants to groundwater from the vadose zone? If not, what do you mean?		Please define each term in the document.	In three of the four IPA documents (RPP-RPT-59197, RPP-ENV-58806, and RPP-ENV-58782), the use of term "aquifer flux" and "aquifer flow" are only used when referring the amounts of volumetric flow of groundwater in the shallow aquifer system beneath WMA C. These terms are not used in RPP-RPT-58329. Its definition is the same as that for groundwater flux which is defined as the rate of groundwater flow per unit area of porous or fractured media measured perpendicular to the direction of flow (10 CFR Part 960.2). We use "groundwater flux " for each instance of term "aquifer flux"
PLES5	Exec Summary, p. ES-5, Table ES-1	Looks like Table ES-2 should read “Table ES-1” to agree with text and as the first table in the Executive Summary.	There is no Table ES-1 in the document.	Revise the table number.	Table was removed from shortened executive summary No disposition provided
PLES6	Exec Summary, p. ES-5 - ES-7	I’m assuming that these are summaries of more detailed work elsewhere in the PA. It would be beneficial if, in a summary such as this, you could indicate where the detailed analyses will be found.		Please refer the reader to section 4 for more details about the cases.	Concur with comment. Have provided some clarification in appropriate parts of the executive summary.

Comment No.	Location	Comment	Basis	Recommendation	Final Disposition
PLES7	Exec Summary, p. ES-7, lines 27-31	How was a heterogeneous model constructed; i.e., what, where and how many lamina/sub-units were added and what properties were they assigned? In how many cells was this heterogeneity introduced? In the modeling sections of the DOE 435.1 PA it appears that input parameters for hydrostratigraphic units are derived from numerical manipulation of laboratory test data to develop hydraulic input parameter values for models; i.e., an upscaling process.	These statements seem counter-intuitive. There are some real measurements of, e.g., moisture, obtained in the field from neutron logging of push holes. This field logging information seems to be ignored in favor of numerical manipulation of lab data to develop input parameter values for "Equivalent Homogenous Media". Intuitively, this seems subject to a high degree of uncertainty. Glaciofluvial sediments underlying C Farm are highly heterogeneous and thin, fine-grained lamina which are volumetrically insignificant but which are functionally significant in flow and transport by creating lateral spreading are ignored. If these thin strata are not included in the process model, they will not be abstracted into the system model.	Please explain or state where this information can be found.	The bullet identified in the comments relates to Case 4a (See discussion of this case in Table 4-1 in Section 4.0 and p. 4-21 in Section 4.4.1). Results for this case are based in ACM II which was an alternative model developed on input and geologic units picks provided by the Nez Perce. The case number based on the heterogeneous model summarized on lines 32-36 on p. ES-7 (See discussion of this case in Table 4-1 in Section 4.0 and p. 4-21 in Section 4.4.1). Information of the development of this model is provided in Appendix F in RPP-ENV-58806. ORP intends to document the development of the range of ACMs, a number of which are considered heterogeneous representations of the subsurface at WMA C, developed as a part of the PA effort in a new WRPS report.
PLES8	Exec Summary, p. ES-7, lines 41-45	Where is the technical basis for these statements?		Please provide the basis here or provide where it can be found.	This bullet removed in shortened executive summary. No dispostion provided/
PLES9	Exec Summary, p. ES-9, lines 5-7	Gross beta, likely Tc-99, was detected in well 299-E27-7 in the mid-1980s, albeit at low levels. Was this considered in your analyses?		Please elaborate.	Gross beta measurements were not considered in our analyses. Gross beta has been detected in the 299-E27-7 well since 1984. Gross beta was first detected in this well about 24 pCi/l in March 1984 and observed at levels ranging between 3 and 7 pCi/l. Tc-99 was first detected in this well in July 1991 and relatively low levels until it began to rise in 1998, reaching its peak of 2760 pCi/l in January 2002. After this peak time, Tc-99 concentration decreased back down to low-levels although they were found at slightly higher levels than observed prior to the rise in concentrations in 1998. While there appears to general correlation between Tc-99 and gross beta results during the overall time frame, this specific analysis focused on observations for Tc-99 and didn't consider the early low trends on gross beta observations. This text can be added to discussion in Section 2.3.3.3, "Groundwater Contamination"
PLES10	Exec Summary, p. ES-10, lines 1-19	Add a bullet summarizing understanding of the fate of contaminants residing in the vadose zone, in particular, how long the vadose zone will continue to contribute contamination to groundwater.	The summary lacks understanding of the fate of contaminants residing in the vadose zone, in particular, how long the vadose zone will continue to contribute contamination to groundwater.	Add a bullet summarizing understanding of the fate of contaminants residing in the vadose zone, in particular, how long the vadose zone will continue to contribute contamination to groundwater.	Concur with comment request. Have provided a bullet that summarizes the time of arrival results, and the projected persistence of the vadose contamination.
PLES11	Exec Summary, p. ES-10, lines 10-12	The first bullet states that "model results indicate that current high concentrations of $^{Tc-99}$ below WMA C are expected to decline over the next several decades as the contamination plume disperses in the aquifer." It seems that this states the obvious, and we had known this without the PA modeling. Please be more specific, i.e., what are the current levels of Tc-99 in downgradient wells and how long will it take for the concentration to reach the MCL?	PA was not needed to conclude that high concentrations of any contaminant in groundwater would decline over the next several decades as the contamination plume disperses in the aquifer.	Recommend deleting this bullet or rewriting it to justify value added of conducting the PA to arrive at the observation that high concentrations of Tc would decline over time due to plume dispersion.	Concur with comment request. Have provided a bullet that summarizes the findings summarized in Section 7.3.3 (Results of Groundwater Pathway Evaluation: Contaminant Flux to Groundwater) in the Revision 2 update of report.
PLES12	Exec Summary, p. ES-	It appears that this should be Table ES-1, not ES-2.		Verify and correct as needed.	Table has been removed in shortened executive summary. No disposition is provided.

Comment No.	Location	Comment	Basis	Recommendation	Final Disposition
	5, Table ES-2				
PLES13	Exec Summary, p. ES-5, Table ES-2	I am not familiar with "Lpm"; a customary notation for liters per minute is L/min. (Case 3c)	editorial	Verify and correct as needed.	Table has been removed in shortened executive summary. No disposition is provided.
PLES14	Exec Summary, p. ES-7, 2nd Bullet	What does ACM stand for?	The use of acronyms should be kept to a minimum, and all acronyms should be defined. Include ACM in the List of Terms.	The use of acronyms should be kept to a minimum, and all acronyms should be defined. Include ACM in the List of Terms.	Table has been removed in shortened executive summary. No disposition is provided.
PLES15	Exec Summary, p. ES-9, lines 33-34	Regarding the following statement: "These three UPRs occurred *later than* the release from tank C-105 and the modeling results exhibit the implications of this." We note the following: According to Table 3-1, the timing of the 1965-1969 UPRs outside the farm (UPR E-82 1.3 Ci and UPR E-86 2.7 Ci) *coincided with* the 1963-1972 major releases inside the farm for Tanks C-105 (10Ci) and C-110 (3.4 Ci).	See Table 3-1	Please resolve this apparent inconsistency and explain potential impacts on the results of your modeling approach.	As a clarification of the comment, Table 3-1 shows the release for C-105 to be from 1963 through 1967. The three UPRs were estimated to have released as follows: UPR-81 (acute release 1969); UPR-82 (acute release 1969) and UPR-86 (Acute release 1971). This formation would support the statement made on line 33-34. Text has been added on ES-9.
PL1-1	Section 1.1, p. 1-4, lines 14-15	As WMA C has impacted groundwater, corrective actions will also be required for groundwater.	WMA C is a RCRA TSD unit which includes the facility, the waste contained therein, and *all media* contaminated by releases from the facility.	Please correct.	Inserted additional text as follows: "Closure decisions for the Hanford Site SST system soils will be made through the *Resource Conservation and Recovery Act of 1976* (RCRA) corrective action process. Corrective measures of groundwater are being undertaken by the CERCLA RI/FS effort in 200-BP-5-OU."
PL1-2	Section 1.3, p. 1-9, Figure 1-3	The oval delineating the Central Plateau is misplaced.	The Central Plateau is the entire expansion bar deposited in impounded water in Missoula style floods.	Please correct.	Concur with comment. Figure has been corrected.
PL2-1	Section 2	There are 11 other UPRs (in addition to UPRs 200-E-81, E-82, and E-86). Also, the Cs-137 in Figure 2-2 is likely to have some associated hazardous waste.	Most of the radioactive waste had nonradionuclide chemicals associated with it.	Include a section on the 11 other UPRs (in addition to UPRs 200-E-81, E-82, and E-86). Also, discuss hazardous waste associated with the Cs-137 shown on Figure 2-2.	Added text from RFI for 16 UPRs. Added footnote to Figure 2-14 to identify 3 of the 16 UPRs not shown. UPR 200-E-115 is the same as UPR 200-E-91 (see text). -Re. Figure 2-2. The additional constituents associated with Cs-137 in the figure are already discussed at the end of Section 2.1. -Added sentence pointing to Table 2-3 and referencing RPP-RPT-42294. Also, added footnote on Table 2-3 and additional text and reference in sentence with callout for Table 2-3. -In addition to changes above, we will include a reference to the inventory information from RPP-RPT-42294. RPP-RPT-42294 Rev. 2 has been added to the Administrative record. https://pdw.hanford.gov/document/0065743H-Associated with PL2-5.
PL2-2	Section 2.1	While push hole logging was conducted at several UPR sites, it is worthy to note that the equipment is limited to radioactive levels below a certain activity for safety precautions. Thus, the "hottest" zones may not have been sampled.		Please consider.	Inserted following text on p. 2-42 before line 2: "While push hole logging was conducted at several UPR sites, it is worthy to note that the equipment is limited to radioactive levels below a certain activity for safety precautions. Thus, the "hottest" zones may not have been sampled at a few locations. However, decisions on sampling due to high levels of radiation was not a pervasive problem in the Phase 2 characterization efforts as indicated by the comment. Changes to original planned due to high radiation levels occurred in only two instances: - Decisions to not pursue the planned direct push borehole Q through the gunite cap at UPR-82 during the Phase 2 characteristic work plan was directly influenced by the knowledge of likely occurrence of high radiation under the gunite at this past release site. Although a vertical push through the Gunite cap had been proposed, it was not implemented due the need to implement radiological control requirements to facilitate the sampling. Instead, four direct push holes were placed to a depth of 61 m (200 ft), one on each side of the unplanned release, and multi-depth electrodes were placed. The basis for this decision is provided in RPP PLAN 39114.

Comment No.	Location	Comment	Basis	Recommendation	Final Disposition
PL2-3	Section 2.1, p. 2-1, lines 27-32	For purposes of environmental insult and soil inventory from releases, it does not matter whether the release is from an overfill, pipeline or cascade line leak. For purposes of tank waste retrieval, liner integrity is significant, and releases may occur from either type event.		Please consider.	Comment noted. No text changes required.
PL2-4	Section 2.1, p. 2-2, lines 3-4	HDW values were adjusted based on ratio of analytical/HDW concentration for a constituent. Values for all constituents were based on the ratio for Cs-137 due to limited analytical data.		Please specify the basis for assuming a constant ratio for all constituents?	Section 2.1, p.2-2, ln 16 states "This ratio is a multiplier or dilution factor comparing the HDW waste type to measured results." Will add. "The ratio assumes that the differences between analytical values and HDW model values for Cs-137 are mostly due to water dilutions. The Cs-137 ratio is not constituent specific and may not apply equally to all constituents if the differences are due to other factors."
PL2-5	Section 2.1, pp. 2-3 & 2-7, Tables 2-1 & 2-3	Table 2-1 lists isotopic uranium as evaluated in the HDW model, yet Table 2-3 only lists inventory for total uranium. Isotopic abundance can potentially be important for risk assessment.		Please specify the assumed isotopic abundance (i.e. natural? or enriched?) and give the reason why.	Added footnote to Table 2-3, "HDW model values for U-Total are the sum of U-isotope values. As shown in Table 2-2, U-235 is low enriched ~4% of U-238." Also provided U isotope specific inventories in Table 2.3. RPP-RPT-42294 Rev. 2 is now in the Administrative record. https://pdw.hanford.gov/document/0065743H- Associated with PL2-1.
PL2-6	Section 2.1.1, p. 2-4, Table 2-2	All of the waste types have been assigned the same mass for uranium except the P2 Stack Drain waste.	It seems like a coincidence that all of the waste types have exactly the same uranium inventories.	Please check and correct if necessary.	The numbers in Table 2-2 are the same as those in HDW Rev. 5 and are OK. Agree that it looks like a mistake, but these are values for supernatant, most of the uranium is partitioned to the solids; HDW Rev. 5 solids values are different for these waste types.
PL2-7	Section 2.1.2, p. 2-7, Table 2-3	Cyanide is present in groundwater at WMA C and C Farm (at least some tanks) was used in the U scavenging process which used $Fe(CN)_6$. First of all $Fe(CN)_6$ is given as zero for all releases.	The cyanide in groundwater is derived from C Farm tanks, likely from the $Fe(CN)_6$ used for U recovery. However, the cyanide may be dissociated from iron in the waste. Cyanide (possibly as the free anion) is a significant hazard in groundwater in the area of WMA C.	Please explain the source of the cyanide in groundwater if it is not from C Farm tanks. Alternatively, provide an estimate, based on usage of iron cyanide, of cyanide in releases.	A new Appendix (Appendix A) has been added that provides additional information on cyanide inventory estimates. This Appendix is referenced in the report at multiple places. Modified the footnote in Table 2-3 to say, "…The Fe(CN)6 was assumed to be insoluble and retained in the solids. However, as discussed in section 2.3.3.3 of this report, low concentrations of cyanide from the tank farms have been observed in groundwater wells. Appendix A provides an estimate of the inventory of cyanide released at WMA C." Text added in Section 2.1 to reference Appendix A. In addition, Appendix A referenced within the document in other sections. The Table of Contents for this Appendix is provided below. The Appendix was provided to Ecology for review. 1.0 INTRODUCTION 2.0 INVENTORY ESTIMATES OF CYANIDE IN PAST RELEASES FROM WMA C 2.1 Cyanide Inventory Estimation Process 2.2 Estimation of Cyanide Inventory in Past Releases at WMA C 3.0 PHASE 2 CHARACTERIZATION RESULTS FOR CYANIDE IN VADOSE ZONE BENEATH WMA C 4.0 GROUNDWATER MONITORING RESULTS FOR CYANIDE SINCE 2000 5.0 EVALUATION OF POTENTIAL IMPACTS TO GROUNDWATER FROM PAST RELEASES OF CYANIDE 6.0 SUMMARY AND CONCLUSIONS 7.0 REFERENCES In addition to the changes recommended, we propose that cyanide inventory estimates taken from Appendix A have been added to Table 2-3. A footnote is added to point to specific sections in Appendix A that provide the basis for the inventories. We concur with the statement provided in the status details by Ecology about some of the limitations of and assumptions made in the HDW model concerning ferrocyanide. Discussions on this specific topic is provided in Section A.2.0 of the new Appendix A. Because of the limitation in the current HDW model assumption about ferrocyanide, we adopted a two-staged approach that is described in Section A2.1 of Appendix A to estimate the supernatant concentration of ferrocyanide with the primary purpose of developing inventory estimates for past discharges at WMA C. The first stage involved conducting a Hanford-specific literature search related to the solubility and dissolution potential of

Comment No.	Location	Comment	Basis	Recommendation	Final Disposition
					precipitated nickel ferrocyanide within the tanks. The second stage involved searching the Tank Waste Information Network System (TWINS) for historical records related to sampling data for cyanide for C Farm tanks. The results from both evaluations are presented in Section A2.1. A summary of the results of evaluation of potential impacts to groundwater from past releases of cyanide provided in Appendix A has been inserted at appropriate locations within Section 7.3 and 7.4 in theRevision 2 update. These results are also summarized in appropriate parts of Section 8.3 and 9.0.
PL2-8	Section 2.1.3, p. 2-8, lines 11-30	It might be prudent to indicate that a better match between time and mass of arrival in groundwater is obtained for a larger inventory release of Cs-137 in one of the modeling scenarios.		Please consider.	The scoping analysis cases are summarized in Table 4-1 in Section 4. That focus was evaluating only Tc-99. The rational for focusing on Tc-99 than other constituents is given at the end of section 3.1 in Section 3.0. We would disagree with the commenter's suggestion that the use of a larger mass release of Cs-137 would be a helpful modeling scenario to include. Have added the following text at the end of Section 2.1. "A series of steady state flow and transport scoping cases evaluated as a part of the past leak analysis are summarized in Table 4-1 in Section 4. The effect of considering transient effects on flow and transport is fully described in Section 5. The focus in the scoping part of the analysis was on evaluating only Tc-99. The rational for focusing on Tc-99 than other constituents is given at the end of section 3.1 in Section 3.0. A set of forward calculations to evaluate the future consequences of the past waste leaks and releases for selected constituents in the past leaks inventory are presented in Section 6.0 to evaluate how the groundwater concentrations may change in the future based on the constraints on the scoping modeling analysis cases established in Section 4.0 and 5.0"
PL2-9	Section 2.1.4, p. 2-9, lines 7-9	There is some uncertainty in determining whether C-108 may have leaked during tank waste retrieval.		Please qualify.	Modified text in Section 2.1.4 and added the following text to last paragraph. "This does not preclude the possibility of a small or slow tank leak or a release from another source that could not be detected by these methods."

Comment No.	Location	Comment	Basis	Recommendation	Final Disposition
PL2-10	Section 2.2.2, p. 2-28, Figure 2-13	What is the basis for this change of boundaries? Please explain the westward "tongue" of the BP-5 boundary that extends almost to the 200 East Area.	This lobe appears to be in the PO-1 Interest Area, but not actually part of the PO-1 Operable Unit.	Please explain.	This is exactly how it appears in the GW Annual Reports. The GW Operable Unit boundaries are determined based on Tri-Party agreement and therefore any discussion of how these are determined is out of scope for this document. The westward "tongue" is actually the boundary for the 200-PO-1 OU, which is based on the 2,000 pCi/L Tritium contour. That shape has been used for the past 15-20 years with more recent discussion provided in DOE/RL-2007-31 and DOE/RL-2009-85 Rev. 1. Additional Reference: See Figure 2.1-1 of the *Hanford Site Groundwater Monitoring for FY 2005*. https://www.pnnl.gov/main/publications/external/technical_reports/PNNL-15670.pdf
PL2-11	Section 2.3, p. 2-30, lines 2-14	This figure appears inconsistent with information given in Sect. 2.1.		Please check and correct as needed.	Text on leaks and releases in Section 2.1 have been made consistent the UPR numbers designated in Figure 2-14
PL2-12	Section 2.3.1, p. 2-32, lines 37-41	An explanation is needed for how these additional conceptual models will be presented and how they will be incorporated into C Farm IPA modeling.		Please elaborate.	The work that has been done by PNNL on alternative conceptual models of heterogeneity with some intercomparion of selected modeling simulation results taken from the PA effort has been documented in PNNL-24740. A more detailed presentation of the intercomparison for modeling results between PNNL and PA related models was provided in the webinar conducted on March 29, 2017. Updates to the IPA documentation provides more information on these additional alternative models and modeling results in a separate planned WRPS document on this topic. A summary of that document will be included in the third document with comments on its relevance to this past leaks analysis. Additional information on the effect of vadose zone heterogeneities on flow and contaminant transport as evaluated in Ecology's Advocacy Alternative Conceptual Model subsurface vadose zone heterogeneity are provided in detail in Section 5 and Appendix B of the Past leaks Analysis in the Revision 2 update of RPP-RPT-59197 Section 5 of RPP-RPT-59197 also provides summaries of these past efforts at WMA C that includes: • Summary of previous work by PNNL documented in PNNL-24740 (Alternative Conceptual Models of the Subsurface at WMA C, 2017) • Summary of previous work by WRPS, PNNL, and INTERA that is in the process of being documented in RPP-RPT-61239 (*Multiple Lines of Evidence and Modeling Results for Heterogeneous Alternative Conceptual Models of the Subsurface at Waste Management Area C*, in preparation)
PL2-13	Section 2.3.2	Spectral gamma logging is mentioned throughout this section, but was any attempt made to determine if alpha or beta emitting radionuclides are present in the vadose zone?	"Vadose zone characterization activities" does not make it clear what type of analyses may have been conducted.	Discuss what radionuclides were analyzed.	As indicated in the text, geophysical logging in dry wells is limited to gamma and high-resolution spectral gamma logging to identify potential depths of contamination from released tank wastes. The major gamma-emitting contaminants associated with WMA C are Cs-137 and Co-60 with lesser amounts of Eu-154. A full suite of alpha, beta, and gamma emitting radionuclides were analyzed for or calculated from soil samples collected in direct push characterization: Americium-241, Antimony-125, Carbon-14, Cesium-137, Cobalt-60, Curium-242, Curium-243/244, Europium-152, Europium-154, Europium-155, Iodine-129, Neptunium-237, Nickel-63, Plutonium-238, Plutonium-239/240, Plutonium-241 (calculated), Selenium-79, Strontium-90, Technetium-99, Thorium-228, Thorium-230, Thorium-232, Thorium-234, Tin-126, Tritium, Uranium-233, Uranium-234, Uranium-235, Uranium-236, Uranium-238. A discussion on key detected (or detected above background) constituents is summarized in Section 2.3.2.5.1 through 2.3.2.5.3.

Comment No.	Location	Comment	Basis	Recommendation	Final Disposition
PL2-14	Section 2.3.2.1, p. 2-33, lines 44-45	The groundwater is contaminated, so the maximum depth of contaminant inventory in the vadose zone is the water table.	The magnitude and extent of the deep vadose zone inventory remains to be determined.	Please rephrase the sentence	Have added following rephrasing. “Consequently, the depth of vadose zone contamination is not known in some areas of WMA C.”
PL2-15	Section 2.3.2.1, p. 2-33, lines 44-45	Text states maximum depth of vadose zone contamination is not known in some areas.		Please specify how this was handled in the model? What concentrations were assumed below the maximum depth of spectral gamma logging?	The approach using in modeling of tank leaks or releases in this analysis is to simulate the release of constituents associated with tank leak or release from the original point of release and not aa an initial condition developed from characterization data or information. The model can then be to estimate the extent of contamination in both the vadose zone and groundwater once it reaches the underlying unconfined aquifer. This approach is described in Section 3.3, "Conceptual Models of Source Term Releases"; Section 3.4 "Vadose Zone Considerations"; Section 3.5, "Aquifer Considerations"; and Section 3.6, Mathematical Models.
PL2-16	Section 2.3.2.4, p. 2-37, lines 16-24	There are no data from directly beneath any tank.	It should be noted that all the characterization boreholes were limited in placement because of infrastructure, and also that, except for UPR 200-E-82, all the boreholes are vertical.	Please clarify.	Have added text after lines 16-24: It should be noted that the placement of all the characterization boreholes was limited because of the tanks, ancillary equipment, and complex infrastructure located in the tank farm. Most direct push boreholes are vertical however, a number of angled direct push boreholes were placed in the vicinity of UPR-82 and Sites A, B, and J. Very little data has been collected directly below the tanks.
PL2-17	Section 2.3.2.4, p. 2-42, lines 9-17	This paragraph refers to Site X, but Site X is not shown on Figure 2-19 which includes other evaluated locations, and I was not able to find another figure that illustrated the location of X. Please include a figure that shows the location of Site X.	Site X location is not identified.	Please include a figure that shows the location of Site X.	Concur with comment. Has been added to figure. (Add Figure 4-10 of the RFI which shows Site X). Figure 2-19 now shows Site X.
PL2-18	Section 2.3.2.5, p. 2-43, lines 11-16	Groundwater is contaminated with cyanide and nickel but the bullets do not include them. Please include them or explain why they are not included.	The bullets do not address cyanide and nickel and it is not clear why.	Please include cyanide and nickel or explain why they are not included.	This section is a summary of what was found in vadose zone characterization that is why groundwater contamination is not discussed. Characterization of cyanide is discussed briefly in Section 2.3.2.5.1, "Mobile Constituents (Kd = 0.0 ml/g). Text describing characterization results for nickel can be added at the end of Section 2.3.2.5.3, Sorbed constituents (Kd > 0.6 ml/g). Proposed text for nickel is as follows: "In the Phase 2 RFI/CMS investigation, nickel was reported above background in nine samples from Investigation Groups E, L1 + L2, P and U at WMA C. The maximum concentration (30,600 µg/kg) was reported at Investigation Area Group P at a depth of 8 m (126 ft) bgs. Nickel was reported above background as follows: • in two samples from Investigation Group E from borehole C7672. The maximum concentration was 25,300 µg/kg at a depth of 23 m (74 ft) bgs (H2). The maximum depth of detection was 23 m (74 ft) bgs (H2). • in one sample from Investigation Group L1 + L2 from borehole C7670 at a concentration of 20,200 µg/kg and a depth of 12 m (40 ft) bgs (backfill). • in five samples from Investigation Group P. The maximum reported concentration was 30,600 µg/kg at a depth of 8 m (26 ft) bgs (H1) from borehole C6392. The maximum depth of detection above background was 52 m (170 ft) bgs (H2) at borehole C6394. • in one sample from Investigation Group U from borehole C7676 with a concentration of 29,400 µg/kg at a depth of 48 m (158 ft) bgs (H2)." Further discussion of cyanide and nickel can be found in Section 2.3.3.3, Groundwater Contamination
PL2-19	Section 2.3.2.5.1, p. 2-46, lines 24-25	This statement indicates that the soil inventory for this COC is unknown.	Cyanide is present in groundwater and the source is WMA C.	Please address.	A new Appendix A concerning Cyanide inventories and impacts has been added to the document.
PL2-20	Section 2.3.2.5.1, p. 2-26, lines 24-25	The text makes reference to background levels for cyanide; cyanide is not a background constituent.	Cyanide is anthropogenic and should not be assigned a background value above its detection or quantitation limit.	Revise the text to discuss detection or quantitation limits.	Concur with comment. Text should have just said that: "Cyanide was not detected in any of the soil samples collected during the Phase 2 soil investigation." The detection limit for cyanide was 0.5 mg/kg.

Comment No.	Location	Comment	Basis	Recommendation	Final Disposition
PL2-21	Section 2.3.2.5.2, p. 2-47, lines 1-28	It is stated that Co-60 is a key constituent indicative of tank waste contamination. It also states that Co-60 was reported above background for many samples but in all cases was considered not detected. Therefore, it appears the detection limit is not low enough to detect if Co-60 exists at concentrations above background. In other words, it cannot be determined if Co-60 tank waste contamination exists. The same problems appear to be present for uranium.		Please discuss the detection limits relative to background for Co-60 and uranium.	Have included the following text: "A summary of results for gross gamma and spectral gamma logging results relevant to Co-60 in drywells and direct push boreholes in each of the investigation areas of the RFI are discussed in Section 5.2 of the RFI (RPP-RPT-58339, Rev. A). All logs used in the RFI are provided in Appendix T of the RFI (RPP-RPT-58339, Rev. A). Cobalt-60 was reported above background in 138 samples across all locations and depths. However, all results were reported as non-detects. The maximum reported concentration was 3.13 [U] pCi/g from Investigation Group P at a depth of 2 m (7 ft.) bgs (shallow). In borehole C-4297 (Phase 1 Characterization), low levels of 60Co (<1 pCi/g) were found at depths from 12 to 20 m (40 to 65 ft.) bgs. Note that detection limits were established during the DQO process and it was understood that based on the limited soil collected through the direct push process that some detection limits would be above site soil background levels. Table 5-4 (Page 5-21) of the RFI identifies the constituents with detection limits established above site soil background levels. Co-60 was one of the constituents having detection limit issues (background level 0.0084 [0.01] pCi/g with a detection limit of 0.05 pCi/g).". For uranium, the DQO identified the target detection limit of 1,000 µg/kg (1 mg/kg) and the SAP identified a required detection limit of 500 µg/kg (0.5 mg/kg). Background for uranium is 3,210 µg/kg (3.21 mg/kg). It should also be noted that the SAP also identified that isotopic uranium analysis may be substituted for total uranium as long as the required detection limit is met. Appendix M of the RFI (Data Quality Assessment) identified the detection limit issues with uranium analysis. Table M-25 provides uranium results estimated from isotopic ratios of uranium radioisotopes. All of the total uranium results (determined from isotopic uranium) were below background with the exception of one sample at Site P (C6404) at a depth of 13 m (43 ft.) bgs and a concentration of 6440 µg/kg. Uranium and Co-60 is not observed in groundwater in concentrations to contribute significantly to current risk. The overall risk contribution from uranium is expected to low in the future due to the combination of its affinity to be sorbed on Hanford sediments and their inventories. In the case of Co-60, its overall risk contribution is expected to low in the future due to its short half-life, low inventory, and its apparent affinity for small amounts of sorption onto Hanford sediments.
PL2-22	Section 2.3.2.5.2, p. 2-47, line 17	A uranium concentration of 101,000 is given with no units. We assume the U associated with this value means not detected, but lab qualifiers are usually given in parentheses, but in this case not.		Please clarify the meaning and the units here, and any data qualifiers.	Text has been corrected to state "… 10,100 ug/kg [U] …."
PL2-23	Section 2.3.2.6, p. 2-49, lines 1-3	Was any attempt made to correlate levels of higher moisture as an indication of continuous fine-grained strata that might influence flow and transport?	This could be helpful in analyzing the effects of heterogeneity in the vadose zone.	Please elaborate.	An alternative conceptual was developed looking at this type of moisture content information. The development of this model is provided in Appendix E in Revision 1 update of RPP-ENV-58806, and in Appendix F in RPP-ENV-58782. This model is one of the many ACMs considered in the scoping analysis of leaks described in Section 4 of this document. An alternative conceptual was also developed by PNNL based on the same moisture content information. The development of that model is summarized in PNNL-24740. This document was not released at the time this document was finalized. This citation will be added to the updated version of this document.
PL2-24	Section 2.3.3.1, p. 2-49, lines 43-44	This is an extremely high value that resulted from aquifer testing near B-BX-BY.	Extrapolation to WMA C does not seem appropriate when the values obtained from WMA C were approximately half that.	Please elaborate on the reasoning.	The text has been updated to better explain the basis for effective saturated hydraulic conductivity. It references Appendix C of RPP-ENV-58806 (*RCRA Closure Analysis of Tank Waste Residuals Impacts at Waste Management Area C, Hanford Site, Washington*). In particular, Section C3.2 is referenced, and relevant text has been added to update the paragraph. Note: The parameter value is not based on pumping test performed near B-BX-BY.
PL2-25	Section 2.3.3.1, p. 2-52, lines 29-30	What specific divide are you meaning? Furthermore, Figure 1-4, p. 1-9 in the Synopsis document shows that the 200-BP-5 groundwater operable unit extends to the Columbia River in the 100 Area. A groundwater divide is developing in the Gable Gap area such that groundwater flow in the 200 East Area is now to the southeast.	Gable Gap is a divide that physically separates the area to the south from the area north to the Columbia River in the 100 Areas.	Please elaborate.	The groundwater divide being discussed here is related to the flow from 200-West area and the flow-path within the 200-East area. The paragraph is now deleted since the discussion related to the location of groundwater divide and its relative shift is not directly relevant to this report. The text above this paragraph is deemed adequate in addressing the flow direction and gradient at WMA C. So, the revised disposition is to delete this paragraph.

Comment No.	Location	Comment	Basis	Recommendation	Final Disposition
		How will this change be incorporated into the domain for 200-BP-5?			
PL2-26	Section 2.3.3.3, p. 2-53, line 39	The text mentions that cyanide is well below the DWS of 200 µg/L. The measured concentration was 14.9 µg/L in December of 2015. This value is over the relevant state standard for cyanide. This also applies to p. 2-55, lines 19-32.	The WAC 173-340-720 Method B groundwater cleanup level for cyanide (hazard quotient = 1) is 9.6 µg/L for CN^- and 4.8 µg/L for HCN.	Please compare with the Method B value and mention the exceedance in the text.	Concur with comment. We have added the following information to this text. "Additionally, cyanide, which is a dangerous waste constituent, is also found in the aquifer at levels above detection limit, which well below the DWS of 200 µg/L but above the WAC 173-340-720 Method B groundwater cleanup level for cyanide (hazard quotient = 1) is 9.6 µg/L for CN- and 4.8 µg/L for HCN in some wells.
PL2-27	Section 2.3.3.3, p. 2-54, lines 19-22	What is the technical basis for suspecting different sources?		Please elaborate.	Added following text changes "Based on evaluation of Tc-99 to nitrate ratios, It is believed the Tc-99 found at wells 299-E27-14 and 299-E27-24 is from a different source than Tc-99 found in the south central region of WMA C (299-E27-4, 299-E27-21, and 299-E27-23). A full discussion of this topic is provided in Section 2.3.4."
PL2-28	Section 2.3.3.3, p. 2-54, lines 24-30	What accounts for the depth distribution of certain contaminants; for instance, density, vertical hydraulic head?		Please elaborate.	Have added following text after line 30 on p. 2-54 The vertical distribution of a plume is affected or influenced by hydrophysical, hydrologic, and geochemical processes. Hydrophysical processes include the rate at which the contaminant enters the aquifer and the volume of water transporting the contaminant. Higher rates and larger volumes provide more of a vertical gradient to the contaminant movement than lower rates and smaller volumes. Hydrologic processes include the irregularly shaped aquifer geometry that may physically control flow paths, and spatially heterogeneous hydrogeologic units that influence transport. Either of these processes may facilitate or impede flow to create vertical gradients and other multidimensional contaminant transport and spreading within the aquifer. Geochemical processes include contaminant solution density, and state (e.g., non-aqueous liquid that may sink or float in water) occurring in the groundwater. The specific factors affecting the increasing contamination with depth observed at wells 299-E27-23 and 299-E27-21 while these wells were being drilled is unknown.
PL2-29	Section 2.3.3.2	Distinguishing sources from current monitoring data seems futile. Also, groundwater flow directions are changing. Without justification, this effort appears invalid. Furthermore, *all* releases from WMA C are to be evaluated, i.e., the sum total of all releases regardless of the source.	There are no groundwater monitoring data directly beneath C Farm. Furthermore, with lateral spreading in the vadose zone, contaminants could spread laterally before reaching groundwater. So, the assumption of proximity of well data to a contaminant source is potentially violated, as this presumes mostly vertical flow.	Please justify this approach or eliminate it.	Added following text at end of the introduction text of Section 2.3.3.3 and before the discussion of Technetium-99 "It should be noted that interpretations of some aspects of groundwater concentration monitoring results, described in the following sections, have been or are generally used to infer that sources for the monitoring well impacts have originated from past source releases from WMA C. However, because the lack of groundwater monitoring wells within the tank farm area and the uncertainties associated with historical knowledge of both natural and anthropogenic sources of recharge, and the past directions and rates of groundwater flow in the unconfined at WMA C, attempts to attribute the impacts observed in groundwater wells to specific source leaks or releases that have occurred in or in the general vicinity of WMA C is not considered to be feasible with current state of data and information ."
PL2-30	Section 2.3.4.3.3, p. 2-63, Figure 2-24	By beginning the plot in 2006, one misses the encroachment of an SO_4 plume from the northeast in 200 East Area. Why the 2006 cutoff date?		Please justify.	Figure 2-24 plots sulfate concentration in Wells at WMA C from 2006-2016, which is the time frame that the 200-BP-5 Remedial Investigation (RI) examined for recent impacts to groundwater at WMA C. This figure is included in the section that summarizes the results of that evaluation, so sulfate concentrations outside that time frame would be out of place.

Comment No.	Location	Comment	Basis	Recommendation	Final Disposition
PL2-31	Section 2.3.4.4.3, p. 2-73, lines 9-28	What is the objective of this calculation?		Include a statement and explanation on the objective of this calculation	Section 2.3.4.4 on page 2-72 provides the objective of the calculation. However, the text has been expanded to better state the objective. The point of Section 2.3.4.4 is to provide published information about the recent estimate of mass flux of Tc-99 from the vadose zone to the saturated zone at WMA C. This is done to provide the reviewer with all relevant information based on evaluation of recent groundwater monitoring data. At the end of the section on page 2-74, a concluding sentence has been added to clarify that this is summary of recent interpretations based on WMA C groundwater chemistry.
PL2-32	Section 2.3.4.4.3, p. 2-73, lines 20-27	The 'second method' model indicates the rate of Tc-99 transport downgradient is equal to rate of transport from vadose zone to saturated zone. This would appear to result in a steady state groundwater concentration. Is this observed in groundwater wells? Can this be used to constrain the model?		Please discuss.	This methodology provides some independent insight about potential inventory in the aquifer based on limited groundwater information on the periphery of the tank farm and cannot accurately account for potential additional inventory in the interior of the tank farm since there are no wells in this areas. This information has been mentioned in the section related to Contaminant Flux to Groundwater (Section 7.3.3 in the Revision 2 update) but, given all of the uncertainties associated with past leaks, we do not believe it is very useful in constraining the range of models that are considered in this analysis. This second method yields an estimate of about 0.14 Ci of Tc-99, whereas, results of modeling of the release of 17.5 Ci of Tc-99 yielded about 2-3 Ci of Tc-99 released to the aquifer by about the 2010 time frame (See Figure 7-24 in the Revision 2 update). Given the uncertainties, these two estimates are in the same ballpark. .
PL3-1	Section 3	Please explain likely impacts of the following assumption on the outcome of modeling "hydraulic conductivities derived from a calibrated model are regarded as more reliable than direct measurements by permeameter, slug, or pump tests." Appendix C of RPP-ENV-58782 (DOE 435.1 PA). In particular, please discuss all 3-day pump tests that have been conducted and compare impacts on the outcome of modeling using hydraulic conductivity data from the 3-day tests against the outcome of modeling using hydraulic conductivities derived from modeling.	Empirical data appears to have been discarded as unreliable.	In particular, please discuss pertinent 3-day pump tests that have been conducted and compare impacts on the outcome of modeling using hydraulic conductivity data from the 3-day tests against the outcome of modeling using hydraulic conductivities derived from modeling.	Hydraulic conductivity estimates from various investigations on the aquifer within the 200 East Area are presented in Figure C-6 of RPP-58782. While groundwater flow can vary spatially due to local changes in hydraulic properties, the peak concentration at a particular location appears to correlate strongly to the mean groundwater flux (i.e., the rate of flow that occurs in a single direction), even in a heterogeneous aquifer (ITRC 2010, "Use and Measurement of Mass Flux and Mass Discharge," Interstate Technology & Regulatory Council; NUREG/CR-6767, *Evaluation of Hydrologic Uncertainty Assessments for Decommissioning Sites Using Complex and Simplified Models*). Permeameter, slug, and even aquifer pumping tests are limited in their ability to quantify spatial averages or trends, and are less likely to produce central measures of flow magnitudes than a regional model, but are important data included during model calibration (ITRC, 2010). Measurements of hydraulic conductivity appear to be dependent on the test scale, and increase as the scale increases, particularly in heterogeneous media ("Scale Dependency of Hydraulic Conductivity Measurements" [Rovey and Cherkauer 1995]; "Scale Dependency of Hydraulic Conductivity in Heterogeneous Media" [Schulze-Makuch et al. 1999]). In-situ measures of aquifer flow and hydraulic properties inferred from hydraulic testing represent relatively small areas compared to the overall scale and dimensions of the model domain, and therefore do not provide representative results appropriate for the field scale (ITRC, 2010). Text has been added to page 3-35.
PL3-2	Section 3, p. 3-1, lines 22-23	There are many other sources of artificial recharge that are not included here but should be.	These include water line breaks and chronic leaks, fire hydrant testing, hydro-excavating, dust control water, among others.	Please include.	A sensitivity case in which the recharge was increased to 150 mm/yr produced results in which the arrival time of the calculated plume appears to be substantially earlier than the observations in the wells, so the 100 mm/yr estimate appears to be adequate. Results for these two cases and others considered in the scoping analysis are presented in Section 4.3 (CASE 3: EFFECT OF CHANGES IN RECHARGE CONDITIONS).
PL3-3	Section 3.1, p. 3-2, lines 1-3	It appears that you are stating that you have only point data and need to extrapolate and interpret the data.		Clarify this wording.	Proposed rewording as follows: • Uncertainties exist in interpreting the groundwater monitoring and vadose zone characterization data on the interpretation of contamination levels observed in ground water and the vadose zone resulting from the past leaks since data represent specific point locations in the subsurface and need to be interpolated in space and time for develop interpretations.

Comment No.	Location	Comment	Basis	Recommendation	Final Disposition
PL3-4	Section 3.1, p. 3-2, lines 5-9	If this does not include sensitivity cases for heterogeneity and/or artificial recharge, then this item is incomplete.		Please clarify.	Both types of cases are included in the scoping analyses. The commenter is referred to Table 4-1 on pp. 4-3 and 4-4 of Section 4.0 for the range of cases considered in the scoping analysis. The heterogeneous case is Case 4b. The cases examining the effects of recharge, including potential effects of anthropogenic sources of recharge are Cases 3a, 3b, and 3c.
PL3-5	Section 3.1, p. 3-2, lines 18-21	The statement regarding the first arrival of contaminants at the water table does not have a basis.	A compliant groundwater monitoring network was not present until 1989, almost a decade after most tanks stopped operating. This fact introduces another element of uncertainty that should be acknowledged.	Provide a basis for this statement (lines 18-21) and acknowledge the uncertainty associated with the lack of monitoring before 1989.	Concur with comment. Have added text that discusses the point of this comment.
PL3-6	Section 3.1, p. 3-2, lines 23-29	If you cannot simulate estimated contaminant release dates and arrival time in groundwater within an order of magnitude to validate the model and to provide some measure of credibility to the modeling effort, then how can your estimates out to 10,000+ years have any reasonable credibility where there are no data at all?		Discuss the validation of your model and the justification for making estimates for 10,000 years when the model cannot express known outputs within an order of magnitude."	One of the most important aspects of the tank waste residual analysis that is relevant is the good general agreement between modeled volumetric moisture results with average field measured volumetric moisture contents for the various hydrogeologic units in the vadose zone at WMA C (See Section 6.4.4 and Appendix B of RPP-ENV-58782 and RPP-ENV-58806). Another aspect that is relevant in the tank waste residual analysis is a very good agreement of simulated contaminant fluxes at the water table between the WMA C PA model and Tank Closure and Waste Management EIS model (See Appendix G of RPP-ENV-58782 and RPP-ENV-58806) when same inventories and release models used for Alternative 2b are evaluated in both models.
PL3-7	Section 3.1, p. 3-2, lines 31-35	As each tank and WMA are unique in terms of contaminant inventory, release inventory, and stratigraphy, the approach of using "templates" should be supported with a basis for using the template		Either clarify or try another approach.	To the extent possible, data were based on WMA C-specific site characterization, sampling, measurements and interpretations, including those for contaminant inventory, geology, hydrology and geochemistry. For estimates of contaminants inventories, due the lack of specific data on specific waste compositions in a tank or in ancillary equipment at the suspected time of the leak, this analysis needed to rely on approaches used in the leak assessment process which involved the use of best basis inventory template compositions developed for waste types suspected to have been in the tank at the time of the suspected leak(s). When characterization data specific to WMA C were not available, data from nearby sites or comparable conditions, as well as data reported in the literature, were used. In all cases, when data are used that are not WMA C-specific, the basis for the use of these alternative sources of information is explained, providing the logical link for their use at WMA C.
PL3-8	Section 3.1, p. 3-2, lines 37-40	Upscaling from bench to field values for parameters introduces another element of uncertainty and does not develop confidence in the model as you state in lines 28, 29.		Please add a discussion in this document about the uncertainty derived from the upscaling process.	Made following change to Bullet 2: • Data were upscaled to represent field-scale processes using scientifically accepted approaches that have been published in peer-reviewed journals. Upscaling techniques use information from small, core-scale measurements to develop parameters that are applicable to large, field-scale models. Details of approaches to upscaling vadose-zone parameters are presented in Appendix B of RPP-ENV-58782 and RPP-ENV-58806. Details of the relationship between local-scale measurements of aquifer properties and the upscaled model representation are presented in Appendix C of RPP-ENV-58782 and RPP-ENV-58806.
PL3-9	Section 3.1, p. 3-3, line 5	Please provide a copy of Internal memorandum 1301789. This sounds like an internal agreement among DOE and contractor, with no Ecology approval or input.		Please include this memorandum as part of the PA documents	Citation of this internal memorandum for establishing acceptance of STOMP code for site- use is not necessary and the sentence where it is cited will be deleted.

Comment No.	Location	Comment	Basis	Recommendation	Final Disposition
PL3-10	Section 3.1, p. 3-3, lines 12-14	No details of the level of effort for validating the simulation model, using data on dates of release of contaminants and dates of arrival of contaminants in groundwater. This is an essential step for affecting the credibility of the model.		Please include.	Revisions were made to model but not related to the context of associated reference to "adjustments". We have added following revision to the first paragraph of Section 3.1 on p. 3-1: "The strategy for this analysis of leaks at WMA C is to define and analyze a suite of scoping cases to evaluate the uncertainties associated with past leaks. The approach has been to compare model results to key data in the groundwater monitoring. No specific adjustments or calibrations to the model to match historical observations were performed; the model was run for a variety of alternative assumptions and input parameters, to evaluate which inputs provided results that were consistent with data, and which inputs provided results that were inconsistent with data. These key uncertainties in the analysis of past leaks can be broadly considered to originate from one of the following sources."
PL3-11	Section 3.1, p. 3-3, lines 28-34	Tc-99 concentrations in groundwater wells are used to evaluate model input conditions consistent with Tc-99 arrival times and concentration levels. Further, why is arrival time the only temporal consideration? What about time of peak concentration and concentration falloff rate?	From the graphs in Section 4, for example Figure 4-34 on Page 4-50, it appears the well concentration levels are not correctly predicted by the model.	Please explain the choice of temporal parameters.	Added following text change beginning at Line 16 of page 3-3. Consequently, the model used in RPP-ENV-58782 and RPP-ENV-58806 was adapted for the past leaks scoping analyses so that the water table was reflective of conditions at WMA C when first arrival of contaminants at the water table was observed. In particular, during the time between when the leaks occurred and when they arrived at the water table, the aquifer was elevated from the addition of water in both 200 East and 200 West Areas. In addition to the water table elevation, it is believed that the flow direction was variable during this time, generally changing from flow to the northwest, shifting to the southeast, with the timing of the shift coinciding with the arrival of contaminants at the water table. Two approaches were used to address the complications the shifting water table causes for the modeling. In the first approach, the water table was assumed to be fixed or at steady state, and directed in the same way as the prospective water table used for future analyses, but at a higher level, which allows the analysis to represent the shorter travel time in the vadose zone that would have existed when the plumes initially arrived. This approach is intended to represent the time of first arrival and the peak of the groundwater plume but is not necessarily to represent the spatial distribution of contamination in the groundwater. Therefore, this first approach can be used to test the model representation of the leaks and vadose-zone behavior, separate from the complications the shifting aquifer causes. The second approach was to introduce a time-varying or transient water table to represent the likely evolution of the aquifer gradient over the simulation period. This second approach requires the introduction of speculation regarding the timing, orientation, and magnitude of the aquifer gradient since these are all unknown. However, it has the benefit that the resulting model can be directly compared to all aspects of the groundwater concentration data. Both of these approaches are described in more detail in Section 4. The model has been initially compared to Tc-99 concentrations in groundwater, since Tc-99 is a key risk driver and the contamination levels observed in groundwater monitoring wells are considered to be the result of WMA C past leaks. The Tc-99 concentration data observed in groundwater monitoring wells have been used to evaluate the input conditions that are consistent with the arrival times and concentration levels of Tc-99 observed historically in the vicinity of WMA C. As discussed in the preceding paragraph, the static water table analyses compared to first arrival time are intended to test how well the model performed in representing the leaks and the vadose zone, while the dynamic water table analyses are intended to test the overall model behavior. The resulting constrained model is then also compared with other contaminant data as appropriate.
PL3-12	Section 3.2, p. 3-4, lines 36-40	These statements need to be qualified.	It's a challenge to determine gradient with periodic measurement of water levels in wells; however, reliable transducers in wells might provide better data to determine a local groundwater gradient at WMA C.	Please use transducers in wells to determine local groundwater gradient. Also, validate the assumption that a similar pattern of behavior has happened at WMA C.	The existing estimates of the hydraulic gradient appear to be sufficient for the purpose of the RCA and past leaks analysis. Adding transducers would not provide particularly useful information applicable to the past leak breakthrough time frame, and the impacts from the tank residuals is not projected to occur for several hundred years.

Comment No.	Location	Comment	Basis	Recommendation	Final Disposition
PL3-13	Section 3.2, p. 3-5, Figure 3-1	There are no drywells or groundwater monitoring wells shown on this schematic. Is the assumption that all drywells and groundwater monitoring wells beneath the barrier have been decommissioned in accordance with WAC 173-160?		Please address.	The schematic is not intended to portray a detailed picture of closure conditions, but a conceptual depiction of the major factors that influence bulk or mean contaminant transport to the water table. It is expected that all drywells and groundwater monitoring wells beneath the barrier will be decommissioned in accordance with the appropriate regulations.
PL3-14	Section 3.2, p. 3-6, Figure 3-2	Important heterogeneities in the stratigraphic units are not shown in the figures and do not appear to be addressed for the past releases.	There are heterogeneities within these stratigraphic units that can influence the pattern of infiltration of water and contaminants that are not shown on this figure.	Cite the locations in the PA documents that discuss how these heterogeneities in the stratigraphy have been addressed in relationship to past releases.	The use of an EHM does not mean uniformity of properties. Credible demonstrations have been made that the heterogeneities do not affect transport. These include The Sisson and Lu experiment, as well as scoping calculations conducted on heterogeneities at WMA C. See our response to comment RC3-3 -Additional information on the effect of vadose zone heterogeneities on flow and contaminant transport as evaluated in Ecology's Advocacy Alternative Conceptual Model subsurface vadose zone heterogeneity are provided in detail in Section 5 and Appendix B in the Revision 2 update of RPP-RPT-59197. Section 5 of RPP-RPT-59197 also provides summaries of other efforts at WMA C that includes: • Summary of previous work by PNNL documented in PNNL-24740 (Alternative Conceptual Models of the Subsurface at WMA C, 2017); • Summary of previous work by WRPS, PNNL, and INTERA that is in the process of being documented in RPP-RPT-61239 (*Multiple Lines of Evidence and Modeling Results for Heterogeneous Alternative Conceptual Models of the Subsurface at Waste Management Area C*, in preparation).
PL3-15	Section 3.3, p. 3-9, lines 19-27	Using estimates of past releases from tanks is a good starting point; however, there are other releases from ancillary equipment and pipelines that will increase the total volume released. And, *all* these releases must be considered.		Please elaborate as to how you plan to treat releases from other non-tank sources.	This analysis has considered all known past losses and releases as described in in Section 2-1 (INVENTORY ESTIMATES FOR PAST WASTE RELEASES TO THE VADOSE ZONE). Each release evaluated has been identified using the correct WID ID number in Table 3-1 consistent with those identified in Figure 2-14. These same releases with correct WIDs ID numbers are used in Section 2.1. Descriptions of UPR's associated with WMA C but not considered in the analysis are also provided in Section 2.1.
PL3-16	Section 3.3, p. 3-9, lines 23-25	Once released, Tc-99 is difficult to detect in soil except by direct sampling.	Cs-137 (and other gamma emitters) are detectable and served to help estimate contaminated soil extent from any release.	Please explain what you mean by using the Tc-99 release, as Cs-137 and Tc-99 travel at very different rates through the soil to groundwater.	The text states: "...the current estimates for Tc-99 releases have been used as the basis for a nominal abstracted leak inventory used in the initial calculations." The intent for the text is simply to identify the current estimates of Tc-99 contained in Revision 4 of RPP-ENV-33418 (mentioned in the first sentence of the section) as the basis for the inventory of Tc-99 used in the past leak analysis.
PL3-17	Section 3.4, p. 3-9, lines 43-46	This is a pretty broad statement that neglects to mention that the effect of clastic dikes on fluid transport is a function of the total volume of release, the rate of release and the relationship of the clastic dike to dominant flow direction. Dikes may serve as both dams and preferential pathways during transport.		Please elaborate.	The following paragraph states: "However, these features may form preferentially faster flow pathways under conditions closer to saturation, such as may have potentially occurred following leak releases. As a result, a specific analysis case has been set up to evaluate the potential effect of a clastic dike on transport of contaminants from past leaks through the vadose zone (see Section 4.4)."
PL3-18	Section 3.5.2, p. 3-11, Table 3-2	The table requires further evaluation and raises several questions.	The Kd for Cs-137 may be lower if high Na is present, as both compete for the same sorption sites. Tributyl phosphate can also result in anionic complexes which alter the Kd of the complexing cation.	Please explain why CN is not modeled when it is already present in the groundwater. Explain why Cs-137 was not modeled. Include a range of Kds for the contaminants whose mobilities are influenced by background cations and complexing agents (ex. Cs-137)	We will elaborate to provide the context for choosing the Kd values. Following discussion has been added and expanded upon. after line 9 on p. 3-11" The Kd based (linear isotherm) sorption model is best used to represent adsorption processes when contaminant concentrations are low relative to the adsorption capacity and variability in mineralogy and geochemical conditions are minimal along the flow path. Since Kd value is a lumped parameter it neglects any time varying and spatially varying chemical conditions that would likely happen near the origin of the tank leak. Some examples of geochemical factors that could influence the mobility of selected constituents in the near field environment impacted by tank wastes could include: - The presence of synthetic chelating agents such as EDTA in some tank wastes that could affect the overall mobility of certain constituents like Co-60 and cyanide or other metals like PU and Am. - The presence of high sodium concentrations and other constituents found in some tank wastes that could affect the overall ion exchange and adsorption process and could lead to enhance the mobility of typically immobile constituents like Cs-137 and other metals. - The direct dissolution of soil components by high pH tank wastes that could impact the potential overall porosity and hydraulic properties of vadose zone sediments. A detailed discussion of important geochemical processes that could affect the overall mobility and transport of key constituents of concern found in tank wastes is provided in Section 6 of PNNL-16663. However, it is

Comment No.	Location	Comment	Basis	Recommendation	Final Disposition
					also recognized from various soil characterization studies that the waste stream-sediment interactions that occur within a short distance of the leak lead to complex mineral dissolution and precipitation reactions that buffer the pH and thereby reduce the variability in local geochemical conditions (from ambient conditions) within a short distance. A discussion of geochemical studies of vadose zone sediments in the vicinity of a postulated leak at tank C-105 and a tank waste losses in the vicinity of the 200-UPR-82, provided in Sections 3.3.1 and 3.3.2 of PNNL-17154, have provided considerable evidence that these geochemical effects that could potentially have affected the mobility of constituents of normally immobile metal constituents were limited to shallow depths that directly came into contact with tank wastes in these location. Given that the vadose zone is much thicker than the extent of the reaction front over which buffering occurs, for the majority of the transport distance in the vadose zone, a Kd based sorption model is deemed adequate due to large sorption capacity compared to the contaminant concentrations. For more details of this approach and applicability of empirical Kd model see discussion in PNNL-17154. For WMA C, the Kd values are chosen that are representative of low-salt, near-neutral waste chemistry assuming "intermediate" impact zones, which are defined as zones (or areas) in which the acidic or basic nature of the released waste was expected to have been largely neutralized by reaction with the natural sediment. However, if the focus of evaluation were on contaminant transport near the leak location at the time of leak, we would have used a more sophisticated sorption model. Given that was not the objective of the study; for the time scales and length scales of evaluation undertaken, a Kd based model is deemed appropriate. Just like any other parameter, the Kd value is uncertain and can vary. The values chosen here (shown in Table 3-2) are the best estimate values. We will clarify and acknowledge the uncertainty in these estimates so that there is no confusion (for example, PNNL-17154 (Table 3-9), provides a minimum and maximum estimates of Kd values besides the best estimate).
PL3-19	Section 3.6.1, p. 3-13, lines 3-6	The document discusses source term contamination masses without mentioning the specific nodes where they are input into the model.	The document makes reference to "nodes representing the estimated location and duration of the occurrence of the leak."	Please explain where these contaminants are entered into the model and the technical basis for this placement.	The text of Section 3.6.1 is changed as follows: "The source term is input directly as a mass of contamination and associated water volume into the STOMP© model at nodes representing the estimated location of the leak. As indicated in Section 2, the tank leaks appear to be associated with cascade lines or spare inlets that occur at or above the shoulders of the tanks. Therefore, source term is applied to the nodes representing the elevation of the tanks approximately halfway between their base and top for the estimated duration of the occurrence. The masses and volumes of the leaks are discussed in Section 2.1."
PL3-20	Section 3.6.2, p. 3-13, line 43	The document gives n as a dimensionless fitting parameter without providing an explanation for it.		Please describe this fitting parameter (n) and its derivation and its variability.	Text is modified as follows: "α = a fitting parameter related to the air entry or bubbling pressure of the soil (cm-1). n = a fitting parameter related to the shape of the retention curve (dimensionless). This parameter is fixed for each HSU. m = a fitting parameter related to the shape of the retention curve assumed equal to 1 - 1/n, per the recommendation in van Genuchten, 1980." The text provides two references to explain the van Genuchten fitting parameters: van Genuchten, 1980, "A Closed-form Equation for Predicting the Hydraulic Conductivity of Unsaturated Soils," and EPA/600/2-91/065, "The RETC Code for Quantifying the Hydraulic Functions of Unsaturated Soils." The text also identifies Mualem, 1976, “A New Model for Predicting the Hydraulic Conductivity of Unsaturated Porous Media,” to explain the "n" parameters use in developing the unsaturated hydraulic conductivity relationship to moisture content and saturation. EPA/600/2-91/065 provides several examples that describe the variability of the fitting parameters.
PL3-21	Section 3.6.2, p. 3-14, lines 9-11	The document gives *l* as a dimensionless pore-connectivity parameter without providing an explanation for it.		Please explain this “pore connectivity” that appears to be constant.	Text is modified as follows: "...l is a pore-connectivity parameter (dimensionless) that accounts for the alignment of pores in the direction of flow, and for the flow path tortuosity. Mualem (1976) estimates the pore-connectivity to be ~0.5 for many soils, and it is assumed to equal 0.5 in this analysis."

Comment No.	Location	Comment	Basis	Recommendation	Final Disposition
PL3-22	Section 3.6.3, p. 3-15, lines 24-26	Without effectively and completely addressing uncertainty in parameter values, the end result is just that much more uncertainty.		Please clarify what is meant.	Text is modified as follows: In the current analysis, it has not been possible to run fully probabilistic analyses of parameter uncertainty because of the large simulation times associated with running the numerical representation of the vadose zone and aquifer systems. Instead, parameter uncertainties have been addressed by performing a range of deterministic calculations that span the range of the parameter uncertainties. The parameters selected in a few of the scoping cases were based on evaluation of uncertainty distributions developed for conducting the uncertainty analysis performed in the RPP-ENV-58782. While this approach is limited in its ability to represent the full parameter space, it illustrates the effects of uncertainties associated with each input parameter. The paragraph will follow the updated first paragraph for Section 3.6.3 proposed in the disposition for comment PL3-25.
PL3-23	Section 3.6.3.1, p. 3-18, line 15	The 11,000 m/d result was obtained in a different part of 200 East Area and project to WMA C without an adequate technical basis.		Explain why this value is used here.	Presumably, the comment refers to the pumping test that was conducted at well 299-E33-268 (DOE/RL-2015-75, 2016 , *Aquifer Treatability Test Report for the 200-BP-5 Groundwater Operable Unit*) where the test results estimated an average hydraulic conductivity of 18,200 m/d (59,711.3 ft/d). The result of this test is not the basis for the hydraulic conductivity value used in the WMA C analysis. The hydraulic conductivity value for the WMA C analysis is derived from estimates developed within the CPGWM (CP-47631, 2015, *Model Package Report: Central Plateau Groundwater Model Version 6.3.3*) that range between 5,802 m/day and 17,000 m/day. Using those hydraulic conductivity estimates and a layer thickness weighted averaging scheme, the effective hydraulic conductivity is estimated to be 11,000 m/day for the entire aquifer around WMA C. Incidentally, CP-47631 (2015) predates DOE/RL-2015-75 (2016) and therefore does not include those results as part of the CPGWM Version 6.3.3 calibration.
PL3-24	Section 3.6.3.2, p. 3-18, lines 25-29	As explained, it seems that the discretization is not carried through if "standard" values of hydrologic parameter values are assigned to multiple cells.		Please elaborate.	The discretization used in the base model does not necessarily affect the assignment of hydraulic properties used for each HSU. Each node in the numerical model (i.e., the discretization) represents a distinct location in space as defined by the unique set of horizontal (x and y) coordinates and vertical (z) elevation. Each node is assigned the hydrogeologic properties associated with the HSU containing it, as determined by the node coordinates and elevation and the three-dimensional extent of the HSU as defined in the RPP-RPT-56356 geologic models. Every node contained within a particular HSU is assigned the hydrogeologic properties associated with that HSU. No changes are recommended to lines 25-29 Propose to insert following text after line 44 on p. 3-18: For one of the cases used the scoping analysis (i.e. heterogeneous model; see Case 4b in Table 4-1in Section 4.0), the assignment of vadose zone hydraulic properties based on moisture contents represented an alternative conceptual model to the base case. Details of the development of this model and how vadose zone properties were assigned to various hydrologic units in this specific model is described in Appendix F of RPP-ENV-58782 and RPP-ENV-58806. This case is meant to examine the effect of heterogeneous treatment of hydraulic properties of sediments in the vadose zone on impacts of past releases. The bulk or mean water flow and contaminant transport in the vadose zone, according to the model results, do appear to remain within the WMA C perimeter fence. However, the model construct in and of itself does not contain contamination within the perimeter fence. The model simulates contaminants associated with the sources moving through the vadose zone in accordance with the hydraulic and transport parameters used in the mathematics of the flow and transport equations. The EHM approach addresses bulk or mean water flow and contaminant transport, in accordance with the intent of the analysis."
PL3-25	Section 3.6.3.2, p. 3-18, lines 31-44	There are numerous thin, volumetrically insignificant lamina/strata that are perhaps discontinuous (i.e., lenses) but which have a significant effect on the infiltration of fluid; in effect, creating a "stair step" pattern of infiltration. These volumetrically		Please add and correct to test the effects of these units on flow and transport.	New paragraph replaces the current first paragraph of Section 3.6.3: "This section describes the implementation of STOMP© in the WMA C PA for evaluation of the groundwater pathway. This model is the starting point for the scoping analyses presented in Sections 4 and 5. The scoping analyses have the same general structure, but have been modified from the model described here to address alternative assumptions in the representation of the transport of contaminants from the leaks. These alternative assumptions include differing hypotheses about the leaks themselves, the geological setting (including consideration of heterogeneous representations of the subsurface), and a number of hydrological parameters. In addition, the

Comment No.	Location	Comment	Basis	Recommendation	Final Disposition
		insignificant, but transport significant units are omitted from these conceptual models.			aquifer gradient changed in magnitude and direction when the leaks were arriving at the water table; consequently, separate scoping analyses have been developed to represent that effect. The model described in this section forms the basis for all these subsequent alternative models." This new paragraph is followed by the text identified in the disposition to comment PL3-22.
PL3-26	Section 3.6.3.2, p. 3-19, Figure 3-6	Implicit in this construct is that contamination in the subsurface is contained within the perimeter fence, a construct that does not represent reality.	With lateral spreading in the vadose zone, contamination has spread beyond the footprint outlined by the perimeter fence.	Please correct and represent an approximation that would provide a conceptual representation of a larger magnitude and extent of a contaminated subsurface.	The bulk or mean water flow and contaminant transport in the vadose zone, according to the model results, do appear to remain within the WMA C perimeter fence. However, the model construct in and of itself does not contain contamination within the perimeter fence. The model simulates contaminants associated with the sources moving through the vadose zone in accordance with the hydraulic and transport parameters used in the mathematics of the flow and transport equations. The EHM approach addresses bulk or mean water flow and contaminant transport, in accordance with the intent of the analysis.
PL3-27	Section 3.6.3.4, pp. 3-25 & 3-26, lines 5-12 & 1-5	This appears to be describing how properties are derived for each HSU. But properties within each HSU can vary significantly, yet you seem to be averaging values that have already been averaged out by your method of “upscaling”, in effect removing heterogeneity that may import to fluid flow and transport.		Please clarify.	The section does describe how properties are derived for each HSU. As stated in the text: "A stochastic model of variable moisture or tension-dependent anisotropy provides the framework for upscaling small-scale measurements to the effective (upscaled) properties for the large-scale vadose zone (Polmann 1990). The upscaling processes factor the inherent spatial variability that occurs on different scales in heterogeneous media into the field scale parameter estimates (“Stochastic analysis of moisture plume dynamics of a field injection experiment” [Ye et al. 2005], 'Estimation of effective unsaturated hydraulic conductivity tensor using spatial moments of observed moisture plume' [Yeh et al. 2005])." The stochastic model mentioned takes small-scale or laboratory measurements and produces EHM parameters applicable to the bulk or mean water flow and contaminant transport on the field scale in each HSU.
PL3-28	Section 3.6.3.4, p. 3-26, lines 11-13	Just before in the text you are describing a process of averaging multiple times that in effect removes the heterogeneity.		Please explain.	The section does describe how properties are derived for each HSU. As stated in the text: "A stochastic model of variable moisture or tension-dependent anisotropy provides the framework for upscaling small-scale measurements to the effective (upscaled) properties for the large-scale vadose zone (Polmann 1990). The upscaling processes factor the inherent spatial variability that occurs on different scales in heterogeneous media into the field scale parameter estimates (“Stochastic analysis of moisture plume dynamics of a field injection experiment” [Ye et al. 2005], 'Estimation of effective unsaturated hydraulic conductivity tensor using spatial moments of observed moisture plume' [Yeh et al. 2005])." The stochastic model mentioned takes small-scale or laboratory measurements and produces EHM parameters applicable to the bulk or mean water flow and contaminant transport on the field scale in each HSU.
PL3-29	Section 3.6.3.4, p. 3-28, Table 3-5	This summarizes various values for each HSU, but each HSU contains multiple cells. How does one go from this to input parameter values for each cell?		Please explain.	The EHM parameters associated with the different HSUs are assigned to each node where the interpolation of the RPP-RPT-56356 geologic models onto the model grid indicates each HSU exists.
PL3-30	Section 3.6.3.5, p. 3-28, lines 13-15	There are multiple paleo-flood channels throughout 200 East Area. Are you talking about the major paleochannel that extends southeast from Gable Gap, or some other? What is the basis for this statement?		Please elaborate.	Concur. Have added a figure showing general interpreted location of the paleochannels relative to WMA C.

Comment No.	Location	Comment	Basis	Recommendation	Final Disposition
PL3-31	Section 3.6.3.5, p. 3-29, lines 1-3	That's the current condition, but it hasn't always been the case when the B Pond mound created a clear and distinct groundwater gradient.		Please correct.	Entire paragraph has been modified as follows: Historically, groundwater flow beneath WMA C was difficult to measure because of the scarcity of monitoring wells, the presence of the hydraulic divide, the hydraulic gradient is very small, and the hydraulic conductivity is very high in this region of the Hanford Site. For example, well 299-E27-7 had been considered an upgradient well, but groundwater contamination detected at this well in the late 1990's raised concern of the representativeness as an upgradient well for WMA C (DOE/RL-2016-67, 2016). In addition, the variable operational liquid discharges at 216-B-3 Pond system and other large discharge sites in 200 East Area impacted the water table. The direction of flow appeared to be primarily to the southwest during operations, although the water table maps were essentially indeterminate with respect to magnitude of the gradient (BNWL-B-360, 1974, "Selected Water Table Contour Maps and Well Hydrographs for the Hanford Reservation, 1944-1973). During the 2000's, groundwater flow direction appears to have been predominantly to the southwest, with a shift to the south-southwest based on observed contaminant migration (DOE/RL-2009-77, 2010). The uneven surface of the basalt bottom of the aquifer also contributes to the difficulty of estimating quantity of flow. The aquifer thickness appears to vary by about ~5.5 m (~18 ft) in the vicinity of WMA C based on the top of basalt contacts in wells 299-E27-7, 299-E27-22, and 299-E27-155 (DOE/RL-2009-77, 2010). The current WMA C monitoring well network consists of three upgradient wells, seven downgradient wells, and two cross-gradient wells (DOE/RL-2016-67, 2016). The water table continues to recover from the operational liquid discharges, and the projected equilibrium state is expected to be similar to its pre-Hanford behavior described in Section 3.1.9.2 and Appendix C of RPP-ENV-58782 and RPP-ENV-58806. As a result of these forecasted changes, the post-closure position of the water table and associated hydraulic gradient can only be evaluated through modeling. Consequently, the groundwater flux in the aquifer beneath WMA C is calculated on the basis of the aquifer hydraulic properties, and the hydraulic gradient projected to exist in the future.
PL3-32	Section 3.6.3.5, p. 3-29, lines 16-17	This statement is true only if natural conditions prevail.	The text states "Appreciable changes in hydraulic gradient are not expected in the future once the hydraulic heads stabilize."	Please clarify this statement.	Entire paragraph has been modified as follows: The hydraulic heads around WMA C are expected to continue declining slowly (Figure 2-11) until they stabilize around 119.5 m (392 ft) (CP-47631). This stabilization is estimated to occur approximately 100 years into the future (CP-47631). The gradient is generally expected to slope from northwest to southeast with a value of ~0.00002 m/m, which is close to the one estimated to have existed prior to start of Hanford operations (Figure 3-10). Appreciable changes in hydraulic gradient are not expected in the future while land use remains as forecast and once the hydraulic heads stabilize.
PL3-33	Section 3.6.3.5, p. 3-29, lines 19-24	This paragraph mixes past behavior during operations with simulated post-closure conditions.	If you can't approximate historical releases and their movement through the vadose zone how can an approximation to 10,000+ be applied or informative.	Please clarify and keep these two separate.	Have modified the 1st sentence of this paragraph to say "…past leaks, from when the leaks occurred to present day conditions…".

Comment No.	Location	Comment	Basis	Recommendation	Final Disposition
PL3-34	Section 3.6.3.5, p. 3-30, lines 1-11	This bullet needs clarification as to what is meant.	Are you saying that the model is not a good predictor of travel time?	Please elaborate and clarify.	Added bullet as follows: • All other scoping analyses have assumed a constant steady-state aquifer gradient magnitude and orientation. These have been chosen to be consistent with the long-term gradient assumed in RPP-ENV-58782 and RPP-ENV-58806 with hydraulic heads representative of past conditions to take account of the shorter travel distance in the vadose zone compared to the post-closure period. Since the orientation of this steady state gradient selected for the scoping cases does not correspond with the transient changes in water table conditions of the past, the concentrations calculated in these analysis cases will not correctly calculate concentrations at any point in space. So, for instance, direct comparison of the concentrations at well 299-E27-23 with model concentrations at the location of 299-E27-23 do not give meaningful comparisons. However, the results of scoping cases are very appropriate for comparison against the first arrival of Tc-99 observed in nearby groundwater wells. Thus, comparisons of modeling results for these cases with this specific observational metric is emphasized for these sets of steady state flow analysis cases. However, they do permit evaluation of peak concentrations as a function of distance from the source.
PL3-35	Section 3.6.3.5, p. 3-30, lines 13-16	This result was obtained as a calibration value based on some pump test data from the area of WMA B-BX-BY.	In an area of highly heterogeneous glaciofluvial sediments, the assumption that this applies everywhere in 200 East is not valid without specific proof from the vicinity of WMA C.	As the value at WMA B-BX-BY comes from a paleochannel, please justify this use at WMA C.	The original comment "This result was obtained as a calibration value based on some pump test data from the area of WMA B-BX-BY" is not factually correct. The development of the aquifer hydraulic properties is presented in Appendix C of RPP-ENV-58806. The WMA C RCA adopted flow hydraulic and contaminant transport properties derived from results developed from the calibrated Central Plateau Groundwater Model (CPGWM, CP-47631, 2015, *Model Package Report: Central Plateau Groundwater Model Version 6.3.3*, Rev. 2, INTERA, Inc., Richland, Washington). The CPGWM calibration places emphasis on matching water level data from the 1940s, early 1950s, and first decade of the 21st century to estimate hydraulic properties using flow conditions relatively unperturbed by site operations. As discussed in Section C.1 of the appendix, the scale of the WMA C RCA requires aquifer flow hydraulic property estimates consistent with large area model calibration studies that are on the appropriate spatial scale. In evaluating available information for the aquifer at WMA C, hydraulic conductivities derived from a calibrated model are regarded as more applicable than direct measurements by permeameter, slug, or pump tests.
PL4-1	Section 4	How do your model predictions agree with models simulating groundwater flow and transport for 200 BP-5? Have you made any comparisons?		Please elaborate.	Groundwater in the vicinity of WMA C has also seen impacts by other COPCs (e.g., nitrate, sulfate, for example), but Tc-99 is the contaminant that accounts for the majority of the past and current dose and risk impacts to groundwater at WMA C. The focus of the analysis cases presented in this section is to provide improved understanding of the phenomena and parameters in the vadose zone that have led to the current state of contamination below and near WMA C. The focus of the analysis cases reported in this section is on Tc-99 contamination, which is unambiguously the result of past UPRs from WMA C. Groundwater in the vicinity of WMA C has also seen impacts by other COPCs (e.g., nitrate, sulfate, for example), but Tc-99 is the contaminant that accounts for the majority of the past and current dose and risk impacts to groundwater at WMA C. The goal of the scoping analyses is to match, to the extent possible, the first arrival times of the contamination at the water table and general concentration levels as observed in monitoring wells. First arrival is primarily influenced by the behavior of the leaks themselves, and by flow and transport behavior in the vadose zone. Changes in the saturated zone affect time to first arrival only in that the changing height of the water table (hence thickness of the vadose zone) needs to be taken into account. Since changes in the water table are not included in the scoping analyses presented in this section, they should not be expected to (and indeed do not) provide good comparisons with either the peak concentrations in well data or the general shapes of the breakthrough curves (sharp rises and falls in concentration). These features of the data are believed to be associated with shifts in the direction of the groundwater flow. This aspect of the breakthrough curves is not well represented by the scoping cases presented in this section, since they all assume a constant groundwater flow rate and direction. Analyses that take account of the changing water table are presented in Section 5, and those analyses are intended to provide insight into the rapid rise and fall of observed data, and how the plume has moved between wells. The scoping analyses presented in this section evaluate changes in calculated groundwater impacts that result from changes in input parameter estimates or changes to a conceptual model, such as the interpretation of the hydrogeologic units. The range of analysis cases are generally intended to evaluate changes in parameters and modeling assumptions, to demonstrate the effect that alternative assumptions and estimates have on the groundwater arrival times and concentrations in and around the tank farm. These scoping analyses have evaluated a variety of alternative assumptions regarding the vadose zone, including extensive evaluations of the effect of spatial heterogeneity

Comment No.	Location	Comment	Basis	Recommendation	Final Disposition
					on transport of contaminants in the leaks. The body of work on vadose-zone heterogeneities has been documented in a separate report (RPP-RPT-61239), the findings of which are incorporated into the current analysis. To emphasize, the scoping cases in this section are focused solely on alternative assumptions about conditions in the vadose zone. The reader is directed to Section 5 for the complete model that takes all of the relevant phenomena into account.
PL4-2	Section 4	Where is the fine scale heterogeneities conceptual model and its analysis? Without such an analysis, the current work is incomplete and unacceptable.		Please correct.	See disposition for Comment PL4-1.
PL4-3	Section 4	The scoping analyses for various cases do not match reality. This means that the model has not been validated with real data and therefore constitutes a poor tool to project out to 10,000+ years. Examination of various input parameters/cases obscures the fact that the basic model is not validated by real data.	For example, the direction of groundwater flow changes are not incorporated, lack of groundwater monitoring data from within the farm (i.e., no wells) where plumes are "originating", mismatch with existing groundwater data on constituents in various wells and times of arrival (shown on various conceptualizations (e.g., Figs. 4-3, 4-5, 4-7, 4-9 etc.).	Please correct.	See disposition for Comment PL4-1.
PL4-4	Section 4	Sensitivity scoping analysis is performed only with Tc-99 in this section. However, in section 9.6 of RPP-ENV-58806 the scoping is done with nitrate and chromium.		The analysis should be included in this document with all the important contaminants of concern.	See Response to PL4-1.
PL4-5	Section 4, p. 4-1, lines 10-12	There are numerous sources of artificial recharge besides the leaks.		Please clarify.	See Response to PL4-1.
PL4-6	Section 4, p. 4-1, lines 26-27	A good approach, but keep in mind that there were no groundwater monitoring wells in place during operation of C Farm.	The existing groundwater monitoring network was started in 1989, with subsequent additions. There were no groundwater monitoring wells in place during the operating years from 1945 to 1980, so it is entirely possible that some episodes of contaminant arrival in groundwater may have occurred, given possible preferential pathways and the volume of artificial recharge—often in large increments. While there are no data, this possibility should be considered.	Please address.	Added a footnote to the following sentence in the 4-1 disposition. The goal of the scoping analyses is to match, to the extent possible, the first arrival times of the contamination at the water table and general concentration levels as observed in monitoring wells. (add footnote) Footnote: The monitoring network was started in 1989, with subsequent additions. There are therefore no observations prior to that time with which to compare. Any contamination that may have reached groundwater during that time is not included in the current assessment. There is no evidence suggesting that any such contamination occurred.
PL4-7	Section 4, pp. 4-3 & 4-4, Table 4-1	It would be useful to restate the assumptions, boundary conditions, and other fixed conditions in the DOE 435.1 PA here. A summary table would be helpful.		Please consider.	All the key assumptions and inputs including boundary conditions are stated in Section 3.6.

Comment No.	Location	Comment	Basis	Recommendation	Final Disposition
PL4-8	Section 4.1.1, p. 4-6, Figure 4-1	Do the calculated and observed curves fit as well for other wells?		Please clarify.	CP-47613, Rev. 2 (CPGWM version 6.3.3) provides in Appendix A hydrograph comparisons of measured data and modeled results for several wells, including wells located near WMA C: 299-E27-12, 299-E27-13, 299-E27-14, 299-E27-15, and 299-E27-21. Figures 4-43 through 4-45 in that document provide information regarding the overall performance of the model calibration in matching the measured data. Figure 4-43 presents the calibration misfit probability density for the two temporal data sets used in the calibration (1948 to 1953 and 2000 to 2009). Figure 4-44 presents the calibration misfit cumulative probability curve, and Figure 4-45 provides a comparative view of the model results and measured data. Table 4-10 in CP-47613, Rev. 2 includes the calibration statistics, indicating that the average error and root mean square error were 0.03 m and 0.86 m, respectively. These values compare favorably to the calibration results for 200 East Area indicated in Figure L-33 of DOE/EIS-0391: residual mean of 0.739 m and root mean square of 1.572 m.
PL4-9	Section 4.2.1, p. 4-9, Figure 4-3	Groundwater flow direction wasn't always to the southeast, as depicted here. This is presumably an assumption for groundwater flow direction. Please clarify. Also, what transverse transmissivity was used in these plume simulations? Or how do you account for the narrow shape of the plume? Does it match current groundwater monitoring data?		Please clarify.	The following paragraphs have been added at the beginning of each case subsection (i.e. Sections 4.1, 4.2, etc.; Yes, this will result in redundancy, but will help clarity): The sensitivity cases presented in this Section represent an attempt to compare alternative modeling assumptions to field data, with a view to identifying modeling assumptions that are either consistent or inconsistent with monitoring data. Monitoring data do not exist prior to 1989, and comparisons of the model with data are only made subsequent to that time. The cases have been run as blind trials; that is, the inputs are best estimates derived as discussed in Sections 2 and 3, and the models run in a forward manner from the time of the leaks to today. There are no fitting parameters in the model, and no adjustments to model inputs have been made to improve the comparisons. The intent is to identify which sets of inputs are contradicted by data, and hence develop improved understanding of the implications of various alternative assumptions on the comparison between the model and data. The model produces spatial distributions of concentrations in groundwater, resulting from the different locations and timing of the leaks. There are no data under WMA C to corroborate these concentration distributions; the model can only be compared to data at the monitoring wells. As discussed in the introduction to this section, because of the complicating effect of the time-varying water table on monitoring data, it is not appropriate to compare the model results in this Section at the location of the monitoring wells. The water table is flat and changing direction, and when concentrations increase in a particular well, it is because the aquifer gradient has shifted in its direction. Similarly, when concentrations begin to decline in a particular well, it is because plume is moving in a different direction. The static gradient applied in the models discussed in this section is not necessarily oriented in the same direction as the real water table at any given time in the analysis. Instead, the model is used primarily for comparison with time of arrival of the plume, and secondarily to calculate concentrations at fixed distances from the releases, and this is used as an indicator of the effect of distance from the leak on groundwater concentrations. The sensitivity cases presented in this Section address alternative assumptions related to the leaks and the vadose zone. Model comparisons with the changing water table are presented in Section 5, along with comparisons with field data. This text would be followed by a few section-specific sentences about the case considered in the section, e.g. Case 3 addresses changes in recharge rate... etc.
PL4-10	Section 4.2.1, p. 4-10, Figure 4-4	I would not call these curves a best fit.		Please elaborate.	See Response to PL4-9.
PL4-11	Section 4.2.2, p. 4-11, Table 4-2	The decline in values for Tc-99 at differing distances downgradient is minimally due to radioactive decay. What longitudinal and transverse disparities were used or other factors that account for both the groundwater flow velocity and decline in concentration?		Please address.	See Response to PL4-9.
PL4-12	Section 4.2.2, p. 4-12,	How do you derive multiple plumes at different starting points within C Farm		Please elaborate.	See Response to PL4-9.

Comment No.	Location	Comment	Basis	Recommendation	Final Disposition
	Figure 4-5	when there are no groundwater monitoring data to corroborate such calculations?			
PL4-13	Section 4.2.2, p. 4-13, Figure 4-6	As well E27-14 is approximately at the fence line, one might expect a closer match with the red curve for 20 m downgradient from C-105.		Explain why this is not the case.	See Response to PL4-9.
PL4-14	Section 4.2.2, p. 4-14, Figure 4-7	The first detection of Tc-99 in the current groundwater monitoring network was in well E27-14, followed by detections on the opposite side of the farm in well E27-15. This does not agree with your modeling in which you generate plumes from C-105 without any groundwater monitoring data from within the farm. This needs either a technically credible explanation, or a re-analysis.		Please elaborate.	See Response to PL4-9.
PL4-15	Section 4.3.2, p. 4-16, lines 23-24	Given that the current groundwater monitoring data begins in 1989-90, the fact that the plume arrives early may be in fact a legitimate case.	There are no groundwater monitoring data available to say that this could not have been the case.	Please qualify and revise conclusions.	See Response to PL4-9.
PL4-16	Section 4.3.2, p. 4-17, Table 4-3	The values for the 20 m downgradient do not match well with actual results either in timing or magnitude. This casts doubt on the credibility of your predictions of arrival times and estimated concentrations at the 60 and 120 m downgradient locations.		Please explain or revise.	See Response to PL4-9.
PL4-17	Section 4.4.1, p. 4-23, Figure 4-13	Figure 4-13 showing arrival times for well 299-E27-14 and well POC's not matching as they do in the other figures.		Explain what the cause of this discrepancy is.	See Response to PL4-9.
PL5-1	Section 5.1	STOMP was used by the TCWMEIS to solve flow equations from 1944 to 1960. Ecology was not aware as stated here that an impractical amount of time was required to solve the equations.		Explain where the decision to not model prior to 1981 came from.	Following new paragraph added at the start of Section 6.1 in the Revision 2 update. As discussed in Section 4, monitoring data for groundwater concentrations are believed to be significantly influenced by transient changes in the water table that have occurred between 1944 and today. In the scoping cases presented in Section 4, these transient effects were ignored, to focus on the representation of the leaks and the vadose zone, while avoiding the complications introduced by the changing water table. The model described in this section is intended to address the changing water table, and to produce a model that can be compared directly with the groundwater monitoring data. Other aspects of the model described in previous sections of the report remain the same. Also, second paragraph to be reworded as follows: The model is run from 1944 forward, with leaks introduced at the times and in the quantities presented in Table 3-1. The representation of the vadose zone is the same as Case 1 in Section 4 and is run beginning in 1944 to produce the antecedent conditions for the leaks. During the time period between 1944 and 1981, data are unavailable for the groundwater levels at WMA C, and any changes that may have occurred during that time would not affect transport of contaminants in the vadose zone during that time. Although the first documented leak occurred in 1960, the groundwater monitoring results indicate that Tc-99 does not reach the water table until after 1981. Therefore, as a simplification and expedient for the model, water table fluctuations before 1981 are omitted from the model, and the period from 1944 to 1981 is simply simulated with the 1981 water table boundary conditions in the aquifer.

Comment No.	Location	Comment	Basis	Recommendation	Final Disposition
PL5-2	General, Section 5.1.1, p. 5-2, lines 7-8,	CPGWM presumably stands for Central Plateau Groundwater Model, but the acronym is not defined and not included in the List of Terms.	The use of acronyms should be kept to a minimum, and all acronyms should be defined.	Include CPGWM in the List of Terms.	This acronym is in the current acronym list.
PL5-3	Sections 5.1.2 & 7	It is not clear why the Central Plateau Groundwater Model and the Plateau to River model, although both using Modflow, are used for different purposes in this document. Explain why both models can or cannot perform the same function. Explain how they are calibrated to perform their intended purpose. A summary outlining the differences and similarities of the two models would be helpful for the public to understand how they are incorporated into the modeling.		Explain why both models can or cannot perform the same function. Explain how they are calibrated to perform their intended purpose. A summary outlining the differences and similarities of the two models would be helpful for the public to understand how they are incorporated into the modeling.	No text changes are recommended but here is the requested information. The Central Plateau Groundwater Model (CPGWM) was developed to evaluate contaminant concentrations in groundwater at decision points within the 200-PO-1, 200-UP-1, 200-BP-5, and 200-ZP-1 Groundwater Operable Units (OU). The intent of the CPGWM includes providing estimates of future groundwater contaminant concentrations to support risk screening, to support the evaluation of the efficacy of remedial alternatives, and to support design and optimization of remedies implemented on the Central Plateau. The CPGW Model calibration places emphasis on matching water level data from the 1940s and early 1950s to estimate hydraulic properties using flow conditions relatively unperturbed by site operations, and on matching water level data from the first decade of the 21st century to establish current flow conditions that typically represent initial conditions for predictive simulations. These goals align well with the goals of the WMA C modeling. The Plateau to River (P2R) model was initially developed to augment the CPGWM to address the fate and transport of contaminants in the 200-PO-1 Groundwater OU that are already outside of the CPGWM domain (DOE/RL-2009-85). The P2R model later supported COPC fate and transport in groundwater as part of the 200-BP-5 Groundwater Operable Unit RI (DOE/RL-2009-127, Draft A). The P2R Model structure was designed to span those portions of the 200-BP-5 and 200-PO-1 OUs that could potentially serve as a future or distant flow path for contaminants in the unconfined aquifer. Calibration of the P2R Model involved a steady state simulation that targeted March and April 2012, and a second calibration of the model that targeted the 6-year time period from 1/1/2006 to 1/1/2012. Although the two models differ in overall size and extent, and the gridding of CPGWM is more highly resolved horizontally (100 m by 100 m compared to 200 m by 200 m in the P2R model), the results of the two models' calibration are similar. Both calibration exercises indicate that the hydraulic conductivity of the material occupying the channel in the aquifer below WMA C is about 17,000 m/day, and the hydraulic conductivity of the Cold Creek material outside of the channel is about 400 m/day (CPGWM) or 109 m/day (P2R). The CPGWM appears to be the better choice as a basis for the hydraulic properties because of its emphasis on the Central Plateau and higher resolution of spacing within the domain, and the more rigorous and detailed hydraulic calibrations. The evaluation of upgradient sources of contamination, which included continuing sources at BX-BY, utilized and adapted the results of the P2R model (DOE/RL-2009-127, Draft A) because they are well suited to the analysis.
PL5-4	Section 5.3	There were *no* groundwater monitoring wells at WMA C during the period of operations (~1945-1980). The first well that was constructed at WMA C was 299-E27-7, located on the northeast side of the farm in what would then have been an upgradient location that would have had contaminant concentrations diluted by the groundwater mound (of very dilute concentrations) extending westward from B Pond that could mask contaminants in C Farm wells even in the 1989 monitoring network. A “compliant” groundwater monitoring network was not established at WMA C until 1989. The model results are being calibrated to known arrival times and concentrations/activities at WMA C wells. Several modeling results were dismissed because the contaminants arrived “too	Given this background it would be hasty to dismiss results showing a too-early arrival in a C Farm groundwater monitoring well if the potential for releases earlier than the establishment of the groundwater monitoring were not at least considered as a possibility.		Text has been added near the start of Section 6 in the Revision 2 updates to clarify that there is considerable uncertainty in impacts to groundwater due to lack of active monitoring at WMA C prior to 1989. There is lack of information (knowledge gap) prior to 1989 to confirm or refute the extent of impact of past leaks from WMA C on the groundwater. We will also add text to clarify that the purpose of Section 6 in the Revision 2 update (and any subsection therein) is not to reconstruct the past water-table conditions but to simply evaluate possible conceptual models of past water-table conditions as it may have fluctuated/shifted directions. There is no specific attempt to calibrate any of the models to historical field data.

Comment No.	Location	Comment	Basis	Recommendation	Final Disposition
		early" to match the existing groundwater monitoring data. The largest leak was at C-105, near the center of the farm. There are no groundwater wells directly beneath WMA C.			
PL5-5	Section 5.3, p. 5-11, lines 17-18	The text states "The results of the modeling provide a basis to evaluate the assumptions and uncertainties associated with the flow direction and magnitude during the operations period." As written, this paragraph, in effect, says that models are more reliable than actual field data. Using models to evaluate assumptions and uncertainties is circular logic and unacceptable because the models contain the inherent assumptions and uncertainties—the equivalent of asking the fox to guard the henhouse.		Please rewrite.	Added following revision to first paragraph of Section 6.3 in the Revision 2 update. The groundwater monitoring data may be interpreted as being the result of changes in flow direction and magnitude during the operations period. By introducing assumptions into the model that reproduce these trends, the model can produce insights as to the timing, magnitude, and orientation of the flow changes. The results also provide a basis to evaluate the estimates regarding inventory and volumes of past leaks for the purpose of better constraining estimates of the existing contamination. These aspects of the modeling analysis help provide some insight into the events and hydraulic conditions responsible for producing the measured concentrations levels and observed changes in the individual wells (e.g., locations and timing of source releases, the timing of changes in flow direction, and the varying magnitude of the hydraulic gradient during the gradual changes in flow directions).
PL5-6	Section 5.3.1, pp. 5-21 & 5-22, Figures 5-9 & 5-10	The figures may reflect an actual accurate monitoring well release of Tc-99 compared to the modeled results. But seeing how poorly the model results fit to the actual well data from the 2004 to 2016 period decreases the confidence that the model can estimate future impacts from past leaks.		More model verification over a longer time period is needed. There are statistical trending tests, like Mann Kendall, that perform a defensible best fit.	Added following new paragraph at the end of Page 6-14 in the Revision 2 update. It is useful to put the comparisons between model and data in Figures 6-9 and 6-10 in perspective. The model and its input parameters were developed almost wholly from inputs independent of the groundwater data. All of these inputs have large amounts of uncertainty in them, with the model implementation containing best estimates from within that uncertainty. These inputs include the structure of the model, the timing and magnitude of the leaks, the stratigraphy of the vadose zone and the parameters needed to represent flow through it. There was no calibration of any of these inputs with the groundwater data; the model was solely run as a forward calculation. To take account of the temporally varying aquifer gradient, reasonable estimates were used for the timing, magnitude, and initial and final orientations of the gradient. The transition of the orientation was represented by a rather simplistic counterclockwise rotation of a flat surface. No attempt was made to optimize these assumptions about the gradient to improve the match between the model and data. Given these observations about the model, and the amount of uncertainty surrounding many of the inputs, the matches between model and data shown in Figures 6-9 and 6-10 are surprisingly good. The model matched the peak concentrations and timing of the peaks in several of the key wells. Furthermore, from a qualitative perspective, the model reproduced the rapid decline in concentration in well 299-E27-23, and the rapid increase in concentration in Well 299-E27-21. As shown in Section 4, these rapid changes in concentration were not well described using a static water table. Where the model deviates from data, a likely cause may be found in the many uncertainties about the leaks: their timing, magnitude, and composition. A second potential cause of deviations between the model and data may be that the aquifer transition may have been considerably more complex than the simplistic rotation used here; such complexity could cause contamination to show up at times and locations not represented in the model. These observations suggest that the general conceptual model (the leaks, their transport through the vadose zone, and their subsequent distribution in the aquifer by a temporally changing gradient) is consistent with

Comment No.	Location	Comment	Basis	Recommendation	Final Disposition
					the groundwater monitoring data. This is not to suggest that this model is the only one that could explain the data. However, any alternative conceptual model would need to produce similar or better fidelity to the data to be considered credible. This is also not to suggest that the fit between the model and data is optimized; by modifying some assumptions in the model, it is likely that a better fit could be produced.
PL5-7	Section 5.3.2, pp. 5-21 & 5-22, Figures 5-9 & 5-10	Graphs in Figures 5-9 and 5-10 do not show a convincing match for field measurements and concentrations of Tc-99 predicted by modeling. Corresponding discussions, while acknowledging the discrepancies, appear to focus on defending the modeling approach.	We appreciate the effort to develop, and describe in the document, a clever and very complex conceptual model involving counterclockwise rotation of the hydraulic gradient. Time will tell how well this model reflects future contaminant fate and transport in the groundwater.	We suggest shifting the focus from defending the conceptual model utilized in modeling to emphasizing the apparent uncertainties and shortcomings of this or any other modeling approach due to the existing data gaps, including uncertainties about the trajectory of plumes moving in the aquifer.	See response to PL5-6.
PL5-8	Section 5.3.3, p. 5-23, lines 28-31	Regarding the following statement: "However, the modeling results do indicate that most of the Tc-99 observed in the monitoring wells located southwest of the farm originated from the sources inside the farm, and not from the UPRs that occurred away from the tanks." (also repeated in RPP-RPT-59625, page ES-9, 3rd paragraph). We note the following: Graphs in Figures 2-22 and 5-9 show an increasing trend of Tc99 concentration in groundwater well 299-E27-13 since 2013 (including recent measurements not shown on the graph). It appears that this increasing trend in 299-E27-13 is associated with the UPRs (1.3 Ci UPR-82 in 1969 and 2.7 Ci UPR-86 in 1971) instead the 1965-1969 releases inside the farm. This observation is consistent with DOE's suggestion of two sources for the Tc-99 contamination: one in the western side of WMA C, associated with the UPRs, and one in the southeast, associated with 100-series tanks (RPP-RPT-59197, page 2-	While the exact magnitudes of the UPRs and the releases inside the farm are unknown, the UPRs have contributed been between 25-50% of all Tc-99 releases into the groundwater, depending on the magnitude of Tc-99 releases inside the tank farm (Table 3-1). Measured concentrations of Tc99 in well 299-E27-13 show an increasing trend since 2013. Model inputs were manipulated to get certain desired results, and time will tell how well the model predicts contaminant fate and transport.	UPRs should not be disregarded as a major source of contamination to groundwater, contrary to the modeling results that UPRs away from the tanks are not major contributors to TC99 in groundwater. The document should include a discussion of model uncertainties regarding the magnitude of UPRs source releases from C-Farm tanks. The document should also acknowledge that the comparison of model simulated Tc99 concentrations in well 299-E27-13 does not reflect empirical data during the period of comparison (since 2000 to 2016).	Added that the release from tank C-105 that was estimated to occur between 1963 and 1967 (See Table 3-1) appears to be the dominant source of Tc-99 observed in groundwater in the monitoring wells. According to the inventory estimates in RPP-RPT-42294, it is the only release large enough and that occurred early enough to bring about the concentration levels observed in the monitoring wells. However, according to the model, most of the Tc-99 observed in the monitoring wells located southwest of the farm originated from the tank leaks, and not from the UPRs that occurred away from the tanks. Releases from UPR-81 (an acute release estimated to occur in 1969); UPR-82 (an acute release estimated to occur in 1969) and UPR-86 (an acute release estimated to occur in 1971) and the leak associated with C-110 (a continuous release 1971-1972) (See timing of these leaks in Table 3-1) occurred later than the release from tank C-105, and the modeling results exhibit the implications of this. Again, according to the model, the concentration of Tc-99 in the wells located nearest the UPRs is dominated by the Tc-99 contained in the release from tank C-105. The concentration of Tc-99 attributed to the Tc-99 contained in three UPRs peaks a few years after the concentration of Tc-99 peaks because of the tank C-105 release. Whether or not the release from tank C-105 is truly the dominant source of Tc-99 observed at the monitoring wells is unknown. Based on assumptions about the timing of releases given above, the modeling that was done suggests that the C-105 source may be the dominate source and that the Tc-99 originating from the UPRs may be a secondary source that has not yet been observed because it has not yet reached the water table. However, given the uncertainties in the timing and of the UPR releases and the magnitude of the overall Tc-99 inventories in 2 of the 3 releases (i.e. 1.3 Ci at UPR-82 and 2.7 Ci at UPR-86), use of other modeling assumptions about the releases at the UPRs relative to the assumed releases at C-105 could lead to different modeling results and conclusions about the relative importance of the UPR releases as major contributing sources to observed contamination to groundwater at WMA C.

Comment No.	Location	Comment	Basis	Recommendation	Final Disposition
		56, Section 2.3.4.2. While the exact magnitudes of the UPRs and the releases inside the farm are unknown, the UPRs have contributed been between 25-50% of all Tc-99 releases into the groundwater, depending on the magnitude of Tc-99 releases inside the tank farm (Table 3-1).			
PL6-1	Section 6	A variety of contaminants are present in the groundwater beneath WMA C. They were listed in Ecology's comments submitted for the WMA C RFI, including RPP-RPT-58297, and were also provided to DOE as comments for the BP-5 supplemental Sampling and Analysis Plan. The contaminants include Tc-99, I-129, tritium, nitrate, nickel, cyanide, arsenic, uranium (total and various isotopes), vanadium, copper, antimony (nonrad), selenium (nonrad), plutonium-239/240, and hexavalent chromium.	No analysis has eliminated WMA C as a source for these contaminants in the groundwater wells around WMA C.	Include all of the contaminants that are currently in the groundwater beneath WMA C as COPCs. See Attachment 3.	We concur with Ecology that a number of contaminants have been detected near or above background in groundwater in the vicinity from C-Farm. Some examples of this category of constituents would include arsenic, chromium, nickel, uranium, and tritium. Of course, observed concentration levels for some of these constituents could just reflect background levels but could also potentially reflect some local influence from past releases or losses from WMA C facilities. In addition, well monitoring results also show that groundwater in the vicinity of WMA C has also been impacted by both local and up gradient plumes that could be influencing the elevated concentration levels of some of these constituents. A thorough analysis of current contamination in vicinity of WMA C should not only include sources originating from WMA C but other contaminant sources nearby and up gradient of WMA C. The responsibility for the evaluation of contaminant sources affecting the unconfined aquifer in areas near and up gradient of WMA C and development of corrective measures for mitigation groundwater contamination has been the responsibility of the 200-BP5 OU Remedial Investigation/Feasibility study. We have made the following modification to the 1st paragraph in Section 2.3.3.3:, "Groundwater Contamination" "In SGW-59669, the results of sampling for 129 constituents across the WMA C monitoring network are provided (See Appendix B of SGW-59669). In that report, six analyses (cyanide, nickel, nitrate, sulfate, Tc-99, and uranium) are discussed in detail. We propose to add the following text after the third paragraph in Section 2.3.3.3, "Groundwater Contamination" "A number of other constituents have been detected at concentration levels near or just above background in groundwater wells near C-Farm. Some examples of these types of constituents include arsenic, chromium, nickel, uranium, and tritium. Concentration levels of some of these constituents may just reflect background levels but could reflect the potential local influences in groundwater from past releases or losses from WMA C tanks and/or ancillary facilities. In addition, past interpretations of well monitoring results in the general area of WMA C do show that groundwater in the vicinity of WMA C has been impacted by both local and up gradient plumes that could also have some potential influence on observed concentration levels for some of these constituents. Current groundwater contamination in vicinity of WMA C has been evaluated as a part of a broader remedial investigation/feasibility study for the 200-BP-5 OU (Cite 200-BP-5 OU RI). The feasibility study part of this evaluation is leading to the development of interim measures designed to mitigate current contamination in groundwater at WMA C as well as other areas of contaminated groundwater within the 200-BP-5 OU."

Comment No.	Location	Comment	Basis	Recommendation	Final Disposition
PL6-2	Section 6.1, p. 6-1, lines 23-25	This statement, in effect, says that the system is not understood well enough to replicate real results.		Please elaborate and correct.	The scoping analyses presented in Section 4 of this report provide comparisons of the STOMP© model to groundwater monitoring data to evaluate the credibility of alternative assumptions for the migration of the leaks from the time of their occurrence to today. As discussed in Section 4, the purpose of these analyses was primarily to compare with first arrival of the contaminant plume, since that metric is affected only by processes in the vadose zone, including the leaks themselves. As noted in Section 4.8, several analysis cases were inconsistent with data and additional analysis cases produced comparable results to each other, all of which were consistent with data. This means that those models could not be differentiated using the data, so none can be ruled out.
PL6-3	Section 6.2, p. 6-2, line 31	Cite PNNL-13895 for Kd "gravel correction" (if this is the case).	The source of the Kd values is not given.	Cite the source of the gravel corrected Kd values.	Have modified Table 3-5 to include the gravel fraction of the HSUs. have added the following sentence to the end of the first paragraph of Section 3.5.2 on Page 3-11: PNNL-17154 (2008), *Geochemical Characterization Data Package for the Vadose Zone in the Single-Shell Tank Waste Management Areas at the Hanford Site*, indicates that Kd values are typically lower for materials that contain significant amounts of gravel and should be corrected according to the equation Kd(gravel corrected) = (1.0-weight fraction gravel) * Kd(value determined using <2 mm material). The gravel weight fractions for the Backfill, Hanford H1/H3, and Hanford H2 HSUs are 0.54, 0.42, and 0.20, respectively (Appendix B of RPP-ENV-58782, 2016). Have included reference to PNNL-17154 (2008) within the parenthetical note, i.e., "(prior to gravel correction, PNNL-17154, 2008)."
PL6-4	Section 6.2, p. 6-2, line 41	Missing figure number should read "Figure 6-2."	The figure number is not given.	Correct the figure number.	Concur. Reference to Figure 7-2 has been added to text on p. 7-2 in the Revision 2 update.
PL6-5	Section 6.2, p. 6-2, line 41-46	The arrival time of contaminants appears highly sensitive to very small changes in Kd values. Going from 0.5 mL/g to 2 mL/g results in an arrival time difference of 9,000 years. For contaminants with Kd > 0, what is the uncertainty of their Kd values? How well are these values known? Just a small error could make a big difference in arrival time.	For example, the slightly sorbed constituents of I-129, Co-60, and uranium are assumed to have Kd values between 0.2 and 0.6.	Please discuss the uncertainty of Kd values and the effects of errors in Kd values on predicted arrival times.	In addition to disposition above, we have added the following text at the end of p. 7-2 in the Revision 2 update: "This screening analysis demonstrates for the setting of WMA C that small changes in Kd can result in a significant changes in the time of arrival at the water table . For example: going from a Kd of 0.5 L/kg to 1.5 L/kg can result in first arrival times increasing from years just over 1,000 yrs to between 6,000 and 7,000 years). For slightly sorbed constituents like I-129 (i.e. assumed Kd of 0.2 l/kg) and U (i. e. assumed Kd of 0.6 l.kg), small changes in assumed Kds can change the first arrival and timing of peak concentrations in the water table."
PL6-6	Section 6.3, pp. 6-4 & 6-5, lines 45-46 & 1-2	The text refers to a 5 m mixing zone.		Justify the assumed "mixing zone" depth in light of the fact that deeper wells show a depth distribution of some contaminants.	have modified sentence as follows: The aquifer mixing zone extends into the upper 5 m (16.4 ft) of the aquifer on the basis of the 5 m mixing zone dimension associated with Equation 747-4 in WAC 173-340-747. The elevated Tc-99 concentrations around WMA C appear to extend throughout the depth of the aquifer, indicating that the plume is well mixed (DOE/RL-2011-01, *Hanford Site Groundwater Monitoring Report for 2010*). Owing to the vertical and lateral dispersivities that are used to represent the contaminant transport through the unconfined aquifer system, the WMA C model groundwater concentration results appear to be relatively constant throughout the depth of the aquifer and there is little difference between the concentrations calculated in the upper 5 meters and those calculated through the entire thickness of the aquifer along the flow path.
PL6-7	Section 6.3.1, pp. 6-5 & 6-6	Text states that the model's predicted concentrations of tritium and Co-60 are not consistent with observed concentrations. In both cases explanations for the discrepancy are given, but these explanations were not developed into the model.		Please explain why the known mass depletion for the tritium transport model and the Kd value of 0.1 mL/g for Co-60 which better fits observed data are not used in the model.	Clarifying text has been added on page 6-6 to indicate that development of detailed fate and transport models for tritium and Co-60 are not undertaken as they are not observed in the groundwater in any significant concentration to be deemed contaminants of potential concern. It is only because of initial conservative modeling assumptions that any groundwater impacts were being predicted.

Comment No.	Location	Comment	Basis	Recommendation	Final Disposition
PL6-8	Section 6.3.1, p. 6-6, lines 2-3	The text discusses that Co is highly immobile in the absence of chelating agents.	There are chelating agents (e.g., CN, TBP) present in C Farm tanks, some of which must be present, as Co-60 is still mobile in several C Farm drywells.	Please justify the choice of this form of Co.	Text has been revised as suggested by Ecology during comment response on 9/4/2018: 'Co-EDTA anionic complexes can undergo dissociation via a complex series of reactions with iron and aluminum oxides in the sediments forming a suite of adsorbates: Co2+, CoIIEDTA2-, FeEDTA, and AlEDTA- that compete for the EDTA and surface adsorption sites. The sorbed Co(II) is then oxidized to the extremely stable but weakly reactive CoIIIEDTA-. In the case of Mn(IV) minerals, such as pyrolusite, the adsorption and subsequent oxidation of CoIIEDTA2- to produce CoIIIEDTA- results in the reduction of Mn(IV) to Mn(III) and the formation of a layer of α-Mn2IIIO2 on the pyrolusite, which eventually limits the production of CoIIIEDTA-. The adsorption behavior of cobalt therefore varies greatly and is a function of pH, oxidation state, sediment interactions, and environmental availability of organic complexants (PNNL-16663).'
PL6-9	Section 6.3.1, p. 6-6, lines 33-37	Re nitrate, sulfate, and Cr+6, text states, "None of these exceed a regulatory standard unless all of the chromium is assumed to be hexavalent." Therefore (alternatively stated), if all Cr is assumed to be hexavalent, Cr+6 concentrations (Figure 6-12) exceed the MTCA Method B groundwater CUL (48 µg/L), as well as the CalEPA MCL (10 µg/L).	Although there is a federal MCL for total Cr (100 µg/L), there is no federal MCL for Cr+6. In the absence of the necessary speciation of chromium, Ecology will assume that all of the chromium is hexavalent. Hexavalent chromium is the soluble form of chromium.	Revise the text to acknowledge that chromium has exceeded the state groundwater standard (MTCA Method B) for hexavalent chromium.	Generally, concur with statement and recommended change. Have added the following text: The maximum concentration of chromium is 0.06 mg/L at PoCal 6 in 2019. If all chromium is assumed to be hexavalent (Figure 6-12) these concentration levels would exceed the MTCA Method B groundwater CUL of 48 µg/L.
PL6-10	Section 6.3.1, p. 6-6, line 40	Text should read "0.6 mg/L" (not "mL/g").	Use concentration units.	Revise the text.	Concur with comment. Units have been corrected as suggested.
PL6-11	Section 6.3.1, p. 6-7, Table 6-1	If U-238 is considered, why is U-234 not considered?	U-234 and U-238 are typically found together in the environment.	Please discuss both of these isotopes.	A footnote has been added to Table 7-1 in the Revision 2 update to indicate that U-234 (and other U isotopes) is not explicitly modeled as its concentration in groundwater can be predicted based on U-238 concentrations and scaling by the U-234/U-238 ratio in the inventory.
PL6-12	Table 6.1, p. 6-7 & 6-8, Table 6-1	It is worth noting that crude mass balances were determined with each tank transfer, and were considered good if the difference was 5,000 gals or less; i.e., less than 2 "liquid level. This could account for some additional inventory; nonetheless, it should be duly noted as a source of uncertainty.		Please include.	The accuracy and precision of volume measurements for a waste transfer is dependent on the specific conditions of waste transfer and would be very challenging to quantify. RPP-ENV-33418 describes an approach that is considered to have less uncertainty. This approach is to estimate the leak primarily from engineered judgment of contaminated sediments in the vadose zone, based on interpretations of spectra gamma measurements of Cs-137 in dry wells and not on specific in-tank measurements of volume levels at the time of the estimated timing of the leaks or losses.
PL6-13	Sections 6.3.1 & 7, pp. 6-10 & general, Figure 6-3	The point of assessment given here (based on the NRC document NUREG-1854, and stated to be "also consistent with the requirements for points of assessment in DOE O 435.1 performance assessment of radiological impacts") is downgradient from the WAC 173-340-720(8)(a) standard point of compliance. It also is not consistent with WAC 173-303-645(6)(a), which gives the point of compliance as "a vertical plane located at the hydraulically down-gradient limit of the waste management area that extends down into the uppermost aquifer underlying the regulated unit." Since this is the RCRA Closure Analysis it will be necessary to show protectiveness that is consistent with WAC 173-303 and the WAC sections it references (including WAC 173-340). The groundwater	See WAC 173-303-610(2)(b)(i), WAC 173-340-720(8), and WAC 173-303-645(6)(a).	Ecology will look at various locations to determine if groundwater concentrations (measured or predicted) exceed regulatory requirements. Remedies will need to be developed for the locations that exceed. This document will need to be revised to be consistent with regulatory definitions of the Point of Compliance, or any negotiated conditional points of compliance. Please provide the predicted concentrations for the groundwater at the edge of the WMA.	This comment appears to be directed towards the RPP-ENV-58806 document rather than the Past Leaks analysis report. The first paragraph in Section 7.3 in the Revision 2 update describes how the highest calculated groundwater concentration at the WMA C fenceline was determined and how the points of calculation are established. As discussed in the comment resolution meetings, we have searched the document and have removed any text reference to the point of compliance. The only discussion would be with regard to the point of calculation.

Comment No.	Location	Comment	Basis	Recommendation	Final Disposition
		protection objective should be analyzed at the regulatory point (or points) of compliance as well as the point of maximum groundwater concentration. Note that section D3.0, p. D-4 states "The point of compliance for this analysis is at the highest concentration or impact, with an allowance for some volume averaging based on projected groundwater use, beyond a 100-m buffer zone around WMA C." If this is considered a conditional point of compliance, it must be negotiated with Ecology (see WAC 173-340-720(8)(c) and (d)).			
PL6-14	Section 6.3.2, p. 6-11, lines 24-34	There appears to be no MCL in EPA's DWS for Se-79, and therefore there is no standard for comparison with the modeled groundwater concentrations. Has an attempt been made to find a Se-79 dose conversion factor, and then use the standard drinking water scenario to calculate a concentration corresponding to 4 mrem/year?		If not, it would be worth investigating if this can be done.	We initially tried but could not establish the MCL due to lack of information in the National Bureau of Standards Handbook 69 (NBS 69). However, we do have the dose coefficients based on water ingestion. Also, Se-79 is not a significant risk driver due to a low inventory.
PL6-15	Section 6.3.2, p. 6-11, lines 24-34	Predicting concentrations to one-tenth of a pCi/L for times thousands of years from now seems ambitious. Are there uncertainties associated with these concentrations and times of peak concentration?	The values are highly sensitive to the Kd values, which must have uncertainties associated with them.	Please adjust predictions based on uncertainties.	The comment is well taken, and some adjustments have been in the section cited. Please keep in mind that these concentrations results are taken from forward predictions of some key constituents using one of the numerical models that did a reasonable job of matching observed first arrival in groundwater. The idea was not to necessarily predict absolute concentrations but to provide overall temporal trends in groundwater impacts. These trends were meant to provide general information inform any remediation of groundwater. Assessing the uncertainty in these predictions is well beyond the scope of what we were intending to accomplish in these analyses. This clarifying text has been added to p. 7.2 in the Revision 2 update
PL6-16	Section 6.3.2, p. 6-11, lines 26-28	I-129 is derived mostly from PUREX cribs, not WMA C. Is I-129 in the vadose zone inventory?		Please explain or correct.	Table 2-3 provides the inventory estimates for I-129 that were modeled to evaluate the impact on groundwater. We changed reference from Table 2-3 to Table 7-1. Reference the RPP-RPT-42294 is provided as a footnote in this table as a source for the modeled inventories
PL6-17	Section 6.3.2, pp. 6-15 through 6-23, Figures 6-4 through 6-12	For this and other similar curves, please explain why these curves are not projected into the post-closure period; i.e., to 10,000 or more years. Also, why aren't curves shown for the fenceline? What is the basis for calculations of the upper 5 m? Is this because of well screen length and placement?		Please elaborate.	These series of curves show cumulative and individual release impacts downgradient of WMA C for a range of mobile constituents evaluated. The time scale of each set of curves was selected to capture the key elements of the impacts. For instance, the impacts for mobile Tc-99 ranges from 1980 to 2120. The timescale could be extended beyond 2120, but it would show a continued decline in concentrations. This same time scale is used for other constituents where a Kd of 0 is used like tritium, Co-60, nitrate, sulfate, chromium. For Tc-99 and tritium, plots are shown at the fenceline in Figures 7-4 and 7-6 to illustrative the relative differences in impacts with results at 100 m downgradient of the fenceline (See Figures 7-5 and 7-7). Tabular summaries of results for all constituents, given in Table 7-4, provide results at the fenceline and at 100 m from the fenceline. For a less mobile constituent like Se-79 (See Figure 7-9) goes from 2040 to 8040. For I-129, U-238, and Total U (See Figures 7-17, 7-18, 7-19 and 7-20, the time scale selected ranges from 6040 to 12040. The concentration in the top 5 m is used in these plots to capture the impacts in the upper part of the unconfined aquifer.
PL6-18	Section 6.3.2, pp. 6-24 through 6-27, Figures	These contour maps do not include any lateral spreading in the subsurface; therefore, they don't match reality.		Please correct.	We disagree with the comment. These model results are based on the use of the assumed hydraulic properties for each of the major hydrogeologic units and consider parameters needed to represent the effects of macrodispersivity and moisture-dependent anisotropy. At the contour levels shown, the results in these plots indicate that past leaks and releases at WMA C which are introduced into the model in just a few nodes at their suspected source locations spread individually well beyond the 75-ft wide tank. Collectively, the cumulative effects of all the sources show impacts to almost the entire tank farm area. We have performed

Comment No.	Location	Comment	Basis	Recommendation	Final Disposition
	6-13 through 6-16				simulations with other alternative conceptual models that we have shared with Ecology on March 29, 2017 during their review of this document. A comparison of results for a simulation of the C-105 leaks with these ACMs, that included a range of heterogeneous models, produced the following general results: -All heterogeneous model simulations of the C-105 Tc-99 leak indicate the center of mass of the Tc-99 plume moved generally downward in response to gravity despite the presence of higher-moisture (finer textured) horizontal features in the models -The Tc-99 plumes originating from the C-105 leak spread laterally in all heterogeneous models to widths of up to 200 ft. as they migrated downward through the vadose zone prior to entering the saturated zone -Results of heterogeneous and EHM representations of the vadose zone generally produced similar results in terms of peak concentrations and the time of occurrence of each peak The slides for that briefing are provided on the WMA C PA website:
PL6-19	Section 6.3.2, pp. 6-36, Table 6-5	It appears that units for peak concentration for Total Uranium should be µg/L for both the fenceline and 100 m downgradient.	Units should be consistent with each other and with units in Figures 6-23 and 6-21.	Revise the total uranium units in the table.	Concur. Have corrected units in Table 7-5.
PL6-20	Section 6.3, pp. 6-4 & 6-5, lines 45-46 & 1-2	The text refers to a 5 m mixing zone.		Justify the assumed “mixing zone” depth in light of the fact that deeper wells show a depth distribution of some contaminants.	See response comment PL6-6.
PL6-21	Section 6.3.3, pp. 6-30 through 6-41	Where is the discussion of CN?		Please correct.	See response to comment PL2-7. Information has been added to this section on potential CN impacts based on information contained in a new Appendix related to CN.
PL6-22	Section 6.4, p. 6-42, line 12	What about Cs-137?		Please elaborate.	This section is focused on the future projected impacts to groundwater from past losses and releases. Due to its affinity for adsorption on to Hanford sediments (see Table 3-2) and its relatively short half-life, Cs-137 has not impacted groundwater nor is it expected to impact groundwater in the future. Information on the Cs-137 developed from spectral gamma logging in dry wells and direct push boreholes as a part of characterization efforts at WMA C are provided in Section 2.3.2 in Section 2.0.
PL6-23	Section 6.4, p. 6-42, line 13-15	The document states: "According to the modeling results, the groundwater concentration of Tc-99 that released from the 100-series tanks peaks around 2019..." However, this numerical finding seems to be contradicted by the measured concentrations of Tc-99 in well 299-E27-21, which exhibit an increasing trend since ~2008, with the rate of increase having risen sharply since ~2012 (see Figure 2-2). Well 299-E27-21 is adjacent to the southern fence line. It is screened from the water table to 34 feet below the water table, while other monitoring wells at WMA C are screened only 15 feet below the water table.		Please address the apparent discrepancy between the findings of numerical modeling and the measured concentrations of $^{Tc-99}$. A solid justification is needed to support the modeling results that show that concentration levels of $^{Tc-99}$ are at or near their peak values.	We added the following text to the beginning of Section 7.4: Simulations projecting into the future assume a steady state water table as a basis for groundwater conditions. This situation differs from the one that produced concentrations measured in individual wells over past few decades. Given the large uncertainties in the timing, volumes and inventories of past releases and the historical changes in the direction and rate of groundwater during the periods when plumes developed in the unconfined aquifer, we would anticipate that many discrepancies in modeling results when compared with past specific concentration levels and trends in individual wells would exist . In spite of the shortcomings, the projected modeling results do provide some useful insights on projected contaminant concentration trends into the future, but the results should be interpreted with understanding of uncertainties inherent in evaluating transport processes in the natural system. In general, what the modeling of the Tc-99 has shown is the following: - The model reasonably approximates the time of first arrival at the aquifer (Section 4), which means that the model provides a consistent representation of processes in the vadose zone. The location and amount of contamination in the vadose zone is key to understanding the persistence of contamination in the future. - The model shows Tc-99 concentration levels well above the DWS. When the model was corrected for the temporally varying water table (Section 5), good agreement was produced with the magnitude of concentrations at the wells.

Comment No.	Location	Comment	Basis	Recommendation	Final Disposition
					- Without implementation of any corrective measures at C-Farm, Tc-99 concentration levels projected by the modeling will continue to be well above the DWS in the near term and will likely remain at levels above the DWS for decades. - The primary contributors to the highest concentration levels seen at the fence line and downgradient are from those plumes that have opportunity to superimpose with one another both temporally and spatially. For the assumed northwest to southeast flow conditions evaluated, the key sources were found to be releases from C-101, C-105, and C-110. Secondary sources included releases at UPR-82, C-104, and C-108".
PL6-24	Section 6.4, p. 6-42, lines 24-26	What is the uncertainty of your "underestimation" of groundwater contaminant concentrations?	The text states "As the gradient provides a proportional indicator of the groundwater flux, and the concentration of contaminants in groundwater is generally inversely proportional to the flux, the application of the estimated steady-state gradient in the model likely contributes to the underestimation of contaminant concentrations in the modeling results. "	Please elaborate.	The uncertainty in the magnitude and direction of the hydraulic gradient during the decline of the 216-B-3 Pond hydraulic mound is essentially impossible to quantify with the data that are available from that time. The text is intended to provide an explanation for why the model results that use a steady state gradient appear to underestimate the observed concentrations. The actual hydraulic gradient during 216-B-3 Pond operations reversed, and is in the process of reversing back, which indicates that the magnitude of the gradient must have at times decreased from the steady state value. Measurements made during 2005 through 2011 provides some insights into the variability in the magnitude of the hydraulic gradient that occurred, and indicate that at times the gradient measured less than one half of the estimated steady-state value while reestablishing a south or southeasterly direction. As the gradient provides a proportional indicator of the groundwater flux, and the concentration of contaminants in groundwater is generally inversely proportional to the flux. Therefore, the application of the estimated steady-state gradient in the model likely contributes to the underestimation of contaminant concentrations in the modeling results compared to the observed values.
PL7-1	Section 7.1, p. 7-1, lines 18-23	There will be remediation at the B complex; it's a matter of when and the effectiveness of such remediation. This is an assumption but necessitates close coordination with activities under the 200-BP-5 groundwater operable unit. BP-5 does not adequately evaluate impacts from upgradient sources for the B complex.	The text states "It is emphasized that existing evaluations of upgradient contamination assume that there will be no remedial activities undertaken at B Complex. They therefore likely provide significant overestimations of future contamination discharges."	Ecology does not agree that the source contributions from B complex have been overestimated. Please evaluate the impact of underestimating B complex contributions by an order of magnitude. This could be a sensitivity case.	This was not work done by the PA effort, but work associated the 200-BP-5 RI. We are merely citing this work. It is beyond the scope of the PA to perform the sensitivity case that is recommended. Some additional text can possibly be added to discuss: - Qualitatively the potential impacts of underestimating B complex contributions in modeling results. - Recent developments with actual remediation that has been initiated in the B-Complex area.
PL7-2	Section 7.1, p. 7-1, lines 37-40	What is the pedigree of the P2R model? Does it match or approximate that of the TWEIS model?		Please add DOE/RL-2009-127 Draft A to the list of references. Also, please justify model calibration for the P2R model. The lack of calibration creates a large uncertainty.	This was not work done by the PA effort, but work associated the 200-BP-5 RI. We are merely citing this work. DOE/RL-2009-127 Draft A is provided in the list of references. Details of the P2R model and its application are provided in this reference.
PL7-3	Section 7.1, p. 702, line 3	ECF-Hanford-15-0011, DOE/RL-2009-127 Draft A, and CP-57037 are not in the references.		Please provide.	The documents are listed in the reference section. On ECF-Hanford-15-0011, this specific document was never released as planned by DOE due to issues on BP-5 groundwater OU. This ECF has now been superseded by ECF-Hanford-18-0023 (*Evaluation of Contaminant Transport for the 200-BP-5 and 200-PO-1 Operable Units Feasibility Study Evaluation of Remedial Alternatives*) in support of the Interim ROD for the BP-5 OU (See disposition related to comment PL7-6).
PL7-4	Section 7.1, p. 7-2, line 8	An unrealistic assumption.	The text states "No continuing source is considered for cyanide and ^{129}I."	Please revise considering the deep vadose zone inventory.	This was not work done by the PA effort, but work associated the 200-BP-5 RI. We are merely citing this work and these assumptions are used in this non-remedial evaluation case. The range of cases evaluated in the 200-BP-5 RI including continuing sources for Tc-99, NO3, and uranium but no specific cases evaluated continuing sources of cyanide and ^{129}I.

Comment No.	Location	Comment	Basis	Recommendation	Final Disposition
PL7-5	Section 7.1, p. 7-2, line 12	TEDF operation and discharges affect the groundwater gradient and possibly direction (slightly), but it will not be operating past Hanford closure. For long term prediction, this is an invalid assumption.	The text states "Discharge from TEDF is assumed to occur."	Please qualify this assumption and discuss how the discontinuation of TEDF discharges will affect contaminant concentrations in groundwater.	This was not work done by the PA effort, but work associated the 200-BP-5 RI. We are merely citing this work, and this is one of the assumptions used in this non-remedial evaluation case. Based on interpretations made from monitoring information during the last couple of years (DOE/RL-2016-67), large operational discharges at TEDF combine with other changes in stage in the Columbia River to the northwest of the gable gap area generally can have a subtle but noticeable effect on reducing the overall hydraulic gradient of the water table in 200 East area. This general information can be added as a footnote to the bullet (• Discharge from TEDF is assumed to occur) on p. 7-2.
PL7-6	Section 7.1, p. 702, line 2-12	The text states "Key features of the remedial evaluation case for the 200 East Feasibility Study include (ECF-Hanford-15-0011): …" Ecology will need to understand if the 200 East Feasibility Study assumptions are justified and consistent with the BP-5 Feasibility Study, which has not been written.	Ecology has not been involved in ECF-Hanford-15-0011.	Provide rationale for key features listed for the remedial evaluation case (ECF-Hanford-15-0011).	This case provides a baseline for assessing the effectiveness of the P&T scenarios. It does consider continuing sources for existing plumes. We acknowledge that the specific remedial evaluation case does utilize assumptions about continuing sources for selected contaminants which may underestimate their impacts. Implementation of a pump & treat system to expedite the remediation of groundwater contaminant plumes at C Farm is under way under the 200 BR-5 OU RI/FS process. The design efforts for this pump and treat system is using continuing sources developed under this past leaks analysis. Some additional text will be added at the
PL7-7	Section 7.1, p. 7-2, line 16	The document states "Depictions of the future plumes from upgradient sources are presented in Appendix B."	The current document (RPP-RPT-59197, Rev 0) does not appear to have an "Appendix B."	Please provide Appendix B for this document or revise the text.	Concur. This sentence has not been deleted. Added text for reference information as to where to find the plume maps in the original source (ECF-Hanford-15-0011).
PL7-8	Section 7.1.1, pp. 7-4 through 7-6, Figure 7-2 through 7-4	These figures illustrate simulations of BP-5 remediation; yet on p. 7-1, you assume no remediation at the B complex, a key source for BP-5. Furthermore, no final remediation has been selected for 200-BP-5.		What are your assumptions and bases for these figures? Please elaborate.	These figures from Figure 7-2 through 7-12 reflect the case described in pp. 7-1 taken from in the original source (ECF-Hanford-15-0011). We have provided a copy of ECF-Hanford-18-0023 as soon as it is released to the ARA. See response to PL7-6 for details.
PL7-9	Section 7.1.1 to 7.2.2, pp. 7-8 & 7-13, Figures 7-6 & 7-11	Both these figures show a sharp drop off in contaminant concentrations just past the yr. 2100.		Please provide a basis for these curves.	That was the extent of the simulations from the ECF-Hanford-15-001. The simulations provided in this document were run out for about 300 yrs.
PL7-10	Section 7.1, p. 7-15, Table 7-1	What is the source of the "calculated remedial evaluation case for upgradient sources"? What is the uncertainty in estimated peak contaminant concentrations?		Please address.	This was not work done by the PA effort, but work associated the 200-BP-5 RI. We are merely citing this work. It is beyond the scope of the PA to perform the evaluation of uncertainty that is recommended. Some additional text can possibly be added to discuss, in general terms, the uncertainty that may exist in the modeling results for this case.
PL7-11	Section 7.1.3, p. 7-15, lines 1-9	CN is a key dangerous waste contaminant arising from WMA C and *must* be included. It's shown on Fig. 7-13, 7-14, 7-15.		Please correct.	This was not work done by the PA effort, but work associated the 200-BP-5 RI. We are merely citing this work so we will not be adding any additional information to these figures. In the updated Past Leaks Analysis, discussion of cyanide from past leaks at WMA C with upgradient sources and residual wastes will be included in a new subsection of Section 8.3 (subsection 8.3.5) in the Revision 2 update
PL7-12	Section 7.1.3, p. 7-14 & 7-16 through	These figures clearly show CN in groundwater beneath WMA C. There are several possible sources in WMA C, as some tanks were used in the U scavenging processing which employed ferrocyanide.		Please add CN^- to the list of COCs for WMA C.	The objective of this work is to support corrective measures of vadose zone sediments that have been contaminated by past leaks and loses at WMA C. CN was below detection in all sediment samples collection as a part of the RFI/CMS characterization efforts. Thus, CN was not retained as a COPC for decisions associated with the RFI/CMS. CN is a COPC of concern for the 200 BP-5 RI/FS and is evaluated in this past leaks analysis.

Comment No.	Location	Comment	Basis	Recommendation	Final Disposition
	7-19, Figures 7-12 through 7-16				
PL7-13	Section 7.1.5, p. 7-15, lines 27-28	The text states information on U-235 concentrations. Was this a mistake? Should it be U-238, not U-235?		Please check and correct if necessary.	Concur. Will correct
PL7-14	Section 7.2.1, p. 7-30, line 30	The MCL for Tc-99 should be provided in this paragraph.	The MCL would keep the Tc-99 discussion consistent with descriptions of nitrate, I-129, and U-238/U-total.	List the MCL for Tc-99 (900 pCi/L) here.	Concur. Will correct
PL7-15	Sections 7.2.1 & 7.2.3, p. 7-30, lines 25-45	Text states that Tc-99 and I-129 are key contaminants in the residual waste PA. However, the modeled peak concentrations are significantly less than DWS MCLs, so it is not clear how these are key contaminants of concern.		Please discuss how Tc-99 and I-129 compare with the MCL and why these are key contaminants for the residual waste.	For purposes of the DOE Order 435.1 PA efforts, comparison of predicted concentrations of Tc-99 and I-129 to MCLs are included in the RPP ENV-58782 and a summary of that comparison can be added here. Clarifying text has been added
PL7-16	Section 7.2.4, pp. 7-38 & 7-39, Figure 7-33	The simulation illustrates that U has not peaked in groundwater by the year 12,000. It would be useful to run the simulation to estimate the year of peak U concentration in groundwater.		Please consider.	They are not in conflict. If you examine the modeling results in this remediation case for uranium, the uranium plume they are discussing originates from B-complex and eventually reaches C-farm during the course of the simulations. There is no plume of uranium at WMA C at the start of the simulation and our simulation of uranium releases in past leaks from C-farm do eventually reach groundwater after year 6040 at very low levels.
PL7-17	Section 7.3, pp. 7-37 through 7-41	Comparison of various sources and their impacts: As stated, “comparison of up-gradient sources, residual wastes, and past leaks data does not correspond to downgradient wells to measured concentrations”. While the current analysis was based mostly on the on the observed data, anomalies found are not explained properly. The results vary in orders of magnitude. There is no attempt to come up with another scenario or scenarios to explain these anomalies.		The document should address these issues.	Following revision to the text added at the beginning of Section 8.3.1: A comparison of results for Tc-99 are presented in Figure 8-34, along with results from the residual waste PA and upgradient sources. The calculation of concentrations from leaks and residual wastes coincide at the same line of analysis at 100 m downgradient, but the upgradient source concentrations are at the PoCals from the P2R model discussed in Section 8.1. The peak concentration of Tc-99 associated with the past leaks is ~2 orders of magnitude higher than for residual wastes, and about a factor of 5 higher than upgradient sources. Caution should be used in interpreting these results. Since the results are generated by two different models with differing spatial discretizations and hydraulic parameters, the concentrations from past leaks analysis and upgradient sources cannot be simply combined in a strict sense, but rather should be evaluated in a qualitative manner.
PL7-18	Section 7.3, pp. 7-37, line 31	Section 8.2 is cited, although there is none.	There is no Section 8.2.	Revise the text.	Concur. This should be Section 8.1 in the Revision 2 update. This has been corrected
PL7-19	Section 7.3.1, p. 7-37, line 39	The document refers to PoCals from the P2R model.	PoCals from the P2R model are not given in this document.	Please specify locations of PoCals from the P2R model here in this document.	Discussion has been added to beginning of Section 8.1 to clarify where the PoCals were selected in the P2R models for purposes of this document. Clarifying text has been added.

Comment No.	Location	Comment	Basis	Recommendation	Final Disposition
PL7-20	Section 7.3.1, p. 7-37, lines 41-44	The document states "It should be noted that because the peak Tc-99 concentration is calculated 100 m downgradient, it does not correspond well to the measured concentrations in monitoring wells, and is about a factor of 4 lower than the highest measured concentration." This is only one possible explanation for the mismatch.	Note that non-correspondence of modeled vs. measured peak Tc-99 in groundwater may be due to location mismatch, as well as model underprediction.	Revise the text to indicate that the explanation provided for the mismatch is only one of the possibilities.	See response to PL7-17.
PL7-21	Section 7.3.1, p. 7-40, Figure 7-34	The tank residual curve label and PoC are not consistent.	The tank residual curve is labelled “3,” while the legend specifies PoC 4 for tank residuals.	Please clarify.	Concur with comment. Necessary changes have been made to correct
PL7-22	Section 7.3.2, p. 7-41, line 7	The text is confusing, as it refers to "both residual wastes."	The prior text referred to residual wastes and upgradient sources.	Insert “upgradient” before “concentration” (if this is correct) and delete “both” before “residual wastes.”	Concur with one of suggested changes. Have made following text change, “The concentration of nitrate from upgradient sources is ~2 orders of magnitude higher than nitrate concentration results from residual wastes.
PL7-23	Section 7.3.3, p. 7-41, line 14	This section is about I-129 yet refers to total uranium instead.		Replace “total uranium” with “I-129.”	Concur. This has been corrected.
PL7-24	Section 7.3.3, p. 7-43, Figure 7-36	The tank residual curve label and PoC are not consistent.	The tank residual curve is labelled “3,” while the legend specifies PoC 4 for tank residuals.	Please clarify.	Concur. This has been corrected.
PL7-25	Section 7.4, p. 7-41, lines 36-37	The title of the section refers to 'contaminants of potential concern'. However, Ecology considers additional contaminants to be contaminants of potential concern.	See Ecology comment on Section 6 (General).	Please rename this section to Summary of Peak Concentrations of Selected Contaminants.	Concur with comment. Have changed to "Summary of Peak Concentrations of Selected Contaminants of Potential Concern."
PL7-26	Section 7.4, p. 7-45, Table 7-2	There is considerable uncertainty associated with these values.	These are simulated maxima.	Please address the uncertainty.	Following text has been added after the first sentence in the first paragraph of Section 8.4: As stated earlier in the beginning of Section 8.3, evaluation of these results need to consider that this summary represents a qualitative comparison between projected concentrations from past leaks, residual wastes, and upgradient sources to give an overview of overall trends from these sources. Given the potential uncertainties in these estimates, caution must be used in drawing too strong conclusions from this comparison, because the purpose and intent of each of the estimates is different, and the underlying assumptions differ.
PL8-1	Section 8	With the uncertainty presented in this Section what is the basis for proposing a protective remediation?		Please address WMA C releases and their impacts, in spite of the upgradient sources. Also, make the remedy assumed in this PA consistent with those in the WMA C CMS.	This analysis of past leaks is intended to provide supporting information that could be relevant to the selection and specific implementation of groundwater mitigation measures being undertaken as a part of the CERCLA RI/FS effort in 200-BP-5-OU. Implementation of a pump & treat system to expedite the remediation of groundwater contaminant plumes at C Farm is also under way under the 200 BR-5 OU RI/FS process. The design of this pump and treat system is using continuing sources of a number of contaminants developed under this past leaks analysis. This analysis also does evaluate the place of engineered surface barrier that is consistent with the general corrective measures identified in the CMS.
PL8-2	Section 8.0, p. 8-1, lines 36-40	Is it a higher flux rate, or an artifact of the changing groundwater flow direction?		Please address.	We have added the following additional text at the end of this paragraph. "It is important to note here that the historical decline in water table conditions, the associated changing direction of groundwater, and related changes in the overall hydraulic gradient have undoubtedly had a significant effect of historical observations of contaminant concentrations found in groundwater at WMA C. However, the actual historical changes in these overall groundwater conditions that have created observed concentrations of selected contaminants at WMA C are uncertain and cannot be reasonably replicated for current monitoring information."

Comment No.	Location	Comment	Basis	Recommendation	Final Disposition
PL8-3	Section 8.0, p. 8-1, line 40	Re Figures 4-34 and 4-35, only 10 curves are discernable, while the legend specifies 14 curves. Also, the legend specifies Case 3d, but there is no Case 3d.	For example, the light blue curve for Case 1a (BaseCase_hi_inv) is difficult to identify.	Please clarify these figures.	Concur with the comments. We have reexamined these plots and have replotted these results to clarify, since a number of the cases overlay on top of each other. The commenter is also correct the legend erroneously includes reference to Case 3d. The legend has been updated to remove Case 3d, since there is no Case 3d.
PL8-4	Section 8.0, p. 8-1, lines 42-46	Although text notes the early arrival of Case 3a (EnhanceRech_150), text fails to note the late arrival of Case 3b (EnhanceRech_100), relative to monitoring data in Figure 4-34.		Discuss the late arrival of Case 3b relative to the monitoring data.	Please keep in mind that the comparisons associated with scoping cases from Section 4 are primarily focused on comparing with the arrival times of the Tc-99 contamination at the water table and only more generally on concentration of Tc-99 levels observed in monitoring wells. These two indicators are regarded as the most reliable and reproducible aspects of the groundwater monitoring data. Given the uncertainties in the estimates and timing of past leaks and complexities of the behavior of the site, it is unrealistic to hope to achieve exact matches with data. Instead, the goal is to provide a reasonable match with data, in a way that provides information and insight into the processes and parameter values that are consistent with observed contamination in monitoring wells at WMA C. The general shapes of the breakthrough curves observed in data (sharp rises and falls in concentration) are believed to be associated with shifts in the direction of the groundwater flow. This aspect of the breakthrough curves is not well represented by the scoping cases presented in this section, since they all assume a constant groundwater flow rate and direction. The scoping case in Section 5 addresses the changing water table and produces much better comparisons with data. Given this context, we will be updated lines 42-46 as follows: "Cases 3a and 3b investigated the general effect of a higher effective recharge rate than used in the other scoping analysis cases. Generally, it was found that the higher recharge rates led to early arrival of the contaminant at the water table. At a rate of 100 mm/y used both within and in the immediate vicinity of the tank farms (Case 3b), the difference in first arrival at contaminants at the water table (See Figure 4-15) resulted in an earlier arrival and peak concentration when compared to the Case 1a results (See Figure 4-4) where the 100 mm/yr was only used within the tank farm area. For the enhanced recharge rate of 150 mm/y (Case 3a) the higher recharge rate generated earlier arrival times that are not consistent with monitoring data observed in key monitoring well locations (see Figures 4-34 and 4-35)."
PL8-5	Section 8.0, p. 8-1, lines 42-46	The text refers to a higher recharge rate for cases 3a and 3b.		Please distinguish natural from artificial recharge.	These cases reflect a combination of recharge from both natural and man-made sources and do not attempt to distinguish or quantify differences of these two types of recharge sources. Given the amount of information we have during the historical period of the operations when these leaks occurred, quantification of differences between anthropogenic and natural sources would an impossible task. These cases are really meant to examine the effect of higher effective rates of combined recharge rates regardless of the sources in arrival of contaminants within leaks and losses at the water. Case 3a reflects a 50% increase in from 100 mm/yr to 150 mm/yr in the tank farm area. Case 3b examines the effect of using a 100 mm/yr rate both within the tank farm and in the immediate areas outside of the tank farm. This clarification can be added to the original text describing these cases in Section 4 and reiterated here after lines 42 and 43 on p. 9-1.
PL8-6	Section 8.0, p. 8-2, lines 7-9	This analysis is about an alternate conceptual model, not about the effect of heterogeneities in the vadose zone.		Please correct.	Have changed text to as follows: "Scoping Cases 4 investigated a number of vadose zone parameters and conceptual models of potential interest, to evaluate the potential for variations in the vadose zone properties to affect the plume development migration".
PL8-7	Section 8.0, p. 8-2, lines 14-17	Contrary to the text, Case 4a (ACM II) appears to coincide with the monitoring data in Figure 4-34 better than Case 1a (BaseCase_hi_inv).		Revise the text to be consistent with the figure.	The conclusions relate to first arrival of contaminants at the water table. Current bullet has been replaced by following proposed text: "The evaluation in Case 4b of ACM using a heterogeneous representation of the vadose zone in Case 4b showed that adding heterogeneity resulted in an earlier arrival time of contamination at the water table than has been observed in monitoring wells and concentrations levels that were slightly higher than concentration levels resulting from Case 1a. Because of the inconsistency of the results from this alternative scoping model with monitoring well data, this case was not identified as a preferred case for further analyses of projected impacts of plumes into the future".

Comment No.	Location	Comment	Basis	Recommendation	Final Disposition
PL8-8	Section 8.0, p. 8-2, lines 19-23	Although text notes the early arrival of Case 4b (ACM_hetero), text fails to note the late peak of Case 1a (BaseCase_hi_inv), relative to monitoring data in Figure 4-34. Also, contrary to text, concentrations in Case 4b are slightly higher than in Case 1a.		Revise the text to discuss the late peak of Case 1a its higher concentration than Case 4b.	The conclusions relate to first arrival of contaminants at the water table. Current bullet has been replaced by following proposed text: "The evaluation in Case 4b of ACM using a heterogeneous representation of the vadose zone in Case 4b showed that adding heterogeneity resulted in an earlier arrival time of contamination at the water table than has been observed in monitoring wells and concentrations levels that were slightly higher than concentration levels resulting from Case 1a. Because of the inconsistency of the results from this alternative scoping model with monitoring well data, this case was not identified as a preferred case for further analyses of projected impacts of plumes into the future".
PL8-9	Section 8.0, p. 8-2, lines 25-31	Contrary to text, Case 4c (vzprop_50%) appears to be a better fit with monitoring data than Case 1a (BaseCase_hi_inv), as shown in Figure 4-34. Also, please clarify how Case 4c (vzprop_50%) evaluates "higher vadose zone hydraulic properties" when these properties are set at 50th percentile values, while Case 4d (vzprop_95%) evaluates "lower vadose zone hydraulic properties" when these properties are set to 95th percentiles (as described in Table 4-1).		Revise the text to address the discrepancies between the text and Figure 4-34. Clarify Case 4c.	From the perspective of first arrival of contaminants at the water table, results from Case 4c show slightly faster transport and contamination arrives a little earlier than Case 1a. Current bullet on p. 9-2 in the Revision 2 update has been replaced by following proposed text: "The evaluation of median values of vadose zone hydraulic properties in Case 4c showed slightly faster transport and earlier arrival time of contaminants and concentration results when compared to arrival time and concentration results simulated for Case 1a. However, the evaluation of 95th percentile values of vadose zone hydraulic properties in Case 4d showed transport and arrival time results that were significantly faster and earlier when compared to the arrival times and concentration levels of Tc-99 concentrations from key monitoring wells. These results showed faster transport and earlier arrival of contaminants at the water table when evaluated against comparable results for Case 1a. Therefore, the use of 95th percentile properties as implemented in Case 4d was not identified as a preferred case for use in further analyses of projected impacts of plumes into the future". With regard to the comment related to Case 4d, the text in Table 4-1 is typo and has been corrected as follows: "Assumes same parameterization and past leak volumes and inventories as Case 1a but with vadose zone hydraulic properties at the 95th percentile values as set in the uncertainty analysis developed for the DOE 435.1 PA. This case evaluates the effect on past releases on vadose zone hydraulic properties that are higher than used in Case 1a and Case 4c."
PL8-10	Section 8.0, p. 8-2, lines 33-37	These results are highly dependent on how the analyses were done.		Please elaborate.	Concur with the thought behind the comment. Have added a sentence referencing where the inputs used to represent these cases may be found in Section 9 in the Revision 2 update and have updated the case descriptions provided in Table 4.1 to provide that same information
PL8-11	Section 8.0, p. 8-3, lines 4-8	Time of arrival is not the only criteria to characterize and distinguish scoping analysis cases (curves).	Criteria should also include time of disappearance, peak amplitude, skewness, kurtosis, and area under the curve.	Discuss the other characteristics of the curves.	The comparisons associated with scoping cases from Section 4 are primarily focused on evaluating the arrival times of the Tc-99 contamination at the water table and general concentration of Tc-99 levels observed in monitoring wells. These two indicators are regarded as the most reliable and reproducible aspects of the groundwater monitoring data. Given the uncertainties in the estimates and timing of past leaks and complexities of the behavior of the site, it is unrealistic to hope to achieve exact matches with data. Instead, the goal is to provide a reasonable match with data, in a way that provides information and insight into the processes and parameter values that are consistent with observed contamination in monitoring wells at WMA C. The general shapes of the breakthrough curves observed in data (sharp rises and falls in concentration) are believed to be associated with shifts in the direction of the groundwater flow. This aspect of the breakthrough curves is not well represented by the scoping cases presented in this section, since they all assume a constant groundwater flow rate and direction. The scoping case in Section 5 addresses the changing water table, and produces much better comparisons with data. Given the transient conditions under which the observed concentrations in wells have developed, we believe that evaluation of the additional criteria suggested by the commenter such time of disappearance, peak amplitude, skewness, kurtosis, and area under the curve would have limited value for the limited objectives of the scoping analysis.
PL8-12	Section 8.0, p. 8-3, lines 4-8	All analyses were compared to groundwater monitoring data obtained from a network that wasn't in place until at least 1989, years after peak operations at C Farm.		Consider a case for releases earlier than what is shown in the groundwater monitoring network.	Some cases have been evaluated that produced these types of results. When we discuss these cases, the relevance of uncertainty associated with the lack of groundwater monitoring data prior to the late 1980's has been mentioned to bring this perspective.

Comment No.	Location	Comment	Basis	Recommendation	Final Disposition
PL8-13	Section 8.0, p. 8-3, lines 4-8	The conclusion that all cases (except Cases 3a, 4b, 4d) produce comparable results is inconsistent with the considerable variation observed in timing and shape of these curves depicted in Figures 4-34 and 4-35.	In particular, this conclusion contradicts the previous observation that results from Case 1b (BaseCase_lo_inv) differ both with results from Case 1a (BaseCase_hi_inv), as well as with monitoring data (p 8-1, lines 29-32).	Discuss Case 1b relative to Case 1a and monitoring data.	Again, the primary focus of the scoping analysis provided in Section 4.0 is on evaluating arrival times of the Tc-99 contamination at the water table and general concentration of Tc-99 levels observed in monitoring wells. These two indicators are regarded as the most reliable and reproducible aspects of the groundwater monitoring data. Given the uncertainties in the estimates and timing of past leaks and complexities of the behavior of the site, it is unrealistic to hope to achieve exact matches with data. Furthermore, the sensitivity cases evaluated in these analyses apply a steady-state aquifer gradient, so they are not expected to reproduce the observed shape and magnitude of contaminant concentrations in monitoring well data perfectly. Instead, the goal is to provide a reasonable match with data, in a way that provides information and insight into the processes and parameter values that are consistent with observed contamination in monitoring wells at WMA C. Improved matches with data were provided in Section 5, taking account of the changing water table conditions. As for Case 1a and Case 1b, concentration levels estimated are quite different primarily resulting from the difference in the assumed inventories for these two cases. It was not possible to reach the concentrations seen in groundwater using a 1 Ci release, whereas the 10 Ci release allowed the potential to match data. However, we believe for the other primary criteria considered in the scoping analysis, i.e. first arrival of contaminants at the water table, results for both Case 1a and 1b produce comparable results. The discussion of those results are provided in Section 4.1. We have updated lines 4 through 8 with the following text as clarification: "The remaining scoping analysis cases evaluated in Section 4 produced comparable results to each other in terms of first arrival of contaminants at the water table and none were obviously superior to others in terms of explaining the arrival of contaminants at the water table observed in monitoring wells. The specific cases that generally had comparable results for first arrival of contaminants at the water table include: - Case 2a, in which a 10th percentile groundwater flux of 0.11 m/d was applied - Case 2b , in which a 90th percentile groundwater flux of 0.33 m/d was applied - Case 3b, in which an enhanced recharge rate of 100 mm/yr was applied in all areas of the WMA C modeling domain - Case 3c, in which enhanced localized recharge (i.e. 72,000 gal. over 4 hrs) was applied at three unplanned releases locations (i.e. UPR-81, UPR-82, and UPR 86) just after initial releases at these UPRs were detected. - Case 4a, in which alternative conceptual model II, where the effect of a finer alternative treatment of major hydrogeologic units in the vadose zone, was implemented - Case 4c, in which a 50th percentile set of vadose zone hydraulic properties was applied - Case 4e, in which a hypothetical clastic dike placed below past leak tank C-105, was considered - Case 4f , in which an inadequately sealed borehole located near past leak tank C-105 was considered. When uncertainties in groundwater fluxes were taken into account, the full range of these scoping analyses cases were each found to be capable of producing both arrival times and concentrations consistent with observed monitoring well data for Tc-99." Have added following to top of case list in previous disposition - Case 1a, in which a 9.8 Ci inventory of Tc-99 and 20,500 gal. was applied for C-105 - Case 1b, in which a 1.0 Ci inventory of Tc-99 and a volume of 10,000 gal was applied was applied for C-105

C2.0 REFERENCES

10 CFR Part 960.2, "General Guidelines for the Preliminary Screening of Potential Sites for a Nuclear Waste Repository – Definitions," *Code of Federal Regulations*, as amended.

17-NWP-085, 2017, "Re: Department of Ecology's (Ecology) Review and Comments of Appendix 1 Performance Assessment for Waste Management Area C (WMA C) Documents" (external letter from J. J. Lyon to C. J. Kemp, U.S. Department of Energy Office of River Protection, July 14), State of Washington Department of Ecology, Richland, Washington.

18-NWP-088, 2018, "Department of Ecology's (Ecology) Comments on the United States Department of Energy (USDOE) Submittal of the Phase 2 RCRA Facility Investigation Report for Waste Management Area C (RFI), RPP-RPT-58339, Revision 0, and Waste Management Area C Phase 2 Corrective Measures Study Report (CMS), RPP-RPT-59379, Revision 0" (external letter from J.J. Lyon to J. Bovier, Office of River Protection, U.S. Department of Energy, June 11), Nuclear Waste Program, State of Washington Department of Ecology, Richland, WA.

BNWL-B-360, 1974, *Selected Water Table Contour Maps and Well Hydrographs for the Hanford Reservation, 1944-1973*, Pacific Northwest Laboratory, Richland, Washington.

Comprehensive Environmental Response, Compensation, and Liability Act of 1980, 42 USC 9601, et seq.

CP-47631, 2011, *Model Package Report: Central Plateau Groundwater Model Version 3.3*, Rev. 0, CH2M HILL Plateau Remediation Company, Richland, Washington.

CP-47631, 2015, *Model Package Report: Central Plateau Groundwater Model Version 6.3.3*, Rev. 2, INTERA, Inc., Richland, Washington.

CP-57037, 2015, *Model Package Report: Plateau to River Groundwater Transport Model Version 7.1*, Rev. 0, CH2M HILL Plateau Remediation Company, Richland, Washington.

DOE/EIS-0391, 2012, *Final Tank Closure and Waste Management Environmental Impact Statement for the Hanford Site, Richland, Washington*, U.S. Department of Energy, Washington, D.C.

DOE O 435.1, 2001, *Radioactive Waste Management*, U.S. Department of Energy, Washington, D.C.

DOE/RL-2007-31, 2008, *Remedial Investigation/Feasibility Study Work Plan for the 200-PO-1 Groundwater Operable Unit*, Rev. 0, U.S. Department of Energy, Richland Operations Office, Richland, Washington.

DOE/RL-2009-77, 2010, *Groundwater Quality Assessment Plan for the Single-Shell Tank Waste Management Area C*, Rev. 0, U.S. Department of Energy, Richland Operations Office, Richland, Washington.

DOE/RL-2009-85, 2010, *Remedial Investigation Report for the 200-PO-1 Groundwater Operable Unit*, Draft A, U.S. Department of Energy, Richland Operations Office, Richland, Washington.

DOE/RL-2009-127, 2015, *Remedial Investigation Report for the 200-BP-5 Groundwater Operable Unit, Draft A*, U.S. Department of Energy, Richland Operations Office, Richland, Washington.

DOE/RL-2011-01, 2011, *Hanford Site Groundwater Monitoring Report for 2010*, Rev. 0, U.S. Department of Energy, Richland Operations Office, Richland, Washington.

DOE/RL-2015-75, 2016, *Aquifer Treatability Test Report for the 200-BP-5 Groundwater Operable Unit*, Rev. 0, Department of Energy, Richland Operations Office, Richland, Washington.

DOE/RL-2016-67, 2017, *Hanford Site Groundwater Monitoring Report for 2016*, Rev. 0, U.S. Department of Energy, Richland Operations Office, Richland, Washington.

ECF-Hanford-15-0011, 2015, *Evaluation of Contaminant Transport for the 200-BP-5 and 200-PO-1 Operable Units*, Rev. 0, CH2M HILL Plateau Remediation Company, Richland, Washington.

ECF-Hanford-18-0023, 2018, *Evaluation of Contaminant Transport for the 200-BP-5 and 200-PO-1 Operable Units Feasibility Study Evaluation of Remedial Alternatives*, Rev. 0, INTERA, Inc., Richland, Washington.

Ecology, EPA, and DOE, 1989, *Hanford Federal Facility Agreement and Consent Order – Tri-Party Agreement*, 2 vols., as amended, State of Washington Department of Ecology, U.S. Environmental Protection Agency, and U.S. Department of Energy, Olympia, Washington.

EMDT-MO-0031. 2019, Environmental Modeling Data Transmittal of an unpublished report entitled, "WMA C Conceptual Model" sent to DOE by the Nez Perce Tribe by email on Wednesday, Nov. 5, 2014 at 2:31 pm PST.

EPA/600/2-91/065, 1991, *The RETC Code for Quantifying the Hydraulic Functions of Unsaturated Soils*, Office of Research and Development, U.S. Environmental Protection Agency, Washington, D.C.

Gee, G. W., M. J. Fayer, M. L. Rockhold, and M. D. Campbell, 1992, "Variations in recharge at the Hanford Site," *Northwest Science*, Vol. 66, pp. 237-250.

Gee, G. W., J. M. Keller, and A. L. Ward, 2005a, 'Measurement and prediction of deep drainage from bare arid sediments at a semi- site," *Vadose Zone J.*," Vol. 4, pp. 32–40.

Gee, G.W., Z.F. Zhang, W.H. Albright, S.W. Tyler, and M.J. Singleton, 2005b, "Chloride mass balance: Cautions in predicting increased recharge rates," *Vadose Zone J.*, Vol. 4, pp. 72–78.

IAMIT 2018-002, 2018, *200-BP-5 and 200-PO-1 Interim Record of Decision (IROD)*, State of Washington Department of Ecology, U.S. Environmental Protection Agency, and U.S. Department of Energy, Richland, Washington.

IAMIT 2019-008, 2019, *Baseline Risk Assessment for Waste Management Area C – Food Chain Pathway*, State of Washington Department of Ecology, U.S. Environmental Protection Agency, and U.S. Department of Energy, Richland, Washington.

ITRC, 2010, "Use and Measurement of Mass Flux and Mass Discharge," Interstate Technology & Regulatory Council, Washington, DC.

Leary, K.D., 1990, "Analysis Techniques for Estimating Potential Recharge and Shallow Unsaturated Zone Water Balance Near Yucca Mountain, Nevada," University of Nevada, Reno, NV.

Mualem, Y., 1976, "A New Model for Predicting the Hydraulic Conductivity of Unsaturated Porous Media," Water Resources Research, Vol. 12, No. 3, pp. 513–522.

Murphy E. M., T. R. Ginn, and J. L. Phillips, 1996. "Geochemical Estimates of Paleorecharge in the PascoBasin: Evaluation of the Chloride Mass-Balance Technique," *Water Resour. Res*., Vol. 32(9), pp. 2853–2868.

NBS Handbook 69, 1963, *Maximum Permissible Body Burdens and Maximum Permissible Concentrations of Radionuclides in Air and in Water for Occupational Exposure*, U.S. National Bureau of Standards, as amended by U.S. Department of Commerce, Washington, D.C.

NUREG/CR-6767, 2002, *Evaluation of Hydrologic Uncertainty Assessments for Decommissioning Sites Using Complex and Simplified Models*, Pacific Northwest Laboratory, Richland, Washington.

PNL-10285, 1995, *Estimated Recharge Rates at the Hanford Site*, Pacific Northwest National Laboratory, Richland, Washington.

PNNL-13033, 1999, *Recharge Data Package for the Immobilized Low-Activity Waste 2001 Performance Assessment*, Pacific Northwest National Laboratory, Richland, Washington.

PNNL-14115, 2003, *Hydrologic Characterizations Using Vadose Zone Monitoring Tools: Status Report*, Pacific Northwest National Laboratory, Richland, Washington.

PNNL-14143, 2002, *The Hanford Site 1000-Year Cap Design Test*, Pacific Northwest National Laboratory, Richland, Washington.

PNNL-14702, 2006, *Vadose Zone Hydrogeology Data Package for Hanford Assessments*, Rev. 1, Pacific Northwest National Laboratory, Richland, Washington.

PNNL-14744, 2004, *Recharge Data Package for the 2005 Integrated Disposal Facility Performance Assessment*, Pacific Northwest National Laboratory, Richland, Washington.

PNNL-15670, 2006, *Hanford Site Groundwater Monitoring for Fiscal Year 2005*, Pacific Northwest National Laboratory, Richland, Washington.

PNNL-16663, 2007, *Geochemical Processes Data Package for the Vadose Zone in the Single-Shell Tank Waste Management Areas at the Hanford Site*, Pacific Northwest National Laboratory, Richland, Washington.

PNNL-16688, 2007, *Recharge Data Package for Hanford Single-Shell Tank Waste Management Areas*, Pacific Northwest National Laboratory, Richland, Washington.

PNNL-17154, 2008, *Geochemical Characterization Data Package for the Vadose Zone in the Single-Shell Tank Waste Management Areas at the Hanford Site*, Pacific Northwest National Laboratory, Richland, Washington.

PNNL-17841, 2008, *Compendium of Data for the Hanford Site (Fiscal Years 2004 to 2008) Applicable to Estimation of Recharge Rates*, Pacific Northwest National Laboratory, Richland, Washington.

PNNL-18807, 2009, *Soil Water Balance and Recharge Monitoring at the Hanford Site –FY09 Status Report*, Pacific Northwest National Laboratory, Richland, Washington.

PNNL-19945, 2010, *Soil Water Balance and Recharge Monitoring at the Hanford Site –FY 2010 Status Report*, Pacific Northwest National Laboratory, Richland, Washington.

PNNL-24740, 2017, *Alternative Conceptual Models of the Subsurface at WMA C*, Rev. 1, Pacific Northwest National Laboratory, Richland, Washington.

Polmann, D. J., 1990, "Application of Stochastic Methods to Transient Flow and Transport in Heterogeneous Unsaturated Soils," Ph.D. Thesis, Massachusetts Institute of Technology, Cambridge, Massachusetts.

Resource Conservation and Recovery Act of 1976, 42 USC 6901, et seq.

Rovey, C. W. II and D. S. Cherkauer, 1995, "Scale Dependency of Hydraulic Conductivity Measurements," *Ground Water*, Vol. 33, No. 5, pp. 769–780.

RPP-19822, 2005, *Hanford Defined Waste Model – Revision 5.0*, Rev. 0-A, CH2M HILL Hanford Group, Inc./Technical Resources International, Inc., Richland, Washington.

RPP-23752, 2005, *Field Investigation Report for Waste Management Areas T and TX-TY*, Rev. 0, CH2M HILL Hanford Group, Inc., Richland, Washington.

RPP-ENV-33418, 2016, *Hanford C-Farm Leak Inventory Assessments Report*, Rev. 4, Washington River Protection Solutions, LLC, Richland, Washington.

RPP-ENV-58782, 2016, *Performance Assessment of Waste Management Area C, Hanford Site, Washington*, Rev. 0, Washington River Protection Solutions, LLC, Richland, Washington.

RPP-ENV-58806, 2016, *RCRA Closure Analysis of Tank Waste Residuals Impacts at Waste Management Area C, Hanford Site, Washington*, Rev. 0, Washington River Protection Solutions, LLC, Richland, Washington.

RPP-RPT-29191, 2006, *Supplemental Information Hanford Tank Waste Leaks*, Rev. 0, CH2M HILL Hanford Group Inc., Richland, Washington.

RPP-RPT-42294, 2016, *Hanford Waste Management Area C Soil Contamination Inventory Estimates*, Rev. 2, Washington River Protection Solutions, LLC, Richland, Washington.

RPP-RPT-44042, 2010, *Recharge and Waste Release within Engineered System in Waste Management Area C*, Rev. 0, Washington River Protection Solutions, LLC, Richland, Washington.

RPP-RPT-46088, 2010, *Flow and Transport in the Natural System at Waste Management Area C*, Rev. 1, Washington River Protection Solutions, LLC/GSI Water Solutions, Inc., Richland, Washington.

RPP-RPT-56356, 2014, *Development of Alternative Digital Geologic Models of Waste Management Area C*, Rev. 0, Freestone Environmental Services Inc./Washington River Protection Solutions, LLC, Richland, Washington.

RPP-RPT-58297, 2014, *Screening-Level Evaluation of Groundwater Monitoring Data Collected in Vicinity of WMA C*, Rev. 0, INTERA, Inc./Washington River Protection Solutions, LLC, Richland, Washington.

RPP-RPT-58329, 2014, *Baseline Risk Assessment for Waste Management Area C*, Rev. 0, INTERA, Inc./Washington River Protection Solutions, LLC, Richland, Washington.

RPP-RPT-58339, 2014, *Phase 2 RCRA Facility Investigation Report for Waste Management Area C*, Draft A, Washington River Protection Solutions, LLC, Richland, Washington.

RPP-RPT-59197, 2016, Analysis of Past Tank Waste Leaks and Losses in the Vicinity of Waste Management Area C at the Hanford Site, Southeast Washington, Rev. 1, Washington River Protection Solutions, LLC, Richland, Washington.

RPP-RPT-59625, 2016, *Synopsis of HFFACO Appendix I Performance Assessment for Waste Management Area C*, Rev. 0, INTERA, Inc./Washington River Protection Solutions, LLC, Richland, Washington.

RPP-RPT-61239, in process, *Multiple Lines of Evidence and Modeling Results for Heterogeneous Alternative Conceptual Models of the Subsurface at Waste Management Area C*, Rev. 0, TecGeo, Inc./Pacific Northwest National Laboratory/INTERA, Inc./ CH2M HILL Plateau Remediation Company/Washington River Protection Solutions, LLC, Richland, Washington.

Scanlon, B.R., K.E. Keese, A.L. Flint, L.E. Flint, C.B. Gaye, W.M. Edmunds, and I. Simmers, 2006, "Global synthesis of groundwater recharge in semiarid and arid regions," *Hydrol. Processes*, Vol. 20, pp. 3335–3370.

Schulze-Makuch, D., D. A. Carlson, D. S. Cherkauer, P. Malik, 1999, "Scale Dependency of Hydraulic Conductivity in Heterogeneous Media," *Ground Water*, Vol. 37, No. 6, pp. 904–919.

Seyfried, M.S., S. Schwinning, M.A. Walvoord, W.T. Pockman, B.D. Newman, R.B. Jackson, and F.M. Phillip, 2005, "Ecohydrological Control of Deep Drainage in Arid and Semiarid Regions," *Ecology*, Vol. 86, pp. 277-287.

SGW-59669, 2016, *WMA C Quarterly October Through December 2015 Quarterly Groundwater Monitoring Report*, Rev. 0, CH2M HILL Plateau Remediation Company, Richland, Washington.

van Genuchten, M. Th., 1980, "A Closed-form Equation for Predicting the Hydraulic Conductivity of Unsaturated Soils," *Soil Science Society of America Journal*, Vol. 44, No. 5, pp. 892–898.

WAC 173-303-610, "Closure and Post-Closure," *Washington Administrative Code*, as amended.

WAC 173-340, "Model Toxics Control Act," *Washington Administrative Code*, as amended.

WAC 173-340-720, "Groundwater Cleanup Standards," *Washington Administrative Code*, as amended.

WAC 173-340-747, "Deriving Soil Concentrations for Groundwater Protection," *Washington Administrative Code*, as amended.

Washington State Department of Ecology Cleanup Levels and Risk Calculation (CLARC), Queried 08/30/2016, [CLARC Data Tables – July 2015, Chemical Parameters], https://fortress.wa.gov/ecy/clarc/FocusSheets/CLARC%20Parameters.pdf.

APPENDIX D

TOC-PRES-19-0068-VA, RESULTS OF ADDITIONAL SCOPING CASE RELATED TO PAST LEAKS ANALYSIS PROPOSED BY ECOLOGY, REVISION 0

This page intentionally left blank.

INFORMATION CLEARANCE REVIEW AND RELEASE APPROVAL

Part I: Background Information

Title: Results of Additional Scoping Case Related to Past Leaks Analysis Proposed by Ecology

Publish to OSTI? Yes ✔ No

Information Category: ☐ Abstract ☐ Internet Full Paper ☐ Journal Article ✔ Visual Aid Report ☐ Summary ☐ Software Other

Trademark/Copyright "Right to Use" Information or Permission Documentation — Yes ☐ NA ✔

Document Number: TOC-PRES-19-0068 -VA Revision 0 — Date: January 2019

Author: Bergeron, Marcel P

Part II: External/Public Presentation Information

Conference Name: Meeting with Ecology

Sponsoring Organization(s): DOE-ORP

Date of Conference: 01/31/2019 — Conference Location: Richland, WA

Will Material be Handed Out? Yes ✔ No — Will Information be Published? Yes ✔ No *(If Yes, attach copy of Conference format instructions/guidance.)*

Part III: WRPS Document Originator Checklist

Description	*Yes*	*N/A*	*Print/Sign/Date*
Information Product meets requirements in TFC-BSM-AD-C-01?	☐	✔	
Document Release Criteria in TFC-ENG-DESIGN-C-25 completed? (Attach checklist)	☐	✔	
If product contains pictures, safety review completed?	☐	✔	

Part IV: WRPS Internal Review

Function	*Organization*	*Date*	*Print Name/Signature/Date*
Subject Matter Expert	WRPS	02/21/2019	Bergeron, Marcel P Workflow data attached
Responsible Manager	WRPS	01/03/2019	Rutland, Paul L Workflow data attached
Other:			

Part V: IRM Clearance Services Review

Description	*Yes*	*No*	*Print Name/Signature*
Document Contains Classified Information?	☐	X	If Answer is "Yes," ADC Approval Required Print Name/Signature/Date
Document Contains Information Restricted by DOE Operational Security Guidelines?	☐	X	Reviewer Signature: Print Name/Signature/Date
Document is Subject to Release Restrictions? *If the answer is "Yes," please mark category at right and describe limitation or responsible organization below:*	☐	X	Document contains: ☐ Applied Technology ☐ Personal/Private Proprietary ☐ Patentable Info. ☐ Predecisional Info. ☐ Restricted by Operational Security Guidelines ☐ Other (Specify) ☐ Protected CRADA ☐ Export Controlled Procurement – Sensitive ☐ OUO ☐ UCNI
Additional Comments from Information Clearance Specialist Review?	☐	☒	Information Clearance Specialist Approval APPROVED By Lynn M. Ayers at 11:23 am, Feb 25, 2019 Print Name/Signature/Date

When IRM Clearance Review is Complete – Return to WRPS Originator for Final Signature Routing (Part VI)

INFORMATION CLEARANCE REVIEW AND RELEASE APPROVAL

Part VI: Final Review and Approvals

Description	*Approved for Release*		*Print Name/Signature*
	Yes	*N/A*	
WRPS External Affairs	☒	☐	McKenna, Mark Workflow data attached
WRPS Office of Chief Counsel	☒	☐	Cherry, Steve Workflow data attached
DOE – ORP Public Affairs/Communications	☒	☐	Davis, Tonja-Maree & Levardi, Yvonne Workflow data attached
Other: ORP Counsel	☒	☐	Silberstein, Mark & King, Grace Workflow data attached
Other: ORP SME	☒	☐	Bovier, Jan B Workflow data attached

Comments Required for WRPS-Indicate Purpose of Document:

This presentation provides a summary of results for an additional scoping case proposed by Ecology as a part of their review of RPP-RPT-59197, Rev. 1, " Analysis of Impacts of Past Tank Waste Leaks and Losses in the Vicinity of Waste Management Area C at the Hanford Site, Southeast Washington". Ecology has requested a copy of these results to support the comment resolutions process and approval of RPP-RPT-59197.

APPROVED
By Lynn M. Ayers at 11:23 am, Feb 25, 2019

Approved for Public Release; Further Dissemination Unlimited

Information Release Station

Was/Is Information Product Approved for Release? ☒ Yes ☐ No

If Yes, what is the Level of Releaser? ☑ Public/Unrestricted ☐ Other (Specify) _____

Date Information Product Stamped/Marked for Release: 02/25/2019

Was/Is Information Product Transferred to OSTI? ☐ Yes ☒ No

Forward Copies of Completed Form to WRPS Originator

```
- <workflow name="(LMA) Normal - TOC-PRES-19-0068-VA" id="234889967">
  - <task name="Clearance Process" id="0" date-initiated="20190103T1130"
      performer="Lynn M Ayers" performer-id="212954838" username="h3998817">
      <comments>DUE: Thursday, January 10, 2019 Please review for public
        release, the PowerPoint presentation submitted by Marcel Bergeron. Thank
        you, Lynn Ayers Information Clearance</comments>
    </task>
    <task name="Add XML" id="1" date-done="20190103T1130" />
    <task name="Manager Approval" id="41" date-due="20190108T1130" date-
      done="20190103T1145" performer="Paul L Rutland" performer-id="140633218"
      username="h4494439" disposition="Approve" authentication="true" />
    <task name="Document Reviewer1" id="54" date-due="20190108T1145" date-
      done="20190108T1347" performer="Mark McKenna" performer-id="182697281"
      username="h1903617" disposition="Public Release" authentication="true" />
    <task name="Document Reviewer2" id="53" date-due="20190108T1145" date-
      done="20190130T0856" performer="Stephen B Cherry" performer-id="1382719"
      username="h0374767" disposition="Public Release" authentication="true" />
    <task name="Doc Owner Clearance Review" id="13" date-due="20190131T0856"
      date-done="20190130T0936" performer="Marcel P Bergeron" performer-
      id="172635544" username="h0006384" disposition="Send On"
      authentication="true" />
    <task name="Milestone 1" id="24" date-done="20190130T0936" />
  - <task name="ORP Document Reviewer1" id="57" date-due="20190201T0936" date-
      done="20190221T1604" performer="Tonja-Maree Davis" performer-
      id="181732204" username="h2711692" disposition="Public Release"
      authentication="true">
      <reviewer performer="Jan B Bovier" performer-id="200441446"
        username="h2359189" />
      <reviewer performer="Mark D Silberstein" performer-id="158207236"
        username="h5490246" />
      <reviewer performer="Grace J King" performer-id="211901436"
        username="h9807759" />
      <reviewer performer="Yvonne M Levardi" performer-id="185346745"
        username="h7131303" />
      <comments>Reviewer's Comments Date: 01/31/2019 10:26 AM Step Name:
        TOC-PRES-19-0068 -VA Rev 0 Results of Additional Scoping Case Related to
        Past Leaks Analysis Proposed by Ecology Performer: Bovier, Jan
        (h2359189) I have reviewed the presentation and I have no comments
        Reviewer's Comments Date: 02/19/2019 08:15 AM Step Name: TOC-PRES-
        19-0068 -VA Rev 0 Results of Additional Scoping Case Related to Past Leaks
        Analysis Proposed by Ecology Performer: Silberstein, Mark (h5490246)
        approve Reviewer's Comments Date: 02/21/2019 02:19 PM Step Name:
        TOC-PRES-19-0068 -VA Rev 0 Results of Additional Scoping Case Related to
        Past Leaks Analysis Proposed by Ecology Performer: Levardi, Yvonne
        (h7131303) no comments</comments>
    </task>
    <task name="Doc Owner Reviews ORP Comments" id="61" date-
      due="20190222T1604" date-done="20190221T1614" performer="Marcel P
      Bergeron" performer-id="172635544" username="h0006384" disposition="Send
      On" authentication="true" />
    <task name="Milestone 2" id="62" date-done="20190221T1614" />
    <task name="Verify Doc Consistency" id="4" date-due="20190222T1614" date-
      done="20190225T1027" performer="Lynn M Ayers" performer-id="212954838"
      username="h3998817" disposition="Cleared" authentication="true" />
  </workflow>
```

TOC-PRES-19-0068-VA
Revision 0

Results of Additional Scoping Case Related to Past Leaks Analysis Proposed by Ecology

Prepared for the U.S. Department of Energy
Assistant Secretary for Environmental Management

Contractor for the U.S. Department of Energy
Office of River Protection under Contract DE-AC27-08RV14800

washingtonriver protectionsolutions

P.O. Box 850
Richland, Washington 99352

Approved for Public Release;
Further Dissemination Unlimited

TOC-PRES-19-0068-VA
Revision 0

Results of Additional Scoping Case Related to Past Leaks Analysis Proposed by Ecology

M. Bergeron
Washington River Protection Solutions

W. McMahon
CH2M HILL Plateau Remediation Company

M. Kozak
INTERA, Inc.

S. Mehta
INTERA, Inc.

Date Published
January 2019

To be Presented at
Meeting with Ecology

DOE-ORP
Richland, WA

01/31/2019

Prepared for the U.S. Department of Energy
Assistant Secretary for Environmental Management

Contractor for the U.S. Department of Energy
Office of River Protection under Contract DE-AC27-08RV14800

washingtonriver protectionsolutions
P.O. Box 850
Richland, Washington 99352

Copyright License
By acceptance of this article, the publisher and/or recipient acknowledges the U.S. Government's right to retain a non exclusive, royalty-free license in and to any copyright covering this paper.

APPROVED
By Lynn M. Ayers at 11:23 am, Feb 25, 2019

Release Approval Date

Approved for Public Release;
Further Dissemination Unlimited

TOC-PRES-19-0068-VA
Revision 0

LEGAL DISCLAIMER

This report was prepared as an account of work sponsored by an agency of the United States Government. Neither the United States Government nor any agency thereof, nor any of their employees, makes any warranty, express or implied, or assumes any legal liability or responsibility for the accuracy, completeness, or any third party's use or the results of such use of any information, apparatus, product, or process disclosed, or represents that its use would not infringe privately owned rights. Reference herein to any specific commercial product, process, or service by trade name, trademark, manufacturer, or otherwise, does not necessarily constitute or imply its endorsement, recommendation, or favoring by the United States Government or any agency thereof or its contractors or subcontractors. The views and opinions of authors expressed herein do not necessarily state or reflect those of the United States Government or any agency thereof.

This report has been reproduced from the best available copy.

Printed in the United States of America

washington river protection solutions

Results of Additional Scoping Case Related to Past Leaks Analysis Proposed by Ecology

washington river protection solutions — Marcel Bergeron

INTERA GEOSCIENCE & ENGINEERING SOLUTIONS — Sunil Mehta, Matt Kozak

CH2MHILL Plateau Remediation Company — Bill McMahon

TOC-PRES-19-0068

1

Background Information

- This additional scoping case was undertaken at the request of the Department of Ecology (Ecology) during a May 18, 2018 meeting with DOE and its prime contractor (WRPS) during review of WMA C Past Leaks Analysis (RPP-RPT-59197, Rev. 1)
- Ecology asked for an additional scoping case that evaluates migration of contaminants under the C Tank Farm due to a doubling of the duration, the volume, and the inventory released from tank C-105 assumed in a current scoping case
- DOE agreed to run the additional scoping case as requested by Ecology

Assumptions used in Additional Scoping Case

- **Recommended revisions to release from 241-C-105 Leak (the largest individual source for Tc-99):**
  - Doubling release duration (*Years 1963 to 1973 versus Years 1963 to 1968*)
  - Doubling of release volume (*41,000 gallons versus 20,500 gallons*)
  - Doubling of Tc-99 release inventory (*19.6 Ci of ^{99}Tc versus 9.8 Ci*)

- **All other sources were assumed to remain the same as assumed in the current scoping case**

Point of Calculation (PoC) and Source Contribution at WMA C Fence line and 100 m Downgradient for Additional Scoping Case

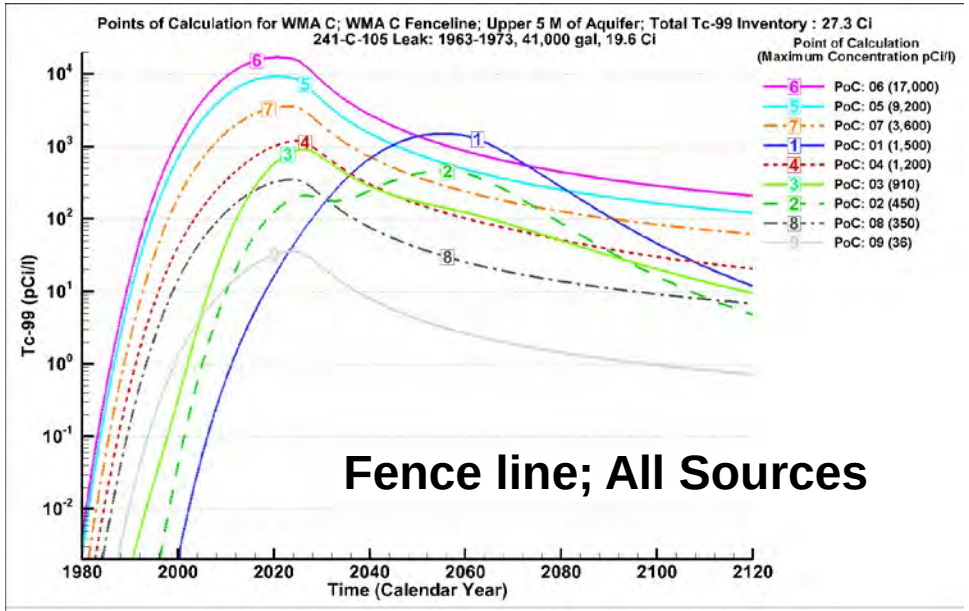

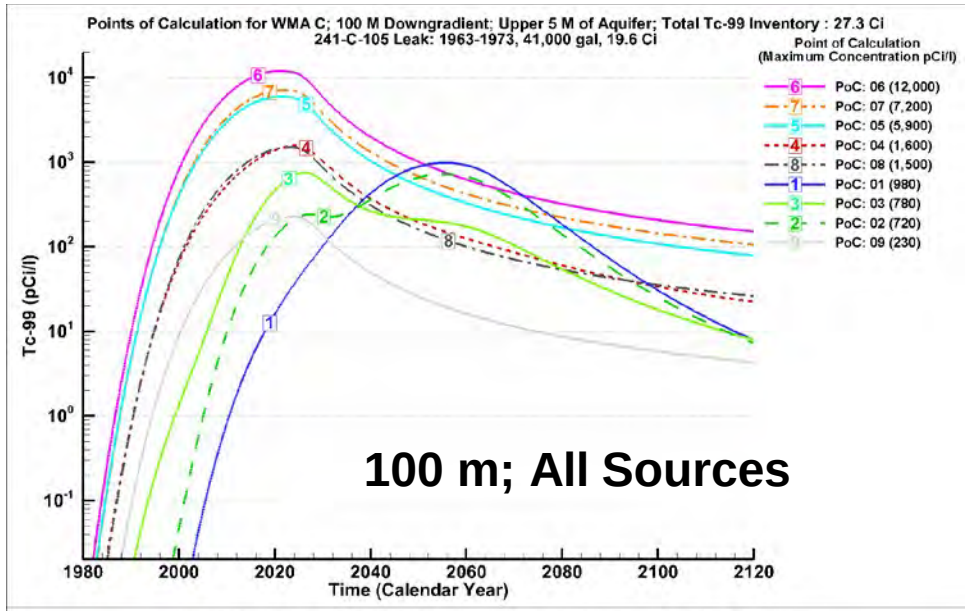

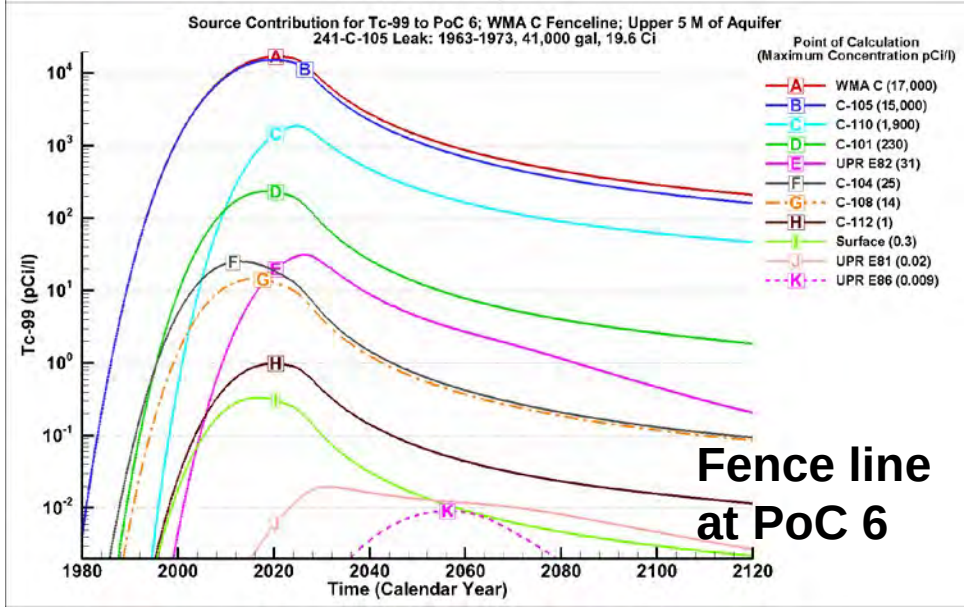

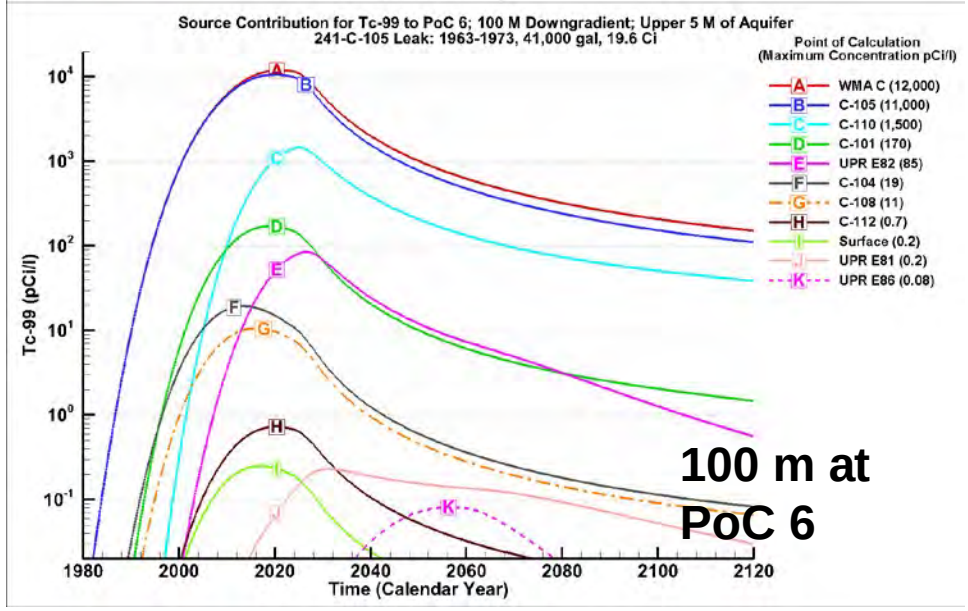

TOC-PRES-19-0068

Results along WMA C Fence line for Additional Scoping Case

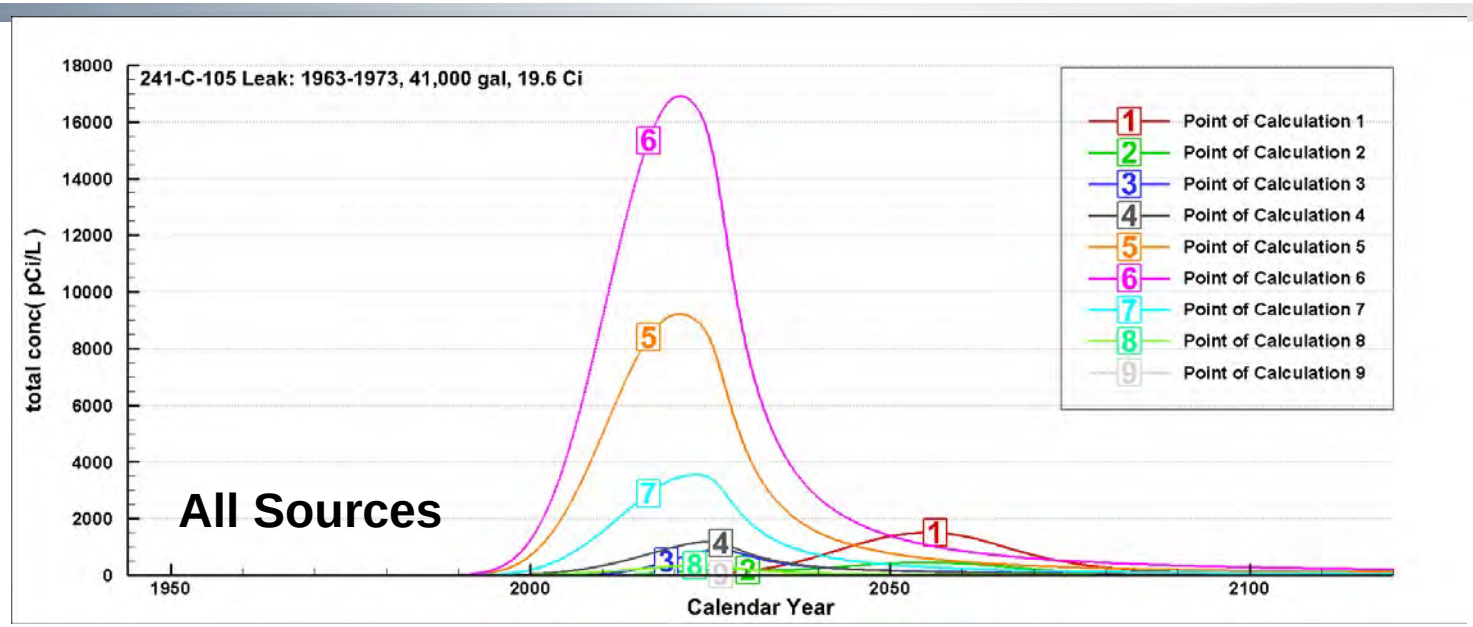

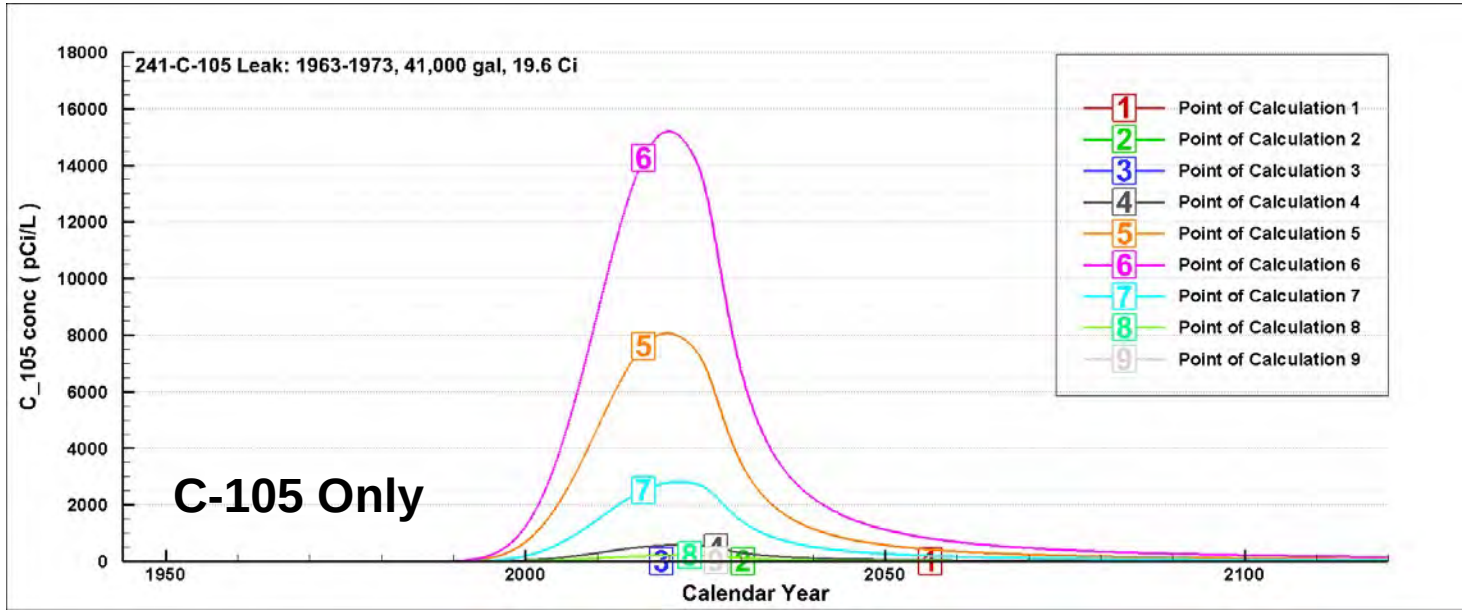

TOC-PRES-19-0068

Comparison of Results for Additional Scoping Case vs. Current Past Leaks Case at WMA C Fence line

	Additional Scoping Case				Current Past Leaks Case			
	All Sources		241-C-105 Source		All Sources		241-C-105 Source	
	Year of Peak	^{99}Tc Peak Concentration (pCi/l)	Year of Peak	^{99}Tc Peak Concentration (pCi/l)	Year of Peak	^{99}Tc Peak Concentration (pCi/l)	Year of Peak	^{99}Tc Peak Concentration (pCi/l)
PoC 1 fence	2055	1,500	2023	0.00004	2055	1,500	2020	0.00002
PoC 2 fence	2055	450	2023	0.004	2055	450	2019	0.002
PoC 3 fence	2026	910	2023	2	2026	910	2019	0.9
PoC 4 fence	2024	1,200	2021	580	2025	880	2018	280
PoC 5 fence	2020	9,200	2019	8,100	2018	5,000	2016	4,100
PoC 6 fence	2020	16,900	2019	15,200	2018	9,400	2016	8,000
PoC 7 fence	2022	3,600	2021	2,800	2022	2,200	2018	1,500
PoC 8 fence	2023	350	2021	220	2023	240	2018	120
PoC 9 fence	2024	36	2021	20	2024	26	2018	11

washington river protection solutions

Summary and Conclusions

- **Doubling of the duration, the volume, and inventory releases assumed in the additional scoping case showed the following results:**
  - The timing of peak concentrations of Tc-99 remained practically unchanged (about Year 2020) when compared to the Current Past Leaks case
    - Peak Concentrations in groundwater at the WMA C fence line and 100 m down gradient occurred about 2 years later
  - The maximum concentrations in groundwater were about 80 and 90 percent higher at the WMA C fence line and 100 m down gradient when compared to the results for the same locations in the Current Past Leaks case
- **As a part of the comment resolution process, DOE agreed to add results of the additional scoping case in Updates to RPP-RPT-59197**